Marine biogeography and evolution: diversity patterns of planktonic gastropods and amphipods

Alice K. Burridge

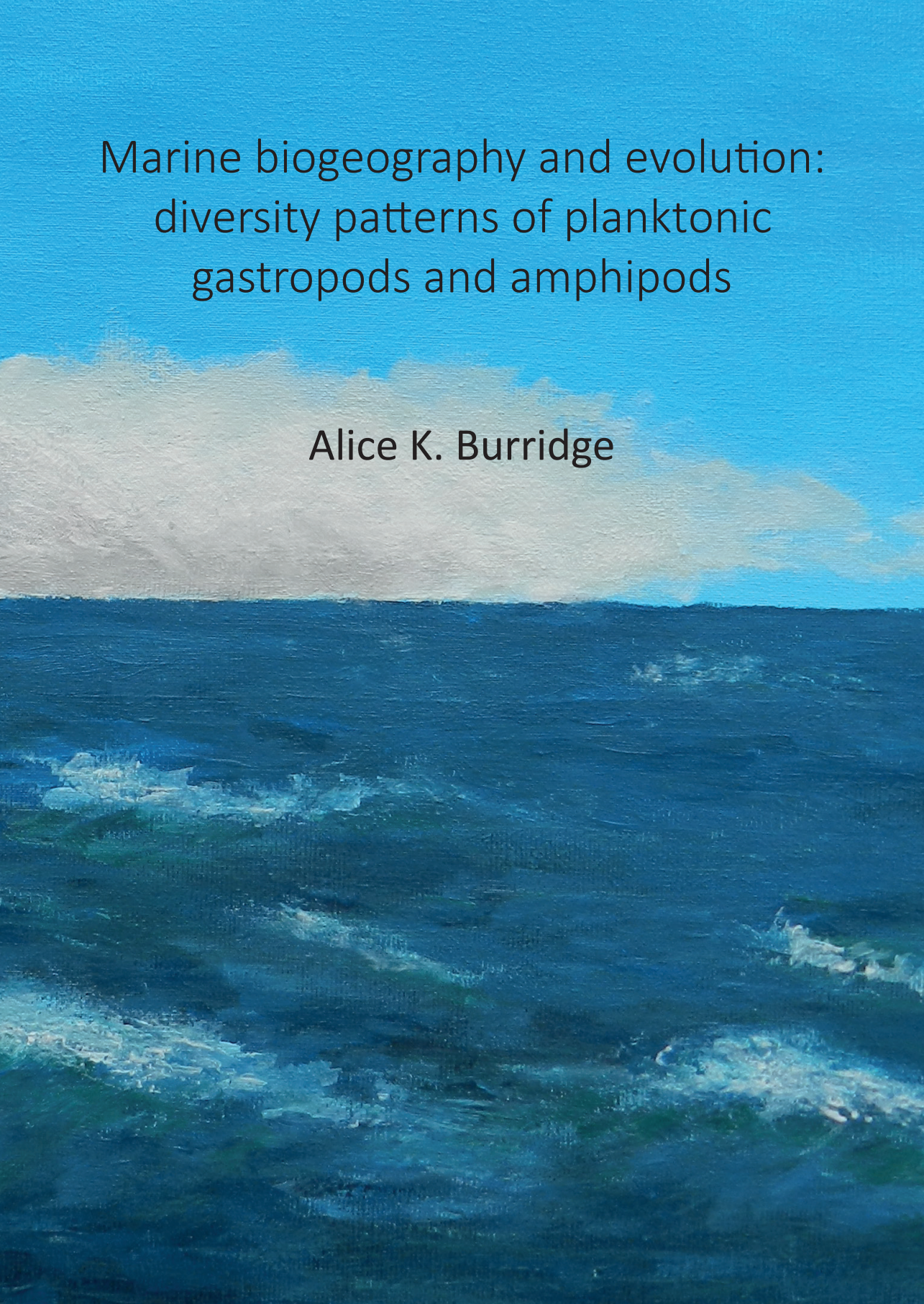

Marine biogeography and evolution: diversity patterns of planktonic gastropods and amphipods

Burridge A.K., 2017. Marine biogeography and evolution: diversity patterns of planktonic gastropods and amphipods

PhD thesis, University of Amsterdam, The Netherlands

This research was carried out at Naturalis Biodiversity Center, Leiden and the Institute for Biodiversity and Ecosystem Dynamics, University of Amsterdam
(Funding is listed in individual chapters)

ISBN: 978-94-91407-51-2

Figures, photos and cover by Alice Karen Burridge
Layout by Jan Bruin (www.bred.nl)
Printed by GvO printers & designers B.V., Ede

Marine biogeography and evolution: diversity patterns of planktonic gastropods and amphipods

ACADEMISCH PROEFSCHRIFT

ter verkrijging van de graad van doctor
aan de Universiteit van Amsterdam
op gezag van de Rector Magnificus
prof. dr. ir. K.I.J. Maex
ten overstaan van een door het College voor Promoties ingestelde commissie,
in het openbaar te verdedigen in de Agnietenkapel

op donderdag 7 december 2017, te 14.00 uur

door

Alice Karen Burridge

geboren te Alphen aan den Rijn

Promotiecommissie

Promotores

Prof. dr. J. Huisman	Universiteit van Amsterdam
Prof. dr. S.B.J. Menken	Universiteit van Amsterdam

Copromotor

Dr. K.T.C.A. Peijnenburg	Naturalis Biodiversity Center

Overige leden

Prof. dr. J.C. Biesmeijer	Universiteit Leiden
Dr. J.A.J. Breeuwer	Universiteit van Amsterdam
Prof. dr. C.P.D. Brussaard	Universiteit van Amsterdam
Prof. dr. M.D. Ohman	University of California, San Diego
Dr. W. Renema	Naturalis Biodiversity Center
Prof. dr. P.C. de Ruiter	Universiteit van Amsterdam
Prof. dr. L.J. Stal	Universiteit van Amsterdam

Faculteit der Natuurwetenschappen, Wiskunde en Informatica

Table of contents

1

Introduction

'I find to my great surprise that a ship is singularly comfortable for all sorts of work. Everything is so close at hand, and being cramped makes one so methodical, that in the end I have been a gainer. I already have got to look at going to sea as a regular quiet place, like going back to home after staying away from it. In short, I find a ship a very comfortable house, with everything you want, and if it was not for sea-sickness the whole world would be sailors.'

Charles Darwin in a letter to his father during the voyage of the Beagle, 1832.
Published in *The life and letters of Charles Darwin*
(edited by his son Francis Darwin, 1887).

In his famous book *The Voyage of the Beagle*, Charles Darwin writes about his adventures and discoveries while sailing across the world's oceans. For centuries, mankind has been wondering what is out there in the seas, and even now, almost 2 centuries after the voyage of the *Beagle*, this question is still awaiting numerous answers from the deep. The magnitude of global marine species diversity has been estimated at 0.7-1.0 million (Appeltans et al., 2012). Of this number, approximately 229,000 species have been described, of which the Animalia constitute approximately 196,000 species (World Register of Marine Species, WoRMS). Marine species are not distributed homogeneously throughout the global ocean, but their distributions are directly or indirectly linked to oceanographic properties like temperature, salinity, and chlorophyll concentration (Van der Spoel and Heyman, 1983; Longhurst, 1998; Norris, 2000; Reygondeau et al., 2013). These properties enable the division of all oceans into biogeochemical provinces that provide a diverse range of ecological niches as well as barriers to dispersal for pelagic species, amongst which the zooplankton (Figure 1; De Vargas et al., 2015; Boltovskoy and Correa, 2016, 2017). Unlike earlier episodes of change throughout the geological time scale, current ocean change is partially caused by human activity. To track the effects of ocean change on zooplankton species diversity, distribution, and across trophic levels, it is essential to gain insights into when current biodiversity evolved, what part of the marine biodiversity is where, and how closely related species can be distinguished.

During 6 weeks in 2014, I was part of an oceanographic expedition from England to the Falkland Islands, hoping to obtain zooplankton samples that would help me address the questions above. Indeed, like Darwin wrote, all utilities were close at hand. The work was methodical and followed a tight schedule. (If you, however, think that being a sailor is the major activity of a modern-day marine biologist, you are wrong: most often they are analyzing data and writing papers or grant proposals). During this expedition, I came to realize the true vastness of the ocean. Oceans cover approximately 71% of the planet's surface. Of the total surface covered by oceans, 46.6% is covered by the Pacific Ocean, followed by the Atlantic (23.5%), Indian (19.5%), Southern (6.1%), and Arctic (4.3%) oceans. The average depth of the ocean has been estimated at 3682 m. Together the oceans contain 97% of the Earth's water (Charette and Smith, 2010).

Twelve animal phyla are prevalent in the marine metazoan holoplankton: Annelida (polychaetes: bristle worms), Arthropoda (predominantly represented by crustaceans: copepods, cladocerans, ostracods, amphipods, mysids, euphausiids), Chaetognatha (arrow worms), Chordata with the subphyla Vertebrata (represented by small fish), Tunicata (salps, pyrosomes, dolioids, appendicularians), and Cephalochordata (lancelets), Cnidaria (amongst which are jellyfish and box jellies), Ctenophora (comb jellies), Mollusca (predominantly represented by the gastropod groups pteropods and heteropods), Nematoda (roundworms), Nemertea (unsegmented, worm-like organisms), Platyhelminthes (flatworms), and Rotifera (wheel animals; Angel, 1993). Arthropoda are consistently the dominant pelagic metazoan group, and most arthropods have been identified as copepods (De Vargas et al., 2015; Pearman and Irigoien, 2015).

In recent years, marine calcifiers have gained considerable attention because of their potential vulnerability to oceanic uptake of carbon dioxide (CO_2; e.g., Drake et al., 2014; Bednaršek et al., 2016; Moya et al., 2016; Hattich et al., 2017; Kroeker et al., 2017; Manno et al., 2017; Riebesell et al., 2017). Major groups of calcifying plankton are pteropods and heteropods with aragonite shells, and coccolithophores and foraminifers with calcite shells (Fabry et al., 2008). Pteropod and heteropod gastropods occur throughout the world's oceans and are especially vulnerable to the effects of ocean acidification because aragonite is more soluble than calcite. However, their use as bioindicators of the effects of ocean acidification is compromised by limited knowledge of their taxonomy and distributions for understanding species-specific responses to ocean change. Accurate insights into their taxonomy,

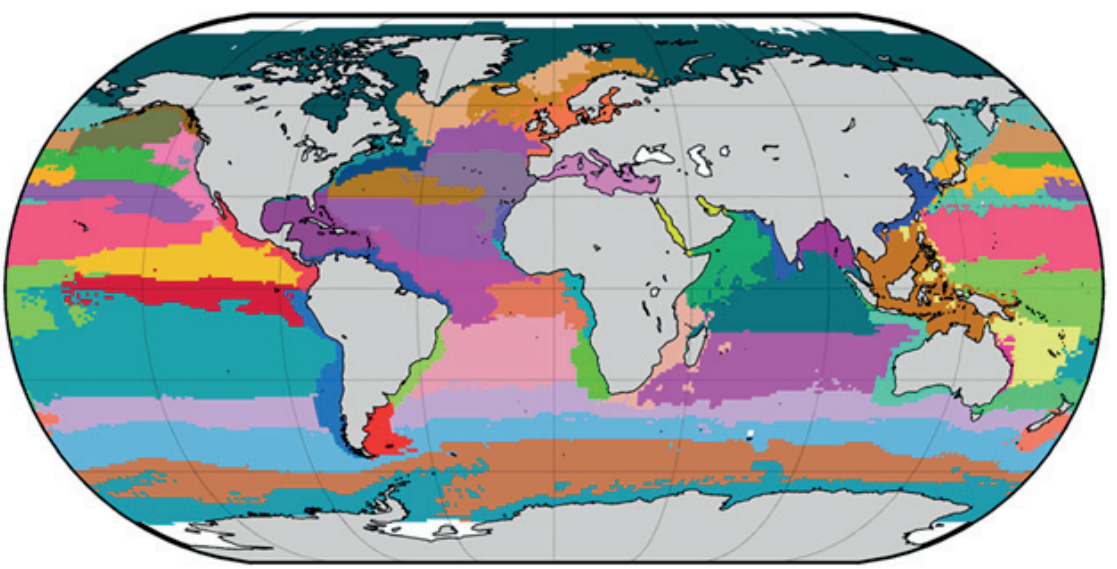

Figure 1. Average distribution of 56 biogeochemical provinces across the global ocean as calculated by Reygondeau et al. (2013) based on the monthly distribution patterns of biogeochemical provinces from January 1998 to December 2007. Edited from Reygondeau et al. (2013), with permission from publisher John Wiley and Sons.

genetic diversity, and biogeography are the essential first steps to predicting the ecological and evolutionary responses of individual species to ocean change.

Atmospheric CO_2 concentrations varied between 180 ppmv during glacials and 280-300 ppmv during interglacials in the last 650,000 years (Siegenthaler et al., 2005). As a consequence of human activity in the past 200 years, the present atmospheric CO_2 concentration is ~410 ppmv (National Oceanic & Atmospheric Administration, 2017) with an expected increase of ~0.5% per year (Forster et al., 2007). Approximately one third of the anthropogenic CO_2 emission is currently stored in the ocean (Sabine et al., 2004). The Southern Ocean will become undersaturated with aragonite and calcite when atmospheric CO_2 concentrations exceed 560 and 900 ppmv, respectively. Given the current rise in atmospheric CO_2 concentrations, it is projected that Southern Ocean surface waters will begin to become undersaturated with respect to aragonite by the year 2050, followed by an extension throughout the entire Southern Ocean, the subpolar Pacific Ocean, and the Arctic Ocean by 2100 (Orr et al., 2005; Comeau et al., 2012). On time scales of several thousands of years, it is estimated that 90% of the anthropogenic CO_2 emissions will end up in the ocean (Sabine et al., 2004). It is expected that pteropods will have difficulty to maintain shells in waters that are undersaturated with respect to aragonite. This may have considerable ecological and biogeochemical impacts, as pteropods serve as food in the diets of a variety of zooplankton and fish species and play a key role in marine calcification.

This thesis aims to understand the diversity, distribution, and evolution of different groups of marine zooplankton in the global ocean. The majority of this thesis (Chapters 2-6) focuses on calcifying zooplankton, more specifically the pelagic gastropods. For instance, I will investigate when current pteropod diversity arose (Chapter 2), how pteropod taxa are related (Chapters 2-5), how species within the pteropod genera *Cuvierina* and *Diacavolinia* can be distinguished and where they occur across the global ocean (Chapters 3-5), and what part of the pteropod and heteropod biodiversity is where in the Atlantic Ocean (Chapter 6). Additionally, Chapter 7 focuses on hyperiid amphipods. They are not marine calcifiers, but are a group of crustaceans that often live as commensals and parasites of gelatinous zooplankton and are an example group of indirect dependence on oceanographic properties. Because hyperiid amphipods were commonly found in zooplankton samples, they allowed for comparison of diversity patterns with pelagic gastropods.

Study organisms

Pteropods

Pteropods are a group of holoplanktonic heterobranch gastropods (Jörger et al., 2010). They comprise the orders Thecosomata, commonly referred to as 'sea butterflies', and Gymnosomata, referred to as 'sea angels' because their two parapodia resemble the shapes of the wings of butterflies or angels (Figure 2). According to WoRMS, there are 83 extant thecosome species and 43 gymnosome

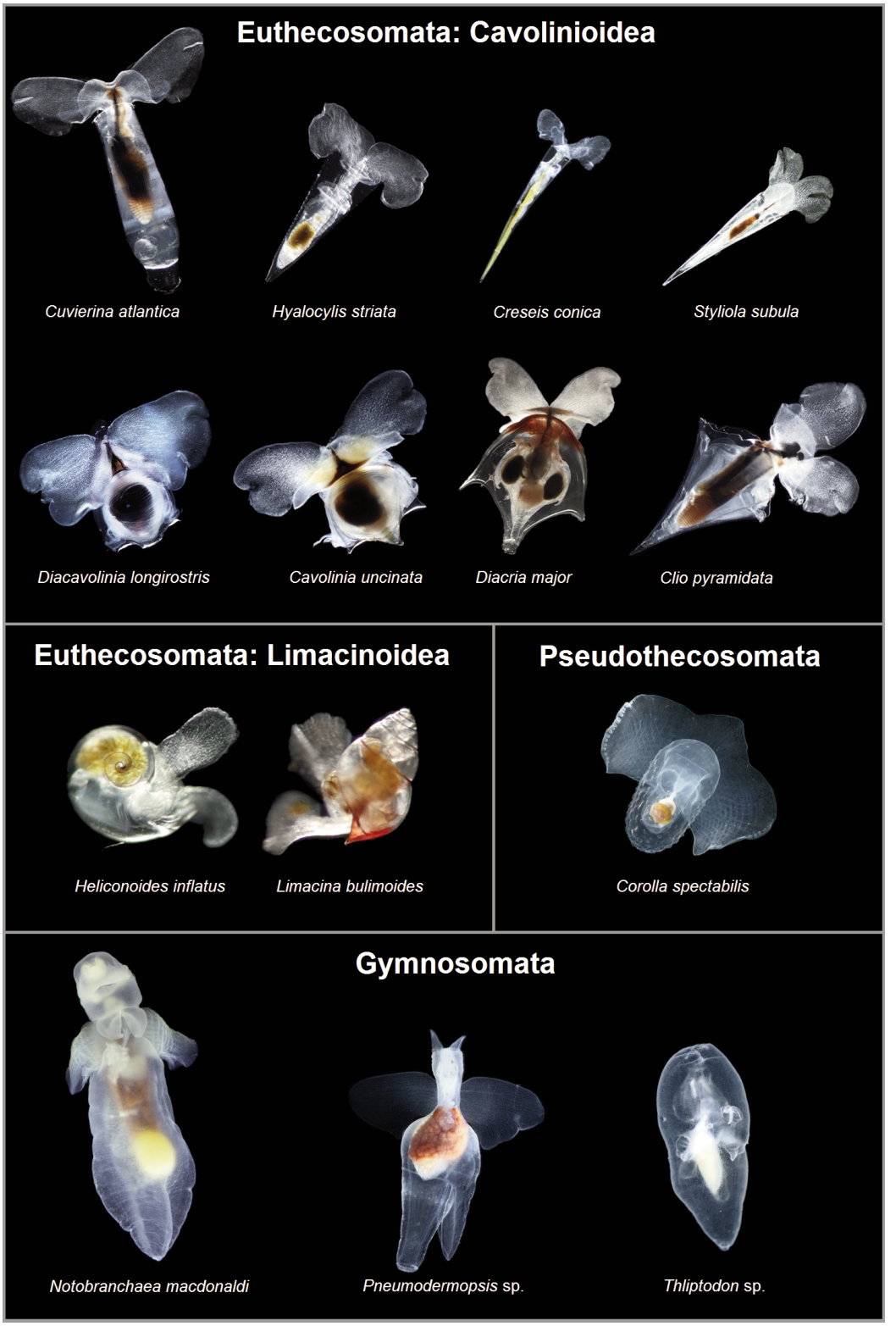

FIGURE 2. Representatives of pteropods (not scaled to relative sizes). Euthecosomata photos taken by K.T.C.A. Peijnenburg and E. Goetze during Atlantic Meridional Transect 22 (2012), Pseudothecosomata and Gymnosomata photos taken by K. Osborne and S. Bush (2012 and 2013).

species worldwide, and many fossil species also have been described (Janssen and Peijnenburg, 2014). Most pteropods are between 0.05 and 2 cm in size. Most pteropod species are epipelagic, but some species are meso- or bathypelagic, and they are vertical migrators moving to shallower depths at night (Van der Spoel and Dadon, 1999; Bé and Gilmer, 1977). The thecosomes feed on microplankton by producing mucus webs, whereas gymnosomes are active predators, often feeding on thecosomes (Gilmer and Harbison, 1986; Van der Spoel and Dadon, 1999). The thecosomes are divided into the suborders Euthecosomata (11 genera, 60 species), with aragonite shells throughout their lives, and Pseudothecosomata (five genera, 23 species), with sinistrally coiled shells or a semi-soft pseudoconch and an aragonite shell during the larval stage (Meisenheimer, 1906; Van der Spoel and Dadon, 1999; Janssen, 2012). Of the euthecosomes, the superfamily Cavolinioidea (eight genera, 52 species) has uncoiled shells, and the superfamily Limacinoidea (three genera, eight species) has coiled shells. Gymnosomes have larval shells that are shed during metamorphosis to the adult stage (Lalli and Conover, 1976; Van der Spoel and Dadon, 1999).

Heteropods

Heteropods are commonly referred to as 'sea elephants' because of their elongate and flexible proboscis and are formally known as Pterotracheoidea (Caenogastropoda). There are three heteropod families: Atlantidae (three genera, 23 species), Carinariidae (three genera, nine species), and Pterotracheidae (two genera, five species; Wall-Palmer et al., 2016a,b,c). The Atlantidae are fully shelled, generally less than 1 cm in size, and are the least efficient swimmers of all heteropods (Figure 3). They can retract their bodies into their keeled, dextrally coiled shells (Seapy et al., 2003). *Atlanta* species have shells composed of aragonite, *Protatlanta* has a shell of aragonite and a keel of conchiolin, and *Oxygyrus* has a shell largely composed of conchiolin (Richter and Seapy, 1999). The Carinariidae have very large, cylindrical bodies that are much larger than their shells and can become up to 50 cm long (Lalli and Gilmer, 1989). The Pterotracheidae have an elongated body that

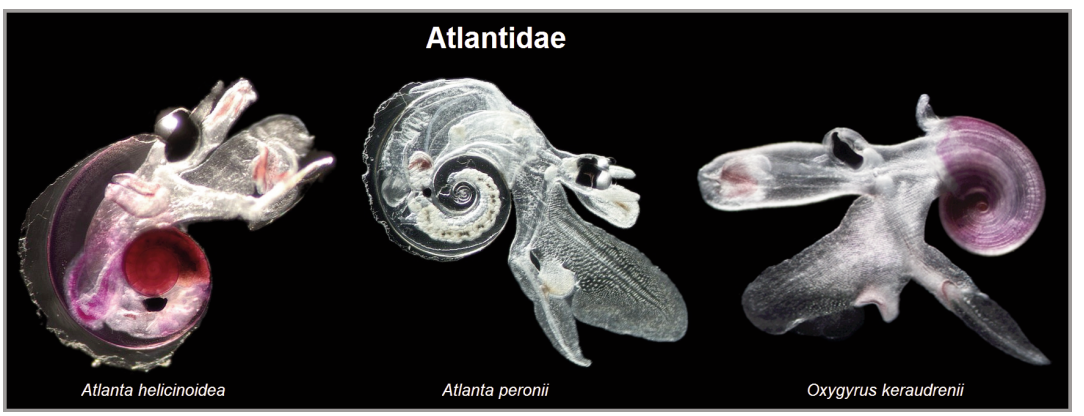

Figure 3. Heteropods (Atlantidae). Note the eye and proboscis in the upper part of the image. Photo taken by K.T.C.A. Peijnenburg and E. Goetze.

can reach a length of 33 cm and only have larval shells (Richter and Seapy, 1999). Heteropods occur primarily at tropical and subtropical latitudes, but *Atlanta ariejansseni* is adapted to the specific conditions of the Southern Subtropical Convergence Zone (Richter and Seapy, 1999; Wall-Palmer et al., 2016a). Heteropods occur in upper mesopelagic and epipelagic waters (Richter and Seapy, 1999). They are visual predators that feed on other zooplankton and small fishes, and as juveniles they feed on small zooplankton and phytoplankton (Lalli and Gilmer, 1989; Seapy et al., 2003). The diversity and abundance of heteropods, predominantly Atlantidae, are studied along a 2014 north-south transect in the Atlantic Ocean in Chapter 6.

Hyperiid amphipods

The amphipod suborder Hyperiidea is an exclusively pelagic group of crustaceans with 292 species currently accepted in WoRMS. Hyperiids are classified into two infraorders, the bathypelagic and mesopelagic Physosomata and the epipelagic and mesopelagic Physocephalata (Figure 4; Vinogradov et al., 1996; Browne et al., 2007; Hurt et al., 2013). The Physocephalata are the most diverse group, with approximately 65% of extant species in 20 families. Most diverse hyperiid families are the Scinidae (Physosomata; 45 species) and the Hyperiidae (Physocephalata; 29 species, WoRMS, 2016). Most hyperiid amphipods are parasitoids and commensals of gelatinous zooplankton, i.e., tunicates, medusae, ctenophores, and siphonophores serve as primary hosts (Harbison et al., 1977; Madin and Harbison, 1977; Laval, 1980; Phleger et al., 1999; Gasca and Haddock, 2004). Some families and genera appear to be restricted to particular host groups while others are less selective (Harbison et al., 1977; Madin and Harbison, 1977; Laval, 1980; Lavaniegos and Ohman, 1999; Gasca et al., 2015; Riascos et al., 2015). Free-living hyperiids occur predominantly in polar environments, where they can dominate the total zooplankton biomass and serve as prey for squids, fishes, and seabirds (Bocher et al., 2001; Laptikhovsky, 2002; Shreeve et al., 2009; Waluda et al., 2010). The diversity and distribution of hyperiids are studied across a 2012 transect in the Atlantic Ocean in Chapter 7.

Study methods

Time-calibrated molecular phylogenies

Pteropods have an extensive fossil record, primarily consisting of euthecosome shells (e.g., Janssen, 2007, 2012; Janssen and Peijnenburg, 2017). In combination with molecular methods for phylogenetic inference, the fossil record improves our understanding of the evolutionary history of pteropods by providing a framework for ages of taxa. Because pteropod shells are fragile, they do not survive significant transportation and are rarely displaced from one sedimentary unit into another. This makes them reliable fossils for fossil-calibrated phylogenetic and biostratigraphic purposes (Janssen and Peijnenburg, 2014). Vicariance events, or the occurrence of physical barriers to dispersal, have had profound effects on marine evolu-

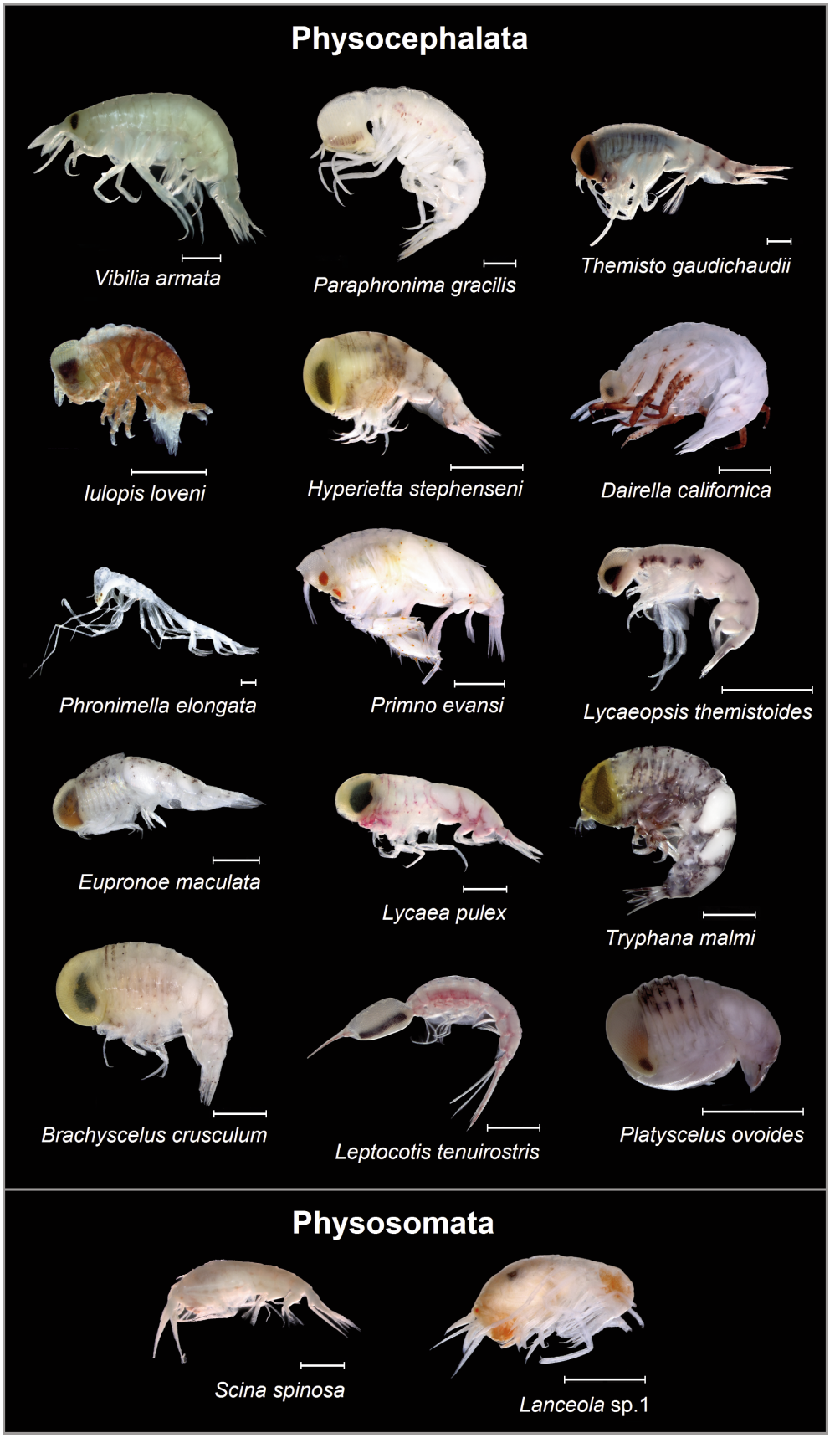
Physocephalata
Vibilia armata
Paraphronima gracilis
Themisto gaudichaudii
Iulopis loveni
Hyperietta stephenseni
Dairella californica
Phronimella elongata
Primno evansi
Lycaeopsis themistoides
Eupronoe maculata
Lycaea pulex
Tryphana malmi
Brachyscelus crusculum
Leptocotis tenuirostris
Platyscelus ovoides
Physosomata
Scina spinosa
Lanceola sp.1

tion. Examples are the Terminal Tethyan Event separating the Atlantic from the Indian Ocean ~19 million years ago (mya), and the formation of the Isthmus of Panama (IOP) between the Atlantic and Pacific oceans ~3 mya (Harzhauser et al., 2007; Bowen et al., 2016; O'Dea et al., 2016). Vicariance events have caused centers of marine diversity to shift and have reduced connectivity by changes in ocean circulation, but the timing of these effects on specific taxa is not fully understood (e.g., Knowlton and Weigt, 1998; Lessios, 2008; Renema et al., 2008; Bowen et al., 2016; O'Dea et al., 2016). Divergence between lineages from different oceans would allow the use of vicariance events as molecular clock calibrations and their comparison with fossil calibrations. However, refinement of fossil as well as biogeographic calibrations will play an important role in strengthening the reliability of molecular clocks (Ho, 2014). In this thesis, I use fossil records of pteropods to calibrate molecular phylogenies in Chapter 2, providing a framework for ages of genera and superfamilies. Additionally, inferred ages of clades are compared based on different calibration methods.

Integrative taxonomy and the species concept

Integrative taxonomy tests species hypotheses using a combination of diverse and sometimes incomplete character and data types. It aims to prevent under- or overestimation of species numbers by describing species based on congruence between morphological and genetic information, with additional supporting characteristics such as geography, behavior, or ecology (McManus and Katz, 2009; Padial et al., 2010; Smith and Hendricks, 2013; Edwards and Knowles, 2014; Karanovic et al., 2016). Recently, novel tools and technologies have improved the application of integrative taxonomy for species discovery, such as advances in high-throughput DNA sequencing, morphometric methods, geographic information systems, and virtual access to museum collections (Vogler and Monaghan, 2006; Leray and Knowlton, 2016). Although statistically identified genetic lineages play a major role in species detection because they are objective tests of species hypotheses that satisfy multiple species concepts, the sole use of genetic information for species detection may fail to delimit the same number of species compared to integrative taxonomic methods (De Queiroz, 2007; Hausdorf, 2011; Edwards and Knowles, 2014; Morard et al., 2016; Sukumaran and Knowles, 2017). Species may go undetected due to a limited set of genetic markers, because they may be distinct only in other genes, morphology, or ecological niche space (Karanovic et al., 2016). I apply an integrative taxonomic species concept in this thesis to study pteropod diversity by using two or three genetic markers combined with geographic information (Chapters 2-5), and additionally, with geometric morphometric information (Chapters 3-5) and ecological niche models (ENM; Chapter 3).

Figure 4. Representatives of the 17 families of hyperiid amphipods that were observed in samples from the Atlantic Meridional Transect 22 (2012). All scale bars represent 1 mm. Edited from Chapter 7.

Geometric morphometrics

Two- or three-dimensional geometric morphometrics is the statistical analysis of shape based on landmark coordinates on a structure (Bookstein, 1991). Shape differences between specimens can be identified by separating shape information from size by Procrustes superimposition, which involves the scaling, translation, and rotation of the landmark coordinates, so that the specimens fit on top of each other in the best possible way. The results can be visualized as actual shapes or shape deformations (Mitteroecker and Gunz, 2009). Landmarks often are point locations that are biologically homologous between species. However, if it is impossible to quantify a shape by homologous landmarks alone, they may be supplemented with smooth curves consisting of semilandmarks that enable quantification of the curve (Gunz and Mitteroecker, 2013). Shelled gastropods have complex and diverse shell shapes that enable detailed geometric morphometric analyses to distinguish species and geographic variation in a powerful way. In this thesis, geometric morphometric methods are applied to multiple orientations of pteropod shells to distinguish between *Cuvierina* species in Chapters 3 and 4 and *Diacavolinia* species in Chapter 5. Geometric morphometric analysis is particularly useful in studies that include historical specimens from, e.g., museum collections for which no genetic information can be obtained (Chapter 5).

Ecological niche modeling

Accurately assessing species distribution patterns is essential for predicting species-specific ecological and evolutionary responses to climate change. Ecological niche modelling (ENM), also referred to as Species Distribution Modelling (SDM), is an important tool to analyze and predict the biogeographical distributions of species based on their response to environmental variables. In contrast to the terrestrial domain, ENM has been applied to the marine environment only since the last ~10 years (Elith and Leathwick, 2009; Dambach and Rödder, 2011; Robinson et al., 2011; Bentlage et al., 2013; Beaugrand et al., 2014). Prior to this, studies of biogeography of marine taxa relied on qualitative estimation of species distributions (e.g., Bé and Gilmer, 1977; Van der Spoel and Heyman, 1983). To estimate ecological tolerances of different taxa, ENM combines presence data of species with spatial data layers of environmental data. The use of presence-only data (i.e., without absence data) is preferred, because collection of sampling locations is often spatially biased toward easily accessible areas and, therefore, the apparent lack of observations of a species in a particular area does not necessarily imply that the species does not occur there (Phillips et al., 2009). Techniques have been developed to allow for significance testing of ENMs based on presence-only data (Raes and Ter Steege, 2007). In this thesis, two-dimensional ENM is applied to quantitatively estimate the ecological tolerances of six *Cuvierina* pteropod morphotypes (Chapter 3).

Species diversity and distribution patterns

An important source of Atlantic zooplankton samples used throughout this thesis is the Atlantic Meridional Transect (AMT), a multidisciplinary expedition for biolo-

gical, chemical, and physical oceanographic research (Figure 5). It is presently an annual transect of >12,000 km between the United Kingdom and the South Atlantic (the Falkland Islands, Chile, or South Africa) and traverses a range of biogeochemical provinces (Rees et al., 2015). For this thesis, I participated in the 2014 expedition and obtained quantitative samples of meso- and macrozooplankton

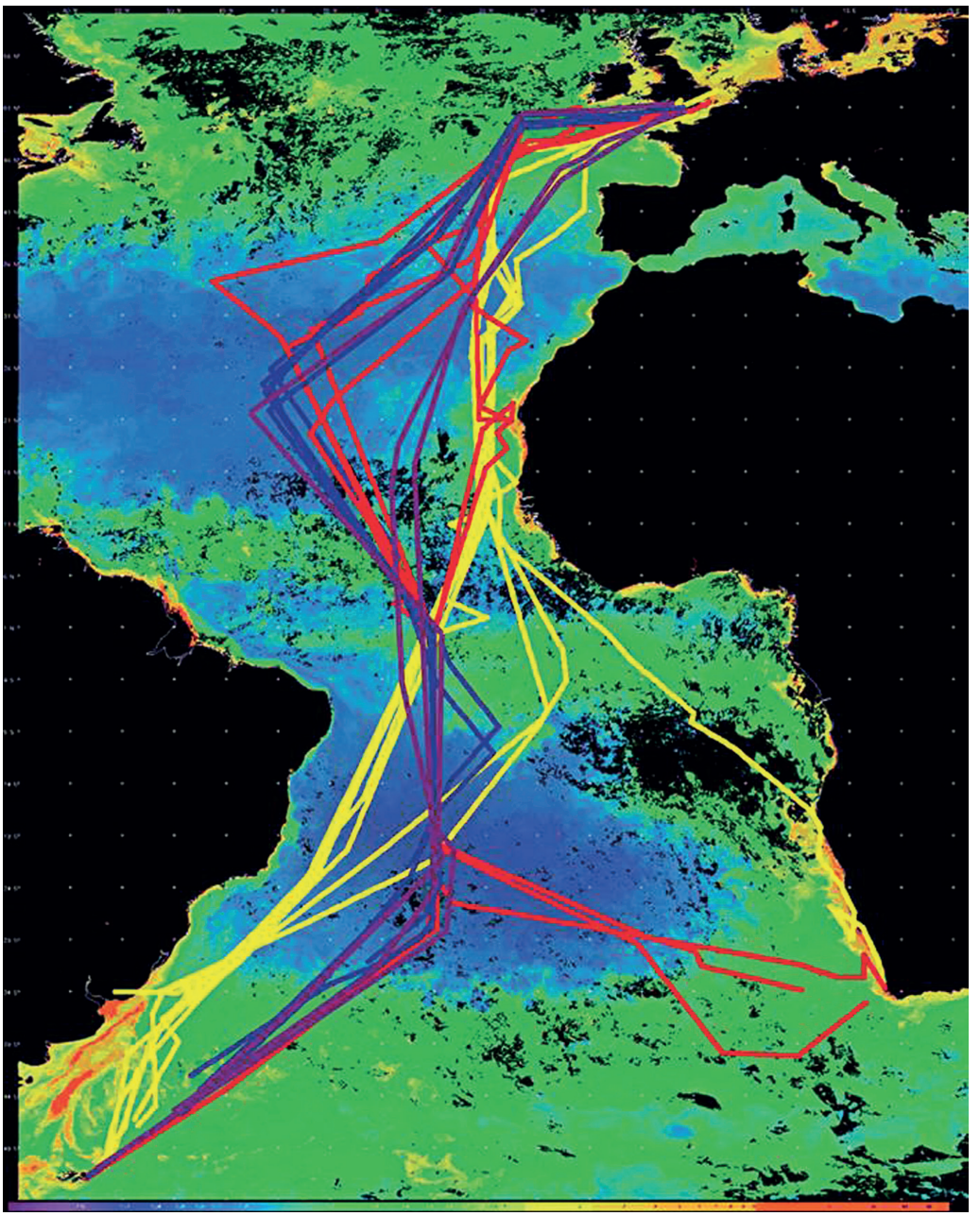

Figure 5. Cruise tracks of AMT1 to AMT25. Transect colors are yellow for AMT1 to 11 (1995-2000), red for AMT12 to AMT17 (2002-2006), blue for AMT18 to 22 (2007-2012), and purple for AMT23 to AMT25 (2012-2015). Ocean colors are from a composite chlorophyll *a* image (courtesy of NEODAAS) for October 2009 (AMT19). From Rees et al. (2015), with permission from publisher John Wiley and Sons.

from the upper ~300 m (AMT24: Chapter 6). I also used non-quantitative zooplankton samples from the upper ~300 m that were collected during the 2012 edition (AMT22: Chapters 2-5 and 7). During both expeditions, samples were obtained by conducting oblique tows at night using a bongo net of 0.71 m diameter and a mesh size of 200 µm (Chapter 6) or 333 µm (Chapter 7).

Biogeochemical provinces of the world's oceans are defined by ecosystem dynamics and biogeochemistry. A total of 56 biogeochemical provinces has been characterized (Longhurst, 1998; Reygondeau et al., 2013). The locations of these biogeochemical provinces are not fixed but fluctuate at seasonal and interannual timescales. It is often assumed that the distributions of distinct species assemblages of marine zooplankton correspond with the distributions of biogeochemical provinces. With the ongoing discovery and collection of marine zooplankton taxa, we gradually obtain a better picture of the biogeographical distributions of pelagic species, and this assumption can be tested by visualization and quantification of similarities in species composition across stations by, e.g., hierarchical clustering, similarity profile analysis, and non-metric multidimensional scaling (Clarke 1993; Clarke and Warwick, 2001; Clarke and Gorley, 2006). Distributions of pelagic species assemblages of pteropods, heteropods, and amphipods are examined in Chapters 6 and 7.

Thesis outline

This thesis aims to improve current understanding of biogeographical and evolutionary patterns in a selection of zooplankton taxa: pteropods, heteropods, and amphipods. I participated in an expedition across the Atlantic Ocean to collect numerous new specimens in addition to using extensive museum collections from all oceans. I obtained new molecular, geometric morphometric and biogeographic information to better comprehend their diversity, distribution, and evolution in the global ocean.

In Chapter 2, I study the phylogenetic relationships of pteropods based on combined analyses of three genetic markers: Cytochrome Oxidase I (COI) mtDNA, 28S rDNA, and 18S rDNA. With a total of 55 included pteropod species spanning the diversity of the group and sampled from each ocean basin, I include molecular data of seven additional euthecosome, two pseudothecosome, and five gymnosome species relative to prior studies. I reconstruct the evolutionary history of pteropods using a fossil-calibrated molecular clock approach.

In Chapter 3, I aim to understand the biogeography and evolution of *Cuvierina* pteropods from the Atlantic, Pacific, and Indian Ocean as a basis for taxonomic revisions by applying an integrative taxonomic approach to this genus for the first time. Geometric morphometric analyses of shell shape variation, phylogenetic analyses based on COI and 28S, and Ecological Niche Modelling are applied to distinguish between and within extant taxa, determine the temporal sequence of evolution in the genus, and explore the current and past biogeographic context of extant *Cuvierina* species.

In Chapter 4, I revise the taxonomy of *Cuvierina* pteropods based on findings from Chapter 3. I reject the earlier proposed subgenera within *Cuvierina* and describe a new species endemic to the Pacific Ocean, *Cuvierina tsudai*.

In Chapter 5, I apply an integrative taxonomic approach to assess species boundaries in *Diacavolinia* pteropods from the Atlantic, Pacific, and Indian Ocean. I develop a method for identifying species boundaries by combining incomplete and varied datasets, and inferences are based on congruence between geometric morphometric analyses of shell shape, phylogenetic analyses based on COI and 28S, and geographic data. This study includes type specimens that were used to describe *Diacavolinia* species.

In Chapter 6, I assess species distributions, abundances, and biogeographical trends in species diversity, as well as biomass of pteropods along a 2014 transect from 46°N to 46°S in the Atlantic Ocean. To my knowledge, this is the most comprehensive study of the diversity and abundance of holoplanktonic gastropods across the Atlantic Ocean to date.

In Chapter 7, I report on the diversity and distribution of hyperiid amphipods across a 2012 transect in the Atlantic Ocean and examine if hyperiid species assemblages are congruent with biogeochemical provinces. This study is among the first to examine their large-scale diversity and distribution patterns in the Atlantic Ocean.

Finally, in Chapter 8, I argue in favor of an integrative taxonomic approach to identifying species in the open ocean compared to the use of morphology or DNA barcoding only, and discuss the powers and pitfalls of next-generation sequencing-based methods. In the second part of this chapter, I provide an overview of recent advances in experimental and genetic research elucidating the sensitivity of pteropods to ocean acidification.

References

Angel M.V., 1993. Biodiversity of the pelagic ocean. Conservation Biology 7, 760–772.

Appeltans W., Ahyong S.T., Anderson G., Angel M.V., Artois T. et al., 2012. The magnitude of global marine species diversity. Current Biology 22, 2189–2202.

Bé A.W.H., Gilmer R.W., 1977. A zoogeographic and taxonomic review of euthecosomatous Pteropoda. In: Ramsay A.T.S. (Ed.), Oceanic Micropaleontology 1. Academic Press, London, pp. 733–808.

Beaugrand G., Goberville E., Luczak C., Kirby R.R., 2014. Marine biological shifts and climate. Proceedings of the Royal Society B 281, 20133350.

Bednaršek N., Harvey C.J., Kaplan I.C., Feely R.A., Možina J., 2016. Pteropods on the edge: cumulative effects of ocean acidification, warming, and deoxygenation. Progress in Oceanography 145, 1–24.

Bentlage B., Townsend Peterson A., Barve N., Cartwright P., 2013. Plumbing the depths: extending ecological niche modelling in three dimensions. Global Ecology and Biogeography 22, 952–961.

Bocher P., Cherel Y., Labat J.-P., Mayzaud P., Razouls S., Jouventin P., 2001. Amphipod-based food web: *Themisto gaudichaudii* caught in nets and by seabirds in Kerguelen waters, southern Indian Ocean. Marine Ecology Progress Series 223, 261–276.

Boltovskoy D., Correa N., 2016. Biogeography of Radiolaria Polycystina (Protista) in the world ocean. Progress in Oceanography 149, 82–105.

Boltovskoy D., Correa N., 2017. Planktonic equatorial diversity throughs: fact or artifact? Latitudinal diversity gradients in Radiolaria. Ecology 98, 112–124.

Bookstein F.L., 1991. Morphometric tools for landmark data: geometry and biology. Cambridge University Press, Cambridge, UK.

Bowen B.W., Gaither M.R., DiBattista J.D., Iacchei M., Andrews K.R. et al., 2016. Comparative phylogeography of the ocean planet. Proceedings of the National Academy of Sciences 113, 7962–7969.

Browne W.E., Haddock S.H.D., Martindale M.Q., 2007. Phylogenetic analysis of lineage relationships among hyperiid amphipods as revealed by examination of the mitochondrial gene, cytochrome oxidase I (COI). Integrative and Comparative Biology 47, 815–830.

Charette M.A., Smith W.H.F., 2010. The volume of Earth's ocean. Oceanography 23, 112–114.

Clarke K.R., 1993. Non-parametric multivariate analyses of changes in community structure. Australian Journal of Ecology 18, 117–143.

Clarke K.R., Gorley R.N., 2006. PRIMER Version 6: User Manual/Tutorial. PRIMER-E, Plymouth, UK.

Clarke K.R., Warwick R.M., 2001. Change in Marine Communities: An Approach to Statistical Analysis an Interpretation. PRIMER-E, Plymouth, UK.

Comeau S., Gattuso J.-P., Nisumaa A.-M., Orr J., 2012. Impact of aragonite saturation state changes on migratory pteropods. Proceedings of the Royal Society B 279, 732–738.

Dambach J., Rödder D., 2011. Applications and future challenges in marine species distribution modeling. Aquatic Conservation: marine and freshwater ecosystems 21, 92–100.

Darwin F., 1887. The life and letters of Charles Darwin. Volumes 1–3. 2nd edition, John Murray, Albemarle Street, London, UK.

De Queiroz K., 2007. Species concepts and species delimitation. Systematic Biology 56, 879–886.

De Vargas C., Audic S., Henry N., Decelle J., Mahé F. et al., 2015. Eukaryotic plankton diversity in the sunlit ocean. Science 348, 1261605.

Drake J.L., Mass T., Falkowski P.G., 2014. The evolution and future of carbonate precipitation in marine invertebrates: Witnessing extinction or documenting resilience in the Anthropocene? Elementa: Science of the Anthropocene 2, 26.

Edwards D.L., Knowles L.L., 2014. Species detection and individual assignment in species delimitation: can integrative data increase efficacy? Proceedings of the Royal Society B 281, 20132765.

Elith J., Leathwick J.R., 2009. Species distribution models: ecological explanation and prediction across space and time. Annual Review of Ecology, Evolution, and Systematics 40, 677–697.

Fabry V.J., Seibel B.A., Feely R.A., Orr J.C., 2008. Impacts of ocean acidification on marine fauna and ecosystem processes. ICES Journal of Marine Science 65, 414–432.

Forster P., Ramaswamy V., Artaxo P., Berntsen T., Betts R. et al., 2007. Changes in atmospheric constituents and in radiative forcing. In: Solomon S., Qin D., Manning M., Chen Z., Marquis M., Averyt K.B., Tignor M., Miller H.L. (Eds.), Climate Change 2007: the physical science basis. Contribution of working group I to the fourth assessment report of the Intergovernmental Panel on Climate Change. Cambridge University Press, Cambridge, pp. 129–234.

Gasca R., Haddock S.H.D., 2004. Associations between gelatinous zooplankton and hyperiid amphipods (Crustacea: Peracarida) in the Gulf of California. Hydrobiologia 530, 529–535.

Gasca R., Hoover R., Haddock S.H.D., 2015. New symbiotic associations of hyperiid amphipods (Peracarida) with gelatinous zooplankton in deep waters off California. Journal of the Marine Biological Association of the United Kingdom 95, 503–511.

Gilmer R.W., Harbison G.R., 1986. Morphology and field behavior of pteropod molluscs: feeding methods in the families Cavoliniidae, Limacinidae and Peraclidae (Gastropoda: Thecosomata). Marine Biology 91, 47–57.

Gunz P., Mitteroecker P., 2013. Semilandmarks: a method for quantifying curves and surfaces. Hystrix, the Italian Journal of Mammalogy 24, 103–109.

Harbison G.R., Biggs D.C., Madin L.P., 1977. The associations of Amphipoda Hyperiidea with gelatinous zooplankton. II. Associations with Cnidaria, Ctenophora and Radiolaria. Deep-Sea Research 24, 465–488.

Harzhauser M., Kroh A., Mandic O., Piller W.E., Göhlich U. et al., 2007. Biogeographic responses to geodynamics: a key study all around the Oligo-Miocene Tethyan Seaway. Zoologischer Anzeiger 246, 241–256.

Hattich G.S.I., Listmann L., Raab J., Ozod-Seradj D., Reusch T.B.H., Matthiessen B., 2017. Inter- and intraspecific phenotypic plasticity of three phytoplankton species in response to ocean acidification. Biology Letters 13, 20160774.

Hausdorf B., 2011. Progress toward a general species concept. Evolution 65, 923–931.

Ho S.Y.W., 2014. The changing face of the molecular evolutionary clock. Trends in Ecology & Evolution 29, 496–503.

Hurt C., Haddock S.H.D., Browne W.E., 2013. Molecular phylogenetic evidence for the reorganization of the Hyperiid amphipods, a diverse group of pelagic crustaceans. Molecular Phylogenetics and Evolution 67, 28–37.

Janssen A.W., 2007. Holoplanktonic Mollusca (Gastropoda) from the Gulf of Aqaba, Red Sea and Gulf of Aden (Late Holocene-Recent). The Veliger 49, 140–195.

Janssen A.W., 2012. Late Quaternary to recent holoplanktonic Mollusca (Gastropoda) from bottom samples of the eastern Mediterranean Sea: systematics, morphology. Bollettino Malacologico 48, 1–105.

Janssen A.W., Peijnenburg K.T.C.A., 2014. Holoplanktonic Mollusca: development in the Mediterranean basin during the last 30 million years and their future. In: Goffredo S., Dubinsky Z. (Eds.), The Mediterranean Sea: Its History and Present Challenges. Springer, Dordrecht, pp. 341–362.

Janssen A.W., Peijnenburg K.T.C.A. 2017. An overview of the fossil record of Pteropoda (Mollusca, Gastropoda, Heterobranchia). Canozoic Research 17, 3–10.

Jörger K.M., Stöger I., Kano Y., Fukuda H., Knebelsberger T., Schrödl M., 2010. On the origin of Acochlidia and other enigmatic euthyneuran gastropods, with implications for the systematics of Heterobranchia. BMC Evolutionary Biology 10, 323.

Karanovic T., Djurakic M., Eberhard S.F., 2016. Cryptic species or inadequate taxonomy? Implementation of 2D geometric morphometrics based on integumental organs as landmarks for delimitation and description of copepod taxa. Systematic Biology 65, 304–327.

Knowlton N., Weigt L.A., 1998. New dates and new rates for divergence across the Isthmus of Panama. Proceedings of the Royal Society B 265, 2257–2263.

Kroeker K.J., Kordas R.L., Harley C.D.G., 2017. Embracing interactions in ocean acidification research: confronting multiple stressor scenarios and context dependence. Biology Letters 13, 20160802.

Lalli C.M., Conover R.J., 1976. Microstructure of the veliger shells of gymnosomatous pteropods (Gastropoda: Opisthobranchia). The Veliger 18, 237–240.

Lalli C.M., Gilmer R.W., 1989. Pelagic Snails: The Biology of Holoplanktonic Gastropod Molluscs. Stanford University Press, Stanford, California.

Laptikhovsky V., 2002. Diurnal feeding rhythm of the short-fin squid *Illex argentines* (Cephalopoda: Ommastrephidae) in the Falkland waters. Fisheries Research 59, 233–237.

Laval P., 1980. Hyperiid amphipods as crustacean parasitoids associated with gelatinous zooplankton. Oceanography and Marine Biology: An Annual Review 18, 11–56.

Lavaniegos B.E., Ohman M.D., 1999. Hyperiid amphipods as indicators of climate change in the California current. In: Schram F.R., Von Vaupel Klein J.C. (Eds.), Proceedings of the Fourth International Crustacean Congress, 1998. Brill, Leiden, pp. 489–509.

Leray M., Knowlton N., 2016. Censusing marine eukaryotic diversity in the twenty-first century. Philosophical Transactions of the Royal Society B 371, 20150331.

Lessios H.A., 2008. The great American schism: divergence of marine organisms after the rise of the Central American Isthmus. Annual Review of Ecology, Evolution, and Systematics 39, 63–91.

Longhurst A.R., 1998. Ecological Geography of the Sea. Academic Press, San Diego.

Madin L.P., Harbison G.R., 1977. The associations of Amphipoda Hyperiidea with gelatinous zooplankton. I. Associations with Salpidae. Deep-Sea Research 24, 449–463.

Manno C., Bednaršek N., Tarling G.A., Peck V.L., Comeau S. et al., 2017. Shelled pteropods in peril: assessing vulnerability in a high CO_2 ocean. Earth-Science Reviews 169, 132–145.

McManus G.B., Katz L.A., 2009. Molecular and morphological methods for identifying plankton: what makes a successful marriage? Journal of Plankton Research 31, 1119–1129.

Meisenheimer J., 1906. Pteropoda. Wissenschaftliche Ergebnisse der Deutschen 769 Tiefsee-Expedition auf dem Dampfer 'Valdivia' 1898-1899, 9, 314 pp.

Mitteroecker P., Gunz P., 2009. Advances in geometric morphometrics. Evolutionary Biology 36, 235–247.

Morard R., Escarguel G., Weiner A.K.M., André A., Douady C.J. et al., 2016. Nomenclature for the nameless: a proposal for an integrative molecular taxonomy of cryptic diversity exemplified by planktonic Foraminifera. Systematic Biology 65, 925–940.

Moya A., Howes E.L., Lacoue-Labarthe T., Forêt S., Bishoy H. et al., 2016. Near-future pH conditions severely impact calcification, metabolism and the nervous system in the pteropod *Heliconoides inflatus*. Global Change Biology 22, 3888–3900.

National Oceanic & Atmospheric Administration (NOAA), Earth System Research Laboratory, Global Monitoring Division https://www.esrl.noaa.gov/gmd/ccgg/trends/index.html

Norris R.D., 2000. Pelagic species diversity, biogeography, and evolution. Paleobiology 26, 236–258.

O'Dea A., Lessios H.A., Coates A.G., Eytan R.I., Restrepo-Moreno S.A. et al., 2016. Formation of the Isthmus of Panama. Science Advances 2, e1600883.

Orr J.C., Fabry V.J., Aumont O., Bopp L., Doney S.C. et al., 2005. Anthropogenic ocean acidification over the twenty-first century and its impact on calcifying organisms. Nature 437, 681–686.

Padial J.M., Miralles A., De la Riva I., Vences M., 2010. The integrative future of taxonomy. Frontiers in Zoology 7, 16.

Pearman J.K., Irigoien X., 2015. Assessment of zooplankton community composition along a depth profile in the central Red Sea. PLoS ONE 10, e0133487.

Phillips S.J., Dudík M., Elith J., Graham C.H., Lehmann A. et al., 2009. Sample selection bias and presence-only distribution models: implications for background and pseudo-absence data. Ecological applications 19, 181–197.

Phleger C.F., Nelson M.M., Mooney B., Nichols P.D., 1999. Lipids of abducted Antarctic pteropods, *Spongiobranchaea australis*, and their hyperiid amphipod host. Comparative Biochemistry and Physiology Part B 124, 295–307.

Raes N., Ter Steege H., 2007. A null-model for significance testing of presence-only species distribution models. Ecography 30, 727–736.

Rees A., Robinson C., Smyth T., Aiken J., Nightingale P., Zubkov M., 2015. 20 Years of the Atlantic Meridional Transect – AMT. Limnology and Oceanography Bulletin 24, 101–107.

Renema W., Bellwood D.R., Braga J.C., Bromfield K., Hall R. et al., 2008. Hopping hotspots: global shifts in marine biodiversity 321, 654–657.

Reygondeau G., Longhurst A., Martinez E., Beaugrand G., Antoine D., Maury O., 2013. Dynamic biogeochemical provinces in the global ocean. Global Biogeochemical Cycles 27, 1–13.

Riascos J.M., Docmac F., Reddin C., Harrod C., 2015. Trophic relationships between the large scyphomedusa *Chrysaora plocamia* and the parasitic amphipod *Hyperia curticephala*. Marine Biology 162, 1841–1848.

Richter G., Seapy R.R., 1999. Heteropoda. In: Boltovskoy, D. (Ed.), South Atlantic Zooplankton. Backhuys Publishers, Leiden, pp. 621–647.

Riebesell U., Bach L.T., Bellerby R.G.J., Monsalve J.R.B., Boxhammer T. et al., 2017. Competitive fitness of a predominant pelagic calcifier impaired by ocean acidification. Nature Geoscience 10, 19–24.

Robinson L.M., Elith J., Hobday A.J., Pearson R.G., Kendall B.E. et al., 2011. Pushing the limits in marine species distribution modelling: lessons from the land present challenges and opportunities. Global Ecology and Biogeography 20, 789–802.

Sabine C.L., Feely R.A., Gruber N., Key R.M., Lee K. et al., 2004. The oceanic sink for anthropogenic CO_2. Science 305, 367–371.

Seapy R.R., Lalli C.M., Wells F.E., 2003. Heteropoda from western Australian waters. In: Wells F.E., Walker D.I., Jones D.S. (Eds.), The Marine Flora and Fauna of Dampier, Western Australia. Western Australian Museum, Perth, pp. 513–546.

Shreeve R.S., Collins M.A., Tarling G.A., Main C.E., Ward P., Johnston N.M., 2009. Feeding ecology of myctophid fishes in the northern Scotia Sea. Marine Ecology Progress Series 385, 221–236.

Siegenthaler U., Stocker T.F., Monnin E., Lüthi D., Schwander J., Stauffer B. et al., 2005. Stable carbon cycle-climate relationship during the Late Pleistocene. Science 310, 1313–1317.

Smith U.E., Hendricks J.R., 2013. Geometric morphometric character suites as phylogenetic data: extracting phylogenetic signal from gastropod shells. Systematic Biology 62, 366–385.

Sukumaran J., Knowles L.L., 2017. Multispecies coalescent delimits structure, not species. Proceedings of the National Academy of Sciences 114, 1607–1612.

Van der Spoel S., Dadon J.R., 1999. Pteropoda. In: Boltovskoy D. (Ed.), South Atlantic Zooplankton. Backhuys Publishers, Leiden, pp. 649–706.

Van der Spoel S., Heyman R.P., 1983. A Comparative Atlas of Zooplankton: Biological Patterns in the Oceans. Springer, New York.

Vinogradov M.E., Volkov A., Semenova T.N., 1996. Hyperiid Amphipods (Amphipoda, Hyperiidea) of the World Oceans. NH, USA, Science Publishers Inc., Lebanon, p. 632.

Vogler A.P., Monaghan M.T., 2006. Recent advances in DNA taxonomy. Journal of Zoological Systematics and Evolutionary Research 45, 1–10.

Wall-Palmer D., Burridge A.K., Peijnenburg K.T.C.A., 2016a. *Atlanta ariejansseni*, a new species of shelled heteropod from the Southern Subtropical Convergence Zone (Gastropoda, Pterotracheoidea). ZooKeys 604, 13–30.

Wall-Palmer D., Burridge A.K., Peijnenburg K.T.C.A., Janssen A.W., Goetze E. et al., 2016b. Evidence for the validity of *Protatlanta sculpta* (Gastropoda: Pterotracheoidea). Contributions to Zoology 85, 423–435.

Wall-Palmer D., Smart C.W., Kirby R., Hart M.B., Peijnenburg K.T.C.A., Janssen A.W., 2016c. A review of the ecology, palaeontology and distribution of atlantid heteropods (Caenogastropoda: Pterotracheoidea: Atlantidae). Journal of Molluscan Studies 82, 221–234.

Waluda C.M., Collins M.A., Black A.D., Staniland I.J., Trathan P.N., 2010. Linking predator and prey behaviour: contrasts between Antarctic fur seals and macaroni penguins at South Georgia. Marine Biology 157, 99–112.

World Register of Marine Species (WoRMS). http://www.marinespecies.org

2

Time-calibrated molecular phylogeny of pteropods

Alice K. Burridge, Christine Hörnlein, Arie W. Janssen, Martin Hughes, Stephanie L. Bush, Ferdinand Marlétaz, Rebeca Gasca, Annelies C. Pierrot-Bults, Ellinor Michel, Jonathan A. Todd, Jeremy R. Young, Karen J. Osborn, Steph B.J. Menken & Katja T.C.A. Peijnenburg

Abstract

Pteropods are a widespread group of holoplanktonic gastropod molluscs and are uniquely suitable for study of long-term evolutionary processes in the open ocean because they are the only living metazoan plankton with a good fossil record. Pteropods have been proposed as bioindicators to monitor the impacts of ocean acidification and in consequence have attracted considerable research interest, however, a robust evolutionary framework for the group is still lacking. Here we reconstruct their phylogenetic relationships and examine the evolutionary history of pteropods based on combined analyses of Cytochrome Oxidase I, 28S, and 18S ribosomal rRNA sequences and a molecular clock calibrated using fossils and the estimated timing of the formation of the Isthmus of Panama. Euthecosomes with uncoiled shells were monophyletic with *Creseis* as the earliest diverging lineage, estimated at 41–38 million years ago (mya). The coiled euthecosomes (*Limacina*, *Heliconoides*, *Thielea*) were not monophyletic contrary to the accepted morphology-based taxonomy; however, due to their high rate heterogeneity no firm conclusions can be drawn. We found strong support for monophyly of most euthecosome genera, but *Clio* appeared as a polyphyletic group, and *Diacavolinia* grouped within *Cavolinia*, making the latter genus paraphyletic. The highest evolutionary rates were observed in *Heliconoides inflatus* and *Limacina bulimoides* for both 28S and 18S partitions. Using a fossil-calibrated phylogeny that sets the first occurrence of coiled euthecosomes at 79–66 mya, we estimate that uncoiled euthecosomes evolved 51–42 mya and that most extant uncoiled genera originated 40–15 mya. These findings are congruent with a molecular clock analysis using the Isthmus of Panama formation as an independent calibration. Although not all phylogenetic relationships could be resolved based on three molecular markers, this study provides a useful resource to study pteropod diversity and provides general insight into the processes that generate and maintain their diversity in the open ocean.

Keywords:
Pteropoda, Plankton evolution, Molecular clock, Fossil record, Isthmus of Panama

This chapter was published as:
Burridge A.K., Hörnlein C., Janssen A.W., Hughes M., Bush S.L., Marlétaz F., Gasca R., Pierrot-Bults A.C., Michel E., Todd J.A., Young J.R., Osborn K.J., Menken S.B.J., Peijnenburg K.T.C.A., 2017. Time-calibrated molecular phylogeny of pteropods. PLoS ONE 12: e0177325.

Introduction

Pteropods are a group of holoplanktonic heterobranch gastropod molluscs (Jörger et al., 2010) that are widespread and abundant in the marine zooplankton (e.g., Bednaršek et al., 2012; Burridge et al., in press: Thesis chapter 6). They have been proposed as bioindicators to monitor the effects of ocean acidification because their aragonite shells are exceptionally vulnerable to rising levels of CO_2 in the global ocean (e.g., Fabry et al., 2008; Comeau et al., 2012; Bednaršek et al., 2016; Moya et al., 2016). It is expected that anthropogenic carbon input into the ocean may affect marine life more severely than in the past, because it is happening much faster than, for instance, at the Paleocene-Eocene thermal maximum (PETM) ~56 million years ago (mya; Zachos et al., 2005; Janssen et al., 2012; Zeebe, 2012). During the PETM, massive amounts of carbon were released into the atmosphere and ocean, leading to ocean acidification and warming, and the ocean's calcite saturation depth shoaled by at least 2 km within 2000 years, a situation that persisted for tens of thousands of years (Doney et al., 2009; Zeebe, 2012). This resulted in major shifts in marine planktonic communities, including foraminifers and calcareous phytoplankton, and a major extinction of benthic foraminifers, but probably not of pteropods (Kelly et al., 1996; Bralower, 2002; Zachos et al., 2005, 2008; Gibbs et al., 2006; Schneider et al., 2013; Janssen et al., 2016).

Pteropods comprise the orders Thecosomata and Gymnosomata (De Blainville, 1824). These groups are ecologically distinct: the thecosomes produce mucus webs to feed on microplankton, whilst gymnosomes are active predators that often feed on thecosomes (Gilmer and Harbison, 1986; Van der Spoel and Dadon, 1999). The thecosomes are further divided into the suborders Euthecosomata and Pseudothecosomata (Meisenheimer et al., 1906). The euthecosomes have aragonite shells throughout their lives while the pseudothecosomes have coiled shells or a semi-soft pseudoconch with an aragonite shell only during the larval stage (Van der Spoel and Dadon, 1999; Janssen, 2012). Within the euthecosomes, the superfamily Limacinoidea has coiled shells, and the superfamily Cavolinioidea has uncoiled shells. Gymnosomes have only larval shells, which they shed during metamorphosis into adults (Lalli and Conover, 1976). Most pteropod species are epipelagic, but some species are meso- or bathypelagic (e.g., *Clio andreae*, *C. chaptalii*, *C. piatkowskii*, *C. polita*, *C. recurva*, *Thielea helicoides*, and *Peracle bispinosa*; Bé and Gilmer, 1977; Van der Spoel and Dadon, 1999).

The taxonomy of thecosomes, and especially that of euthecosomes, has been revised frequently and remains disputed, especially at the (super)family level. The most widely used taxonomy (as accepted by the World Register of Marine Species, WoRMS) was proposed by Janssen (2003). In this classification, the Limacinidae (with extant genera *Heliconoides*, *Limacina*, and *Thielea*) are the only family within the superfamily Limacinoidea, whereas most other classifications included the Limacinidae in the Cavolinioidea (Van der Spoel, 1967; Bouchet and Rocroi, 2005). The superfamily Cavolinioidea contains the extant families Cavoliniidae (*Cavolinia*, *Diacavolinia*, *Diacria*), Cliidae (*Clio*), Creseidae (*Creseis*, *Hyalocylis*, *Styliola*), and

Cuvierinidae (*Cuvierina*; Janssen, 2003). In other studies, Cavolinioidea has been ranked as the family Cavoliniidae with three subfamilies: Cavoliniinae (*Cavolinia*, *Diacavolinia*, *Diacria*), Clionae (*Clio*, *Creseis*, *Hyalocylis*, *Styliola*), and Cuvierininae (*Cuvierina*; Van der Spoel, 1967, 1987; Bouchet and Rocroi, 2005). Finally, according to Rampal (1973, 1975, 2011) there are two families within the Cavolinioidea: Creseidae (*Creseis*, *Hyalocylis*, *Styliola*) and Cavoliniidae, comprising the subfamilies Cavoliniinae (*Cavolinia*, *Diacavolinia*, *Diacria*, *Clio*) and Cuvierininae (*Cuvierina*).

Several recent studies have tested pteropod taxonomic hypotheses using genetic data. Pteropods were confirmed as a monophyletic group within the Opisthobranchia based on a sampling of 10 euthecosome and three gymnosome taxa using the three molecular markers Cytochrome Oxidase subunit I (COI) mitochondrial DNA, nuclear 28S, and 18S rRNA (28S and 18S respectively; Klussmann-Kolb and Dinapoli, 2006). Anaspidea was proposed as the most likely sister group of pteropods (Klussmann-Kolb and Dinapoli, 2006), and this was confirmed by phylogenomic analyses of gastropods (Zapata et al., 2014). Within the pteropods, the uncoiled euthecosomes and gymnosomes were recognized as monophyletic groups in molecular phylogenetic analyses (Klussmann-Kolb and Dinapoli, 2006; Corse et al., 2013). Jennings et al. (2010) constructed phylogenies based on COI sequences of 30 pteropod species. They demonstrated that phylogenetic relationships of pteropods above the species level could not be reliably established using COI as the only molecular marker because of the high rate heterogeneity and limited phylogenetic signal of this marker. Corse et al. (2013) proposed an evolutionary scenario for thecosome pteropods based on a cladistic analysis of morphological data of extant species and separate phylogenetic analyses of COI and 28S genes, with pseudo- and euthecosomes splitting first, and coiled euthecosomes as a paraphyletic group from which uncoiled euthecosomes evolved. Based solely on 28S, both Klussmann-Kolb and Dinapoli (2006) and Corse et al. (2013) reported *Creseis* as the earliest diverging member of the uncoiled euthecosomes.

Some euthecosome taxa have been studied in more detail using molecular methods. Based on COI sequences, Hunt et al. (2010) found that Arctic and Antarctic *Limacina helicina* populations represented genetically distinct species. The Creseidae were studied by Gasca and Janssen (2014), who found monophyly of the genera *Creseis*, *Hyalocylis*, and *Styliola* based on COI data. *Cuvierina* and *Diacavolinia* have been studied using integrative taxonomic approaches combining COI and/or 28S data, morphological analyses of shells, and/or geographic information (Maas et al., 2013; Burridge et al., 2015: Thesis chapter 3, in prep.: Thesis chapter 5). Six *Cuvierina* morphotypes with distinct geographic distributions were distinguished based on geometric morphometric analyses of shell shapes (Burridge et al., 2015: Thesis chapter 3), one of which was described as a new species (Burridge et al., 2016: Thesis chapter 4). Burridge et al. (in prep.: Thesis chapter 5) found evidence for a reduction in the number of described *Diacavolinia* species from 24 to a maximal estimate of 13 species based on integrative taxonomic analyses using recently collected specimens as well as museum specimens, including type material.

Pteropods have an extensive fossil record that largely consists of euthecosome shells and larval gymnosome shells (e.g., Janssen, 2007, 2012). Because their fragile shells do not survive significant transport, they are rarely reworked from one sedimentary unit into another, which makes them reliable fossils for biostratigraphic purposes (e.g., Janssen and Peijnenburg, 2014). Combining their fossil record with molecular methods for phylogenetic inference can improve our understanding of the evolutionary history of pteropods, and provides a framework for assessing past and present responses to global change.

Vicariance events in the global ocean, such as the Terminal Tethyan Event (TTE) and uplift of the Isthmus of Panama (IOP), have had profound effects on the evolution of marine organisms (e.g., Lessios, 2008; Cowman and Bellwood, 2013; Bacon et al., 2015; Bowen et al., 2016; O'Dea et al., 2016). These include reduced connectivity by changes in ocean circulation and shifts in centers of marine diversity. However, the onset of these land barriers has been complex and the timing of events is widely debated, with the IOP formation most commonly estimated at ~3 mya (e.g., Harzhauser et al., 2002, 2007; Bacon et al., 2015; O'Dea et al., 2016). Hence, a better understanding of when these events occurred has important implications for using vicariance events for calibrating molecular clocks for different species as well as for cross-validating fossil-calibrated molecular clocks. Jennings et al. (2010) demonstrated that several pteropod species had interspecific levels of sequence divergence between lineages from different ocean basins. Divergent clades for Atlantic and Pacific sister taxa would allow the use of the IOP as a molecular clock calibration.

Here we shed new light on the evolutionary history of pteropods by performing a combined analysis of three molecular markers: COI, 28S and 18S genes. We include 55 pteropod species spanning the diversity of the group and sampled from each ocean basin, including molecular data of seven additional euthecosome, two pseudothecosome, and five gymnosome species relative to prior studies. We use fossil evidence and the dating of the formation of the Isthmus of Panama to reconstruct the evolutionary history of pteropods, thus enabling comparisons between different calibration methods. Our aims are to (1) examine the phylogenetic relationships of pteropods sampled from the global ocean based on COI, 28S, and 18S sequence data and (2) reconstruct the evolutionary history of pteropods using a molecular clock approach.

Materials and methods

Sampling and specimens

A total of 55 pteropod species were included in this study (treating subspecies as separate species here and subsequently; Table S1). Of these, 27 species are uncoiled euthecosomes and eight are coiled euthecosomes, together representing up to 56% of all currently recognized extant euthecosome species, as well as all eight uncoiled and all three coiled genera. In addition, eight pseudothecosome species

are included (35% of all species), representing all five genera. Twelve gymnosome species (23% of all species) are included, representing eight of the 19 genera. Pteropods were collected at a total of 90 stations: 58 in the Atlantic Ocean (40 species), 14 in the Pacific Ocean (14 species), 10 in the Indian Ocean (10 species), six in the Southern Ocean (seven species), and two in the Arctic Ocean (two species; Figure 1; Table S1). New samples for this study were collected from the Atlantic Ocean and Caribbean Sea during the AMT18, AMT22, ECO-CH-Z, and MAR-ECO expeditions between 2004 and 2012, and from net tows, remotely operated vehicles and bluewater SCUBA dives in the Northwest Atlantic Ocean, Northeast Pacific Ocean, and Gulf of California in 2012 and 2013. Permits were available for sampling in the Gulf of California (permits DAPA / 2 / 080211 / 00217 by Comisión Nacional de Acuacultura y Pesca, CTC / 001340 by La Secretaria de Relacione Exteriores, and H00 / INAPESCA / DGIPPN / 831 by Secretaria de Agricultura, Ganaderia, Desarrollo Rural, Pesca Y Alimentacion) and the NE Pacific Ocean (California Department of Fish and Wildlife Scientific Collecting Permit SC-2316). No permits were required for other plankton collections, and the work did not involve any endangered or protected species.

The majority of pteropod specimens were collected from the epi- to upper mesopelagic layer (500–0 m depth) using different types of plankton nets. Sampling details can be obtained from shipboard reports available online (e.g., Atlantic Meridional Transect cruise reports for AMT cruises, Wenneck et al. (2008) for the MAR-ECO cruise, and The University-National Oceanographic Laboratory System (UNOLS), National Oceanic and Atmospheric Administration (NOAA), and Monterey Bay Aquarium Research Institute (MBARI)). Pteropod sequences from remaining locations were available from Klussmann-Kolb and Dinapoli (2006), Hunt et al. (2010), Jennings et al. (2010), Corse et al. (2013), Maas et al. (2013), Gasca and Janssen (2014), Zapata et al. (2014), and Burridge et al. (2015: Thesis chapter 3). Sampling information for all specimens in this study, including collection dates, geographical coordinates, cruise and station numbers, if reported in previous work, are collated in Table S1. Images of newly collected specimens are deposited in the Dryad digital repository at DOI: 10.5061/dryad.bp106.

DNA extraction, amplification, and sequencing

Genomic DNA was extracted from muscle tissue or entire individuals (when smaller than 3 mm) using the DNeasy blood & tissue Kit (Qiagen). Alternatively, genomic DNA from specimens collected in 2012 and 2013 from the Northwest Atlantic and Northeast Pacific oceans and the Gulf of California was extracted using an AutoGenprep965 high throughput system (AutoGen, Holliston, MA, USA) using manufacturer protocols.

A fragment of ~600 basepairs (bp) of COI was amplified using the primers LCO-1490 (5'-GGTCAACAAATCATAAAGATATTGG-3') and HCO-2198 (5'-TAAACTTCAGGGT GACCAAAAAATCA-3'; Folmer et al., 1994). A fragment of ~1000 bp of 28S was amplified using primers C1-F (5'-ACCCGCTGAATTTAAGCAT-3'; Dayrat et al., 2001) and D3-R (5'-GACGATCGATTTGCACGTCA-3'; Vonnemann et al., 2005). The 18S

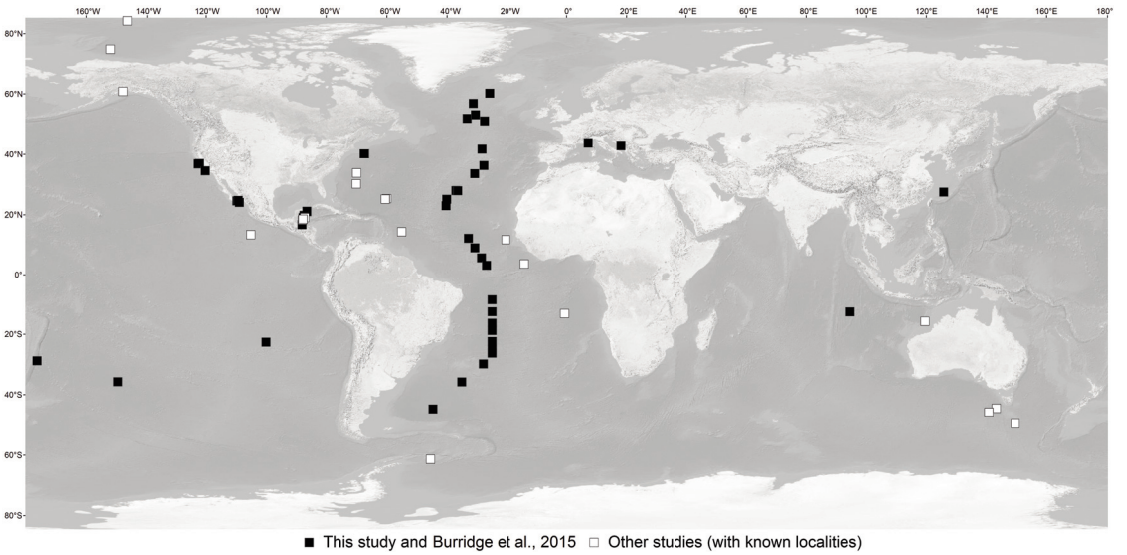

Figure 1. Overview of sampling locations. Black squares indicate sampling locations of new specimens in this study and white squares indicate all known locations of specimens used from other studies. Sampling locations from Klussmann-Kolb and Dinapoli (2006), Hunt et al. (2010), and Corse et al. (2013), are not indicated because no exact localities were given (see Table S1).

region of ~1800 bp was amplified by two overlapping fragments for most samples (overlap of ~500 bp). The two fragments were amplified using the primer pairs A1-F (5'-CTGGTTGATCCTGCCAGTCATATGC-3'; Vonnemann et al., 2005) and 18S-KP-R (5'-TTCCCGTGTTGAGTCAAATTAAG-3'; this study) and 18S-KP-F (5'-TGGAGGGCAAG TCTGGTG-3'; this study) and 1800R (5'-GATCCTTCCGCAGGTTCACCTACG-3'; Vonnemann et al., 2005).

PCR amplification of COI was performed using 25 µl volumes containing 15.7 µl ddH_2O, 2.5 µl 10x PCR buffer, 2.5 µl DNTPs (1 mM each), 1 µl $MgCl_2$, 0.2 µl BSA (10 mg/ml), 0.2 µl of each primer, 0.2 µl Super*Taq*, and 2.5 µl template DNA, or using illustraTM puReTaq Ready-To-Go PCR Beads (GE Healthcare) requiring 20 µl ddH_2O, 1 µl of each primer, and 3 µl template DNA. The PCR cycling steps were an initial denaturation step of 94°C for 180 s followed by 35 cycles of 94°C for 45 s, 45°C for 60 s, and 72°C for 120 s, and a final extension of 72°C for 600 s. Alternatively, for specimens collected in 2012 and 2013 from the Northwest Atlantic and Northeast Pacific oceans, PCR amplification of COI was performed in 10 µl volumes containing 5.95 µl ddH_2O, 0.6 µl $MgCl_2$, 0.5 µl dNTPs, 0.25 µl BSA, 0.3 µl of each primer, 0.1 µl Biolase DNA polymerase (BioLine, Taunton, MA, USA), 1 µl manufacturer-provided buffer, and 1 µl template DNA, with an initial denaturation at 95°C for 300 s, 40 cycles of 95°C for 30 s, 48°C for 30 s, and 72°C for 45 s, with a final extension at 72°C for 300 s. For most specimens, PCR amplification of both 18S and 28S was performed in 20 µl volumes containing 8.8 µl ddH_2O, 4 µl 5x Phire buffer (Phire), 2 µl dNTPs (1 mM each), 1.4 µl 100% DMSO, 0.2 µl BSA (10 mg/ml), 0.5 µl of each primer (18S: A1-F and 1800R or A1-F and KP-R and KP-F

and 1800-R, 28S: C1-F and D3-R), 0.2 µl Hot Start *Taq* (Phire) and 2.4 µl template DNA. Alternatively, 25 µl volumes were used, containing 7 µl ddH_2O, 2.5 µl BSA, 1 µl of each primer, 12.5 µl Amplitaq Gold Fast *Taq* (Life Technologies, Grand Island, NY, USA), and 1 µl template DNA. PCR cycling steps were an initial denaturation step of 98°C for 30 s, 35 cycles of 98°C for 5 s, 48°C for 5 s and 72°C for 20 s, a final extension step of 72°C for 60 s, and a cooling step of 4°C for 180 s. Bands were checked on agarose gel followed by a purification step of the PCR product using the QIAquick gel extraction kit (Qiagen, Germany). After a final cycle sequencing reaction using ABI BigDye Terminator cycle sequencing kit v.1.1 (Life Technologies, USA) according to the manufactures protocol, PCR products were sequenced by Macrogen Europe, The Netherlands, the Laboratories of Analytical Biology at the Smithsonian National Museum of Natural History, USA, or the Monterey Bay Aquarium Research Institute, USA.

Sequence alignments

We aimed to include as many complete COI, 28S, and 18S fragments for available taxa as possible in our sequence alignments. The data collected in this study was complemented by sequences from prior studies (Table S1). For some specimens we combined partitions from different specimens of the same species and the same ocean for the multi-gene alignments (Table S1). For inclusion in multi-gene alignments, sequences of at least two of the three markers per taxon had to be available.

We obtained a total of 53 COI, 53 28S, and 46 18S sequences in this study, and used an additional 65 COI, 35 28S, and six 18S sequences from prior studies for various purposes (Table S1). We included two outgroup species sequenced by Klussmann-Kolb and Dinapoli (2006) in all alignments: the large sea slug *Aplysia californica* (Anaspidea), and the shelled gastropod *Bulla striata* (Cephalaspidea). These species were chosen as outgroups because *Aplysia californica* is a representative of the most likely sister group of the Pteropoda, and *Bulla striata* represents a possible sister group to Anaspidea + Pteropoda (Klussmann-Kolb and Dinapoli, 2006).

Nucleotide sequences of COI, 28S, and 18S were examined in MEGA 6 (Tamura et al., 2013) and aligned using MAFFT v7. The amino acid alignment of COI (AACOI) was aligned using the MUSCLE algorithm (Edgar, 2004) in MEGA 6. All sites were used for COI as well as for the AACOI alignment. For 28S and 18S, sites with a coverage of <80% in the alignments were removed using trimAl (Capella-Gutiérrez et al., 2009) in Phylemon 2.0 (Sánchez et al., 2011). This resulted in final alignment lengths of 656 bp or 218 amino acids for COI, 941 bp for 28S, and 1683 bp for 18S. To estimate evolutionary relationships among taxa based on single-gene trees, we used an alignment of $N = 117$ sequences representing 53 pteropod species for COI, $N = 87$ sequences (44 species) for 28S, and $N = 52$ sequences (28 species) for 18S. For the multi-gene phylogeny, we used AACOI, 28S, and 18S partitions comprising a subset of 78 specimens to have a more even taxon sampling across groups (42 pteropod species; a maximum of two taxa per species per ocean). The 28S partition was complete and for the other partitions, 77 AACOI sequences were available (only missing for *Limacina bulimoides*), as well as 52 18S sequences (representing all

euthecosome genera except *Thielea*, representing the pseudothecosome genera *Corolla* and *Peracle*, but missing for *Cymbulia*, *Gleba*, and *Desmopterus*, and representing six gymnosome genera except *Notobranchaea* and *Schizobrachium*, regarding only the genera included elsewhere in this study). To produce a time-calibrated phylogeny, we used a subset of 46 sequences (40 pteropod species, a maximum of one sequence per species per ocean) consisting of AACOI (*N* = 45), 28S (*N* = 46), and 18S (*N* = 34) partitions, because the Yule tree prior assumes that all taxa are independent (i.e., reproductively isolated; Gernhard, 2008).

Phylogenetic analyses

We first estimated phylogenetic relationships based on single-gene Maximum Likelihood (ML) analyses, followed by multi-gene ML analyses, and Bayesian, time-calibrated analyses. To estimate evolutionary relationships among taxa based on single as well as combined genes, we applied a ML approach (Felsenstein, 1981) in RaxmlGUI 1.3 (Stamatakis, 2006; Silvestro and Michalak, 2012). We tested for the most appropriate model of sequence evolution per gene separately using the Akaike Information Criterion (AIC) in jModelTest 2.1.3 (Darriba et al., 2012) based on 88 models, and this approach always selected the GTR (General Time Reversible) model with a proportion of invariable sites (I) and gamma distributed rate variation among sites (Γ). For the AACOI alignment, we used the MtZoa model of evolution, because it best represents the evolutionary process and reduces systematic bias (Rota-Stabelli et al., 2009).

For the single-gene ML phylogenies, we applied a ML search followed by a non-parametric bootstrap analysis with 1500, 2000, and 3000 replicates for COI, 28S, and 18S, respectively. For the multi-gene combined ML phylogeny, we used the MtZoa model of evolution for AACOI and GTR + Γ + I for 28S as well as 18S, and applied a ML search followed by 1500 bootstrap replicates. To examine the effect of long-branch taxa on the phylogenetic signal, an additional tree of 75 specimens (40 pteropod species) was generated excluding *Limacina bulimoides* and *Heliconoides inflatus*.

Prior to producing a time-calibrated phylogeny, we independently tested the topology of the dataset in RaxmlGUI using the same methods as described above. We subsequently applied relaxed Bayesian molecular clock analyses with uncorrelated log-normal rates in BEAUti and BEAST 1.81 (Drummond et al., 2012). Because the MtZoa model of evolution was not available in BEAUti 1.81, we instead used the WAG model (Whelan and Goldman, 2001) for AACOI and GTR + Γ + I for 28S and 18S.

The molecular clock analyses used the Yule Process of speciation (Gernhard, 2008) and were calibrated using three different methods as summarized in Table 1 (see also Drummond et al., 2012). In all three methods, the stem node of the pteropods was calibrated using a normally distributed secondary calibration derived from a phylogenomic gastropod study by Zapata et al. (2014), and the crown node of the euthecosomes was calibrated using a log-normal distribution based on the geological age of the first known euthecosome pteropod, *Heliconoides* sp., from the Late Cretaceous (Janssen and Goedert, 2016). In the first calibration approach (Method 1), we used the geological ages of the oldest known fossils

TABLE 1. Overview of molecular clock calibration settings using three different methods.

Calibrated node	Calibration type	Calibration method 1	2	3	Calibration age mya
Clio pyramidata (excl.*C. p. antarctica*)	IOP: Atlantic – Pacific			Crown	3.1
Hyalocylis striata	IOP: Atlantic – Pacific			Crown	3.1
Cliopsis krohni	IOP: Atlantic – Pacific			Crown	3.1
Hyalocylis	Fossil: *Hyalocylis marginata*	Crown	Stem		3.6–2.6
Diacria	Fossil: *Diacria sangiorgii*	Crown	Stem		11.6–7.2
Cavolinia – Diacavolinia	Fossil: *Cavolinia zamboninii*	Crown	Stem		16–13.8
Cuvierina	Fossil: *Cuvierina torpedo*	Crown	Stem		23–20.4
Creseis	Fossil: *Creseis corpulenta*	Crown	Stem		38–41
Limacina	Fossil: *Limacina gormani*	Crown			56–47.8
Euthecosomata	Fossil: *Heliconoides* sp.	Crown	Crown	Crown	79–66
Pteropods vs. outgroup taxa	Secondary: *Clione antarctica* vs. *Aplysia californica*	Stem	Stem	Stem	170–90

Method 1 uses fossil ages as crown calibrations, Method 2 uses fossil ages as stem calibrations, and Method 3 uses the formation of the Isthmus of Panama (IOP) as crown calibrations. mya = million years ago; Prior dist. = Prior distribution; SD = Standard deviation.

presumed to belong to the extant euthecosome genera *Hyalocylis*, *Diacria*, *Cavolinia*, *Cuvierina*, *Creseis*, and *Limacina* as log-normally distributed crown calibrations (TABLE 1; Meyer, 1887; Marshall, 1918; Checchia-Rispoli, 1921; Scarsella, 1934; Curry, 1982; Janssen, 2005, 2007; Cahuzac and Janssen, 2010; Janssen and Goedert, 2016). These fossils were of Eocene, Miocene, or Pliocene age (TABLE 1). In the second approach (Method 2), we set these crown calibrations as genus stem calibrations instead, excluding the *Limacina* calibration. The significant genetic differentiation between Atlantic and Pacific populations of the euthecosomes *Clio pyramidata* and *Hyalocylis striata*, and the gymnosome *Cliopsis krohni* was likely a consequence of the emergence of the Isthmus of Panama (IOP). Hence, in a third calibration approach (Method 3) we used the IOP as a normally distributed prior with a mean of 3.1 mya and a standard deviation of 1 million years, accounting for the debated IOP timing (O'Dea et al., 2016). For all approaches, two MCMC chains were run of 10^8 generations each. We sampled trees and log-likelihood values at 10^4-generation intervals. Sets of trees obtained during independent runs were combined in LogCombiner 1.8.1 (Drummond et al., 2012), and the maximum clade credibility trees were select-

Calibration age Epoch: age	Prior settings Prior dist.	Offset	Mean	Log (SD)	SD	References
Pliocene: Piacenzian	Normal		3.1		1	O'Dea et al., 2016
Pliocene: Piacenzian	Normal		3.1		1	O'Dea et al., 2016
Pliocene: Piacenzian	Normal		3.1		1	O'Dea et al., 2016
Pliocene: Piacenzian	Log-normal	2.6	0.8	0.7		Janssen, 2007
Miocene: Tortonian	Log-normal	7.2	2.5	0.7		Scarsella, 1934
Miocene: Langhian	Log-normal	13.8	1.5	0.7		Checchia-Rispoli, 1921
Miocene: Aquitanian	Log-normal	20.4	1.5	0.7		Marshall, 1918; Janssen, 2005
Eocene: Bartonian	Log-normal	38	1.5	0.7		Meyer, 1887; Cahuzac and Janssen, 2010
Eocene: M-L Ypresian	Log-normal	48	8	0.7		Curry, 1982; Cahuzac and Janssen, 2010
Late Cretaceous: Late Campanian/ Maastrichtian	Log-normal	65.5	3	0.7		Janssen and Goedert, 2016
	Normal		130		14	Zapata et al., 2014

ed using TreeAnnotator 1.8.1 (Drummond et al., 2012). To cross-validate calibrations and derive independent ages of these nodes, we performed additional runs of 10^8 generations while leaving out one calibration at a time.

Results

Sequence alignments

The numbers of indels in the COI, 28S, and 18S sequence alignments vary considerably between euthecosomes, pseudothecosomes, and gymnosomes. No stop codons or frameshift mutations are present in the COI alignment (656 bp). The same consecutive three codons are missing for all *Limacina*, *Corolla*, *Cymbulia*, and *Gleba* species. Additional deletions of one or two codons are observed for *Hyalocylis* and *Limacina* species. No insertions or deletions are observed in gymnosome sequences. In the trimmed 28S alignment (941 bp), the number of species or genus-specific gaps is highly variable. Within the euthecosomes, *Heliconoides inflatus* sequences have the highest number of gaps (20 bp), followed by 6–15 bp

for *Limacina bulimoides*, *L. trochiformis*, all *Creseis* species, and *Hyalocylis striata*. Within the pseudothecosomes, 15 bp are missing for *Desmopterus* sp., followed by 3–7 bp for *Cymbulia* sp., *Corolla spectabilis*, and *Peracle reticulata*. Of the gymnosomes, only *Spongiobranchaea australis* has a gap (1 bp). In the trimmed 18S alignment (1683 bp), a large number of gaps is found for *Limacina bulimoides* (47 bp), followed by *Creseis clava* (13 bp), and *Heliconoides inflatus* (11 bp). Few gaps are present within the pseudothecosome sequences (1–3 bp for *Corolla spectabilis* and *Peracle reticulata*). Contrary to COI and 28S alignments of gymnosome taxa, some gaps remain in the 18S alignment of the gymnosomes *Pneumoderma atlantica* (10 bp), and 1–2 bp for *Pneumodermopsis* sp., *Spongiobranchaea australis*, *Clione limacina antarctica*, and *Thliptodon* sp.

Individual gene trees

Gene trees recovered from separate ML analyses of COI, AACOI, 28S, and 18S datasets generally recover species and genera with moderate to high bootstrap support (>80%), however, higher-level groupings are unstable and unsupported (Figures S1–S4). In both COI gene trees (Figures S1 and S2 for nucleotides and amino acids, respectively) the coiled *Heliconoides inflatus* and *Thielea helicoides* group with the uncoiled euthecosomes, rendering both superfamilies of Euthecosomata, uncoiled Cavolinoidea and coiled Limacinoidea, polyphyletic. This could be due to long branches of all *Limacina* taxa (coiled), and *Styliola subula* and *Hyalocylis striata* (uncoiled). Higher-level taxa such as the Euthecosomata, Pseudothecosomata, and Gymnosomata are not significantly supported and their relationships are unresolved based on COI. Supported geographic subclades within species sampled from different ocean basins are recovered for Atlantic and Pacific populations of *Cavolinia uncinata*, *Clio pyramidata*, and *Hyalocylis striata* (euthecosomes), and the gymnosome *Cliopsis krohni* (Figure S1). In the 28S tree, all genera are recovered with moderate to high bootstrap support, except *Clio* (Figure S3). There is one well-supported clade with *Clio pyramidata* and *C. convexa* (96% bootstrap support), with *C. cuspidata* and *C. recurva* falling into the basal polytomy. Relationships between different genera are mostly unresolved, but the genus *Cavolinia* is monophyletic only when *Diacavolinia* is included within *Cavolinia*. *Heliconoides inflatus* is on an exceptionally long branch. Similarly, the 18S tree supports most genera but does not resolve any of the higher-level groupings, likely because of extremely long branches of two species, *Heliconoides inflatus* and *Limacina bulimoides* (Figure S4).

Multi-gene phylogenies

Combining COI, 28S, and 18S sequences into a single phylogenetic analysis with the three genes as separate partitions (partially) compensates for the effects of rate heterogeneity within specific partitions between taxa and improves phylogenetic resolution. Concatenated datasets both including (Figure S5) and excluding the long-branch taxa *H. inflatus* and *L. bulimoides* (Figure 2) have very similar topologies. Both phylogenies recover Pteropoda as a monophyletic group (100 and 99% support, respectively) as well as Euthecosomata (99% in both phylogenies) and

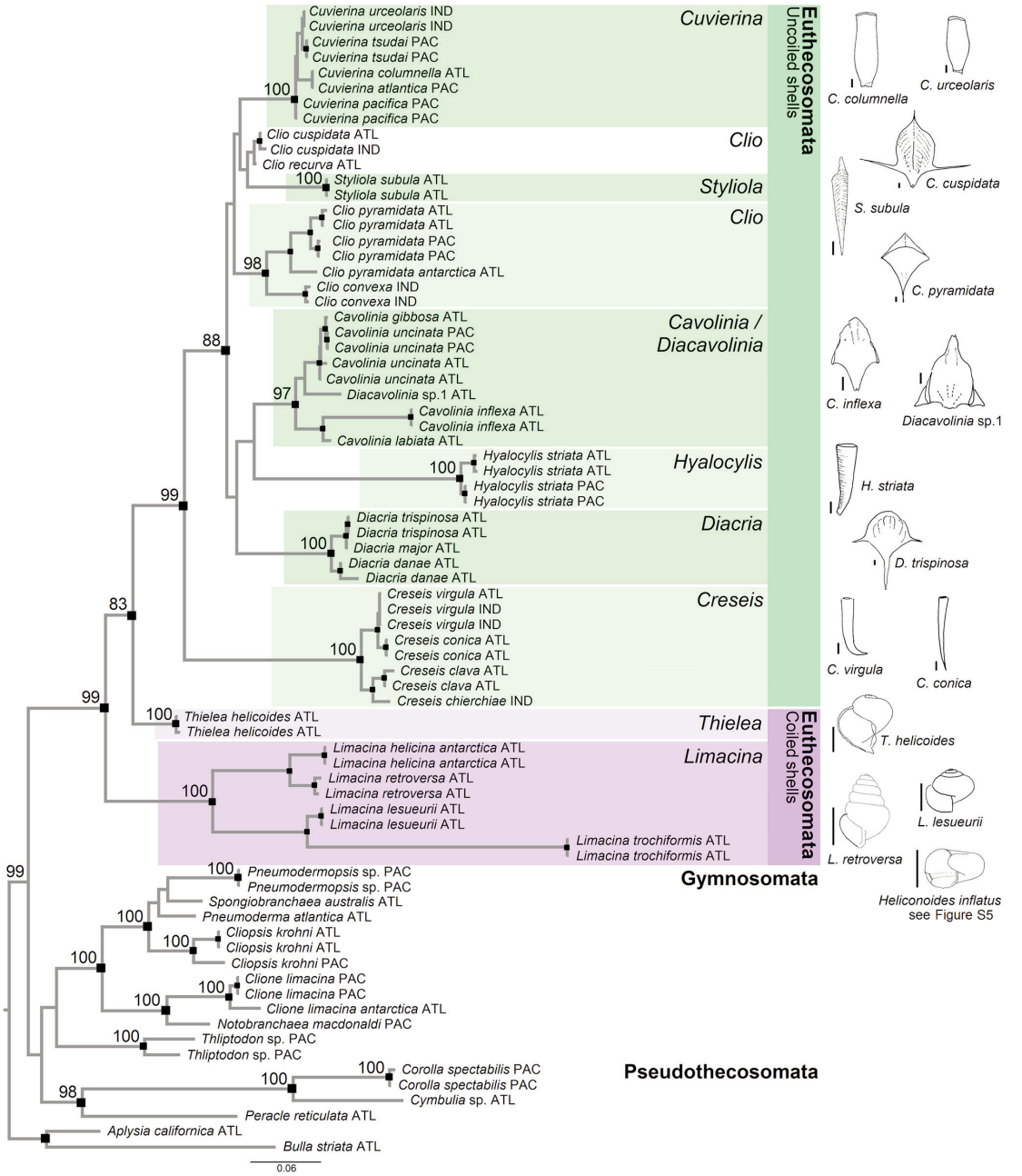

Figure 2. Maximum Likelihood phylogeny of pteropods based on the concatenated dataset of Cytochrome Oxidase I (amino acid alignment) and ribosomal genes 28S and 18S (nucleotide alignments) excluding the long-branch taxa *Heliconoides inflatus* and *Limacina bulimoides*. Black squares represent a bootstrap support of ≥80%, with small, medium and large black squares representing support within genera, of genera, and above genus level, respectively. Supported euthecosome genera are highlighted in coloured boxes, and representative shell shapes of species are drawn on the right, with all scale bars representing 1 mm. Maximum Likelihood phylogeny including the long-branch taxa *Heliconoides inflatus* and *Limacina bulimoides* is shown in Figure S5. Abbreviations ATL, PAC, and IND denote Atlantic, Pacific, and Indian Ocean origins, respectively, including their sectors in the Southern Ocean.

Pseudothecosomata (99% and 98%, respectively). However, in both phylogenies the monophyly of Gymnosomata is not supported due to the exclusion of *Thliptodon* from the clade. The phylogenetic relationships between euthecosomes, pseudothecosomes, and gymnosomes are unresolved based on these three genes.

The uncoiled euthecosomes (eight genera, superfamily Cavolinioidea) are a well-supported monophyletic group (99% support) in the analyses that exclude long-branch taxa, and *Creseis* is the sister group to all other genera within this clade (Figure 2). However, relationships between other uncoiled euthecosome genera are unresolved. The coiled euthecosome genera *Thielea* and *Limacina* (superfamily Limacinoidea) are not supported as a clade but represent the earliest diverging branches within Euthecosomata (Figure 2), and the phylogenetic position of *Heliconoides* remains unknown. In the phylogeny with long-branch taxa removed (Figure 2), the bathypelagic coiled species *Thielea helicoides* is the sister group of all uncoiled euthecosomes with moderate bootstrap support (83%).

Most species and genera are recovered as monophyletic groups in multi-gene phylogenies except *Clio* and *Cavolinia* (Figures 2 and S5). *Clio pyramidata*, *C. pyramidata antarctica*, and *C. convexa* represent one well-supported clade and *C. cuspidata* and *C. recurva* represent another unsupported group with unresolved affinities. *Diacavolinia* sp. groups with *Cavolinia* species rendering the genus *Cavolinia* paraphyletic. Within Pseudothecosomata, the pseudoconch genera *Corolla* and *Cymbulia* group separately (100% bootstrap) from the shelled *Peracle* species. The genus *Thliptodon* does not form a supported clade with other gymnsosome genera that do represent a well-supported monophyletic group (*Clione*, *Cliopsis*, *Notobranchaea*, *Pneumoderma*, *Pneumodermopsis*, and *Spongiobranchaea*). The latter clade consists of two subclades, one comprising *Clione* and *Notobranchaea* (100% support), and the other containing *Cliopsis*, *Pneumoderma*, *Pneumodermopsis*, and *Spongiobranchaea* (100% support, Figures 2 and S5).

Time-calibrated phylogenies

For molecular clock analyses, we reduced the number of taxa in the concatenated dataset to one taxon per species per ocean basin, and kept the long-branch taxa *Heliconoides inflatus* and *Limacina bulimoides*. We first performed a ML analysis to confirm that tree topologies were identical with previous multi-gene phylogenies. This is clearly the case, and Gymnosomata also represent a well-supported clade in this analysis (Figure S6).

The topologies of Bayesian time-calibrated phylogenies based on three approaches are identical and match unconstrained ML analyses (Figures 3, S7 and S8), for calibration methods 1, 2, and 3, respectively). Posterior probabilities of clade support are high for most nodes (>0.95), including the monophyletic euthecosome, pseudothecosome, and gymnosome clades. Within the uncoiled euthecosomes, significant support is observed for several additional clades compared to the ML phylogenies: the *Clio cuspidata*/*recurva* group, the *Cuvierina* + *Clio cuspidata*/*recurva* + *Styliola* group, the *Cavolinia*/*Diacavolinia* + *Hyalocylis* group (only for Methods 1 and 3), and the *Cavolinia*/*Diacavolinia* + *Hyalocylis* + *Diacria* group.

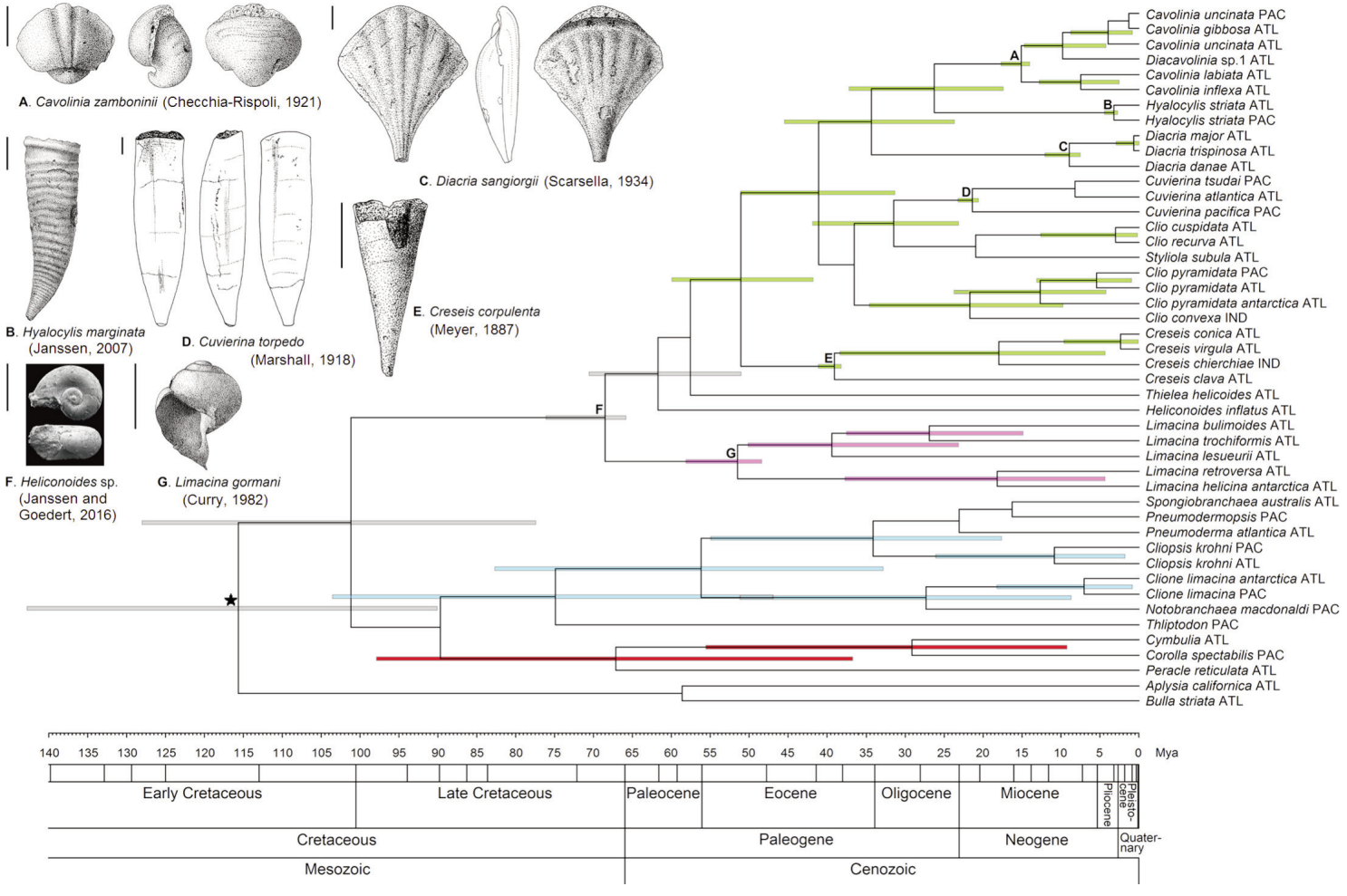

FIGURE 3. Fossil-calibrated phylogeny of pteropods (46 taxa, maximum one sequence per taxon per ocean) following Method 1 with crown calibrations based on the oldest known fossils of *Hyalocylis*, *Diacria*, *Cavolinia*, *Cuvierinia*, *Creseis*, *Limacina*, and euthecosomes (see TABLE 1). Drawings of fossils used for calibration are shown on the left, with all scale bars representing 1 mm, and calibrations are indicated with letters A to G. Error bars (95%) are shown only for clades with posterior probabilities ≥0.95 in green for uncoiled euthecosomes, purple for coiled euthecosomes, red for pseudothecosomes, and blue for gymnosomes. Abbreviations ATL, PAC, and IND denote Atlantic, Pacific, and Indian Ocean origins, respectively, including their sectors in the Southern Ocean.

TABLE 2. Overview of node ages as calibrated, as derived from independent runs without specific node calibrations, and as derived from two runs using all calibrations from a specific method.

Group	Calibration type	Calibrated/derived age
Euthecosomata	Fossil: *Heliconoides* sp.	Calibrated
		Derived
Cavolinioidea[1]		*Derived*
Cavolinia – Diacavolinia	Fossil: *Cavolinia zamboninii*	Calibrated
		Derived
Clio pyramidata (excl. f. *antarctica*)	IOP closure: Atlantic – Pacific	Calibrated
		Derived
Clio convexa/pyramidata group	None	*Derived*
Clio cuspidata/recurva group[2]	None	*Derived*
Creseis	Fossil: *Creseis corpulenta*	Calibrated
		Derived
Cuvierina	Fossil: *Cuvierina torpedo*	Calibrated
		Derived
Diacria	Fossil: *Diacria sangiorgii*	Calibrated
		Derived
Hyalocylis	Fossil: *Hyalocylis marginata*	Calibrated
		Derived
Hyalocylis striata	IOP closure: Atlantic – Pacific	Calibrated
		Derived
Limacina	Fossil: *Limacina gormani*	Calibrated
		Derived
Pseudothecosomata	None	*Derived*
Cymbuliidae	None	*Derived*
Gymnosomata[2]	None	*Derived*
Cliopsis krohni	IOP closure: Atlantic – Pacific	Calibrated
		Derived
Pteropods vs. outgroup taxa	Secondary: *Clione antarctica* vs. *Aplysia californica*	Calibrated
		Derived

The Gymnosomata and of the *Clio cuspidata/recurva* group are supported in time-calibrated, but not in unconstrained multi-gene Maximum Likelihood analyses. The monophyly of uncoiled Euthecosomata (Cavolinioidea) is not supported with a posterior probability of >95 in calibration Method 2 (see TABLE 1). mya = million years ago.

The node ages of pteropod genera derived from molecular clocks are less variable than node ages at higher taxonomic levels. The crown group ages of euthecosome genera based on fossil ages (Method 1) correspond well with the ages based on IOP calibrations (Method 3), and fossil-based stem calibrations (Method 2) generally lead to much younger crown group ages than other calibration methods (FIGURES 3, S7 and S8; TABLE 2). Cross-validation analyses, in which we left out one of the fossil crown calibrations at a time, show that the derived node ages correspond well with the calibrated ages (Method 1) for *Hyalocylis* (Pliocene), *Diacria*, *Cavolinia*/*Diacavolinia* (Miocene), and *Limacina* (Eocene). This was not the case for *Cuvierina* (Miocene) and *Creseis* (Eocene), for which crown ages appeared to be

Age of crown group (95% confidence intervals; mya)			Calibration age (mya)
Method 1	Method 2	Method 3	
68.54 (76.1–65.9)	67.91 (73.2–65.8)	68.11 (74.4–65.8)	79–66
89.62 (116.3–66.4)[3]	*75.79 (101.2–53.0)*[3]	*86.55 (116.6–57.4)*[3]	
51.0 (60.0–41.75)[4]		*42.5 (56.5–28.75)*[4]	
15.05 (17.6–14.0)	10.61 (14.1–6.5)		16–13.8
18.62 (29.1–10.2)[3]	*10.45 (20.0–4.1)*[3]	*14.35 (23.0–7.2)*[4]	
		3.11 (4.9–1.5)	3.1
5.44 (13.0–0.9)[4]	*3.72 (8.7–0.6)*[4]	*4.01 (9.9–0.9)*[3]	
21.75 (34.5–9.75)[4]	*14.5 (23.25–6.75)*[4]	*14.25 (25.75–6.75)*[4]	
3.0 (12.5–0.25)[4]	*2.0 (8.5–0.25)*[4]	*2.0 (7.75–0.25)*[4]	
39.04 (41.0–38.2)	9.36 (21.9–2.3)		41–38
12.12 (26.2–3.0)[3]	*9.09 (20.2–2.67)*[3]	*9.6 (22.0–2.9)*[4]	
21.27 (23.1–20.6)	3.72 (10.0–0.7)		23–20.4
4.42 (11.2–0.8)[3]	*3.37 (8.7–0.5)*[3]	*3.66 (9.2–0.8)*[4]	
8.88 (12.0–7.5)	4.14 (11.0–0.7)		11.6–7.2
7.43 (20.6–1.1)[3]	*5.19 (12.6–0.9)*[3]	*5.39 (15.0–0.9)*[4]	
3.19 (4.3–2.7)	2.25 (6.0–0.3)		3.6–2.6
3.82 (10.5–0.4)[3]	*2.52 (6.5–0.3)*[3]	*See H. striata.*	
		2.85 (4.6–1.1)	3.1
See Hyalocylis.	*See Hyalocylis.*	*2.99 (8.3–0.4)*[3]	
51.48 (58.1–48.3)			56–47.8
52.82 (66.5–35.2)[3]	*50.33 (64.3–33.6)*[4]	*49.69 (64.2–32.7)*[4]	
67.25 (98.0–36.5)[4]	*56.75 (84.75–29.0)*[4]	*58.25 (86.0–30.25)*[4]	
29.0 (55.5–9.25)[4]	*23.0 (46.0–7.0)*[4]	*23.75 (46.0–7.0)*[4]	
75.0 (103.75–47.0)[4]	*63.25 (89.25–38.5)*[4]	*65.25 (92.0–40.25)*[4]	
		3.47 (5.2–1.8)	3.1
10.8 (26.0–1.8)[4]	*7.69 (19.3–1.0)*[4]	*8.62 (21.2–0.8)*[3]	
115.63 (142.8–90.1)	104.47 (130.7–80.6)	105.96 (132.1–82.0)	170–90
94.14 (134.4–68.3)[3]	*74.95 (94.2–66.3)*[3]	*74.63 (90.3–66.5)*[3]	

[1] Not supported with posterior probability of >0.95 in molecular clock Method 2
[2] Supported monophyly in molecular clock, but not in ML analyses
[3] Derived from independent run without calibration of this node (100 million generations, 10% burn-in)
[4] Derived from 2 runs using all calibrations from specific method (2 * 100 million generations, 10% burn-in each)

younger than the fossil evidence, derived at 4.42 and 12.12 mya, respectively. Derived crown group ages based on leaving out one fossil stem calibration per independent run (Method 2) are ~1–3 million years younger than ages derived in Method 1 for *Hyalocylis*, *Diacria*, *Cuvierina*, and *Creseis*, and ~8 million years younger for *Cavolinia*/*Diacavolinia* (Table 2). Derived ages from independent runs that left out one of the three IOP-calibrations each (Method 3) correspond best for *Hyalocylis striata* (derived at 2.99 mya), but are slightly older for *Clio pyramidata* (4.01 mya), and much older for the gymnosome *Cliopsis krohni* (8.62 mya). These ages correspond well with the ages of uncalibrated nodes in Methods 1 and 2 (Table 2).

At the higher taxonomic levels (Pteropoda, Euthecosomata, Pseudothecosomata, Gymnosomata) node ages are more variable. The derived age of pteropods versus the outgroup taxa *Aplysia californica* and *Bulla striata* results in a younger age compared to the secondary calibration of this node: 94–74 mya instead of 116–104 mya with large 95% error ranges (Table 2). When not used as a fossil crown calibration, the derived age of the euthecosomes appears to be overestimated by all three calibration methods compared to its fossil age (90–75 mya instead of 79–66 mya), but all with large 95% error ranges of 50–59 million years. Derived ages of the pseudothecosomes are 67.25, 56.75, and 58.25 mya, and for the gymnosomes they are 75.0, 63.25, and 65.25 mya, based on calibration methods 1, 2, and 3, respectively (Figures 3, S7 and S8).

Discussion

Taxonomy of Pteropoda

Generally, our reconstructed molecular phylogenies match the current morphology-based taxonomy of pteropods. Most species and genera are well resolved and confirmed to be monophyletic and hence provide a useful framework for ecological and evolutionary studies of the group. A taxonomic division of pteropods into euthecosomes, pseudothecosomes, and gymnosomes is also consistent with our data, although their phylogenetic interrelationships remain unresolved. We cannot confirm that euthecosomes are more closely related to pseudothecosomes than they are to gymnosomes, as reflected in current taxonomy, in which the eu- and pseudothecosomes represent the order Thecosomata based on shared morphological characters that set them apart from the order Gymnosomata. The parapodia (wing-like structures) of thecosomes are positioned differently compared to gymnosomes with respect to the head, mouth, and foot-lobes (Pafort-van Iersel and Van der Spoel, 1979; Van der Spoel, 1982). Resolving higher-level taxonomic relationships in pteropods will require additional molecular evidence, such as could be provided by transcriptome data that enable a phylogenomic approach.

All our analyses recover the monophyly of uncoiled euthecosomes supporting the validity of the superfamily Cavolinioidea. We see no reason for changing this name to Orthoconcha, as suggested by Corse et al. (2013). However, the current taxonomy of families within the Cavolinioidea was not supported by our phylogenetic analyses. Currently valid families are Cavoliniidae (*Cavolinia*, *Diacavolinia*, *Diacria*), Cliidae (*Clio*), Creseidae (*Creseis*, *Hyalocylis*, *Styliola*), and Cuvierinidae (*Cuvierina*). This classification corresponds with the overall shape of shells: complex and round for Cavoliniidae, wide and conical for Cliidae, narrow and conical for Creseidae, and bottle-shaped for Cuvierinidae (Figure 2). We only found one supported subdivision within Cavolinioidea based on ML phylogenies, with *Creseis* as a monophyletic group and sister clade to the cluster of genera comprising *Cavolinia*, *Clio*, *Cuvierina*, *Diacavolinia*, *Diacria*, *Hyalocylis*, and *Styliola* (Figure 2). The time-calibrated phylogenies support additional subdivisions within Cavolinioidea (e.g., *Cavolinia* + *Diacavolinia* + *Hyalocylis*); however, they do not reflect current family-level taxonomy either.

The genus *Clio* was paraphyletic in the multi-gene phylogenies, with the well-resolved clade comprising *Clio convexa*, *C. pyramidata*, and *C. pyramidata antarctica*, being sister to another clade comprising *C. cuspidata* and *C. recurva* that was only supported in time-calibrated Bayesian phylogenies. Morphological characteristics of the two groups support this division: *Clio convexa*, *C. pyramidata*, and *C. pyramidata antarctica* have an elongated protoconch (larval shell) with a subtle transition into the apical spine (larval shell tip), whereas *Clio cuspidata* and *C. recurva* have a round protoconch with a sharp transition into the apical spine (e.g., Janssen, 2012). More genetic information is required to clarify the phylogenetic position of *C. cuspidata* and *C. recurva*, and additional *Clio* taxa should be included in the analysis, such as the deep-dwelling *C. andreae*, *C. chaptalii*, *C. polita*, and *C. piatkowskii*.

Diacavolinia, introduced as a genus by Van der Spoel (1987) was previously included in *Cavolinia* as the single species *Cavolinia longirostris*. We recovered *Diacavolinia* as nested within *Cavolinia*. Specimens identified as *Diacavolinia* sp. 1 were from the Atlantic Ocean and match the Atlantic sequences from Maas et al. (2013) and *Diacavolinia* Group 1 in Burridge et al. (in prep.: Thesis chapter 5). Pacific individuals used in single-gene COI analyses (*Diacavolinia* sp. 2) match the Pacific sequences from Maas et al. (2013) as well as *Diacavolinia* Group 12 in Burridge et al. (in prep.: Thesis chapter 5). The high levels of morphological and genetic diversity found for both *Diacavolinia* and *Cavolinia* suggests that more taxon sampling across all oceans and additional genetic markers are needed to resolve their taxonomy.

The coiled euthecosomes or Limacinoidea consist of a single family, the Limacinidae, which appears to be paraphyletic with respect to the uncoiled euthecosomes. The genera *Heliconoide*s, *Limacina*, and *Thielea* are genetically more divergent than the Cavolinioidea genera. This may be a result of their earlier origin compared to uncoiled euthecosomes, and/or higher evolutionary rates, as observed for the conservative markers 28S and 18S. Corse et al. (2013) proposed to rename *Heliconoides inflatus* (listed in their study as *Limacina inflata*) to *Embolus inflata* to emphasize a putative soft polytomy between *Heliconoides inflatus* and other coiled euthecosomes, however, based on the available evidence, we consider the position of *Heliconoides* as unresolved. Moreover, earliest fossil occurrences do not support the presence of a hard polytomy of coiled euthecosome genera (Janssen, 2012; Janssen and Goedert, 2016; Janssen et al., 2016; see next section). Finally, *Embolus* is currently considered a synonym of *Heliconoides* and represents an invalid junior homonym of *Embolus*, a genus of echinoderm (WoRMS).

The single and multi-gene trees strongly supported the taxonomy of the pseudothecosome families Peraclidae (*Peracle*) and Cymbuliidae (*Cymbulia*, *Corolla*, *Gleba*). However, pseudothecosome species remain poorly studied compared to euthecosomes, and additional taxon sampling of all genera, including *Desmopterus*, is required to resolve their taxonomy.

Only four out of six families and eight of 19 genera of Gymnosomata were included in our analyses, and thus phylogenetic relationships should be regarded

as tentative. Our analyses did not support the current taxonomy of the gymnosome families examined: Clionidae (*Clione*, *Thliptodon*), Cliopsidae (*Cliopsis*), Notobranchaeidae (*Notobranchaea*), and Pneumodermatidae (*Pneumoderma*, *Pneumodermopsis*, *Schizobrachium*, *Spongiobranchaea*). We found *Clione* as the most likely sister taxon of *Notobranchaea*, and *Thliptodon* grouped separately from all other gymnosome taxa.

Evolutionary history

Based on a molecular clock approach using fossils and the IOP as calibrations, we propose a scenario of pteropod evolution, in which this group originated during the Late Cretaceous, and most extant genera evolved during the Late Oligocene and Miocene. The euthecosomes, pseudothecosomes, and gymnosomes most likely evolved during the final stages of the Late Cretaceous (79–66 mya) from which the first *Heliconoides* euthecosome fossil is known (Janssen and Goedert, 2016). Interestingly, this is earlier than previously thought as the time of divergence between the euthecosomes and pseudothecosomes was estimated at 58.6 / 57.3 mya by Corse et al. (2013) based on two different molecular clock methods. However, this may be due to their incorrect assumption that the Early-Eocene (Ypresian) thecosome genus *Altaspiratella* belongs to the Pseudothecosomata.

Among the coiled euthecosomes, the evolution of *Heliconoides* in the Late Cretaceous was followed by the origin of *Limacina* in the Early Eocene at ~56 mya based on fossil records and our time-calibrated molecular phylogeny. The Paleocene-Eocene thermal maximum (PETM) at ~56 mya was probably a critical event in pteropod evolution. Although some studies have suggested that modern pteropod families appeared only after the PETM (e.g., Doney et al., 2009), a recent study of a PETM assemblage of pteropods demonstrated the presence of *Limacina* and *Heliconoides* as well as the extinct genus *Altaspiratella* in this period (Janssen et al., 2016). Based on fossil evidence, it was suggested that most genera that originated after the PETM went extinct before the end of the Eocene at 33.9 mya, when global ocean temperatures dropped (Hodgkinson et al., 1992; Janssen and Peijnenburg, 2017).

We estimated that uncoiled euthecosomes evolved during the Early to Middle Eocene at 51–42 mya, probably from a coiled euthecosome ancestor, as was earlier suggested by Curry (1965) and Curry and Rampal (1979). Putative successive stages of despiralisation have been observed in some pteropod species from the Eocene (Ypresian, 56.0–47.8 mya; Lutetian, 47.8–41.3 mya), as in particular species of the limacinid genus *Altaspiratella*, leading to the creseid genera *Camptoceratops* and *Euchilotheca* (Janssen and Peijnenburg, 2014). *Camptoceratops priscus* was used by Corse (2013) to calibrate the origin of the euthecosomes, but based on its intermediate morphology between coiled and uncoiled taxa its phylogenetic position is considered uncertain. *Creseis* appeared as the first extant uncoiled genus at 41–38 mya (Middle Eocene: Bartonian), followed by a *Clio* representative at 38–34 mya (Late Eocene: Priabonian; Bernasconi and Robba, 1982; Janssen, 1990).

During the Oligocene and Miocene, the (sub)tropical connectivity between the Atlantic and Indian oceans decreased and finally ceased as a result of closure of the

Miocene Tethys Sea (Terminal Tethyan Event TTE; Harzhauser et al., 2002, 2007), and during this period of oceanographic and climatic change many extant pteropod genera appeared. The uncoiled euthecosome genera *Cavolinia*, *Cuvierina*, *Diacria*, *Styliola*, and the *Clio convexa*/*pyramidata* group originated during the late Oligocene and Miocene between 40 and 15 mya. Corse et al. (2013) estimated that the family Cavoliniidae evolved 47.1 / 30.0 mya, but we did not find evidence for its monophyly. Most pseudothecosome and gymnosome genera probably originated during the Late Oligocene and Miocene (Janssen, 2010). We could not estimate the age of the bathypelagic, coiled euthecosome *Thielea*, but rare fossil evidence suggests at least a Miocene (Tortonian, 11.6–7.2 mya) origin (Janssen, 2012).

The uncoiled euthecosomes *Hyalocylis*, *Diacavolinia* and the *Clio cuspidata* / *recurva* group appear to be of more recent, Pliocene origin, when the Isthmus of Panama (IOP) became totally emergent, and fossil evidence supports this age (5.3–2.6 mya; Janssen, 2007, 2012). Hence, the age of *Hyalocylis* appears to have been overestimated by Corse et al. (2013) at 38.5 / 16.1 mya. This age rather corresponds with the Late Eocene origin of *Praehyalocylis*, which is the supposed ancestor of *Hyalocylis* (Janssen, 2010). The IOP emergence led to a further reduction in (sub)tropical connectivity between the Atlantic and Indo-Pacific oceans. Isolation of (sub)tropical Atlantic and Pacific populations probably did not occur at the same time for all species. For example, the gymnosome *Cliopsis krohni* may require deeper maximum depths than *Hyalocylis striata* and *Clio pyramidata*, occurring as deep as 1500 m (Troschel, 1854). This could explain the earlier divergence between Atlantic and Pacific populations of *Cliopsis krohni* compared to *Hyalocylis striata* and *Clio pyramidata*. Recent molecular studies of the (sub)tropical *Cuvierina* and *Diacavolinia* taxa also suggested isolation of Atlantic and Indo-Pacific taxa (Maas et al., 2013; Burridge et al., 2015: Thesis chapter 3, in prep.: Thesis chapter 5).

Pteropods in the Anthropocene

We present a framework for understanding the evolutionary relationships among pteropods with a focus on shelled euthecosome species based on an integrated analysis of three molecular markers, fossil evidence, and vicariance events. Although not all phylogenetic relationships could be resolved, this study provides new data on the diversity of pteropods, which is an essential first step for their use as bioindicators of the ongoing effects of ocean acidification (e.g., Bednaršek et al., 2016). Recent advances in high-throughput sequencing will allow sampling across the entire genome and will result in better resolved and more robust phylogenies, especially at higher taxonomic levels. Anthropogenic carbon input into the atmosphere and the ocean is occurring over the course of just hundreds instead of thousands of years. Hence, the impacts on surface ocean pH are more precipitous now than during the PETM (Zachos et al., 2005; Zeebe, 2012). Although the PETM may be the most comparable ocean acidification event in the past, its preceding climate conditions were very different from the present day. Continents were configured differently and the global climate was warmer (Zeebe, 2012; Dietmar Müller et al., 2016). Stuecker and Zeebe (2010) found that the current sensitivity

of marine ecosystems to carbon perturbation is likely higher than during the PETM because the ocean's chemistry might have differed substantially. All in all, it is likely that the effects of ocean acidification on pteropods will be unprecedented, and this key group of the zooplankton community will be among the most severely affected.

Acknowledgements

We thank J. Huisman for comments on this manuscript, P. Kuperus, B. Voetdijk, L. Dong, and K. Walz for technical assistance in the molecular lab, C. Mennes and V. Merckx for advice regarding phylogenetic and molecular clock analyses, and E. Goetze and A. Tsuda for providing samples. We thank the Southeast Area and Monitoring Program (SEAMAP) for providing samples from their surveys. L. Vásquez (ECOSUR) and J. Lamkin (NOAA) kindly allowed R. Gasca to examine these samples. The authors also thank the captain and crew of the NOAA ship 'Gordon Gunter 1101'. This is contribution number 308 of the Atlantic Meridional Transect Programme. This work was supported by a Netherlands Organisation for Scientific Research (NWO) cruise participation grant, Veni and Vidi grants 863.08.024 and 016.161351 (http://www.nwo.nl), respectively, to K.T.C.A. Peijnenburg. M. Hughes was supported by the Natural History Museum of London / Imperial College Biosystematics Mres programme and John Templeton Foundation grant 43915 (https://www.templeton.org). S.L. Bush was funded by the Smithsonian Women's Committee grants and Smithsonian research funds to K.J. Osborn, and the Monterey Bay Aquarium. The David and Lucile Packard Foundation provided funding for numerous cruises to the Monterey Bay Aquarium Research Institute in which K.J. Osborn and S.L. Bush participated. Plankton collections for this study were (partially) supported by National Science Foundation (USA) grants OCE-1230900 to the UNOLS Training Program and OCE-1029478 and OCE-1338959 (https://www.nsf.gov) to E. Goetze, National Ocean and Atmospheric Administration's Northeast Fisheries Science Center to NOAA/National Marine Fisheries Service and M. Vecchione, and the UK Natural Environmental Research Council National Capability funding to Plymouth Marine Laboratory and the National Oceanography Centre, Southampton. Funding for SEAMAP surveys was provided by NOAA. This is contribution number 308 of the Atlantic Meridional Transect Programme. The funders had no role in study design, data collection and analysis, decision to publish, or preparation of the manuscript. The authors have declared that no competing interests exist.

References

Atlantic Meridional Transect cruise reports. http://www.amt-uk.org

Bacon C.D., Silvestro D., Jaramillo C., Tilston Smith B., Chakrabarty P., Antonelli A., 2015. Biological evidence supports an early and complex emergence of the Isthmus of Panama. Proceedings of the National Academy of Sciences 112, 6110–6115.

Bé A.W.H., Gilmer R.W., 1977. A zoogeographic and taxonomic review of euthecosomatous Pteropoda. In: Ramsay A.T.S. (Ed.), Oceanic Micropaleontology 1. Academic Press, London, pp. 733–808.

Bednaršek N., Harvey C.J., Kaplan I.C., Feely R.A., Možina J., 2016. Pteropods on the edge: cumulative effects of ocean acidification, warming, and deoxygenation. Progress in Oceanography 145, 1–24.

Bednaršek N., Možina J., Vogt M., O'Brien C., Tarling G.A., 2012. The global distribution of pteropods and their contribution to carbonate and carbon biomass in the modern ocean. Earth System Science Data 4, 167–186.

Bernasconi M.P., Robba E., 1982. The thecosomatous pteropods: a contribution toward the Cenozoic Tethyan paleobiogeography. Bollettino della Società Paleontologica Italiana 21, 2–3.

Bouchet P., Rocroi J.-P., 2005. Classification and nomenclator of gastropod families. Malacologia 47, 1–397.

Bowen B.W., Gaither M.R., DiBattista J.D., Iacchei M., Andrews K.R. et al., 2016. Comparative phylogeography of the ocean planet. Proceedings of the National Academy of Sciences 113, 7962–7969.

Bralower T.J., 2002. Evidence of surface water oligotrophy during the Paleocene-Eocene thermal maximum: Nannofossil assemblage data from Ocean Drilling Program Site 690, Maud Rise, Weddel Sea. Paleoceanography 17, 1023.

Burridge A.K., Goetze E., Raes N., Huisman J., Peijnenburg K.T.C.A., 2015. Global biogeography and evolution of *Cuvierina* pteropods. BMC Evolutionary Biology 15, 39. Thesis chapter 3.

Burridge A.K., Goetze E., Wall-Palmer D., Le Double S.L., Huisman J., Peijnenburg K.T.C.A., in press. Diversity and abundance of pteropods and heteropods along a latitudinal gradient across the Atlantic Ocean. Progress in Oceanography, published online in 2016. Thesis chapter 6.

Burridge A.K., Janssen A.W., Peijnenburg K.T.C.A., 2016. Revision of the genus *Cuvierina* Boas, 1886 based on integrative taxonomic data, including the description of a new species from the Pacific Ocean (Gastropoda, Thecosomata). ZooKeys 619, 1–12. Thesis chapter 4.

Burridge A.K., Van der Hulst R., Goetze E., Peijnenburg K.T.C.A., in prep. Assessing species boundaries in the open sea: applying an integrative taxonomic approach to a genus of pelagic molluscs. Thesis chapter 5.

Cahuzac B., Janssen A.W., 2010. Eocene to Miocene holoplanktonic Mollusca (Gastropoda) of the Aquitaine Basin, southwest France. Scripta Geologica 141, 1–193.

Capella-Gutiérrez S., Silla-Martínez J.M., Gabaldón T., 2009. TrimAl: a tool for automated alignment trimming in large-scale phylogenetic analyses. Bioinformatics 25, 1972–1973.

Checchia-Rispoli G., 1921. I pteropodi del Miocene garganico. Bollettino del R. Comitato Geologico d'Italia 48, 1–28.

Comeau S., Gattuso J.-P., Nisumaa A.-M., Orr J., 2012. Impact of aragonite saturation state changes on migratory pteropods. Proceedings of the Royal Society B 279, 732–738.

Corse E., Rampal J., Cuoc C., Peck N., Perez Y., Gilles A, 2013. Phylogenetic analysis of Thecosomata Blainville, 1824 (Holoplanktonic Opisthobranchia) using morphological and molecular data. PLoS ONE 8, e59439.

Cowman P.E., Bellwood D.R., 2013. Vicariance across major marine biogeographic barriers: temporal concordance and the relative intensity of hard versus soft barriers. Proceedings of the Royal Society B 280, 20131541.

Curry D., 1965. The English Palaeogene pteropods. Proceedings of the Malacological Society of London 36, 357–371.

Curry D., 1982. Ptéropodes éocènes de la tuilerie de Gan (Pyrénées-Atlantiques) et de quelques Autres localités du SW de la France. Cahiers de Micropaléontologie 4, 35–44.

Curry D., Rampal J., 1979. Shell microstructure in fossil thecosome pteropods. Malacologia 18, 23–25.

Darriba D., Taboada G.L., Doallo R., Posada D., 2012. jModelTest 2: more models, new heuristics and parallel computing. Nature Methods. 9, 772.

Dayrat B., Tillier A., Lecointre G., Tillier S., 2001. New clades of euthyneuran gastropods (Mollusca) from 28S rRNA sequences. Molecular Phylogenetics and Evolution 19, 225–235.

De Blainville H.M.D., 1824. Mollusques, Mollusca (Malacoz.). Dictionnaire des Sciences Naturelles 7, 105–108.

Dietmar Müller R., Seton M., Zahirovic S., Williams S.E., Matthews K.J., et al., 2016. Ocean basin evolution and global-scale plate reorganization events since Pangaea breakup. Annual Review of Earth and Planetary Sciences 44, 107–138.

Doney S.C., Fabry V.J., Feely R.A., Kleypas J.A, 2009. Ocean acidification: the other CO_2 problem. Annual Review of Marine Science 1, 169–192.

Drummond A.J., Suchard M.A., Xie D., Rambaut A., 2012. Bayesian phylogenetics with BEAUti and the BEAST 1.7. Molecular Biology and Evolution 29, 1969–1973.

Edgar R.C., 2004. MUSCLE: multiple sequence alignment with high accuracy and high throughput. Nucleic Acids Research 32, 1792–1797.

Fabry V.J., Seibel B.A., Feely R.A., Orr J.C., 2008. Impacts of ocean acidification on marine fauna and ecosystem processes. ICES Journal of Marine Science 65, 414–432.

Felsenstein J., 1981. Evolutionary trees from DNA sequences: a maximum likelihood approach. Journal of Molecular Evolution 17, 368–376.

Folmer O., Black M., Hoeh W., Lutz R., Vrijenhoek R., 1994. DNA primers for amplification of mitochondrial Cytochrome c Oxidase subunit I from diverse metazoan invertebrates. Molecular Marine Biology and Biotechnology 3, 294–299.

Gasca R., Janssen A.W., 2014. Taxonomic review, molecular data and key to the species of Creseidae from the Atlantic Ocean. Journal of Molluscan Studies 80, 35–42.

Gernhard T., 2008. The conditioned restructured process. Journal of Theoretical Biology 253, 769–778.

Gibbs S.J., Bown P.R., Sessa J.A., Bralower T.J., Wilson P.A., 2006. Nannoplankton extinction and origination across the Paleocene-Eocene Thermal Maximum. Science 314, 1770–1773.

Gibbs S.J., Bralower T.J., Bown P.R., Zachos J.C., Bybell L.M., 2006. Shelf and open-ocean calcareous phytoplankton assemblages across the Paleocene-Eocene Thermal Maximum: implications for global productivity gradients. Geology 34, 233–236.

Gilmer R.W., Harbison G.R., 1986. Morphology and field behavior of pteropod molluscs: feeding methods in the families Cavoliniidae, Limacinidae and Peraclididae (Gastropoda: Thecosomata). Marine Biology 91, 47–57.

Harzhauser M., Kroh A., Mandic O., Piller W.E., Göhlich U. et al., 2007. Biogeographic responses to geodynamics: a key study all around the Oligo-Miocene Tethyan Seaway. Zoologischer Anzeiger 246, 241–256.

Harzhauser M., Piller W.E., Steiniger F.F., 2002. Circum-Mediterranean Oligo-Miocene biogeographic evolution–the gastropods' point of view. Palaeogeography, Palaeoclimatology, Palaeoecology, 183, 103–133.

Hodgkinson K.A., Garvie C.L., Bé A.W.H, 1992. Eocene euthecosomatous Pteropoda (Gastropoda) of the Gulf and eastern coasts of North America. Bulletins of American Paleontology 103, 5–62.

Hunt B., Strugnell J., Bednaršek N., Linse K., John Nelson R., et al., 2010. Poles apart: The 'bipolar' pteropod species *Limacina helicina* is genetically distinct between the Arctic and Antarctic Oceans. PLoS ONE 5, e9835.

Janssen A.W., 1990. Pteropoda (Gastropoda, Euthecosomata) from the Australian Cainozoic. Scripta Geologica 91, 1–76.

Janssen A.W., 2003. Notes on the systematics, morphology and biostratigraphy of fossil holoplanktonic Mollusca, 13. Considerations on a subdivision of Thecosomata, with the emphasis on genus group classification of Limacinidae. Cainozoic Research 2, 163–170.

Janssen A.W., 2005. Development of Cuvierinidae (Mollusca, Euthecosomata, Cavolinioidea) during the Cainozoic: a non-cladistic approach with a re-interpretation of Recent taxa. Basteria 69, 25–72.

Janssen A.W., 2007. Holoplanktonic Mollusca (Gastropoda: Pterotracheoidea, Janthinoidea, Thecosomata and Gymnosomata) from the Pliocene of Pangasinan (Luzon, Philippines). Scripta Geologica 135, 29–177.

Janssen A.W., 2010. Systematics and biostratigraphy of holoplanktonic Mollusca from the Oligo-Miocene of the Maltese Archipelago. Bollettino del Museo Regionale di Scienze Naturali Torino 28, 197–601.

Janssen A.W., 2012. Late Quaternary to recent holoplanktonic Mollusca (Gastropoda) from bottom samples of the eastern Mediterranean Sea: systematics, morphology. Bollettino Malacologico 48, 1–105.

Janssen A.W., Goedert J.L., 2016. Notes on the systematics, morphology and biostratigraphy of fossil holoplanktonic Mollusca, 24. First observation of a genuinely Late Mesozoic thecosomatous pteropod. Basteria 80, 59–63.

Janssen A.W., Peijnenburg K.T.C.A., 2014. Holoplanktonic Mollusca: development in the Mediterranean basin during the last 30 million years and their future. In: Goffredo S., Dubinsky Z. (Eds.), The Mediterranean Sea: Its History and Present Challenges. Springer, Dordrecht, pp. 341–362.

Janssen A.W., Peijnenburg K.T.C.A. 2017. An overview of the fossil record of Pteropoda (Mollusca, Gastropoda, Heterobranchia). Cainozoic Research 17, 3–10.

Janssen A.W., Sessa J.A., Thomas E., 2016. Pteropoda (Mollusca, Gastropoda, Thecosomata) from the Paleocene-Eocene Thermal Maximum (United States Atlantic Coastal Plain). Palaeontologia Electronica 19, 1–26.

Jennings R.M., Bucklin A., Ossenbrügger H., Hopcroft R.R., 2010. Species diversity of planktonic gastropods (Pteropoda and Heteropoda) from six ocean regions based on DNA barcode analysis. Deep-Sea Research II 57, 2199–2210.

Jörger K.M., Stöger I., Kano Y., Fukuda H., Knebelsberger T., Schrödl M., 2010. On the origin of Acochlidia and other enigmatic euthyneuran gastropods, with implications for the systematics of Heterobranchia. BMC Evolutionary Biology 10, 323.

Kelly D.C., Bralower T.J., Zachos J.C., Premoli Silva I., Thomas E., 1996. Rapid diversification of planktonic foraminifera in the tropical Pacific (ODP Site 865) during the late Paleocene thermal maximum. Geology 24, 423–426.

Klussmann-Kolb A., Dinapoli A., 2006. Systematic position of the pelagic Thecosomata and Gymnosomata within Opisthobranchia (Mollusca, Gastropoda)–revival of the Pteropoda. Journal of Zoological Systematics and Evolutionary Research 44, 118–129.

Lalli C.M., Conover R.J., 1976. Microstructure of the veliger shells of gymnosomatous pteropods (Gastropoda: Opisthobranchia). The Veliger 18, 237–240.

Lessios H.A., 2008. The great American schism: divergence of marine organisms after the rise of the Central American Isthmus. Annual Review of Ecology, Evolution, and Systematics 39, 63–91.

Maas A.E., Blanco-Bercial L., Lawson G.L., 2013. Reexamination of the species assignment of *Diacavolinia* pteropods using DNA barcoding. PLoS ONE 8, e53889.

MAFFT version 7. Multiple alignment program for amino acid or nucleotide sequences. http://mafft.cbrc.jp/alignment/server

Marshall P., 1918. The Tertiary molluscan fauna of Pakaurangi Point, Kaipara Harbour. Transactions of the New Zealand Institute 50, 263–278.

Meisenheimer J., 1906. Pteropoda. Wissenschaftliche Ergebnisse der Deutschen 769 Tiefsee-Expedition auf dem Dampfer 'Valdivia' 1898-1899, 9, 314 pp.

Meyer O., 1887. Beitrag zur Kenntnis der Fauna des Alttertiärs von Mississippi und Alabama. Vorträge und Abhandlungen 2, 3–22.

Monterey Bay Aquarium Research Institute (MBARI). http://www.mbari.org/at-sea/expeditions

Moya A., Howes E.L., Lacoue-Labarthe T., Forêt S., Bishoy H. et al., 2016. Near-future pH conditions severely impact calcification, metabolism and the nervous system in the pteropod *Heliconoides inflatus*. Global Change Biology 22, 3888–3900.

National Oceanic and Atmospheric Administration (NOAA). http://www.noaa.gov

O'Dea A., Lessios H.A., Coates A.G., Eytan R.I., Restrepo-Moreno S.A. et al., 2016. Formation of the Isthmus of Panama. Science Advances 2, e1600883.

Pafort-van Iersel T., Van der Spoel S., 1979. The structure of the columellar muscle system in *Clio pyramidata* and *Cymbulia peroni* (Thecosomata, Gastropoda) with a note on the phylogeny of both species. Bijdragen tot de Dierkunde 48, 111–126.

Rampal J., 1973. Phylogénie des Ptéropodes Thécosomes d'après la structure de la coquille et la morphologie du manteau. Comptes Rendus de l'Académie des Sciences – Series II 277, 1345–1348.

Rampal J., 1975. Les thécosomes (mollusques pélagiques). Systématique et évolution–écologie et biogéographie méditerranéennes. PhD thesis, Université de Provence, U.E.R. Scientifiques (Aix-Marseille 1).

Rampal J., 2011. Clés de détemination des ptéropodes thécosomes de Méditerranée et de l'atlantique euroafricain. Revue des Travaux l'institut des pêches maritimes 37, 369–381.

Rota-Stabelli O., Yang Z., Telford M.J., 2009. MtZoa: A general mitochondrial amino acid substitution model for animal evolutionary stories. Molecular Phylogenetics and Evolution 52, 268–272.

Sánchez R., Serra F., Tárraga J., Medina I., Carbonell J., et al., 2011. Phylemon 2.0: a suite of web-tools for molecular evolution, phylogenetics, phylogenomics and hypothesis testing. Nucleic Acids Research 39, W470–W474.

Scarsella F., 1934. Di una nuova specie di pteropodo del Miocene appenninico. Bollettino della Società Geologica Italiana 53, 177–181.

Schneider L.J., Bralower T.J., Kump L.R., Patzkowsky M.E., 2013. Calcareous nannoplankton ecology and community change across the Paleocene-Eocene Thermal Maximum. Paleobiology 39, 628–647.

Silvestro D., Michalak I., 2012. RaxmlGUI: a graphical front-end for RAxML. Organisms Diversity & Evolution 12, 335–337.

Stamatakis A., 2006. RAxML-VI-HPS: maximum likelihood-based phylogenetic analyses with thousands of taxa and mixed models. Bioinformatics 22, 2688–2690.

Stuecker M.F., Zeebe R.E., 2010. Ocean chemistry and atmospheric CO_2 sensitivity to carbon perturbations throughout the Cenozoic. Geophysical Research Letters 37, L03609.

Tamura K., Stecher G., Peterson D., Filipski A., Kumar S., 2013. MEGA6: Molecular Evolutionary Genetics Analysis Version 6.0. Molecular Biology and Evolution 30, 2725–2729.

The University-National Oceanographic Laboratory System (UNOLS). https://www.unols.org

Troschel F.H., 1854. Beitrage zur Kenntniss der Pteropoden. Archiv für Naturgeschichte 20, 196–241.

Van der Spoel S., 1967. Euthecosomata, a group with remarkable developmental stages (Gastropoda, Pteropoda). PhD thesis, University of Amsterdam. Noorduijn en Zoon, Gorinchem.
Van der Spoel S., 1982. Are pteropods really ptero-pods? (Mollusca, Gastropoda, Pteropoda). Bulletin of the Zoological Museum of the University of Amsterdam 9, 1–6.
Van der Spoel S., 1987. *Diacavolinia* nov. gen. separated from *Cavolinia* (Pteropoda, Gastropoda). Bulletin of the Zoological Museum of the University of Amsterdam 11, 77–79.
Van der Spoel S., Dadon J.R., 1999. Pteropoda. In: Boltovskoy D. (Ed.), South Atlantic Zooplankton. Backhuys Publishers, Leiden, pp. 649–706.
Vonnemann V., Schrödl M., Klussmann-Kolb A., Wägele H., 2005. Reconstruction of the phylogeny of the Opisthobranchia (Mollusca: Gastropoda) by means of 18S and 28S rRNA gene sequences. Journal of Molluscan Studies 71, 113–125.
Wenneck T.L., Falkenhaug T., Bergstad O.A., 2008. Strategies, methods, and technologies adopted on the R.V. G.O. Sars MAR-ECO expedition to the Mid-Atlantic ridge in 2004. Deep-Sea Research II 55, 6–28.
Whelan S., Goldman N., 2001. A general empirical model of protein evolution derived from multiple protein families using a maximum-likelihood approach. Molecular Biology and Evolution 18, 691–699.
World Register of Marine Species (WoRMS). http://www.marinespecies.org
Zachos J.C., Dickens G.R., Zeebe R.E., 2008. An early Cenozoic perspective on greenhouse warming and carbon- cycle dynamics. Nature 451, 279–283.
Zachos J.C., Röhl U., Schellenberg S.A., Sluijs A., Hodell D.A., et al., 2005. Rapid acidification of the ocean during the Paleocene-Eocene Thermal Maximum. Science 308, 1611–1615.
Zapata F., Wilson N.G., Howison M., Andrade S.C.S., Jörger K.M., et al., 2014. Phylogenomic analyses of deep gastropod relationships reject Orthogastropoda. Proceedings of the Royal Society B 281, 20141739.
Zeebe R.E., 2012. History of seawater carbonate chemistry, atmospheric CO_2, and ocean acidification. Annual Review of Earth and Planetary Sciences 40, 141–165.

SUPPLEMENTARY INFORMATION

Photographs of pteropod specimens used in this study are available in the Dryad Digital Repository at DOI: 10.5061/dryad.bp106. DNA sequences have been deposited at GenBank under the following accession numbers: MF048913–MF049064.

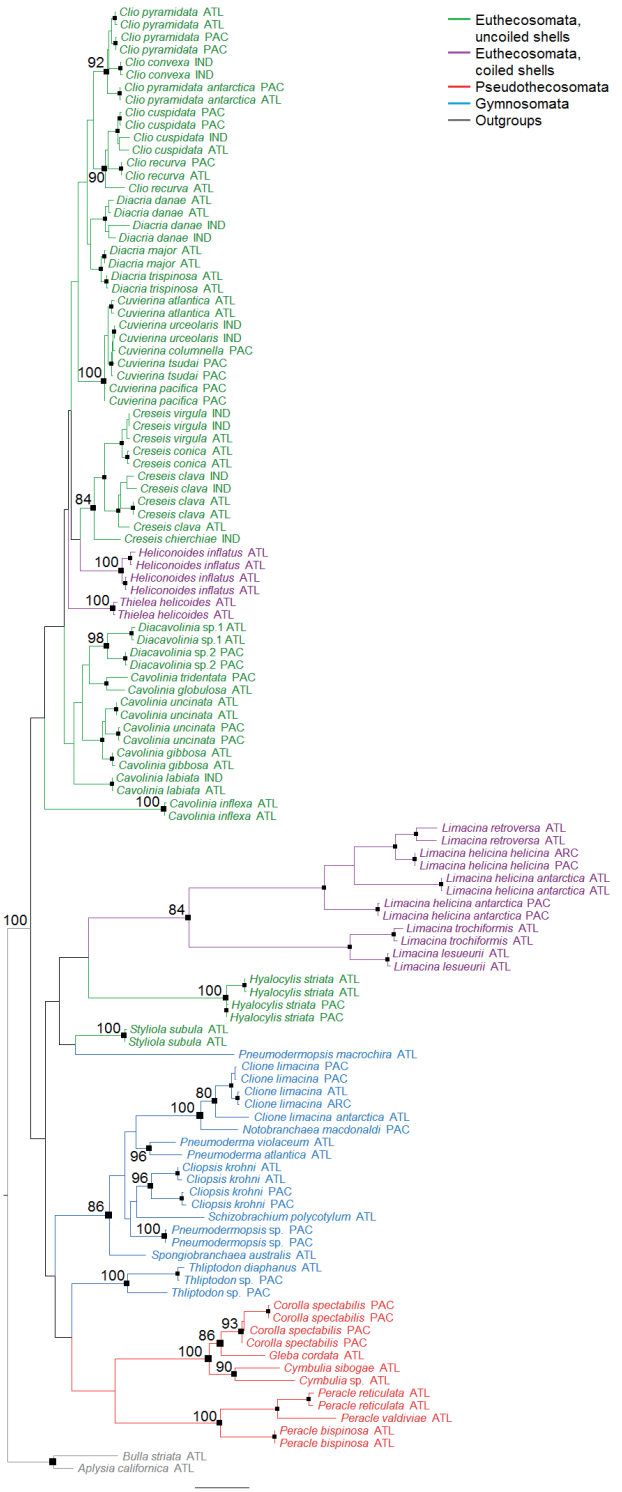

FIGURE S1. Maximum Likelihood phylogeny of pteropods based on Cytochrome Oxidase I sequences (*N* = 117 sequences of 656 basepairs). Black squares represent a bootstrap support of ≥80%, with small, medium and large black squares representing support within genera, of genera, and above genus level, respectively. Abbreviations ATL, PAC, and IND denote Atlantic, Pacific, and Indian Ocean origins, respectively, including their sectors in the Southern Ocean; ARC denotes the Arctic Sea.

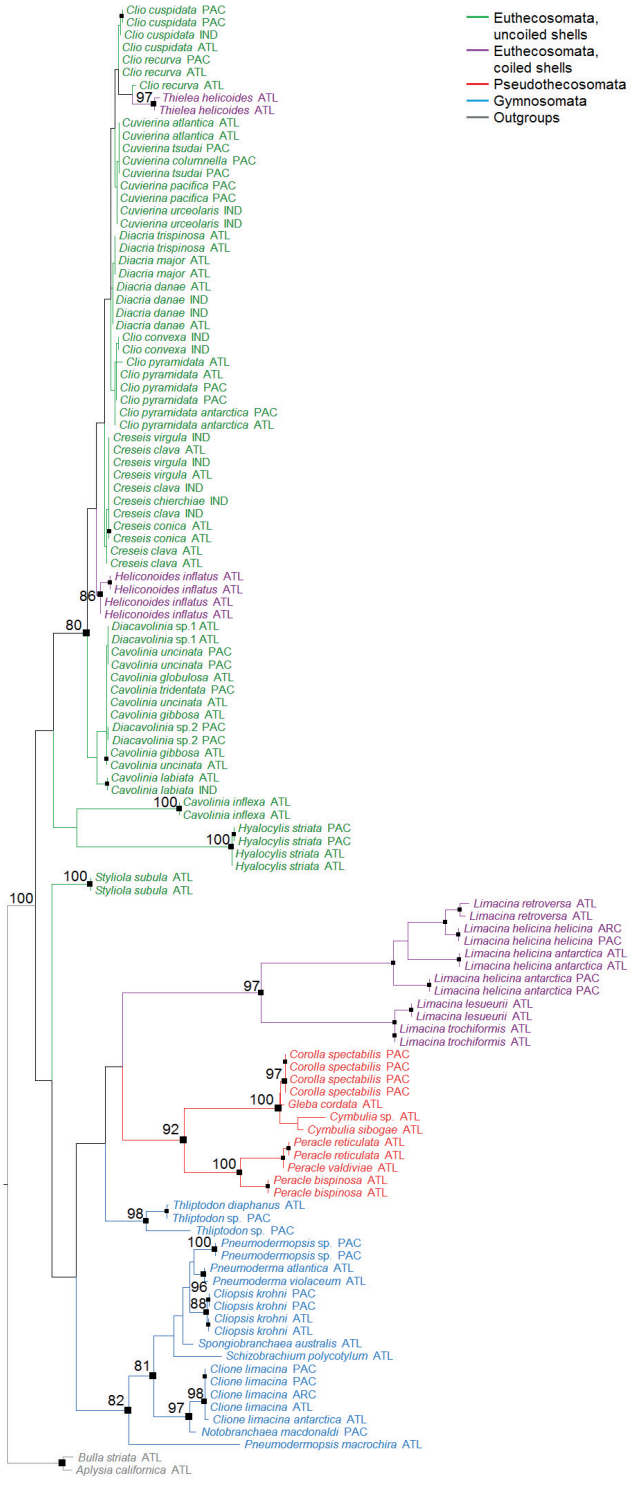

FIGURE S2. Maximum Likelihood phylogeny of pteropods based on Cytochrome Oxidase I protein sequences (*N* = 117 sequences of 218 amino acids). Black squares represent a bootstrap support of ≥80%, with small, medium and large black squares representing support within genera, of genera, and above genus level, respectively. Abbreviations ATL, PAC, and IND denote Atlantic, Pacific, and Indian Ocean origins, respectively, including their sectors in the Southern Ocean; ARC denotes the Arctic Sea.

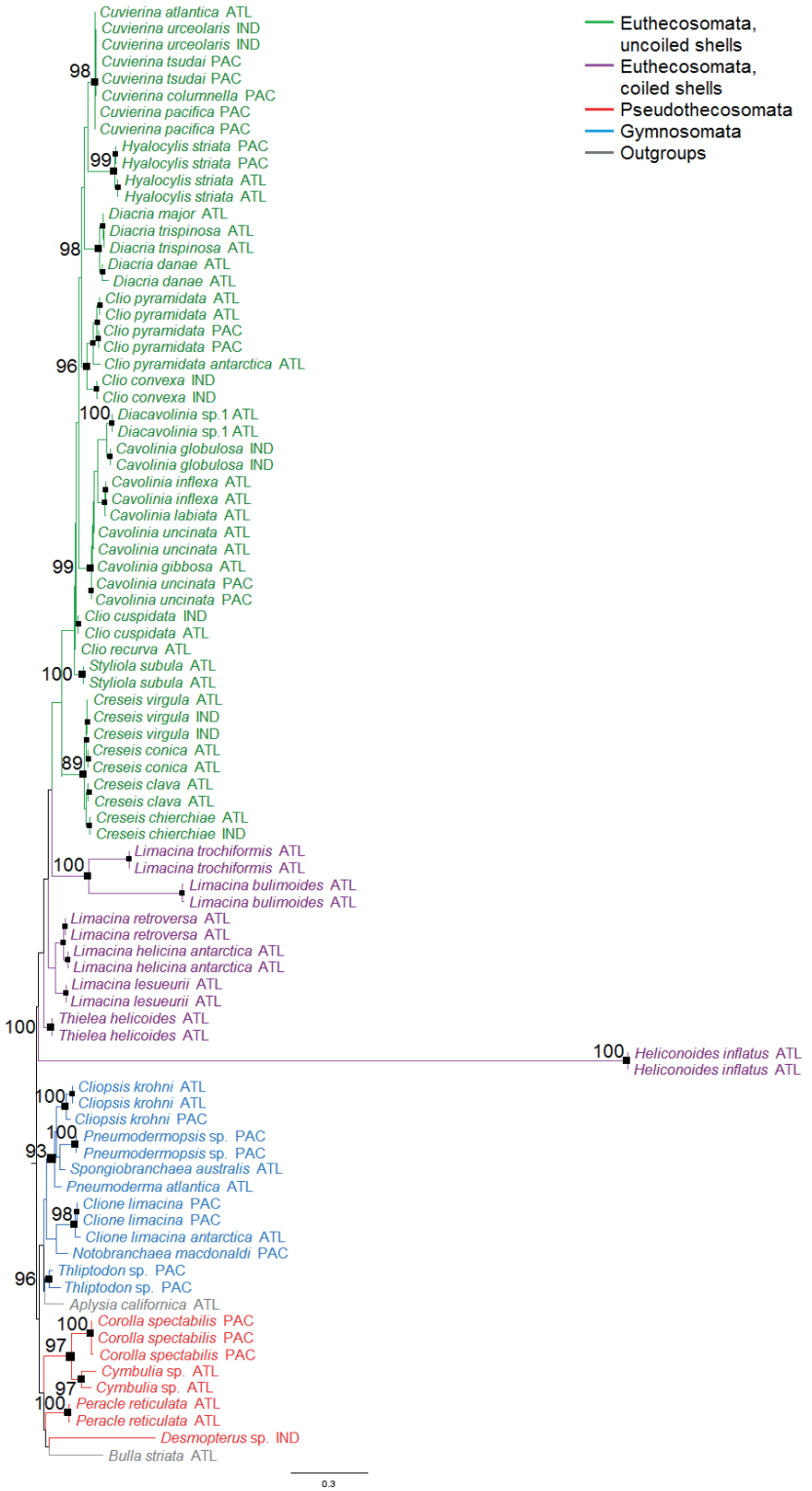

FIGURE S3. Maximum Likelihood phylogeny of pteropods based on 28S sequences (*N* = 87 sequences of 941 basepairs). Black squares represent a bootstrap support of ≥80%, with small, medium and large black squares representing support within genera, of genera, and above genus level, respectively. Abbreviations ATL, PAC, and IND denote Atlantic, Pacific, and Indian Ocean origins, respectively, including their sectors in the Southern Ocean.

FIGURE S4. Maximum Likelihood phylogeny of pteropods based on 18S sequences (*N* = 52 sequences of 1683 basepairs). Black squares represent a bootstrap support of ≥80%, with small, medium and large black squares representing support within genera, of genera, and above genus level, respectively. Abbreviations ATL, PAC, and IND denote Atlantic, Pacific, and Indian Ocean origins, respectively, including their sectors in the Southern Ocean.

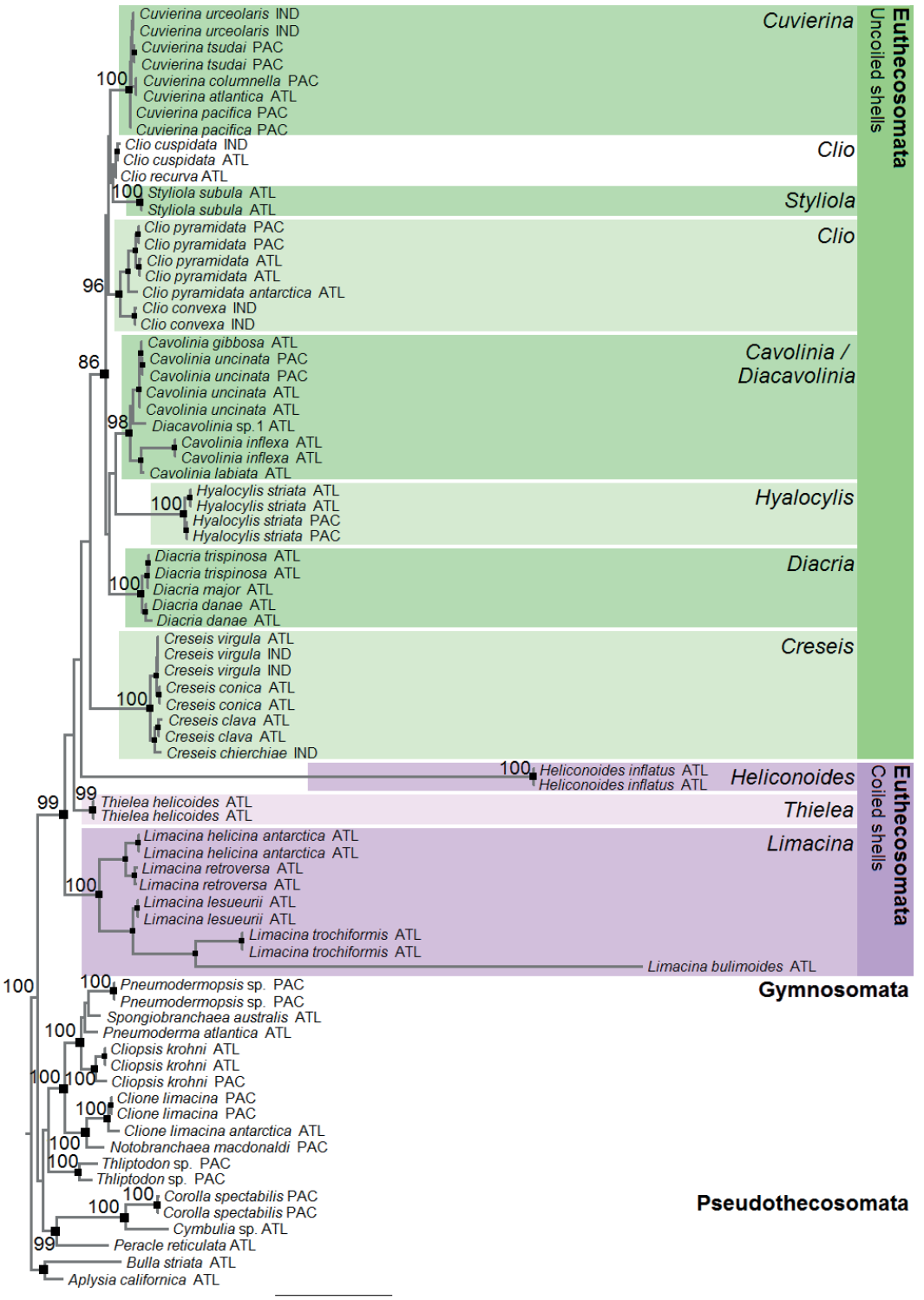

FIGURE S5. Combined Maximum Likelihood tree based on Cytochrome Oxidase I protein sequences and 28S and 18S DNA sequences including long-branch taxa (*N* = 78 sequences, max. two sequences per taxon per ocean). Black squares represent bootstrap support ≥80%, with small, medium and large black squares representing support within genera, of genera, and above genus level, respectively. Abbreviations ATL, PAC, and IND denote Atlantic, Pacific, and Indian Ocean origins, respectively, including their sectors in the Southern Ocean.

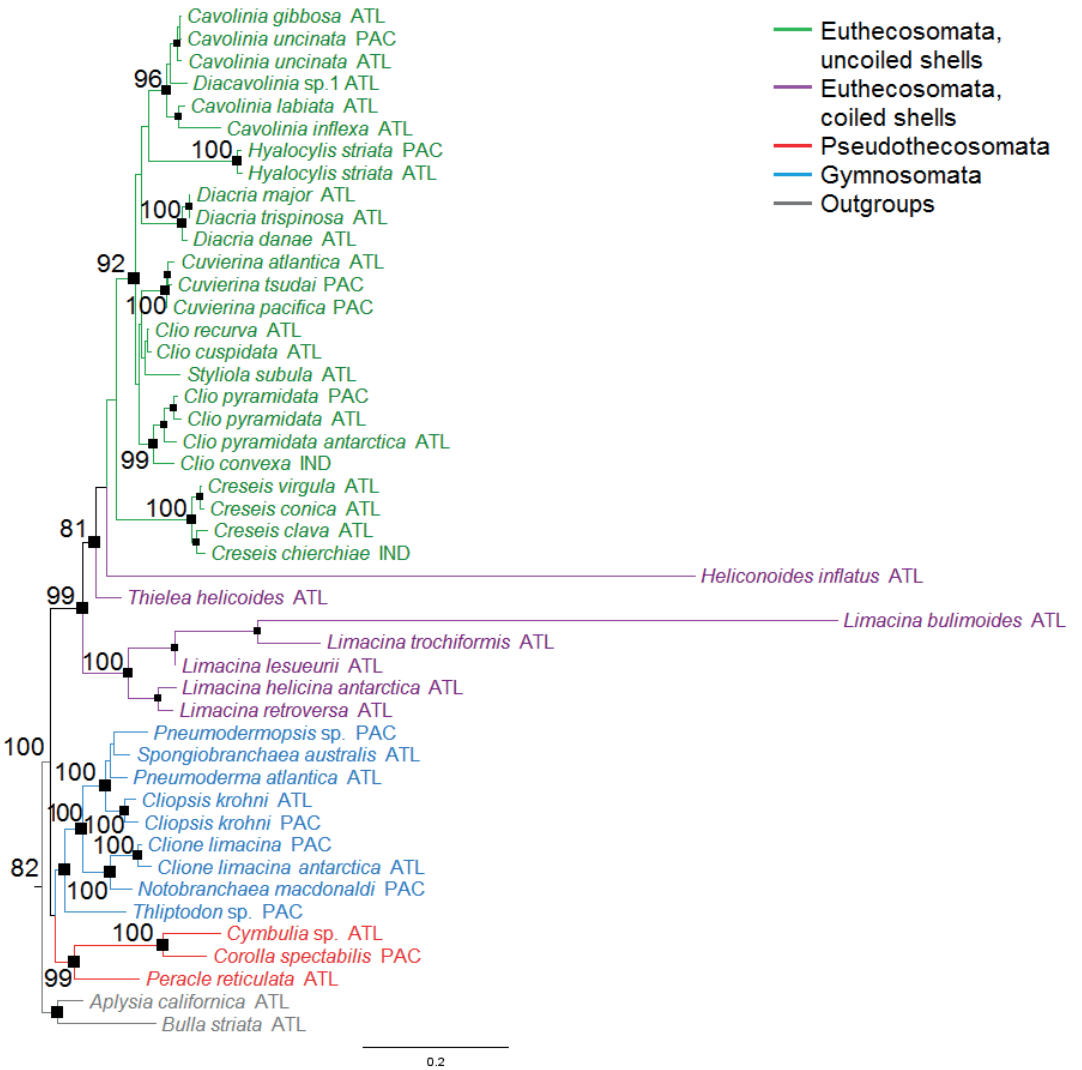

FIGURE S6. Combined Maximum Likelihood phylogeny using the same dataset as for the molecular clock analyses (*N* = 46 sequences, max. one sequence per taxon per ocean). Black squares represent bootstrap support ≥80%, with small, medium and large black squares representing support within genera, of genera, and above genus level, respectively. Abbreviations ATL, PAC, and IND denote Atlantic, Pacific, and Indian Ocean origins, respectively, including their sectors in the Southern Ocean.

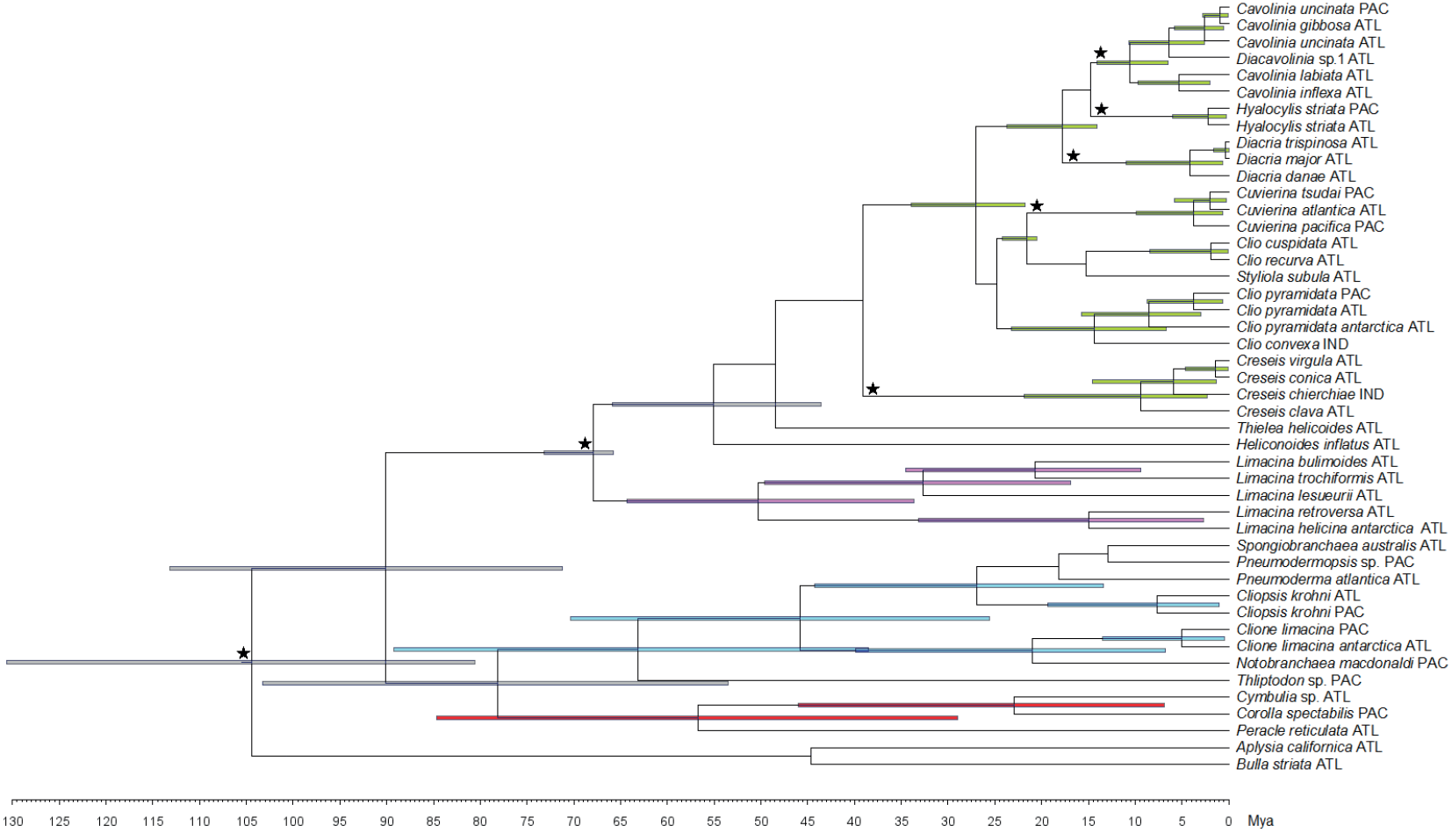

FIGURE S7. Pteropod phylogeny based on a fossil-calibrated molecular clock approach (46 sequences, max. one sequence per taxon per ocean) following Method 2 with stem calibrations based on the oldest known fossils of *Hyalocylis*, *Diacria*, *Cavolinia*, *Cuvierinia*, *Creseis*, and euthecosomes (see TABLE 1). Calibrations are indicated with stars. Error bars (95%) are shown only for clades with posterior probabilities ≥0.95 in green for uncoiled euthecosomes, purple for coiled euthecosomes, red for pseudothecosomes, and blue for gymnosomes. Abbreviations ATL, PAC, and IND denote Atlantic, Pacific, and Indian Ocean origins, respectively, including their sectors in the Southern Ocean.

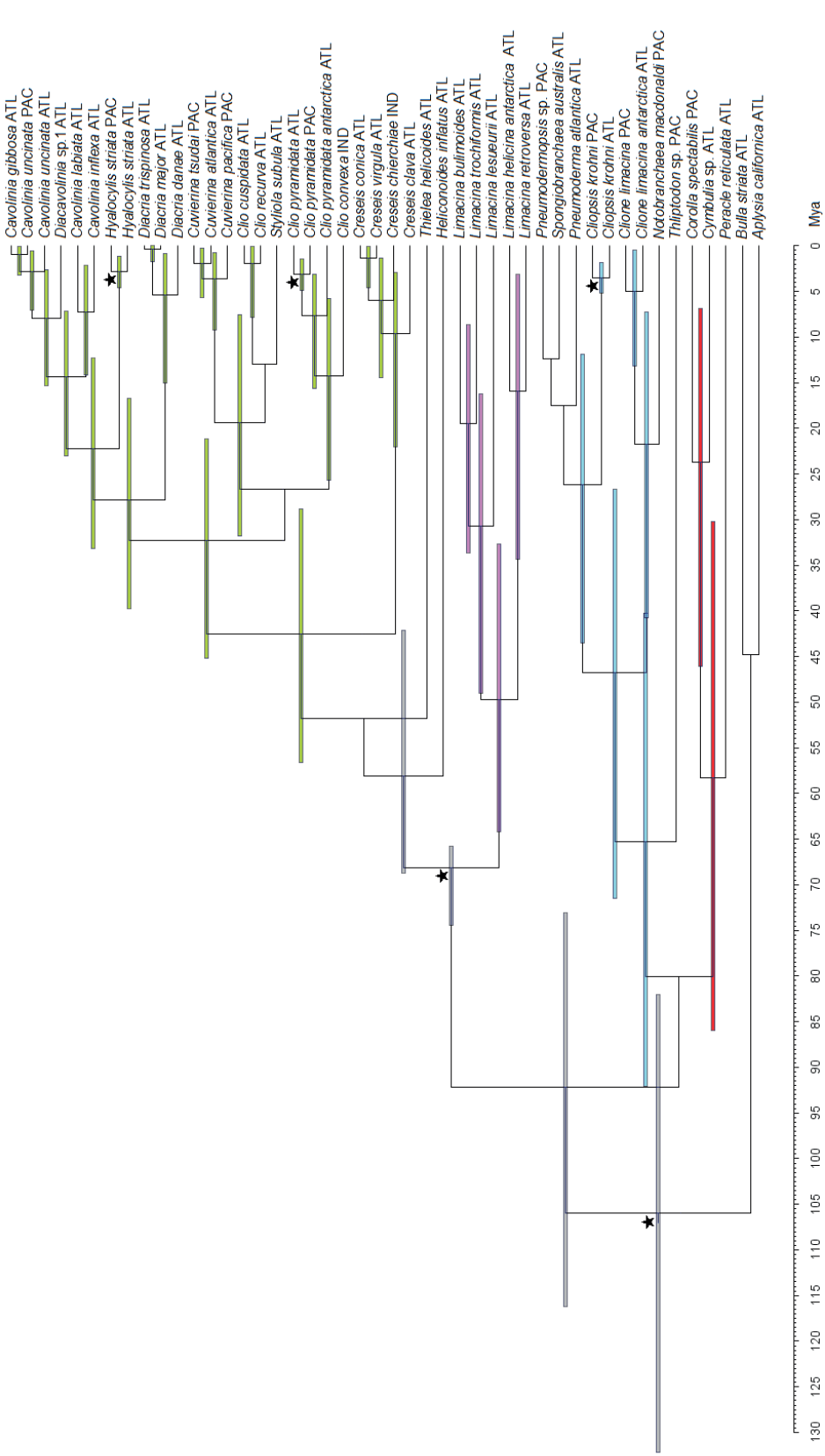

FIGURE S8. Time-calibrated molecular phylogeny of pteropods (46 sequences, max. one sequence per taxon per ocean) following Method 3 with crown calibrations of *Clio pyramidata*, *Hyalocylis striata*, and *Cliopsis krohni* based on the formation of the Isthmus of Panama (IOP) and the oldest known euthecosome fossil (see TABLE 1). Calibrations are indicated with stars. Error bars (95%) are shown only for clades with posterior probabilities ≥0.95 in green for uncoiled euthecosomes, purple for coiled euthecosomes, red for pseudothecosomes, and blue for gymnosomes. Abbreviations ATL, PAC, and IND denote Atlantic, Pacific, and Indian Ocean origins, respectively, including their sectors in the Southern Ocean.

TABLE S1. Overview of sequences used in combined and/or as single-gene phylogenetic analyses based on Cytochrome Oxidase I, 28S rRNA, and 18S rRNA. Numbers in the 9th column indicate their use in (1) single-gene Maximum Likelihood (ML), combined ML and combined Bayesian phylogenies, (2) single-gene ML and combined ML phylogenies, or (3) single-gene ML phylogenies. An asterisk indicates long-branch taxa that were excluded in separate multi-gene ML phylogenetic analyses. Bp = number of basepairs per sequence. *Clione limacina antarctica* sequences were obtained from a transcriptome (T). Picture numbers indicated with an asterisk represent juvenile specimens (available in the Dryad digital repository at DOI: 10.5061/dryad.bp106).

	Sample information				
	Reference	Collection date	Latitude	Longitude	Cruise
Taxonomy & Species					
Thecosomata, Euthecosomata					
Cavolinoidea					
Cavolinia gibbosa	Corse et al., 2013	-	-	-	ECOSUR
Cavolinia gibbosa	Jennings et al., 2010	2006-04-13	33°31'N	69°58'W	RHB0603
Cavolinia globulosa	Corse et al., 2013	-	-	-	TARA
Cavolinia globulosa	Corse et al., 2013	-	-	-	TARA
Cavolinia globulosa	Jennings et al., 2010	2006-04-25	14°00'N	55°00'W	RHB0603
Cavolinia inflexa	This study	2008-10-20	11°49'N	32°49'W	AMT18
Cavolinia inflexa	This study	2008-10-20	11°49'N	32°49'W	AMT18
Cavolinia labiata	Corse et al., 2013	-	-	-	TARA
Cavolinia labiata	Corse et al., 2013	-	-	-	TARA
Cavolinia tridentata atlantica	Jennings et al., 2010	2007-01-22	46°21'S	140°32'E	Aurora_Australis_2007.3
Cavolinia uncinata	This study	2011-01-31	18°07'N	87°44'W	GU1101
Cavolinia uncinata	This study	2012-09-04	39°55'N	67°27'W	NOAA PC201205
Cavolinia uncinata	This study	2012-02-24	24°22'N	109°13'W	MBARI GOC 2012
Cavolinia uncinata	This study	2012-02-24	24°22'N	109°13'W	MBARI GOC 2012
Clio convexa	Corse et al., 2013	-	-	-	TARA
Clio convexa	Corse et al., 2013	-	-	-	TARA
Clio cuspidata	Burridge et al., 2015	2008-10-27	12°50'S	25°00'W	AMT18
Clio cuspidata	Corse et al., 2013	-	-	-	TARA
Clio cuspidata	Jennings et al., 2010	2007-02-08	50°00'S	149°25'E	Aurora_Australis_2007.3
Clio cuspidata	Jennings et al., 2010	2007-02-08	50°00'S	149°25'E	Aurora_Australis_2007.3
Clio pyramidata antarctica	This study	2008-11-07	45°13'S	44°37'W	AMT18
Clio pyramidata antarctica	Jennings et al., 2010	2007-02-08	50°00'S	149°25'E	Aurora_Australis_2007.3
Clio pyramidata lanceolata	This study	2000-03	43°30'N	07°12'E	KP
Clio pyramidata pyramidata	Burridge et al., 2015; this study	2008-10-15	24°45'N	40°05'W	AMT18
Clio pyramidata	This study	2012-02-17	24°11'N	109°38'W	MBARI GOC 2012
Clio pyramidata	This study	2012-02-17	24°11'N	109°38'W	MBARI GOC 2012
Clio recurva	Burridge et al., 2015; this study	2004-06-09	59°58'N	25°45'W	MAR-ECO
Clio recurva	This study	2004-06-19	51°34'N	33°17'W	MAR-ECO
Clio recurva	Jennings et al., 2010	2007-01-20	45°00'S	142°59'E	Aurora_Australis_2007.3
Creseis chierchiae	Corse et al., 2013	-	-	-	CRER 2
Creseis chierchiae	Corse et al., 2013	-	-	-	TARA
Creseis clava	This study	2011-01-25	18°43'N	87°40'W	GU1101
Creseis clava	Gasca and Janssen, 2014	2007-01-21	18°47'N	87°08'W	GU0701
Creseis clava	Corse et al., 2013	-	-	-	TARA

Station	Ocean/sea/region	Used for	Genetics CO1	28S	18S	Pictures *N*
-	Caribbean Sea	1	KC774033	KC774104		
-	North Atlantic Ocean	3	FJ876856			
41	Gulf of Aden	3		KC774101		
42	Indian Ocean (Maldives)	3		KC774141		
-	North Atlantic Ocean	3	FJ876857			
44	North Atlantic Ocean	2	MF048913	MF048966		2
44	North Atlantic Ocean	1	MF048914	MF048967		2
52	Indian Ocean (East of Madagascar)	3	KC774038			
66	South Atlantic Ocean (Cape Town)	1	KC774037	KC774099		
-	Southern Ocean (South of Australia)	3	FJ876861			
91	Caribbean Sea	1	MF048915	MF048968	MF049019	9
ST23P4	Northwest Atlantic Ocean	2	MF048916	MF048969	MF049020	1
D342BW	Gulf of California	1	MF048917	MF048970	MF049021	1
D342BW	Gulf of California	2	MF048918	MF048971	MF049022	
42	Indian Ocean (Maldives)	1	KC774063	KC774105		
53	Indian Ocean (East of Madagascar)	2	KC774069	KC774093		
66	South Atlantic Ocean	1	KP292789	KP292650		2
42	Indian Ocean (Maldives)	2	KC774064	KC774098		
-	Southern Ocean (South of Australia)	3	FJ876869			
-	Southern Ocean (South of Australia)	3	FJ876870			
101	South Atlantic / Southern Ocean	1	MF048919	MF048972	MF049023	1
-	Southern Ocean (South of Australia)	3	FJ876876			
-	Mediterranean Sea (Ligurian Sea: Villefranche-Sur-Mer)	2	MF048920	MF048973	MF049024	
27	North Atlantic Ocean	1	KP292791	KP292652	MF049025	2
D333T	Gulf of California	1	MF048921	MF048974	MF049026	
D333T	Gulf of California	2	MF048922	MF048975	MF049027	
2	North Atlantic Ocean	1	KP292790	KP292651	MF049028	
16	North Atlantic Ocean	3	MF048923			1
-	Southern Ocean (South of Australia)	3	FJ876880			
-	Caribbean Sea (Yucatan/Belize)	3		KC774136		
41	Gulf of Aden	1	KC774044	KC774137		
53	Caribbean Sea	1			MF049029	5
35	Caribbean Sea	3	HM385035			1
41	Gulf of Aden	3	KC774052			

TABLE S1. Continued

Taxonomy & Species	Sample information Reference	Collection date	Latitude	Longitude	Cruise
Creseis clava	Corse et al., 2013	-	-	-	CRER 2
Creseis clava	Corse et al., 2013	-	-	-	ANTEDON
Creseis clava	Jennings et al., 2010	2006-11-17	16°01'S	119°19'E	Galathea_2006
Creseis conica	This study	2011-01-31	18°07'N	87°44'W	GU1101
Creseis conica	This study	2011-01-31	18°07'N	87°44'W	GU1101
Creseis conica	This study	2011-01-31	18°07'N	87°44'W	GU1101
Creseis virgula	Corse et al., 2013	-	-	-	ECOSUR
Creseis virgula	Corse et al., 2013	-	-	-	TARA
Creseis virgula	Corse et al., 2013	-	-	-	TARA
Cuvierina atlantica	Burridge et al., 2015; this study	2004-07-01	41°29'N	28°19'W	MAR-ECO
Cuvierina atlantica	Burridge et al., 2015	2004-07-01	41°29'N	28°19'W	MAR-ECO
Cuvierina columnella	Burridge et al., 2015	2001-12-24	36°05'S	149°29'W	DRFT07RR
Cuvierina tsudai	Burridge et al., 2015; this study	2010-09-29	27°08'N	125°33'E	R/V Tansei-Maru KT-10-20
Cuvierina tsudai	Burridge et al., 2015; this study	2010-09-29	27°08'N	125°33'E	R/V Tansei-Maru KT-10-20
Cuvierina tsudai	Burridge et al., 2015	2010-09-29	27°08'N	125°33'E	R/V Tansei-Maru KT-10-20
Cuvierina pacifica	Burridge et al., 2015	2012-01-18	23°00'S	100°00'W	KH-11-10
Cuvierina pacifica	Burridge et al., 2015	2001-10-14	29°05'S	176°09'W	COOK14MV
Cuvierina urceolaris	Burridge et al., 2015	2003-06-06	12°52'S	94°26'E	VANC10MV
Cuvierina urceolaris	Corse et al., 2013	-	-	-	TARA
Diacavolinia longirostris (sp. 1)	Corse et al., 2013	-	-	-	ECOSUR
Diacavolinia sp. 1	This study	2008-10-22	5°20'N	28°31'W	AMT18
Diacavolinia sp. 1	This study	2008-10-23	2°47'N	26°51'W	AMT18
Diacavolinia van-utrechti (sp. 2)	Maas et al., 2013	2007-10&11	13°01'N	105°01'W	RV Seward
Diacavolinia van-utrechti (sp. 2)	Maas et al., 2013	2007-10&11	13°01'N	105°01'W	RV Seward
Diacria danae	This study	2008-10-30	22°47'S	25°01'W	AMT18
Diacria danae	Corse et al., 2013	-	-	-	CRER 2
Diacria danae	Corse et al., 2013	-	-	-	TARA
Diacria danae	Corse et al., 2013	-	-	-	TARA
Diacria danae	Klussmann-Kolb and Dinapoli, 2006	-	-	-	-
Diacria major	This study	2008-10-14	27°38'N	37°02'W	AMT18
Diacria major	This study	2008-10-16	22°36'N	40°16'W	AMT18
Diacria trispinosa	This study	2011-01-28	16°22'N	88°02'W	GU1101
Diacria trispinosa	This study	2011-01-28	16°22'N	88°02'W	GU1101
Hyalocylis striata	This study	2008-10-11	36°01'N	27°44'W	AMT18
Hyalocylis striata	This study	2011-01-16	20°44'N	86°24'W	GU1101
Hyalocylis striata	This study	2011-01-16	20°44'N	86°24'W	GU1101
Hyalocylis striata	This study	2011-01-16	20°44'N	86°24'W	GU1101
Hyalocylis striata	This study	2012-02-17	24°11'N	109°38'W	MBARI GOC 2012
Hyalocylis striata	This study	2012-02-17	24°11'N	109°38'W	MBARI GOC 2012
Styliola subula	This study	2008-10-28	16°38'S	25°00'W	AMT18
Styliola subula	This study	2011-01-19	19°21'N	87°22'W	GU1101
Styliola subula	Gasca and Janssen, 2014	2007-01-24	17°54'N	87°54'W	-
Styliola subula	Gasca and Janssen, 2014	2007-01-29	18°11'N	87°45'W	-

Station	Ocean/sea/region	Used for	Genetics CO1	28S	18S	Pictures *N*
-	Caribbean Sea (Yucatan/Belize)	1	KC774053	KC774125		
-	Mediterranean Sea (Gulf of Lyon, Cassidaigne)	2	KC774054	KC774126		
-	Indian Ocean	3	FJ876888			
91	Caribbean Sea	1		MF048976	MF049030	2
91	Caribbean Sea	1	MF048924	MF048977		2
91	Caribbean Sea	2	MF048925		MF049031	2
-	Caribbean Sea (Yucatan/Belize)	1	KC774045	KC774128		
34	Red Sea	2	KC774046	KC774129		
42	Indian Ocean (Maldives)	2	KC774047	KC774130		
36	North Atlantic Ocean	1	KP292669		MF049032	2
36	North Atlantic Ocean	1	KP292675	KP292622		2
11	South Pacific Ocean	2	KP292728	KP292634		2
5	Northwest Pacific Ocean (East China Sea)	2		KP292642	MF049033	2
5	Northwest Pacific Ocean (East China Sea) Ocean (East China	1	KP292767	MF048978	MF049034	2
5	Northwest Pacific Ocean (East China Sea)	2	KP292768			2
21	South Pacific Ocean	1	KP292780	KP292647		2
19	South Pacific Ocean	2	KP292785	KP292648		2
22	Indian Ocean	2	KP292729	KP292635		2
52	Indian Ocean (East of Madagascar)	2	KC774071	KC774107		
-	Caribbean Sea (Yucatan/Belize)	3		KC774118		
50	North Atlantic Ocean	1	MF048926	MF048979	MF049035	
56	North Atlantic Ocean	3	MF048927			
-	East Pacific Ocean	3	JX183614			3
-	East Pacific Ocean	3	JX183616			3
79	South Atlantic Ocean	1	MF048928	MF048980	MF049036	1*
-	Caribbean Sea (Yucatan/Belize)	3	KC774075	KC774113		
50	Indian Ocean (North)	3	KC774076			
58	Indian Ocean (Southwest, Mozambique)	3	KC774077			
-	North Atlantic Ocean (Canary Islands)	2	DQ238001	DQ237987	DQ237968	
24	North Atlantic Ocean	1	MF048929	MF048981	MF049037	1*
32	North Atlantic Ocean	3	MF048930			1*
77	Caribbean Sea	1	MF048931	MF048982	MF049038	4
77	Caribbean Sea	2	MF048932	MF048983	MF049039	4
15	North Atlantic Ocean	2		MF048984		2
10	Caribbean Sea	1	MF048933			2
10	Caribbean Sea	1		MF048985	MF049040	2
10	Caribbean Sea	2	MF048934		MF049041	2
D333T	Gulf of California	2	MF048935	MF048986	MF049042	1
D333T	Gulf of California	1	MF048936	MF048987	MF049043	
70	South Atlantic Ocean	2		MF048988	MF049044	1
29	Caribbean Sea	1		MF048989	MF049045	3
-	Caribbean Sea	1	KF200174			1
-	Caribbean Sea	2	KF200175			1

TABLE S1. Continued

Taxonomy & Species	Sample information Reference	Collection date	Latitude	Longitude	Cruise
Limaciniidae					
Heliconoides inflatus	This study	2008-10-21	8°39'N	30°43'W	AMT18
Heliconoides inflatus	This study	2008-10-26	08°50'S	25°00'W	AMT18
Heliconoides inflatus	This study	2008-10-26	08°50'S	25°00'W	AMT18
Heliconoides inflatus	This study	2008-11-04	36°10'S	35°03'W	AMT18
Heliconoides inflatus	This study	2008-11-04	36°10'S	35°03'W	AMT18
Heliconoides inflatus	This study	2008-11-04	36°10'S	35°03'W	AMT18
Heliconoides inflatus	This study	2010-03-25	42°37'N	18°06'E	KP
Limacina bulimoides	This study	2008-10-20	11°49'N	32°49'W	AMT18
Limacina bulimoides	This study	2008-10-31	26°33'S	25°00'W	AMT18
Limacina helicina antarctica	This study	2008-11-07	45°13'S	44°37'W	AMT18
Limacina helicina antarctica	This study	2008-11-07	45°13'S	44°37'W	AMT18
Limacina helicina antarctica	Hunt et al., 2010	-	-	-	-
Limacina helicina antarctica	Hunt et al., 2010	-	-	-	-
Limacina helicina helicina	Jennings et al., 2010	2003-12-03	60°32'N	147°48'W	Alpha-Helix-2003
Limacina helicina helicina	Jennings et al., 2010	2007-09-04	87°01'N	146°21'W	PS-ARK-23-2
Limacina lesueurii	This study	2008-10-20	11°49'N	32°49'W	AMT18
Limacina lesueurii	This study	2008-10-20	11°49'N	32°49'W	AMT18
Limacina lesueurii	This study	2012-11-09	25°29'S	25°00'W	AMT22
Limacina lesueurii	This study	2012-11-09	25°29'S	25°00'W	AMT22
Limacina retroversa	This study	2004-06-12	56°35'N	31°14'W	MAR-ECO
Limacina retroversa	This study	2004-06-23	50°42'N	27°31'W	MAR-ECO
Limacina trochiformis	This study	2012-10-21	27°36'N	36°22'W	AMT22
Limacina trochiformis	This study	2012-11-12	30°10'S	27°54'W	AMT22
Limacina trochiformis	This study	2011-01-22	18°52'N	87°17'W	GU1101
Limacina trochiformis	This study	2011-01-22	18°52'N	87°17'W	GU1101
Thielea helicoides	This study	2004-06-21	52°45'N	30°30'W	MAR-ECO
Thielea helicoides	This study	2004-06-23	50°42'N	27°31'W	MAR-ECO
Thecosomata, Pseudothecosomata					
Cymbuliidae					
Corolla spectabilis	This study	2012-11-12	34°15'N	120°09'W	UNOLS CSTC 2012
Corolla spectabilis	This study	2012-11-12	34°15'N	120°09'W	UNOLS CSTC 2012
Corolla spectabilis	This study	2012-02-24	24°22'N	109°13'W	MBARI GOC 2012
Corolla spectabilis	This study	2012-02-24	24°22'N	109°13'W	MBARI GOC 2012
Cymbulia sibogae	Jennings et al., 2010	2007-11-11	3°13'N	14°04'W	PS-ANT-24-1
Cymbulia sp.	Corse et al., 2013	-	-	-	ECOSUR
Cymbulia sp.	Corse et al., 2013	-	-	-	TARA
Gleba cordata	Jennings et al., 2010	2006-04-19	25°00'N	59°57'W	RHB0603
Desmopteridae					
Desmopterus sp.	Corse et al., 2013	-	-	-	TARA

Station	Ocean/sea/region	Used for	Genetics CO1	28S	18S	Pictures *N*
47	North Atlantic Ocean	1*	MF048937		MF049046	1
63	South Atlantic Ocean	3	MF048938			1
63	South Atlantic Ocean	2*		MF048990		
94	South Atlantic Ocean	2*			MF049047	
94	South Atlantic Ocean	2*	MF048939			1
94	South Atlantic Ocean	3	MF048940			1
4	Mediterranean Sea (Adriatic Sea: Dubrovnik)	1*		MF048991		
44	North Atlantic Ocean	3		MF048992		1
83	South Atlantic Ocean	1*		MF048993	MF049048	
101	South Atlantic / Southern Ocean	1	MF048941	MF048994	MF049049	2
101	South Atlantic / Southern Ocean	2	MF048942	MF048995		2
-	Southern Ocean (Amundsen Sea)	3	GQ861824			
-	Southern Ocean (Amundsen Sea)	3	GQ861825			
-	Gulf of Alaska (Prince Williams Sound)	3	FJ876923			
-	Arctic Ocean	3	FJ876924			
44	North Atlantic Ocean	2		MF048996		2
44	North Atlantic Ocean	1		MF048997	MF049050	2
56A	South Atlantic Ocean	2	MF048943			
56A	South Atlantic Ocean	1	MF048944			
6	North Atlantic Ocean	1	MF048945	MF048998	MF049051	
22	North Atlantic Ocean	2	MF048946	MF048999	MF049052	
19	North Atlantic Ocean	1	MF048947			
60	South Atlantic Ocean	2	MF048948			
34	Caribbean Sea	1		MF049000		2
34	Caribbean Sea	2		MF049001		2
20	North Atlantic Ocean	1	MF048949	MF049002		2
22	North Atlantic Ocean	2	MF048950	MF049003		
SB2SB3 MOC	Northeast Pacific Ocean (Southern California)	3	MF048951	MF049004		
SB2SB3 MOC	Northeast Pacific Ocean (Southern California)	2	MF048952	MF049005	MF049053	
D342BW	Gulf of California	3	MF048953			1
D342BW	Gulf of California	1	MF048954	MF049006	MF049054	
-	North Atlantic Ocean	3	FJ876932			
-	Caribbean Sea (Yucatan/Belize)	3		KC774158		
30	Mediterranean Sea (East)	1	KC774090	KC774159		
-	North Atlantic Ocean	3	FJ876933			
40	Gulf of Aden	3		KC774167		

TABLE S1. Continued

Taxonomy & Species	Sample information Reference	Collection date	Latitude	Longitude	Cruise
Peraclidae					
Peracle bispinosa	Jennings et al., 2010	2007-11-11	3°31'N	14°01'W	PS-ANT-24-1
Peracle bispinosa	Jennings et al., 2010	2007-11-11	3°31'N	14°01'W	PS-ANT-24-1
Peracle reticulata	This study	2008-10-12	33°18'N	30°48'W	AMT18
Peracle reticulata	This study	2008-10-29	19°07'S	25°00'W	AMT18
Peracle reticulata	Corse et al., 2013	-	-	-	CRER 2
Peracle reticulata	Corse et al., 2013	-	-	-	ANTEDON
Peracle valdiviae	Jennings et al., 2010	2007-11-17	13°25'S	0°39'W	PS-ANT-24-1
Gymnosomata					
Clionidae					
Clione limacina antarctica	Zapata et al., 2014	2009-02-20	61°46'S	45°27'W	Nerida Wilson
Clione limacina	This study	2012-07-17	36°42'N	122°03'N	MBARI MW 2012
Clione limacina	This study	2012-07-17	36°42'N	122°03'N	MBARI MW 2012
Clione limacina	Jennings et al., 2010	2006-04-13	33°31'N	69°58'W	RHB0603
Clione limacina	Jennings et al., 2010	2005-07-11	74°35'N	151°56'W	Healy 05/2
Thliptodon sp.	This study	2012-02-24	24°22'N	109°13'W	MBARI GOC 2012
Thliptodon sp.	This study	2013-06-09	36°35'N	122°31'W	MBARI MW 2013
Thliptodon diaphanus	Jennings et al., 2010	2006-04-20	24°50'N	60°27'W	RHB0603
Cliopsidae					
Cliopsis krohni	This study	2013-06-09	36°34'N	122°31'W	MBARI MW 2013
Cliopsis krohni	This study	2013-06-09	36°34'N	122°31'W	MBARI MW 2013
Cliopsis krohni	This study	2013-08-30	39°56'N	67°17'W	NOAA PC201205
Cliopsis krohni	This study	2012-09-04	39°57'N	67°27'W	NOAA PC201205
Notobranchaeidae					
Notobranchaea macdonaldi	This study	2013-03-22	36°41'N	122°10'W	MBARI MW 2013
Pneumodermatidae					
Pneumoderma atlantica	Klussmann-Kolb and Dinapoli, 2006	-	-	-	-
Pneumoderma violaceum	Jennings et al., 2010	2007-11-08	11°23'N	20°21'W	PS-ANT-24-1
Pneumodermopsis macrochira	Jennings et al., 2010	2006-04-16	29°52'N	70°05'W	RHB0603
Pneumodermopsis sp.	This study	2012-02-12	23°42'N	108°49'W	MBARI GOC 2012
Pneumodermopsis sp.	This study	2012-02-12	23°42'N	108°49'W	MBARI GOC 2012
Schizobrachium polycotylum	Jennings et al., 2010	2007-11-11	3°31'N	14°01'W	PS-ANT-24-1
Spongiobranchaea australis	Klussmann-Kolb and Dinapoli, 2006	-	-	-	-
Outgroup taxa					
Cephalaspidea, Bulloidea, Bullidae					
Bulla striata	Klussmann-Kolb and Dinapoli, 2006	-	-	-	-
Anaspidea, Aplysioidea, Aplysiidae					
Aplysia californica	Klussmann-Kolb and Dinapoli, 2006	-	-	-	-

Station	Ocean/sea/region	Used for	Genetics CO1	28S	18S	Pictures *N*
-	North Atlantic Ocean	3	FJ876936			
-	North Atlantic Ocean	3	FJ876938			
19	North Atlantic Ocean	3		MF049007		1
75	South Atlantic Ocean	1		MF049008	MF049055	2
-	Caribbean Sea (Yucatan/Belize)	1	KC774088			
-	Mediterranean Sea (Gulf of Lyon, Cassidaigne)	3	KC774089			
-	South Atlantic Ocean	3	FJ876940			
-	Southern Ocean (South Orkney Islands)	1	CEF048	CEF048	CEF048	
D416T.11	Northeast Pacific Ocean (Northern California)	1	MF048955	MF049009	MF049056	1
D416T.15	Northeast Pacific Ocean (Northern California)	2	MF048956	MF049010	MF049057	
-	North Atlantic Ocean	3	FJ876941			
-	Arctic Ocean (Canadian Basin)	3	FJ876944			
D342BW	Gulf of California	1	MF048957	MF049011	MF049058	1
D484D3	Northeast Pacific Ocean (Northern California)	2	MF048958	MF049012	MF049059	1
-	North Atlantic Ocean	3	FJ876950			
D484T	Northeast Pacific Ocean (Northern California)	1	MF048959	MF049013	MF049060	1
D484T	Northeast Pacific Ocean (Northern California)	3	MF048960			1
NWAT1	Northwest Atlantic Ocean	1	MF048961	MF049014	MF049061	1
NWAT20	Northwest Atlantic Ocean	2	MF048962	MF049015	MF049062	1
D448T	Northeast Pacific Ocean (Northern California)	1	MF048963	MF049016		1
-	North Atlantic / Indian / Pacific Ocean (USA/Australia)	1	DQ238003	DQ237989	DQ237970	
-	North Atlantic Ocean	3	FJ876945			
-	North Atlantic Ocean	3	FJ876946			
D339T	Gulf of California	1	MF048964	MF049017	MF049063	1
D339T	Gulf of California	2	MF048965	MF049018	MF049064	
-	North Atlantic Ocean	3	FJ876949			
-	Southern Ocean (Scotia Arc)	1	DQ238002	DQ237988	DQ237969	
-	North Atlantic Ocean (Bermuda)	1	DQ238005	AY427477	AY427512	
-	Atlantic Ocean	1	AF077759	AY026366	AY039804	

3

Global biogeography and evolution of *Cuvierina* pteropods

Alice K. Burridge, Erica Goetze, Niels Raes,
Jef Huisman & Katja T.C.A. Peijnenburg

Abstract

Shelled pteropods are planktonic gastropods that are potentially good indicators of the effects of ocean acidification. They also have high potential for the study of zooplankton evolution because they are metazoan plankton with a good fossil record. We investigated phenotypic and genetic variation in pteropods belonging to the genus *Cuvierina* in relation to their biogeographic distribution across the world's oceans. We aimed to assess species boundaries and to reconstruct their evolutionary history. We distinguished six morphotypes based on geometric morphometric analyses of shells from 926 museum and 113 fresh specimens. These morphotypes have distinct geographic distributions across the Atlantic, Pacific and Indian oceans, and belong to three major genetic clades based on COI and 28S DNA sequence data. Using a fossil-calibrated phylogeny, we estimated that these clades separated in the Late Oligocene and Early to Middle Miocene. We found evidence for ecological differentiation among all morphotypes based on ecological niche modelling with sea surface temperature, salinity and phytoplankton biomass as primary determinants. Across all analyses, we found highly congruent patterns of differentiation suggesting species level divergences between morphotypes. However, we also found distinct morphotypes (e.g., in the Atlantic Ocean) that were ecologically, but not genetically differentiated. Given the distinct ecological and phenotypic specializations found among both described and undescribed *Cuvierina* taxa, they may not respond equally to future ocean changes and may not be equally sensitive to ocean acidification. Our findings support the view that ecological differentiation may be an important driving force in the speciation of zooplankton.

Keywords:

Zooplankton, Integrative taxonomy, Geometric morphometrics, Molecular clock, Ecological niche modelling

This chapter was published as:

Burridge A.K., Goetze E., Raes N., Huisman J., Peijnenburg K.T.C.A., 2015. Global biogeography and evolution of *Cuvierina* pteropods. BMC Evolutionary Biology 15, 39.

Background

Shelled pteropods (Mollusca, Gastropoda: Thecosomata) are potentially good bioindicators of the effects of ocean acidification, but their application as such is hampered by limited knowledge of their taxonomy, genetic diversity, ecology and distribution patterns. Pteropods are a group of heterobranch gastropods (Jörger et al., 2010) that are a common component of the marine zooplankton. They affect the ocean carbon cycle by producing aragonite shells that can accelerate the export of organic matter from the surface into the deep ocean. Because of their delicate aragonite shells, pteropods have been identified as exceptionally vulnerable to rising CO_2 (e.g., Feely et al., 2004; Orr et al., 2005; Fabry et al., 2008), and hence are widely used to explore the effects of ocean acidification (e.g., Roger et al., 2011; Bednaršek et al., 2012a, 2014; Comeau et al., 2012). Shelled pteropods also may be a particularly informative model system for the study of long-term marine evolutionary processes, because they are metazoan plankton with an abundant fossil record (e.g., Lalli and Gilmer, 1989; Janssen and Peijnenburg, 2014).

Recent studies suggest that marine plankton have higher evolutionary potential than originally thought and may be well poised for evolutionary responses to global change (e.g., Lohbeck et al., 2012; Jin et al., 2013; Peijnenburg and Goetze, 2013). A recent review of population genetic studies of oceanic zooplankton showed that genetic isolation can be achieved at the scale of gyre systems, and appears to be linked to the particular ecological requirements of the organisms (Sa'ez et al., 2003). Molecular phylogenetic studies on calcifying plankton have suggested greater specificity in oceanographic habitat preferences than previously supposed, e.g., in coccolithophores (e.g., De Vargas et al., 2004; Aurahs et al., 2011) and foraminifers (e.g., Darling and Wade, 2008; Aurahs et al., 2011; Seears et al., 2012; Ujiié et al., 2012; Weiner et al., 2012). The evolutionary potential of calcifying plankton is further supported by long-term selection experiments, which have demonstrated rapid functional genetic divergence in response to elevated CO_2 concentrations (Lohbeck et al., 2012; Jin et al., 2013). Hence, calcifying plankton may be capable of rapid evolutionary as well as ecological responses to changing ocean conditions, including future changes driven by global warming and ocean acidification.

The taxonomy of shelled pteropods has generally been based on shell morphology, although some studies have also examined soft parts (e.g., Van der Spoel, 1967; Van der Spoel et al., 1993). Several pteropod taxa have been identified using the traditional approach of univariate measurements of shell dimensions (e.g., Van der Spoel, 1970, 1974; Van der Spoel et al., 1993; Janssen, 2005). Yet, the complex and highly diverse shell morphologies of pteropods also enable detailed geometric morphometric analyses. Several studies have shown that geometric morphometrics can be more powerful in distinguishing taxa than univariate measurements (e.g., Aiello et al., 2007; Mitteroecker and Gunz, 2009; Klingenberg, 2010). Molecular phylogenetic studies suggested that taxonomic revisions will be required (Klussmann-Kolb and Dinapoli, 2006; Jennings et al., 2010; Corse et al., 2013). These studies showed a well-supported separation of species and genera, but relation-

ships among genera are poorly resolved. The first genus-level study of pteropods focused on DNA barcoding of *Diacavolinia*, and emphasized the inadequacy of current systematic understanding of this genus (Maas et al., 2013). The taxonomy of *Creseis*, *Hyalocylis* and *Styliola* was reviewed by Gasca and Janssen (2014).

This study focuses on the genus *Cuvierina*, an excellent model group for an integrative study of zooplankton because it has a worldwide distribution, it is abundantly present in museum collections, and has a well-described fossil record (Janssen, 2005). Moreover, the bottle-shaped adult shells (6-11 mm long) do not change during adult life, and can be easily distinguished from juvenile shells that are shed once the animal is mature (Bé et al., 1972; Lalli and Gilmer, 1989). Extant *Cuvierina* pteropods occur from 45°N to 40°S, in ocean regions with surface water temperatures above ~17°C (Van der Spoel, 1967). Recent taxa are absent from the Mediterranean and Red Seas (Bé and Gilmer, 1977; Janssen, 2005). *Cuvierina* taxa have a diel vertical migration pattern and prefer epipelagic depths, with highest abundance between 100 and 250 m (Bé and Gilmer, 1977). *Cuvierina* taxa are hermaphrodites and internal fertilizers (Lalli and Gilmer, 1989). The most recent taxonomic revision of *Cuvierina* was based on univariate shell measurements and a description of shell micro-ornamentation (Janssen, 2005, 2006a). Based on fossil evidence, Janssen (2005) proposed that extant *Cuvierina* species evolved 5-4 million years ago (mya), with the origin of the first fossil species estimated at 25-24 mya. Janssen (2005) proposed a subdivision of five extant morphospecies divided in two subgenera: *Cuvierina* (*Urceolarica*) *cancapae* (Janssen, 2005), *Cuvierina* (*Urceolarica*) *urceolaris* (Mörch, 1850), *Cuvierina* (*Cuvierina*) *columnella* (Rang, 1827), *Cuvierina* (*Cuvierina*) *atlantica* (Bé et al., 1972), and *Cuvierina* (*Cuvierina*) *pacifica* (Janssen, 2005). However, recent studies of pteropods have not implemented this species-level revision, resulting in considerable taxonomic confusion (Klussmann-Kolb and Dinapoli, 2006; Jennings et al., 2010; Bednaršek et al., 2012b; Corse et al., 2013). Here, we follow and test the morphological taxonomy of Janssen (2005), referring to the proposed *Cuvierina* taxa as morphotypes.

The overall aim of this study was to obtain a framework of phenotypic, genetic and geographic information to assess species boundaries and the evolutionary history of *Cuvierina* pteropods. To this end, we first applied geometric morphometric analyses of shell outlines using an extensive collection of museum and fresh specimens from the Pacific, Atlantic, and Indian oceans. Secondly, we sequenced a portion of mitochondrial DNA (mtDNA) comprising a fragment of the cytochrome oxidase I (COI) subunit, as well as a portion of the nuclear 28S rDNA gene. Thirdly, we plotted global distribution patterns of *Cuvierina* morphotypes and applied ecological niche modelling to estimate their ecological tolerances. Our specific objectives were (1) to distinguish between and within extant taxa using an integrative approach (as suggested by, e.g., McManus and Katz, 2009), (2) to determine the temporal sequence of evolution in the genus using a fossil-calibrated molecular phylogeny, and (3) to explore the current and past biogeographic context of extant *Cuvierina* taxa.

Methods

Samples

An overview of all *Cuvierina* samples is listed in Table 1 (more detailed information can be found in Table S1). Museum samples included specimens from the Natural History Museum of Denmark in Copenhagen (ZMUC) and Naturalis Biodiversity Center (NBC, Leiden, formerly Zoological Museum of Amsterdam (ZMA)). Museum samples were stored in 70% ethanol, but all museum samples had initially been fixed in formalin rendering them unsuitable for genetic analyses. Geographic locations of museum samples were either provided with the samples or obtained from Schmidt (1934), Gibbs (1971), Gibbs et al. (1971), Krueger et al. (1976) or Van Couwelaar (1998). Samples from ZMUC (*N* = 712 from 80 locations, 1-46 specimens per sample) were identified and sorted per morphospecies by A.W. Janssen (2001-2005; Janssen, 2005) and served as reference museum samples for geometric morphometric analyses in this study (Figure 1; Tables 1 and S1). Reference samples were collected during the Danish DANA expeditions between 1911 and 1934 during all seasons (53 locations), and during various other expeditions between 1846 and 1912 (27 locations) such as Leg. Andrea (Table S1). Samples from NBC (*N* = 214 from 32 locations, 1-23 specimens per sample) were not identified according to the taxonomic revision of *Cuvierina* by Janssen (2005) and are referred to as unidentified museum samples (Figure 1; Table 1). These samples were collected during the DANA expeditions between 1911 and 1933 (21 locations), ACRE expeditions (1967-1968, five locations), and Project 101A (1980, six locations; Table S1). Fresh samples (*N* = 133 from 53 locations, 1-23 specimens per sample) were collected between 2001 and 2012 during the following expeditions: MP3 (2001, three locations), 0106TRAN

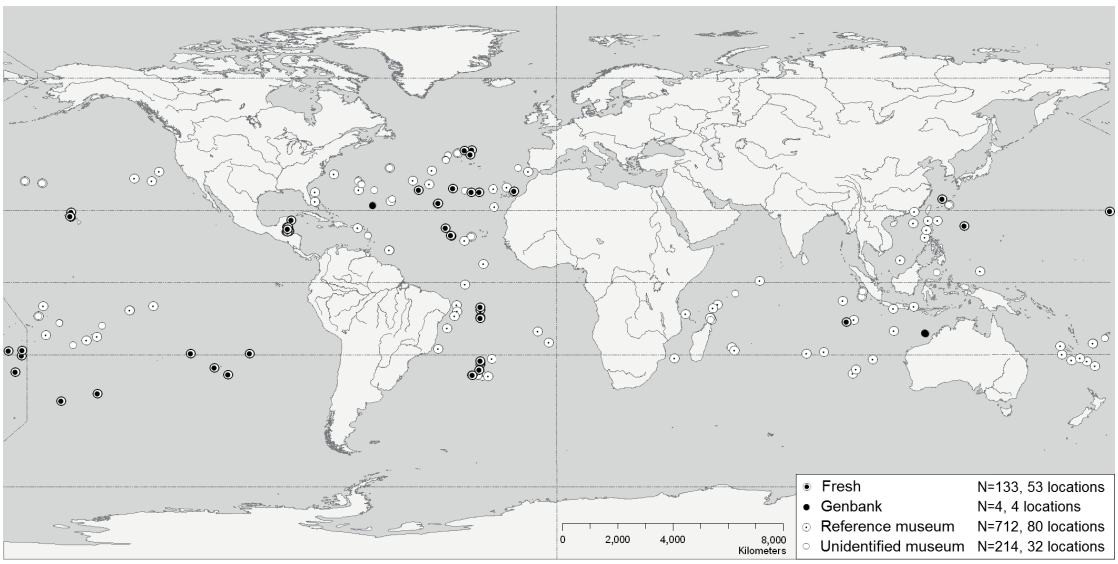

Figure 1. Geographic overview of all *Cuvierina* specimens used in this study. Some sampling locations of reference and unidentified museum samples overlap.

Table 1. Overview of *Cuvierina* samples used in this study.

Morphotype	Ocean	Morphometrics		COI	28S
		Ventral	Apertural		
	Total	1039	550	136	31
Reference museum samples		712	352		
C. atlantica		226	83		
	North Atlantic	218	75		
	South Atlantic	8	8		
C. cancapae		103	43		
	Central Atlantic	103	43		
C. columnella		65	39		
	Indian	30	20		
	Pacific	35	19		
C. urceolaris		226	95		
	Indian	137	49		
	Pacific	89	46		
C. pacifica N		34	34		
	Pacific	34	34		
C. pacifica S		58	58		
	South Pacific	58	58		
		58	58		
Unidentified museum samples		214	83		
	Atlantic	168	37		
	Pacific	33	33		
	Indian	13	13		
Unidentified fresh samples		113	115	133	30
	Atlantic	60	61	72	14
	Pacific	52	53	60	15
	Indian	1	1	1	1
GenBank sequences*				3	1
	Atlantic			1	1
	Indian			2	0

*GenBank sequences: COI, Atlantic: FJ876895, Indian: FJ876896-7 (Jennings et al., 2010); 28S, Atlantic: DQ237984 (Klussmann-Kolb and Dinapoli, 2006)

(2001, one location), COOK11MV and 14MV (2001, five locations), DRFT07RR (2001, three locations), VANC10MV (2003, one location), MARECO (2004, three locations), ECO-CH-Z (2007, nine locations, provided by R.A. Gasca Serrano, Unidad Chetumal, Mexico), AMT18 (2008, three locations), R/V Tansei-Maru KT-10-20 (2010, one location, provided by H. Miyamoto, University of Tokyo, Japan), Kilo Moana 1109 (2011, four locations), AMT22 (2012, 14 locations), and KH-11-10 (2011-2012, six locations, provided by A. Tsuda, University of Tokyo, Japan; Figure 1; Table S1). The collection nets used had mesh sizes between 0.2 and 1 cm. Fresh samples were stored in 96% ethanol. Only mature individuals with intact shells, both museum and fresh specimens, were used for geometric morphometric analyses. All fresh individuals were used for genetic analyses (*N* = 133; Tables 1 and S1).

Geometric morphometrics

Specimens were photographed in two orientations: ventral and apertural (Figure 2). Photographs were taken with a Nikon D100 6 mpx camera (Micro-Nikkor lens 55 mm / 3.5, aperture f / 16, shutter speed 1 / 8s ISO 200, fixed zoom), which was attached to a stand. For ventral photography, specimens were mounted on photographic film with methyl glucose (60%) to standardize the orientation. For apertural photography, shells were put into small disposable pipette tips. Photographs were adjusted in Adobe Photoshop Lightroom 2-2008 on white balance, sharpness, vibrancy and noise. Files containing pictures selected for analysis were prepared using tpsUtil (Rohlf, 2006). Only well-focused, undamaged adult shells in standardized orientation were used.

Because there are no true landmarks on *Cuvierina* shells, we used semi-landmarks for outlining shells (Gunz and Mitteroecker, 2013). Ventral shell outlines were created tpsDig (Rohlf, 2006) for a total of 1039 specimens, and apertural outlines were applied to a subset of 550 specimens (Figure 2; Table 1). The ventral outline was created by starting and ending at the distinct transitions from the outside of the shell to the aperture. One separate semi-landmark was placed at the top of the aperture. Using tpsUtil (Rohlf, 2006) the outline was converted to 75 semi-landmarks, separated by equal length, enabling further analyses (Figure 2). The apertural outline started with the semi-landmark in the middle of the aperture edge (the upper semi-landmark shown for typical specimens in Figure 2), being one of 35 semi-landmarks in which the apertural outline was converted. TpsRelw (Rohlf, 2006) was used to rotate, translate and scale semi-landmark coordinates through generalized least square Procrustes superimposition (GLS; Kendall, 1977, in Zelditch et al., 2004). GLS provided centroid sizes (a size measure depending on surface area) and multiple relative warp axes (RWs; ventral $N = 148$; apertural $N = 70$) per specimen. RWs contain information on shape, with the first RW containing the most shape information. To test for repeatability of RWs, a selection of 44 specimens was photographed in two subsequent series. Intraclass correlation coefficients (ICCs) between the two series were calculated for the first 10 RWs in Past 3.0 (Hammer et al., 2001). RWs were considered repeatable when ICC > 0.80. The outline method for geometric morphometric analyses on *Cuvierina* shells was highly repeatable (ICC > 0.89 for ventral RWs 1, 2, 4, 5, 6 and centroid size; ICC > 0.82 for apertural RWs 1, 2, 4, 5, and centroid size). Only repeatable RWs were used in further analyses of shell shape. To test whether sliding semi-landmarks provided more consistent results, ICCs were also calculated after transformation of semi-landmarks separated by equal-length intervals into sliding semi-landmarks with estimated positions on the outline. This did not improve repeatability; hence only semi-landmarks were used in this study.

The *a priori* classification of reference museum specimens (those identified by Janssen, 2005), was compared to results of clustering by linear discriminant analyses (LDA) in R 3.0.1 (R Development Core Team, 2013). Parameters for identifying morphotypes using LDA were ventral centroid size and ventral RWs 1, 2, 4, 5, 6.

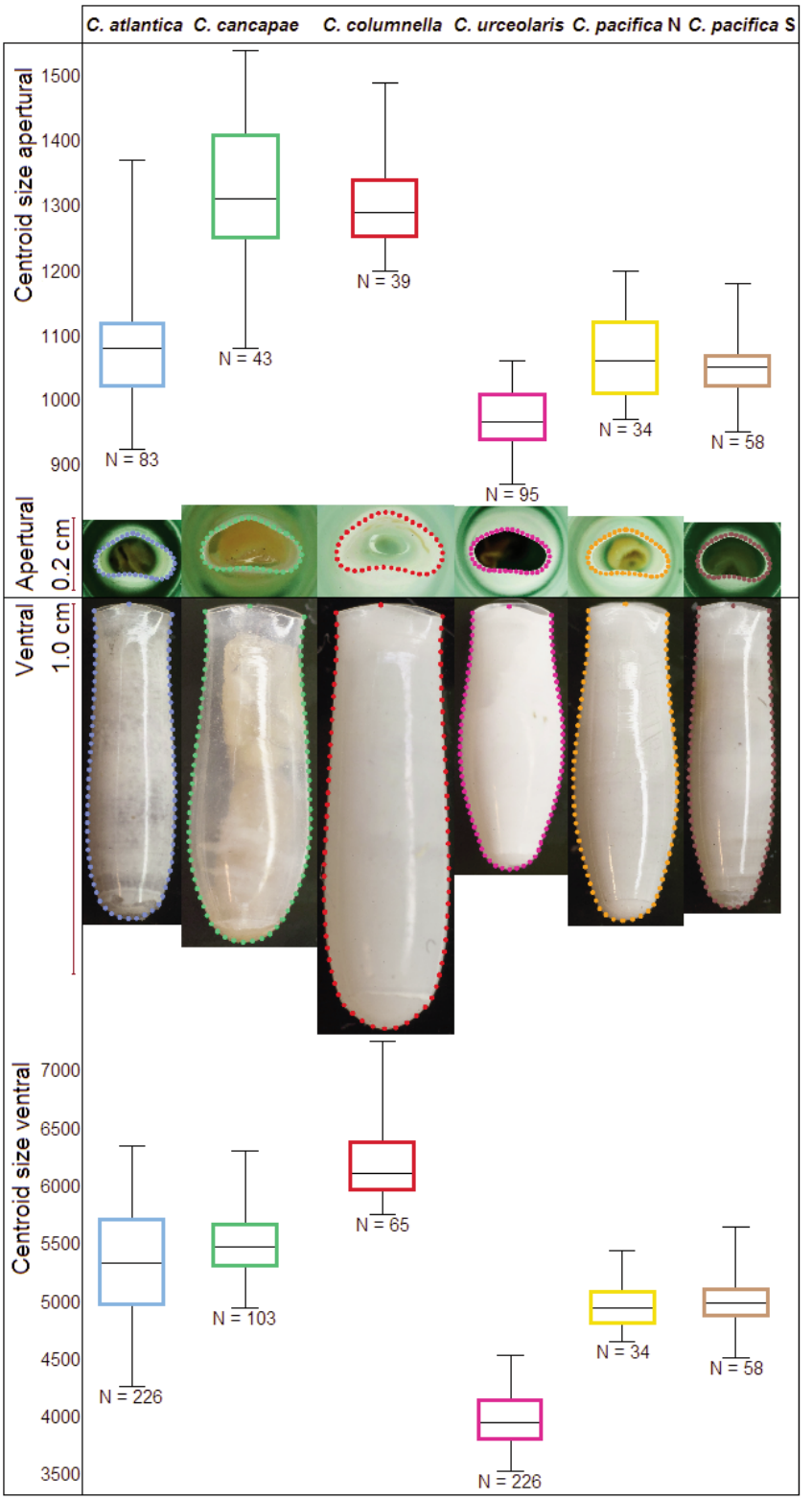

FIGURE 2. Centroid size variation for reference museum specimens of *Cuvierina* in ventral (*N* = 712) and apertural (*N* = 352) orientations. Typical specimens of six morphotypes are shown with outlines transformed to semi-landmarks to allow for geometric morphometric analysis. Lengths of *Cuvierina* shells were between 0.6 and 1.1 cm.

Subsequently, we compared our manual morphotype identifications of previously unidentified museum and fresh specimens to results of LDA-assignment of these specimens to morphotypes. Our manual identification of unidentified specimens was based on ventral centroid size, ventral RWs 1, 2, 4, 5, 6, and if available, apertural centroid size and apertural RWs 1, 3, 4, 5. The performance of the LDA algorithm was tested by cross-validation using a jackknifed confusion matrix in Past 2.17c (Hammer et al., 2011).

To test for significant differentiation between *a priori* defined groups of *Cuvierina* (morphotypes or geographic distributions), we applied non-parametric permutational multivariate analyses of variance (PerMANOVA; Anderson, 2001) in Past 2.17c. We used Euclidean distances applied to ventral and apertural centroid sizes and RWs with ICC > 0.80 (representing 96.75% of shell shape variation). The PerMANOVA *F*-statistic was tested against 9999 non-parametric mutations.

Genetics

To assess levels of genetic variation within *Cuvierina*, we sequenced 133 individuals for COI mtDNA and 21 individuals for 28S rDNA (Table 1). Entire juveniles (*N* = 4) and 2 × 2 mm of tissue of adults (*N* = 129) were individually placed in BLB buffer (250 mM EDTA, 5% SDS, 50 mM Tris-HCl pH 8.0; Holland, 1993) for at least 24 h. Total DNA was extracted from BLB buffer using the DNeasy blood & tissue kit (Qiagen Benelux B.V., 2006). The extract was resuspended in 100 µl AE-buffer (Qiagen Benelux B.V.). A 658bp fragment of COI was amplified using the primers LCO1490 (5'-GGTCAACAAATCATAAAGATATTGG-3') and HCO2198 (5'-TAAACTTCAGGGTGACCAAAAAATCA-3'; Folmer et al., 1994). For a subset of 31 individuals, a 965bp 28S rDNA fragment was amplified using the primers 28SC1F (5'-ACCCGCTGAATTTAAGCAT-3') and 28SD3R (5'-GACGATCGATTTGCACGTCA-3'; Dayrat et al., 2001). Most polymerase chain reactions (PCR) of COI and 28S, with total volumes of 25 µl, contained PCR Beads (GE Healthcare Europe GmbH) with 3 µl template DNA, 0.5 µl of each primer, and 21 µl ddH_2O. Alternatively for COI, PCR solutions (25 µl) contained 3 µl template DNA, 2.5 µl 10x reaction buffer (HT Biotechnology, Cambridge, U.K.), 1 µl $MgCl_2$ (25 mM), 2.5 µl dNTPs (GATC 1 mM each), 0.3 µl of each primer (10 µM), 0.15 µl Taq polymerase (HT Biotechnology), 0.2 µl BSA (10 mg/ml) and 15.05 µl ddH_2O. Amplifications were carried out in a PTC-200 DNA Engine Cycler (Bio-Rad Laboratories B.V.) with an initial denaturation of 3 min at 94°C, 35 cycles of 45 s at 94°C, 1 min at 45°C, and 1.5 min at 72°C, followed by final extensions of 10 min at 72°C and 5 min at 4°C. Sequencing of PCR products was carried out using both PCR primers by Macrogen Europe. The genus-level identities of all sequences were confirmed by BLAST searching GenBank (Altschul et al., 1997). Sequences were aligned in CodonCode Aligner 4.1 (CodonCode Corporation, USA, 2013). Additional GenBank sequences were added, namely three for COI ('*C. columnella*'): FJ876895-7 (Jennings et al., 2010) and one for 28S ('*C. columnella*'): DQ237984 (Klussmann-Kolb and Dinapoli, 2006).

To estimate evolutionary relationships among COI haplotypes, we applied a Maximum Likelihood (ML) approach (Felsenstein, 1981) in raxmlGUI 1.3, which

only provides GTR-related models of rate heterogeneity for nucleotide data (Stamatakis, 2006; Silvestro and Michalak, 2012). We tested for the most appropriate model of sequence evolution for this dataset using AIC in jModelTest 2.1.3 (Darriba et al., 2012) based on 88 models and the GTR + Γ + I was selected. However, we use 3 codon positions (CP) instead of Γ + I because it is a biologically realistic model for protein coding sequences (following Shapiro et al., 2006). We applied a ML search followed by a non-parametric bootstrap analysis with 2000 replicates. Additionally, we calculated pairwise genetic distances for COI in MEGA 6.0 using the *p*-distance model of evolution (Tamura et al., 2013).

To test for congruence of mitochondrial clades with nuclear DNA, we reconstructed alleles from 28S genotypes using the PHASE algorithm (Stephens et al., 2001; Stephens and Donelly, 2003) in DnaSP v5 (Librado and Rozas, 2009) and used these to calculate pairwise genetic distances with the *p*-distance model of evolution in MEGA 6.0.

We further explored the population genetic structure of *Cuvierina* in the Atlantic Ocean based on the COI fragment using a total of 60 fresh specimens for which morphotypes were assigned (northern *C. atlantica* (*N* = 34), southern *C. atlantica* (*N* = 21) and central Atlantic *C. cancapae* (*N* = 5); Table S1). The number of fresh specimens from the Indian and Pacific Oceans was insufficient for population genetic analyses. We obtained haplotype diversity (H) and nucleotide diversity (π: Tajima, 1983; Nei, 1987) for each population sample and pooled samples per morphotype and/or geographic region using Arlequin 3.5.1.3 (Excoffier et al., 2005). We tested for differentiation between Atlantic morphotypes and between geographic regions within morphotypes (e.g., North Atlantic versus South Atlantic) using ϕ_{ST} based on pairwise differences. These were tested for divergence from the null distribution of no differentiation with 10,000 permutations, as implemented in Arlequin. For all analyses involving multiple simultaneous tests, significance levels were adjusted by application of a sequential Bonferroni correction with an initial alpha of 0.05 (Rice, 1989).

To reconstruct evolution within *Cuvierina* and to provide a phylogenetic perspective of outgroup relationships, 30 *Cuvierina* sequences were compared to other Cavoliniid taxa. This approach was applied to combined partitions of COI (658bp) and 28S (989bp). Outgroup taxa were *Creseis conica*, *Clio pyramidata*, *C. cuspidata*, *C. recurva, Diacria danae* and *D. trispinosa*. The AIC in jModeltest 2.1.3 based on 88 models suggested the use of GTR + Γ + I for COI and GRT + Γ for 28S. Firstly, we applied a ML search followed by non-parametric bootstrap analysis with 3500 replicates in raxmlGUI 1.3. For this purpose, we used the GTR + CP substitution model for COI following (Shapiro et al., 2006). Secondly, we applied a relaxed Bayesian molecular clock analysis to combined COI and 28S partitions with uncorrelated lognormal rates in BEAUti and BEAST 1.7.5 (Drummond et al., 2012). For this we used the models suggested by jModelTest 2.13, because CP-based reconstructions failed to reach an Effective sample size (ESS) > 100 for the posterior statistic after two runs of 10^9 generations (burn-in 2×10^8 generations), as visual-

ized in Tracer 1.5 (Rambaut and Drummond, 2009). The tree prior was set to the Yule Process of speciation (Gernhard, 2008) with a random starting tree. Because our dataset consists of intraspecific as well as interspecific sequences, we limited our dataset to one individual per taxon, but used two individuals of *C. pacifica* S to calculate the TMRCA of this clade. We included the most basally positioned individuals for each morphotype based on the ML-phylogeny of COI and 28S combined. Two fossil calibrations were used, one on the root node of the tree (= stem Cavolinoidea) and one for the time of most recent common ancestry (TMRCA) of extant *Cuvierina*. For the first calibration we used the first fossil occurrence of the now extinct Cavoliniid *Camptoceratops priscus* (Wenz, 1923), 47.8-56 mya (Ypresian stage, A.W. Janssen, pers. comm. and in accordance with Corse et al., 2013) and set a lognormal distributed prior [log (Mean) = 8.0; log (Stdev) = 0.7; offset = 48.0]. For the crown ode of *Cuvierina* we set a lognormal distributed prior [log (Mean) = 3.0; log (Stdev) = 0.5; offset = 23.0] based on the first occurrence of *Cuvierina torpedo* in the fossil record at 20.4-23 mya (Janssen, 2005, 2006b). The preliminary MCMC chain was 10^7 generations (burn-in 10^6 generations), followed by six runs of 2.5×10^8 generations (burn-in 2.5×10^6 generations each). We sampled trees and log-likelihood values at 10,000-generation intervals. Sets of trees obtained during independent runs were combined in LogCombiner 1.7.5 (Drummond et al., 2012) and the maximum clade credibility tree was selected using TreeAnnotator 1.7.5 (Drummond et al., 2012).

Ecological niche modelling

To test whether *Cuvierina* morphotypes were ecologically differentiated based on their biogeographic distributions, we applied ecological niche modelling (ENM) to estimate their ecological tolerances. Based on geometric morphometric analyses, we plotted global morphotype occurrences on maps containing marine environmental data from the Bio-ORACLE dataset (Tyberghein et al., 2012) in a WGS1984 coordinate system in ArcMap 10.0 (ESRI, USA, 2011) to obtain an indication of geographic distributions in relation to the ecological variables. The number of georeferenced sampling locations for each morphotype was 69 for *C. atlantica*, 14 for *C. cancapae*, 17 for *C. columnella*, 30 for *C. urceolaris*, 20 for *C. pacifica* N, and 20 for *C. pacifica* S, respectively. We calculated Spearman rank correlation coefficients (ρ) between the environmental variables and performed a principal component analysis (PCA) on all Bio-ORACLE data layers. The PCA was used to select the most informative ecological variables from sets of correlated variables. This reduced the effect of collinearity of environmental variables (Dormann et al., 2013). Six uncorrelated data layers (with ρ ranging from -0.48 to 0.72), all with a special resolution of 5 arcmin (*ca*. 9.2 km), were selected for ENM: maximum monthly sea surface temperature (SST), annual SST range, annual average sea surface salinity (SSS), annual average surface pH, maximum monthly photosynthetically active radiation reaching the ocean surface (PAR) and maximum monthly near-surface chlorophyll *a* concentration. The Bio-ORACLE layers SST, chlorophyll *a* and PAR were based on remotely sensed data (Tyberghein et al., 2012). Maximum monthly

chlorophyll *a* concentration was set to a maximum of 10 mg/m^3 and annual average SSS was set to a minimum of 30 PSU as seen in nature. Although *Cuvierina* taxa are most abundant between 100 and 250 m, they migrate daily between surface waters and greater depths (Bé and Gilmer, 1977). It is therefore likely that sea surface variables are an important dimension of *Cuvierina*'s niche. Using MaxEnt 3.3.3 k (Phillips et al., 2006; Elith et al., 2011) we created response curves for these six ecological variables, performed jackknife tests to measure the importance of individual environmental variables in explaining the modelled distribution of each morphotype, and estimated potential niches per morphotype. Response curves were not extrapolated outside the range of observed values. We used the default settings and all presence records (N = 170) for training our model. Accuracy of ENMs per morphotype was examined using a null-model methodology using 99 randomisations that allows for significance testing of ENMs (Raes and Ter Steege, 2007). This test corrects for collection bias by restricting the randomly drawn points to all known sampling locations (presence-only data). Niche overlap between pairs of morphotypes was calculated by the Schoener's D statistic (Schoener, 1968; Warren et al., 2008) in ENMTools (Warren et al., 2010). A D-value of 1 indicates that two species share the same environmental space and a D-value of 0 suggests no overlap.

Results

Phenotypic variation

We distinguished six morphotypes in the pteropod genus *Cuvierina* based on geometric morphometric analyses of shell shape and size of reference specimens (Figures 2 and 3). Because we found a separation between North and South *C. pacifica* morphotypes (Figures 2, 3 and S1, respectively), these were separated in further analyses and are referred to as *C. pacifica* N and *C. pacifica* S. All morphotypes were significantly different from each other in terms of centroid size (ventral F = 731.7; p < 0.001) except *C. pacifica* N and *C. pacifica* S (Figure 2). Separation in size and shape was most evident in ventral orientation. Here, the overall shell shape variation between six morphotypes was significant after strict Bonferroni correction (N = 712, 96.89% of shape variation; F = 1364; p < 0.001). Extremes on the first RW axis (explaining 91.53% of ventral shell shape variation) were represented by the cylindrical *C. atlantica* and the bottle-shaped *C. urceolaris*, respectively (Figure 3). Extremes on the second RW axis (explaining 3.61% of ventral shell shape variation) were *C. pacifica* S with a narrow shell bottom (septum) and *C. cancapae* with a broad septum, respectively. In an apertural orientation, two of the six morphotypes (*C. urceolaris* and *C. pacifica* S) were significantly differentiated (N = 352; 84.59% of shape variation; F = 232.1; p < 0.001).

We also found significant variation in shell shape and size *within* morphotypes for *C. columnella* and *C. urceolaris* from different geographic regions. *C. columnella* specimens from the Indian Ocean (N = 30) were larger than Pacific specimens (N = 35; F =

25.44; $p < 0.001$). The opposite was true for *C. urceolaris*: specimens from the Indian Ocean ($N = 137$) were smaller than Pacific specimens ($N = 89$; $F = 123.7$; $p < 0.001$). We found no significant shape and size differences between *C. atlantica* specimens from the northern ($N = 255$) and southern ($N = 28$) Atlantic populations.

Linear Discriminant Analyses (LDA) almost completely matched manual morphotype identifications based on geometric morphometric analyses of unidentified specimens and showed high correspondence with *a priori* classification of reference museum samples. Without assigning samples to ocean basins *a priori*, 96% of all reference specimens ($N = 712$) were assigned to the same morphotype as determined *a priori*. Confidence increased to 99% when samples from the Atlantic and Indo-Pacific were analyzed separately. We compared this assignment method to LDA and found that without separating samples from the Atlantic and Indo-Pacific basins, 91% of all fresh specimens ($N = 113$) and 96% of all unidentified museum specimens ($N = 214$) were assigned to the same morphotypes as in manual identifications. This accuracy increased when samples were distinguished geographically: 96% of all fresh specimens and 99.5% of unidentified museum specimens were assigned to the same morphotype as with our manual method. We chose our manual method as the final identification method because a few specimens could not be identified unambiguously by LDA. These specimens had either shapes or centroid sizes that were on the edges of the total size-range or morphospace of a specific morphotype. Cross-validation demonstrated a high accuracy of the LDA algorithm itself: 98% of Atlantic and 99.5% of Indo-Pacific reference museum samples were identified as true positives.

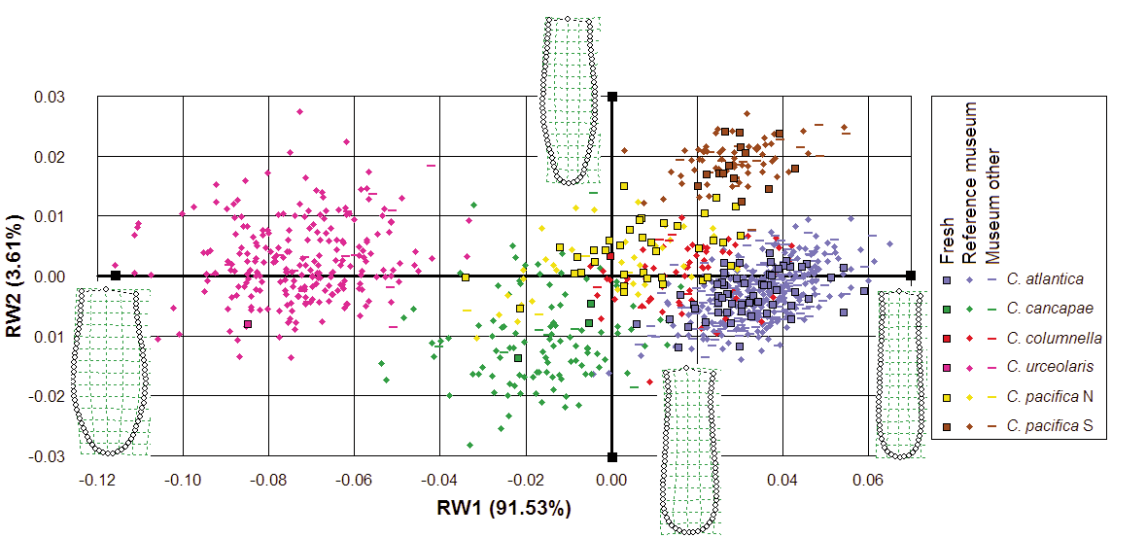

FIGURE 3. Ordination of uncorrected Relative Warp (RW) data of *Cuvierina* in a ventral orientation. Fresh ($N = 113$), reference museum ($N = 712$) and other museum specimens ($N = 214$) are included. Relative Warp 1 explains 91.53% of the total shape variation; RW2 explains 3.61%. Corresponding thin plate splines of the most positive and negative deformations along the axes are indicated to depict the variation in shell shape. Six distinguished morphotypes are indicated in the legend.

Genetic variation

We found high levels of mitochondrial diversity in a data set of 136 COI sequences collected from global samples of *Cuvierina*, including 127 different haplotypes represented by 166 polymorphic sites (GenBank accession numbers KP292656-KP292788; Table S1). We translated COI sequences into amino acids and discarded the possibility of pseudogenes because we found no stop codons and no insertions or deletions. Phylogenetic analysis of COI sequences indicated the presence of three major mitochondrial clades (Figures 4 and S2). These three monophyletic clades were highly supported (bootstrap values of 84-99%) and largely congruent with morphotypes as well as geographic distributions (Figure 5). The three major clades were named after their geographic distributions; viz., Atlantic, Indo-Pacific and South Pacific (Figures 4 and 5). The Atlantic clade contains both the *C. atlantica* and *C. cancapae* morphotypes: we did not find any grouping of these morphotypes, nor did we find any grouping of individuals from either the North or South Atlantic. The Indo-Pacific clade consists of *C. urceolaris*, *C. pacifica* N and *C. columnella* morphotypes. Within this clade, *C. pacifica* N was paraphyletic. Our single specimen of the *C. urceolaris* morphotype grouped with two GenBank sequences from the Indian Ocean (both reported as *C. columnella*, Jennings et al., 2010). The South Pacific clade consists entirely of the *C. pacifica* S morphotype. Average pairwise genetic distances of COI were 4.5-5.1% between major clades and 2.0, 1.7 and 0.8% within clades for the Atlantic, Indo-Pacific and South Pacific, respectively (Table S2).

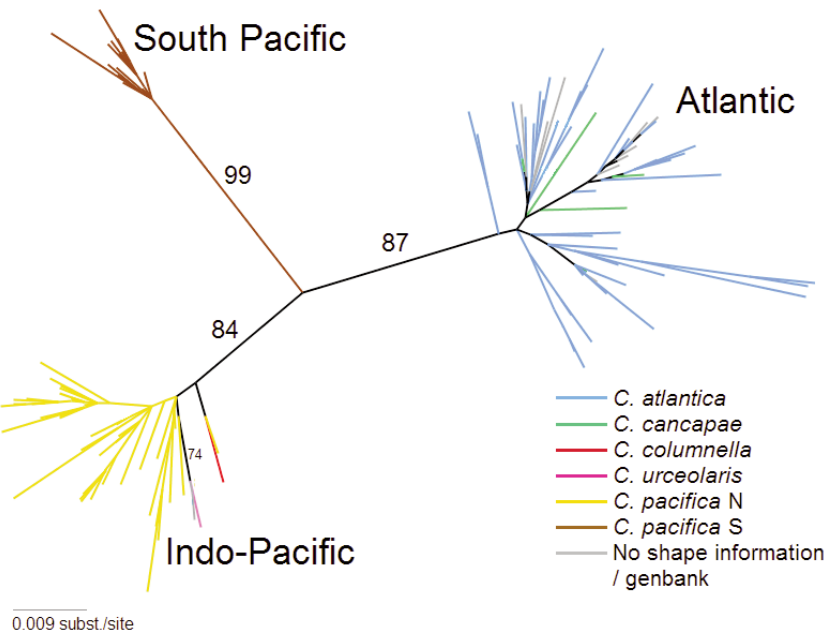

Figure 4. Unrooted maximum likelihood tree of 136 Cytochrome Oxidase I gene sequences of *Cuvierina*. Three sequences are from GenBank: FJ876895, Atlantic; FJ876896-7, Indian Ocean. Numbers indicate bootstrap support (only bootstrap values of major clades are shown). Symbols indicate major genetic clades; colors indicate distinct morphotypes (also see Figure 5).

Genetic patterns in 28S were not in conflict with our COI data but contained much less variation (0.8% for *N* = 31 representing six morphotypes). We found 11 diploid genotypes represented by 13 phased alleles and a total of eight polymorphic sites (GenBank accession numbers KP292620-KP292649; Tables S1 and S2). Most *Cuvierina* morphotypes shared 28S sequences, however, *C. pacifica* S and our single *C. urceolaris* specimen had unique single substitutions at positions 866 and 678, respectively (both C instead of T). Average pairwise genetic distances of 28S were 0.03, 0.1 and 0.09% within the Atlantic, Indo-Pacific and South Pacific mitochondrial clades, and 0.14-0.26% between major clades (Table S2).

Because we found *C. atlantica* populations in the northern as well as southern Atlantic Ocean, which are separated geographically by *C. cancapae* (Figure 5), we tested for spatial genetic structuring. Overall, we found high levels of genetic diversity in Atlantic *Cuvierina* samples (haplotype diversities ranged from 0.99 to 1.0 per sample). Nucleotide diversities were comparable for northern *C. atlantica* (π = 0.020 ± 0.01, *N* = 34), southern *C. atlantica* (π = 0.022 ± 0.01, *N* = 21) and *C. cancapae* (π = 0.020 ± 0.01, *N* = 5). We found significant population genetic structuring of northern versus southern *C. atlantica* populations (ϕ_{ST} = 0.047, *p* = 0.008), but not between *C. cancapae* and any *C. atlantica* population. This could be due to low sample size of *C. cancapae*.

We reconstructed evolution within the genus *Cuvierina* based on ML and fossil-calibrated Bayesian phylogenetic analyses of the combined COI + 28S sequence

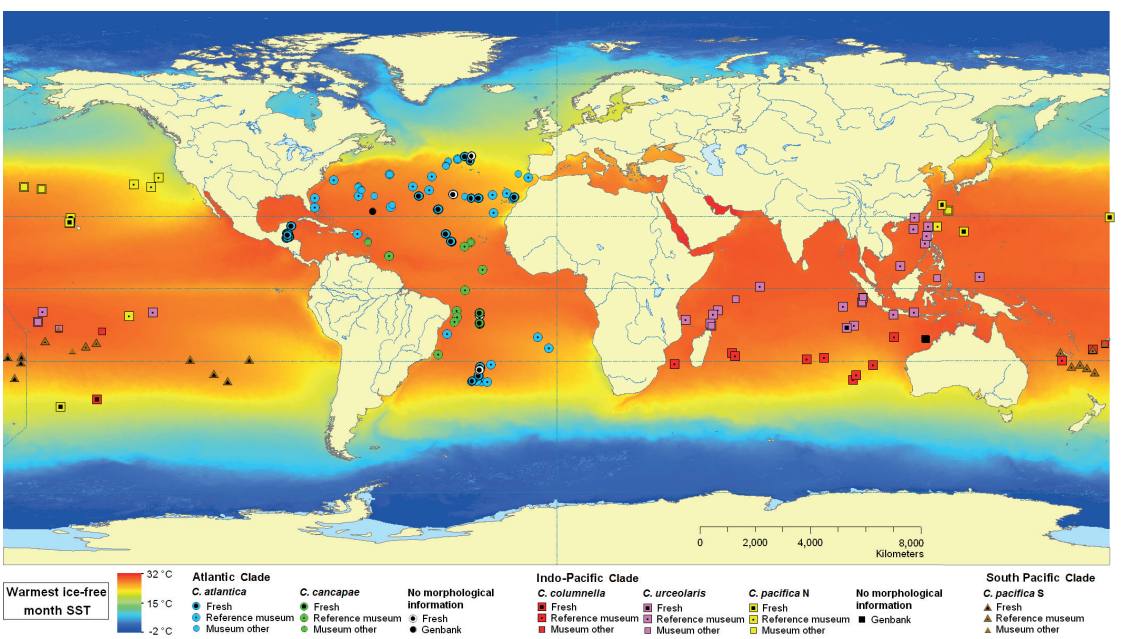

Figure 5. Geographic overview of all *Cuvierina* specimens used in this study. Sampling locations are projected on a map of sea surface temperatures (SST) of the warmest ice-free month (MARSPEC data set, Sbrocco and Barber, 2013). See legend for explanation of symbols and colors.

data (Figures 6 and S2, respectively). The ML and Bayesian reconstructions established a well-supported monophyly of *Cuvierina* versus outgroup taxa (GenBank accession numbers KP292650-KP292655 and KP292789-KP292794; Table S1). Within *Cuvierina*, the South Pacific clade appears basal in both reconstructions, followed by a split between the Atlantic and Indo-Pacific. We found that evolutionary rates of COI and 28S in outgroup taxa were highly variable and outgroup relationships remained largely unresolved (PP < 0.50; ML bootstraps < 40). *Creseis*, the sister taxon of *Cuvierina* based on interpretation of fossil evidence by Janssen (2005), had the fastest evolutionary rate with respect to the other taxa based on our Bayesian analyses (Figure 6). Following the TMRCA of 25.3 (28-23, 95% confidence interval) mya (Oligocene) for the genus *Cuvierina*, the first divergence most likely took place between the South Pacific and the Indo-Pacific / Atlantic clades. The Indo-Pacific and Atlantic clades diverged ~16.1 (24.5-7) mya (Miocene). The TMRCA for recent taxa within these three major clades was estimated to be at least 4.7 (13.5-1) mya for the Atlantic, 6.8 (15-2) mya for the Indo-Pacific, and 3.4 (14.5-0.5) mya for the South Pacific clades.

Biogeography

Cuvierina morphotypes are restricted to warm tropical and subtropical oceanic waters between ca. 43° north and ca. 40° south (Figure 5). We found little range overlap between *Cuvierina* morphotypes, especially in the Atlantic and Indian Oceans. However, Pacific distributions of morphotypes of the Indo-Pacific clade (*C. columnella*, *C. pacifica* N and *C. urceolaris*) partly overlapped (Figure 5). In the Atlantic Ocean, the *C. cancapae* morphotype is found in equatorial waters, extending as far as 23° south, whereas *C. atlantica* appears in subtropical waters up to 43° north and 35° south. In the Indian Ocean, *C. urceolaris* is found in equatorial waters, whereas *C. columnella* appears in subtropical waters up to 35° south. In the Pacific Ocean, *C. urceolaris* is found in equatorial waters, but *C. columnella* appears in equatorial as well as southern waters up to 40° south. The *C. pacifica* N morphotype has a much wider distribution pattern. It is confined to the Pacific Ocean and has been observed in northern subtropical waters up to 38° north, but also at a few equatorial and southern sampling sites. The *C. pacifica* S morphotype is confined to the large South Pacific gyre (Figure 5).

Based on response curves, MaxEnt jackknife scores and Schoener's *D* values, we found evidence for ecological differentiation among all six morphotypes (Figure 7; Tables 2 and S3). The relative contributions of individual oceanographic variables in explaining distribution patterns differed across morphotypes (Table 2). In the Atlantic Ocean, maximum monthly SST was most important in explaining the range of *C. cancapae* (41.9% contribution), indicative of its preference for warm waters (Figure 7). Other range-explaining variables were annual SST range (22.8%) and annual average SSS (34.6%). The distributional range of *C. atlantica*, however, was predominantly explained by annual average SSS (73.9%), and to a much smaller extent by maximum monthly SST (7.7%). The Indo-Pacific ranges of *C. urceolaris* were to a great extent explained by maximum monthly SST (86.3%), indicating a

preference for warm waters (FIGURE 7), whereas maximum monthly PAR reaching the ocean surface (high) and chlorophyll *a* concentration (low) were important to the distribution of *C. columnella*. No single oceanographic variable was found to predominantly explain the broad range of *C. pacifica* N, but maximum monthly SST and near-surface chlorophyll *a* concentration (both 30.8%) and SSS (21.5%) contributed most. The distribution of *C. pacifica* S was predominantly defined by maximum monthly chlorophyll *a* concentration (57.1%; TABLE 2), indicative of a

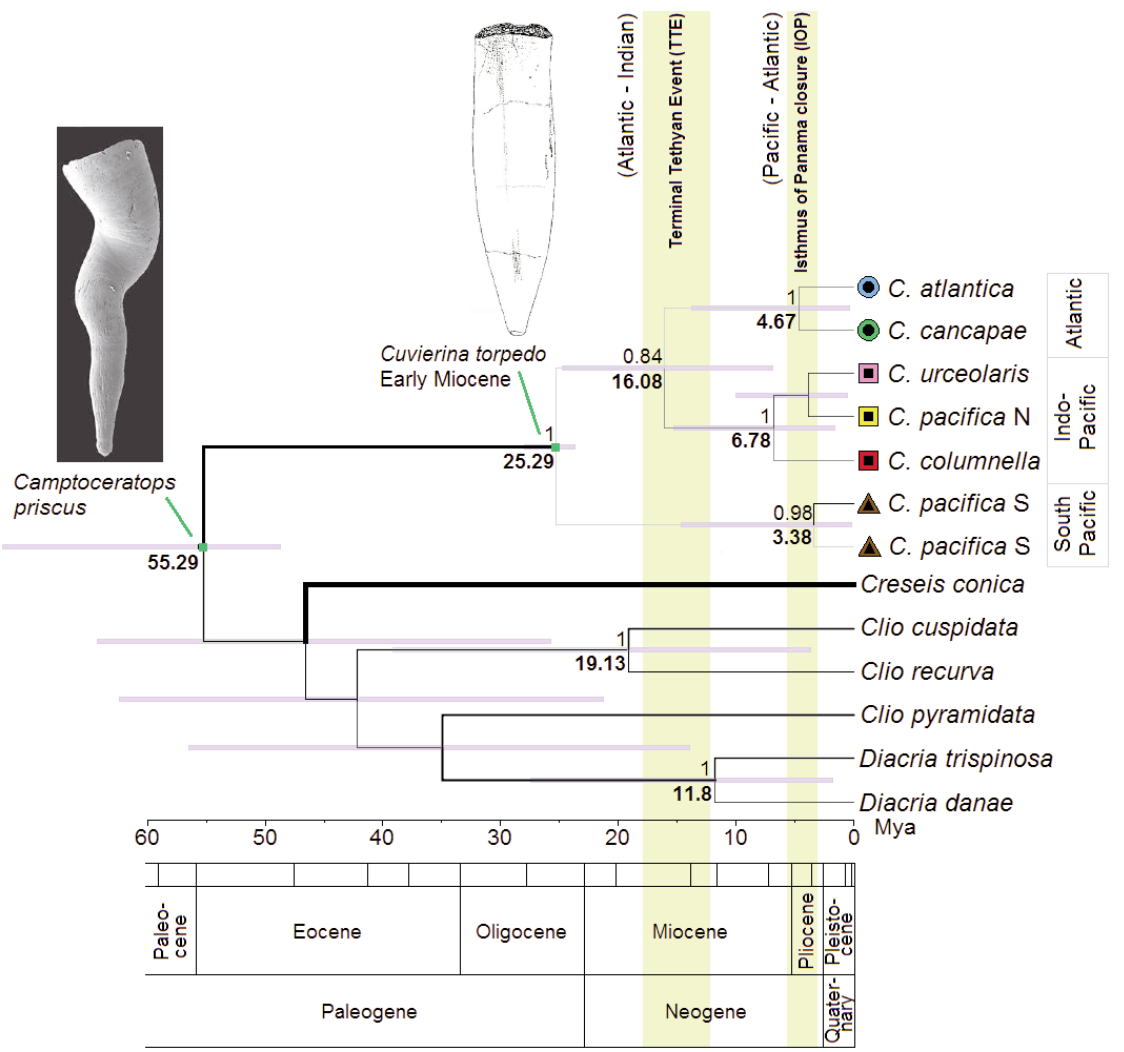

FIGURE 6. Fossil-calibrated Bayesian phylogeny of 7 *Cuvierina* and 6 outgroup taxa using COI (658bp) and 28S (989bp). The reconstruction was calibrated by the earliest occurrences in the fossil record of *Camptoceratops priscus* and *Cuvierina torpedo*, indicated by green dots on the nodes. Numbers above major branches indicate posterior probabilities (only values > 0.95 are shown); numbers below major branches indicate ages in million years ago. Branch widths correspond to substitution rates, with thick branches indicating high substitution rates. Symbols for *Cuvierina* indicate major genetic clades; colors indicate morphotypes (also see FIGURE 5). Image of *C. priscus*: Cahuzak and Janssen (2010); and *C. torpedo*: Janssen (2006b). The TTE and IOP are highlighted after estimations by Cowman and Bellwood (2013).

Table 2. MaxEnt Jackknife scores representing the relative importance of environmental variables in explaining distribution patterns of *Cuvierina* morphotypes.

% contribution	*C. atlantica*	*C. cancapae*	*C. columnella*	*C. urceolaris*	*C. pacifica* N	*C. pacifica* S
SST max.	7.7	41.9	9.1	86.3	30.8	12.5
Chlorophyll *a* max.	3.9	0.7	53.4	3.3	30.8	57.1
SSS average	73.9	34.6	1.6	5.9	21.5	7.0
PAR max.	4.1	0.0	31.5	0.0	12.3	7.5
SST range	9.3	22.8	2.6	0.7	4.6	2.0
pH average	1.1	0.0	1.8	3.8	0.0	13.9

SST max. = maximum monthly sea surface temperature (SST), Chlorophyll *a* max. = maximum monthly near-surface chlorophyll *a* concentration (set to a maximum of 10 mg/m^3), SSS average = annual average sea surface salinity (SSS, set to a minimum of 30 PSU), PAR max. = maximum monthly photosynthetically active radiation reaching the ocean surface (PAR), SST range = annual SST range, pH average = annual average pH. Highest Jackknife scores represent largest contributions of environmental variables to explaining geographic distributions of morphotypes, but do not provide information on values of selected environmental variables.

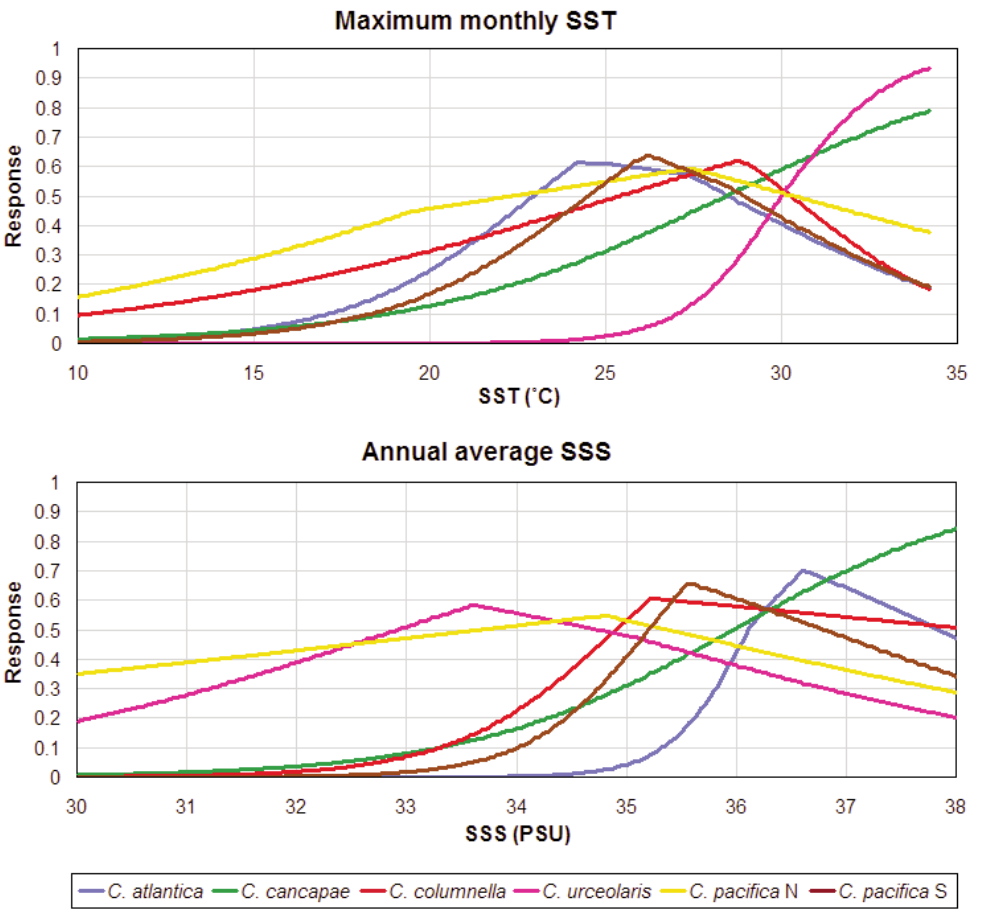

Figure 7. Ecological niche modelling response curves for each *Cuvierina* morphotype. Only response curves for maximum monthly Sea Surface Temperature (SST) and annual average Sea Surface Salinity (SSS) are shown.

preference for waters with low surface phytoplankton biomass. All six ENMs per morphotype were accurate according to significance testing using presence-only data (AUC-values 0.884-0.9588; $p = < 0.03$).

Discussion

Species boundaries

By conducting a global study combining phenotypic, genetic and biogeographic analyses of a zooplankton taxon, we show that the approach of integrative taxonomy can greatly improve our understanding of biodiversity and evolution in the open ocean. We have revealed congruent morphological, genetic and ecological patterns in *Cuvierina*, which all proved to be informative for distinguishing between taxa. We found evidence for six distinct morphotypes based on variation in shell shape and size (Figure 3; Table 1). This is one more than was formally described by Janssen (2005), although he mentioned the existence of two geographic types of *C. pacifica*. We distinguished three major genetic clades: the Atlantic clade with morphotypes *C. atlantica* and *C. cancapae*, the Indo-Pacific clade with *C. columnella*, *C. urceolaris* and *C. pacifica* N, and the South Pacific clade that consisted entirely of *C. pacifica* S (Figure 4). Morphotypes *C. atlantica* and *C. cancapae* are endemic to the Atlantic, *C. pacifica* N and *C. pacifica* S are restricted to the Pacific, and *C. columnella* and *C. urceolaris* occur in both the Indian and Pacific oceans (Figure 5). All six morphotypes were clearly disjunct in terms of the combination of shell shape and size, and could be consistently distinguished by LDA. Notably, morphotypes within the same genetic clade were usually the most divergent in morphometric characters. We also found differences in oceanographic habitat preferences, with differences particularly notable within the same genetic clades and ocean basins (see Figures 5, 7 and S3). In contrast to the terrestrial domain, the application of ecological niche models for depicting ecological tolerances of pelagic taxa has been rare (e.g., Provan et al., 2009; Robinson et al., 2011). Our ecological niche models have not taken into account diel vertical migration, dispersal limitation and biotic interactions in the prediction of the potential realized niche of the six morphotypes (Robinson et al., 2011). This may explain why morphotypes were not observed throughout their entire modelled potential niches.

Given the widely documented importance of shell morphology in the adaptation of gastropods (e.g., Vermeij, 2002; Rólan-Alvarez et al., 2004), the phenotypic variation found in *Cuvierina* taxa may reflect the interplay between genetic adaptation as well as plasticity in response to environmental conditions. For example, at present there is no genetic evidence for concluding that the *C. atlantica* and *C. cancapae* morphotypes are distinct species. However, genetic differentiation may well be present in other parts of the genome and would be an interesting topic for future research. We hypothesize that interbreeding between *C. atlantica* and *C. cancapae* is unlikely given the clearly disjunct morphologies of adult shells congruent with their respective geographic distributions. The preference of *C. cancapae*

for warmer waters with lower viscosities may explain its more bottle-shaped morphology with a larger surface to body weight-ratio compared to *C. atlantica*. This could be an adaptation to increase drag and thereby reduce sinking rates in warmer waters (Power, 1989). Furthermore, *C. cancapae* has pronounced shell micro-ornamentation which may also increase drag, whereas *C. atlantica* shells are completely smooth. All extinct *Cuvierina* and *Ireneia* taxa had pronounced shell micro-ornamentation and occurred in warm waters (Janssen, 2005), suggesting that micro-ornamentation is the ancestral character state. Common garden studies of other gastropod molluscs have shown that axes of shell shape variation often have a large genetic component, such as *Nucella lapillus* (h^2 of 0.51: Colson et al., 2006) and *Littorina saxatilis* (h^2 of 0.35-0.7: Conde-Padin et al., 2007).

We tentatively consider interbreeding between morphotypes within the Indo-Pacific clade unlikely as well, pending additional sampling and molecular data. We find clearly disjunct morphologies, extreme size differences and strong ecological preferences of *C. urceolaris* (warm tropical waters), *C. columnella* and *C. pacifica* N (both in subtropical, oligotrophic gyres) morphotypes. The shell of *C. urceolaris* is bottle-shaped with pronounced micro-ornamentation similar to *C. cancapae*. This may be explained by the same hypothesis as for *C. cancapae* in the Atlantic Ocean, because *C. urceolaris* also occurs in the warmest waters with lowest viscosities in the Indo-Pacific. Similar to our findings, other studies have reported much stronger phenotypic divergence than (neutral) genetic divergence in marine populations (e.g., Mariani et al., 2012), in particular in taxa with high dispersal potential (e.g., Luttikhuizen et al., 2003; Hollander, 2008; André et al., 2011; Yebra et al., 2011).

Ecological barriers to dispersal and similar distribution patterns as for *Cuvierina* are found in several other open ocean plankton taxa, such as *Diacavolinia* pteropods, foraminifers, krill and copepods. *Diacavolinia flexipes*, *D. angulosa* and *D. grayi* show a zonation of equatorial and subtropical distribution patterns in the Indian Ocean similar to *C. urceolaris* and *C. columnella* distributions (Van der Spoel et al., 1993). Like *C. pacifica* S, the krill species *Euphausia gibba* is endemic to the large South-Pacific gyre (Van der Spoel and Heyman, 1983). The presence of a disjunct distribution pattern as for *C. atlantica* in the Atlantic Ocean is also observed for the pelagic copepod genus *Pleuromamma* (Goetze, 2011; Halbert et al., 2013) and the mesopelagic copepod *Haloptilus longicornis* (Norton and Goetze, 2013). However, unlike *H. longicornis*, the *C. atlantica* morphotype is unable to reach the Indian Ocean around South Africa, where a warm current from the Indian Ocean impinges a cold current from the Southern Ocean. Numerous clades of planktonic foraminifers also have distribution patterns that are predominantly based on latitudinal zonation of water masses (e.g., Darling and Wade, 2008).

Based on results from this study, we do not find support for a subdivision into the subgenera *Cuvierina* (containing *C. atlantica*, *C. columnella*, *C. pacifica* N and *C. pacifica* S) and the more bottle-shaped *Urceolarica* (*C. urceolaris* and *C. cancapae*) as proposed by Janssen (2005, 2006a). We find evidence that *C. pacifica* N and *C. pacifica* S are distinct species because they belong to different genetic clades (COI

and 28S) and are morphologically disjunct. Because the holotype of *C. pacifica* belongs to the *C. pacifica* S morphotype, we propose a limitation of the description of *C. pacifica* to *C. pacifica* S and a new taxonomic description for the *C. pacifica* N morphotype (Burridge et al., 2016: Thesis chapter 4). However, because we found no molecular evidence to support the species status of morphotypes within the Atlantic and Indo-Pacific clades, we consider it possible that they represent ecophenotypic varieties or incipient species.

Evolution in *Cuvierina*

Based on a fossil-calibrated molecular phylogeny, we propose a biogeographic scenario for the evolution of *Cuvierina* morphotypes that is influenced by decreasing connectivity between the three world oceans since the Miocene (Figure 6). The now extinct ancestral genera *Spoelia*, *Johnjagtia* and *Ireneia* originated during the Oligocene at 34-33 mya as an offshoot of the Creseidae according to Janssen (2005). The first *Cuvierina* was thought to have originated directly from *Ireneia* (Janssen, 2005). However, the outgroup relationships of *Cuvierina* remain poorly resolved possibly because ancestral genera, as well as many Miocene and Pliocene *Cuvierina* taxa, are now extinct (e.g., *C. torpedo*, *C. paronai*, *C. grandis*, *C. curryi*, *C. intermedia*, *C. jagti*, *C. inflata*, *C. ludbrooki*, *C. astesana*, and *C. miyakiensis*; Janssen, 2005, 2006a,c, 2007, 2012). There was high connectivity between the three world oceans at the time of divergence between the South Pacific genetic clade and the Atlantic and Indo-Pacific *Cuvierina* clades at 25.3 (28-23) mya (Late Oligocene), but it is unknown for how long the South Pacific clade has been endemic to the large South Pacific gyre. The divergence between the Atlantic and Indo-Pacific clades of 16.1 (24.5-7) mya (Miocene) coincides with the Tethys Sea closure, suggesting a vicariant model of divergence, with the Indo-Pacific clade diverging from the Atlantic clade in the Indian Ocean and later dispersing to the Pacific basin. Until the Terminal Tethyan Event (TTE, 12-18 mya, Cowman and Bellwood, 2013), the Atlantic and Indian oceans were connected through the Tethyan Seaway, but pelagic connectivity was probably reduced from ± 21 mya onwards (Harzhauser et al., 2002, 2007). Dispersal between the Atlantic and Pacific oceans was possible until ± 3.1 mya with the final closure of the Isthmus of Panama (IOP, Cowman and Bellwood, 2013). However, there are no clear indications of vicariance events of Atlantic and Pacific *Cuvierina* associated with the IOP (Figure 6). The estimated TMRCAs of the three extant clades correspond very nicely with the estimates based on fossil evidence (5-4 mya: Janssen, 2005).

Connectivity between the three major oceans is now much more restricted at tropical and subtropical latitudes than in the Early Miocene. The Indo-West-Pacific region (IWP) does not seem to represent a physical barrier today, but could have functioned as such between Indian and Pacific populations of *C. columnella* and *C. urceolaris* during glacial periods when sea levels dropped (e.g., Gaither et al., 2010). This is a possible explanation for the subtle morphometric differences between Indian and Pacific *C. urceolaris* and *C. columnella* specimens. The IWP has also been considered an intermittent barrier to dispersal for several copepods

(Goetze, 2005, 2011). In these studies, significant population genetic structuring was found between Indian and Pacific populations of *Eucalanus hyalinus* and *E. spinifer* (Goetze, 2005) and *Pleuromamma xiphias* (Goetze, 2011).

Physical and ecosystem properties of different Atlantic water masses may be key to incipient speciation within the Atlantic clade. Our population genetic analyses of *C. atlantica* suggest that there is a significant degree of structuring between populations in the northern and southern subtropical gyre systems in the Atlantic Ocean. If genetic structure is interpreted in light of gene flow, this implies a more limited dispersal than expected for open ocean holoplankton. Combined with the disjunct distribution of *C. atlantica* populations, this suggest that the equatorial upwelling waters in the Atlantic represent a significant barrier to dispersal. This equatorial dispersal barrier was also found for the mesopelagic copepod *Haloptilus longicornis*, for which a genetic break was observed between populations in the northern and southern oligotrophic Atlantic gyres (Norton and Goetze, 2013). By contrast, the equatorial Atlantic offers an ecological niche for *C. cancapae*.

Conclusion

Given the distinct ecological and phenotypic specializations found among both described and undescribed *Cuvierina* taxa, they may not respond equally to future ocean changes and may not be equally sensitive to ocean acidification. Because the presence and strength of open ocean dispersal barriers depends on the ecological niche of a species, the capacity of a species to adapt to or to track a suitable habitat may vary across closely-related taxa (Peijnenburg and Goetze, 2013). Although open ocean evolution is partially driven by vicariance, our findings support the view that ecological differentiation may also be a major driving force of speciation for zooplankton.

Acknowledgements

We are grateful to A.W. Janssen for his ideas, inspiration for this research, and many articles on pteropod fossils. We are indepted to H. Miyamoto, A. Tsuda and R.A. Gasca Serrano who generously provided freshly collected *Cuvierina* samples from diverse regions in the world. We thank J. van Arkel for his assistance concerning specimen photography, to P. Meirmans for his introduction to statistical analyses in R, to V. Merckx for his advice on phylogenetic methods and to L. Dong, B. Voetdijk, and P. Kuperus for technical assistance in the IBED molecular lab. Finally, we thank P. Tarroso, A.W. Janssen, S.B.J. Menken, B.W. Hoeksema and the anonymous reviewers for their helpful comments on this manuscript, and W. Renema, E. Michel, J. Todd, Y. Young and O.S. Tendal for insightful discussions and inspiration. This study was partially supported by the UK Natural Environment Research Council National Capability funding to Plymouth Marine Laboratory and the National Oceanography Centre, Southampton. This is contribution number 264 of the AMT programme. A.K. Burridge was supported by The Malacological Society of London Research grant, N. Raes by the Netherlands Research Council NOW-ALW grant 819.01.014, E. Goetze by NSF grants OCE-1029478 and OCE-1338959, and K.T.C.A. Peijnenburg by SYNTHESYS grant DK-TAF-5199 and NWO-VENI grant 863.08.024. The authors declare that they have no competing interests.

References

Aiello G., Barratolo F., Barra D., Fiorito G., Mazzarella A., et al., 2007. Fractal analysis of ostracod shell variability: a comparison withg eometric and classic morphohometrics. Acta Palaeontologica Polonica 52, 563–573.

Altschul S.F., Madden T.L., Schäfer A.A., Zhang J., Zhang Z., et al., 1997. Gapped BLAST and PSI-BLAST: a new generation of protein database search programs. Nucleic Acids Research 25, 3389–3402.

Anderson M.J., 2001. A new method for non-parametric multivariate analysis of variance. Austral Ecology 26, 32–46.

André C., Larsson L.C., Laikre L., Bekkevold D., Brigham J., et al., 2011. Detecting population structure in a high gene flow species, Atlantic herring (*Clupea harengus*): direct, simultaneous evaluation of neutral vs. putatively selected loci. Heredity 106, 270–280.

Aurahs R., Treis Y., Darling K., Kucera M., 2011. A revised taxonomic and phylogenetic concept for the planktonic foraminifer species *Globigerinoides ruber* based on molecular and morphometric evidence. Marine Micropaleontology 79, 1–14.

Bé A.W.H., Gilmer R.W., 1977. A zoogeographic and taxonomic review of euthecosomatous Pteropoda. In: Ramsay A.T.S. (Ed.), Oceanic Micropaleontology 1. Academic Press, London, pp. 733–808.

Bé A.W.H., MacClintock C., Currie D.C., 1972. Helical shell structure and growth of the pteropod *Cuvierina columnella* (Rang) (Mollusca, Gastropoda). Biomineralization Research Reports 4, 47–79.

Bednaršek N., Feely R.A., Reum J.C.P., Peterson B., Menkel J. et al., 2014. *Limacina helicina* shell dissolution as an indicator of declining habitat suitability owing to ocean acidification in the California Current Ecosystem. Proceedings of the Royal Society B 281, 20140123.

Bednaršek N., Možina J., Vogt M., O'Brien C., Tarling G.A., 2012b. The global distribution of pteropods and their contribution to carbonate and carbon biomass in the modern ocean. Earth System Science Data 4, 167–186.

Bednaršek N., Tarling G.A., Bakker D.C.E., Fielding S., Jones E.M., et al., 2012a. Extensive dissolution of live pteropods in the Southern Ocean. Nature Geoscience 5, 881–885.

Burridge A.K., Janssen A.W., Peijnenburg K.T.C.A., 2016. Revision of the genus *Cuvierina* Boas, 1886 based on integrative taxonomic data, including the description of a new species from the Pacific Ocean (Gastropoda, Thecosomata). ZooKeys 619, 1–12. *Thesis chapter 4.*

Cahuzak B., Janssen A.W., 2010. Eocene to Miocene holoplanktonic Mollusca (Gastropoda) of the Aquitaine Basin, southwest France. Scripta Geologica 141, 1–193.

Colson I., Guerra-Valela J., Hughes R.N., Rolán-Alvarez E., 2006. Using molecular and quantitative variation for assessing genetic impacts on *Nucella lapillus* populations after local extinction and recolonization. Integrative Zoology 1, 104–107.

Comeau S., Gattuso J.-P., Nisumaa A.-M., Orr J., 2012. Impact of aragonite saturation state changes on migratory pteropods. Proceedings of the Royal Society B 279, 732–738.

Conde-Padin P., Carvajal-Rodriquez A., Carballo M., Caballero A., Rolán-Alvarez E., 2007. Genetic variation for shell traits in a direct-developing marine snail involved in a putative sympatric ecological speciation process. Evolutionary Ecology 21, 635–650.

Corse E., Rampal J., Cuoc C., Peck N., Perez Y., Gilles A, 2013. Phylogenetic analysis of Thecosomata Blainville, 1824 (Holoplanktonic Opisthobranchia) using morphological and molecular data. PLoS ONE 8, e59439.

Cowman P.E., Bellwood D.R., 2013. Vicariance across major marine biogeographic barriers: temporal concordance and the relative intensity of hard versus soft barriers. Proceedings of the Royal Society B 280, 20131541.

Darling K.F., Wade C.M., 2008. The genetic diversity of planktic foraminifera and the global distribution of ribosomal RNA genotypes. Marine Micropaleontology 67, 216–238.

Darriba D., Taboada G.L., Doallo R., Posada D., 2012. jModelTest 2: more models, new heuristics and parallel computing. Nature Methods 9, 772.

Dayrat B., Tillier A., Lecointre G., Tillier S., 2001. New clades of euthyneuran gastropods (Mollusca) from 28S rRNA sequences. Molecular Phylogenetics and Evolution 19, 225–235.

De Vargas C., Zaez A.G., Medlin L.K., Thierstein H.R., 2004. Super-species in the calcareous plankton. In: Thierstein H.R., Young Y.R. (Eds.), Coccolithophores: from molecular processes to global impact. Springer, Berlin, pp. 271–298.

Dormann C.F., Elith J., Bacher S., Buchmann C., Carl G., et al., 2013. Collinearity: a review of methods to deal with it and a simulation study evaluating their performance. Ecography 36, 27–46.

Drummond A.J., Suchard M.A., Xie D., Rambaut A., 2012. Bayesian phylogenetics with BEAUti and the BEAST 1.7. Molecular Biology and Evolution 29, 1969–1973.

Elith J., Phillips S.J., Hastie T., Dudik M., En Shee Y., Yates C.J., 2011. A statistical explanation of maxent for ecologists. Diversity and Distributions 17, 43–57.

Excoffier L., Laval G., Schneider S., 2005. Arlequin ver,3.0: an integrated software package for population genetics and data analysis. Evolutionary Bioinformatics Online 1, 47–50.

Fabry V.J., Seibel B.A., Feely R.A., Orr J.C., 2008. Impacts of ocean acidification on marine fauna and ecosystem processes. ICES Journal of Marine Science 65, 414–432.

Feely R.A., Sabine C.L., Lee K., Berelson W., Kleypas J., et al., 2004. Impact of anthropogenic CO_2 on the $CaCO_3$ system in the oceans. Science 305, 362–366.

Felsenstein J., 1981. Evolutionary trees from DNA sequences: a maximum likelihood approach. Journal of Molecular Evolution 17, 368–376.

Folmer O., Black M., Hoeh W., Lutz R., Vrijenhoek R., 1994. DNA primers for amplification of mitochondrial Cytochrome c Oxidase subunit I from diverse metazoan invertebrates. Molecular Marine Biology and Biotechnology 3, 294–299.

Gaither M.R., Toonen R.J., Robertson D.R., Planes S., Bowen B.W., 2010. Genetic evaluation of marine biogeographical barriers: perspectives from two widespread Indo-Pacific snappers (*Lutjanus kasmira* and *Lutjanus fulvus*). Journal of Biogeography 37, 133–147.

Gasca R., Janssen A.W., 2014. Taxonomic review, molecular data and key to the species of Creseidae from the Atlantic Ocean. Journal of Molluscan Studies 80, 35–42.

Gernhard T., 2008. The conditioned restructured process. Journal of Theoretical Biology 253, 769–778.

Gibbs R.H., 1971. Cruise report on ACRE12, R/V Delaware II.

Gibbs R.H., Roper C.F.E., Brown D.W., Goodyear R.W., 1971. Biological studies of the Bermuda Ocean ACRE I. Station data, methods and equipment for cruises 1 through 11, October 1967 – January 1971. Report to the U.S. Navy Underwater Systems Center.

Goetze E., 2005. Global population genetic structure and biogeography of the oceanic copepods *Eucalanus hyalinus* and *E.spinifer*. Evolution 59, 2378–2398.

Goetze E., 2011. Population differentiation in the open sea: insights from the pelagic copepod *Pleuromamma xiphias*. Integrative and Comparative Biology 51, 580–597.

Gunz P., Mitteroecker P., 2013. Semilandmarks: a method for quantifying curves and surfaces. Hystrix, the Italian Journal of Mammalogy 24, 103–109.

Halbert K.M.K., Goetze E., Carlon D.B., 2013. High cryptic diversity across the global range of the migratory planktonic copepods *Pleuromamma piseki* and *P. gracilis*. PLoS ONE 8, e77011.

Hammer Ø., Harper D.A.T., Ryan P.D., 2001. PAST: paleontological statistics software package for education and data analysis. Palaeontologia Electronica 4, 1–9.

Harzhauser M., Kroh A., Mandic O., Piller W.E., Göhlich U. et al., 2007. Biogeographic responses to geodynamics: a key study all around the Oligo-Miocene Tethyan Seaway. Zoologischer Anzeiger 246, 241–256.

Harzhauser M., Piller W.E., Steiniger F.F., 2002. Circum-Mediterranean Oligo-Miocene biogeographic evolution–the gastropods' point of view. Palaeogeography, Palaeoclimatology, Palaeoecology 183, 103–133.

Holland P.W.H., 1993. Cloning genes using the polymerase chain reaction. In: Stern C.D., Holland P.W.H. (Eds.), Developmental biology: a practical approach. Oxford University Press, Oxford, pp. 243–255.

Hollander J., 2008. Testing the grain-size model for the evolution of phenotypic plasticity. Evolution 62, 1381–1389.

Janssen A.W., 2005. Development of Cuvierinidae (Mollusca, Euthecosomata, Cavolinioidea) during the Cainozoic: a non-cladistic approach with a re-interpretation of Recent taxa. Basteria 69, 25–72.

Janssen A.W., 2006a. Notes on the systematics, morphology and biostratigraphy of fossil holoplanktonic Mollusca, 16. Some additional notes and amendments on Cuvierinidae and on classification of Thecosomata (Mollusca, Euthecosomata). Basteria 70, 67–70.

Janssen A.W., 2006b. Notes on the systematics, morphology and biostratigraphy of fossil holoplanktonic mollusca, 17. On the status of some pteropods (Gastropoda, Euthecosomata) from the Miocene of New Zealand, referred to as species of *Vaginella*. Basteria 70, 71–83.

Janssen A.W., 2006c. Notes on the systematics, morphology and biostratigraphy of fossil holoplanktonic Mollusca. On the status of *Cuvierina* (*Cuvierina*) *ludbrooki* and *C.* (*C.*) *jagti* (Gastropoda, Euthecosomata). Basteria 70, 85–88.

Janssen A.W., 2007. Holoplanktonic Mollusca (Gastropoda: Pterotracheoidea, Janthinoidea, Thecosomata and Gymnosomata) from the Pliocene of Pangasinan (Luzon, Philippines). Scripta Geologica 135, 29–177.

Janssen A.W., 2012. Late Quaternary to recent holoplanktonic Mollusca (Gastropoda) from bottom samples of the eastern Mediterranean Sea: systematics, morphology. Bollettino Malacologico 48, 1–105.

Janssen A.W., Peijnenburg K.T.C.A., 2014. Holoplanktonic Mollusca: development in the Mediterranean basin during the last 30 million years and their future. In: Goffredo S., Dubinsky Z. (Eds.), The Mediterranean Sea: Its History and Present Challenges. Springer, Dordrecht, pp. 341–362.

Jennings R.M., Bucklin A., Ossenbrügger H., Hopcroft R.R., 2010. Species diversity of planktonic gastropods (Pteropoda and Heteropoda) from six ocean regions based on DNA barcode analysis. Deep-Sea Research II 57, 2199–2210.

Jin P., Gao K., Beardall J., 2013. Evolutionary responses of a coccolithophorid *Gephyrocapsa oceanica* to ocean acidification. Evolution 67, 1869–1878.

Jörger K.M., Stöger I., Kano Y., Fukuda H., Knebelsberger T., Schrödl M., 2010. On the origin of Acochlidia and other enigmatic euthyneuran gastropods, with implications for the systematics of Heterobranchia. BMC Evolutionary Biology 10, 323.

Kendall D., 1977. The diffusion of shape. Advances in Applied Probability 9, 428–430.

Klingenberg C.P., 2010. Evolution and development of shape: integrating quantitative approaches. Nature Reviews. Genetics 11, 623–635.

Klussmann-Kolb A., Dinapoli A., 2006. Systematic position of the pelagic Thecosomata and Gymnosomata within Opisthobranchia (Mollusca, Gastropoda)–revival of the Pteropoda. Journal of Zoological Systematics and Evolutionary Research 44, 118–129.

Krueger W.H., Gibbs R.H., Kleckner R.C., Keller A.A., Keene M.J., 1976. Distribution and abundance of mesopelagic fishes on cruises 2 and 3 at Deepwater Dumpsite 106. Includes appendix table with station data from cruises 1–4. Cruise report. University of Rhode Island, Kingston, Washington and National Museum of Natural History, Smithsonian Institution.

Lalli C.M., Gilmer R.W., 1989. The thecosomes. Shelled pteropods. In: Lalli C.M., Gilmer R.W. (Eds.), Pelagic snails. The biology of holoplanktonic gastropod molluscs. Stanford University Press, Stanford, California, pp. 58–166.

Librado P., Rozas J., 2009. DnaSP v5: a software for comprehensive analysis of DNA polymorphism data. Bioinformatics 25, 1451–1452.

Lohbeck K.T., Riebesell U., Collins S., Reusch T.B.H., 2012. Functional genetic divergence in high CO_2 adapted *Emiliana huxleyi* populations. Evolution 67, 1892–1900.

Luttikhuizen P.C., Drent J., Van Delden W., Piersma T., 2003. Spatially structured genetic variation in a broadcast spawning bivalve: quantitative vs. molecular traits. Journal of Evolutionary Biology 16, 260–272.

Maas A.E., Blanco-Bercial L., Lawson G.L., 2013. Reexamination of the species assignment of *Diacavolinia* pteropods using DNA barcoding. PLoS ONE 8, e53889.

Mariani S., Peijnenburg K.T.C.A., Weetman D., 2012. Independence of neutral and adaptive divergence in a low dispersal marine mollusc. Marine Ecology Progress Series 446, 173–187.

McManus G.B., Katz L.A., 2009. Molecular and morphological methods for identifying plankton: what makes a successful marriage? Journal of Plankton Research 31, 1119–1129.

Mitteroecker P., Gunz P., 2009. Advances in geometric morphometrics. Evolutionary Biology 36, 235–247.

Mörch O.A.L., 1850. Catalogus conchyliorum quae reliquit C.P. Kierulf, md. dr. nunc publica auctione X Decembris MDCCCL Hafniae Dividenda. Hafniae, Trieri.

Nei M., 1987. Molecular evolutionary genetics. Columbia University Press, New York.

Norton E.L., Goetze E., 2013. Equatorial dispersal barriers and limited population connectivity among oceans in a planktonic copepod. Limnology and Oceanography 58, 1581–1596.

Orr J.C., Fabry V.J., Aumont O., Bopp L., Doney S.C., et al., 2005. Anthropogenic ocean acidification over the twenty-first century and its impact on calcifying organisms. Nature 437, 681–686.

Peijnenburg K.T.C.A., Goetze E., 2013. High evolutionary potential of marine zooplankton. Ecology and Evolution 3, 2765–2781.

Phillips S.J., Anderson R.P., Schapire R.E., 2006. Maximum entropy modelling of species geographic distributions. Ecological Modelling 190, 231–259.

Power J.H., 1989. Sink or swim: growth dynamics and zooplankton hydromechanics. The American Naturalist 133, 706–721.

Provan J., Beatty G.E., Keating S.L., Maggs C.A., Savidge G., 2009. High dispersal potential has maintained long-term population stability in the North Atlantic copepod *Calanus finmarchicus*. Proceedings of the Royal Society B 276, 301–307.

R Development Core Team. R. A language and environment for statistical computing. 2013. http://www.R-project.org

Raes N., Ter Steege H., 2007. A null-model for significance testing of presence-only species distribution models. Ecography 30, 727–736.

Rambaut A., Drummond A.J., 2009. Tracerv1.5. http://beast.bio.ed.ac.uk/Tracer

Rang P.C.A.L., 1827. Description de deux genres nouveaux (*Cuvieria* et *Euribia*) appartenant à la classe des ptéropodes. Annales des Sciences Naturelles 12, 320–329. [pl. 45B dated 1826]

Rice W.R., 1989. Analyzing tables of statistical tests. Evolution 43, 223–225.

Robinson L.M., Elith J., Hobday A.J., Pearson R.G., Kendall B.E. et al., 2011. Pushing the limits in marine species distribution modelling: lessons from the land present challenges and opportunities. Global Ecology and Biogeography 20, 789–802.

Roger L.M., Richardson A.J., McKinnon A.D., Knott B., Matear R., Scadding C., 2011. Comparison of the shell structure of two tropical Thecosomata (*Creseis acicula* and *Diacavolinia longirostris*) from 1963 to 2009: potential implications of declining aragonite saturation. ICES Journal of Marine Science 69, 465–474.

Rohlf F.J., 2006. Tps series. http://life.bio.sunysb.edu/morph

Rolán-Alvarez E., Carballo M., Galindo J., Morán P., Fernández B., et al., 2004. Nonallopatric and parallel origin of local reproductive barriers between two snail ecotypes. Molecular Ecology 13, 3415–3424.

Sa'ez A.G., Probert I., Gelsen M., Quinn P., Young J.R., Medlin L.K., 2003. Pseudo-cryptic speciation in coccolithophores. Proceedings of the National Academy of Sciences 100, 7163–7168.

Sbrocco E.J., Barber P.H., 2013. MARSPEC: ocean climate layers for marine spatial ecology. Ecology 94, 979.

Schmidt J. Dana-Report Vol. I 1932-1934: the Carlsberg foundation's oceanographic expedition round the world 1928-1939, and previous 'Dana' expeditions. C.A. Reitzels Vorlag, Oxford University Press, London.

Schoener T.W., 1968. The Anolis lizards of Bimini: resource partitioning in a complex fauna. Ecology 49, 704–726.

Seears H.A., Darling K.F., Wade C.M., 2012. Ecological partitioning and diversity in tropical planktonic foraminifera. BMC Evolutionary Biology 12, 54.

Shapiro B., Rambaut A., Drummond A.J., 2006. Choosing appropriate substitution models for the phylogenetic analysis of protein-coding sequences. Molecular Biology and Evolution 23, 7–9.

Silvestro D., Michalak I., 2012. RaxmlGUI: a graphical front-end for RAxML. Organisms Diversity & Evolution 12, 335–337.

Stamatakis A., 2006. RAxML-VI-HPS: maximum likelihood-based phylogenetic analyses with thousands of taxa and mixed models. Bioinformatics 22, 2688–2690.

Stephens M., Donelly P., 2003. A comparison of Bayesian methods for haplotype reconstruction from population genotype data. The American Journal of Human Genetics 73, 1162–1169.

Stephens M., Smith N., Donelly P., 2001. A new statistical method for haplotype reconstruction from population data. The American Journal of Human Genetics 68, 978–989.

Tajima F., 1983. Evolutionary relationship of DNA sequences in finite populations. Genetics 105, 437–60.

Tamura K., Stecher G., Peterson D., Filipski A., Kumar S., 2013. MEGA6: Molecular Evolutionary Genetics Analysis Version 6.0. Molecular Biology and Evolution 30, 2725–2729.

Tyberghein L., Verbruggen H., Pauly K., Troupin C., Mineur F., DeClerck O., 2012. Bio-ORACLE: a global environmental dataset for marine species distribution modelling. Global Ecology and Biogeography 21, 272–281.

Ujiié Y., Asami T., De Garidel-Thoron T., Liu H., Ishitani Y., De Vargas C., 2012. Longitudinal differentiation among pelagic populations in a planktic foraminifer. Ecology and Evolution 2, 1725–1737.

Van Couwelaar M., 1998. Pelagic faunas in monsoon ruled seas. PhD thesis, University of Amsterdam, Amsterdam.

Van der Spoel S., 1967. Euthecosomata, a group with remarkable developmental stages (Gastropoda, Pteropoda). PhD thesis, University of Amsterdam. Noorduijn en Zoon, Gorinchem.
Van der Spoel S., 1970. Morphometric data on Cavoliniidae, with notes on a new form of *Cuvierina columnella* (Rang,1827) (Gastropoda, Pteropoda). Basteria 34, 103–151.
Van der Spoel S., 1974. Geographical variation in *Cavolinia tridentata* (Mollusca, Pteropoda). Bijdragen tot de Dierkunde 44, 100–112.
Van der Spoel S., Bleeker J., Kobayasi H., 1993. From *Cavolinia longirostris* to twenty-four *Diacavolinia* taxa, with a phylogenetic discussion (Mollusca, Gastropoda). Bijdragen tot de Dierkunde 62, 127–166.
Van der Spoel S., Heyman R.P., 1983. A Comparative Atlas of Zooplankton: Biological Patterns in the Oceans. Springer, New York.
Vermeij G.J., 2002. Characters in context: molluscan shells and the forces that mold them. Paleobiology 28, 41–54.
Warren D.L., Glor R.E., Turelli M., 2008. Environmental niche equivalency versus conservatism: quantitative approaches to niche evolution. Evolution 62, 2868–2883.
Warren D.L., Glor R.E., Turelli M., 2010. ENMTools: a toolbox for comparative studies of environmental niche models. Ecography. 33, 607–611.
Weiner A., Aurahs R., Kurasawa A., Kitazaho H., Kucera M., 2012. Vertical niche partitioning between cryptic sibling species of a cosmopolitan marine planktonic protist. Molecular Ecology 21, 4063–4073.
Wenz W., 1923. Gastropoda extramarina tertiaria, 5. Animalia. Fossilium Catalogus 22, 1421–1734.
Yebra L., Bonnet D., Harris R.P., Lindeque P., Peijnenburg K.T.C.A., 2011. Barriers in the pelagic: population structuring of *Calanus helgolandicus* and *C. euxinus* in European waters. Marine Ecology Progress Series 428, 135–149.
Zelditch M.L., Swiderski D.L., Sheets H.D., Fink W.L., 2004. Geometric morphometrics for biologists. Elsevier Academic Press, San Diego and London.

Supplementary information

The data set supporting the results of this article is available at the Dryad Digital Repository at DOI: 10.5061/dryad.7n1q4, and DNA sequences have been deposited at GenBank under the following accession numbers: KP292620-KP292794.

Supplementary information 1. Centroid size and uncorrected RW (Relative warp) data of all *Cuvierina* shells in ventral as well as apertural orientations. Relative contributions of RW axes to shell shape variation are included. The first sheet contains ventral data of 113 fresh, 712 reference museum, and 214 other museum specimens. The second sheet contains apertural data of 115 fresh, 352 reference museum, and 83 other museum specimens.

Supplementary information 2. Photographs of 1039 *Cuvierina* shells in a ventral orientation used for geometric morphometric analyses in this study.

Supplementary information 3. Photographs of 550 *Cuvierina* shells in an apertural orientation used for geometric morphometric analyses in this study.

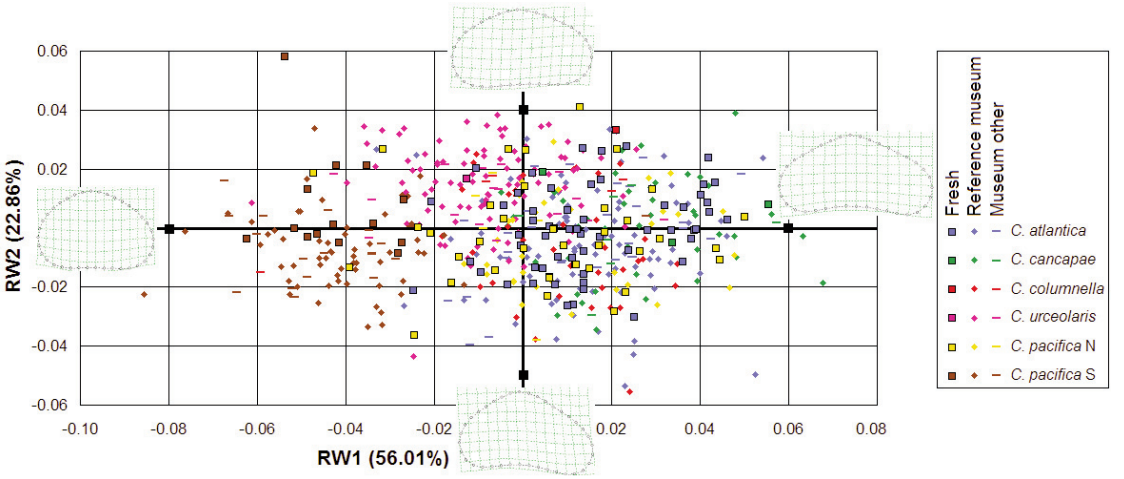

FIGURE S1. Ordination of uncorrected RW data of *Cuvierina* in an apertural orientation. Fresh (*N* = 115), reference museum (*N* = 352) and other museum specimens (*N* = 83) are included. Relative Warp 1 explains 56.01% of the total shape variation; RW2 explains 22.86%. Corresponding thin plate splines of the most positive and negative deformations along the axes are indicated to depict the variation in shell shape. Six distinguished morphotypes are indicated in the legend.

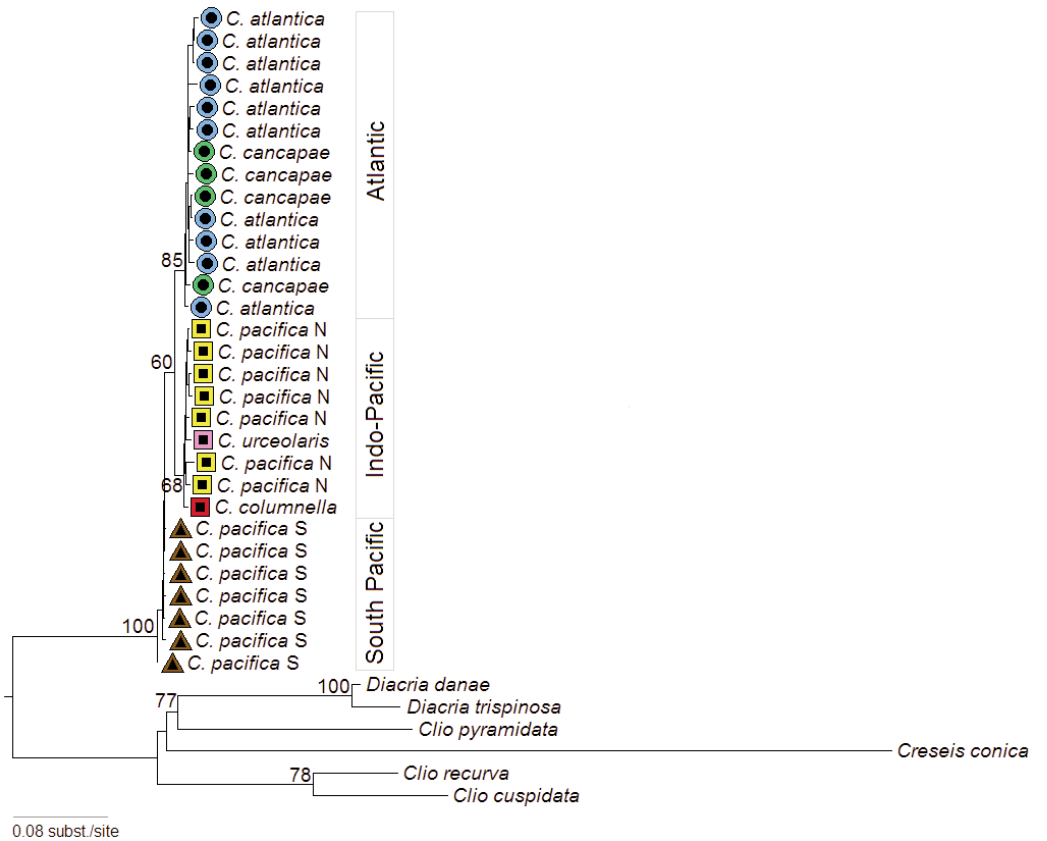

FIGURE S2. Maximum likelihood tree of 30 *Cuvierina* specimens and six outgroup taxa using COI (658bp) and 28S (989bp). Numbers indicate bootstrap support (only bootstrap values of major clades are shown). Symbols for *Cuvierina* indicate major genetic clades; colors indicate distinct morphotypes (also see FIGURE 5).

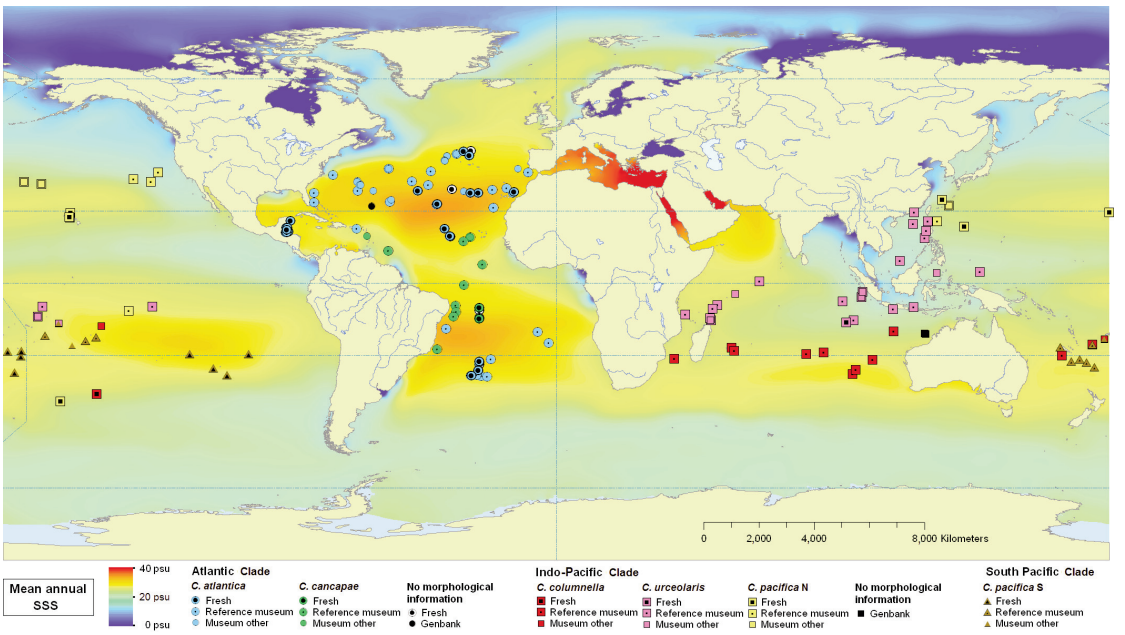

FIGURE S3. Geographic overview of all *Cuvierina* specimens used in this study. Sampling locations are projected on a map of annual average sea surface salinities (SSS; MARSPEC data set, Sbrocco and Barber, 2013). See legend for explanation of symbols and colors.

TABLE S1. Extended summary of *Cuvierina* samples used in this study. Available from http://www.biomedcentral.com/content/supplementary/s12862-015-0310-8-s1.xls

TABLE S2. Pairwise genetic distances within and between *Cuvierina* morphotypes based on COI and 28S. Available from http://www.biomedcentral.com/content/supplementary/s12862-015-0310-8-s4.xls

TABLE S3. Assessment of ecological niche overlap between *Cuvierina* morphotypes using Schoener's *D*.

N		*C. atlantica*	*C. cancapae*	*C. pacifica* S	*C. pacifica* N	*C. columnella*
69	*C. atlantica*					
14	*C. cancapae*	0.406				
20	*C. pacifica* S	0.427	0.489			
20	*C. pacifica* N	0.316	0.436	0.525		
17	*C. columnella*	0.390	0.558	0.714	0.716	
30	*C. urceolaris*	0.194	0.490	0.324	0.481	0.422

4

Revision of the genus *Cuvierina* Boas, 1886 based on integrative taxonomic data, including the description of a new species from the Pacific Ocean (Gastropoda, Thecosomata)

Alice K. Burridge, Arie W. Janssen & Katja T.C.A. Peijnenburg

Abstract

Shelled pteropods (Gastropoda, Thecosomata, Euthecosomata) are a group of holoplanktonic gastropods that occur predominantly in the surface layers of the world's oceans. Accurate species identifications are essential for tracking changes in species assemblages of planktonic gastropods, because different species are expected to have different sensitivities to ocean changes. The genus *Cuvierina* has a worldwide warm water distribution pattern between ~36°N and ~39°S. Based on an integrative taxonomic approach combining morphometric, genetic, and biogeographic information, the two subgenera of *Cuvierina*, *Cuvierina s. str.* and *Urceolarica*, are rejected. A new species is introduced: *Cuvierina tsudai* **sp. n.**, which has to date been considered the same species as *Cuvierina pacifica*. *Cuvierina tsudai* **sp. n.** is endemic to the Pacific Ocean and is characterised by a shell height of 7.2-8.0 mm, a moderately cylindrical shell shape, the absence of micro-ornamentation and a triangular aperture. *Cuvierina pacifica* is restricted to the centre of the oligotrophic southern Pacific gyre, has a shell height of 6.6-8.5 mm, a more cylindrical shell shape, no micro-ornamentation and a less triangular aperture than *C. tsudai* **sp. n.**

Keywords:
Integrative taxonomy, DNA barcoding, Geometric morphometrics, Pteropods, Biogeography

This chapter was published as:
Burridge A.K., Janssen A.W., Peijnenburg K.T.C.A., 2016. Revision of the genus *Cuvierina* Boas, 1886 based on integrative taxonomic data, including the description of a new species from the Pacific Ocean (Gastropoda, Thecosomata). ZooKeys 619, 1-12.

Introduction

Pteropods are holoplanktonic heterobranch gastropods classified in a superorder comprised of the orders Thecosomata and Gymnosomata, commonly referred to as 'sea butterflies' and 'sea angels', respectively (Lalli and Gilmer, 1989; Pierrot-Bults and Peijnenburg, 2015). The order Thecosomata consists of Euthecosomata that have sinistrally coiled or straight, bilaterally symmetrical shells, and Pseudothecosomata that have either sinistrally coiled shells, an internal gelatinous pseudoconch, or are shell-less in the adult stage (Meisenheimer, 1905; Tesch, 1913). Pteropods play an important role in marine food webs (Jörger et al., 2010), and although most species occur in warm tropical and subtropical waters, the highest abundances have been observed for some (sub)polar cold water species (Bé and Gilmer, 1977; Van der Spoel and Heyman, 1983; Bednaršek et al., 2012; Burridge et al., in press: Thesis chapter 6). Because of their thin-walled, aragonite shells, euthecosomes are exceptionally vulnerable to the effects of ocean acidification (e.g., Fabry et al., 2008; Bednaršek and Ohman, 2015; Gattuso et al., 2015; Moya et al., 2016).

The genus *Cuvierina* is a remarkable group of shelled pteropods with relatively large (5.1-11.1 mm), straight, bottle-shaped shells (Janssen, 2005). Ever since *Cuvierina* was described as a mollusc genus (as *Cuvieria* Rang, 1827, emended by Boas, 1886), it has often been considered to consist of a single species, *C. columnella* (Rang, 1827), the type species of the genus by monotypy. The first taxonomic division within the genus came with the description of a second *Cuvierina* species, introduced as *Cuvieria urceolaris* (Mörch, 1850), but in later literature it was often interpreted as a form or subspecies of *C. columnella* (e.g., Tesch, 1913; Van der Spoel, 1967; Rampal, 1975). A third form, *Cuvierina columnella* f. *atlantica*, was described by Van der Spoel (1970), and validated as a taxon of the species group by Bé et al. (1972). Bé and Gilmer (1977) interpreted the morphological differences between the three taxa as infraspecific variability. Contrarily, Rampal (2002) distinguished these taxa as independent species but introduced the taxon *C. spoeli* to replace the taxonomically invalid *Cuvierina columnella* f. *atlantica*. Because the holotype of *C. spoeli* was from the Indian Ocean, where *C. atlantica* is absent, it rather represented *C. columnella* and was rejected as a valid species by Janssen (2005). Two further extant species, *C. cancapae* and *C. pacifica*, were described by Janssen (2005).

According to the most recent taxonomic revision of *Cuvierina*, five extant species were assigned to two subgenera based on shell morphology and supposed lineages of fossil occurrences since the early Miocene (Janssen, 2005, 2006). The subgenus *Cuvierina s. str.* consisted of *C. atlantica*, *C. columnella*, and *C. pacifica*, which are characterised by relatively slender, cylindrical shells, triangular rather than kidney-shaped apertures and the presence (*C. columnella*) or absence (*C. atlantica, C. pacifica*) of micro-ornamentation. Two geographical varieties were recognised within *C. pacifica*, one from the North Pacific and the other from the South Pacific, but were not formally introduced as new species. The subgenus

Urceolarica, containing *C. cancapae* and *C. urceolaris*, is characterised by more inflated, bottle-shaped rather than cylindrical shells, pronounced micro-ornamentation, and kidney-shaped rather than triangular apertures.

All extant *Cuvierina* species are restricted to the surface layers of tropical and subtropical waters from ~45°N to ~40°S. In the Atlantic Ocean, *C. atlantica* occurs in the subtropical gyres and *C. cancapae* is found in tropical waters. In the Indian Ocean, *C. columnella* is found in the southern subtropical zone and *C. urceolaris* occurs in tropical waters and further south along Madagascar towards South Africa. *Cuvierina columnella* and *C. urceolaris* also occur in the Pacific Ocean along with *C. pacifica* (Janssen, 2005; Burridge et al., 2015: Thesis chapter 3).

Burridge et al. (2015: Thesis chapter 3) examined the diversity, distribution, and evolution of *Cuvierina* taxa using integrative geometric morphometric, molecular, and biogeographic methods. They confirmed that the five species described for *Cuvierina* species have significantly different shell shapes and that *C. pacifica* consists of two disjunct morphometric groups, registered as *C. pacifica* N and *C. pacifica* S in their study. Three genetic lineages were distinguished based on mitochondrial Cytochrome Oxidase I DNA: the Atlantic lineage with *C. atlantica* and *C. cancapae*, the Indo-Pacific lineage with *C. columnella*, *C. urceolaris*, and *C. pacifica* N, and the South Pacific lineage with *C. pacifica* S. A new taxonomic description of *C. pacifica* N is required because the holotype of *C. pacifica* has the shell shape of *C. pacifica* S.

Based on the findings of Janssen (2005) and the integrative approach of Burridge et al. (2015: Thesis chapter 3) the taxonomy of the genus *Cuvierina* is revised. The subgenera *Cuvierina s. str.* and *Urceolarica* are rejected, a new species, *C. tsudai*, is described from the Pacific Ocean, and the species description of *C. pacifica* is restricted to the South Pacific lineage. A taxonomic key is provided for the identification of *Cuvierina* species.

Methods

Two approaches were used to distinguish between *C. tsudai* and *C. pacifica* based on differences in shell shape. First, simple measurements of shell height and width, aperture diameters, and position of maximum shell width as applied to museum specimens by Janssen (2005) were used to distinguish between *C. tsudai* and *C. pacifica*. Second, geometric morphometric data of shell shapes in ventral and apertural orientations were used for 168 adult specimens of *Cuvierina* that were registered as *C. pacifica* N or *C. pacifica* S in Burridge et al. (2015: Thesis chapter 3). The specimens corresponded to museum specimens as identified and measured by Janssen (2005, *N* = 92), additional museum specimens (*N* = 24), and recently collected fresh specimens (*N* = 52). Geometric morphometric methods consisted of digitising shell outlines using tpsDig and tpsUtil (Rohlf, 2006) to contain 76 ventral and 37 apertural semi-landmarks per shell, after which a generalised least square Procrustes superimposition was applied (GLS, Kendall, 1977 in Zelditch et al., 2004) to rotate, translate, and scale the semi-landmark coordinates. A subsequent thin-plate spline (TPS) analysis (e.g., Zelditch et al., 2004) provided centroid sizes, a size

measure depending on surface area, and multiple relative warp axes per specimen, containing information on shape. To describe the new species *C. tsudai* as well as to reject the validity of the *Cuvierina* subgenera, Cytochrome Oxidase I mitochondrial (COI) DNA and 28S ribosomal DNA sequence data from Burridge et al. (2015: Thesis chapter 3) were used.

Results and discussion

Distinction between *Cuvierina tsudai* and *C. pacifica*

Cuvierina tsudai and *C. pacifica* are similar in size but have different shell shapes, COI mtDNA and 28S rDNA. Because of their Pacific distributions and similarities in shell size, *C. tsudai* and *C. pacifica* have to date been considered the same species. Although Janssen (2005) demonstrated their presence as morphological varieties within *C. pacifica*, the congruence between morphometric and genetic differentiation supports the separation into two species (Figures 1A-J and 2; figure 4 in Burridge et al., 2015: Thesis chapter 3). Shell heights of *C. tsudai* specimens are between 7.2 and 8.8 mm, showing a large overlap with *C. pacifica*, which measures between 6.6 and 8.5 mm (Janssen, 2005). However, in terms of shell shape, *C. pacifica* and *C. tsudai* are significantly different (figure 29 lower left in Janssen, 2005; Burridge et al., 2015: Thesis chapter 3). The shell of *C. tsudai* is wider (more inflated) than the slender and more cylindrical *C. pacifica* (Figure 2). *Cuvierina pacifica* has a larger height/width-ratio between 3.25 and 3.96 (mean 3.50) compared to *C. tsudai*, which has a ratio between 2.77 and 3.46 (mean 3.14). The position of maximum shell width is located at 34-45% (mean 40%) of the shell height from the septum upwards for *C.*

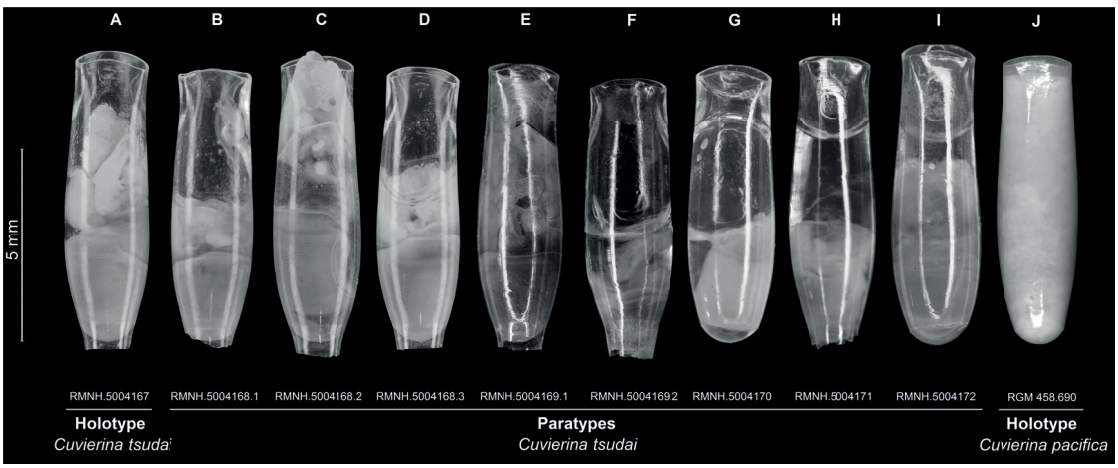

Figure 1. Holotype and paratypes of *C. tsudai* and holotype of *C. pacifica*. A Holotype (RMNH.5004167) and B-I paratypes (RMNH.5004168-72) of *C. tsudai* and J holotype of *C. pacifica* (RGM 458.690) photographed in a ventral view. Photographs of RMNH.5004169-72 from Burridge et al. (2015); RMNH.5004167-68 taken by R. van der Hulst and RGM 458.692 taken by E.F. de Vogel, this study. RMNH = Naturalis Biodiversity Center, mollusc collection and RGM = Naturalis Biodiversity Center, fossil planktonic mollusc collection, Leiden.

pacifica and at 33-42% (mean 37%) for *C. tsudai* (Janssen, 2005). The aperture of *C. tsudai* is wider, more triangular and more concave on the ventral side than in *C. pacifica*. The overall shape variation is larger for *C. tsudai* than for *C. pacifica* (Figure 2). The average pairwise genetic distance of COI mtDNA (658bp fragment) between *C. tsudai* (*N* = 16) and *C. pacifica* (*N* = 43) is 4.5%. The genetic variation of COI within *C. tsudai* is 1.6% compared to 0.8% within *C. pacifica*. The 28S rDNA fragment (965bp) of *C. tsudai* differs at least at one position compared with other *Cuvierina* species, except for *C. columnella* (Burridge et al., 2015: Thesis chapter 3).

The larger genetic and shell shape variation for *C. tsudai* compared to *C. pacifica* coincides with a much larger Pacific distribution and lower ecological specificity of *C. tsudai*. *Cuvierina pacifica* is restricted to the centre of the oligotrophic

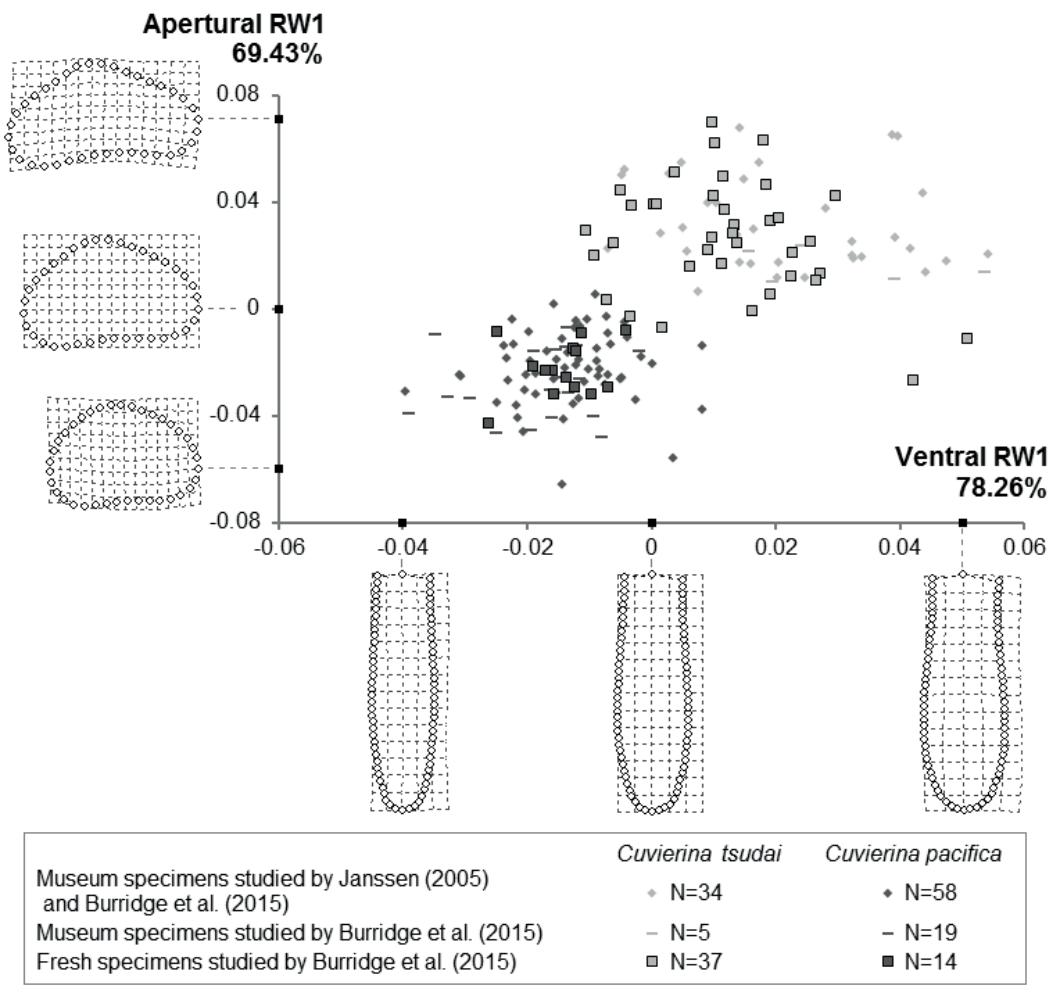

Figure 2. Shape variation in *C. tsudai* and *C. pacifica* by means of Relative Warp (RW) data. Ordination of RW data of *C. tsudai* and *C. pacifica* for the first ventral and apertural RWs (*N* = 167 excluding one specimen with only one orientation). On the X-axis, RW1 depicts 78.26% of the total ventral shape variation. On the Y-axis, 69.43% of the apertural shape variation is explained by its RW1. Shape variations depicted by ventral and apertural RW1 (with subsequent RWs = 0) are shown.

southern Pacific gyre and occupies a more specialised ecological niche based on ecological niche modelling (ENM) than *C. tsudai* (Burridge et al., 2015: Thesis chapter 3). This study used presence-only data and six uncorrelated environmental parameters, of which ocean surface temperature and chlorophyll *a* concentration were the most important. The distribution of *C. tsudai* was mostly explained by maximum monthly sea surface temperatures (SST) and near-surface chlorophyll *a* concentrations (both 30.8%). The distribution of *C. pacifica* was best explained by low maximum monthly chlorophyll *a* concentrations (57.1%).

Description of *Cuvierina tsudai* sp. n.

Superfamily Cavolinioidea Gray, 1840
Family Cuvierinidae Gray, 1840
Genus *Cuvierina* Boas, 1886 (= replacement name for *Cuvieria* Rang, 1827 non Lesueur & Petit, 1807, pl. 30 (Coelenterata))
Type species. *Cuvieria columnella* Rang, 1827, p. 323, pl. 45 figures 1-3, by monotypy.

Cuvierina tsudai sp. n.

http://zoobank.org/B33A28E9-BCDE-4F2B-9349-F3E18CCD87BE

Cuvieria columnella Rang, 1827: 323 (partim).

Cuvierina columnella: Boas, 1886: 132, 217, pl. 6 figure 95g (*partim*, *non* Rang); Rampal, 2002: 214 (*partim*, *non* Rang).

Cuvierina columnella (Rang, 1827) forma *columnella* (Rang, 1827) – Van der Spoel, 1967: 79 (*partim, non* Rang); Van der Spoel, 1970: 120, figure 19 (*partim*, *non* Rang).

Cuvierina (Cuvierina) pacifica Janssen, 2005: 46, figures 18-20 (*partim*, northern Pacific specimens only, *non* figures 14-17 = *C. pacifica*).

Cuvierina pacifica N (Janssen, 2005): Burridge et al., 2015: 5, figure 2.

Holotype. RMNH.5004167, also see Figure 1A and Table 1.
Type locality. 8°47'N, 158°49'W.
Paratypes. See Figure 1B-I and Table 1 for all specimen information. Three specimens from the type locality (RMNH.5004168); three specimens from the Zoological Museum of the University of Copenhagen, Denmark (ZMUC, not registered) illustrated by Janssen (2005, figures 18-20); five specimens from four locations (RMNH.5004169-72) studied by Burridge et al. (2015: Thesis chapter 3, referred to as *C. pacifica* N therein). The latter five specimens have COI mtDNA and 28S rDNA sequences available at GenBank (see Table 1).
Additional material examined. Specimens recorded as *C. pacifica* from the North Pacific Ocean in Janssen (2005: 49, 71), housed in the Muséum National d'Histoire Naturelle (MNHN, Paris, France) and ZMUC (Copenhagen, Denmark). Specimens from Burridge et al. (2015: Thesis chapter 3), referred to as *C. pacifica* N in Table S1 therein, with photographs deposited at the Dryad repository (DOI: 10.5061/dryad.7n1q4) and COI mtDNA (KP292730-72) and 28S rDNA sequences (KP292636-42)

Table 1. Voucher and sampling information of type specimens of *C. tsudai* including the holotype of *C. pacifica*.

Museum voucher	Image voucher	Collection date	Latitude	Longitude
Holotype of *C. tsudai*				
RMNH.5004167	C_PNE_SE1201_21_01	2012-05-15	8°47'N	158°49'W
Paratypes of *C. tsudai*				
RMNH.5004168.1	C_PNE_SE1201_21_02	2012-05-15	8°47'N	158°49'W
RMNH.5004168.2	C_PNE_SE1201_21_03	2012-05-15	8°47'N	158°49'W
RMNH.5004168.3	C_PNE_SE1201_21_04	2012-05-15	8°47'N	158°49'W
RMNH.5004169.1	C_PNE_KH1110_08_01	2011-12-19	22°47'N	158°06'W
RMNH.5004169.2	C_PNE_KH1110_08_20	2011-12-19	22°47'N	158°06'W
RMNH.5004170	C_PNE_KM1109_02_02	2011-03-04	21°14'N	158°11'W
RMNH.5004171	C_PNE_KM1109_08_01	2011-03-06	21°20'N	158°22'W
RMNH.5004172	C_PNW_TMKT1020_05_01	2010-09-29	27°08'N	125°33'E
ZMUC, not registered	Figure 18	1933-08-21	33°45'N	137°30'W
ZMUC, not registered	Figure 19	1934-02-12	32°56'N	131°50'W
ZMUC, not registered	Figure 20	1929-05-25	20°04'N	125°59'E
Holotype of *C. pacifica*				
RGM 458.692	Figure 15	1986-04/05	18°39'S	172°12'W

deposited at GenBank. These specimens are housed in Naturalis Biodiversity Center (Leiden, The Netherlands) and ZMUC (Copenhagen, Denmark). Registration numbers, if available, from Janssen (2005).

Diagnosis. Shell moderately small, adult specimens 7.2-8.8 mm high, height/width-ratio 2.77-3.46 (mean 3.14), position of maximum shell width 33-42% (mean 37%) of shell height from septum upwards. Aperture triangular. No longitudinal micro-ornamentation.

Description. The shell shape of *Cuvierina tsudai* differs from other *Cuvierina* species. Its shell height is smaller than in *C. columnella*, *C. cancapae*, and *C. atlantica*, but larger than in *C. urceolaris*, and of similar size compared to *C. pacifica*. The position of maximum shell width is distinctly higher than for *C. columnella* and *C. atlantica* and lower than for *C. pacifica*. It is more cylindrical in shape than the inflated (bottle-shaped) *C. urceolaris* but less cylindrical than *C. atlantica* and *C. pacifica*. It differs from *C. urceolaris* and *C. cancapae* by the absence of micro-ornamentation. It has a more triangular and wider aperture than *C. urceolaris* and *C. pacifica* (Figure 3; Janssen, 2005; Burridge et al., 2015: Thesis chapter 3).

Distribution. *Cuvierina tsudai* has a wide, exclusively Pacific distribution between 36°N and 39°S, in which it co-exists with *C. columnella*, *C. urceolaris*, and *C. pacifica*. It has been found most often in the North Pacific, but also occurs in the South Pacific. It has not been found thus far in the central, oligotrophic parts of the South Pacific subtropical gyre, the southeast Pacific, the coral triangle west of the Philippines or southwest of Papua New Guinea.

Etymology. Named after Atsushi Tsuda, professor in biological oceanography at the University of Tokyo, Japan, for sending us pteropod samples from the Pacific Ocean and in recognition of his services to the zooplankton research community.

Cruise	Station	COI GenBank	28S GenBank	First studied
SE1201	21			This study
SE1201	21			This study
SE1201	21			This study
SE1201	21			This study
KH-11-10	8	KP292730	KP292636	Burridge et al., 2015
KH-11-10	8	KP292748	KP292637	Burridge et al., 2015
Kilo Moana 1109	2	KP292755	KP292639	Burridge et al., 2015
Kilo Moana 1109	8	KP292759	KP292640	Burridge et al., 2015
R/V Tansei-Maru KT-10-20	5	KP292766	KP292642	Burridge et al., 2015
DANA	4794			Janssen, 2005
DANA	4807			Janssen, 2005
DANA	3718 V			Janssen, 2005
Manihiki Plateau Expedition	U351a			Janssen, 2005

Rejection of the subgenera *Cuvierina*

Two subgenera of *Cuvierina* were described that supposedly evolved since the early Miocene (Aquitanian, 23 million years ago): *Cuvierina s. str.*, with extant species *C. atlantica*, *C. columnella*, and *C. pacifica*, and *Urceolarica* with extant species *C. cancapae* and *C. urceolaris* (see Janssen, 2005, 2006). They were based on distinguishing shell characteristics in fossil species such as the position of maximum shell width, aperture shape and presence or absence of micro-ornamentation. However, the morphology and molecular phylogenetic information of recent species are in conflict with this separation. *Cuvierina columnella*, typically a *Cuvierina s. str.* species, has distinct micro-ornamentation, which was considered one of the distinguishing characters of the subgenus *Urceolarica*. It was shown that there are three divergent and well-supported lineages based on genetic data: the Atlantic (*C. atlantica* and *C. cancapae*), Indo-Pacific (*C. columnella*, *C. urceolaris* and *C. tsudai*), and South Pacific (*C. pacifica*) lineages (figure 4 in Burridge et al., 2015: Thesis chapter 3). Hence, we reject the two subgenera within *Cuvierina*.

Taxonomic key to *Cuvierina* pteropods

The following taxonomic key identifies adult *Cuvierina* pteropod species based on distinctive shell shape characteristics and shell sizes. Photographs of typical adult shells are shown in Figure 3.

1	Micro-ornamentation present	2
–	Micro-ornamentation absent	4
2	Strongly inflated shell shape, shell height 5.1-6.7 mm	*C. urceolaris*
–	Moderately inflated or cylindrical shell shape, shell height 7.5-11.1 mm	3

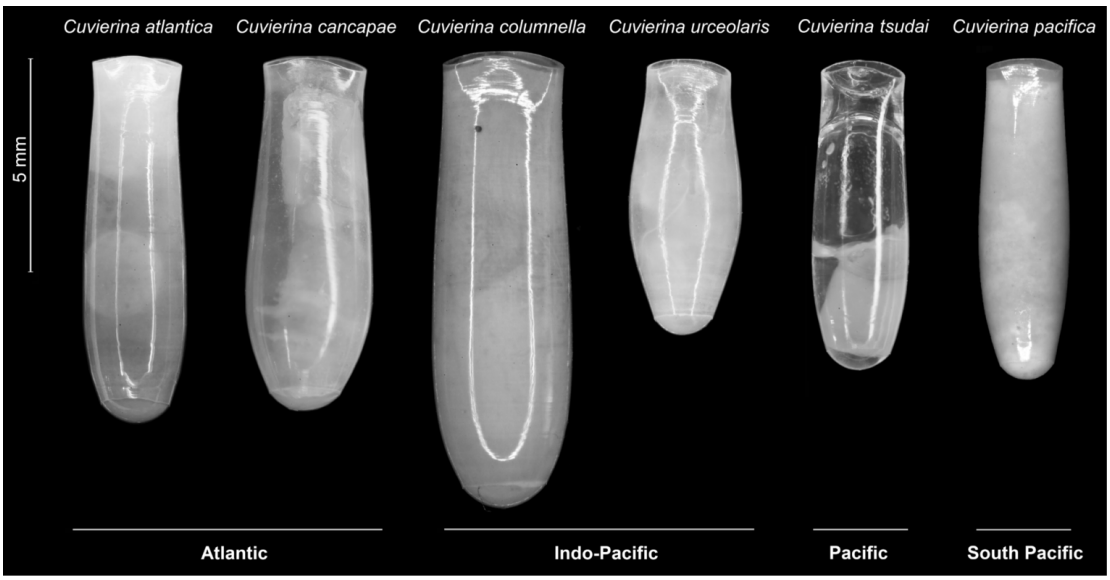

FIGURE 3. Typical specimens of six *Cuvierina* species.

3	Cylindrical shell shape, shell height 8.8-11.1 mm	*C. columnella*
–	Moderately inflated shell shape, shell height 7.5-9.3 mm	*C. cancapae*
4	Cylindrical shell shape and triangular aperture, shell height 6.7-10.5 mm	*C. atlantica*
–	Moderately inflated or cylindrical shell shape, triangular to kidney-shaped aperture, shell height 6.6-8.8 mm	5
5	Cylindrical shell shape and kidney-shaped aperture, shell height 6.6-8.5 mm	*C. pacifica*
–	Moderately inflated shell shape and triangular aperture, shell height 7.2-8.8 mm	*C. tsudai*

CONCLUSIONS

Morphometric, genetic, and biogeographic information has led to the introduction of a new species of the warm water pteropod genus *Cuvierina* and the rejection of its subgenera. We encourage a combined evidence approach of taxonomy to more accurately identify species boundaries and higher taxonomic relationships in planktonic gastropods. Accurate taxonomic identification is a prerequisite to assess to what extent species are affected by ocean changes and to potentially use them as bioindicators.

ACKNOWLEDGEMENTS

We thank A. Tsuda, H. Miyamoto, E. Goetze, D. Kobayashi, L. Giuseffi, and E. Norton for contributing specimens from the Pacific Ocean, R. van der Hulst and E.F. de Vogel for photographing the holotype and some paratypes of *C. tsudai*, and J. Goud and B. van der Bijl for adding the type material to the collections of Naturalis Biodiversity Center. Finally, we are grateful to Deborah Wall-Palmer, Maria Moreno-Alcántara and Nathalie Yonow for constructive comments on this manuscript.

References

Bé A.W.H., Gilmer R.W., 1977. A zoogeographic and taxonomic review of euthecosomatous Pteropoda. In: Ramsay A.T.S. (Ed.), Oceanic Micropaleontology 1. Academic Press, London, pp. 733–808.

Bé A.W.H., MacClintock C., Currie D.C., 1972. Helical shell structure and growth of the pteropod *Cuvierina columnella* (Rang) (Mollusca, Gastropoda). Biomineralization Research Reports 4, 47–79.

Bednaršek N., Možina J., Vogt M., O'Brien C., Tarling G.A., 2012. The global distribution of pteropods and their contribution to carbonate and carbon biomass in the modern ocean. Earth System Science Data 4, 167–186.

Bednaršek N., Ohman M.D., 2015. Changes in pteropod distributions and shell dissolution across a frontal system in the California Current System. Marine Ecology Progress Series 523, 93–103.

Boas J.E.V., 1886. *Spolia atlantica*. Bidrag til Pteropodernes. Morfologi og Systematik samt til Kundskaben om deres geografiske Udbredelse. Videnskabernes Selskap Skrifter 6. Naturvidenskabelig og mathematisk Afdeling 4, 1–231.

Burridge A.K., Goetze E., Raes N., Huisman J., Peijnenburg K.T.C.A., 2015. Global biogeography and evolution of *Cuvierina* pteropods. BMC Evolutionary Biology 15, 39. *Thesis chapter 3.*

Burridge A.K., Goetze E., Wall-Palmer D., Le Double S.L., Huisman J., Peijnenburg K.T.C.A., in press. Diversity and abundance of pteropods and heteropods along a latitudinal gradient across the Atlantic Ocean. Progress in Oceanography, published online in 2016. *Thesis chapter 6.*

Fabry V.J., Seibel B.A., Feely R.A., Orr J.C., 2008. Impacts of ocean acidification on marine fauna and ecosystem processes. ICES Journal of Marine Science 65, 414–432.

Gattuso J.-P., Magnan A., Billé R., Cheung W.W.L., Howes E.L., et al., 2015. Contrasting futures for ocean and society from different anthropogenic CO_2 emissions scenarios. Science 349, 1–10.

Gray J.E., 1840. Shells of molluscous animals. In: Synopsis of the contents of the British Museum, 42, 105–152.

Janssen A.W., 2005. Development of Cuvierinidae (Mollusca, Euthecosomata, Cavolinioidea) during the Cainozoic: a non-cladistic approach with a re-interpretation of Recent taxa. Basteria 69, 25–72.

Janssen A.W., 2006. Notes on the systematics, morphology and biostratigraphy of fossil holoplanktonic Mollusca, 16. Some additional notes and amendments on Cuvierinidae and on classification of Thecosomata (Mollusca, Euthecosomata). Basteria 70, 67–70.

Jörger K.M., Stöger I., Kano Y., Fukuda H., Knebelsberger T., Schrödl M., 2010. On the origin of Acochlidia and other enigmatic euthyneuran gastropods, with implications for the systematics of Heterobranchia. BMC Evolutionary Biology 10, 323.

Kendall D., 1977. The diffusion of shape. Advances in Applied Probability 9, 428–430.

Lalli C.M., Gilmer R.W., 1989. Pelagic Snails: The Biology of Holoplanktonic Gastropod Molluscs. Stanford University Press, Stanford, California.

Lesueur C.A., Petit N., 1807. Voyage de découvertes aus terres Australes exécuté par ordre de S. M. l'Empereur et Roi. Langlois, Paris; atlas, part 1, 40 pls.

Meisenheimer J., 1906. Pteropoda. Wissenschaftliche Ergebnisse der Deutschen 769 Tiefsee-Expedition auf dem Dampfer 'Valdivia' 1898-1899, 9, 314 pp.

Mörch O.A.L., 1850. Catalogus conchyliorum quae reliquit C.P. Kierulf, md. dr. nunc publica auctione X Decembris MDCCCL Hafniae Dividenda. Hafniae, Trieri.

Moya A., Howes E.L., Lacoue-Labarthe T., Forêt S., Bishoy H. et al., 2016. Near-future pH conditions severely impact calcification, metabolism and the nervous system in the pteropod *Heliconoides inflatus*. Global Change Biology 22, 3888–3900.

Pierrot-Bults A.C., Peijnenburg K.T.C.A., 2015. Pteropods. In: Harff J., Meschede M., Petersen S., Thiede J. (Eds.), Encyclopedia of marine geosciences. Springer, Dordrecht, pp. 1–10.

Rampal J., 1975. Les thécosomes (mollusques pélagiques). Systématique et évolution–écologie et biogéographie méditerranéennes. PhD thesis, Université de Provence, U.E.R. Scientifiques (Aix-Marseille 1).

Rampal J., 2002. Biodiversité et biogéographie chez les Cavoliniidae (Mollusca, Gastropoda, Opisthobranchia, Euthecosomata). Régions faunistiques marines. Zoosystema 24, 209–258.

Rang P.C.A.L., 1827. Description de deux genres nouveaux (*Cuvieria* et *Euribia*) appartenant à la classe des ptéropodes. Annales des Sciences Naturelles 12, 320–329. [pl. 45B dated 1826]

Rohlf F.J., 2006. Tps series. http://life.bio.sunysb.edu/morph

Tesch J.J., 1913. Mollusca, Pteropoda. In: Schulze F.E. (Ed.), Das Tierreich. Eine Zusammenstellung und Kennzeichnung der rezenten Tierformen, 36. Friedländer & Sohn, Berlin.

Van der Spoel S., 1967. Euthecosomata, a group with remarkable developmental stages (Gastropoda, Pteropoda). PhD thesis, University of Amsterdam. Noorduijn en Zoon, Gorinchem.

Van der Spoel S., 1970. Morphometric data on Cavoliniidae, with notes on a new form of *Cuvierina columnella* (Rang, 1827) (Gastropoda, Pteropoda). Basteria 34: 103–151.

Van der Spoel S., Heyman R.P., 1983. A Comparative Atlas of Zooplankton: Biological Patterns in the Oceans. Springer, New York.

Zelditch M.L., Swiderski D.L., Sheets H.D., Fink W.L., 2004. Geometric morphometrics for biologists. Elsevier Academic Press, San Diego and London.

5

Assessing species boundaries in the open sea: applying an integrative taxonomic approach to a genus of pelagic molluscs

Alice K. Burridge, Remy van der Hulst,
Erica Goetze & Katja T.C.A. Peijnenburg

Abstract

To track changes in pelagic biodiversity in response to ocean change, it is essential to accurately define species boundaries using integrative taxonomic methods based on diverse data types. A particularly suitable, yet challenging, group for integrative taxonomy is the pteropod genus *Diacavolinia*, shelled holoplanktonic gastropods with a circumglobal distribution. With 24 described species, they are the most speciose pteropod genus. We applied an integrative approach to assess species boundaries in this genus, with inferences based on congruence between geometric morphometric analyses of shell shape variation, genetic data (cytochrome *c* oxidase subunit I, 28S rRNA sequences), and geographic data. With observations on 969 museum and freshly-collected specimens, including holo- or paratype specimens for 14 taxa, we found evidence for a reduction in the number of described species from 24 to a maximum of 13 species. In the Atlantic Ocean, two species were well-supported in contrast to eight currently described, and in the Indo-Pacific we found a maximum of 11 species, comprising 13 of the described species. The higher species diversity in the Indo-Pacific compared to the Atlantic Ocean supports the hypothesis of an Indo-Pacific origin for *Diacavolinia* pteropods. The most important biogeographic barriers for the distribution of species were between the Atlantic and Indo-Pacific oceans, and between the East and Central Pacific. Biogeographic distributions of revised *Diacavolinia* species were as follows: Atlantic (two endemic species), warm waters south of South Africa (one endemic species), Western Indian Ocean (four species), Red Sea and Gulf of Aden (three species), Indo-West Pacific (six species, one endemic), Hawaiian waters (three species, one endemic), Sino-Japanese waters (three species), and the Eastern Tropical Pacific (three endemic species). These distributions were congruent with several well-known biogeographic provinces, and provide important information on the range of environmental variation experienced by each species. Our integrative taxonomic framework enabled more accurate assessment of species boundaries in *Diacavolinia*, a crucial step to assessing the diversity, distributions, and impact of ocean changes on these important bioindicators of ocean acidification.

Keywords:
Zooplankton, Pteropods, Integrative taxonomy, Biogeography, Geometric morphometrics, mtCOI, 28S rRNA

This chapter is to be submitted

Introduction

Integrative taxonomy aims to rigorously delimit species and prevent under- or overestimation of species numbers by statistically testing species hypotheses with diverse, sometimes incomplete, character and data types (Edwards and Knowles, 2014; Karanovic et al., 2016). An increasing number of species is described each year as a result of the incorporation of new tools for species discovery, including virtual access to museum collections, advances in DNA sequencing, morphometric methods, and geographic information systems (Vogler and Monaghan, 2006; Knapp, 2008). Such tools have enabled integrative taxonomic approaches, in which species are described based on congruence between morphological and genetic information, with additional supporting characteristics such as behavior, ecology, or geography (McManus and Katz, 2009; Padial et al., 2010; Smith and Hendricks, 2013; Edwards and Knowles, 2014). Statistical identification of genetic lineages plays a pivotal role in species detection and satisfies multiple species concepts, because it treats species as hypotheses using objective tests (De Queiroz, 2007; Hausdorf, 2011; Morard et al., 2016). However, the usefulness of statistical approaches in the taxonomic description of species remains under debate (e.g., Bauer et al., 2011; Fujita and Leaché, 2011; Fujita et al., 2012). The sole use of genetic information in species delimitation may fail to detect the same number of species as methods that combine multiple lines of evidence (Edwards and Knowles, 2014; Burridge et al., 2015: Thesis chapter 3; Karanovic et al., 2016). Species may go undetected based on a limited set of selected genetic markers, because they may be distinct only in other genes, morphology, or ecological niche space. Advances in geometric morphometric methods may especially benefit studies based on incomplete datasets, such as fossil taxa and valuable museum specimens for which genetic information could not be obtained (Karanovic et al., 2016). Developing integrative taxonomic frameworks for assessing species boundaries will enable the inclusion of museum specimens originally used to describe species combined with fresh samples for which genetic information is available.

Tracking changes in marine biodiversity in response to ocean change on a global scale requires accurate assessment of species boundaries and distributions (e.g., Goetze and Ohman, 2010; Burridge et al., 2015: Thesis chapter 3; Wall-Palmer et al., 2016). Range shifts of planktonic taxa have been among the most rapid, have occurred over the largest spatial scales in comparison to other marine and terrestrial groups, and may affect higher trophic levels in the marine food web (Richardson, 2008; Beaugrand et al., 2012, 2014, 2015; Parmesan et al., 2013; Brown et al., 2016). Plankton distributions are often concordant with biogeochemical provinces at the level of species and communities (e.g., Valentin and Monteiro-Ribas, 1993; Longhurst, 1998; Reygondeau et al., 2013; Dolan et al., 2016; Burridge et al., in press: Thesis chapter 6, in press: Thesis chapter 7), as well as at the level of population genetic structure within species (e.g., Norton and Goetze, 2013; Goetze et al., 2015, in press; Hirai et al., 2015). Persistent dispersal barriers may limit range shifts of some taxa in response to changing ocean conditions, while

other taxa may be able to adapt and occupy new ecological niches. Integrative taxonomy will improve the accuracy of marine species delimitation, enable the identification of rare taxa, and provide insights in current species distributions. It may be applied to a wide array of morphologically diverse marine taxa and is an essential first step to predicting species-specific ecological and evolutionary responses to ocean change, for example using Ecological Niche Modelling (Elith and Leathwick, 2009; Dambach and Rödder, 2011; Robinson et al., 2011).

Holoplanktonic gastropods are a marine group that has been identified as exceptionally vulnerable to ocean acidification (Fabry et al., 2008; Bednaršek et al., 2016). Euthecosome pteropods have aragonitic shells, and form a diverse group of organisms that are common in marine zooplankton from polar to equatorial pelagic habitats (Lalli and Gilmer, 1989). Pteropods have an extensive fossil record (Janssen, 2007a,b, 2012), and are commonly used to explore the effects of ocean acidification on marine life (Roger et al., 2011; Comeau et al., 2012; Bednaršek and Ohman, 2015; Maas et al., 2016; Moya et al., 2016). However, their usefulness as bio-indicators of the effects of ocean acidification is compromised by limited historical context for understanding species-specific long-term exposure to variations in ocean chemistry. Accurate knowledge of their taxonomy, genetic diversity, and biogeography is the essential first step to predicting ecological and evolutionary responses to ocean change.

We illustrate an integrative taxonomic approach using shelled pteropods of the genus *Diacavolinia*, which have particularly problematic systematics and are usually not identified below genus level, or are listed as *Cavolinia* sp. or *Diacavolinia longirostris* in recent studies (Jennings et al., 2010; Roger et al., 2011; Corse et al., 2013). A new taxonomic assessment of species boundaries in *Diacavolinia* pteropods is important because they are morphologically diverse, and some taxa occur in low pH regions, including the California Current coastal upwelling ecosystem (Maas et al., 2013). A study of *Diacavolinia* pteropods from Australian tropical waters found a significant increase in shell porosity along with a 10% local decline of the aragonite saturation level between the 1960s and 2000s (Roger et al., 2011), suggesting sensitivity of this taxon to contemporary changes in the ocean's aragonite saturation state.

Previously known as a single species within *Cavolinia* (*Cavolinia longirostris*), *Diacavolinia* was described as a separate genus by Van der Spoel (1987) on the basis of a distinct shell shape and shell growth compared to *Cavolinia* taxa. *Diacavolinia* is the most speciose genus of pteropods with a total of 24 extant species, of which 18 were introduced by Van der Spoel et al. (1993). Species boundaries were primarily based on shell size and small variations in shell shape that were sometimes found among sympatric taxa. *Diacavolinia* taxa occur in tropical and subtropical waters between ~17-28°C in the Atlantic, Pacific, and Indian oceans and the Red Sea, at depths of ~200 m by day and ~75 m at night across oceans (Wormelle, 1962; Van der Spoel, 1967; Bé and Gilmer, 1977). They have complex, bilaterally symmetrical shells (0.4-1.2 cm adult size), and adult shells are

easily distinguished from juveniles (Van der Spoel et al., 1993). This enables detailed geometric morphometric analyses of shell shape, which can be a very powerful tool for distinguishing taxa (Mitteroecker and Gunz, 2009; Klingenberg, 2010). Maas et al. (2013) distinguished four *Diacavolinia* species from the Northeast Atlantic and one from the Eastern Tropical Pacific based on morphological characteristics. However, they observed that Atlantic specimens were not genetically distinct (<3% divergence), whereas specimens from the Atlantic and Pacific were much more divergent (~19% divergence) based on a fragment of the cytochrome *c* oxidase subunit I mitochondrial gene (COI). The authors concluded that broader geographic sampling and a combination of genetic and morphological information were needed to resolve species boundaries in this genus (Maas et al., 2013).

We apply an integrative approach to assess species boundaries in *Diacavolinia*, with inferences based on congruence between genetic, geometric morphometric, and geographic data (Figure 1). To identify as many species as possible, we link datasets comprising fresh specimens for which both genetic and morphometric information is available to morphometric information from museum specimens (969 specimens), including holo- and/or paratype specimens from 14 species. We aim to (1) develop an objective method for identifying species boundaries by combining incomplete and varied datasets; (2) assess species boundaries and distribution patterns of *Diacavolinia* taxa by applying an integrative framework of genetic, morphometric, and geographic information; and (3) examine consistency of results obtained with this framework across the 24 *Diacavolinia* taxa as described by Van der Spoel et al. (1993). We find evidence to support a reduction in the number of *Diacavolinia* species, with at least eight of the species described

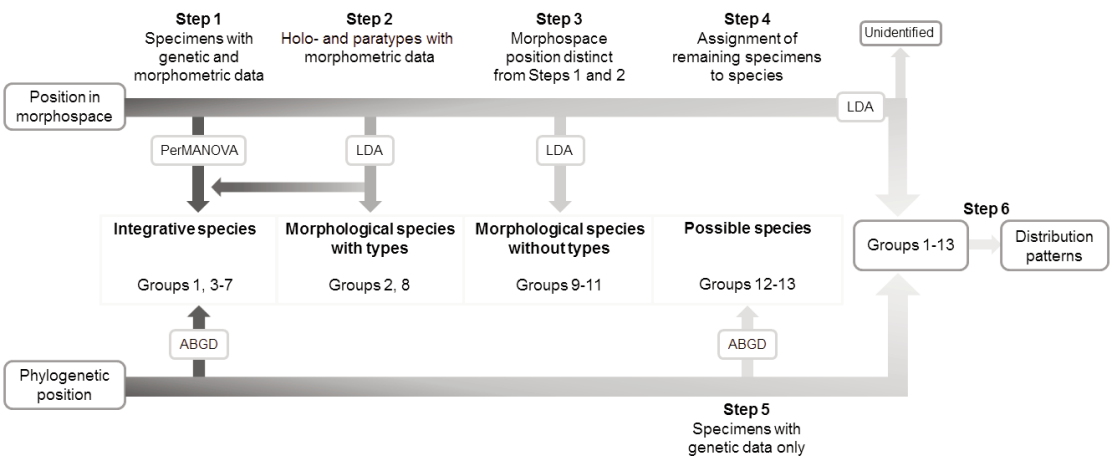

Figure 1. Schematic overview of the integrative taxonomic approach as applied to *Diacavolinia* pteropods. Distinct groups that are identified in each step are indicated. Phylogenetic position was determined based on Cytochrome *c* Oxidase I (COI) and 28S molecular markers. LDA = Linear Discriminant Analysis; PerMANOVA = non-parametric permutational multivariate analysis of variance; ABGD = Automatic Barcode Gap Discovery.

by Van der Spoel likely representing taxonomic over-splitting. We provide systematic and biogeographic descriptions of the global component of species in this complex genus.

Materials and methods

Specimens

969 *Diacavolinia* specimens were included in this study, with collections from 152 locations between 40°N and 35°S in the Atlantic, Pacific, and Indian oceans (Figure 2). Of these, 263 fresh specimens suitable for genetics were obtained from 40 Atlantic, 27 Pacific, and 7 Indian Ocean locations (Table 1). Our fresh material was collected using plankton nets during nine oceanographic expeditions between 2001 and 2012 (Table S1). All fresh specimens were preserved in 96% ethanol and stored at -20°C. We also examined 706 specimens from museum collections at the Naturalis Biodiversity Center, Leiden, The Netherlands (NBC) and Zoological Museum of the University of Copenhagen, Denmark (ZMUC). These museum specimens were collected at 78 locations during ten expeditions between 1909 and 1993 and stored in 70% ethanol following initial fixation in formaldehyde (Table 1). Most of the museum specimens (*N* = 425) were collected during the Danish DANA expeditions between 1921 and 1932 (Table S1). The available museum specimens were identified by Van der Spoel et al. (1993) as 23 of the 24 described *Diacavolinia* taxa, including holo- and/or paratype specimens (*N* = 79) of 14 taxa, providing a critical link between prior and current work (Table S2). Specimens of *Diacavolinia robusta* were not available. Use of this historical material enabled us to make direct comparisons of species boundaries as identified by our methods versus those considered by Van der Spoel et al. (1993).

Integrative approach to assessing species boundaries

We combined genetic, geometric morphometric, and geographic observations on single *Diacavolinia* specimens wherever possible, with the approach outlined in

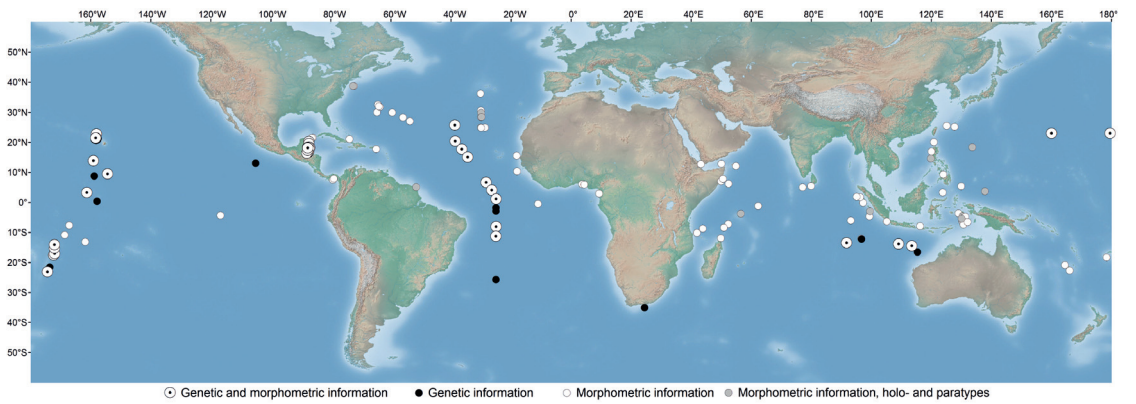

Figure 2. Geographic overview of collection locations for all *Diacavolinia* specimens used in this study, with the type of information obtained from specimens at each location.

Table 1. Overview of *Diacavolinia* specimens used in this study. For ventral and lateral geometric morphometrics, numbers of specimens for which morphometric data was obtained are indicated per number of landmarks (LM).

	Total	Atlantic	Pacific	Indian
Diacavolinia specimens (museum and fresh)	969	374	421	174
Ventral photographs	920	368	381	171
of which Ventral geom. morph. 23 LMs	646	268	260	118
of which Ventral geom. morph. 38 LMs	314	140	115	59
Lateral photographs	903	363	376	164
of which Lateral geom. morph. 15 LMs	752	325	292	135
of which Lateral geom. morph. 49 LMs	549	267	190	92
Diacavolinia fresh specimens[1]	263	109	136	18
Sequenced reference (Steps 1 and 5)[1]	176	65	100	11
of which COI (Steps 1 and 5)[1]	89	56	25	8
of which 28S (Step 1)	138	35	94	9
Identified by LDA (Step 4)	48	33	15	0
Unidentified	39	11	21	7
Diacavolinia museum specimens	706	265	285	156
Holo- and paratype reference (Step 2)	79	34	36	9
Added reference, no types (Step 3)	26	0	15	11
Identified by LDA (Step 4)	423	195	139	89
Unidentified	178	36	95	47
Outgroup sequences (COI and 28S)[2]	4	2	2	0
Cavolinia uncinata[2]	4	2	2	0
Diacavolinia locations[1]	152	67	56	29
Diacavolinia fresh locations[1]	74	40	27	7
Diacavolinia museum locations	78	27	29	22

[1]Includes 3 Pacific sequences / 1 location from Maas et al. (2013).
[2]Outgroup sequences from Burridge et al. (2017).

Figure 1. The information obtained for each specimen varied, but this framework allowed for the combination of partial observations from each specimen. Morphometric measurements consisted of a partial shell shape outline of 49 landmarks (LMs) in lateral orientation and/or 23 LMs in a ventral orientation per specimen (photographs and geometric morphometric data: Supplementary information 1 and 2). For some specimens it was possible to obtain an additional 15 ventral LMs to outline the shape of the ventral lip, in cases where the soft tissue did not obscure the ventral lip (also see next paragraph; E in Figure 3; Table 1). Phylogenies were inferred from cytochrome *c* oxidase subunit I mtDNA (COI; 658 bp) and/or 28S DNA (901 bp) gene fragments (Table 1).

Our approach included six steps for the discovery of and assignment to species (Figure 1). The first step consisted of identifying integrative groups by linking genetic and morphometric information using fresh specimens (*N* = 173). To test for significant morphometric differences between genetic clades with >5 specimens, we applied non-parametric permutational multivariate analyses of variance to shell shape or size parameters (PerMANOVA based on Euclidean distances; Anderson, 2001) in Past 2.17c (Hammer et al., 2001). The PerMANOVA *F*-statistic was tested against 10^4 non-parametric permutations. A significantly different result provided

evidence for the presence of integrative species, with concordance observed among genetic and morphometric characters. In the second step, we examined the morphospace position of the holo- and paratype specimens identified by Van der Spoel et al. (1993), for which no genetic information is available. Geometric morphometric measurements were obtained for 79 type specimens from 14 described taxa (Tables 1 and S2). We applied Linear Discriminant Analysis (LDA) in R 3.0.1 (R Development Core Team, 2013) to identify morphological species based on types, merge different types into a single morphological species, or merge types with integrative species as identified in Step 1. We performed separate LDAs for shape and size data of the different orientations to include as many specimens as possible and to limit the presence of correlated lateral and ventral size variables within the same LDA. Morphometric assignment criteria for synonymization with integrative groups and/or conservation of holo- and paratypes as distinct morphological species were: at least 80% confidence of belonging to a group for lateral 49 LMs, and/or 95% for ventral 23 LMs, and/or 85% for ventral 38 LMs and no contradictory assignment between orientations. These cutoff values were chosen to reflect the relatively higher information content of the shell outline of the lateral compared to the ventral orientation. If synonymized, we did so for all type specimens of the same species, based on a positively assigned majority, while also including unassigned minorities, because they were always from the same location. In this way, we reduced the number of distinct groups identified in Step 2. The third step was to identify morphological species without holo- or paratypes based on distinct positions in morphospace not covered by specimens from Steps 1 and 2, using LDA

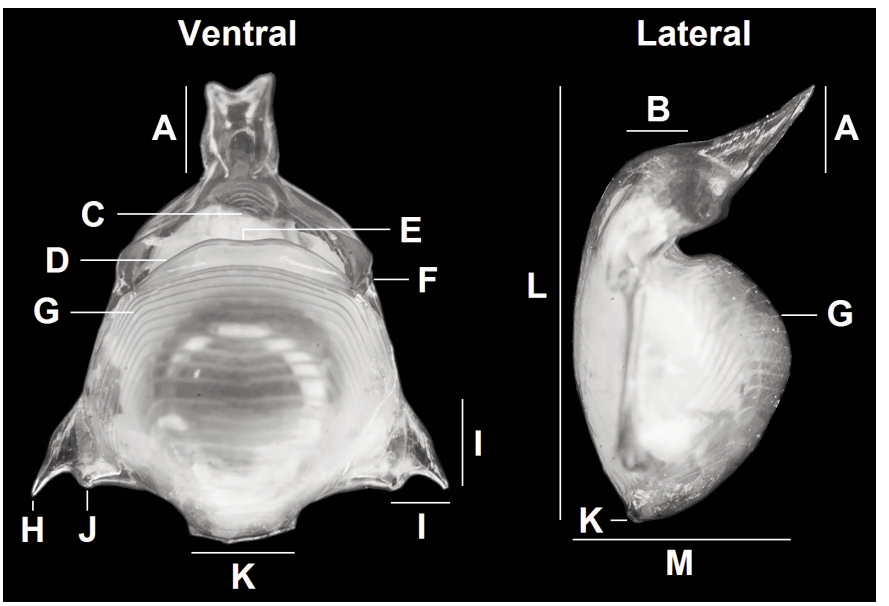

Figure 3. Morphology of *Diacavolinia* shells in ventral and lateral orientations, with (A) rostrum, (B) outer hump, (C) aperture, (D) ventral lip, (E) median lip depression, (F) lock area, (G) ventral ribs, (H) spine tip, (I) spine surface, (J) gutter corner, (K) caudal joint, (L) dorsal side, and (M) maximum shell width as marked.

to justify this distinction. The fourth step was the LDA assignment of the remaining specimens for which morphometric information was available to the groups identified in Steps 1-3. Remaining specimens were either non-sequenced fresh or non-type specimens from museum collections. Individuals remained unidentified if they did not meet the assignment criteria or were assigned ambiguously between orientations. In the fifth step, we identified possible species based on individuals with genetic, but without morphometric information. These are treated as separate groups because their genetic data could not be linked to morphological data from other groups, although they may be synonymous to groups identified in Steps 2-3. Finally, in the sixth step, we plot sampling locations of all identified species and possible species of *Diacavolinia*.

Geometric morphometrics

For quantitative analyses of *Diacavolinia* shell shapes and sizes, fresh and museum specimens were photographed in lateral (*N* = 904) and ventral (*N* = 919) orientations using a Nikon D100 6 mpx camera (Micro-Nikkor lens 55 mm / 3.5, aperture f / 11, shutter speed 1 / 1.3s, ISO 200, fixed zoom) attached to a stand. To standardize the ventral orientation, specimens were mounted on photographic film using 60% methyl glucose. For lateral standardization we used fine black sand, free from organic material. For geometric morphometric analyses, we selected photographs of all fully developed adults and excluded specimens that were not well-focused or in standard orientation. We also excluded specimens that were damaged or obscured at relevant positions by soft tissue that could not be removed without damaging the shell. Selected photographs were compiled for further analysis using tpsUtil software (Rohlf, 2006).

We used a combination of landmarks and semi-landmarks for partially outlining shell shapes in tpsDig (Rohlf, 2006) to cover as much shell shape variation as possible for as many specimens as possible (Gunz and Mitteroecker, 2013). To assess the shape variation in the laterally photographed shells, two partial outlines were created, which were connected at the caudal joint between its ventral and dorsal parts at the bottom of the shell (also see Figure 3 for shell anatomy). The first partial outline started at the position of maximum width of the ventral part, ended at the caudal joint and was standardized per specimen to 15 LMs separated by equal length. The second partial outline started at the top of the shell rostrum, ended at the caudal joint via the dorsal part of the shell and was standardized to 35 LMs. Because of the mutual landmark at the caudal joint, this resulted in a total lateral outline of 49 LMs. Creating the first partial outline of 15 LMs was possible for 752 specimens and creating both (49 LMs) was possible for a subset of 549 specimens (Table 1). To assess shape variation in a ventral orientation, two LMs were placed at the left and right gutter corners and a third LM was placed at the caudal joint. Subsequently, left and right partial outlines of 10 LMs each were generated from the lock areas left and right of the shell aperture downwards to the closest position without overlap between ventral and dorsal shell parts, the upper start of the dorsal spine surface (also see Figure 3). This resulted in a total of 23 LMs

for 646 specimens. No landmarks were created on the two spine tips because these were often damaged. For a subset of 314 specimens it was possible to create an additional 15 LM outline of the ventral lip, resulting in a total of 38 LMs.

We used tpsRelw software (Rohlf, 2006) to rotate, translate, and scale LM coordinates through generalized least-square Procrustes superimposition (GLS; Kendall, 1977). This provided centroid sizes, a size measure depending on the surface area within all LMs, and multiple relative warp (RW) axes containing information on shape variation, with the first RW containing most information. The morphospace of the lateral orientation was represented by 26 relative warps (RWs) for 15 LMs and 94 RWs for 49 LMs. In ventral orientation, there were 42 RWs for 23 LMs and 72 RWs for 38 LMs.

To test for repeatability of RWs, a selection of 19 museum specimens was photographed in two subsequent series for lateral 15 LMs and 49 LMs and ventral 23 LMs, of which 10 could also be used for ventral 38 LMs. Intra-class correlation coefficients (ICCs) between the two series were calculated for the centroid sizes and first 10 RWs in Past 3.0 (Hammer et al., 2001). RWs were considered repeatable when ICC > 0.80, and only repeatable RWs were used in further analyses of shell shape. Centroid sizes were always repeatable (ICC > 0.99). For 15 LMs, the first two RWs were repeatable (ICC > 0.94) and contained 95.96% of the shape variation for this part of the shell. For 49 LMs, RWs 1-8 and 10 were repeatable (ICC > 0.91), accounting for 98.29% of the shell shape variation. In a ventral orientation, repeatable RWs for 23 LMs were 1-5 and 8 (ICC > 0.83; 92.36% of shape variation) and 1-5 (ICC > 0.81; 83.17%) for 38 LMs, respectively.

Genetics

To assess genetic diversity and phylogenetic relationships within *Diacavolinia*, we obtained 86 COI mtDNA (GenBank accession numbers MF974762-MF974847) and 138 28S DNA (GenBank accession numbers MF974624-MF974761) sequences from a total of 173 specimens, following photography of shells of the same individuals for morphometric measurements. Tissue fragments of one mm^3 for DNA extraction could only be obtained by damaging the shells. DNA extraction was performed using the EZNA Mollusc DNA Kit (Omega Biotek 2013), as recommended by Maas et al. (2013). We followed the manufacturer's recommended methods without freeze-drying of tissue before DNA extraction.

A 658 bp fragment of COI was amplified using the primers LCO1490 (5'-GGTCA ACAAATCATAAAGATATTGG-3') and HCO2198 (5'-TAAACTTCAGGGTGACCAAAAAAT CA-3'; Folmer et al., 1994). Reactions were run in 25 µl volumes consisting of 15.75 µl MilliQ, 2.5 µl 10x PCR buffer containing 1.5 mM $MgCl_2$ (Qiagen), 0.5 µl $MgCl_2$ (25 mM), 2.0 µl dNTPs (2.5 mM per nucleotide), 0.25 µl Taq (Qiagen), 1.0 µl (10 mM) of each primer, and 2.0 µl DNA template. A 901 bp fragment of the nuclear 28S ribosomal gene was amplified using the primers 28SC1F (5'-ACCCGCTGAATTTAAG CAT-3') and 28SD3R (5'-GACGATCGATTTGCACGTCA-3'; Dayrat et al., 2001). The 25 µl reaction consisted of 15.25 µl MilliQ, 2.5 µl 10x PCR buffer containing 1.5 mM

$MgCl_2$ (Qiagen), 0.5 µl $MgCl_2$ (25 mM), 2.5 µl dNTPs (2.5 mM per nucleotide), 0.25 µl Taq polymerase (Qiagen), 1.0 µl (10 mM) of each primer, and 2.0 µl DNA template. PCR was performed applying an initial denaturation of 4 min at 94°C, 35 cycles of 1 min at 94°C, 30 s at 50°C, 1 min at 72°C and finally 5 min at 72°C for final extension, followed by ~1 h at 12°C. If the initial PCR failed, an anti-inhibitor treatment (PCR Inhibition Removal Kit, Zymo Research, USA) was applied. Sanger sequencing of PCR products was performed using an ABI3730XL sequencer (Life Technologies; outsourced to BaseClear, Leiden, The Netherlands).

Forward and reverse COI and 28S sequences were assembled in MEGA 6.0 (Tamura et al., 2013) and CodonCode Aligner 4.1 (CodonCode Corporation, USA, 2013). For 28S, double peaks were registered as ambiguous when apparent in both forward and reverse sequences and with a secondary peak that was at least 1/3 of the height of the primary peak. Assembled sequences were aligned using the MAFFT algorithm (MAFFT version 7) and their identities as shelled pteropods were checked by BLAST against the NCBI nt database (Altschul et al., 1997). Three Pacific *Diacavolinia* sequences from Maas et al. (2013; GenBank accession numbers JX183614-JX183616) were included in the COI alignment, as well as two Atlantic and two Pacific *Cavolinia uncinata* specimens (Burridge et al., 2017: Thesis chapter 2; GenBank accession numbers MF048915-MF048918 for COI and MF048968-MF048971 for 28S) in both alignments.

Maximum Likelihood (ML; Felsenstein, 1981) was used to infer phylogenetic relationships among specimens for both the COI and 28S alignments. For COI, we used a General Time Reversible (GTR) substitution model with different evolutionary rates for the three codon positions (CP), because this is a biologically realistic model for protein coding sequences (Shapiro et al., 2006). GTR with a proportion of invariable sites (I) and gamma distributed rate variation among sites (Γ) was selected from 24 models using the Akaike Information Criterion (AIC) in JModeltest 2.1.7, in which CP-models were not available (Darriba et al., 2012). For 28S, the most appropriate substitution model selected using AIC was GTR + I. Molecular phylogenies were inferred using Maximum Likelihood followed by non-parametric bootstrap analyses with 1000 bootstraps in RaxMLGUI 1.3 (Stamatakis, 2006; Silvestro and Michalak, 2012).

To quantify differences between and within genetic clades, we calculated pairwise genetic distances between COI haplotypes as well as 28S alleles using the K2P + Γ distance model of evolution that assumes equal evolutionary rates among all transitions as well as among all transversions (Kimura, 1980) in MEGA 6.0 (Tamura et al., 2013). Among the available models in MEGA 6.0, this model most closely represented our sequence data according to the AIC for COI and 28S. We reconstructed alleles from 28S genotypes using the PHASE algorithm (Stephens et al., 2001; Stephens and Donelly, 2003) in DnaSP v5 (Librado et al., 2009).

We first identified molecular operational taxonomic units (MOTUs) based on COI and 28S sequences separately, using the online version of ABGD (Automatic Barcode Gap Discovery; Puillandre et al., 2012). Subsequently, integrative species

were defined based on a pairwise genetic distance of at least 5% divergence for COI, combined with the ability to distinguish groups morphologically using geometric morphometric methods. If COI sequences were not available, additional groups were identified based on the presence of unique 28S mutations. If morphologies between different MOTUs could not be distinguished, they were treated as a single group.

Results

Integrative approach to assessing species boundaries

Geometric morphometric data demonstrate large variation in shell sizes and shapes among *Diacavolinia* specimens, especially in the Indo-Pacific (Figures 3-5 and S1). The first three lateral RWs captured 43.38, 21.95, and 14.97% of the total shell shape variation, respectively (Figures 4 and S1A). For ventral RWs (23 LMs) these results were 43.38, 27.20, and 10.79% (Figures 5A,B and S1B).

There were 251 polymorphic sites in the COI nucleotide alignment of *Diacavolinia* (*N* = 89; 658 bp; GenBank accession numbers MF974762-MF974847). For 28S (*N* = 138; 901 bp; GenBank accession numbers MF974624-MF974761) there were 28 polymorphic sites of which 10 contained ambiguous base assignments, all based on transitions of C-T (Y) and A-G (R).

Step 1: Identification of integrative species

We identified six integrative species based on combined genetic and geometric morphometric information on fresh specimens in step 1: Groups 1 (Atlantic), 3-5 (Indo-Pacific), 6 (Pacific), and 7 (Indian Ocean; Figure 6; groups numbered sequentially for Atlantic followed by Indo-Pacific throughout). The COI phylogeny included Groups 1 (*N* = 56; 1 MOTU), 3 (*N* = 21; 1 MOTU), 5 (*N* = 6; 2 MOTUs), 6 (*N* = 1; 1 MOTU), and 7 (*N* = 1; 1 MOTU; Figure 6A). For Group 4, COI sequences failed to amplify in PCR. Groups 12 and 13, for which we obtained COI sequences but lack morphological data, are discussed in Step 5. Pairwise genetic distances of COI haplotypes between these groups were high with averages of 18.6-43.8% (Table S3). Pairwise distances were small within Groups 1 (average 1.4%, range 0-2.7%) and 3 (0.4%, 0-1.1%), and larger within Group 5 (6.3%, 0.5-15.6%). Within Group 5, a single specimen was assigned to a different MOTU based on COI sequences, but because no geometric morphometric differences could be detected it was not treated as a separate group. Without this specimen, pairwise distances within Group 5 were 2.0% (0.5-3.0%). The Atlantic COI sequences from Maas et al. (2013) all corresponded to Group 1 (NCBI BLAST-search; not included in counts or analyses). Other groups with COI sequences but without morphological data are discussed in Step 5. The 28S phylogeny included Groups 1 (*N* = 35), 3 (*N* = 17), 4 (*N* = 78), 5 (*N* = 6), 6 (*N* = 1), and 7 (*N* = 1) and no additional groups without morphological data were identified based on this genetic marker. Two well-supported *Diacavolinia* clades were present, each representing one 28S MOTU as identified by ABGD (Figure 6B). The first clade contained Groups 1, 3, 6, and 7 (*N* = 54) from all three

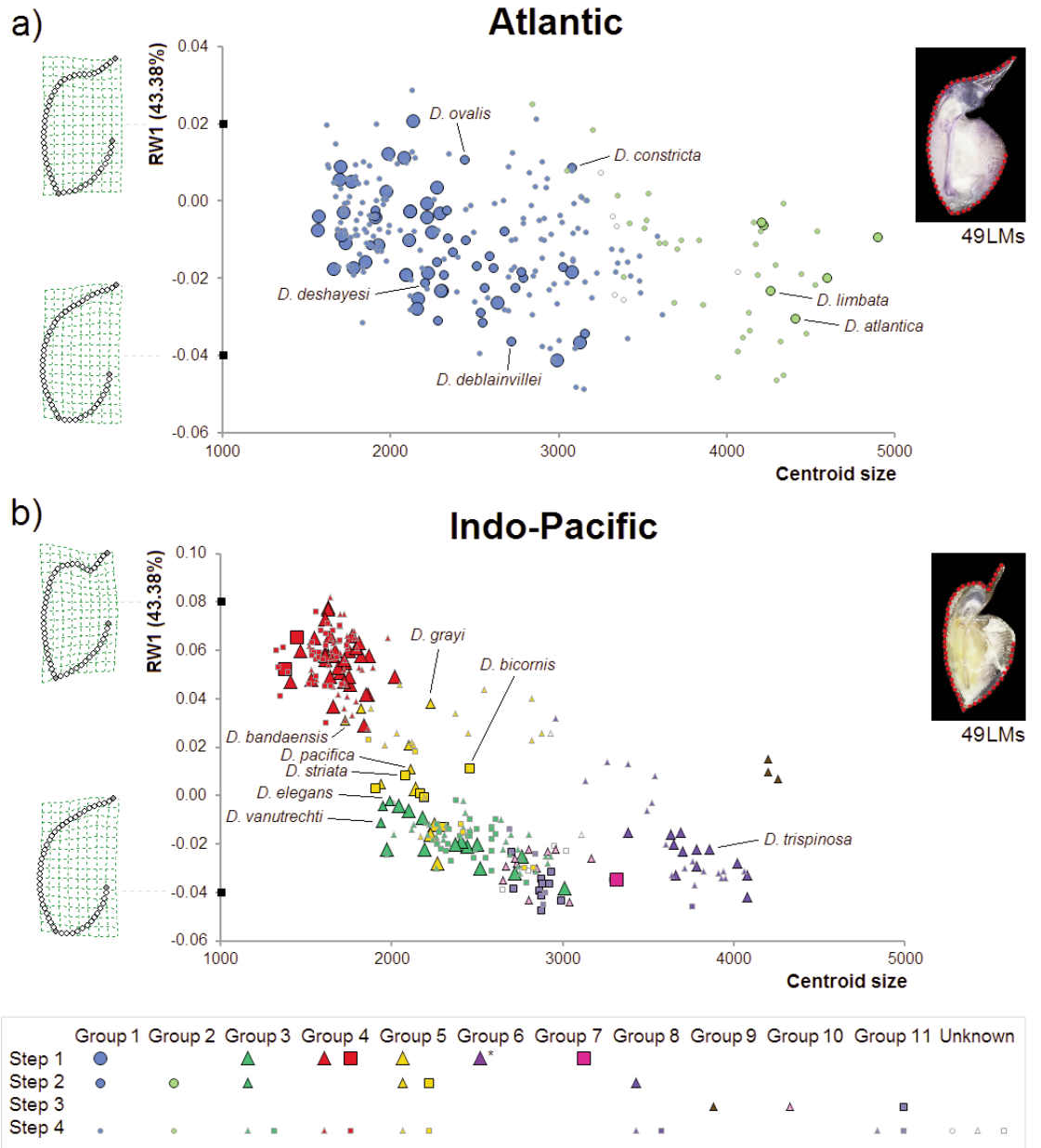

FIGURE 4. Ordination of centroid sizes and the first Relative Warp (RW) axis of *Diacavolinia* in a lateral orientation with 49 landmarks (LMs) for (A) Atlantic specimens and (B) Indo-Pacific specimens. The morphospace positions are indicated as circles for Atlantic (*N* = 267), triangles for Pacific (*N* = 190), and squares for Indian Ocean (*N* = 92) specimens. Colors indicate distinct groups. Symbol sizes represent the steps in the integrative taxonomic approach in which specimens were assigned to a group (see legend). Corresponding thin plate splines of the most positive and negative deformations are indicated along RW1 to depict the variation in shell shape, with images of shells and LM positions shown on the right. Names of holotypes, and if not available, representative paratypes, are indicated. Groups 12 and 13 are not shown because no morphological data was available.

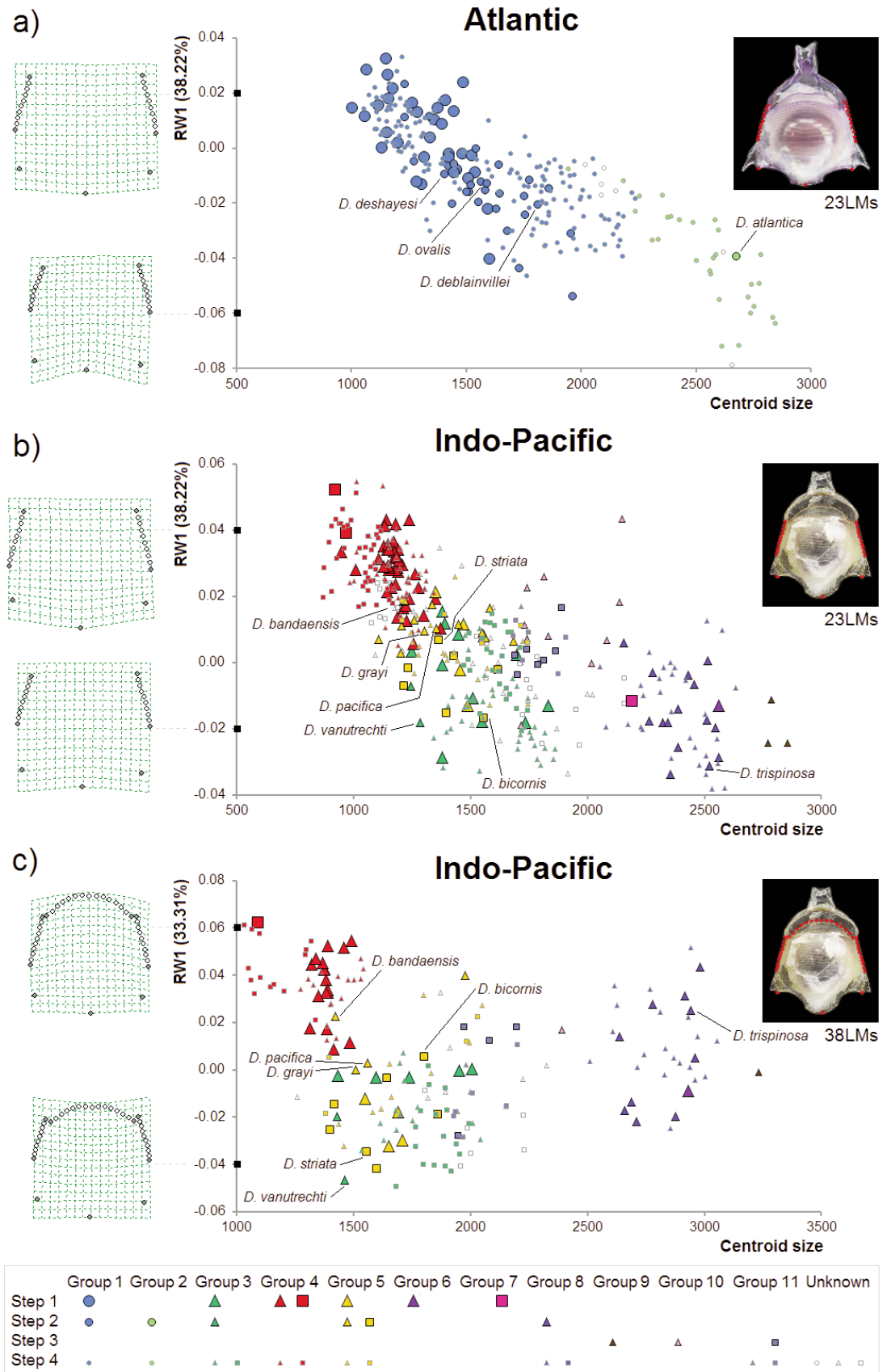
a)
Atlantic
RW1 (38.22%)
0.04
0.02
0.00
-0.02
-0.04
-0.06
-0.08
500
1000
1500
2000
2500
3000
Centroid size
D. deshayesi
D. ovalis
D. deblainvillei
D. atlantica
23LMs
b)
Indo-Pacific
RW1 (38.22%)
0.06
0.04
0.02
0.00
-0.02
-0.04
500
1000
1500
2000
2500
3000
Centroid size
D. striata
D. bandaensis
D. grayi
D. pacifica
D. vanutrechti
D. bicornis
D. trispinosa
23LMs
c)
Indo-Pacific
RW1 (33.31%)
0.08
0.06
0.04
0.02
0.00
-0.02
-0.04
-0.06
1000
1500
2000
2500
3000
3500
Centroid size
D. bandaensis
D. bicornis
D. pacifica
D. grayi
D. striata
D. vanutrechti
D. trispinosa
38LMs
Group 1
Group 2
Group 3
Group 4
Group 5
Group 6
Group 7
Group 8
Group 9
Group 10
Group 11
Unknown
Step 1
Step 2
Step 3
Step 4

FIGURE 5. Ordination of centroid sizes and the first Relative Warp (RW) axis of *Diacavolinia* in a ventral orientation for (A) Atlantic specimens with 23 landmarks (LMs, *N* = 268), (B) Indo-Pacific specimens with 23 LMs (*N* = 378), and (C) a subset of Indo-Pacific specimens with 38 LMs (*N* = 174). See FIGURE 4 for symbol definitions. Corresponding thin plate splines of the most positive and negative deformations are indicated along RW1 to depict the variation in shell shape, with shell image and LM positions shown on the right. Names of holotypes, and if not available, representative paratypes, are indicated.

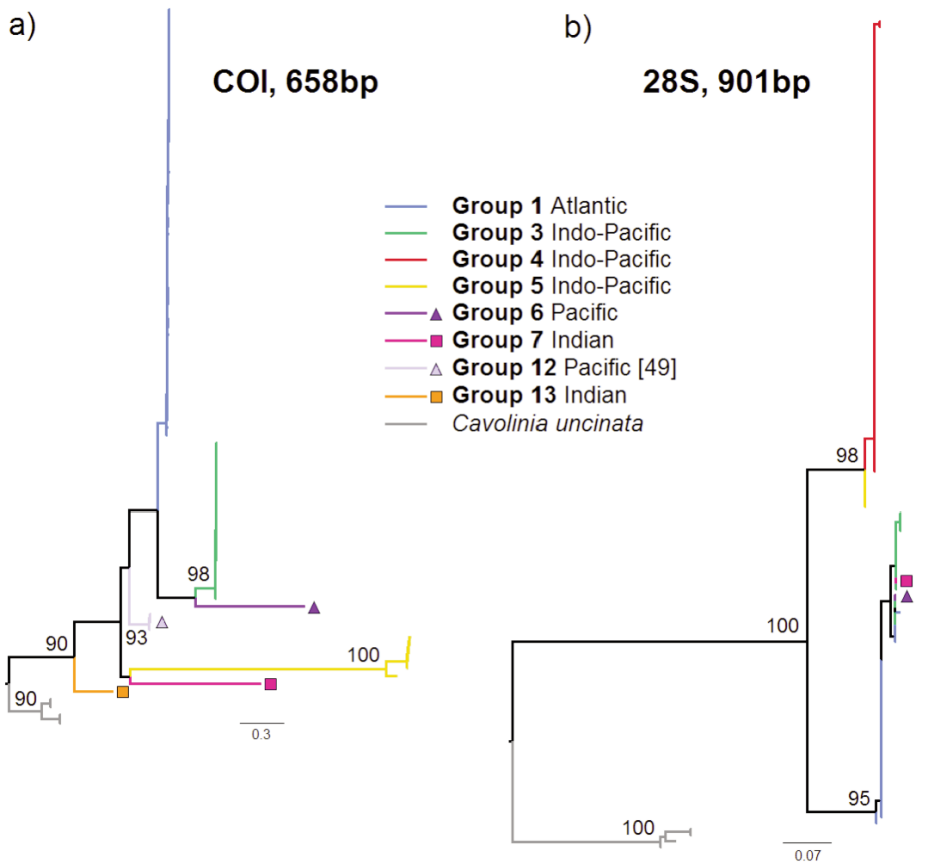

FIGURE 6. Maximum likelihood trees of (A) cytochrome *c* oxidase I (COI) mtDNA sequences (*N* = 89) and (B) nuclear 28S rDNA sequences (*N* = 138) of *Diacavolinia*. The COI phylogeny (A) includes Groups 1 (*N* = 56), 3 (*N* = 21), 5 (*N* = 6), 6 (*N* = 1), 7 (*N* = 1), 12 (*N* = 3, from Maas et al., 2013; GenBank accession numbers JX183614-JX183616; Pacific Ocean), and 13 (*N* = 1). The 28S phylogeny (B) includes Groups 1 (*N* = 35), 3 (*N* = 17), 4 (*N* = 78), 5 (*N* = 6), 6 (*N* = 1), and 7 (*N* = 1). Four *Cavolinia uncinata* outgroup sequences are included to root each tree (Genbank accession numbers MF048915-MF048918 for COI and MF048968-MF048971 for 28S from Burridge et al., 2017: Thesis chapter 2). Numbers indicate bootstrap support in ML analyses (only bootstrap values >=90 are shown). Colors indicate distinct genetic groups; symbols indicate rare genetic groups (triangle = Pacific; square = Indian Ocean). Not all groups were amplified in PCR for both markers.

oceans. The second clade consisted of Groups 4 and 5 (*N* = 84) and was restricted to the Indo-Pacific. The average genetic distance between alleles of the two clades was 2.4% (1.7-3.0%). Within the first clade, this was 0.2% (0-0.6%), and within the second clade it was 0.1% (0-0.4%). The groups within the first clade could not unequivocally be distinguished from one another based on 28S alone. Groups 4 and 5 within the second clade could always be distinguished from each other (0.3%, 0.2-0.4% genetic distance between alleles; Table S3).

Geometric morphometric and genetic data were congruent for the integrative species identified (Figures 4-6 and S1). Across all orientations, LDA demonstrated a 100% correspondence between geometric morphometric and genetic data for Groups 1 and 5. Accuracy was 92.9% for Group 3 and 95.9% for Group 4, with the remaining individuals not reaching the assignment criteria for unambiguous identification (Table S4). We obtained geometric morphometric measurements of shell shape and size for 112 sequenced individuals with *N* = 89 for lateral 49 LMs, *N* = 94 for ventral 23 LMs, and *N* = 57 for ventral 38 LMs (Table S1). The shell shapes of Groups 1 and 3-5 were significantly different in all orientations (Bonferroni-corrected $p < 0.001$ for all orientations; $F = 45.84$ for lateral 49 LMs; $F = 17.49$ for ventral 23 LMs; $F = 17.69$ for ventral 38 LMs). Some, but not all shell sizes were significantly different based on centroid size measurements. For lateral 49 LMs, Group 4 was significantly smaller than Groups 1, 3, and 5 ($p < 0.001$, 0.001, and 0.01; $F = 36.75$, 127.1, and 59.15, respectively). The same was true for 38 LMs ($p < 0.05$, 0.01, and 0.01; $F = 8.217$, 31.74, and 35.23, same order) and for ventral 23 LMs ($p < 0.001$ for all combinations; $F = 27.04$, 75.07, and 48.57). Additionally, Group 1 was significantly smaller than Group 3 in this orientation ($p < 0.01$; $F = 9.318$).

Step 2: Identification of morphological species with holo- and paratypes

In the Atlantic Ocean, holo- and paratypes of *D. atlantica* and *D. limbata africana* were identified as Group 2 with 100% confidence. Holo- and paratypes of *D. deblainvillei*, *D. deshayesi*, *D. constricta*, and *D. ovalis* were placed into Group 1 with a confidence of 96.4% (Figures 1, 4A and 5A; Table S4). We did not use the ventral orientation with 38 LMs for identifying Atlantic specimens because this part of the shell was always obscured by soft tissue for Group 2.

In the Pacific Ocean, *D. triangulata* holo- and paratypes were identified as Group 8 with 100% confidence. Based on geometric morphometric data from the Indo-Pacific, seven taxa were placed into groups from Step 1 (Figures 1, 4B, 5B,C and S1; Table S4). *Diacavolinia elegans* and *D. vanutrechti vanutrechti* paratypes from the Pacific fit into Group 3 (75% confidence). The Pacific *D. grayi*, *D. bandaensis*, and *D. pacifica* holo- and paratypes as well as the Indian Ocean *D. striata* and *D. bicornis* paratypes were identified as belonging to Group 5 (64% confidence). The higher fraction of ambiguous type specimens in Group 5 may be due to the relatively large morphospace covered by this group, in which we could not distin-

guish any subgroups, and for which at least two MOTUs were identified by ABGD based on COI sequences.

Step 3: Identification of morphological species without types

We distinguished three additional morphological species based on the morphospace position of non-type museum specimens from the Indo-Pacific (Groups 9-11; *N* = 26; Figures 1, 4B, 5B,C and S1). For all three groups, there was a 100% correspondence between their estimated position in morphospace and their LDA assignment (Table S4). Non-type specimens were previously identified by Van der Spoel et al. (1993) as Pacific *D. strangulata* (Group 9), Pacific *D. mcgowani* and *D. longirostris* (Group 10), and *D. longirostris* from the Indian Ocean (Group 11). Group 9 was distinguished by a strongly ventrally directed shell rostrum and large size, Group 10 was identified by large spines and a triangular appearance in a ventral orientation, and Group 11 was recognized by a subtle outer hump combined with a ventrally directed shell rostrum.

Step 4: Assignment of remaining specimens to morphogroups

Of our fresh specimens with morphometric but without genetic data, all Atlantic specimens (*N* = 33) were assigned to Group 1 by LDA. Pacific specimens (*N* = 15; 94.8%) were assigned to Group 4 (1 specimen was ambiguous). We thus infer that a representative number of specimens from Groups 1 and 4 were sequenced in Step 1. Of our remaining museum specimens, 423 specimens (88%) were successfully assigned to groups, and 58 (12%) were not (Table S4).

Step 5: Identification of possible species

Two additional groups were identified based on COI sequences alone, each representing one MOTU (Groups 12 and 13; Figure 6A; Table S4). Group 12 contained all three Eastern Tropical Pacific sequences from Maas et al. (2013; listed as *D. vanutrechti*). Group 13 contained a single sequence from the Indian Ocean near South Africa and its phylogenetic position was between other *Diacavolinia* groups and *Cavolinia uncinata*. No morphological information was available for these groups because Group 12 was solely represented by sequences from Maas et al. (2013) and Group 13 was represented by a single juvenile specimen with a damaged shell.

Step 6: Global biogeography

Biogeographic ranges of the identified groups were diverse and varied in size (Figure 7). In the Atlantic ocean, two groups occur: Group 1 (*N* = 276) is present across the entire range (39°N-26°S) including the Caribbean Sea and Group 2 (*N* = 51) is found only in the northern hemisphere and predominantly around the Azores, near the Cape Verde Islands, and in the Gulf of Guinea. Groups 3-5 are the most common groups in the Indo-Pacific (*N* = 100; 172; 64), and they all have wide Indo-Pacific distributions. Less common are Group 8 (*N* = 49), predominantly occurring in the central Indo-Pacific but also extending west to the Red Sea, and Group 11 (*N* = 19) from the southern part of the central Indo-Pacific and in and near the Gulf of Aden. Of the remaining, rare groups, Group 6 (*N* = 1) is found

south of Hawaii at 14°N and Groups 9 (*N* = 3), 10 (*N* = 12), and 12 (*N* = 3) all occur in the Eastern Tropical Pacific (ETP), of which Group 10 (*N* = 12) was sampled near the coast of Panama. Groups 7 and 13 were each found once in the Indian Ocean, with Group 7 occurring close to the Cocos-Keeling Islands and Group 13 occurring in warm waters near South Africa (Figure 7).

Synthesis

Following our integrative approach, a total of 752 specimens (77.6% of 969 available specimens) were assigned to 13 groups (Figures 1 and 8; Table S4). We distinguished two groups in the Atlantic Ocean and 11 groups in the Indo-Pacific. We

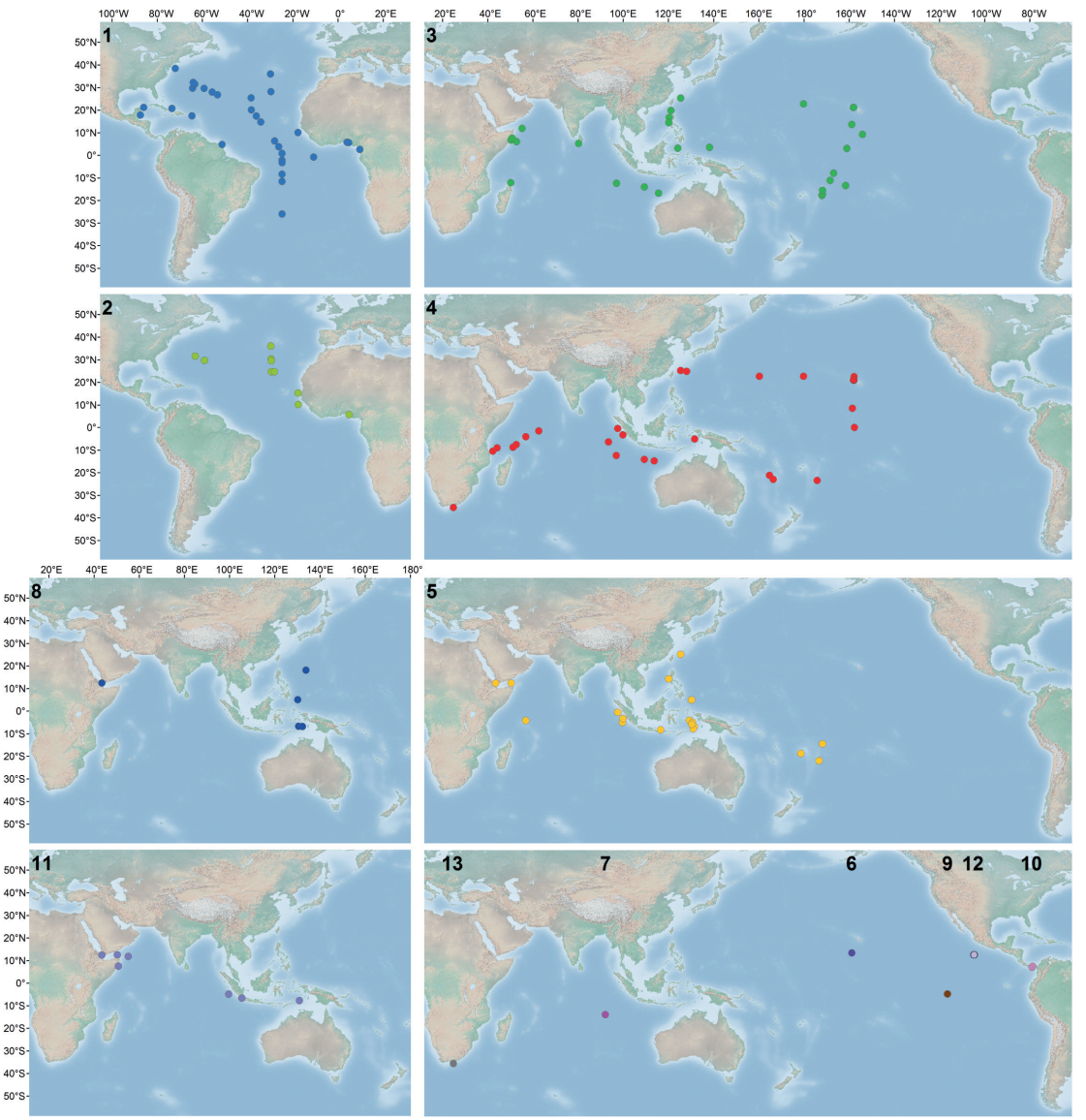

Figure 7. Distribution of *Diacavolinia* groups 1-13 as identified in this study. A presence record was mapped if at least one specimen from that locality was positively identified. Group # numbers are indicated at the top of each map.

consider there to be sufficient genetic and morphometric evidence for the validity of the Atlantic Group 1 and Indo-Pacific Groups 3-5 as integrative species, with possible additional diversity within Group 5. Although we had only one specimen each for Groups 6 and 7, they likely also represent separate species based on genetic and morphometric data. We identified Atlantic Group 2 and Indo-Pacific Groups 8-11 as morphological species, but they were not sampled in our recent collection and we lack genetic information for these taxa. Hence, we could not link them to possible species of Groups 12 and 13, for which we only had genetic information. We consider it, however, unlikely that Group 13 represents any morphological species based on its South African locality with none of Groups 8-11 occurring nearby. Of the unassigned individuals (*N* = 217), 158 specimens provided no evi-

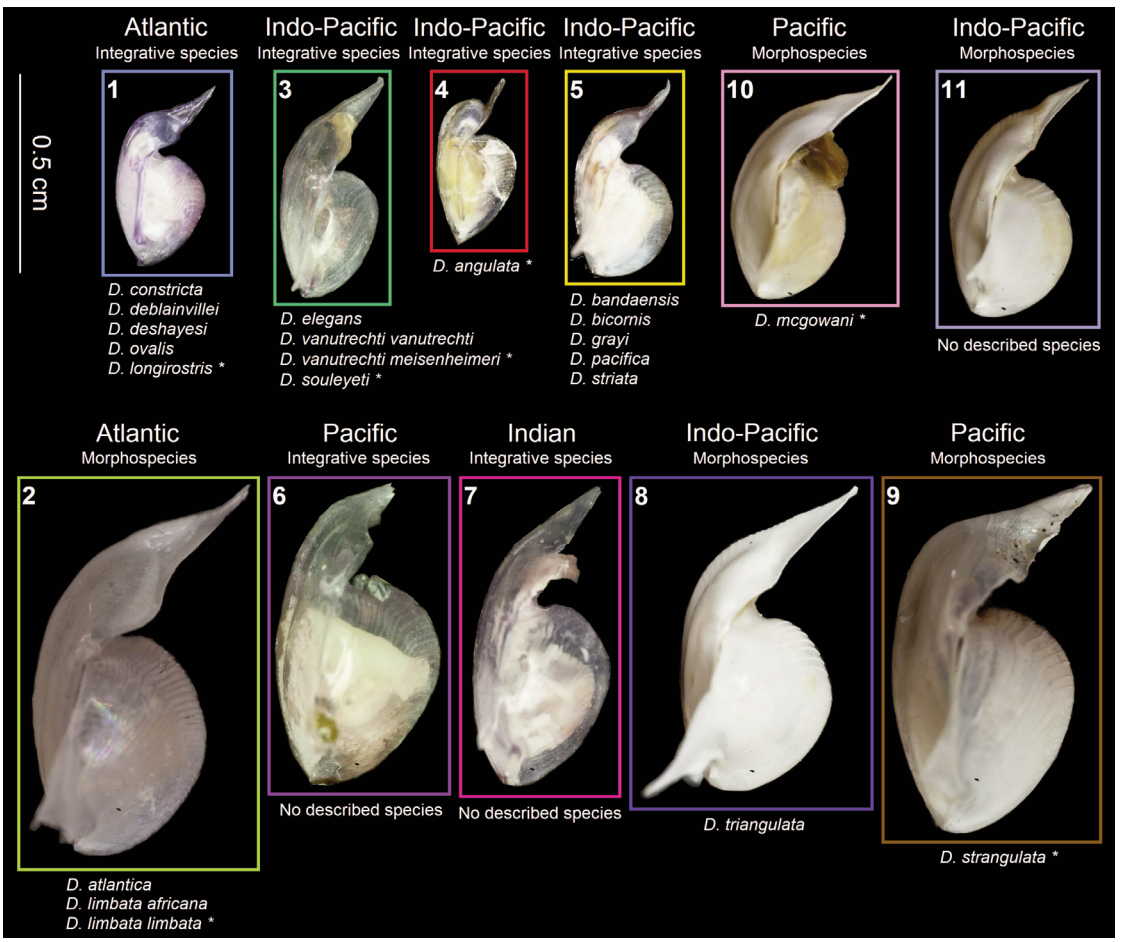

FIGURE 8. Overview of *Diacavolinia* revised taxonomy with example specimens of groups 1-11 shown in a lateral orientation. Species names as (re)described by Van der Spoel et al. (1993) are listed below each group based on holo- and paratype specimens. For species with an (*) no type specimens were included in this study, but they are listed below the group to which the majority of specimens identified as such was assigned in Steps 3 and 4, and are listed only if the species was originally described from the same ocean basin. Photo sizes are standardized to the 0.5-cm scale bar. Groups 12 and 13 are not shown because no morphological data was available.

dence to either determine their position in morphospace (no photographs, or unusable photographs), or to determine their molecular phylogenetic position. A further 59 specimens for which geometric morphometric measurements were available, of which 50 from the Indo-Pacific, could not be confidently assigned to a group and may represent additional diversity.

Figure 8 gives an overview of typical adult shell shapes (in lateral orientation) and sizes for Groups 1-11. Important morphological characteristics for distinguishing between *Diacavolinia* species are the presence of an outer hump (B in Figure 3), direction of the shell rostrum (A in Figure 3) and spines (H in Figure 3) relative to the rest of the shell, convexity of the dorsal (L in Figure 3) and ventral parts as seen in lateral orientation, and shell size.

Discussion

Integrative taxonomy and pteropod diversity

To our knowledge, this is the first time a global collection of samples, including recent and museum type specimens of a marine zooplankton group, have been combined into a single dataset for integrative taxonomic purposes. We successfully linked 969 specimens belonging to the pteropod genus *Diacavolinia* for which there was morphological and/or genetic information available. Using museum material also used by Van der Spoel et al. (1993) allowed for direct comparison with previous taxonomies. In this way, we more accurately and objectively resolved species boundaries and species distributions than has been possible in prior work.

Our findings suggest that the 24 taxa described by Van der Spoel et al. (1993) should be reduced to a maximum of 13 species. Especially in the Atlantic Ocean, the number of species should be reduced from eight to two, with one species comprising *D. constricta*, *D. deblainvillei*, *D. deshayesi*, *D. ovalis*, and *D. longirostis*, and the other comprising *D. atlantica*, *D. limbata africana*, and *D. limbata limbata* (Figure 8). New taxonomic descriptions should reflect the larger morphological variation covered by each group. Although the overall morphological diversity in the Atlantic was large, we found little structure in our morphometric data and low levels of genetic diversity, in contrast to the Indo-Pacific. In the Indo-Pacific, we found a maximum of 11 species, comprising 13 of the original taxa described by Van der Spoel et al. (1993). Based on our findings, *D. angulata*, *D. triangulata*, *D. strangulata*, and *D. mcgowani* are confirmed as valid species. Nine original taxa should be merged into two species: one species comprising *D. elegans*, *D. vanutrechti vanutrechti*, *D. vanutrechti meisenheimeri*, and *D. souleyeti*, and one comprising *D. bandaensis*, *D. bicornis*, *D. grayi*, *D. pacifica*, and *D. striata*. The latter species may comprise additional unresolved diversity. Furthermore, three Indo-Pacific groups identified in this study require taxonomic names (Figure 8). Despite the global distribution of our samples, some taxonomic uncertainties remain, especially in the Indo-Pacific, Eastern Tropical Pacific (ETP), and Red Sea. The sampling coverage in the Atlantic Ocean was higher than in the Indo-Pacific. The species status of three original,

described taxa remains unknown: *D. aspina*, *D. robusta*, and *D. flexipes*, described from the Indian Ocean, Pacific Ocean, and Red Sea, respectively (Van der Spoel et al., 1993). We failed to assign non-type material identified as *D. aspina* (*N* = 1) by Van der Spoel et al. (1993) to any group unambiguously and did not have *D. robusta* specimens available. Finally, we did not have the type material nor other material identified as *D. flexipes* from the Red Sea. However, Janssen (2007b) suggested that the species status of *D. flexipes* based on subtle morphological differences is doubtful, and rather represents intraspecific variation.

The higher overall species diversity in the Indo-Pacific compared to the Atlantic supports the hypothesis of an Indo-Pacific origin for *Diacavolinia* as outlined in Van der Spoel et al. (1993). *Diacavolinia* was already present in the Indo-Pacific in the Pliocene (Piacenzian, 3.6-2.6 million years ago (mya)), based on fossils from northern Philippine sediments described as *Diacavolinia pristina* (Janssen, 2007a). It is unknown how long *Diacavolinia* has been present in the Atlantic Ocean. The ratio between the number of *Diacavolinia* species found in the Atlantic versus the Indo-Pacific is 0.18 based on our integrative analysis compared to 0.7 in previous research (Van der Spoel et al., 1993). Members of other, older euthecosome genera than *Diacavolinia* may have been able to disperse more easily at (sub)tropical latitudes at their times of origin, because the Isthmus of Panama and Tethys Sea were still open (closing at ~3.5 and ~13.5 mya, respectively; Bowen et al., 2016). Atlantic:Indo-Pacific species ratios of other genera appear to increase with time of origin (data from Checchia-Rispoli, 1921; Scarsella, 1934; Bernasconi and Robba, 1982; Janssen, 1990, 2005, 2006, 2007a; Cahuzac and Janssen, 2010; Burridge et al., 2015: Thesis chapter 3, 2016: Thesis chapter 4; Bowen et al., 2016; World Register of Marine Species (WoRMS)). When only considering extant, epipelagic, warm water species, ratios of straight-shelled genera (Cavolinioidea) containing more than one such species are 0.43 for *Diacria* (Miocene: Tortonian, 7.2-11.6 mya), 0.5 for *Cuvierina* (Miocene: Aquitanian, 20.4-23 mya), 0.67 for *Cavolinia* (Miocene: Langhian, 13.8-16 mya), 0.75 for *Clio* (Eocene: Priabonian, 33.9-38.0 mya), and 1 for *Creseis* (Eocene: Bartonian, 38-41 mya). *Creseis* is the oldest extant straight-shelled genus. All epipelagic, warm water species of the coiled genera *Limacina* and *Heliconoides* (Limacinoidea) also appear to have circumglobal distributions and Atlantic:Indo-Pacific species ratios of 1, with the first representative being described from the Late Cretaceous: Campanian (83.5-72.1 mya; Janssen and Goedert, 2016). These observations suggest an increased Atlantic:Indo-Pacific species ratio for pteropod genera with a longer evolutionary history.

Barriers to dispersal

Persistent dispersal barriers may limit range shifts of some taxa in response to changing ocean conditions, while other taxa may be able to adapt and occupy new ecological niches. The most important biogeographic barriers for *Diacavolinia*, as inferred from distinct species assemblages, were between the Atlantic and Indo-Pacific oceans and the East and Central Pacific. Biogeographic distributions of

revised *Diacavolinia* species were as follows: Atlantic (two endemic species), warm waters south of South Africa (one endemic species), Western Indian Ocean (four species), Red Sea and Gulf of Aden (three species), Indo-West Pacific (six species, one endemic), Hawaiian waters (three species, one endemic), Sino-Japanese waters (three species), and Eastern Tropical Pacific (three endemic species). Species distributions were less patchy and disjunct compared to Van der Spoel et al. (1993) and may better reflect ecological and/or habitat preferences of *Diacavolinia* taxa. The distribution patterns of the revised *Diacavolinia* species were congruent with several well-known biogeographic provinces for other holoplankton or benthic species with pelagic larvae, and provide important information on the range of environmental variation experienced by each species (e.g., Kulbicki et al., 2013; Bowen et al., 2016; Iacchei et al., 2016). Kitidis (in press) observed evidence of ocean acidification along a longitudinal transect across the Atlantic Ocean, and estimated an annual rate of pH decrease of 0.0013 ± 0.0009 units. Jiang et al. (2015) observed that the aragonite saturation depth was deeper in the North and South Atlantic (~1000-2500 m), South Indian (~750-1500 m), and Southwest Pacific Ocean (~500-1500 m) compared to the North Indian (350-600 m), North Pacific (~200-750 m), and Southeast Pacific Ocean (~150-500 m). They also observed that in the Atlantic and Pacific oceans the aragonite saturation state in waters shallower than 100 m depth decreased by ~0.40% on average from the decade spanning 1989-1998 to the decade spanning 1998-2010. These findings suggest that *Diacavolinia* species in the East Pacific, the endemic Groups 9, 10, and 12, may be more exposed and vulnerable to future ocean acidification than other *Diacavolinia* species.

The Agulhas Current in the Indian Ocean intermittently forces warm eddies into the Atlantic (Hutchings et al., 2009; Villar et al., 2015). Although distributions of two *Diacavolinia* taxa extended to waters south of South Africa, we did not find evidence for recent dispersal among the Atlantic and Indian Oceans along this pathway. Hence, the degree of connection of *Diacavolinia* in the Atlantic and Indo-Pacific basins appears to have been overestimated by Van der Spoel et al. (1993), who reported that five of the 24 originally described *Diacavolinia* taxa occurred in both the Atlantic and the Indo-Pacific. For *Cuvierina* pteropods, also no evidence of recent dispersal from the Indian Ocean into the Atlantic Ocean was found (Janssen, 2005; Burridge et al., 2015: Thesis chapter 3). More rigorous molecular examination of other warm-water euthecosomes may identify higher numbers of endemic species in the Atlantic and Indo-Pacific ocean basins than have been described to date. Other pelagic examples for which Atlantic taxa are isolated from the Indo-Pacific include several copepods (e.g., Hirai et al., 2015; Goetze, 2011) and populations of two-wing flyfish (Lewallen et al., 2016). Conversely, evidence of Agulhas leakage among ocean basins has increased over the last decade (Biastoch et al., 2009). Sporadic dispersal through Agulhas rings has been demonstrated, e.g., for moray eels and glasseye fish (Reece et al., 2010; Gaither et al., 2015). Additionally, Villar (2015) demonstrated an overlap in metabarcode MOTUs of the plankton community within Agulhas rings between the Indian and South Atlantic oceans.

We found evidence for endemism of *Diacavolinia* species in the Eastern Tropical Pacific (ETP). Other genetic studies of East Pacific plankton showed that some, but not all taxa demonstrated East Pacific endemism, and it is likely that cryptic diversity is present within what are now considered single species or species complexes. Within another group of planktonic gastropods (heteropods, Pterotracheoidea), *Atlanta californiensis* is restricted to the East Pacific (Seapy et al., 2003). Some endemic cryptic diversity within the ETP also was found in the *Pleuromamma piseki – P. gracilis* copepod species complex (Halbert et al., 2013). Taxa with pelagic larval stages sometimes demonstrated East Pacific isolation, such as the reef-building coral *Porites lobata* (Baums et al., 2012) and the spiny lobster *Panulirus penicillatus* (Iacchei et al., 2016), but not always, such as the echinoderm *Echinothrix diadema* (Lessios et al., 1998).

Red Sea endemism appears to have multiple causes, with a cold, nutrient-rich barrier separating the Gulf of Aden from the rest of the Arabian Sea, and a narrow strait separating the Red Sea from the Gulf of Aden. Moreover, circulation patterns and environmental gradients may provide additional isolating barriers to dispersal (DiBattista et al., 2016). We found indications for isolation of Red Sea fauna for *Diacavolinia* based on geometric morphometric information, because specimens from the Gulf of Aden and entrance of the Red Sea were always assigned to multiple groups per location (18% unassigned). Because no genetic information was available, we could not infer whether the Red Sea has exported *Diacavolinia* biodiversity over time, or if it is an area of incipient speciation and local endemism due to its pheripheral position and unique oceanographic conditions within a wide Indo-Pacific distribution. Fossil records have indicated that the latter is more likely for pelagic taxa because of loss of plankton diversity in the central Red Sea during low sea level stands in Pleistocene glacial maxima, and hypersaline conditions caused by almost complete isolation from the Indian Ocean (Fenton et al., 2000). Conversely, there is also evidence that some taxa increased in abundance due to freshwater dilution in the Gulf of Aqaba, such as observed in *Creseis* pteropods and siliceous diatoms (Reiss et al., 1980; Fenton et al., 2000; Almogi-Labin et al., 2008). Furthermore, some Red Sea lineages are older than their respective sister lineages in the Indian Ocean, suggesting export of biodiversity from the Red Sea, such as for some reef fishes (DiBattista et al., 2013). Peripheral speciation was observed for the spiny lobster *Panulirus penicillatus* with a 9-month larval stage, as well as for several reef fish taxa (Liu et al., 2014; Fernandez-Silva et al., 2015; Iacchei et al., 2016).

The high number of *Diacavolinia* taxa in the Indo-West Pacific (IWP) reflects the high overall marine diversity in the area (e.g., Renema et al., 2008; Becking et al., 2016). We found that the most common taxa were distributed across a broad range in the Sino-Japanese, Central Pacific, and Indian Ocean waters. There are no large-scale environmental gradients in the Indo-West Pacific that limit the distributions of *Diacavolinia* taxa, such as observed in the Red Sea, and present-day waters would appear to be deep enough to enable diel vertical migration in the epi- and

upper mesopelagic zones. However, more genetic sampling in this area is needed to further resolve species boundaries in *Diacavolinia*, clarify the high genetic and presumably cryptic diversity within Group 5, and explore IWP endemism. Also for genetic lineages of *Pleuromamma xiphias* copepods, which are deep diel migrators (>400 m), broad distributions as well as one endemic clade were found within the IWP (Goetze, 2011).

Across all oceans, we observed no obvious equatorial dispersal barriers separating the distributions of extant *Diacavolinia* taxa, but our Group 2 (no genetic information available) only occurred in the subtropical Atlantic waters north of the equator. We also found no evidence for equatorial genetic breaks within groups. Equatorial dispersal barriers may be important drivers of pelagic evolution for other taxa, such as shown for subtropical Atlantic copepods (Goetze et al., 2015, in press) and pteropods (Burridge et al., 2015: Thesis chapter 3).

Conclusions

Combining varied datasets in an integrative taxonomic approach may be suitable for a wide array of morphologically diverse marine taxa and is an essential first step to predicting species-specific ecological and evolutionary responses to ocean change. Museum collections prove to be an invaluable reference for assessing species boundaries and biogeographic distributions using modern techniques, enabling comparison of our findings with prior works based on the same specimens. We assessed species boundaries in *Diacavolinia* pteropods based on rigorous sampling over a time period of 104 years and data collection across the Atlantic, Pacific, and Indian oceans. Our results show that taxonomic revisions of *Diacavolinia* are needed, and will be reported on in subsequent work. However, still not all species boundaries are resolved and some rare species were only sampled once.

Acknowledgements

We thank A. Tsuda and R.A. Gasca Serrano for generously providing freshly collected *Diacavolinia* samples from the Atlantic and Pacific oceans, J. van Arkel for his assistance in specimen photography, and M. Eurlings, K. Beentjes, M.K. Dijkstra, O.D. Schaap, L. Dong, B. Voetdijk, and P. Kuperus for technical assistance in the molecular lab. We are grateful to A.W. Jansen for his ideas, thorough knowledge of pteropod fossils, and comments on this manuscript. Finally, we thank J. Huisman and S.B.J. Menken for their helpful comments on this manuscript. This work was supported by the Royal Netherlands Institute for Sea Research (NIOZ) for cruise participation, the Royal Netherlands Academy of Sciences Ecology Fund (KNAW Fonds Ecologie) Research grant 0205510763, and The Malacological Society of London Research grant to A.K. Burridge, a Netherlands Organisation for Scientific Research (NWO) cruise participation grant, and VENI grant 863.08.024 to K.T.C.A. Peijnenburg. E. Goetze and collections in this study were supported under National Science Foundation grants OCE-1029478, OCE-1255697 and OCE-1338959, as well as Hawaii state support for ship time on R/V Kilo Moana in 2011 (U Hawaii OCN627 student training cruise, KM1109). We also thank the Sea Education Association (S226), and D. Kobayashi and L. Giuseffi (SE1201) for assistance with collections. This is contribution number 294 of the Atlantic Meridional Transect Programme. The authors declare that they have no competing interests.

References

Almogi-Labin A., Edelman-Furstenberg Y., Hemleben C., 2008. Variations in biodiversity of thecosomatous pteropods during the Late Quaternary as a response to environmental changes in the Gulf of Aden-Red Sea-Gulf of Aqaba ecosystems. In: Por D. (Ed.), Aqaba-Eilat, the improbable Gulf. Environment, biodiversity and preservation. The Hebrew University Press, Jerusalem, pp. 31–48.

Altschul S.F., Madden T.L., Schäfer A.A., Zhang J., Zhang Z., et al., 1997. Gapped BLAST and PSI-BLAST: a new generation of protein database search programs. Nucleic Acids Research 25, 3389–3402.

Anderson M.J., 2001. A new method for non-parametric multivariate analysis of variance. Austral Ecology 26, 32–46.

Bauer A.M., Parham J.F., Brown R.M., Stuart B.L., Grismer L., et al., 2011. Availability of new Bayesian-delimited gecko names and the importance of character-based species descriptions. Proceedings of the Royal Society B 278, 490–492.

Baums I.B., Boulay J.N., Polato N.R., Hellberg M.E., 2012. No gene flow across the Eastern Pacific Barrier in the reef-building coral *Porites lobata*. Molecular Ecology 21, 5418–5433.

Bé A.W.H., Gilmer R.W., 1977. A zoogeographic and taxonomic review of euthecosomatous Pteropoda. In: Ramsay A.T.S. (Ed.), Oceanic Micropaleontology 1. Academic Press, London, pp. 733–808.

Beaugrand G., Edwards M., Rayboud V., Goberville E., Kirby R.R., 2015. Future vulnerability of marine biodiversity compared with contemporary and past changes. Nature Climate Change 5, 695–701.

Beaugrand G., Goberville E., Luczak C., Kirby R.R., 2014. Marine biological shifts and climate. Proceedings of the Royal Society B 281, 20133350.

Beaugrand G., McQuatters-Gollop A., Edwards M., Goverville E., 2012. Long-term responses of North Atlantic calcifying plankton to climate change. Nature Climate Change 3, 263–267.

Becking L.E., De Leeuw C.A., Knegt B., Maas D.L., De Voogd N.J., et al., 2016. Highly divergent mussel lineages in isolated Indonesian marine lakes. PeerJ 4, e2496.

Bednaršek N., Harvey C.J., Kaplan I.C., Feely R.A., Možina J., 2016. Pteropods on the edge: cumulative effects of ocean acidification, warming, and deoxygenation. Progress in Oceanography 145, 1–24.

Bednaršek N., Ohman M.D., 2015. Changes in pteropod distributions and shell dissolution across a frontal system in the California Current System. Marine Ecology Progress Series 523, 93–103.

Bernasconi M.P., Robba E., 1982. The thecosomatous pteropods: a contribution toward the Cenozoic Tethyan paleobiogeography. Bollettino della Società Paleontologica Italiana 21, 2–3.

Biastoch A., Böning C.W., Schwarzkopf F.U., Lutjeharms J.R., 2009. Increase in Agulhas leakage due to poleward shift of southern hemisphere westerlies. Nature 462, 495–498.

Bowen B.W., Gaither M.R., DiBattista J.D., Iacchei M., Andrews K.R. et al., 2016. Comparative phylogeography of the ocean planet. Proceedings of the National Academy of Sciences 113, 7962–7969.

Brown C.J., O'Connor M.I., Poloczanska E., Schoeman D.S., Buckley L.B., et al., 2016. Ecological and methodological drivers of species' distribution and phenology responses to climate change. Global Change Biology 22, 1548–1560.

Burridge A.K., Goetze E., Raes N., Huisman J., Peijnenburg K.T.C.A., 2015. Global biogeography and evolution of *Cuvierina* pteropods. BMC Evolutionary Biology 15, 39. *Thesis chapter 3.*

Burridge A.K., Goetze E., Wall-Palmer D., Le Double S.L., Huisman J., Peijnenburg K.T.C.A., in press. Diversity and abundance of pteropods and heteropods along a latitudinal gradient across the Atlantic Ocean. Progress in Oceanography, published online in 2016. *Thesis chapter 6.*

Burridge A.K., Hörnlein C., Janssen A.W., Hughes M., Bush S., et al., 2017. Time-calibrated molecular phylogeny of pteropods. PLoS ONE 12, e0177325. *Thesis chapter 2.*

Burridge A.K., Janssen A.W., Peijnenburg K.T.C.A., 2016. Revision of the genus *Cuvierina* Boas, 1886 based on integrative taxonomic data, including the description of a new species from the Pacific Ocean (Gastropoda, Thecosomata). ZooKeys 619, 1–12. *Thesis chapter 4.*

Burridge A.K., Tump M., Vonk R., Goetze E., Peijnenburg K.T.C.A., in press. Diversity and distribution of hyperiid amphipods along a latitudinal gradient in the Atlantic Ocean. Progress in Oceanography, published online in 2016. *Thesis chapter 7.*

Cahuzak B., Janssen A.W., 2010. Eocene to Miocene holoplanktonic Mollusca (Gastropoda) of the Aquitaine Basin, southwest France. Scripta Geologica 141, 1–193.

Checchia-Rispoli G., 1921. I pteropodi del Miocene garganico. Bollettino del R. Comitato Geologico d'Italia 48, 1–28.

Comeau S., Gattuso J.-P., Nisumaa A.-M., Orr J., 2012. Impact of aragonite saturation state changes on migratory pteropods. Proceedings of the Royal Society B 279, 732–738.

Corse E., Rampal J., Cuoc C., Peck N., Perez Y., Gilles A, 2013. Phylogenetic analysis of Thecosomata Blainville, 1824 (Holoplanktonic Opisthobranchia) using morphological and molecular data. PLoS ONE 8, e59439.

Dambach J., Rödder D., 2011. Applications and future challenges in marine species distribution modeling. Aquatic Conservation: Marine and Freshwater Ecosystems 21, 92–100.

Darriba D., Taboada G.L., Doallo R., Posada D., 2012. jModelTest 2: more models, new heuristics and parallel computing. Nature Methods 9, 772.

Dayrat B., Tillier A., Lecointre G., Tillier S., 2001. New clades of euthyneuran gastropods (Mollusca) from 28S rRNA sequences. Molecular Phylogenetics and Evolution 19, 225–235.

D'Orbigny A., 1836–1846. Voyage dans l'Amérique médionale (le Brésil, la république orientale de l'Uruguay, la république Argentine, la Patagonie, la république du Chili, la république de Bolivia la république du Pérou), exécuté pendant les années 1826, 1827, 1828, 1829, 1830, 1831, 1832 et 1833, 5. Bertrand, Paris; Levrault, Strasbourg.

De Blainville H.M.D., 1821. Hyale, Hyaloea (Malacoz.). Dictionnaire des Sciences Naturelles 22, 65–83.

De Queiroz K., 2007. Species concepts and species delimitation. Systematic Biology 56, 879–886.

Deshayes G.P., 1823. Cléodore. *Cleodora*. Moll. Dictionnaire classique d'Histoire Naturelle 4, 203–204.

DiBattista J.D., Berumen M.L., Gaither M.R., Rocha L.A., Eble J.A., et al., 2013. After continents divide: comparative phylogeography of reef fishes from the Red Sea and Indian Ocean. Journal of Biogeography 40, 1170–1181.

DiBattista J.D., Howard Choat J., Gaither M.J., Hobbs J.-P.A., Lozano-Cortés D.J., et al., 2016. On the origin of endemic species in the Red Sea. Journal of Biogeography 43, 13–30.

Dolan J.R., Yang E.J., Kang S.-H., Rhee T.S., 2016. Declines in both redundant and trace species characterize the latitudinal diversity gradient in tintinnid ciliates. The ISME Journal 10, 2174–2183.

Edwards D.L., Knowles L.L., 2014. Species detection and individual assignment in species delimitation: can integrative data increase efficacy? Proceedings of the Royal Society B 281, 20132765.

Elith J., Leathwick J.R., 2009. Species distribution models: ecological explanation and prediction across space and time. Annual Review of Ecology, Evolution, and Systematics 40, 677–697.

Fabry V.J., Seibel B.A., Feely R.A., Orr J.C., 2008. Impacts of ocean acidification on marine fauna and ecosystem processes. ICES Journal of Marine Science 65, 414–432.

Felsenstein J., 1981. Evolutionary trees from DNA sequences: a maximum likelihood approach. Journal of Molecular Evolution 17, 368–376.

Fenton M., Geiselhart S., Rohling E., Hemleben C., 2000. Aplanktonic zones in the Red Sea. Marine Micropaleontology 40, 277–294.

Fernandez-Silva I., Randall J.E., Coleman R.R., DiBattista J.D., Rocha L.A., et al., 2015. Yellow tails in the Red Sea: phylogeography of the Indo-Pacific goatfish *Mulloidichthys flavolineatus* reveals isolation in pheripheral provinces and cryptic evolutionary lineages. Journal of Biogeography 42, 2402–2413.

Folmer O., Black M., Hoeh W., Lutz R., Vrijenhoek R., 1994. DNA primers for amplification of mitochondrial Cytochrome c Oxidase subunit I from diverse metazoan invertebrates. Molecular Marine Biology and Biotechnology 3, 294–299.

Fujita M.K., Leaché A.D., 2011. A coalescent perspective on delimiting and naming species: a reply to Bauer *et al*. Proceedings of the Royal Society B 278, 493–495.

Fujita M.K., Leaché A.D., Burbrink F.T., McGuire J.A., Moritz C., 2012. Coalescent-based species delimitation in an integrative taxonomy. Trends in Ecology & Evolution 27, 480–488.

Gaither M.R., Bernal M.A., Fernandez-Silva I., Mwale M., Jones S.A., et al., 2015. Two deep evolutionary lineages in the circumtropical glasseye *Heteropriacanthus cruentatus* (Teleostei, Priacanthidae) with admixture in the south-western Indian Ocean. Journal of Fish Biology 87, 715–727.

Goetze E., 2011. Population differentiation in the open sea: insights from the pelagic copepod *Pleuromamma xiphias*. Integrative and Comparative Biology 51, 580–597.

Goetze E., Andrews K.R., Peijnenburg K.T.C.A., Portner E., Norton E., 2015. Temporal stability of genetic structure in a mesopelagic copepod. PLoS ONE 10, e0136087.

Goetze E., Hüdepohl P.T., Chang C., Van Woudenberg L., Iacchei M., Peijnenburg K.T.C.A., in press. Ecological dispersal barrier across the equatorial Atlantic in a migratory planktonic copepod. Progress in Oceanography, published online in 2016.

Goetze E., Ohman M., 2010. Integrated molecular and morphological biogeography of the calanoid copepod family Eucalanidae. Deep-Sea Research II 57, 2110–2129.

Gray J.E., 1850. Catalogue of the Mollusca in the collection of the British Museum, 2. Pteropoda. British Museum/E. Newman, London, pp. 1–45.
Gunz P., Mitteroecker P., 2013. Semilandmarks: a method for quantifying curves and surfaces. Hystrix, the Italian Journal of Mammalogy 24, 103–109.
Halbert K.M.K., Goetze E., Carlon D.B., 2013. High cryptic diversity across the global range of the migratory planktonic copepods *Pleuromamma piseki* and *P. gracilis*. PLoS ONE 8, e77011.
Hammer Ø., Harper D.A.T., Ryan P.D., 2001. PAST: paleontological statistics software package for education and data analysis. Palaeontologia Electronica 4, 1–9.
Hausdorf B., 2011. Progress toward a general species concept. Evolution 65, 923–931.
Hirai J., Tsuda A., Goetze E., 2015. Extensive genetic diversity and endemism across the global range of the oceanic copepod *Pleuromamma abdominalis*. Progress in Oceanography 138, 77–90.
Hutchings I., Van der Lingen C.D., Shannon L.J., Crawford R.J.M., Verheye H.M.S., et al., 2009. The Benguela Current: an ecosystem of four components. Progress in Oceanography 83, 15–32.
Iacchei M., Gaither M.R., Bowen B.W., Toonen R.J., 2016. Testing dispersal limits in the sea: range-wide phylogeography of the pronghorn spiny lobster *Panulirus penicillatus*. Journal of Biogeography 43, 1032–1044.
Janssen A.W., 1990. Pteropoda (Gastropoda, Euthecosomata) from the Australian Cainozoic. Scripta Geologica 91, 1–76.
Janssen A.W., 2005. Development of Cuvierinidae (Mollusca, Euthecosomata, Cavolinioidea) during the Cainozoic: a non-cladistic approach with a re-interpretation of Recent taxa. Basteria 69, 25–72.
Janssen A.W., 2006. Notes on the systematics, morphology and biostratigraphy of fossil holoplanktonic Mollusca, 16. Some additional notes and amendments on Cuvierinidae and on classification of Thecosomata (Mollusca, Euthecosomata). Basteria 70, 67–70.
Janssen A.W., 2007a. Holoplanktonic Mollusca (Gastropoda: Pterotracheoidea, Janthinoidea, Thecosomata and Gymnosomata) from the Pliocene of Pangasinan (Luzon, Philippines). Scripta Geologica 135, 29–177.
Janssen A.W., 2007b. Holoplanktonic Mollusca (Gastropoda) from the Gulf of Aqaba, Red Sea and Gulf of Aden (Late Holocene-Recent). The Veliger 49, 140–195.
Janssen A.W., 2012. Late Quaternary to recent holoplanktonic Mollusca (Gastropoda) from bottom samples of the eastern Mediterranean Sea: systematics, morphology. Bollettino Malacologico 48, 1–105.
Janssen A.W., Goedert J.L., 2016. Notes on the systematics, morphology and biostratigraphy of fossil holoplanktonic Mollusca, 24. First observation of a genuinely Late Mesozoic thecosomatous pteropod. Basteria 80, 59–63.
Jennings R.M., Bucklin A., Ossenbrügger H., Hopcroft R.R., 2010. Species diversity of planktonic gastropods (Pteropoda and Heteropoda) from six ocean regions based on DNA barcode analysis. Deep-Sea Research II 57, 2199–2210.
Jiang L.-Q., Feely R.A., Carter B.R., Greeley D.J., Gledhill D.K., Arzayus K.M., 2015. Climatological distribution of aragonite saturation state in the global oceans. Global Biogeochemical Cycles 29, 1656–1673.
Karanovic T., Djurakic M., Eberhard S.F., 2016. Cryptic species or inadequate taxonomy? Implementation of 2D geometric morphometrics based on integumental organs as landmarks for delimitation and description of copepod taxa. Systematic Biology 65, 304–327.
Kendall D., 1977. The diffusion of shape. Advances in Applied Probability 9, 428–430.
Kimura M., 1980. A simple method for estimating evolutionary rate of base substitutions through comparative studies of nucleotide sequences. Journal of Molecular Evolution 16, 111–120.
Kitidis V., Brown I., Hardman-Mountford N., Lefèvre N., in press. Surface ocean carbon dioxide during the Atlantic Meridional Transect (1995-2013); evidence of ocean acidification. Progress in Oceanography, published online in 2016.
Klingenberg C.P., 2010. Evolution and development of shape: integrating quantitative approaches. Nature Reviews. Genetics 11, 623–635.
Knapp S., 2008. Taxonomy as a team sport. In: Wheeler Q.D. (Ed.), The new taxonomy. CRC Press, Taylor & Francis Group, Boca Raton, pp. 33–53.
Kulbicki M., Parravicini V., Bellwood D.R., Arias-Gonzàlez E., Chabanet P., et al., 2013. Global biogeography of reef fishes: a hierarchical quantitative delineation of regions. PLoS ONE 8, e81847.
Lalli C.M., Gilmer R.W., 1989. Pelagic Snails: The Biology of Holoplanktonic Gastropod Molluscs. Stanford University Press, Stanford, California.

Lessios H.A., Kessing B.D., Robertson D.R., 1998. Massive gene flow across the world's most potent marine biogeographic barrier. Proceedings of the Royal Society B 265, 583–588.

Lewallen E.A., Bohonak A.J., Bonin C.A., Van Wijnen A.J., Pitman R.L., Lovejoy N.R., 2016. Population genetic structure of the tropical two-wing flyingfish (*Exocoetus volitans*). PLoS ONE 11, e0163198.

Librado P., Rozas J., 2009. DnaSP v5: a software for comprehensive analysis of DNA polymorphism data. Bioinformatics 25, 1451–1452.

Liu S.-Y.V., Chang F.-T., Borsa P., Chen W.-J., Dai C.-F., 2014. Phylogeography of the humbug damselfish, *Dascyllus aruanus* (Linnaeus, 1758): evidence of Indo-Pacific vicariance and genetic differentiation of pheripheral populations. Biological Journal of the Linnean Society 113, 931–942.

Longhurst A.R., 1998. Ecological Geography of the Sea. Academic Press, San Diego.

Maas A.E., Blanco-Bercial L., Lawson G.L., 2013. Reexamination of the species assignment of *Diacavolinia* pteropods using DNA barcoding. PLoS ONE 8, e53889.

Maas A.E., Lawson G.L., Aleck Wang Z., 2016. The metabolic response of thecosome pteropods from the North Atlantic and North Pacific oceans to high CO_2 and low O_2. Biogeosciences 13, 6191–6210.

MAFFT version 7. Multiple alignment program for amino acid or nucleotide sequences. http://mafft.cbrc.jp/alignment/server

Marine Species Identification Portal (MSIP). http://species-identification.org

McManus G.B., Katz L.A., 2009. Molecular and morphological methods for identifying plankton: what makes a successful marriage? Journal of Plankton Research 31, 1119–29.

Mitteroecker P., Gunz P., 2009. Advances in geometric morphometrics. Evolutionary Biology 36, 235–247.

Morard R., Escarguel G., Weiner A.K.M., André A., Douady C.J. et al., 2016. Nomenclature for the nameless: a proposal for an integrative molecular taxonomy of cryptic diversity exemplified by planktonic Foraminifera. Systematic Biology 65, 925–940.

Moya A., Howes E.L., Lacoue-Labarthe T., Forêt S., Bishoy H. et al., 2016. Near-future pH conditions severely impact calcification, metabolism and the nervous system in the pteropod *Heliconoides inflatus*. Global Change Biology 22, 3888–3900.

Norton E.L., Goetze E., 2013. Equatorial dispersal barriers and limited population connectivity among oceans in a planktonic copepod. Limnology and Oceanography 58, 1581–1596.

Padial J.M., Miralles A., De la Riva I., Vences M., 2010. The integrative future of taxonomy. Frontiers in Zoology 7, 16.

Parmesan C., Burrows M.T., Duarte C.M., Poloczanska E.S., Richardson A.J., et al., 2013. Beyond climate change attribution in conservation and ecological research. Ecology Letters 16, 58–71.

Puillandre N., Lambert A., Brouillet S., Achaz G., 2012. ABGD, Automatic Barcode Gap Discovery for primary species delimitation. Molecular Ecology 21, 1864–1877.

R Development Core Team. R. A language and environment for statistical computing. 2013. http://www.R-project.org

Reece J.S., Bowen B.W., Smith D.G., Larson A., 2010. Molecular phylogenetics of moray eels (Muraenidae) demonstrates multiple origins of a shell-crushing jaw (*Gymnomuraena*, *Echidna*) and multiple colonizations of the Atlantic Ocean. Molecular Phylogenetics and Evolution 57, 829–835.

Reiss Z., Luz B., Almogi-Labin A., Halicz E., Winter A., et al., 1980. Late Quaternary paleoceanography of the Gulf of Aqaba (Elat), Red Sea. Quaternary Research 14, 294–308.

Renema W., Bellwood D.R., Braga J.C., Bromfield K., Hall R. et al., 2008. Hopping hotspots: global shifts in marine biodiversity 321, 654–657.

Reygondeau G., Longhurst A., Martinez E., Beaugrand G., Antoine D., Maury O., 2013. Dynamic biogeochemical provinces in the global ocean. Global Biogeochemical Cycles 27, 1–13.

Richardson A.J., 2008. In hot water: zooplankton and climate change. ICES Journal of Marine Science 65, 279–295.

Robinson L.M., Elith J., Hobday A.J., Pearson R.G., Kendall B.E. et al., 2011. Pushing the limits in marine species distribution modelling: lessons from the land present challenges and opportunities. Global Ecology and Biogeography 20, 789–802.

Roger L.M., Richardson A.J., McKinnon A.D., Knott B., Matear R., Scadding C., 2011. Comparison of the shell structure of two tropical Thecosomata (*Creseis acicula* and *Diacavolinia longirostris*) from 1963 to 2009: potential implications of declining aragonite saturation. ICES Journal of Marine Science 69, 465–474.

Rohlf F.J., 2006. Tps series. http://life.bio.sunysb.edu/morph
Scarsella F., 1934. Di una nuova specie di pteropodo del Miocene appenninico. Bollettino della Società Geologica Italiana 53, 177–181.
Seapy R.R., Richter G., 2003. *Atlanta californiensis*, a new species of atlantid heteropod (Mollusca: Gastropoda) from the California Current. The Veliger 36, 389–398.
Shapiro B., Rambaut A., Drummond A.J., 2006. Choosing appropriate substitution models for the phylogenetic analysis of protein-coding sequences. Molecular Biology and Evolution 23, 7–9.
Silvestro D., Michalak I., 2012. RaxmlGUI: a graphical front-end for RAxML. Organisms Diversity & Evolution 12, 335–337.
Smith U.E., Hendricks J.R., 2013. Geometric morphometric character suites as phylogenetic data: extracting phylogenetic signal from gastropod shells. Systematic Biology 62, 366–385.
Souleyet F.L.A., 1852. In: Eydoux F., Souleyet F.L.A. (Eds.). Voyage autour du monde execute pendant les années 1836 and 1837 sur la corvette 'La Bonite', commandée par M. Vaillant, capitaine de vaisseau, publié par ordre du Gouvernement sous les auspices du département de la marine. Zoologie, 2. Bertrand, Paris, pp. 1–664.
Stamatakis A., 2006. RAxML-VI-HPS: maximum likelihood-based phylogenetic analyses with thousands of taxa and mixed models. Bioinformatics 22, 2688–2690.
Stephens M., Donelly P., 2003. A comparison of Bayesian methods for haplotype reconstruction from population genotype data. The American Journal of Human Genetics 73, 1162–1169.
Stephens M., Smith N., Donelly P., 2001. A new statistical method for haplotype reconstruction from population data. The American Journal of Human Genetics 68, 978–989.
Tamura K., Stecher G., Peterson D., Filipski A., Kumar S., 2013. MEGA6: Molecular Evolutionary Genetics Analysis Version 6.0. Molecular Biology and Evolution 30, 2725–2729.
Valentin J.L., Monteiro-Ribas W.M., 1993. Zooplankton community structure on the east-southeast Brazilian continental shelf (18–23°S latitude). Continental Shelf Research 13, 407–424.
Van der Spoel S., 1967. Euthecosomata, a group with remarkable developmental stages (Gastropoda, Pteropoda). PhD thesis, University of Amsterdam. Noorduijn en Zoon, Gorinchem.
Van der Spoel S., 1971. New forms of *Diacria quadridentata* (De Blainville, 1821), *Cavolinia longirostris* (De Blainville, 1821) and *Cavolinia uncinata* (Rang, 1829) from the Red Sea and the East Pacific Ocean (Mollusca, Pteropoda). Beaufortia 19, 1–20.
Van der Spoel S., 1973. Variation in *Cavolinia longirostris* (De Blainville, 1821) from the Pacific Ocean with description of a new forma (Mollusca, Pteropoda). Bulletin of the Zoological Museum of the University of Amsterdam 3, 99–102.
Van der Spoel S., 1987. *Diacavolinia* nov. gen. separated from *Cavolinia* (Pteropoda, Gastropoda). Bulletin of the Zoological Museum of the University of Amsterdam 11, 77–79.
Van der Spoel S., Bleeker J., Kobayasi H., 1993. From *Cavolinia longirostris* to twenty-four *Diacavolinia* taxa, with a phylogenetic discussion (Mollusca, Gastropoda). Bijdragen tot de Dierkunde 62, 127–166.
Villar E., Farrant G.K., Follows M., Garczarek L., Speich S., et al., 2015. Environmental characteristics of Agulhas rings affect interocean plankton transport. Science 348, 1261447.
Vogler A.P., Monaghan M.T., 2006. Recent advances in DNA taxonomy. Journal of Zoological Systematics and Evolutionary Research 45, 1–10.
Wall-Palmer D., Burridge A.K., Peijnenburg K.T.C.A., 2016a. *Atlanta ariejansseni*, a new species of shelled heteropod from the Southern Subtropical Convergence Zone (Gastropoda, Pterotracheoidea). ZooKeys 604, 13–30.
World Register of Marine Species (WoRMS). http://www.marinespecies.org
Wormelle R.L., 1962. A survey of the standing crop of plankton of the Florida current. VI. A study of the distribution of the pteropods of the Florida current. Bulletin of Marine Science 12, 93–136.

Supplementary information

The data set supporting the results of this chapter is available upon request and will be deposited at the Dryad Digital Repository once this manuscript is accepted for publication in a peer-reviewed journal. DNA sequences have been deposited at GenBank under the following accession numbers: MF974624-MF974847.

Supplementary information 1. Photographs of *Diacavolinia* specimens included in this study in (A) ventral and (B) lateral orientations.

Supplementary information 2. Geometric morphometric data of *Diacavolinia* specimens: centroid sizes and relative warps in ventral (A: 23 and B: 38 landmarks) and lateral orientations (C: 15 and D: 49 landmarks).

Figure S1. Ordination of the second and third relative warps (RWs) of *Diacavolinia* for Indo-Pacific specimens for (A) lateral orientation with 49 landmarks (LMs; *N* = 282), (B) ventral orientation with 23 LMs (*N* = 378), and (C) ventral orientation of a subset with 38 LMs (*N* = 174). See Figure 4 for symbol definitions. Corresponding thin plate splines of the most positive and negative deformations are indicated along the axes to depict the variation in shell shape.

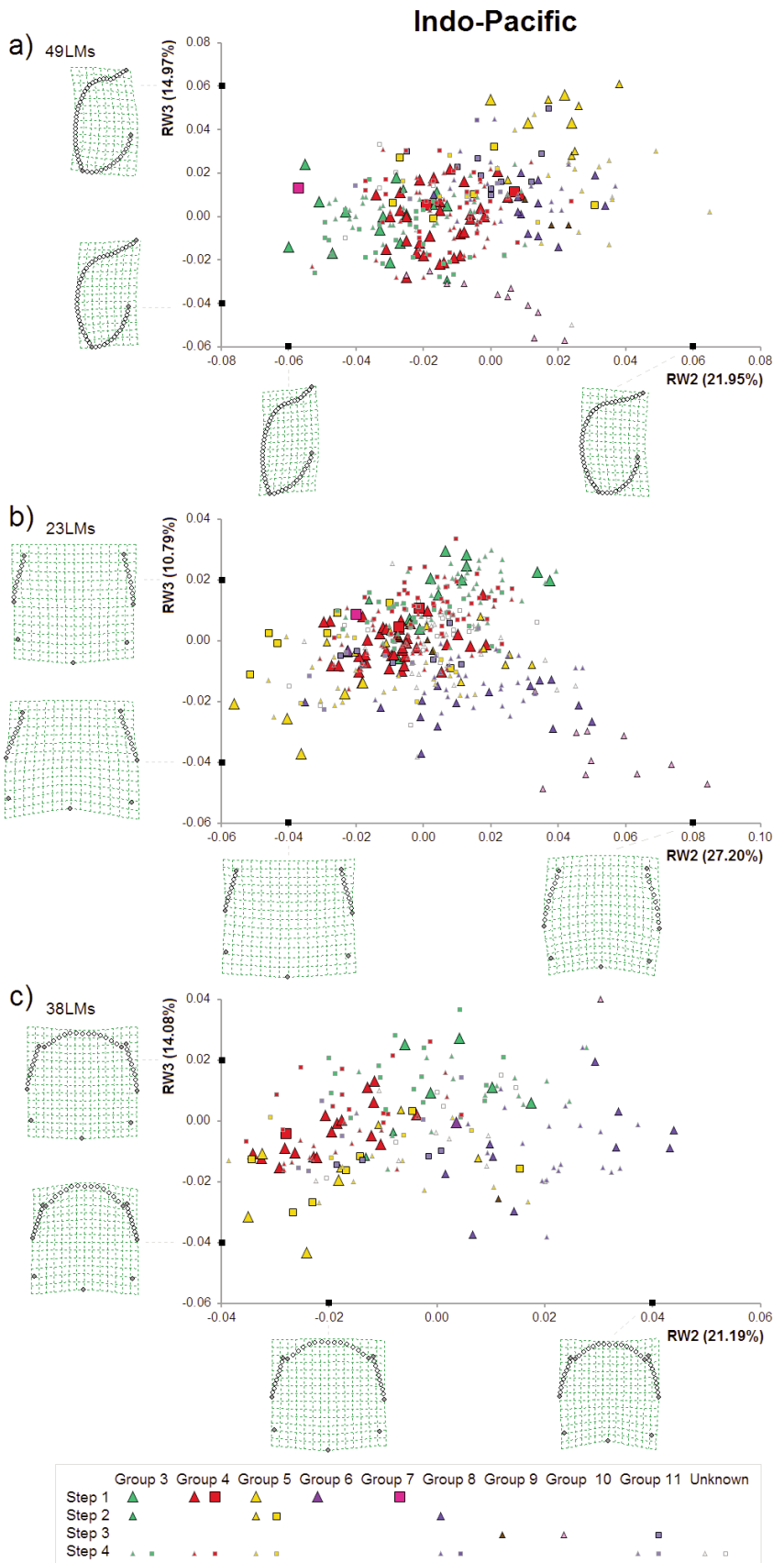
Indo-Pacific
a) 49LMs
RW3 (14.97%)
RW2 (21.95%)
b) 23LMs
RW3 (10.79%)
RW2 (27.20%)
c) 38LMs
RW3 (14.08%)
RW2 (21.19%)
Group 3 Group 4 Group 5 Group 6 Group 7 Group 8 Group 9 Group 10 Group 11 Unknown
Step 1
Step 2
Step 3
Step 4

TABLE S1. Sample collection information, group assignment using integrative approach, data usage for geometric morphometric analyses, and GenBank accession codes for each *Diacavolinia* specimen used in this study. Amb. = Ambiguous LDA assignment; Unkn. = Unknown integrative group; N.A. = Not available.; *D. v.* = *Diacavolinia vanutrechti*.

Sample information					
Specimen ID	Cruise	Station	Latitude	Longitude	Collection date
Atlantic Ocean					
D_ANE_AMT22_21a_01	AMT22	21a	25°42'N	38°43'W	2012-10-21
D_ANE_AMT22_25_01	AMT22	25	20°24'N	38°37'W	2012-10-24
D_ANE_AMT22_27_01	AMT22	27	17°42'N	36°27'W	2012-10-25
D_ANE_AMT22_29_01	AMT22	29	15°03'N	34°28'W	2012-10-26
D_ANE_AMT22_29_02	AMT22	29	15°03'N	34°28'W	2012-10-26
D_ANE_AMT22_29a_01	AMT22	29a	15°18'N	34°40'W	2012-10-26
D_ANE_AMT22_29a_02	AMT22	29a	15°18'N	34°40'W	2012-10-26
D_ANE_AMT22_35_01	AMT22	35	6°37'N	28°19'W	2012-10-29
D_ANE_AMT22_35_02	AMT22	35	6°37'N	28°19'W	2012-10-29
D_ANE_AMT22_35_03	AMT22	35	6°37'N	28°19'W	2012-10-29
D_ANE_AMT22_35_04	AMT22	35	6°37'N	28°19'W	2012-10-29
D_ANE_AMT22_35_05	AMT22	35	6°37'N	28°19'W	2012-10-29
D_ANE_AMT22_35_06	AMT22	35	6°37'N	28°19'W	2012-10-29
D_ANE_AMT22_35_07	AMT22	35	6°37'N	28°19'W	2012-10-29
D_ANE_AMT22_35_08	AMT22	35	6°37'N	28°19'W	2012-10-29
D_ANE_AMT22_35_09	AMT22	35	6°37'N	28°19'W	2012-10-29
D_ANE_AMT22_35_10	AMT22	35	6°37'N	28°19'W	2012-10-29
D_ANE_AMT22_35_11	AMT22	35	6°37'N	28°19'W	2012-10-29
D_ANE_AMT22_35_12	AMT22	35	6°37'N	28°19'W	2012-10-29
D_ANE_AMT22_35_13	AMT22	35	6°37'N	28°19'W	2012-10-29
D_ANE_AMT22_35_14	AMT22	35	6°37'N	28°19'W	2012-10-29
D_ANE_AMT22_35_15	AMT22	35	6°37'N	28°19'W	2012-10-29
D_ANE_AMT22_35_16	AMT22	35	6°37'N	28°19'W	2012-10-29
D_ANE_AMT22_35_17	AMT22	35	6°37'N	28°19'W	2012-10-29
D_ANE_AMT22_35_18	AMT22	35	6°37'N	28°19'W	2012-10-29
D_ANE_AMT22_35_19	AMT22	35	6°37'N	28°19'W	2012-10-29
D_ANE_AMT22_35_20	AMT22	35	6°37'N	28°19'W	2012-10-29
D_ANE_AMT22_35_21	AMT22	35	6°37'N	28°19'W	2012-10-29
D_ANE_AMT22_35_22	AMT22	35	6°37'N	28°19'W	2012-10-29
D_ANE_AMT22_35_23	AMT22	35	6°37'N	28°19'W	2012-10-29
D_ANE_AMT22_35_24	AMT22	35	6°37'N	28°19'W	2012-10-29
D_ANE_AMT22_35_25	AMT22	35	6°37'N	28°19'W	2012-10-29
D_ANE_AMT22_35_26	AMT22	35	6°37'N	28°19'W	2012-10-29
D_ANE_AMT22_35_27	AMT22	35	6°37'N	28°19'W	2012-10-29
D_ANE_AMT22_35_28	AMT22	35	6°37'N	28°19'W	2012-10-29
D_ANE_AMT22_35_29	AMT22	35	6°37'N	28°19'W	2012-10-29
D_ANE_AMT22_35_30	AMT22	35	6°37'N	28°19'W	2012-10-29
D_ANE_AMT22_35_31	AMT22	35	6°37'N	28°19'W	2012-10-29
D_ANE_AMT22_35_32	AMT22	35	6°37'N	28°19'W	2012-10-29
D_ANE_AMT22_35_33	AMT22	35	6°37'N	28°19'W	2012-10-29
D_ANE_AMT22_35_34	AMT22	35	6°37'N	28°19'W	2012-10-29
D_ANE_AMT22_35_35	AMT22	35	6°37'N	28°19'W	2012-10-29
D_ANE_AMT22_35_36	AMT22	35	6°37'N	28°19'W	2012-10-29
D_ANE_AMT22_37_01	AMT22	37	4°03'N	26°28'W	2012-10-30
D_ANE_AMT22_37_02	AMT22	37	4°03'N	26°28'W	2012-10-30

Identification				Geometric morphometrics						Genetics	
Specimen type (F, Fresh; M, Museum)	Genetic clade / Species (Van der Spoel et al., 1993)	LDA group	Integrative group	Ventral photo	Ventral 23LMs	Ventral 38LMs	Lateral photo	Lateral 15LMs	Lateral 49LMs	COI	28S
F Step 1	Group 1	Group 1	Group 1	✓			✓	✓	✓		MF974624
F Step 1	Group 1	Group 1	Group 1	✓	✓	✓	✓	✓			MF974625
F Step 1	Group 1	Group 1	Group 1	✓	✓	✓	✓	✓	✓	MF974762	MF974626
F Step 1	Group 1	Group 1	Group 1	✓	✓	✓	✓	✓			MF974627
F Step 1	Group 1	Group 1	Group 1	✓	✓	✓	✓	✓	✓	MF974763	MF974628
F Step 1	Group 1	N.A.	Group 1	✓			✓			MF974764	
F Step 1	Group 1	N.A.	Group 1	✓			✓			MF974765	
F Step 1	Group 1	Group 1	Group 1	✓			✓	✓	✓	MF974766	MF974629
F Step 4	N.A.	Group 1	Group 1	✓	✓	✓	✓	✓	✓		
F unknown	N.A.	N.A.	Unkn.	✓			✓				
F Step 1	Group 1	N.A.	Group 1	✓			✓			MF974767	MF974630
F unknown	N.A.	N.A.	Unkn.	✓			✓				
F Step 1	Group 1	N.A.	Group 1	✓			✓			MF974768	
F Step 1	Group 1	Group 1	Group 1	✓	✓	✓	✓	✓	✓	MF974769	
F unknown	N.A.	N.A.	Unkn.	✓			✓				
F Step 4	N.A.	Group 1	Group 1	✓			✓	✓	✓		
F unknown	N.A.	N.A.	Unkn.	✓			✓	✓			
F Step 1	Group 1	Group 1	Group 1	✓			✓	✓	✓		MF974631
F Step 1	Group 1	N.A.	Group 1	✓			✓	✓			MF974632
F Step 4	N.A.	Group 1	Group 1	✓			✓	✓	✓		
F Step 1	Group 1	N.A.	Group 1	✓			✓	✓		MF974770	MF974633
F Step 4	N.A.	Group 1	Group 1	✓			✓	✓	✓		
F Step 1	Group 1	N.A.	Group 1	✓			✓	✓		MF974771	
F unknown	N.A.	N.A.	Unkn.								
F Step 1	Group 1	N.A.	Group 1							MF974772	
F unknown	N.A.	N.A.	Unkn.								
F Step 1	Group 1	N.A.	Group 1							MF974773	
F Step 1	Group 1	N.A.	Group 1							MF974774	
F Step 1	Group 1	N.A.	Group 1							MF974775	
F Step 1	Group 1	Group 1	Group 1	✓			✓	✓	✓	MF974776	
F Step 1	Group 1	Group 1	Group 1	✓	✓	✓	✓	✓		MF974777	
F Step 1	Group 1	Group 1	Group 1	✓	✓	✓	✓	✓	✓	MF974778	
F Step 4	N.A.	Group 1	Group 1	✓	✓	✓	✓	✓	✓		
F Step 1	Group 1	Group 1	Group 1	✓	✓	✓	✓	✓	✓	MF974779	MF974634
F Step 1	Group 1	Group 1	Group 1	✓			✓	✓	✓	MF974780	
F unknown	N.A.	N.A.	Unkn.	✓			✓	✓			
F Step 4	N.A.	Group 1	Group 1	✓	✓		✓	✓	✓		
F Step 4	N.A.	Group 1	Group 1	✓	✓	✓	✓	✓	✓		
F Step 1	Group 1	Group 1	Group 1	✓	✓		✓	✓	✓	MF974781	
F Step 1	Group 1	N.A.	Group 1	✓			✓			MF974782	
F Step 1	Group 1	Group 1	Group 1	✓	✓	✓	✓	✓	✓	MF974783	
F Step 1	Group 1	Group 1	Group 1	✓	✓	✓	✓	✓	✓	MF974784	
F unknown	N.A.	N.A.	Unkn.	✓			✓	✓			
F Step 1	Group 1	Group 1	Group 1	✓	✓		✓			MF974785	MF974635
F Step 1	Group 1	N.A.	Group 1	✓			✓			MF974786	

TABLE S1. Continued

Sample information					
Specimen ID	Cruise	Station	Latitude	Longitude	Collection date
Atlantic Ocean					
D_ANE_AMT22_37_03	AMT22	37	4°03'N	26°28'W	2012-10-30
D_ANE_AMT22_37_04	AMT22	37	4°03'N	26°28'W	2012-10-30
D_ANE_AMT22_37_05	AMT22	37	4°03'N	26°28'W	2012-10-30
D_ANE_AMT22_37_06	AMT22	37	4°03'N	26°28'W	2012-10-30
D_ANE_AMT22_37a_01	AMT22	37a	4°16'N	26°37'W	2012-10-30
D_ANE_AMT22_39_01	AMT22	39	1°08'N	25°00'W	2012-10-31
D_ANE_AMT22_39_02	AMT22	39	1°08'N	25°00'W	2012-10-31
D_ANE_AMT22_39_03	AMT22	39	1°08'N	25°00'W	2012-10-31
D_ASW_AMT22_41_01	AMT22	41	1°51'S	25°01'W	2012-11-01
D_ASW_AMT22_42_01	AMT22	42	2°55'S	25°01'W	2012-11-01
D_ASW_AMT22_42_02	AMT22	42	2°55'S	25°01'W	2012-11-01
D_ASW_AMT22_42_03	AMT22	42	2°55'S	25°01'W	2012-11-01
D_ASW_AMT22_45_01	AMT22	45	8°05'S	25°02'W	2012-11-03
D_ASW_AMT22_47a_01	AMT22	47a	11°18'S	25°03'W	2012-11-03
D_ASW_AMT22_47a_02	AMT22	47a	11°18'S	25°03'W	2012-11-03
D_ASW_AMT22_56_01	AMT22	56	25°44'S	25°00'W	2012-11-10
D_ANW_ECO_01_01	GU1101	1	21°35'N	86°00'W	2007-01-14
D_ANW_ECO_01_02	GU1101	1	21°35'N	86°00'W	2007-01-14
D_ANW_ECO_02_01	GU1101	2	21°30'N	86°17'W	2007-01-14
D_ANW_ECO_19_01	GU1101	19	20°13'N	87°20'W	2007-01-17
D_ANW_ECO_25_01	GU1101	25	19°44'N	87°16'W	2007-01-18
D_ANW_ECO_25_02	GU1101	25	19°44'N	87°16'W	2007-01-18
D_ANW_ECO_27_01	GU1101	27	19°35'N	87°22'W	2007-01-18
D_ANW_ECO_37_01	GU1101	37	18°47'N	86°59'W	2007-01-22
D_ANW_ECO_40_01	GU1101	40	18°29'N	87°17'W	2007-01-22
D_ANW_ECO_40_02	GU1101	40	18°29'N	87°17'W	2007-01-22
D_ANW_ECO_40_03	GU1101	40	18°29'N	87°17'W	2007-01-22
D_ANW_ECO_41_01	GU1101	41	18°16'N	87°01'W	2007-01-22
D_ANW_ECO_41_02	GU1101	41	18°16'N	87°01'W	2007-01-22
D_ANW_ECO_41_03	GU1101	41	18°16'N	87°01'W	2007-01-22
D_ANW_ECO_41_04	GU1101	41	18°16'N	87°01'W	2007-01-22
D_ANW_ECO_41_05	GU1101	41	18°16'N	87°01'W	2007-01-22
D_ANW_ECO_43_01	GU1101	43	18°22'N	87°23'W	2007-01-23
D_ANW_ECO_46_01	GU1101	46	18°16'N	87°49'W	2007-01-23
D_ANW_ECO_51_01	GU1101	51	18°42'N	87°25'W	2007-01-24
D_ANW_ECO_53_01	GU1101	53	18°43'N	87°39'W	2007-01-24
D_ANW_ECO_58_01	GU1101	58	17°43'N	87°17'W	2007-01-25
D_ANW_ECO_62_01	GU1101	62	16°49'N	87°11'W	2007-01-26
D_ANW_ECO_62_02	GU1101	62	16°49'N	87°11'W	2007-01-26
D_ANW_ECO_65_01	GU1101	65	16°42'N	87°29'W	2007-01-26
D_ANW_ECO_66_01	GU1101	66	16°41'N	87°40'W	2007-01-26
D_ANW_ECO_72_01	GU1101	72	16°28'N	87°48'W	2007-01-27
D_ANW_ECO_74_01	GU1101	74	16°34'N	87°59'W	2007-01-27
D_ANW_ECO_74_02	GU1101	74	16°34'N	87°59'W	2007-01-27
D_ANW_ECO_75_01	GU1101	75	16°34'N	87°59'W	2007-01-27
D_ANW_ECO_77_01	GU1101	77	16°22'N	88°02'W	2007-01-27
D_ANW_ECO_77_02	GU1101	77	16°22'N	88°02'W	2007-01-27
D_ANW_ECO_77_03	GU1101	77	16°22'N	88°02'W	2007-01-27
D_ANW_ECO_77_04	GU1101	77	16°22'N	88°02'W	2007-01-27

Identification				Geometric morphometrics						Genetics	
Specimen type (F, Fresh; M, Museum)	Genetic clade / Species (Van der Spoel et al., 1993)	LDA group	Integrative group	Ventral photo	Ventral 23LMs	Ventral 38LMs	Lateral photo	Lateral 15LMs	Lateral 49LMs	COI	28S
F Step 1	Group 1	Group 1	Group 1	✓	✓	✓	✓	✓	✓	MF974787	MF974636
F Step 1	Group 1	Group 1	Group 1	✓			✓	✓	✓	MF974788	
F Step 4	N.A.	Group 1	Group 1	✓	✓	✓	✓	✓	✓		
F Step 4	N.A.	Group 1	Group 1	✓	✓		✓	✓	✓		
F Step 1	Group 1	N.A.	Group 1	✓			✓			MF974789	
F unknown	N.A.	N.A.	Unkn.	✓			✓	✓			
F Step 1	Group 1	Group 1	Group 1	✓	✓	✓	✓	✓	✓	MF974790	MF974637
F Step 1	Group 1	Group 1	Group 1	✓	✓	✓	✓	✓	✓	MF974791	
F Step 1	Group 1	N.A.	Group 1	✓			✓	✓		MF974792	MF974638
F Step 1	Group 1	N.A.	Group 1	✓			✓			MF974793	MF974639
F Step 1	Group 1	N.A.	Group 1	✓			✓			MF974794	MF974640
F Step 1	Group 1	N.A.	Group 1	✓			✓			MF974795	MF974641
F Step 1	Group 1	Group 1	Group 1	✓	✓	✓	✓	✓			MF974642
F Step 1	Group 1	Group 1	Group 1	✓			✓	✓	✓	MF974796	MF974643
F Step 1	Group 1	N.A.	Group 1	✓			✓			MF974797	
F Step 1	Group 1	N.A.	Group 1	✓			✓			MF974798	MF974644
F Step 4	N.A.	Group 1	Group 1	✓	✓	✓	✓	✓	✓		
F Step 4	N.A.	Group 1	Group 1	✓	✓	✓	✓				
F Step 4	N.A.	Group 1	Group 1	✓	✓	✓	✓	✓	✓		
F Step 1	Group 1	Group 1	Group 1	✓	✓	✓	✓	✓	✓		MF974645
F Step 4	N.A.	Group 1	Group 1	✓	✓	✓	✓	✓	✓		
F Step 4	N.A.	Group 1	Group 1	✓	✓	✓	✓	✓	✓		
F Step 1	Group 1	Group 1	Group 1	✓	✓	✓	✓	✓	✓	MF974799	MF974646
F Step 4	N.A.	Group 1	Group 1	✓	✓	✓	✓	✓	✓		
F Step 4	N.A.	Group 1	Group 1	✓	✓	✓	✓	✓	✓		
F Step 4	N.A.	Group 1	Group 1	✓	✓	✓	✓	✓	✓		
F Step 4	N.A.	Group 1	Group 1	✓	✓		✓	✓	✓		
F Step 1	Group 1	N.A.	Group 1	✓			✓	✓		MF974800	MF974647
F Step 4	N.A.	Group 1	Group 1	✓	✓	✓	✓	✓	✓		
F Step 1	Group 1	Group 1	Group 1	✓	✓	✓	✓	✓	✓	MF974801	
F Step 1	Group 1	Group 1	Group 1	✓	✓		✓	✓	✓	MF974802	
F Step 4	N.A.	Group 1	Group 1	✓	✓	✓	✓	✓	✓		
F Step 1	Group 1	Group 1	Group 1	✓			✓	✓	✓		MF974648
F Step 1	Group 1	Group 1	Group 1	✓	✓	✓	✓	✓	✓	MF974803	MF974649
F unknown	N.A.	N.A.	Unkn.	✓			✓	✓			
F Step 4	N.A.	Group 1	Group 1	✓	✓	✓	✓	✓	✓		
F Step 1	Group 1	Group 1	Group 1	✓	✓	✓	✓	✓	✓	MF974804	MF974650
F Step 4	N.A.	Group 1	Group 1	✓	✓		✓	✓	✓		
F Step 4	N.A.	Group 1	Group 1	✓	✓	✓	✓	✓	✓		
F Step 1	Group 1	Group 1	Group 1	✓	✓	✓	✓	✓	✓	MF974805	MF974651
F Step 1	Group 1	Group 1	Group 1	✓	✓	✓	✓	✓	✓	MF974806	MF974652
F Step 1	Group 1	N.A.	Group 1	✓			✓	✓		MF974807	
F Step 1	Group 1	Group 1	Group 1	✓	✓	✓	✓	✓	✓	MF974808	MF974653
F Step 4	N.A.	Group 1	Group 1	✓	✓	✓	✓	✓	✓		
F Step 1	Group 1	Group 1	Group 1	✓	✓	✓	✓	✓	✓	MF974809	
F Step 1	Group 1	Group 1	Group 1	✓	✓		✓	✓	✓	MF974810	MF974654
F Step 1	Group 1	Group 1	Group 1	✓	✓	✓	✓	✓	✓	MF974811	MF974655
F Step 1	Group 1	Group 1	Group 1	✓	✓	✓	✓	✓	✓	MF974812	MF974656
F Step 1	Group 1	Group 1	Group 1	✓	✓		✓	✓	✓	MF974813	

TABLE S1. Continued

Sample information					
Specimen ID	Cruise	Station	Latitude	Longitude	Collection date
Atlantic Ocean					
D_ANW_ECO_77_05	GU1101	77	16°22'N	88°02'W	2007-01-27
D_ANW_ECO_77_06	GU1101	77	16°22'N	88°02'W	2007-01-27
D_ANW_ECO_82_01	GU1101	82	17°19'N	87°46'W	2007-01-28
D_ANW_ECO_82_02	GU1101	82	17°19'N	87°46'W	2007-01-28
D_ANW_ECO_82_03	GU1101	82	17°19'N	87°46'W	2007-01-28
D_ANW_ECO_83_01	GU1101	83	17°23'N	87°38'W	2007-01-28
D_ANW_ECO_84_01	GU1101	84	18°19'N	87°46'W	2007-01-28
D_ANW_ECO_87_01	GU1101	87	18°12'N	87°45'W	2007-01-29
D_ANW_ECO_87_02	GU1101	87	18°12'N	87°45'W	2007-01-29
D_ANW_ECO_88_01	GU1101	88	18°08'N	87°48'W	2007-01-29
D_ANW_ECO_88_02	GU1101	88	18°08'N	87°48'W	2007-01-29
D_ANW_ECO_90_01	GU1101	90	18°07'N	87°44'W	2007-01-30
D_ANW_ECO_90_02	GU1101	90	18°07'N	87°44'W	2007-01-30
D_ANW_ECO_90_03	GU1101	90	18°07'N	87°44'W	2007-01-30
D_ANW_ECO_90_04	GU1101	90	18°07'N	87°44'W	2007-01-30
DANG_ANW_DANA_1243_01	DANA	1243	21°04'N	73°48'W	1922-02-16
DANG_ANW_DANA_1243_02	DANA	1243	21°04'N	73°48'W	1922-02-16
DANG_ANW_DANA_1243_03	DANA	1243	21°04'N	73°48'W	1922-02-16
DANG_ANW_DANA_1243_04	DANA	1243	21°04'N	73°48'W	1922-02-16
DANG_ANW_DANA_1243_05	DANA	1243	21°04'N	73°48'W	1922-02-16
DANG_ANW_DANA_1243_06	DANA	1243	21°04'N	73°48'W	1922-02-16
DANG_ANW_DANA_1243_07	DANA	1243	21°04'N	73°48'W	1922-02-16
DANG_ANW_DANA_1243_08	DANA	1243	21°04'N	73°48'W	1922-02-16
DANG_ANW_DANA_1243_09	DANA	1243	21°04'N	73°48'W	1922-02-16
DANG_ANW_DANA_1243_10	DANA	1243	21°04'N	73°48'W	1922-02-16
DANG_ANW_DANA_1243_11	DANA	1243	21°04'N	73°48'W	1922-02-16
DANG_ANW_DANA_1243_12	DANA	1243	21°04'N	73°48'W	1922-02-16
DANG_ANW_DANA_1243_13	DANA	1243	21°04'N	73°48'W	1922-02-16
DANG_ANW_DANA_1243_14	DANA	1243	21°04'N	73°48'W	1922-02-16
DANG_ANW_DANA_1243_15	DANA	1243	21°04'N	73°48'W	1922-02-16
DATL_ANE_101A_23_01	Projekt 101A	23 Tr.4	30°34'N	30°01'W	1980-04-28
DATL_ANE_101A_23_02	Projekt 101A	23 Tr.4	30°34'N	30°01'W	1980-04-28
DATL_ANE_101A_23_03	Projekt 101A	23 Tr.4	30°34'N	30°01'W	1980-04-28
DATL_ANE_AMN_25_01	AMNAPE	25	28°24'N	29°56'W	1980-04-30
DBIC_ANW_DANA_1322_01	DANA	1322 XXXVIII	27°02'N	53°39'W	1922-05-01
DCON_ANE_101A_89_01	Projekt 101A	89 Tr.4	24°50'N	29°58'W	1983-05-30
DCON_ANE_AMN_88_01	AMNAPE	88	28°28'N	29°51'W	1983-06-01
DCON_ANE_AMN_88_02	AMNAPE	88	28°28'N	29°51'W	1983-06-01
DCON_ANE_AMN_88_03	AMNAPE	88	28°28'N	29°51'W	1983-06-01
DCON_ANE_AMN_88_04	AMNAPE	88	28°28'N	29°51'W	1983-06-01
DCON_ANE_AMN_88_05	AMNAPE	88	28°28'N	29°51'W	1983-06-01
DCON_ANW_ACRE_0109_01	ACRE	1-9B	32°33'N	64°21'W	1967-10-28
DCON_ANW_DANA_1355_01	DANA	1355 I III	31°48'N	63°38'W	1922-05-30
DCON_ANW_DANA_1355_02	DANA	1355 I III	31°48'N	63°38'W	1922-05-30
DCON_ANW_DANA_1355_03	DANA	1355 I III	31°48'N	63°38'W	1922-05-30
DCON_ANW_DANA_1355_04	DANA	1355 I III	31°48'N	63°38'W	1922-05-30
DCON_ANW_DANA_1355_05	DANA	1355 I III	31°48'N	63°38'W	1922-05-30
DCON_ANW_DANA_1355_06	DANA	1355 I III	31°48'N	63°38'W	1922-05-30
DCON_ANW_DANA_1355_07	DANA	1355 I III	31°48'N	63°38'W	1922-05-30

Identification				Geometric morphometrics						Genetics	
Specimen type (F, Fresh; M, Museum)	Genetic clade / Species (Van der Spoel et al., 1993)	LDA group	Integrative group	Ventral photo	Ventral 23LMs	Ventral 38LMs	Lateral photo	Lateral 15LMs	Lateral 49LMs	COI	28S
F Step 4	N.A.	Group 1	Group 1	✓	✓	✓	✓	✓	✓		
F Step 4	N.A.	Group 1	Group 1	✓	✓		✓	✓	✓		
F Step 1	Group 1	Group 1	Group 1	✓	✓	✓	✓	✓		MF974814	MF974657
F Step 1	Group 1	Group 1	Group 1	✓	✓	✓	✓	✓	✓	MF974815	
F unknown	N.A.	N.A.	Unkn.	✓			✓	✓			
F Step 4	N.A.	Group 1	Group 1	✓	✓	✓	✓	✓	✓		
F Step 4	N.A.	Group 1	Group 1	✓	✓	✓	✓	✓	✓		
F Step 4	N.A.	Group 1	Group 1	✓	✓	✓	✓	✓	✓		
F Step 4	N.A.	Group 1	Group 1	✓	✓	✓	✓	✓	✓		
F Step 4	N.A.	Group 1	Group 1	✓	✓	✓	✓	✓	✓		
F Step 4	N.A.	Group 1	Group 1	✓	✓	✓	✓	✓	✓		
F Step 1	Group 1	Group 1	Group 1	✓	✓	✓	✓	✓	✓		MF974658
F Step 1	Group 1	N.A.	Group 1	✓			✓			MF974816	
F Step 1	Group 1	Group 1	Group 1	✓	✓	✓	✓	✓	✓	MF974817	
F Step 4	N.A.	Group 1	Group 1	✓	✓	✓	✓	✓	✓		
M Step 4	*D. angulata*	Group 1	Group 1	✓	✓		✓	✓	✓		
M Step 4	*D. angulata*	Group 1	Group 1	✓	✓		✓	✓	✓		
M Step 4	*D. angulata*	Group 1	Group 1	✓	✓	✓	✓	✓			
M Step 4	*D. angulata*	Group 1	Group 1	✓	✓		✓	✓	✓		
M Step 4	*D. angulata*	Group 1	Group 1	✓	✓		✓	✓	✓		
M Step 4	*D. angulata*	Group 1	Group 1	✓	✓		✓	✓			
M Step 4	*D. angulata*	Group 1	Group 1	✓	✓		✓	✓	✓		
M Step 4	*D. angulata*	Group 1	Group 1	✓	✓		✓	✓	✓		
M Step 4	*D. angulata*	Group 1	Group 1	✓	✓		✓	✓	✓		
M Step 4	*D. angulata*	Group 1	Group 1	✓	✓	✓	✓	✓	✓		
M Step 4	*D. angulata*	Group 1	Group 1	✓	✓		✓	✓	✓		
M Step 4	*D. angulata*	Group 1	Group 1	✓	✓		✓	✓	✓		
M Step 4	*D. angulata*	Group 1	Group 1	✓	✓		✓	✓	✓		
M Step 4	*D. angulata*	Group 1	Group 1	✓	✓		✓	✓			
M Step 4	*D. angulata*	Group 1	Group 1	✓	✓		✓	✓	✓		
M Step 4	*D. atlantica*	Group 2	Group 2	✓	✓		✓				
M Step 4	*D. atlantica*	Group 2	Group 2	✓	✓		✓				
M Step 4	*D. atlantica*	Group 2	Group 2	✓	✓		✓	✓	✓		
M Step 2	*D. atlantica*	Group 2	Group 2	✓	✓		✓	✓	✓		
M Step 4	*D. bicornis*	Group 1	Group 1	✓	✓	✓	✓	✓	✓		
M Step 4	*D. constricta*	Group 2	Group 2	✓			✓	✓	✓		
M Step 2	*D. constricta*	Group 1	Group 1	✓			✓	✓	✓		
M unknown	*D. constricta*	N.A.	Unkn.	✓			✓				
M unknown	*D. constricta*	N.A.	Unkn.	✓			✓				
M unknown	*D. constricta*	N.A.	Unkn.	✓			✓				
M unknown	*D. constricta*	N.A.	Unkn.	✓			✓				
M unknown	*D. constricta*	N.A.	Unkn.	✓			✓	✓			
M Step 4	*D. constricta*	Group 1	Group 1	✓	✓		✓	✓	✓		
M unknown	*D. constricta*	N.A.	Unkn.	✓			✓	✓			
M unknown	*D. constricta*	N.A.	Unkn.	✓			✓	✓			
M Step 4	*D. constricta*	Group 1	Group 1	✓	✓		✓	✓	✓		
M unknown	*D. constricta*	Amb.	Unkn.	✓	✓		✓	✓	✓		
M Step 4	*D. constricta*	Group 1	Group 1	✓	✓	✓	✓	✓	✓		
M Step 4	*D. constricta*	Group 1	Group 1	✓	✓	✓	✓	✓	✓		

TABLE S1. Continued

Sample information					
Specimen ID	Cruise	Station	Latitude	Longitude	Collection date
Atlantic Ocean					
DCON_ANW_DANA_1355_08	DANA	1355 I III	31°48'N	63°38'W	1922-05-30
DCON_ANW_DANA_1355_09	DANA	1355 I III	31°48'N	63°38'W	1922-05-30
DCON_ANW_DANA_1355_10	DANA	1355 I III	31°48'N	63°38'W	1922-05-30
DCON_ANW_DANA_1355_11	DANA	1355 I III	31°48'N	63°38'W	1922-05-30
DCON_ANW_DANA_1355_12	DANA	1355 I III	31°48'N	63°38'W	1922-05-30
DCON_ANW_DANA_1355_13	DANA	1355 I III	31°48'N	63°38'W	1922-05-30
DCON_ANW_DANA_1355_14	DANA	1355 I III	31°48'N	63°38'W	1922-05-30
DCON_ANW_DANA_1355_15	DANA	1355 I III	31°48'N	63°38'W	1922-05-30
DCON_ANW_DANA_1355_16	DANA	1355 I III	31°48'N	63°38'W	1922-05-30
DCON_ANW_DANA_1355_17	DANA	1355 I III	31°48'N	63°38'W	1922-05-30
DCON_ANW_DANA_1355_18	DANA	1355 I III	31°48'N	63°38'W	1922-05-30
DCON_ANW_DANA_1355_19	DANA	1355 I III	31°48'N	63°38'W	1922-05-30
DCON_ANW_DANA_1355_20	DANA	1355 I III	31°48'N	63°38'W	1922-05-30
DCON_ANW_DANA_1355_21	DANA	1355 I III	31°48'N	63°38'W	1922-05-30
DCON_ANW_DANA_1355_22	DANA	1355 I III	31°48'N	63°38'W	1922-05-30
DCON_ANW_DANA_1355_23	DANA	1355 I III	31°48'N	63°38'W	1922-05-30
DCON_ANW_DANA_1355_24	DANA	1355 I III	31°48'N	63°38'W	1922-05-30
DCON_ANW_DANA_1355_25	DANA	1355 I III	31°48'N	63°38'W	1922-05-30
DCON_ANW_DANA_1355_26	DANA	1355 I III	31°48'N	63°38'W	1922-05-30
DCON_ANW_DANA_1355_27	DANA	1355 I III	31°48'N	63°38'W	1922-05-30
DCON_ANW_DANA_1355_28	DANA	1355 I III	31°48'N	63°38'W	1922-05-30
DCON_ANW_DANA_1355_29	DANA	1355 I III	31°48'N	63°38'W	1922-05-30
DCON_ANW_DANA_1355_30	DANA	1355 I III	31°48'N	63°38'W	1922-05-30
DCON_ANW_DANA_1355_31	DANA	1355 I III	31°48'N	63°38'W	1922-05-30
DCON_ANW_DANA_1355_32	DANA	1355 I III	31°48'N	63°38'W	1922-05-30
DDEB_ANW_DANA_1192_01	DANA	1192 VII	17°43'N	64°54'W	1929-12-15
DDEB_ANW_DANA_1192_02	DANA	1192 VII	17°43'N	64°54'W	1929-12-15
DDEB_ANW_DANA_1192_03	DANA	1192 VII	17°43'N	64°54'W	1929-12-15
DDEB_ANW_DANA_1192_04	DANA	1192 VII	17°43'N	64°54'W	1929-12-15
DDEB_ANW_DANA_1192_05	DANA	1192 VII	17°43'N	64°54'W	1929-12-15
DDEB_ANW_DANA_1192_06	DANA	1192 VII	17°43'N	64°54'W	1929-12-15
DDEB_ANW_DANA_1192_07	DANA	1192 VII	17°43'N	64°54'W	1929-12-15
DDEB_ANW_DANA_1192_08	DANA	1192 VII	17°43'N	64°54'W	1929-12-15
DDEB_ANW_DANA_1192_09	DANA	1192 VII	17°43'N	64°54'W	1929-12-15
DDEB_ANW_DANA_1192_10	DANA	1192 VII	17°43'N	64°54'W	1929-12-15
DDEB_ANW_DANA_1192_11	DANA	1192 VII	17°43'N	64°54'W	1929-12-15
DDEB_ANW_DANA_1192_12	DANA	1192 VII	17°43'N	64°54'W	1929-12-15
DDEB_ANW_DANA_1192_13	DANA	1192 VII	17°43'N	64°54'W	1929-12-15
DDEB_ANW_DANA_1192_14	DANA	1192 VII	17°43'N	64°54'W	1929-12-15
DDEB_ANW_DD106_67_01	DD106	67M	38°45'N	72°20'W	1975-07-31
DDEB_ANW_DD106_67_02	DD106	67M	38°45'N	72°20'W	1975-07-31
DDEB_ANW_DD106_67_03	DD106	67M	38°45'N	72°20'W	1975-07-31
DDEB_ANW_DD106_67_04	DD106	67M	38°45'N	72°20'W	1975-07-31
DDEB_ANW_DD106_67_05	DD106	67M	38°45'N	72°20'W	1975-07-31
DDEB_ANW_DD106_67_06	DD106	67M	38°45'N	72°20'W	1975-07-31
DDEB_ANW_DD106_67_07	DD106	67M	38°45'N	72°20'W	1975-07-31
DDEB_ANW_DD106_67_08	DD106	67M	38°45'N	72°20'W	1975-07-31
DDEB_ANW_DD106_67_09	DD106	67M	38°45'N	72°20'W	1975-07-31
DDEB_ANW_DD106_67_10	DD106	67M	38°45'N	72°20'W	1975-07-31

Identification				Geometric morphometrics						Genetics	
Specimen type (F, Fresh; M, Museum)	Genetic clade / Species (Van der Spoel et al., 1993)	LDA group	Integrative group	Ventral photo	Ventral 23LMs	Ventral 38LMs	Lateral photo	Lateral 15LMs	Lateral 49LMs	COI	28S
M unknown	*D. constricta*	Amb.	Unkn.	✓	✓		✓	✓	✓		
M Step 4	*D. constricta*	Group 1	Group 1	✓	✓		✓	✓	✓		
M Step 4	*D. constricta*	Group 1	Group 1	✓	✓	✓	✓	✓			
M Step 4	*D. constricta*	Group 1	Group 1	✓	✓	✓	✓	✓	✓		
M Step 4	*D. constricta*	Group 1	Group 1	✓	✓		✓	✓	✓		
M Step 4	*D. constricta*	Group 2	Group 2	✓	✓	✓	✓	✓	✓		
M Step 4	*D. constricta*	Group 1	Group 1	✓	✓		✓	✓	✓		
M Step 4	*D. constricta*	Group 1	Group 1	✓			✓	✓	✓		
M Step 4	*D. constricta*	Group 1	Group 1	✓	✓	✓	✓	✓	✓		
M Step 4	*D. constricta*	Group 1	Group 1	✓	✓		✓	✓			
M unknown	*D. constricta*	N.A.	Unkn.	✓			✓	✓			
M Step 4	*D. constricta*	Group 1	Group 1	✓	✓		✓	✓	✓		
M Step 4	*D. constricta*	Group 1	Group 1	✓	✓	✓	✓	✓	✓		
M Step 4	*D. constricta*	Group 1	Group 1	✓	✓		✓	✓	✓		
M Step 4	*D. constricta*	Group 1	Group 1	✓			✓	✓	✓		
M unknown	*D. constricta*	Amb.	Unkn.	✓	✓		✓	✓	✓		
M Step 4	*D. constricta*	Group 1	Group 1	✓			✓	✓	✓		
M Step 4	*D. constricta*	Group 1	Group 1	✓	✓		✓	✓	✓		
M Step 4	*D. constricta*	Group 1	Group 1	✓	✓		✓	✓	✓		
M Step 4	*D. constricta*	Group 1	Group 1	✓	✓	✓	✓	✓	✓		
M Step 4	*D. constricta*	Group 1	Group 1	✓	✓	✓	✓	✓	✓		
M Step 4	*D. constricta*	Group 1	Group 1	✓	✓	✓	✓	✓	✓		
M unknown	*D. constricta*	Amb.	Unkn.	✓	✓	✓	✓				
M unknown	*D. constricta*	Amb.	Unkn.	✓			✓	✓	✓		
M Step 4	*D. constricta*	Group 1	Group 1	✓	✓		✓	✓	✓		
M Step 4	*D. deblainvillei*	Group 1	Group 1	✓	✓		✓	✓	✓		
M Step 4	*D. deblainvillei*	Group 1	Group 1	✓	✓		✓	✓	✓		
M Step 4	*D. deblainvillei*	Group 1	Group 1	✓	✓		✓	✓	✓		
M Step 4	*D. deblainvillei*	Group 1	Group 1	✓	✓	✓	✓	✓	✓		
M Step 4	*D. deblainvillei*	Group 1	Group 1	✓	✓		✓	✓	✓		
M Step 4	*D. deblainvillei*	Group 1	Group 1	✓	✓	✓	✓	✓	✓		
M Step 4	*D. deblainvillei*	Group 1	Group 1	✓	✓		✓	✓	✓		
M Step 4	*D. deblainvillei*	Group 1	Group 1	✓	✓	✓	✓	✓			
M Step 4	*D. deblainvillei*	Group 1	Group 1	✓	✓	✓	✓	✓	✓		
M Step 4	*D. deblainvillei*	Group 1	Group 1	✓	✓	✓	✓	✓	✓		
M Step 4	*D. deblainvillei*	Group 1	Group 1	✓	✓		✓	✓	✓		
M Step 4	*D. deblainvillei*	Group 1	Group 1	✓	✓		✓	✓	✓		
M Step 4	*D. deblainvillei*	Group 1	Group 1	✓	✓		✓	✓	✓		
M Step 4	*D. deblainvillei*	Group 1	Group 1	✓	✓		✓	✓	✓		
M Step 2	*D. deblainvillei*	Group 1	Group 1	✓	✓	✓	✓	✓	✓		
M Step 2	*D. deblainvillei*	Group 1	Group 1	✓	✓	✓	✓	✓	✓		
M Step 2	*D. deblainvillei*	Group 1	Group 1	✓	✓	✓	✓	✓	✓		
M Step 2	*D. deblainvillei*	Group 1	Group 1	✓	✓	✓	✓	✓	✓		
M Step 2	*D. deblainvillei*	Group 1	Group 1	✓	✓		✓	✓	✓		
M Step 2	*D. deblainvillei*	Group 1	Group 1	✓	✓		✓	✓	✓		
M Step 2	*D. deblainvillei*	Group 1	Group 1	✓	✓		✓	✓	✓		
M Step 2	*D. deblainvillei*	Group 1	Group 1	✓	✓	✓	✓	✓	✓		
M Step 2	*D. deblainvillei*	Group 1	Group 1	✓	✓	✓	✓	✓	✓		
M Step 2	*D. deblainvillei*	Group 1	Group 1	✓	✓		✓	✓	✓		

TABLE S1. Continued

Sample information					
Specimen ID	Cruise	Station	Latitude	Longitude	Collection date
Atlantic Ocean					
DDEB_ANW_DD106_67_11	DD106	67M	38°45'N	72°20'W	1975-07-31
DDEB_ANW_DD106_67_12	DD106	67M	38°45'N	72°20'W	1975-07-31
DDEB_ANW_DD106_67_13	DD106	67M	38°45'N	72°20'W	1975-07-31
DDEB_ANW_DD106_67_14	DD106	67M	38°45'N	72°20'W	1975-07-31
DDEB_ANW_DD106_67_15	DD106	67M	38°45'N	72°20'W	1975-07-31
DDEB_ANW_DD106_67_16	DD106	67M	38°45'N	72°20'W	1975-07-31
DDEB_ANW_DD106_67_17	DD106	67M	38°45'N	72°20'W	1975-07-31
DDEB_ANW_DD106_67_18	DD106	67M	38°45'N	72°20'W	1975-07-32
DDES_ANW_ACRE_0427_01	ACRE	4-27D	31°58'N	64°01'W	1968-09-08
DDES_ANW_ACRE_0427_02	ACRE	4-27D	31°58'N	64°01'W	1968-09-08
DDES_ANW_ACRE_0427_03	ACRE	4-27D	31°58'N	64°01'W	1968-09-08
DDES_ANW_ACRE_0427_04	ACRE	4-27D	31°58'N	64°01'W	1968-09-08
DDES_ANW_ACRE_0427_05	ACRE	4-27D	31°58'N	64°01'W	1968-09-08
DDES_ANW_ACRE_0427_06	ACRE	4-27D	31°58'N	64°01'W	1968-09-08
DDES_ANW_ACRE_0427_07	ACRE	4-27D	31°58'N	64°01'W	1968-09-08
DDES_ANW_ACRE_0427_08	ACRE	4-27D	31°58'N	64°01'W	1968-09-08
DDES_ANW_ACRE_0427_09	ACRE	4-27D	31°58'N	64°01'W	1968-09-08
DDES_ANW_DANA_1175_01	DANA	1175 III	5°06'N	51°35'W	1929-09-17
DDES_ANW_DANA_1175_02	DANA	1175 III	5°06'N	51°35'W	1929-09-17
DDES_ANW_DANA_1175_03	DANA	1175 III	5°06'N	51°35'W	1929-09-17
DDES_ANW_DANA_1175_04	DANA	1175 III	5°06'N	51°35'W	1929-09-17
DDES_ANW_DANA_1175_05	DANA	1175 III	5°06'N	51°35'W	1929-09-17
DDES_ANW_DANA_1175_06	DANA	1175 III	5°06'N	51°35'W	1929-09-17
DDES_ANW_DANA_1175_07	DANA	1175 III	5°06'N	51°35'W	1929-09-17
DDES_ANW_DANA_1175_08	DANA	1175 III	5°06'N	51°35'W	1929-09-17
DDES_ANW_DANA_1322_01	DANA	1322 XXXVIII	27°02'N	53°39'W	1922-05-01
DDES_ANW_DANA_1322_02	DANA	1322 XXXVIII	27°02'N	53°39'W	1922-05-01
DDES_ANW_DANA_1322_03	DANA	1322 XXXVIII	27°02'N	53°39'W	1922-05-01
DDES_ANW_DANA_1356_01	DANA	1356 VI	29°56'N	59°33'W	1922-06-01
DDES_ANW_DANA_1356_02	DANA	1356 VI	29°56'N	59°33'W	1922-06-01
DDES_ANW_DANA_1356_03	DANA	1356 VI	29°56'N	59°33'W	1922-06-01
DDES_ANW_DANA_1358_01	DANA	1358 XIII XIV	28°15'N	56°00'W	1922-06-02/03
DDES_ANW_DANA_1358_02	DANA	1358 XIII XIV	28°15'N	56°00'W	1922-06-02/03
DDES_ANW_DANA_1358_03	DANA	1358 XIII XIV	28°15'N	56°00'W	1922-06-02/03
DDES_ANW_DANA_1358_04	DANA	1358 XIII XIV	28°15'N	56°00'W	1922-06-02/03
DDES_ANW_DANA_1358_05	DANA	1358 XIII XIV	28°15'N	56°00'W	1922-06-02/03
DDES_ANW_DANA_1358_06	DANA	1358 XIII XIV	28°15'N	56°00'W	1922-06-02/03
DDES_ANW_DANA_1358_07	DANA	1358 XIII XIV	28°15'N	56°00'W	1922-06-02/03
DDES_ANW_DANA_1358_08	DANA	1358 XIII XIV	28°15'N	56°00'W	1922-06-02/03
DDES_ANW_DANA_1358_09	DANA	1358 XIII XIV	28°15'N	56°00'W	1922-06-02/03
DDES_ANW_DANA_1358_10	DANA	1358 XIII XIV	28°15'N	56°00'W	1922-06-02/03
DDES_ANW_DANA_1358_11	DANA	1358 XIII XIV	28°15'N	56°00'W	1922-06-02/03
DDES_ANW_DANA_1358_12	DANA	1358 XIII XIV	28°15'N	56°00'W	1922-06-02/03
DDES_ANW_DANA_1358_13	DANA	1358 XIII XIV	28°15'N	56°00'W	1922-06-02/03
DDES_ANW_DANA_1358_14	DANA	1358 XIII XIV	28°15'N	56°00'W	1922-06-02/03
DDES_ANW_DANA_1358_15	DANA	1358 XIII XIV	28°15'N	56°00'W	1922-06-02/03
DDES_ANW_DANA_1358_16	DANA	1358 XIII XIV	28°15'N	56°00'W	1922-06-02/03
DDES_ANW_DANA_1358_17	DANA	1358 XIII XIV	28°15'N	56°00'W	1922-06-02/19
DELE_ANW_DD106_67_01	DD106	67M	38°45'N	72°20'W	1975-07-31

Identification				Geometric morphometrics						Genetics	
Specimen type (F, Fresh; M, Museum)	Genetic clade / Species (Van der Spoel et al., 1993)	LDA group	Integrative group	Ventral photo	Ventral 23LMs	Ventral 38LMs	Lateral photo	Lateral 15LMs	Lateral 49LMs	COI	28S
M Step 2	*D. deblainvillei*	Group 1	Group 1	✓	✓		✓	✓	✓		
M Step 2	*D. deblainvillei*	Group 1	Group 1	✓	✓		✓	✓	✓		
M Step 2	*D. deblainvillei*	Group 1	Group 1	✓	✓		✓	✓	✓		
M Step 2	*D. deblainvillei*	Group 1	Group 1	✓	✓	✓	✓	✓	✓		
M Step 2	*D. deblainvillei*	Group 1	Group 1	✓	✓		✓	✓	✓		
M Step 2	*D. deblainvillei*	Group 1	Group 1	✓	✓	✓	✓	✓	✓		
M Step 2	*D. deblainvillei*	Group 1	Group 1	✓	✓	✓	✓	✓	✓		
M Step 2	*D. deblainvillei*	Group 1	Group 1	✓	✓						
M Step 4	*D. deshayesi*	Group 1	Group 1	✓	✓	✓	✓	✓	✓		
M Step 4	*D. deshayesi*	Group 1	Group 1	✓	✓	✓	✓				
M Step 4	*D. deshayesi*	Group 1	Group 1	✓			✓	✓	✓		
M Step 4	*D. deshayesi*	Group 1	Group 1	✓	✓	✓	✓	✓	✓		
M Step 4	*D. deshayesi*	Group 1	Group 1	✓	✓	✓	✓	✓	✓		
M Step 4	*D. deshayesi*	Group 1	Group 1	✓			✓	✓	✓		
M Step 4	*D. deshayesi*	Group 1	Group 1	✓	✓	✓	✓	✓	✓		
M Step 4	*D. deshayesi*	Group 1	Group 1	✓	✓	✓	✓	✓	✓		
M Step 4	*D. deshayesi*	Group 1	Group 1	✓	✓	✓	✓	✓	✓		
M Step 2	*D. deshayesi*	Group 1	Group 1	✓	✓	✓	✓	✓	✓		
M Step 2	*D. deshayesi*	Group 1	Group 1	✓	✓		✓	✓	✓		
M Step 2	*D. deshayesi*	Group 1	Group 1	✓	✓		✓	✓	✓		
M Step 2	*D. deshayesi*	Group 1	Group 1	✓	✓		✓	✓	✓		
M Step 2	*D. deshayesi*	Group 1	Group 1	✓	✓		✓	✓	✓		
M Step 2	*D. deshayesi*	Group 1	Group 1	✓	✓		✓	✓	✓		
M Step 2	*D. deshayesi*	Group 1	Group 1	✓	✓	✓	✓	✓	✓		
M Step 2	*D. deshayesi*	Group 1	Group 1	✓	✓						
M Step 4	*D. deshayesi*	Group 1	Group 1	✓	✓	✓	✓				
M Step 4	*D. deshayesi*	Group 1	Group 1	✓	✓	✓	✓	✓	✓		
M Step 4	*D. deshayesi*	Group 1	Group 1	✓	✓	✓	✓	✓	✓		
M Step 4	*D. deshayesi*	Group 1	Group 1	✓	✓		✓	✓			
M Step 4	*D. deshayesi*	Group 2	Group 2	✓	✓	✓	✓	✓	✓		
M Step 4	*D. deshayesi*	Group 1	Group 1	✓	✓		✓	✓	✓		
M Step 4	*D. deshayesi*	Group 1	Group 1	✓	✓		✓	✓	✓		
M Step 4	*D. deshayesi*	Group 1	Group 1	✓	✓		✓	✓	✓		
M unknown	*D. deshayesi*	N.A.	Unkn.	✓			✓				
M Step 4	*D. deshayesi*	Group 1	Group 1	✓	✓		✓	✓	✓		
M Step 4	*D. deshayesi*	Group 1	Group 1	✓	✓	✓	✓	✓	✓		
M Step 4	*D. deshayesi*	Group 1	Group 1	✓	✓	✓	✓	✓	✓		
M Step 4	*D. deshayesi*	Group 1	Group 1	✓	✓		✓	✓	✓		
M Step 4	*D. deshayesi*	Group 1	Group 1	✓	✓		✓				
M Step 4	*D. deshayesi*	Group 1	Group 1	✓	✓	✓	✓	✓	✓		
M Step 4	*D. deshayesi*	Group 1	Group 1	✓	✓	✓	✓	✓	✓		
M Step 4	*D. deshayesi*	Group 1	Group 1	✓	✓	✓	✓				
M Step 4	*D. deshayesi*	Group 1	Group 1	✓	✓	✓	✓	✓	✓		
M Step 4	*D. deshayesi*	Group 1	Group 1	✓	✓		✓	✓	✓		
M Step 4	*D. deshayesi*	Group 1	Group 1	✓	✓	✓	✓	✓	✓		
M Step 4	*D. deshayesi*	Group 1	Group 1	✓	✓		✓	✓	✓		
M Step 4	*D. deshayesi*	Group 1	Group 1	✓	✓	✓	✓	✓	✓		
M Step 4	*D. deshayesi*	Group 1	Group 1	✓	✓		✓	✓	✓		
M Step 4	*D. elegans*	Group 1	Group 1	✓	✓		✓	✓	✓		

TABLE S1. Continued

Sample information					
Specimen ID	Cruise	Station	Latitude	Longitude	Collection date
Atlantic Ocean					
DELE_ANW_DD106_67_02	DD106	67M	38°45'N	72°20'W	1975-07-31
DELE_ANW_DD106_67_03	DD106	67M	38°45'N	72°20'W	1975-07-31
DELE_ANW_DD106_67_04	DD106	67M	38°45'N	72°20'W	1975-07-31
DELE_ANW_DD106_67_05	DD106	67M	38°45'N	72°20'W	1975-07-31
DELE_ANW_DD106_67_06	DD106	67M	38°45'N	72°20'W	1975-07-31
DELE_ANW_DD106_67_07	DD106	67M	38°45'N	72°20'W	1975-07-31
DELE_ANW_DD106_67_08	DD106	67M	38°45'N	72°20'W	1975-07-31
DELE_ANW_DD106_67_09	DD106	67M	38°45'N	72°20'W	1975-07-31
DELE_ANW_DD106_67_10	DD106	67M	38°45'N	72°20'W	1975-07-31
DELE_ANW_DD106_67_11	DD106	67M	38°45'N	72°20'W	1975-07-31
DELE_ANW_DD106_67_12	DD106	67M	38°45'N	72°20'W	1975-07-31
DELE_ANW_DD106_67_13	DD106	67M	38°45'N	72°20'W	1975-07-31
DLIA_ANE_101A_23_01	Projekt 101A	23 Tr.4	30°34'N	30°01'W	1980-04-28
DLIA_ANE_101A_23_02	Projekt 101A	23 Tr.4	30°34'N	30°01'W	1980-04-28
DLIA_ANE_101A_23_03	Projekt 101A	23 Tr.4	30°34'N	30°01'W	1980-04-28
DLIA_ANE_101A_23_04	Projekt 101A	23 Tr.4	30°34'N	30°01'W	1980-04-28
DLIA_ANE_101A_27_01	Projekt 101A	27 Tr.20	24°54'N	28°37'W	1980-05-02
DLIA_ANE_101A_27_02	Projekt 101A	27 Tr.20	24°54'N	28°37'W	1980-05-02
DLIA_ANE_101A_27_03	Projekt 101A	27 Tr.20	24°54'N	28°37'W	1980-05-02
DLIA_ANE_101A_27_04	Projekt 101A	27 Tr.20	24°54'N	28°37'W	1980-05-02
DLIA_ANE_101A_27_05	Projekt 101A	27 Tr.20	24°54'N	28°37'W	1980-05-02
DLIA_ANE_101A_27_06	Projekt 101A	27 Tr.20	24°54'N	28°37'W	1980-05-02
DLIA_ANE_101A_27_07	Projekt 101A	27 Tr.20	24°54'N	28°37'W	1980-05-02
DLIA_ANE_101A_27_08	Projekt 101A	27 Tr.20	24°54'N	28°37'W	1980-05-02
DLIA_ANE_101A_27_09	Projekt 101A	27 Tr.20	24°54'N	28°37'W	1980-05-02
DLIA_ANE_AMN_24_01	AMNAPE	24	29°48'N	29°58'W	1980-04-29
DLIA_ANE_AMN_24_02	AMNAPE	24	29°48'N	29°58'W	1980-04-29
DLIA_ANE_AMN_24_03	AMNAPE	24	29°48'N	29°58'W	1980-04-29
DLIA_ANE_AMN_24_04	AMNAPE	24	29°48'N	29°58'W	1980-04-29
DLIA_ANE_AMN_24_05	AMNAPE	24	29°48'N	29°58'W	1980-04-29
DLIA_ANE_AMN_24_06	AMNAPE	24	29°48'N	29°58'W	1980-04-29
DLIA_ANE_AMN_24_07	AMNAPE	24	29°48'N	29°58'W	1980-04-29
DLIL_ANE_101A_26_01	Projekt 101A	26 Tr.4	24°52'N	30°00'W	1980-05-01
DLIL_ANE_101A_26_02	Projekt 101A	26 Tr.4	24°52'N	30°00'W	1980-05-01
DLIL_ANE_101A_26_03	Projekt 101A	26 Tr.4	24°52'N	30°00'W	1980-05-01
DLIL_ANE_101A_26_04	Projekt 101A	26 Tr.4	24°52'N	30°00'W	1980-05-01
DLIL_ANE_101A_26_05	Projekt 101A	26 Tr.4	24°52'N	30°00'W	1980-05-01
DLIL_ANE_101A_26_06	Projekt 101A	26 Tr.4	24°52'N	30°00'W	1980-05-01
DLIL_ANE_101A_26_07	Projekt 101A	26 Tr.4	24°52'N	30°00'W	1980-05-01
DLIL_ANE_101A_26_08	Projekt 101A	26 Tr.4	24°52'N	30°00'W	1980-05-01
DLIL_ANE_DANA_4006_01	DANA	4006 IV	15°31'N	18°05'W	1930-01-13
DLIL_ANE_DANA_4006_02	DANA	4006 IV	15°31'N	18°05'W	1930-01-13
DLIL_ANE_DANA_4006_03	DANA	4006 IV	15°31'N	18°05'W	1930-01-13
DLIL_ANE_DANA_4006_04	DANA	4006 IV	15°31'N	18°05'W	1930-01-13
DLIL_ANE_DANA_4006_05	DANA	4006 IV	15°31'N	18°05'W	1930-01-13
DLIL_ANE_DANA_4006_06	DANA	4006 IV	15°31'N	18°05'W	1930-01-13
DLIL_ANE_DANA_4006_07	DANA	4006 IV	15°31'N	18°05'W	1930-01-13
DLIL_ANE_DANA_4006_08	DANA	4006 IV	15°31'N	18°05'W	1930-01-13
DLIL_ANE_HAV_628_01	Komm.Havunders	628	36°16'N	30°10'W	1912-10-15

Identification				Geometric morphometrics						Genetics	
Specimen type (F, Fresh; M, Museum)	Genetic clade / Species (Van der Spoel et al., 1993)	LDA group	Integrative group	Ventral photo	Ventral 23LMs	Ventral 38LMs	Lateral photo	Lateral 15LMs	Lateral 49LMs	COI	28S
M Step 4	*D. elegans*	Group 1	Group 1	✓	✓		✓	✓	✓		
M Step 4	*D. elegans*	Group 1	Group 1	✓	✓		✓	✓	✓		
M Step 4	*D. elegans*	Group 1	Group 1	✓	✓	✓	✓	✓	✓		
M Step 4	*D. elegans*	Group 1	Group 1	✓	✓	✓	✓	✓	✓		
M Step 4	*D. elegans*	Group 1	Group 1	✓	✓	✓	✓	✓	✓		
M Step 4	*D. elegans*	Group 1	Group 1	✓	✓		✓	✓	✓		
M Step 4	*D. elegans*	Group 1	Group 1	✓	✓		✓	✓	✓		
M Step 4	*D. elegans*	Group 1	Group 1	✓	✓		✓	✓	✓		
M Step 4	*D. elegans*	Group 1	Group 1	✓	✓		✓	✓	✓		
M Step 4	*D. elegans*	Group 1	Group 1	✓	✓	✓	✓	✓	✓		
M unknown	*D. elegans*	N.A.	Unkn.	✓			✓				
M Step 4	*D. elegans*	Group 1	Group 1	✓	✓	✓	✓	✓			
M unknown	*D. limbata africana*	N.A.	Unkn.	✓			✓	✓			
M unknown	*D. limbata africana*	N.A.	Unkn.	✓			✓	✓			
M Step 4	*D. limbata africana*	Group 2	Group 2	✓			✓	✓	✓		
M Step 4	*D. limbata africana*	Group 2	Group 2	✓			✓	✓	✓		
M Step 4	*D. limbata africana*	Group 2	Group 2	✓			✓	✓	✓		
M Step 4	*D. limbata africana*	Group 2	Group 2	✓			✓	✓	✓		
M Step 4	*D. limbata africana*	Group 2	Group 2	✓			✓	✓	✓		
M Step 4	*D. limbata africana*	Group 2	Group 2	✓	✓	✓	✓	✓	✓		
M Step 4	*D. limbata africana*	Group 2	Group 2	✓	✓	✓	✓	✓	✓		
M Step 4	*D. limbata africana*	Group 2	Group 2	✓	✓		✓	✓	✓		
M Step 4	*D. limbata africana*	Group 2	Group 2	✓			✓	✓	✓		
M unknown	*D. limbata africana*	N.A.	Unkn.	✓			✓	✓			
M Step 4	*D. limbata africana*	Group 2	Group 2	✓	✓	✓					
M Step 2	*D. limbata africana*	Group 2	Group 2	✓			✓	✓	✓		
M Step 2	*D. limbata africana*	Group 2	Group 2	✓			✓	✓	✓		
M Step 2	*D. limbata africana*	Group 2	Group 2	✓			✓	✓	✓		
M Step 2	*D. limbata africana*	Group 2	Group 2	✓			✓	✓	✓		
M unknown	*D. limbata africana*	N.A.	Unkn.	✓			✓	✓			
M Step 2	*D. limbata africana*	Group 2	Group 2	✓			✓	✓	✓		
M unknown	*D. limbata africana*	N.A.	Unkn.	✓							
M unknown	*D. limbata limbata*	N.A.	Unkn.	✓			✓	✓			
M unknown	*D. limbata limbata*	N.A.	Unkn.	✓			✓				
M unknown	*D. limbata limbata*	Amb.	Unkn.	✓	✓	✓	✓	✓			
M unknown	*D. limbata limbata*	N.A.	Unkn.	✓			✓	✓			
M unknown	*D. limbata limbata*	N.A.	Unkn.	✓			✓	✓			
M Step 4	*D. limbata limbata*	Group 2	Group 2	✓	✓		✓	✓			
M Step 4	*D. limbata limbata*	Group 2	Group 2	✓			✓	✓	✓		
M Step 4	*D. limbata limbata*	Group 2	Group 2	✓	✓		✓				
M Step 4	*D. limbata limbata*	Group 2	Group 2	✓			✓	✓	✓		
M Step 4	*D. limbata limbata*	Group 2	Group 2	✓	✓	✓	✓	✓	✓		
M Step 4	*D. limbata limbata*	Group 2	Group 2	✓	✓	✓	✓	✓	✓		
M Step 4	*D. limbata limbata*	Group 2	Group 2	✓	✓		✓	✓	✓		
M unknown	*D. limbata limbata*	N.A.	Unkn.	✓			✓				
M Step 4	*D. limbata limbata*	Group 2	Group 2	✓	✓		✓				
M Step 4	*D. limbata limbata*	Group 2	Group 2	✓	✓	✓	✓	✓	✓		
M Step 4	*D. limbata limbata*	Group 2	Group 2	✓	✓	✓	✓	✓			
M Step 4	*D. limbata limbata*	Group 2	Group 2	✓	✓		✓	✓	✓		

TABLE S1. Continued

Sample information					
Specimen ID	Cruise	Station	Latitude	Longitude	Collection date
Atlantic Ocean					
DLIL_ANE_HAV_628_02	Komm.Havunders	628	36°16'N	30°10'W	1912-10-15
DLIL_ANE_HAV_628_03	Komm.Havunders	628	36°16'N	30°10'W	1912-10-15
DLIL_ANE_HAV_628_04	Komm.Havunders	628	36°16'N	30°10'W	1912-10-15
DLIL_ANE_HAV_628_05	Komm.Havunders	628	36°16'N	30°10'W	1912-10-15
DLIL_ANE_HAV_628_06	Komm.Havunders	628	36°16'N	30°10'W	1912-10-15
DLIL_ANE_HAV_628_07	Komm.Havunders	628	36°16'N	30°10'W	1912-10-15
DLIL_ANE_HAV_628_08	Komm.Havunders	628	36°16'N	30°10'W	1912-10-15
DLIL_ANE_HAV_628_09	Komm.Havunders	628	36°16'N	30°10'W	1912-10-15
DLIL_ANE_HAV_628_10	Komm.Havunders	628	36°16'N	30°10'W	1912-10-15
DLIL_ANE_HAV_628_11	Komm.Havunders	628	36°16'N	30°10'W	1912-10-15
DLIL_ANE_HAV_628_12	Komm.Havunders	628	36°16'N	30°10'W	1912-10-15
DLIL_ANE_HAV_628_13	Komm.Havunders	628	36°16'N	30°10'W	1912-10-15
DLIL_ANE_HAV_628_14	Komm.Havunders	628	36°16'N	30°10'W	1912-10-15
DLIL_ANE_HAV_628_15	Komm.Havunders	628	36°16'N	30°10'W	1912-10-15
DLIL_ANE_HAV_628_16	Komm.Havunders	628	36°16'N	30°10'W	1912-10-15
DLON_ANW_DANA_1339_01	DANA	1339 V	30°00'N	64°38'W	1922-05-10
DLON_ANW_DANA_1355_01	DANA	1355 I	31°48'N	63°38'W	1922-05-30
DLON_ASE_DANA_4000_01	DANA	4000 V	0°31'S	11°02'W	1930-03-04
DLON_ASE_DANA_4000_02	DANA	4000 V	0°31'S	11°02'W	1930-03-04
DLON_ASE_DANA_4000_03	DANA	4000 V	0°31'S	11°02'W	1930-03-04
DLON_ASE_DANA_4000_04	DANA	4000 V	0°31'S	11°02'W	1930-03-04
DLON_ASE_DANA_4000_05	DANA	4000 V	0°31'S	11°02'W	1930-03-04
DLON_ASE_DANA_4000_06	DANA	4000 V	0°31'S	11°02'W	1930-03-04
DLON_ASE_DANA_4000_07	DANA	4000 V	0°31'S	11°02'W	1930-03-04
DLON_ASE_DANA_4000_08	DANA	4000 V	0°31'S	11°02'W	1930-03-04
DLON_ASE_DANA_4000_09	DANA	4000 V	0°31'S	11°02'W	1930-03-04
DLON_ASE_DANA_4000_10	DANA	4000 V	0°31'S	11°02'W	1930-03-04
DLON_ASE_DANA_4000_11	DANA	4000 V	0°31'S	11°02'W	1930-03-04
DLON_ASE_DANA_4000_12	DANA	4000 V	0°31'S	11°02'W	1930-03-04
DLON_ASE_DANA_4000_13	DANA	4000 V	0°31'S	11°02'W	1930-03-04
DLON_ASE_DANA_4000_14	DANA	4000 V	0°31'S	11°02'W	1930-03-04
DLON_ASE_DANA_4000_15	DANA	4000 V	0°31'S	11°02'W	1930-03-04
DLON_ASE_DANA_4000_16	DANA	4000 V	0°31'S	11°02'W	1930-03-04
DOVA_ANW_DD106_67_01	DD106	67M	38°45'N	72°20'W	1975-07-31
DOVA_ANW_DD106_76_01	DD106	76M	38°47'N	72°38'W	1975-08-01
DOVA_ANW_DD106_76_02	DD106	76M	38°47'N	72°38'W	1975-08-01
DOVA_ANW_DD106_76_03	DD106	76M	38°47'N	72°38'W	1975-08-01
DOVA_ANW_DD106_76_04	DD106	76M	38°47'N	72°38'W	1975-08-01
DOVA_ANW_DD106_76_05	DD106	76M	38°47'N	72°38'W	1975-08-01
DOVA_ANW_DD106_76_06	DD106	76M	38°47'N	72°38'W	1975-08-01
DOVA_ANW_DD106_76_07	DD106	76M	38°47'N	72°38'W	1975-08-01
DOVA_ANW_DD106_76_08	DD106	76M	38°47'N	72°38'W	1975-08-01
DSTA_ANE_ATL_097_01	Atlantide	97	6°06'N	3°41'E	1946-02-14
DSTA_ANE_ATL_098_01	Atlantide	98	5°56'N	4°26'E	1946-02-15
DSTA_ANE_ATL_098_02	Atlantide	98	5°56'N	4°26'E	1946-02-15
DSTA_ANE_ATL_098_03	Atlantide	98	5°56'N	4°26'E	1946-02-15
DSTA_ANE_ATL_098_04	Atlantide	98	5°56'N	4°26'E	1946-02-15
DSTA_ANE_ATL_098_05	Atlantide	98	5°56'N	4°26'E	1946-02-15
DSTA_ANE_ATL_098_06	Atlantide	98	5°56'N	4°26'E	1946-02-15

Identification				Geometric morphometrics						Genetics	
Specimen type (F, Fresh; M, Museum)	Genetic clade / Species (Van der Spoel et al., 1993)	LDA group	Integrative group	Ventral photo	Ventral 23LMs	Ventral 38LMs	Lateral photo	Lateral 15LMs	Lateral 49LMs	COI	28S
M Step 4	*D. limbata limbata*	Group 2	Group 2	✓			✓	✓	✓		
M Step 4	*D. limbata limbata*	Group 2	Group 2	✓	✓	✓	✓	✓			
M Step 4	*D. limbata limbata*	Group 2	Group 2	✓			✓	✓	✓		
M Step 4	*D. limbata limbata*	Group 2	Group 2	✓	✓		✓	✓	✓		
M Step 4	*D. limbata limbata*	Group 1	Group 1	✓	✓	✓	✓	✓	✓		
M Step 4	*D. limbata limbata*	Group 2	Group 2	✓	✓		✓	✓	✓		
M Step 4	*D. limbata limbata*	Group 2	Group 2	✓			✓	✓	✓		
M Step 4	*D. limbata limbata*	Group 2	Group 2	✓	✓		✓	✓	✓		
M Step 4	*D. limbata limbata*	Group 1	Group 1	✓			✓	✓	✓		
M Step 4	*D. limbata limbata*	Group 2	Group 2	✓	✓	✓	✓	✓	✓		
M Step 4	*D. limbata limbata*	Group 2	Group 2	✓	✓		✓	✓	✓		
M Step 4	*D. limbata limbata*	Group 1	Group 1	✓	✓		✓	✓	✓		
M Step 4	*D. limbata limbata*	Group 2	Group 2	✓	✓		✓	✓	✓		
M unknown	*D. limbata limbata*	Amb.	Unkn.	✓	✓		✓	✓	✓		
M unknown	*D. limbata limbata*	N.A.	Unkn.	✓			✓	✓			
M Step 4	*D. longirostris*	Group 1	Group 1	✓	✓	✓	✓	✓	✓		
M Step 4	*D. longirostris*	Group 1	Group 1	✓	✓		✓	✓			
M Step 4	*D. longirostris*	Group 1	Group 1	✓			✓	✓	✓		
M Step 4	*D. longirostris*	Group 1	Group 1	✓	✓		✓	✓	✓		
M Step 4	*D. longirostris*	Group 1	Group 1	✓			✓	✓	✓		
M Step 4	*D. longirostris*	Group 1	Group 1	✓	✓		✓	✓	✓		
M Step 4	*D. longirostris*	Group 1	Group 1	✓	✓		✓	✓	✓		
M Step 4	*D. longirostris*	Group 1	Group 1	✓	✓		✓	✓			
M Step 4	*D. longirostris*	Group 1	Group 1	✓	✓		✓	✓			
M Step 4	*D. longirostris*	Group 1	Group 1	✓	✓		✓	✓	✓		
M Step 4	*D. longirostris*	Group 1	Group 1	✓	✓		✓	✓	✓		
M Step 4	*D. longirostris*	Group 1	Group 1	✓	✓		✓	✓	✓		
M Step 4	*D. longirostris*	Group 1	Group 1	✓	✓		✓	✓	✓		
M Step 4	*D. longirostris*	Group 1	Group 1	✓	✓	✓	✓	✓	✓		
M Step 4	*D. longirostris*	Group 1	Group 1	✓	✓		✓	✓	✓		
M Step 4	*D. longirostris*	Group 1	Group 1	✓	✓	✓	✓	✓	✓		
M Step 4	*D. longirostris*	Group 1	Group 1	✓	✓		✓	✓	✓		
M Step 4	*D. longirostris*	Group 1	Group 1	✓	✓		✓	✓	✓		
M Step 2	*D. ovalis*	Group 1	Group 1	✓	✓		✓	✓	✓		
M Step 4	*D. ovalis*	Group 1	Group 1	✓	✓		✓	✓			
M unknown	*D. ovalis*	N.A.	Unkn.	✓			✓	✓			
M Step 4	*D. ovalis*	Group 1	Group 1	✓	✓		✓	✓	✓		
M Step 4	*D. ovalis*	Group 1	Group 1	✓	✓	✓	✓	✓	✓		
M Step 4	*D. ovalis*	Group 1	Group 1	✓	✓	✓	✓				
M Step 4	*D. ovalis*	Group 1	Group 1	✓	✓	✓	✓	✓			
M Step 4	*D. ovalis*	Group 1	Group 1	✓	✓		✓	✓	✓		
M unknown	*D. ovalis*	N.A.	Unkn.	✓			✓	✓			
M Step 4	*D. strangulata*	Group 1	Group 1	✓	✓	✓	✓	✓			
M Step 4	*D. strangulata*	Group 1	Group 1	✓	✓		✓	✓	✓		
M Step 4	*D. strangulata*	Group 1	Group 1	✓	✓	✓	✓	✓	✓		
M Step 4	*D. strangulata*	Group 2	Group 2	✓			✓	✓	✓		
M Step 4	*D. strangulata*	Group 1	Group 1	✓	✓	✓	✓	✓	✓		
M Step 4	*D. strangulata*	Group 1	Group 1	✓	✓	✓	✓	✓	✓		
M Step 4	*D. strangulata*	Group 1	Group 1	✓	✓		✓	✓			

TABLE S1. Continued

Sample information					
Specimen ID	Cruise	Station	Latitude	Longitude	Collection date
Atlantic Ocean					
DSTA_ANE_ATL_098_07	Atlantide	98	5°56'N	4°26'E	1946-02-15
DSTA_ANE_ATL_119_01	Atlantide	119	2°55'N	9°21'E	1946-02-28
DSTA_ANE_ATL_119_02	Atlantide	119	2°55'N	9°21'E	1946-02-28
DSTA_ANW_DANA_1293_01	DANA	1293 III	17°43'N	64°56'W	1922-04-17
DSTA_ANW_DANA_1293_02	DANA	1293 III	17°43'N	64°56'W	1922-04-17
DVUM_ANE_DANA_4004_01	DANA	4004 IV	10°21'N	17°59'W	1930-03-11
DVUM_ANE_DANA_4004_02	DANA	4004 IV	10°21'N	17°59'W	1930-03-11
DVUM_ANE_DANA_4004_03	DANA	4004 IV	10°21'N	17°59'W	1930-03-11
DVUM_ANE_DANA_4004_04	DANA	4004 IV	10°21'N	17°59'W	1930-03-11
DVUM_ANE_DANA_4004_05	DANA	4004 IV	10°21'N	17°59'W	1930-03-11
DVUM_ANE_DANA_4004_06	DANA	4004 IV	10°21'N	17°59'W	1930-03-11
DVUM_ANE_DANA_4004_07	DANA	4004 IV	10°21'N	17°59'W	1930-03-11
DVUM_ANE_DANA_4004_08	DANA	4004 IV	10°21'N	17°59'W	1930-03-11
DVUM_ANE_DANA_4004_09	DANA	4004 IV	10°21'N	17°59'W	1930-03-11
DVUM_ANE_DANA_4004_10	DANA	4004 IV	10°21'N	17°59'W	1930-03-11
DVUM_ANE_DANA_4004_11	DANA	4004 IV	10°21'N	17°59'W	1930-03-11
DVUM_ANE_DANA_4004_12	DANA	4004 IV	10°21'N	17°59'W	1930-03-11
DVUM_ANE_DANA_4004_13	DANA	4004 IV	10°21'N	17°59'W	1930-03-11
DVUM_ANE_DANA_4004_14	DANA	4004 IV	10°21'N	17°59'W	1930-03-11
DVUU_ANW_DANA_1192_01	DANA	1192 XI	17°43'N	64°54'W	1921-12-16
DVUU_ANW_DANA_1192_02	DANA	1192 XI	17°43'N	64°54'W	1921-12-16
DVUU_ANW_DANA_1192_03	DANA	1192 XI	17°43'N	64°54'W	1921-12-16
DVUU_ANW_DANA_1192_04	DANA	1192 XI	17°43'N	64°54'W	1921-12-16
DVUU_ANW_DANA_1192_05	DANA	1192 XI	17°43'N	64°54'W	1921-12-16
DVUU_ANW_DANA_1192_06	DANA	1192 XI	17°43'N	64°54'W	1921-12-16
DVUU_ANW_DANA_1192_07	DANA	1192 XI	17°43'N	64°54'W	1921-12-16
DVUU_ANW_DANA_1192_08	DANA	1192 XI	17°43'N	64°54'W	1921-12-16
DVUU_ANW_DANA_1192_09	DANA	1192 XI	17°43'N	64°54'W	1921-12-16
DVUU_ANW_DANA_1192_10	DANA	1192 XI	17°43'N	64°54'W	1921-12-16
DVUU_ANW_DANA_1192_11	DANA	1192 XI	17°43'N	64°54'W	1921-12-16
DVUU_ANW_DANA_1192_12	DANA	1192 XI	17°43'N	64°54'W	1921-12-16
DVUU_ANW_DANA_1192_13	DANA	1192 XI	17°43'N	64°54'W	1921-12-16
DVUU_ANW_DANA_1192_14	DANA	1192 XI	17°43'N	64°54'W	1921-12-16
DVUU_ANW_DANA_1192_15	DANA	1192 XI	17°43'N	64°54'W	1921-12-16
DVUU_ANW_DANA_1192_16	DANA	1192 XI	17°43'N	64°54'W	1921-12-16
Pacific Ocean					
D_PNW_KH1110_02_01	KH1110	2	23°00'N	160°00'E	2011-12-07
D_PNW_KH1110_02_02	KH1110	2	23°00'N	160°00'E	2011-12-07
D_PNW_KH1110_02_03	KH1110	2	23°00'N	160°00'E	2011-12-07
D_PNW_KH1110_02_04	KH1110	2	23°00'N	160°00'E	2011-12-07
D_PNW_KH1110_02_05	KH1110	2	23°00'N	160°00'E	2011-12-07
D_PNW_KH1110_02_06	KH1110	2	23°00'N	160°00'E	2011-12-07
D_PNW_KH1110_02_07	KH1110	2	23°00'N	160°00'E	2011-12-07
D_PNW_KH1110_02_08	KH1110	2	23°00'N	160°00'E	2011-12-07
D_PNW_KH1110_02_09	KH1110	2	23°00'N	160°00'E	2011-12-07
D_PNW_KH1110_02_10	KH1110	2	23°00'N	160°00'E	2011-12-07
D_PNW_KH1110_02_11	KH1110	2	23°00'N	160°00'E	2011-12-07
D_PNW_KH1110_02_12	KH1110	2	23°00'N	160°00'E	2011-12-07
D_PNW_KH1110_02_13	KH1110	2	23°00'N	160°00'E	2011-12-07

Identification				Geometric morphometrics						Genetics	
Specimen type (F, Fresh; M, Museum)	Genetic clade / Species (Van der Spoel et al., 1993)	LDA group	Integrative group	Ventral photo	Ventral 23LMs	Ventral 38LMs	Lateral photo	Lateral 15LMs	Lateral 49LMs	COI	28S
M Step 4	*D. strangulata*	Group 1	Group 1	✓	✓		✓	✓	✓		
M Step 4	*D. strangulata*	Group 1	Group 1	✓	✓	✓	✓	✓	✓		
M Step 4	*D. strangulata*	Group 1	Group 1	✓	✓	✓	✓	✓	✓		
M Step 4	*D. strangulata*	Group 1	Group 1	✓			✓	✓	✓		
M Step 4	*D. strangulata*	Group 1	Group 1	✓	✓	✓	✓				
M Step 4	*D. v. meisenheimeri*	Group 2	Group 2	✓	✓		✓	✓			
M Step 4	*D. v. meisenheimeri*	Group 2	Group 2	✓	✓	✓	✓	✓			
M unknown	*D. v. meisenheimeri*	N.A.	Unkn.	✓			✓				
M unknown	*D. v. meisenheimeri*	N.A.	Unkn.	✓			✓	✓			
M Step 4	*D. v. meisenheimeri*	Group 2	Group 2	✓	✓		✓	✓			
M Step 4	*D. v. meisenheimeri*	Group 2	Group 2	✓			✓	✓	✓		
M unknown	*D. v. meisenheimeri*	Amb.	Unkn.	✓	✓		✓	✓	✓		
M Step 4	*D. v. meisenheimeri*	Group 2	Group 2	✓			✓	✓	✓		
M Step 4	*D. v. meisenheimeri*	Group 1	Group 1	✓	✓		✓	✓	✓		
M Step 4	*D. v. meisenheimeri*	Group 2	Group 2	✓			✓	✓	✓		
M Step 4	*D. v. meisenheimeri*	Group 2	Group 2	✓	✓	✓	✓	✓	✓		
M unknown	*D. v. meisenheimeri*	N.A.	Unkn.	✓			✓	✓			
M Step 4	*D. v. meisenheimeri*	Group 1	Group 1	✓			✓	✓	✓		
M unknown	*D. v. meisenheimeri*	Amb.	Unkn.	✓			✓	✓	✓		
M unknown	*D. v. vanutrechti*	N.A.	Unkn.	✓			✓	✓			
M Step 4	*D. v. vanutrechti*	Group 1	Group 1	✓	✓	✓	✓	✓	✓		
M Step 4	*D. v. vanutrechti*	Group 1	Group 1	✓	✓		✓	✓	✓		
M Step 4	*D. v. vanutrechti*	Group 1	Group 1	✓	✓		✓	✓	✓		
M Step 4	*D. v. vanutrechti*	Group 1	Group 1	✓	✓		✓	✓			
M Step 4	*D. v. vanutrechti*	Group 1	Group 1	✓	✓		✓	✓	✓		
M Step 4	*D. v. vanutrechti*	Group 1	Group 1	✓	✓		✓	✓	✓		
M Step 4	*D. v. vanutrechti*	Group 1	Group 1	✓	✓	✓	✓	✓	✓		
M Step 4	*D. v. vanutrechti*	Group 1	Group 1	✓	✓	✓	✓	✓	✓		
M Step 4	*D. v. vanutrechti*	Group 1	Group 1	✓	✓		✓	✓	✓		
M Step 4	*D. v. vanutrechti*	Group 1	Group 1	✓	✓	✓	✓	✓	✓		
M Step 4	*D. v. vanutrechti*	Group 1	Group 1	✓	✓		✓	✓			
M Step 4	*D. v. vanutrechti*	Group 1	Group 1	✓	✓	✓	✓	✓	✓		
M Step 4	*D. v. vanutrechti*	Group 1	Group 1	✓	✓		✓	✓	✓		
M Step 4	*D. v. vanutrechti*	Group 1	Group 1	✓	✓	✓	✓	✓	✓		
M Step 4	*D. v. vanutrechti*	Group 1	Group 1	✓	✓						
F Step 1	Group 4	Group 4	Group 4	✓	✓	✓	✓	✓	✓		MF974659
F Step 1	Group 4	Group 4	Group 4	✓			✓	✓	✓		MF974660
F Step 1	Group 4	Group 4	Group 4	✓	✓	✓	✓	✓			MF974661
F Step 1	Group 4	Group 4	Group 4	✓	✓		✓	✓	✓		MF974662
F Step 1	Group 4	Group 4	Group 4	✓	✓	✓	✓	✓			MF974663
F Step 1	Group 4	Group 4	Group 4	✓	✓	✓	✓	✓			MF974664
F Step 4	N.A.	Group 4	Group 4	✓	✓	✓	✓				
F Step 1	Group 4	Group 4	Group 4	✓	✓	✓	✓	✓	✓		MF974665
F Step 1	Group 4	Group 4	Group 4	✓	✓		✓	✓	✓		MF974666
F Step 1	Group 4	Group 4	Group 4	✓	✓		✓	✓			MF974667
F Step 4	N.A.	Group 4	Group 4	✓	✓		✓				
F Step 1	Group 4	Group 4	Group 4	✓	✓	✓	✓	✓			MF974668
F Step 1	Group 4	N.A.	Group 4	✓			✓	✓			MF974669

TABLE S1. Continued

Sample information					
Specimen ID	Cruise	Station	Latitude	Longitude	Collection date
Pacific Ocean					
D_PNW_KH1110_02_14	KH1110	2	23°00'N	160°00'E	2011-12-07
D_PNW_KH1110_05_01	KH1110	5	23°00'N	180°00'E	2011-12-14
D_PNW_KH1110_05_02	KH1110	5	23°00'N	180°00'E	2011-12-14
D_PNW_KH1110_05_03	KH1110	5	23°00'N	180°00'E	2011-12-14
D_PNW_KH1110_05_04	KH1110	5	23°00'N	180°00'E	2011-12-14
D_PNW_KH1110_05_05	KH1110	5	23°00'N	180°00'E	2011-12-14
D_PNW_KH1110_05_06	KH1110	5	23°00'N	180°00'E	2011-12-14
D_PNW_KH1110_05_07	KH1110	5	23°00'N	180°00'E	2011-12-14
D_PNW_KH1110_05_08	KH1110	5	23°00'N	180°00'E	2011-12-14
D_PNW_KH1110_05_09	KH1110	5	23°00'N	180°00'E	2011-12-14
D_PNW_KH1110_05_10	KH1110	5	23°00'N	180°00'E	2011-12-14
D_PNW_KH1110_05_11	KH1110	5	23°00'N	180°00'E	2011-12-14
D_PNW_KH1110_05_12	KH1110	5	23°00'N	180°00'E	2011-12-14
D_PNW_KH1110_05_13	KH1110	5	23°00'N	180°00'E	2011-12-14
D_PNW_KH1110_05_14	KH1110	5	23°00'N	180°00'E	2011-12-14
D_PNW_KH1110_05_15	KH1110	5	23°00'N	180°00'E	2011-12-14
D_PNW_KH1110_05_16	KH1110	5	23°00'N	180°00'E	2011-12-14
D_PNW_KH1110_05_17	KH1110	5	23°00'N	180°00'E	2011-12-14
D_PNW_KH1110_05_18	KH1110	5	23°00'N	180°00'E	2011-12-14
D_PNW_KH1110_05_19	KH1110	5	23°00'N	180°00'E	2011-12-14
D_PNW_KH1110_05_20	KH1110	5	23°00'N	180°00'E	2011-12-14
D_PNW_KH1110_05_21	KH1110	5	23°00'N	180°00'E	2011-12-14
D_PNE_KH1110_08_01	KH1110	8	22°47'N	158°06'W	2011-12-19
D_PNE_KM1109_01_01	KM1109	1	21°15'N	158°11'W	2011-03-04
D_PNE_KM1109_01_02	KM1109	1	21°15'N	158°11'W	2011-03-04
D_PNE_KM1109_01_03	KM1109	1	21°15'N	158°11'W	2011-03-04
D_PNE_KM1109_01_04	KM1109	1	21°15'N	158°11'W	2011-03-04
D_PNE_KM1109_01_05	KM1109	1	21°15'N	158°11'W	2011-03-04
D_PNE_KM1109_02_01	KM1109	2	21°15'N	158°11'W	2011-03-04
D_PNE_KM1109_02_02	KM1109	2	21°15'N	158°11'W	2011-03-04
D_PNE_KM1109_02_03	KM1109	2	21°15'N	158°11'W	2011-03-04
D_PNE_KM1109_02_04	KM1109	2	21°15'N	158°11'W	2011-03-04
D_PNE_KM1109_02_05	KM1109	2	21°15'N	158°11'W	2011-03-04
D_PNE_KM1109_02_06	KM1109	2	21°15'N	158°11'W	2011-03-04
D_PNE_KM1109_03_01	KM1109	3	21°16'N	158°13'W	2011-03-05
D_PNE_KM1109_03_02	KM1109	3	21°16'N	158°13'W	2011-03-05
D_PNE_KM1109_03_03	KM1109	3	21°16'N	158°13'W	2011-03-05
D_PNE_KM1109_03_04	KM1109	3	21°16'N	158°13'W	2011-03-05
D_PNE_KM1109_03_05	KM1109	3	21°16'N	158°13'W	2011-03-05
D_PNE_KM1109_04_01	KM1109	4	21°25'N	158°18'W	2011-03-05
D_PNE_KM1109_06_01	KM1109	6	21°27'N	158°23'W	2011-03-05
D_PNE_KM1109_06_02	KM1109	6	21°27'N	158°23'W	2011-03-05
D_PNE_KM1109_07_01	KM1109	7	21°27'N	158°15'W	2011-03-06
D_PNE_KM1109_07_02	KM1109	7	21°27'N	158°15'W	2011-03-06
D_PNE_KM1109_07_03	KM1109	7	21°27'N	158°15'W	2011-03-06
D_PNE_KM1109_07_04	KM1109	7	21°27'N	158°15'W	2011-03-06
D_PNE_KM1109_07_05	KM1109	7	21°27'N	158°15'W	2011-03-06
D_PNE_KM1109_07_06	KM1109	7	21°27'N	158°15'W	2011-03-06
D_PNE_KM1109_07_07	KM1109	7	21°27'N	158°15'W	2011-03-06

Identification				Geometric morphometrics						Genetics	
Specimen type (F, Fresh; M, Museum)	Genetic clade / Species (Van der Spoel et al., 1993)	LDA group	Integrative group	Ventral photo	Ventral 23LMs	Ventral 38LMs	Lateral photo	Lateral 15LMs	Lateral 49LMs	COI	28S
F Step 1	Group 4	N.A.	Group 4	✓			✓	✓			MF974670
F Step 1	Group 3	Group 3	Group 3	✓	✓	✓	✓	✓	✓	MF974818	MF974671
F Step 1	Group 3	Group 3	Group 3	✓	✓		✓	✓	✓	MF974819	MF974672
F Step 1	Group 3	N.A.	Group 3	✓			✓	✓		MF974820	MF974673
F Step 1	Group 4	N.A.	Group 4	✓			✓				MF974674
F Step 1	Group 4	Group 4	Group 4	✓	✓		✓				MF974675
F Step 4	N.A.	Group 4	Group 4	✓	✓	✓	✓	✓	✓		
F Step 1	Group 4	Group 4	Group 4	✓	✓		✓	✓	✓		MF974676
F unknown	N.A.	N.A.	Unkn.	✓			✓	✓			
F unknown	N.A.	N.A.	Unkn.	✓			✓				
F Step 1	Group 4	Group 4	Group 4	✓			✓	✓	✓		MF974677
F Step 1	Group 4	Group 4	Group 4	✓	✓		✓				MF974678
F Step 1	Group 4	Group 4	Group 4	✓			✓	✓	✓		MF974679
F Step 1	Group 4	N.A.	Group 4	✓			✓				MF974680
F Step 1	Group 4	N.A.	Group 4	✓			✓				MF974681
F Step 1	Group 4	N.A.	Group 4	✓			✓				MF974682
F Step 1	Group 4	Group 4	Group 4	✓	✓		✓				MF974683
F Step 1	Group 4	Group 4	Group 4	✓	✓	✓	✓				MF974684
F Step 1	Group 4	N.A.	Group 4	✓			✓	✓			MF974685
F Step 4	N.A.	Group 4	Group 4	✓	✓	✓	✓	✓			
F Step 1	Group 4	N.A.	Group 4	✓			✓	✓			MF974686
F Step 4	N.A.	Group 4	Group 4	✓	✓	✓	✓				
F Step 1	Group 4	Group 4	Group 4	✓	✓		✓	✓	✓		MF974687
F Step 1	Group 4	Group 4	Group 4	✓	✓		✓				MF974688
F Step 1	Group 4	Group 4	Group 4	✓	✓	✓	✓	✓	✓		MF974689
F Step 1	Group 4	Group 4	Group 4	✓	✓	✓	✓				MF974690
F Step 1	Group 4	Group 4	Group 4	✓	✓	✓	✓	✓	✓		MF974691
F Step 1	Group 4	Group 4	Group 4	✓	✓	✓	✓	✓	✓		MF974692
F Step 4	N.A.	Group 4	Group 4	✓	✓		✓	✓	✓		
F unknown	N.A.	N.A.	Unkn.								
F Step 1	Group 4	Group 4	Group 4	✓			✓	✓	✓		MF974693
F unknown	N.A.	N.A.	Unkn.								
F unknown	N.A.	N.A.	Unkn.								
F Step 4	N.A.	Group 4	Group 4	✓	✓	✓	✓	✓	✓		
F Step 1	Group 4	Group 4	Group 4	✓	✓		✓	✓	✓		MF974694
F Step 1	Group 4	Group 4	Group 4	✓			✓	✓	✓		MF974695
F Step 1	Group 4	Group 4	Group 4	✓	✓		✓	✓	✓		MF974696
F unknown	N.A.	N.A.	Unkn.								
F unknown	N.A.	N.A.	Unkn.								
F Step 4	N.A.	Group 4	Group 4	✓	✓		✓	✓	✓		
F Step 1	Group 3	Group 3	Group 3	✓	✓	✓	✓	✓	✓	MF974821	
F Step 1	Group 4	Group 4	Group 4	✓	✓		✓	✓	✓		MF974697
F Step 1	Group 4	N.A.	Group 4								MF974698
F Step 1	Group 4	N.A.	Group 4								MF974699
F Step 1	Group 4	N.A.	Group 4								MF974700
F Step 1	Group 4	Group 4	Group 4	✓	✓	✓	✓	✓	✓		MF974701
F Step 1	Group 4	N.A.	Group 4								MF974702
F Step 1	Group 4	N.A.	Group 4								MF974703
F Step 1	Group 4	N.A.	Group 4								MF974704

TABLE S1. Continued

Sample information					
Specimen ID	Cruise	Station	Latitude	Longitude	Collection date
Pacific Ocean					
D_PNE_KM1109_07_08	KM1109	7	21°27'N	158°15'W	2011-03-06
D_PNE_KM1109_07_09	KM1109	7	21°27'N	158°15'W	2011-03-06
D_PNE_KM1109_07_10	KM1109	7	21°27'N	158°15'W	2011-03-06
D_PNE_KM1109_07_11	KM1109	7	21°27'N	158°15'W	2011-03-06
D_PNE_KM1109_07_12	KM1109	7	21°27'N	158°15'W	2011-03-06
D_PNE_KM1109_07_13	KM1109	7	21°27'N	158°15'W	2011-03-06
D_PNE_KM1109_07_14	KM1109	7	21°27'N	158°15'W	2011-03-06
D_PNE_KM1109_07_15	KM1109	7	21°27'N	158°15'W	2011-03-06
D_PNE_KM1109_07_16	KM1109	7	21°27'N	158°15'W	2011-03-06
D_PNE_KM1109_07_17	KM1109	7	21°27'N	158°15'W	2011-03-06
D_PNE_KM1109_07_18	KM1109	7	21°27'N	158°15'W	2011-03-06
D_PNE_KM1109_08_01	KM1109	8	21°20'N	158°22'W	2011-03-06
D_PNE_KM1109_08_02	KM1109	8	21°20'N	158°22'W	2011-03-06
D_PNE_KM1109_08_03	KM1109	8	21°20'N	158°22'W	2011-03-06
D_PNE_KM1109_08_04	KM1109	8	21°20'N	158°22'W	2011-03-06
D_PNE_KM1109_08_05	KM1109	8	21°20'N	158°22'W	2011-03-06
D_PNE_KM1109_08_06	KM1109	8	21°20'N	158°22'W	2011-03-06
D_PNE_KM1109_08_07	KM1109	8	21°20'N	158°22'W	2011-03-06
D_PNE_KM1109_10_01	KM1109	10	21°25'N	158°21'W	2011-03-07
D_PNE_KM1109_10_02	KM1109	10	21°25'N	158°21'W	2011-03-07
D_PNE_KM1109_10_03	KM1109	10	21°25'N	158°21'W	2011-03-07
D_PNE_KM1109_10_04	KM1109	10	21°25'N	158°21'W	2011-03-07
D_PNE_KM1109_10_05	KM1109	10	21°25'N	158°21'W	2011-03-07
D_PNE_KM1109_10_06	KM1109	10	21°25'N	158°21'W	2011-03-07
D_PNE_KM1109_10_07	KM1109	10	21°25'N	158°21'W	2011-03-07
D_PNE_KM1109_10_08	KM1109	10	21°25'N	158°21'W	2011-03-07
D_PNE_KM1109_10_09	KM1109	10	21°25'N	158°21'W	2011-03-07
D_PNE_KM1109_10_10	KM1109	10	21°25'N	158°21'W	2011-03-07
D_PNE_KM1109_10_11	KM1109	10	21°25'N	158°21'W	2011-03-07
D_PNE_KM1109_10_12	KM1109	10	21°25'N	158°21'W	2011-03-07
D_PNE_KM1109_10_13	KM1109	10	21°25'N	158°21'W	2011-03-07
D_PNE_KM1109_10_14	KM1109	10	21°25'N	158°21'W	2011-03-07
D_PNE_KM1109_10_15	KM1109	10	21°25'N	158°21'W	2011-03-07
D_PNE_KM1109_10_16	KM1109	10	21°25'N	158°21'W	2011-03-07
D_PNE_KM1109_10_17	KM1109	10	21°25'N	158°21'W	2011-03-07
D_PNE_KM1109_10_18	KM1109	10	21°25'N	158°21'W	2011-03-07
D_PNE_KM1109_10_19	KM1109	10	21°25'N	158°21'W	2011-03-07
D_PNE_KM1109_10_20	KM1109	10	21°25'N	158°21'W	2011-03-07
D_PNE_KM1109_10_21	KM1109	10	21°25'N	158°21'W	2011-03-07
D_PNE_KM1109_11_01	KM1109	11	21°25'N	158°21'W	2011-03-07
D_PNE_KM1109_11_02	KM1109	11	21°25'N	158°21'W	2011-03-07
D_PNE_KM1109_11_03	KM1109	11	21°25'N	158°21'W	2011-03-07
D_PNE_KM1109_11_04	KM1109	11	21°25'N	158°21'W	2011-03-07
D_PNE_KM1109_13_01	KM1109	13	21°25'N	158°21'W	2011-03-07
D_PNE_KM1109_13_02	KM1109	13	21°25'N	158°21'W	2011-03-07
D_PNE_KM1109_13_03	KM1109	13	21°25'N	158°21'W	2011-03-07
D_PNE_KM1109_13_04	KM1109	13	21°25'N	158°21'W	2011-03-07
D_PSW_COOK11MV_05_01	COOK11MV	5	2°14'S	145°13'E	2001-08-16
D_PSE_COOK14MV_29_01	COOK14MV	29	23°08'S	174°26'W	2001-10-22

Identification				Geometric morphometrics						Genetics	
Specimen type (F, Fresh; M, Museum)	Genetic clade / Species (Van der Spoel et al., 1993)	LDA group	Integrative group	Ventral photo	Ventral 23LMs	Ventral 38LMs	Lateral photo	Lateral 15LMs	Lateral 49LMs	COI	28S
F Step 1	Group 4	Group 4	Group 4	✓	✓		✓	✓	✓		MF974705
F Step 1	Group 4	N.A.	Group 4								MF974706
F Step 4	N.A.	Group 4	Group 4	✓	✓	✓	✓	✓	✓		
F Step 4	N.A.	Group 4	Group 4	✓	✓	✓	✓	✓	✓		
F unknown	N.A.	Amb.	Unkn.	✓	✓		✓				
F Step 1	Group 4	N.A.	Group 4								MF974707
F Step 1	Group 4	N.A.	Group 4								MF974708
F Step 1	Group 4	Group 4	Group 4	✓	✓	✓	✓	✓	✓		MF974709
F Step 1	Group 4	N.A.	Group 4								MF974710
F Step 1	Group 4	N.A.	Group 4								MF974711
F Step 1	Group 4	N.A.	Group 4								MF974712
F unknown	N.A.	N.A.	Unkn.								
F unknown	N.A.	N.A.	Unkn.								
F Step 4	N.A.	Group 4	Group 4	✓			✓	✓	✓		
F unknown	N.A.	N.A.	Unkn.								
F Step 1	Group 4	Group 4	Group 4	✓	✓		✓	✓	✓		MF974713
F Step 1	Group 4	N.A.	Group 4								MF974714
F Step 1	Group 4	N.A.	Group 4								MF974715
F unknown	N.A.	N.A.	Unkn.								
F Step 4	N.A.	Group 4	Group 4	✓	✓		✓	✓	✓		
F Step 1	Group 4	Group 4	Group 4	✓	✓		✓	✓	✓		MF974716
F Step 1	Group 4	N.A.	Group 4								MF974717
F Step 1	Group 4	Group 4	Group 4	✓	✓	✓	✓				MF974718
F Step 4	N.A.	Group 4	Group 4	✓			✓	✓	✓		
F Step 4	N.A.	Group 4	Group 4	✓	✓		✓	✓	✓		
F Step 1	Group 4	N.A.	Group 4								MF974719
F Step 1	Group 4	Group 4	Group 4	✓	✓	✓	✓				MF974720
F Step 4	N.A.	Group 4	Group 4	✓	✓		✓	✓	✓		
F Step 1	Group 4	Group 4	Group 4	✓	✓		✓	✓	✓		MF974721
F Step 1	Group 4	Group 4	Group 4	✓	✓	✓	✓	✓			MF974722
F Step 1	Group 4	Group 4	Group 4	✓	✓		✓	✓	✓		MF974723
F Step 1	Group 4	Group 4	Group 4	✓	✓		✓	✓	✓		MF974724
F Step 1	Group 4	N.A.	Group 4								MF974725
F unknown	N.A.	N.A.	Unkn.								
F Step 1	Group 4	N.A.	Group 4								MF974726
F unknown	N.A.	N.A.	Unkn.								
F Step 1	Group 4	N.A.	Group 4								MF974727
F unknown	N.A.	N.A.	Unkn.								
F Step 1	Group 4	N.A.	Group 4								MF974728
F Step 1	Group 4	Group 4	Group 4	✓	✓		✓	✓	✓		MF974729
F unknown	N.A.	N.A.	Unkn.								
F Step 1	Group 4	Group 4	Group 4	✓			✓	✓	✓		MF974730
F unknown	N.A.	N.A.	Unkn.								
F Step 1	Group 3	Group 3	Group 3	✓	✓		✓	✓	✓	MF974822	
F unknown	N.A.	N.A.	Unkn.								
F unknown	N.A.	N.A.	Unkn.								
F Step 1	Group 4	Group 4	Group 4	✓	✓		✓	✓	✓		MF974731
F unknown	N.A.	N.A.	Unkn.	✓			✓				
F Step 1	Group 4	Group 4	Group 4	✓	✓	✓	✓	✓	✓		MF974732

TABLE S1. Continued

Sample information					
Specimen ID	Cruise	Station	Latitude	Longitude	Collection date
Pacific Ocean					
D_PSE_COOK14MV_31_01	COOK14MV	31	21°36'S	173°36'W	2001-10-24
D_PSE_COOK14MV_34_01	COOK14MV	34	17°36'S	172°21'W	2001-10-25
D_PSE_COOK14MV_34_02	COOK14MV	34	17°36'S	172°21'W	2001-10-25
D_PSE_COOK14MV_35_01	COOK14MV	35	17°03'S	172°04'W	2001-10-25
D_PSE_COOK14MV_38_01	COOK14MV	38	15°15'S	172°08'W	2001-10-27
D_PSE_COOK14MV_38_02	COOK14MV	38	15°15'S	172°08'W	2001-10-27
D_PSE_COOK14MV_38_03	COOK14MV	38	15°15'S	172°08'W	2001-10-27
D_PSE_COOK14MV_40_01	COOK14MV	40	14°06'S	172°08'W	2001-10-27
D_PSE_COOK14MV_40_02	COOK14MV	40	14°06'S	172°08'W	2001-10-27
D_PSE_COOK14MV_40_03	COOK14MV	40	14°06'S	172°08'W	2001-10-27
D_PSE_COOK14MV_40_04	COOK14MV	40	14°06'S	172°08'W	2001-10-27
D_PSE_COOK14MV_40_05	COOK14MV	40	14°06'S	172°08'W	2001-10-27
D_PNE_S226_09_01	S226	9	13°52'N	159°07'W	2009-12-02
D_PNE_S226_09_02	S226	9	13°52'N	159°07'W	2009-12-02
D_PNE_S226_09_03	S226	9	13°52'N	159°07'W	2009-12-02
D_PNE_S226_23_01	S226	23	3°17'N	161°21'W	2009-12-10
D_PNE_S226_34_01	S226	34	0°21'N	157°54'W	2009-12-15
D_PNE_S226_34_02	S226	34	0°21'N	157°54'W	2009-12-15
D_PNE_S226_34_03	S226	34	0°21'N	157°54'W	2009-12-15
D_PNE_S226_45_01	S226	45	9°28'N	154°25'W	2009-12-24
D_PSE_SE1201_13_01	SE1201	13	XXX S	XXX W	2012-04-26
D_PNE_SE1201_21_01	SE1201	21	8°47'N	158°49'W	2012-05-15
D_PNE_JX183614	Ga32.16		13°01'N	105°01'W	2007-10/11
D_PNE_JX183615	Ga32.16		13°01'N	105°01'W	2007-10/11
D_PNE_JX183616	Ga32.16		13°01'N	105°01'W	2007-10/11
DANG_PSW_DANA_3613_01	DANA	3613 IV	22°43'S	166°06'E	1928-11-28
DANG_PSW_DANA_3613_02	DANA	3613 IV	22°43'S	166°06'E	1928-11-28
DANG_PNW_DANA_3723_01	DANA	3723 IV	25°31'N	125°08'E	1929-05-30
DANG_PNW_DANA_3723_02	DANA	3723 IV	25°31'N	125°08'E	1929-05-30
DANG_PNW_DANA_3723_03	DANA	3723 IV	25°31'N	125°08'E	1929-05-30
DANG_PNW_DANA_3723_04	DANA	3723 IV	25°31'N	125°08'E	1929-05-30
DANG_PNW_DANA_3723_05	DANA	3723 IV	25°31'N	125°08'E	1929-05-30
DANG_PNW_DANA_3723_06	DANA	3723 IV	25°31'N	125°08'E	1929-05-30
DANG_PNW_DANA_3723_07	DANA	3723 IV	25°31'N	125°08'E	1929-05-30
DANG_PNW_DANA_4761_01	DANA	4761	25°10'N	127°45'E	1932-04-19
DANG_PNW_DANA_4761_02	DANA	4761	25°10'N	127°45'E	1932-04-19
DANG_PNW_DANA_4761_03	DANA	4761	25°10'N	127°45'E	1932-04-19
DANG_PNW_DANA_4761_04	DANA	4761	25°10'N	127°45'E	1932-04-19
DANG_PNW_DANA_4761_05	DANA	4761	25°10'N	127°45'E	1932-04-19
DANG_PNW_DANA_4761_06	DANA	4761	25°10'N	127°45'E	1932-04-19
DANG_PNW_DANA_4761_07	DANA	4761	25°10'N	127°45'E	1932-04-19
DANG_PNW_DANA_4761_08	DANA	4761	25°10'N	127°45'E	1932-04-19
DANG_PNW_DANA_4761_09	DANA	4761	25°10'N	127°45'E	1932-04-19
DANG_PSW_SNEL_03_01	Snellius II	3 Tr.1	3°41'S	129°06'E	1984-08-01
DANG_PSW_SNEL_03_02	Snellius II	3 Tr.1	3°41'S	129°06'E	1984-08-01
DANG_PSW_SNEL_03_03	Snellius II	3 Tr.1	3°41'S	129°06'E	1984-08-01
DASP_PNW_DANA_3751_01	DANA	3751 IV	3°41'N	137°53'E	1929-07-12
DBAN_PSW_SNEL_09_01	Snellius II	9	4°36'S	130°22'E	1984-08-02
DBAN_PSW_SNEL_09_02	Snellius II	9	4°36'S	130°22'E	1984-08-02

Identification				Geometric morphometrics						Genetics	
Specimen type (F, Fresh; M, Museum)	Genetic clade / Species (Van der Spoel et al., 1993)	LDA group	Integrative group	Ventral photo	Ventral 23LMs	Ventral 38LMs	Lateral photo	Lateral 15LMs	Lateral 49LMs	COI	28S
F Step 1	Group 5	N.A.	Group 5	✓			✓	✓		MF974823	MF974733
F Step 1	Group 3	Group 3	Group 3	✓	✓	✓	✓	✓	✓	MF974824	MF974734
F Step 1	Group 3	Group 3	Group 3	✓			✓	✓	✓	MF974825	MF974735
F Step 1	Group 3	Group 3	Group 3	✓	✓	✓	✓	✓	✓	MF974826	MF974736
F Step 1	Group 3	Group 3	Group 3	✓	✓	✓	✓	✓	✓	MF974827	MF974737
F Step 1	Group 3	Group 3	Group 3	✓	✓		✓	✓		MF974828	MF974738
F Step 1	Group 3	Group 3	Group 3	✓			✓	✓	✓	MF974829	MF974739
F Step 1	Group 5	Group 5	Group 5	✓	✓	✓	✓	✓	✓	MF974830	MF974740
F Step 1	Group 5	Group 5	Group 5	✓	✓	✓	✓	✓		MF974831	MF974741
F Step 1	Group 5	Group 5	Group 5	✓	✓	✓	✓	✓	✓	MF974832	MF974742
F Step 1	Group 5	Group 5	Group 5	✓	✓	✓	✓	✓	✓	MF974833	MF974743
F Step 1	Group 5	Group 5	Group 5	✓	✓		✓	✓	✓	MF974834	MF974744
F Step 1	Group 6	Group 6	Group 6	✓	✓	✓	✓	✓		MF974835	MF974745
F Step 1	Group 3	Group 3	Group 3	✓			✓	✓	✓	MF974836	MF974746
F Step 1	Group 3	Group 3	Group 3	✓	✓		✓	✓	✓	MF974837	
F Step 1	Group 3	Group 3	Group 3	✓	✓		✓	✓	✓	MF974838	MF974747
F Step 1	Group 4	Group 4	Group 4	✓	✓		✓	✓	✓		MF974748
F Step 1	Group 4	Group 4	Group 4	✓			✓	✓	✓		MF974749
F unknown	N.A.	N.A.	Unkn.								
F Step 1	Group 3	Group 3	Group 3	✓	✓		✓	✓	✓	MF974839	MF974750
F Step 1	Group 4	Group 4	Group 4	✓	✓		✓	✓	✓		MF974751
F Step 1	Group 4	Group 4	Group 4	✓	✓		✓	✓	✓		MF974752
F Step 5	Group 12	N.A.	Group 12							JX183614	
F Step 5	Group 12	N.A.	Group 12							JX183615	
F Step 5	Group 12	N.A.	Group 12							JX183616	
M unknown	*D. angulata*	Amb.	Unkn.	✓	✓		✓	✓			
M Step 4	*D. angulata*	Group 4	Group 4	✓	✓	✓	✓	✓	✓		
M Step 4	*D. angulata*	Group 4	Group 4	✓	✓	✓	✓	✓	✓		
M Step 4	*D. angulata*	Group 4	Group 4	✓	✓		✓	✓	✓		
M Step 4	*D. angulata*	Group 4	Group 4	✓	✓		✓	✓	✓		
M Step 4	*D. angulata*	Group 4	Group 4	✓	✓		✓	✓	✓		
M Step 4	*D. angulata*	Group 4	Group 4	✓	✓		✓	✓	✓		
M Step 4	*D. angulata*	Group 4	Group 4	✓	✓		✓	✓	✓		
M Step 4	*D. angulata*	Group 4	Group 4	✓	✓		✓	✓	✓		
M Step 4	*D. angulata*	Group 4	Group 4	✓	✓	✓	✓	✓	✓		
M Step 4	*D. angulata*	Group 4	Group 4	✓	✓	✓	✓	✓	✓		
M Step 4	*D. angulata*	Group 4	Group 4	✓	✓		✓	✓	✓		
M Step 4	*D. angulata*	Group 4	Group 4	✓	✓	✓	✓	✓			
M Step 4	*D. angulata*	Group 4	Group 4	✓	✓	✓	✓	✓	✓		
M Step 4	*D. angulata*	Group 4	Group 4	✓	✓	✓	✓	✓	✓		
M Step 4	*D. angulata*	Group 4	Group 4	✓			✓	✓	✓		
M Step 4	*D. angulata*	Group 4	Group 4	✓	✓	✓	✓	✓			
M Step 4	*D. angulata*	Group 4	Group 4	✓	✓	✓	✓	✓	✓		
M Step 4	*D. angulata*	Group 5	Group 5	✓	✓		✓				
M unknown	*D. angulata*	N.A.	Unkn.	✓			✓	✓			
M unknown	*D. angulata*	N.A.	Unkn.	✓			✓				
M unknown	*D. aspina*	Amb.	Unkn.	✓	✓	✓					
M Step 2	*D. bandaensis*	Group 5	Group 5	✓	✓		✓	✓			
M unknown	*D. bandaensis*	N.A.	Unkn.	✓			✓				

TABLE S1. Continued

Sample information					
Specimen ID	Cruise	Station	Latitude	Longitude	Collection date
Pacific Ocean					
DBAN_PSW_SNEL_09_03	Snellius II	9	4°36'S	130°22'E	1984-08-02
DBAN_PSW_SNEL_09_04	Snellius II	9	4°36'S	130°22'E	1984-08-02
DBAN_PSW_SNEL_09_05	Snellius II	9	4°36'S	130°22'E	1984-08-02
DBAN_PSW_SNEL_09_06	Snellius II	9	4°36'S	130°22'E	1984-08-02
DBAN_PSW_SNEL_09_07	Snellius II	9	4°36'S	130°22'E	1984-08-02
DBAN_PSW_SNEL_09_08	Snellius II	9	4°36'S	130°22'E	1984-08-02
DBAN_PSW_SNEL_09_09	Snellius II	9	4°36'S	130°22'E	1984-08-02
DELE_PNW_DANA_3723_01	DANA	3723 IV	25°31'N	125°08'E	1929-05-30
DELE_PNW_DANA_3723_02	DANA	3723 IV	25°31'N	125°08'E	1929-05-30
DELE_PNW_DANA_3723_03	DANA	3723 IV	25°31'N	125°08'E	1929-05-30
DELE_PNW_DANA_3723_04	DANA	3723 IV	25°31'N	125°08'E	1929-05-30
DELE_PNW_DANA_3729_01	DANA	3729 V	20°03'N	120°50'E	1929-06-14
DELE_PNW_DANA_3729_02	DANA	3729 V	20°03'N	120°50'E	1929-06-14
DELE_PNW_DANA_3729_03	DANA	3729 V	20°03'N	120°50'E	1929-06-14
DELE_PNW_DANA_3729_04	DANA	3729 V	20°03'N	120°50'E	1929-06-14
DELE_PNW_DANA_3729_05	DANA	3729 V	20°03'N	120°50'E	1929-06-14
DELE_PNW_DANA_3729_06	DANA	3729 V	20°03'N	120°50'E	1929-06-14
DELE_PNW_DANA_3751_01	DANA	3751 IV	3°41'N	137°53'E	1929-07-12
DELE_PNW_DANA_3751_02	DANA	3751 IV	3°41'N	137°53'E	1929-07-12
DELE_PNW_DANA_3751_03	DANA	3751 IV	3°41'N	137°53'E	1929-07-12
DELE_PSW_SNEL_39_01	Snellius II	39 Tr.2	7°25'S	130°44'E	1984-08-08
DELE_PSW_SNEL_39_02	Snellius II	39 Tr.2	7°25'S	130°44'E	1984-08-08
DELE_PSW_SNEL_39_03	Snellius II	39 Tr.2	7°25'S	130°44'E	1984-08-08
DELE_PSW_SNEL_39_04	Snellius II	39 Tr.2	7°25'S	130°44'E	1984-08-08
DELE_PSW_SNEL_39_05	Snellius II	39 Tr.2	7°25'S	130°44'E	1984-08-08
DELE_PSW_SNEL_39_06	Snellius II	39 Tr.2	7°25'S	130°44'E	1984-08-08
DELE_PSW_SNEL_39_07	Snellius II	39 Tr.2	7°25'S	130°44'E	1984-08-08
DELE_PSW_SNEL_39_08	Snellius II	39 Tr.2	7°25'S	130°44'E	1984-08-08
DFLE_PSE_DANA_3585_01	DANA	3585 VI	7°40'S	167°10'W	1928-10-31
DFLE_PSE_DANA_3585_02	DANA	3585 VI	7°40'S	167°10'W	1928-10-31
DFLE_PSE_DANA_3585_03	DANA	3585 VI	7°40'S	167°10'W	1928-10-31
DFLE_PSE_DANA_3585_04	DANA	3585 VI	7°40'S	167°10'W	1928-10-31
DFLE_PSE_DANA_3585_05	DANA	3585 VI	7°40'S	167°10'W	1928-10-31
DFLE_PSE_DANA_3585_06	DANA	3585 VI	7°40'S	167°10'W	1928-10-31
DFLE_PSE_DANA_3585_07	DANA	3585 VI	7°40'S	167°10'W	1928-10-31
DFLE_PSE_DANA_3585_08	DANA	3585 VI	7°40'S	167°10'W	1928-10-31
DFLE_PSE_DANA_3585_09	DANA	3585 VI	7°40'S	167°10'W	1928-10-31
DFLE_PSE_DANA_3585_10	DANA	3585 VI	7°40'S	167°10'W	1928-10-31
DFLE_PSE_DANA_3585_11	DANA	3585 VI	7°40'S	167°10'W	1928-10-31
DFLE_PSE_DANA_3585_12	DANA	3585 VI	7°40'S	167°10'W	1928-10-31
DFLE_PSE_DANA_3585_13	DANA	3585 VI	7°40'S	167°10'W	1928-10-31
DFLE_PSE_DANA_3585_14	DANA	3585 VI	7°40'S	167°10'W	1928-10-31
DFLE_PSE_DANA_3585_15	DANA	3585 VI	7°40'S	167°10'W	1928-10-31
DGRA_PSW_DANA_3800_01	DANA	3800 IV	7°55'S	116°18'E	1929-08-28
DGRA_PSW_DANA_3800_02	DANA	3800 IV	7°55'S	116°18'E	1929-08-28
DGRA_PSW_DANA_3800_03	DANA	3800 IV	7°55'S	116°18'E	1929-08-28
DGRA_PSW_DANA_3800_04	DANA	3800 IV	7°55'S	116°18'E	1929-08-28
DGRA_PSW_DANA_3800_05	DANA	3800 IV	7°55'S	116°18'E	1929-08-28
DGRA_PSW_DANA_3800_06	DANA	3800 IV	7°55'S	116°18'E	1929-08-28

Identification				Geometric morphometrics						Genetics	
Specimen type (F, Fresh; M, Museum)	Genetic clade / Species (Van der Spoel et al., 1993)	LDA group	Integrative group	Ventral photo	Ventral 23LMs	Ventral 38LMs	Lateral photo	Lateral 15LMs	Lateral 49LMs	COI	28S
M Step 2	*D. bandaensis*	Group 5	Group 5	✓	✓		✓	✓			
M unknown	*D. bandaensis*	N.A.	Unkn.	✓			✓	✓			
M unknown	*D. bandaensis*	N.A.	Unkn.	✓			✓	✓			
M Step 2	*D. bandaensis*	Group 5	Group 5	✓	✓		✓	✓			
M Step 2	*D. bandaensis*	Group 5	Group 5	✓	✓		✓	✓	✓		
M Step 2	*D. bandaensis*	Group 5	Group 5	✓	✓	✓	✓	✓			
M Step 2	*D. bandaensis*	Group 5	Group 5	✓	✓		✓	✓	✓		
M Step 4	*D. elegans*	Group 5	Group 5	✓	✓	✓	✓	✓			
M unknown	*D. elegans*	N.A.	Unkn.	✓			✓				
M unknown	*D. elegans*	Amb.	Unkn.	✓	✓	✓	✓				
M unknown	*D. elegans*	N.A.	Unkn.	✓			✓	✓			
M unknown	*D. elegans*	N.A.	Unkn.	✓			✓	✓			
M unknown	*D. elegans*	N.A.	Unkn.	✓			✓	✓			
M unknown	*D. elegans*	N.A.	Unkn.	✓			✓				
M unknown	*D. elegans*	N.A.	Unkn.	✓			✓	✓			
M unknown	*D. elegans*	N.A.	Unkn.	✓			✓	✓			
M unknown	*D. elegans*	N.A.	Unkn.	✓			✓	✓			
M unknown	*D. elegans*	N.A.	Unkn.	✓			✓				
M Step 2	*D. elegans*	Group 3	Group 3	✓			✓	✓	✓		
M unknown	*D. elegans*	N.A.	Unkn.	✓			✓				
M Step 4	*D. elegans*	Group 11	Group 11	✓	✓	✓	✓	✓			
M unknown	*D. elegans*	N.A.	Unkn.	✓			✓	✓			
M unknown	*D. elegans*	N.A.	Unkn.	✓			✓				
M Step 4	*D. elegans*	Group 5	Group 5	✓	✓	✓	✓				
M unknown	*D. elegans*	N.A.	Unkn.	✓			✓				
M unknown	*D. elegans*	N.A.	Unkn.	✓			✓				
M Step 4	*D. elegans*	Group 5	Group 5	✓	✓	✓	✓				
M Step 4	*D. elegans*	Group 5	Group 5	✓	✓		✓	✓	✓		
M Step 4	*D. flexipes*	Group 3	Group 3	✓	✓		✓	✓	✓		
M Step 4	*D. flexipes*	Group 3	Group 3	✓	✓		✓	✓	✓		
M Step 4	*D. flexipes*	Group 3	Group 3	✓	✓		✓	✓	✓		
M Step 4	*D. flexipes*	Group 3	Group 3	✓	✓		✓	✓	✓		
M Step 4	*D. flexipes*	Group 3	Group 3	✓	✓		✓	✓			
M Step 4	*D. flexipes*	Group 3	Group 3	✓	✓		✓	✓	✓		
M Step 4	*D. flexipes*	Group 3	Group 3	✓	✓		✓	✓			
M Step 4	*D. flexipes*	Group 3	Group 3	✓	✓		✓	✓	✓		
M Step 4	*D. flexipes*	Group 3	Group 3	✓	✓		✓	✓	✓		
M unknown	*D. flexipes*	N.A.	Unkn.	✓			✓	✓			
M Step 4	*D. flexipes*	Group 3	Group 3	✓	✓	✓	✓	✓	✓		
M Step 4	*D. flexipes*	Group 3	Group 3	✓	✓		✓				
M Step 4	*D. flexipes*	Group 3	Group 3	✓	✓		✓	✓			
M Step 4	*D. flexipes*	Group 3	Group 3	✓	✓		✓	✓	✓		
M unknown	*D. flexipes*	N.A.	Unkn.	✓			✓	✓			
M unknown	*D. grayi*	Amb.	Unkn.	✓	✓		✓				
M unknown	*D. grayi*	Amb.	Unkn.	✓	✓		✓				
M Step 4	*D. grayi*	Group 5	Group 5	✓	✓		✓	✓	✓		
M unknown	*D. grayi*	Amb.	Unkn.	✓	✓		✓	✓			
M Step 4	*D. grayi*	Group 5	Group 5	✓	✓		✓	✓	✓		
M unknown	*D. grayi*	N.A.	Unkn.	✓			✓				

TABLE S1. Continued

Sample information					
Specimen ID	Cruise	Station	Latitude	Longitude	Collection date
Pacific Ocean					
DGRA_PSW_DANA_3800_07	DANA	3800 IV	7°55'S	116°18'E	1929-08-28
DGRA_PSW_DANA_3800_08	DANA	3800 IV	7°55'S	116°18'E	1929-08-28
DGRA_PSW_SNEL_27_01	Snellius II	27 Tr.1	4°48'S	131°21'E	1984-08-05
DGRA_PSW_SNEL_27_02	Snellius II	27 Tr.1	4°48'S	131°21'E	1984-08-05
DGRA_PSW_SNEL_27_03	Snellius II	27 Tr.1	4°48'S	131°21'E	1984-08-05
DGRA_PSW_SNEL_27_04	Snellius II	27 Tr.1	4°48'S	131°21'E	1984-08-05
DGRA_PSW_SNEL_27_05	Snellius II	27 Tr.1	4°48'S	131°21'E	1984-08-05
DGRA_PSW_SNEL_27_06	Snellius II	27 Tr.1	4°48'S	131°21'E	1984-08-05
DGRA_PSW_SNEL_27_07	Snellius II	27 Tr.1	4°48'S	131°21'E	1984-08-05
DGRA_PSW_SNEL_27_08	Snellius II	27 Tr.1	4°48'S	131°21'E	1984-08-05
DGRA_PSW_SNEL_27_09	Snellius II	27 Tr.1	4°48'S	131°21'E	1984-08-05
DGRA_PSW_SNEL_27_10	Snellius II	27 Tr.1	4°48'S	131°21'E	1984-08-05
DGRA_PSW_SNEL_45_01	Snellius II	45 Tr.1	6°33'S	132°06'E	1984-08-08
DGRA_PSW_SNEL_45_02	Snellius II	45 Tr.1	6°33'S	132°06'E	1984-08-08
DGRA_PSW_SNEL_45_03	Snellius II	45 Tr.1	6°33'S	132°06'E	1984-08-08
DGRA_PSW_SNEL_45_04	Snellius II	45 Tr.1	6°33'S	132°06'E	1984-08-08
DGRA_PSW_SNEL_45_05	Snellius II	45 Tr.1	6°33'S	132°06'E	1984-08-08
DGRA_PSW_SNEL_45_06	Snellius II	45 Tr.1	6°33'S	132°06'E	1984-08-08
DGRA_PSW_SNEL_45_07	Snellius II	45 Tr.1	6°33'S	132°06'E	1984-08-08
DGRA_PSW_SNEL_45_08	Snellius II	45 Tr.1	6°33'S	132°06'E	1984-08-08
DGRA_PSW_SNEL_45_09	Snellius II	45 Tr.1	6°33'S	132°06'E	1984-08-08
DGRA_PSW_SNEL_45_10	Snellius II	45 Tr.1	6°33'S	132°06'E	1984-08-08
DGRA_PSW_SNEL_C2_01	Snellius II	C Tr.2	5°23'S	130°05'E	1984-08-28
DGRA_PSW_SNEL_C2_02	Snellius II	C Tr.2	5°23'S	130°05'E	1984-08-28
DGRA_PSW_SNEL_C2_03	Snellius II	C Tr.2	5°23'S	130°05'E	1984-08-28
DGRA_PSW_SNEL_C2_04	Snellius II	C Tr.2	5°23'S	130°05'E	1984-08-28
DGRA_PSW_SNEL_C2_05	Snellius II	C Tr.2	5°23'S	130°05'E	1984-08-28
DGRA_PSW_SNEL_C2_06	Snellius II	C Tr.2	5°23'S	130°05'E	1984-08-28
DGRA_PSW_SNEL_C2_07	Snellius II	C Tr.2	5°23'S	130°05'E	1984-08-28
DGRA_PSW_SNEL_C2_08	Snellius II	C Tr.2	5°23'S	130°05'E	1984-08-28
DGRA_PSW_SNEL_C2_09	Snellius II	C Tr.2	5°23'S	130°05'E	1984-08-28
DGRA_PSW_SNEL_C2_10	Snellius II	C Tr.2	5°23'S	130°05'E	1984-08-28
DGRA_PSW_SNEL_C2_11	Snellius II	C Tr.2	5°23'S	130°05'E	1984-08-28
DGRA_PSW_SNEL_C2_12	Snellius II	C Tr.2	5°23'S	130°05'E	1984-08-28
DGRA_PSW_SNEL_C2_13	Snellius II	C Tr.2	5°23'S	130°05'E	1984-08-28
DLON_PNE_DANA_3553_01	DANA	3553 I	7°55'N	79°02'W	1928-09-05
DLON_PNE_DANA_3553_02	DANA	3553 I	7°55'N	79°02'W	1928-09-05
DLON_PNE_DANA_3553_03	DANA	3553 I	7°55'N	79°02'W	1928-09-05
DLON_PNE_DANA_3553_04	DANA	3553 I	7°55'N	79°02'W	1928-09-05
DLON_PNE_DANA_3553_05	DANA	3553 I	7°55'N	79°02'W	1928-09-05
DLON_PNE_DANA_3553_06	DANA	3553 I	7°55'N	79°02'W	1928-09-05
DLON_PSW_SNEL_45_01	Snellius II	45 Tr.1	6°33'S	132°06'E	1984-08-08
DLON_PSW_SNEL_45_02	Snellius II	45 Tr.1	6°33'S	132°06'E	1984-08-08
DLON_PSW_SNEL_45_03	Snellius II	45 Tr.1	6°33'S	132°06'E	1984-08-08
DLON_PSW_SNEL_45_04	Snellius II	45 Tr.1	6°33'S	132°06'E	1984-08-08
DLON_PSW_SNEL_45_05	Snellius II	45 Tr.1	6°33'S	132°06'E	1984-08-08
DLON_PSW_SNEL_45_06	Snellius II	45 Tr.1	6°33'S	132°06'E	1984-08-08
DLON_PSW_SNEL_45_07	Snellius II	45 Tr.1	6°33'S	132°06'E	1984-08-08
DLON_PSW_SNEL_45_08	Snellius II	45 Tr.1	6°33'S	132°06'E	1984-08-08

Identification				Geometric morphometrics						Genetics	
Specimen type (F, Fresh; M, Museum)	Genetic clade / Species (Van der Spoel et al., 1993)	LDA group	Integrative group	Ventral photo	Ventral 23LMs	Ventral 38LMs	Lateral photo	Lateral 15LMs	Lateral 49LMs	COI	28S
M Step 4	*D. grayi*	Group 5	Group 5	✓			✓	✓	✓		
M unknown	*D. grayi*	Amb.	Unkn.	✓	✓		✓	✓			
M unknown	*D. grayi*	N.A.	Unkn.	✓			✓	✓			
M unknown	*D. grayi*	N.A.	Unkn.	✓			✓	✓			
M Step 4	*D. grayi*	Group 4	Group 4	✓	✓		✓	✓	✓		
M Step 4	*D. grayi*	Group 4	Group 4	✓	✓		✓	✓	✓		
M unknown	*D. grayi*	N.A.	Unkn.	✓			✓				
M Step 4	*D. grayi*	Group 4	Group 4	✓	✓		✓	✓	✓		
M Step 4	*D. grayi*	Group 4	Group 4	✓	✓		✓	✓			
M unknown	*D. grayi*	N.A.	Unkn.	✓			✓				
M unknown	*D. grayi*	Amb.	Unkn.	✓	✓		✓				
M Step 4	*D. grayi*	Group 4	Group 4	✓	✓		✓				
M unknown	*D. grayi*	N.A.	Unkn.	✓			✓	✓			
M unknown	*D. grayi*	N.A.	Unkn.	✓			✓	✓			
M unknown	*D. grayi*	N.A.	Unkn.	✓			✓				
M unknown	*D. grayi*	N.A.	Unkn.	✓			✓				
M unknown	*D. grayi*	N.A.	Unkn.	✓			✓	✓			
M unknown	*D. grayi*	Amb.	Unkn.	✓	✓		✓				
M unknown	*D. grayi*	N.A.	Unkn.	✓			✓				
M unknown	*D. grayi*	N.A.	Unkn.	✓			✓				
M unknown	*D. grayi*	N.A.	Unkn.	✓			✓	✓			
M unknown	*D. grayi*	N.A.	Unkn.	✓			✓	✓			
M Step 2	*D. grayi*	Group 5	Group 5	✓	✓	✓	✓				
M Step 2	*D. grayi*	Group 5	Group 5	✓			✓	✓	✓		
M Step 2	*D. grayi*	Group 5	Group 5	✓			✓	✓	✓		
M Step 2	*D. grayi*	Group 5	Group 5	✓	✓	✓	✓	✓			
M Step 2	*D. grayi*	Group 5	Group 5	✓	✓		✓				
M unknown	*D. grayi*	N.A.	Unkn.	✓			✓				
M unknown	*D. grayi*	N.A.	Unkn.	✓			✓				
M Step 2	*D. grayi*	Group 5	Group 5	✓			✓	✓	✓		
M unknown	*D. grayi*	N.A.	Unkn.	✓			✓	✓			
M Step 2	*D. grayi*	Group 5	Group 5	✓	✓		✓				
M Step 2	*D. grayi*	Group 5	Group 5	✓	✓		✓				
M unknown	*D. grayi*	N.A.	Unkn.	✓			✓				
M unknown	*D. grayi*	N.A.	Unkn.	✓							
M Step 3	*D. longirostris*	Group 10	Group 10	✓	✓		✓				
M Step 3	*D. longirostris*	Group 10	Group 10	✓	✓	✓	✓	✓	✓		
M Step 3	*D. longirostris*	Group 10	Group 10	✓	✓		✓	✓	✓		
M Step 3	*D. longirostris*	Group 10	Group 10	✓	✓		✓	✓	✓		
M Step 3	*D. longirostris*	Group 10	Group 10	✓			✓	✓	✓		
M unknown	*D. longirostris*	N.A.	Unkn.	✓			✓	✓			
M Step 4	*D. longirostris*	Group 8	Group 8	✓	✓	✓	✓	✓			
M Step 4	*D. longirostris*	Group 8	Group 8	✓	✓	✓	✓	✓	✓		
M Step 4	*D. longirostris*	Group 8	Group 8	✓	✓	✓	✓	✓			
M Step 4	*D. longirostris*	Group 8	Group 8	✓	✓	✓	✓	✓	✓		
M Step 4	*D. longirostris*	Group 8	Group 8	✓	✓	✓	✓				
M Step 4	*D. longirostris*	Group 8	Group 8	✓	✓		✓	✓	✓		
M Step 4	*D. longirostris*	Group 8	Group 8	✓	✓	✓	✓	✓	✓		
M Step 4	*D. longirostris*	Group 8	Group 8	✓	✓	✓	✓	✓	✓		

TABLE S1. Continued

Sample information					
Specimen ID	Cruise	Station	Latitude	Longitude	Collection date
Pacific Ocean					
DLON_PSW_SNEL_45_09	Snellius II	45 Tr.1	6°33'S	132°06'E	1984-08-08
DLON_PSW_SNEL_45_10	Snellius II	45 Tr.1	6°33'S	132°06'E	1984-08-08
DLON_PSW_SNEL_45_11	Snellius II	45 Tr.1	6°33'S	132°06'E	1984-08-08
DLON_PSW_SNEL_45_12	Snellius II	45 Tr.1	6°33'S	132°06'E	1984-08-08
DLON_PSW_SNEL_45_13	Snellius II	45 Tr.1	6°33'S	132°06'E	1984-08-08
DLON_PSW_SNEL_45_14	Snellius II	45 Tr.1	6°33'S	132°06'E	1984-08-08
DLON_PSW_SNEL_45_15	Snellius II	45 Tr.1	6°33'S	132°06'E	1984-08-08
DLON_PSW_SNEL_45_16	Snellius II	45 Tr.1	6°33'S	132°06'E	1984-08-08
DLON_PSW_SNEL_45_17	Snellius II	45 Tr.1	6°33'S	132°06'E	1984-08-08
DLON_PSW_SNEL_45_18	Snellius II	45 Tr.1	6°33'S	132°06'E	1984-08-08
DLON_PSW_SNEL_45_19	Snellius II	45 Tr.1	6°33'S	132°06'E	1984-08-08
DLON_PSW_SNEL_45_20	Snellius II	45 Tr.1	6°33'S	132°06'E	1984-08-08
DMCG_PNE_DANA_1203_01	DANA	1203 V	7°30'N	79°19'W	1922-01-11
DMCG_PNE_DANA_1203_02	DANA	1203 V	7°30'N	79°19'W	1922-01-11
DMCG_PNE_DANA_1203_03	DANA	1203 V	7°30'N	79°19'W	1922-01-11
DMCG_PNE_DANA_1203_04	DANA	1203 V	7°30'N	79°19'W	1922-01-11
DMCG_PNE_DANA_1203_05	DANA	1203 V	7°30'N	79°19'W	1922-01-11
DMCG_PNE_DANA_1203_06	DANA	1203 V	7°30'N	79°19'W	1922-01-11
DMCG_PNE_DANA_1203_07	DANA	1203 V	7°30'N	79°19'W	1922-01-11
DMCG_PNW_DANA_3736_01	DANA	3736 IV	9°17'N	123°58'E	1929-06-28
DMCG_PSW_DANA_3601_01	DANA	3601 IV	18°21'S	178°21'E	1928-11-20
DMCG_PSW_DANA_3601_02	DANA	3601 IV	18°21'S	178°21'E	1928-11-20
DMCG_PSW_DANA_3601_03	DANA	3601 IV	18°21'S	178°21'E	1928-11-20
DMCG_PSW_DANA_3601_04	DANA	3601 IV	18°21'S	178°21'E	1928-11-20
DMCG_PSW_DANA_3601_05	DANA	3601 IV	18°21'S	178°21'E	1928-11-20
DMCG_PSW_DANA_3601_06	DANA	3601 IV	18°21'S	178°21'E	1928-11-20
DMCG_PSW_DANA_3601_07	DANA	3601 IV	18°21'S	178°21'E	1928-11-20
DMCG_PSW_DANA_3601_08	DANA	3601 IV	18°21'S	178°21'E	1928-11-20
DMCG_PSW_DANA_3601_09	DANA	3601 IV	18°21'S	178°21'E	1928-11-20
DMCG_PSW_DANA_3601_10	DANA	3601 IV	18°21'S	178°21'E	1928-11-20
DMCG_PSW_DANA_3601_11	DANA	3601 IV	18°21'S	178°21'E	1928-11-20
DMCG_PSW_DANA_3601_12	DANA	3601 IV	18°21'S	178°21'E	1928-11-20
DPAC_PSW_DANA_3611_01	DANA	3611 V	20°53'S	164°30'E	1928-11-26
DPAC_PSW_DANA_3611_02	DANA	3611 V	20°53'S	164°30'E	1928-11-26
DPAC_PSW_DANA_3611_03	DANA	3611 V	20°53'S	164°30'E	1928-11-26
DPAC_PSW_DANA_3611_04	DANA	3611 V	20°53'S	164°30'E	1928-11-26
DPAC_PSW_DANA_3611_05	DANA	3611 V	20°53'S	164°30'E	1928-11-26
DPAC_PSW_DANA_3611_06	DANA	3611 V	20°53'S	164°30'E	1928-11-26
DPAC_PSW_DANA_3611_07	DANA	3611 V	20°53'S	164°30'E	1928-11-26
DPAC_PSW_DANA_3611_08	DANA	3611 V	20°53'S	164°30'E	1928-11-26
DPAC_PSW_DANA_3611_09	DANA	3611 V	20°53'S	164°30'E	1928-11-26
DPAC_PSW_DANA_3611_10	DANA	3611 V	20°53'S	164°30'E	1928-11-26
DPAC_PSW_DANA_3611_11	DANA	3611 V	20°53'S	164°30'E	1928-11-26
DPAC_PSW_DANA_3611_12	DANA	3611 V	20°53'S	164°30'E	1928-11-26
DPAC_PSW_DANA_3611_13	DANA	3611 V	20°53'S	164°30'E	1928-11-26
DPAC_PSW_DANA_3611_14	DANA	3611 V	20°53'S	164°30'E	1928-11-26
DPAC_PNW_DANA_3731_01	DANA	3731 IV	14°37'N	119°52'E	1929-06-16
DPAC_PNW_DANA_3731_02	DANA	3731 IV	14°37'N	119°52'E	1929-06-16
DPAC_PNW_DANA_3731_03	DANA	3731 IV	14°37'N	119°52'E	1929-06-16

Identification				Geometric morphometrics						Genetics	
Specimen type (F, Fresh; M, Museum)	Genetic clade / Species (Van der Spoel et al., 1993)	LDA group	Integrative group	Ventral photo	Ventral 23LMs	Ventral 38LMs	Lateral photo	Lateral 15LMs	Lateral 49LMs	COI	28S
M Step 4	*D. longirostris*	Group 8	Group 8	✓	✓	✓	✓	✓	✓		
M Step 4	*D. longirostris*	Group 8	Group 8	✓	✓	✓	✓	✓	✓		
M Step 4	*D. longirostris*	Group 8	Group 8	✓	✓	✓	✓	✓	✓		
M Step 4	*D. longirostris*	Group 8	Group 8	✓	✓	✓	✓				
M Step 4	*D. longirostris*	Group 8	Group 8	✓	✓	✓	✓	✓	✓		
M Step 4	*D. longirostris*	Group 8	Group 8	✓	✓		✓				
M Step 4	*D. longirostris*	Group 8	Group 8	✓	✓	✓	✓	✓			
M Step 4	*D. longirostris*	Group 8	Group 8	✓	✓	✓	✓				
M Step 4	*D. longirostris*	Group 8	Group 8	✓	✓	✓	✓	✓			
M Step 4	*D. longirostris*	Group 8	Group 8	✓	✓	✓	✓	✓	✓		
M Step 4	*D. longirostris*	Group 8	Group 8	✓	✓	✓	✓				
M Step 4	*D. longirostris*	Group 8	Group 8	✓	✓	✓	✓	✓	✓		
M Step 3	*D. mcgowani*	Group 10	Group 10	✓	✓		✓	✓	✓		
M Step 3	*D. mcgowani*	Group 10	Group 10	✓	✓		✓	✓	✓		
M Step 3	*D. mcgowani*	Group 10	Group 10	✓			✓	✓	✓		
M Step 3	*D. mcgowani*	Group 10	Group 10	✓	✓		✓	✓	✓		
M Step 3	*D. mcgowani*	Group 10	Group 10	✓	✓		✓	✓	✓		
M Step 3	*D. mcgowani*	Group 10	Group 10	✓	✓		✓	✓	✓		
M Step 3	*D. mcgowani*	Group 10	Group 10	✓	✓		✓	✓	✓		
M unknown	*D. mcgowani*	Amb.	Unkn.	✓	✓	✓	✓	✓			
M Step 4	*D. mcgowani*	Group 5	Group 5	✓	✓	✓	✓	✓			
M Step 4	*D. mcgowani*	Group 5	Group 5	✓	✓		✓				
M Step 4	*D. mcgowani*	Group 5	Group 5	✓			✓	✓	✓		
M Step 4	*D. mcgowani*	Group 5	Group 5	✓	✓	✓	✓				
M unknown	*D. mcgowani*	N.A.	Unkn.	✓			✓				
M Step 4	*D. mcgowani*	Group 5	Group 5	✓	✓	✓	✓	✓			
M unknown	*D. mcgowani*	N.A.	Unkn.	✓			✓				
M Step 4	*D. mcgowani*	Group 5	Group 5	✓	✓	✓	✓				
M unknown	*D. mcgowani*	N.A.	Unkn.	✓			✓	✓			
M Step 4	*D. mcgowani*	Group 5	Group 5	✓	✓		✓	✓	✓		
M Step 4	*D. mcgowani*	Group 5	Group 5	✓	✓		✓				
M unknown	*D. mcgowani*	N.A.	Unkn.	✓			✓				
M Step 4	*D. pacifica*	Group 4	Group 4	✓			✓	✓	✓		
M Step 4	*D. pacifica*	Group 4	Group 4	✓	✓		✓				
M unknown	*D. pacifica*	Amb.	Unkn.	✓	✓		✓				
M Step 4	*D. pacifica*	Group 4	Group 4	✓	✓		✓				
M unknown	*D. pacifica*	N.A.	Unkn.	✓			✓	✓			
M Step 4	*D. pacifica*	Group 4	Group 4	✓	✓		✓	✓	✓		
M Step 4	*D. pacifica*	Group 4	Group 4	✓	✓		✓	✓			
M Step 4	*D. pacifica*	Group 4	Group 4	✓	✓		✓	✓			
M Step 4	*D. pacifica*	Group 4	Group 4	✓			✓	✓	✓		
M unknown	*D. pacifica*	N.A.	Unkn.	✓			✓				
M Step 4	*D. pacifica*	Group 4	Group 4	✓	✓		✓	✓	✓		
M Step 4	*D. pacifica*	Group 4	Group 4	✓	✓		✓	✓	✓		
M Step 4	*D. pacifica*	Group 4	Group 4	✓	✓		✓				
M Step 4	*D. pacifica*	Group 4	Group 4	✓	✓		✓	✓	✓		
M unknown	*D. pacifica*	N.A.	Unkn.	✓			✓				
M unknown	*D. pacifica*	N.A.	Unkn.	✓			✓	✓			
M unknown	*D. pacifica*	Amb.	Unkn.	✓	✓	✓	✓	✓			

TABLE S1. Continued

Sample information					
Specimen ID	Cruise	Station	Latitude	Longitude	Collection date
Pacific Ocean					
DPAC_PNW_DANA_3731_04	DANA	3731 IV	14°37'N	119°52'E	1929-06-16
DPAC_PNW_DANA_3731_05	DANA	3731 IV	14°37'N	119°52'E	1929-06-16
DPAC_PNW_DANA_3731_06	DANA	3731 IV	14°37'N	119°52'E	1929-06-16
DPAC_PNW_DANA_3731_07	DANA	3731 IV	14°37'N	119°52'E	1929-06-16
DPAC_PNW_DANA_3731_08	DANA	3731 IV	14°37'N	119°52'E	1929-06-16
DPAC_PNW_DANA_3739_01	DANA	3739 IV	3°20'N	123°50'E	1929-07-02
DPAC_PNW_SNEL_05_01	Snellius II	C Tr.5	5°22'N	129°56'E	1984-08-26
DPAC_PNW_SNEL_05_02	Snellius II	C Tr.5	5°22'N	129°56'E	1984-08-26
DPAC_PNW_SNEL_05_03	Snellius II	C Tr.5	5°22'N	129°56'E	1984-08-26
DPAC_PNW_SNEL_05_04	Snellius II	C Tr.5	5°22'N	129°56'E	1984-08-26
DPAC_PNW_SNEL_05_05	Snellius II	C Tr.5	5°22'N	129°56'E	1984-08-26
DPAC_PNW_SNEL_05_06	Snellius II	C Tr.5	5°22'N	129°56'E	1984-08-26
DPAC_PNW_SNEL_05_07	Snellius II	C Tr.5	5°22'N	129°56'E	1984-08-26
DPAC_PNW_SNEL_05_08	Snellius II	C Tr.5	5°22'N	129°56'E	1984-08-26
DPAC_PNW_SNEL_05_09	Snellius II	C Tr.5	5°22'N	129°56'E	1984-08-26
DPAC_PNW_SNEL_05_10	Snellius II	C Tr.5	5°22'N	129°56'E	1984-08-26
DPAC_PNW_SNEL_05_11	Snellius II	C Tr.5	5°22'N	129°56'E	1984-08-26
DPAC_PNW_SNEL_05_12	Snellius II	C Tr.5	5°22'N	129°56'E	1984-08-26
DPAC_PNW_SNEL_05_13	Snellius II	C Tr.5	5°22'N	129°56'E	1984-08-26
DPAC_PNW_SNEL_05_14	Snellius II	C Tr.5	5°22'N	129°56'E	1984-08-26
DPAC_PNW_SNEL_05_15	Snellius II	C Tr.5	5°22'N	129°56'E	1984-08-26
DPAC_PNW_SNEL_05_16	Snellius II	C Tr.5	5°22'N	129°56'E	1984-08-26
DPAC_PSW_SNEL_33_01	Snellius II	33	6°30'S	131°09'E	1984-08-06
DPAC_PSW_SNEL_33_02	Snellius II	33	6°30'S	131°09'E	1984-08-06
DPAC_PSW_SNEL_33_03	Snellius II	33	6°30'S	131°09'E	1984-08-06
DSTA_PSE_DANA_3561_01	DANA	3561 IX	4°20'S	116°46'W	1928-09-24
DSTA_PSE_DANA_3561_02	DANA	3561 IX	4°20'S	116°46'W	1928-09-24
DSTA_PSE_DANA_3561_03	DANA	3561 IX	4°20'S	116°46'W	1928-09-24
DTRI_PNW_APE_01_01	Albatr.Phil.Exp.		Philippine Sea		1909-09-18
DTRI_PNW_APE_01_02	Albatr.Phil.Exp.		Philippine Sea		1909-09-18
DTRI_PNW_APE_01_03	Albatr.Phil.Exp.		Philippine Sea		1909-09-18
DTRI_PNW_APE_01_04	Albatr.Phil.Exp.		Philippine Sea		1909-09-18
DTRI_PNW_APE_01_05	Albatr.Phil.Exp.		Philippine Sea		1909-09-18
DTRI_PNW_APE_01_06	Albatr.Phil.Exp.		Philippine Sea		1909-09-18
DTRI_PNW_APE_01_07	Albatr.Phil.Exp.		Philippine Sea		1909-09-18
DTRI_PNW_APE_01_08	Albatr.Phil.Exp.		Philippine Sea		1909-09-18
DTRI_PNW_APE_01_09	Albatr.Phil.Exp.		Philippine Sea		1909-09-18
DTRI_PNW_APE_01_10	Albatr.Phil.Exp.		Philippine Sea		1909-09-18
DTRI_PNW_APE_01_11	Albatr.Phil.Exp.		Philippine Sea		1909-09-18
DTRI_PNW_APE_01_12	Albatr.Phil.Exp.		Philippine Sea		1909-09-18
DTRI_PNW_APE_01_13	Albatr.Phil.Exp.		Philippine Sea		1909-09-18
DTRI_PNW_APE_01_14	Albatr.Phil.Exp.		Philippine Sea		1909-09-18
DTRI_PNW_APE_01_15	Albatr.Phil.Exp.		Philippine Sea		1909-09-18
DTRI_PNW_APE_01_16	Albatr.Phil.Exp.		Philippine Sea		1909-09-18
DTRI_PNW_APE_01_17	Albatr.Phil.Exp.		Philippine Sea		1909-09-18
DTRI_PSW_SNEL_21_01	Snellius II	21 Tr.1	6°24'S	130°20'E	1984-08-04
DTRI_PSW_SNEL_21_02	Snellius II	21 Tr.1	6°24'S	130°20'E	1984-08-04
DTRI_PSW_SNEL_21_03	Snellius II	21 Tr.1	6°24'S	130°20'E	1984-08-04
DTRI_PSW_SNEL_21_04	Snellius II	21 Tr.1	6°24'S	130°20'E	1984-08-04

Identification				Geometric morphometrics						Genetics	
Specimen type (F, Fresh; M, Museum)	Genetic clade / Species (Van der Spoel et al., 1993)	LDA group	Integrative group	Ventral photo	Ventral 23LMs	Ventral 38LMs	Lateral photo	Lateral 15LMs	Lateral 49LMs	COI	28S
M unknown	*D. pacifica*	N.A.	Unkn.	✓			✓	✓			
M Step 4	*D. pacifica*	Group 5	Group 5	✓	✓	✓	✓	✓			
M unknown	*D. pacifica*	N.A.	Unkn.	✓			✓	✓			
M unknown	*D. pacifica*	N.A.	Unkn.	✓			✓				
M unknown	*D. pacifica*	N.A.	Unkn.	✓			✓				
M unknown	*D. pacifica*	N.A.	Unkn.	✓			✓	✓			
M unknown	*D. pacifica*	Amb.	Unkn.	✓	✓		✓	✓	✓		
M Step 4	*D. pacifica*	Group 8	Group 8	✓	✓		✓	✓	✓		
M Step 4	*D. pacifica*	Group 8	Group 8	✓	✓		✓	✓			
M Step 4	*D. pacifica*	Group 8	Group 8	✓			✓	✓	✓		
M Step 4	*D. pacifica*	Group 5	Group 5	✓			✓	✓	✓		
M Step 4	*D. pacifica*	Group 5	Group 5	✓	✓	✓	✓	✓	✓		
M unknown	*D. pacifica*	Amb.	Unkn.	✓	✓		✓	✓			
M Step 4	*D. pacifica*	Group 5	Group 5	✓	✓		✓	✓	✓		
M Step 4	*D. pacifica*	Group 5	Group 5	✓			✓	✓	✓		
M Step 4	*D. pacifica*	Group 5	Group 5	✓	✓		✓	✓	✓		
M unknown	*D. pacifica*	Amb.	Unkn.	✓	✓		✓	✓			
M Step 4	*D. pacifica*	Group 5	Group 5	✓	✓	✓	✓				
M Step 4	*D. pacifica*	Group 5	Group 5	✓			✓	✓	✓		
M unknown	*D. pacifica*	N.A.	Unkn.	✓			✓				
M unknown	*D. pacifica*	N.A.	Unkn.	✓			✓	✓			
M Step 4	*D. pacifica*	Group 5	Group 5	✓	✓		✓	✓	✓		
M Step 2	*D. pacifica*	Group 5	Group 5	✓	✓	✓	✓	✓	✓		
M unknown	*D. pacifica*	N.A.	Unkn.	✓			✓				
M Step 2	*D. pacifica*	Group 5	Group 5	✓	✓		✓	✓			
M Step 3	*D. strangulata*	Group 9	Group 9	✓	✓		✓	✓	✓		
M Step 3	*D. strangulata*	Group 9	Group 9	✓	✓	✓	✓	✓	✓		
M Step 3	*D. strangulata*	Group 9	Group 9	✓	✓		✓	✓	✓		
M Step 2	*D. triangulata*	Group 8	Group 8	✓	✓	✓					
M unknown	*D. triangulata*	N.A.	Unkn.	✓			✓	✓			
M Step 2	*D. triangulata*	Group 8	Group 8	✓	✓	✓	✓	✓	✓		
M Step 2	*D. triangulata*	Group 8	Group 8	✓	✓		✓	✓			
M Step 2	*D. triangulata*	Group 8	Group 8	✓	✓	✓	✓	✓	✓		
M Step 2	*D. triangulata*	Group 8	Group 8	✓			✓	✓	✓		
M Step 2	*D. triangulata*	Group 8	Group 8	✓	✓	✓	✓	✓	✓		
M Step 2	*D. triangulata*	Group 8	Group 8	✓	✓	✓	✓	✓	✓		
M Step 2	*D. triangulata*	Group 8	Group 8	✓	✓	✓	✓	✓	✓		
M Step 2	*D. triangulata*	Group 8	Group 8	✓	✓	✓	✓	✓	✓		
M Step 2	*D. triangulata*	Group 8	Group 8	✓	✓		✓	✓	✓		
M Step 2	*D. triangulata*	Group 8	Group 8	✓	✓	✓	✓	✓	✓		
M Step 2	*D. triangulata*	Group 8	Group 8	✓	✓	✓	✓	✓	✓		
M Step 2	*D. triangulata*	Group 8	Group 8	✓	✓		✓	✓	✓		
M Step 2	*D. triangulata*	Group 8	Group 8	✓	✓		✓	✓	✓		
M Step 2	*D. triangulata*	Group 8	Group 8	✓	✓	✓	✓	✓			
M Step 2	*D. triangulata*	Group 8	Group 8	✓	✓						
M Step 4	*D. triangulata*	Group 8	Group 8	✓			✓	✓	✓		
M Step 4	*D. triangulata*	Group 8	Group 8	✓	✓		✓	✓			
M unknown	*D. triangulata*	N.A.	Unkn.	✓			✓	✓			
M Step 4	*D. triangulata*	Group 8	Group 8	✓	✓		✓				

TABLE S1. Continued

Sample information					
Specimen ID	Cruise	Station	Latitude	Longitude	Collection date
Pacific Ocean					
DTRI_PSW_SNEL_21_05	Snellius II	21 Tr.1	6°24'S	130°20'E	1984-08-04
DTRI_PSW_SNEL_21_06	Snellius II	21 Tr.1	6°24'S	130°20'E	1984-08-04
DTRI_PSW_SNEL_21_07	Snellius II	21 Tr.1	6°24'S	130°20'E	1984-08-04
DTRI_PSW_SNEL_21_08	Snellius II	21 Tr.1	6°24'S	130°20'E	1984-08-04
DTRI_PSW_SNEL_21_09	Snellius II	21 Tr.1	6°24'S	130°20'E	1984-08-04
DTRI_PSW_SNEL_21_10	Snellius II	21 Tr.1	6°24'S	130°20'E	1984-08-04
DTRI_PNW_SNEL_C5_01	Snellius II	C Tr.5	5°22'N	129°56'E	1984-08-26
DTRI_PNW_SNEL_C5_02	Snellius II	C Tr.5	5°22'N	129°56'E	1984-08-26
DTRI_PNW_SNEL_C5_03	Snellius II	C Tr.5	5°22'N	129°56'E	1984-08-26
DTRI_PNW_SNEL_C5_04	Snellius II	C Tr.5	5°22'N	129°56'E	1984-08-26
DVUM_PSE_DANA_3583_01	DANA	3583 VI	13°11'S	161°51'W	1928-10-28
DVUM_PSE_DANA_3583_02	DANA	3583 VI	13°11'S	161°51'W	1928-10-28
DVUM_PSE_DANA_3583_03	DANA	3583 VI	13°11'S	161°51'W	1928-10-28
DVUM_PSE_DANA_3583_04	DANA	3583 VI	13°11'S	161°51'W	1928-10-28
DVUM_PSE_DANA_3583_05	DANA	3583 VI	13°11'S	161°51'W	1928-10-28
DVUM_PSE_DANA_3583_06	DANA	3583 VI	13°11'S	161°51'W	1928-10-28
DVUM_PSE_DANA_3583_07	DANA	3583 VI	13°11'S	161°51'W	1928-10-28
DVUM_PSE_DANA_3583_08	DANA	3583 VI	13°11'S	161°51'W	1928-10-28
DVUM_PSE_DANA_3583_09	DANA	3583 VI	13°11'S	161°51'W	1928-10-28
DVUM_PSE_DANA_3583_10	DANA	3583 VI	13°11'S	161°51'W	1928-10-28
DVUM_PSE_DANA_3583_11	DANA	3583 VI	13°11'S	161°51'W	1928-10-28
DVUM_PSE_DANA_3584_01	DANA	3584 V	10°52'S	168°40'W	1928-10-29
DVUM_PSE_DANA_3584_02	DANA	3584 V	10°52'S	168°40'W	1928-10-29
DVUM_PSE_DANA_3584_03	DANA	3584 V	10°52'S	168°40'W	1928-10-29
DVUM_PNW_DANA_3723_01	DANA	3723 IV	25°31'N	125°08'E	1929-05-30
DVUM_PNW_DANA_3723_02	DANA	3723 IV	25°31'N	125°08'E	1929-05-30
DVUM_PNW_DANA_3723_03	DANA	3723 IV	25°31'N	125°08'E	1929-05-30
DVUM_PNW_DANA_3723_04	DANA	3723 IV	25°31'N	125°08'E	1929-05-30
DVUM_PNW_DANA_3723_05	DANA	3723 IV	25°31'N	125°08'E	1929-05-30
DVUM_PNW_DANA_3723_06	DANA	3723 IV	25°31'N	125°08'E	1929-05-30
DVUM_PNW_DANA_4761_01	DANA	4761	25°10'N	127°45'E	1932-04-19
DVUM_PNW_DANA_4761_02	DANA	4761	25°10'N	127°45'E	1932-04-19
DVUU_PNE_DANA_1203_01	DANA	1203 V	7°30'N	179°19'W	1922-01-11
DVUU_PNE_DANA_1203_02	DANA	1203 V	7°30'N	179°19'W	1922-01-11
DVUU_PNE_DANA_1203_03	DANA	1203 V	7°30'N	179°19'W	1922-01-11
DVUU_PNW_DANA_3729_01	DANA	3729 V	20°03'N	120°50'E	1929-06-14
DVUU_PNW_DANA_3729_02	DANA	3729 V	20°03'N	120°50'E	1929-06-14
DVUU_PNW_DANA_3729_03	DANA	3729 V	20°03'N	120°50'E	1929-06-14
DVUU_PNW_DANA_3730_01	DANA	3730 V	16°55'N	120°03'E	1929-06-15
DVUU_PNW_DANA_3730_02	DANA	3730 V	16°55'N	120°03'E	1929-06-15
DVUU_PNW_DANA_3730_03	DANA	3730 V	16°55'N	120°03'E	1929-06-15
DVUU_PNW_DANA_3730_04	DANA	3730 V	16°55'N	120°03'E	1929-06-15
DVUU_PNW_DANA_3730_05	DANA	3730 V	16°55'N	120°03'E	1929-06-15
DVUU_PNW_DANA_3730_06	DANA	3730 V	16°55'N	120°03'E	1929-06-15
DVUU_PNW_DANA_3730_07	DANA	3730 V	16°55'N	120°03'E	1929-06-15
DVUU_PNW_DANA_3730_08	DANA	3730 V	16°55'N	120°03'E	1929-06-15
DVUU_PNW_DANA_3730_09	DANA	3730 V	16°55'N	120°03'E	1929-06-15
DVUU_PNW_DANA_3730_10	DANA	3730 V	16°55'N	120°03'E	1929-06-15
DVUU_PNW_DANA_3730_11	DANA	3730 V	16°55'N	120°03'E	1929-06-15

Identification				Geometric morphometrics						Genetics	
Specimen type (F, Fresh; M, Museum)	Genetic clade / Species (Van der Spoel et al., 1993)	LDA group	Integrative group	Ventral photo	Ventral 23LMs	Ventral 38LMs	Lateral photo	Lateral 15LMs	Lateral 49LMs	COI	28S
M Step 4	*D. triangulata*	Group 8	Group 8	✓	✓		✓	✓			
M unknown	*D. triangulata*	N.A.	Unkn.	✓			✓	✓			
M Step 4	*D. triangulata*	Group 8	Group 8	✓	✓	✓	✓	✓	✓		
M Step 4	*D. triangulata*	Group 8	Group 8	✓	✓		✓	✓	✓		
M Step 4	*D. triangulata*	Group 8	Group 8	✓	✓		✓	✓			
M unknown	*D. triangulata*	N.A.	Unkn.	✓			✓				
M Step 4	*D. triangulata*	Group 5	Group 5	✓			✓	✓	✓		
M unknown	*D. triangulata*	N.A.	Unkn.	✓			✓	✓			
M Step 4	*D. triangulata*	Group 8	Group 8	✓	✓	✓	✓	✓	✓		
M Step 4	*D. triangulata*	Group 8	Group 8	✓	✓		✓	✓	✓		
M Step 4	*D. v. meisenheimeri*	Group 3	Group 3	✓	✓	✓	✓	✓			
M Step 4	*D. v. meisenheimeri*	Group 3	Group 3	✓	✓	✓	✓	✓	✓		
M Step 4	*D. v. meisenheimeri*	Group 3	Group 3	✓	✓	✓	✓	✓			
M Step 4	*D. v. meisenheimeri*	Group 3	Group 3	✓	✓	✓	✓	✓			
M Step 4	*D. v. meisenheimeri*	Group 3	Group 3	✓	✓		✓	✓	✓		
M Step 4	*D. v. meisenheimeri*	Group 3	Group 3	✓			✓	✓	✓		
M Step 4	*D. v. meisenheimeri*	Group 3	Group 3	✓	✓	✓	✓	✓			
M unknown	*D. v. meisenheimeri*	N.A.	Unkn.	✓			✓				
M unknown	*D. v. meisenheimeri*	N.A.	Unkn.	✓			✓	✓			
M Step 4	*D. v. meisenheimeri*	Group 3	Group 3	✓			✓	✓	✓		
M Step 4	*D. v. meisenheimeri*	Group 3	Group 3	✓	✓		✓	✓			
M Step 4	*D. v. meisenheimeri*	Group 3	Group 3	✓	✓		✓	✓	✓		
M Step 4	*D. v. meisenheimeri*	Group 3	Group 3	✓	✓	✓	✓	✓	✓		
M Step 4	*D. v. meisenheimeri*	Group 3	Group 3	✓	✓		✓	✓	✓		
M unknown	*D. v. meisenheimeri*	Amb.	Unkn.	✓	✓		✓	✓			
M Step 4	*D. v. meisenheimeri*	Group 3	Group 3	✓	✓		✓	✓	✓		
M Step 4	*D. v. meisenheimeri*	Group 3	Group 3	✓	✓		✓	✓	✓		
M Step 4	*D. v. meisenheimeri*	Group 3	Group 3	✓	✓	✓	✓	✓	✓		
M Step 4	*D. v. meisenheimeri*	Group 3	Group 3	✓	✓		✓	✓	✓		
M unknown	*D. v. meisenheimeri*	Amb.	Unkn.	✓	✓		✓	✓			
M unknown	*D. v. meisenheimeri*	Amb.	Unkn.	✓	✓	✓	✓	✓	✓		
M unknown	*D. v. meisenheimeri*	Amb.	Unkn.	✓	✓	✓	✓	✓			
M unknown	*D. v. vanutrechti*	Amb.	Unkn.	✓	✓		✓	✓			
M unknown	*D. v. vanutrechti*	Amb.	Unkn.	✓	✓		✓	✓	✓		
M unknown	*D. v. vanutrechti*	N.A.	Unkn.	✓			✓	✓			
M Step 4	*D. v. vanutrechti*	Group 3	Group 3	✓			✓	✓	✓		
M Step 4	*D. v. vanutrechti*	Group 3	Group 3	✓			✓	✓	✓		
M Step 4	*D. v. vanutrechti*	Group 3	Group 3	✓	✓	✓	✓				
M unknown	*D. v. vanutrechti*	Amb.	Unkn.	✓	✓		✓				
M Step 4	*D. v. vanutrechti*	Group 3	Group 3	✓	✓		✓	✓	✓		
M Step 4	*D. v. vanutrechti*	Group 3	Group 3	✓	✓	✓	✓	✓	✓		
M Step 4	*D. v. vanutrechti*	Group 3	Group 3	✓	✓	✓	✓	✓	✓		
M Step 4	*D. v. vanutrechti*	Group 3	Group 3	✓	✓		✓	✓	✓		
M unknown	*D. v. vanutrechti*	Amb.	Unkn.	✓	✓		✓				
M Step 4	*D. v. vanutrechti*	Group 3	Group 3	✓	✓	✓	✓	✓	✓		
M Step 4	*D. v. vanutrechti*	Group 3	Group 3	✓	✓		✓	✓	✓		
M Step 4	*D. v. vanutrechti*	Group 3	Group 3	✓	✓	✓	✓	✓	✓		
M unknown	*D. v. vanutrechti*	Amb.	Unkn.	✓	✓	✓	✓	✓			
M Step 4	*D. v. vanutrechti*	Group 3	Group 3	✓			✓	✓	✓		

TABLE S1. Continued

Sample information					
Specimen ID	Cruise	Station	Latitude	Longitude	Collection date
Pacific Ocean					
DVUU_PNW_DANA_3730_12	DANA	3730 V	16°55'N	120°03'E	1929-06-15
DVUU_PNW_DANA_3730_13	DANA	3730 V	16°55'N	120°03'E	1929-06-15
DVUU_PNW_DANA_3730_14	DANA	3730 V	16°55'N	120°03'E	1929-06-15
DVUU_PNW_DANA_3730_15	DANA	3730 V	16°55'N	120°03'E	1929-06-15
DVUU_PNW_DANA_3730_16	DANA	3730 V	16°55'N	120°03'E	1929-06-15
DVUU_PNW_DANA_3731_01	DANA	3731 IV	14°37'N	119°52'E	1929-06-16
DVUU_PNW_DANA_3731_02	DANA	3731 IV	14°37'N	119°52'E	1929-06-16
DVUU_PNW_DANA_3731_03	DANA	3731 IV	14°37'N	119°52'E	1929-06-16
DVUU_PNW_DANA_3739_01	DANA	3739 IV	3°20'N	123°50'E	1929-07-02
DVUU_PNW_DANA_3739_02	DANA	3739 IV	3°20'N	123°50'E	1929-07-02
DVUU_PNW_DANA_3739_03	DANA	3739 IV	3°20'N	123°50'E	1929-07-02
DVUU_PNW_DANA_3739_04	DANA	3739 IV	3°20'N	123°50'E	1929-07-02
DVUU_PNW_DANA_3739_05	DANA	3739 IV	3°20'N	123°50'E	1929-07-02
DVUU_PNW_DANA_3739_06	DANA	3739 IV	3°20'N	123°50'E	1929-07-02
DVUU_PNW_DANA_3739_07	DANA	3739 IV	3°20'N	123°50'E	1929-07-02
DVUU_PNW_DANA_3739_08	DANA	3739 IV	3°20'N	123°50'E	1929-07-02
Indian Ocean					
D_ISW_VANC10MV_01_01	VANC10MV	1	35°03'S	23°44'E	2003-05-16
D_ISW_VANC10MV_01_02	VANC10MV	1	35°03'S	23°44'E	2003-05-16
D_ISW_VANC10MV_01_03	VANC10MV	1	35°03'S	23°44'E	2003-05-16
D_ISW_VANC10MV_01_04	VANC10MV	1	35°03'S	23°44'E	2003-05-16
D_ISW_VANC10MV_01_05	VANC10MV	1	35°03'S	23°44'E	2003-05-16
D_ISW_VANC10MV_02_01	VANC10MV	2	35°04'S	24°30'E	2003-05-16
D_ISW_VANC10MV_02_02	VANC10MV	2	35°04'S	24°30'E	2003-05-16
D_ISW_VANC10MV_02_03	VANC10MV	2	35°04'S	24°30'E	2003-05-16
D_ISW_VANC10MV_02_04	VANC10MV	2	35°04'S	24°30'E	2003-05-16
D_ISE_VANC10MV_21_01	VANC10MV	21	13°30'S	91°46'E	2003-06-05
D_ISE_VANC10MV_23_01	VANC10MV	23	12°13'S	96°47'E	2003-06-07
D_ISE_VANC10MV_23_02	VANC10MV	23	12°13'S	96°47'E	2003-06-07
D_ISE_VANC10MV_23_03	VANC10MV	23	12°13'S	96°47'E	2003-06-07
D_ISE_VANC10MV_23_04	VANC10MV	23	12°13'S	96°47'E	2003-06-07
D_ISE_VANC10MV_25_01	VANC10MV	25	13°51'S	109°03'E	2003-06-10
D_ISE_VANC10MV_25_02	VANC10MV	25	13°51'S	109°03'E	2003-06-10
D_ISE_VANC10MV_26_01	VANC10MV	26	14°29'S	113°27'E	2003-06-11
D_ISE_VANC10MV_27_01	VANC10MV	27	16°35'S	115°23'E	2003-06-12
DANG_ISE_DANA_3844_01	DANA	3844 VII	12°05'S	96°41'E	1929-10-11
DANG_ISW_DANA_3925_01	DANA	3925 V	7°13'S	52°22'E	1929-12-16
DANG_ISW_DANA_3925_02	DANA	3925 V	7°13'S	52°22'E	1929-12-16
DANG_ISW_DANA_3925_03	DANA	3925 V	7°13'S	52°22'E	1929-12-16
DANG_ISW_DANA_3925_04	DANA	3925 V	7°13'S	52°22'E	1929-12-16
DANG_ISW_DANA_3925_05	DANA	3925 V	7°13'S	52°22'E	1929-12-16
DANG_ISW_DANA_3925_06	DANA	3925 V	7°13'S	52°22'E	1929-12-16
DANG_ISW_DANA_3925_07	DANA	3925 V	7°13'S	52°22'E	1929-12-16
DANG_ISW_DANA_3925_08	DANA	3925 V	7°13'S	52°22'E	1929-12-16
DANG_ISW_DANA_3925_09	DANA	3925 V	7°13'S	52°22'E	1929-12-16
DANG_ISW_DANA_3925_10	DANA	3925 V	7°13'S	52°22'E	1929-12-16
DANG_ISW_DANA_3925_11	DANA	3925 V	7°13'S	52°22'E	1929-12-16
DANG_ISW_DANA_3925_12	DANA	3925 V	7°13'S	52°22'E	1929-12-16
DANG_ISW_DANA_3925_13	DANA	3925 V	7°13'S	52°22'E	1929-12-16

Identification				Geometric morphometrics						Genetics	
Specimen type (F, Fresh; M, Museum)	Genetic clade / Species (Van der Spoel et al., 1993)	LDA group	Integrative group	Ventral photo	Ventral 23LMs	Ventral 38LMs	Lateral photo	Lateral 15LMs	Lateral 49LMs	COI	28S
M Step 4	*D. v. vanutrechti*	Group 3	Group 3	✓	✓	✓	✓	✓	✓		
M unknown	*D. v. vanutrechti*	Amb.	Unkn.	✓	✓	✓	✓	✓			
M Step 4	*D. v. vanutrechti*	Group 3	Group 3	✓	✓		✓	✓	✓		
M unknown	*D. v. vanutrechti*	Amb.	Unkn.	✓	✓		✓				
M Step 4	*D. v. vanutrechti*	Group 3	Group 3	✓	✓	✓					
M Step 2	*D. v. vanutrechti*	Group 3	Group 3	✓	✓	✓	✓	✓			
M Step 2	*D. v. vanutrechti*	Group 3	Group 3	✓			✓	✓	✓		
M Step 2	*D. v. vanutrechti*	Group 3	Group 3	✓	✓	✓	✓	✓	✓		
M Step 4	*D. v. vanutrechti*	Group 3	Group 3	✓			✓	✓	✓		
M unknown	*D. v. vanutrechti*	N.A.	Unkn.	✓			✓	✓			
M Step 4	*D. v. vanutrechti*	Group 3	Group 3	✓			✓	✓	✓		
M unknown	*D. v. vanutrechti*	N.A.	Unkn.	✓			✓				
M unknown	*D. v. vanutrechti*	N.A.	Unkn.	✓			✓	✓			
M Step 4	*D. v. vanutrechti*	Group 3	Group 3	✓	✓		✓	✓			
M unknown	*D. v. vanutrechti*	N.A.	Unkn.	✓			✓				
M Step 4	*D. v. vanutrechti*	Group 3	Group 3	✓			✓	✓	✓		
F unknown	N.A.	N.A.	Unkn.								
F unknown	N.A.	N.A.	Unkn.	✓							
F unknown	N.A.	N.A.	Unkn.	✓							
F unknown	N.A.	N.A.	Unkn.	✓							
F unknown	N.A.	N.A.	Unkn.	✓							
F unknown	N.A.	N.A.	Unkn.	✓			✓				
F unknown	N.A.	N.A.	Unkn.								
F Step 5	Group 13	N.A.	Group 13	✓						MF974840	
F Step 1	Group 4	N.A.	Group 4	✓			✓				MF974753
F Step 1	Group 7	Group 7	Group 7	✓	✓		✓	✓	✓	MF974841	MF974754
F Step 1	Group 3	N.A.	Group 3	✓			✓			MF974842	MF974755
F Step 1	Group 3	N.A.	Group 3	✓			✓			MF974843	MF974756
F Step 1	Group 3	N.A.	Group 3	✓						MF974844	
F Step 1	Group 3	N.A.	Group 3	✓						MF974845	MF974757
F Step 1	Group 3	N.A.	Group 3	✓			✓	✓		MF974846	MF974758
F Step 1	Group 4	Group 4	Group 4	✓	✓	✓	✓	✓	✓		MF974759
F Step 1	Group 4	Group 4	Group 4	✓	✓		✓	✓	✓		MF974760
F Step 1	Group 3	N.A.	Group 3	✓			✓			MF974847	MF974761
M Step 4	*D. angulata*	Group 4	Group 4	✓	✓		✓	✓	✓		
M Step 4	*D. angulata*	Group 4	Group 4	✓	✓		✓	✓			
M Step 4	*D. angulata*	Group 4	Group 4	✓	✓		✓	✓	✓		
M Step 4	*D. angulata*	Group 4	Group 4	✓			✓	✓	✓		
M unknown	*D. angulata*	Amb.	Unkn.	✓	✓		✓	✓			
M Step 4	*D. angulata*	Group 4	Group 4	✓	✓		✓	✓	✓		
M unknown	*D. angulata*	N.A.	Unkn.	✓			✓	✓			
M Step 4	*D. angulata*	Group 4	Group 4	✓			✓	✓	✓		
M Step 4	*D. angulata*	Group 4	Group 4	✓	✓	✓	✓	✓			
M Step 4	*D. angulata*	Group 4	Group 4	✓	✓		✓	✓	✓		
M Step 4	*D. angulata*	Group 4	Group 4	✓	✓		✓	✓	✓		
M unknown	*D. angulata*	N.A.	Unkn.	✓			✓	✓			
M Step 4	*D. angulata*	Group 4	Group 4	✓	✓		✓				
M Step 4	*D. angulata*	Group 4	Group 4	✓	✓		✓				

TABLE S1. Continued

Sample information					
Specimen ID	Cruise	Station	Latitude	Longitude	Collection date
Indian Ocean					
DANG_ISW_DANA_3925_14	DANA	3925 V	7°13'S	52°22'E	1929-12-16
DANG_ISW_DANA_3925_15	DANA	3925 V	7°13'S	52°22'E	1929-12-16
DANG_ISW_DANA_3925_16	DANA	3925 V	7°13'S	52°22'E	1929-12-16
DANG_ISW_DANA_3925_17	DANA	3925 V	7°13'S	52°22'E	1929-12-16
DANG_ISW_DANA_3925_18	DANA	3925 V	7°13'S	52°22'E	1929-12-16
DANG_ISW_DANA_3925_19	DANA	3925 V	7°13'S	52°22'E	1929-12-16
DANG_ISW_DANA_3925_20	DANA	3925 V	7°13'S	52°22'E	1929-12-16
DANG_ISW_DANA_3939_01	DANA	3939 III	8°44'S	43°54'E	1929-11-23
DANG_ISW_DANA_3939_02	DANA	3939 III	8°44'S	43°54'E	1929-11-23
DANG_ISW_DANA_3939_03	DANA	3939 III	8°44'S	43°54'E	1929-11-23
DANG_ISW_DANA_3939_04	DANA	3939 III	8°44'S	43°54'E	1929-11-23
DANG_ISW_DANA_3939_05	DANA	3939 III	8°44'S	43°54'E	1929-11-23
DANG_ISW_DANA_3939_06	DANA	3939 III	8°44'S	43°54'E	1929-11-23
DANG_ISW_DANA_3948_01	DANA	3948 I	10°11'S	41°57'E	1930-01-06
DBIC_INE_DANA_3910_01	DANA	3910 IV	5°28'N	79°57'E	1929-11-23
DBIC_INE_DANA_3910_02	DANA	3910 IV	5°28'N	79°57'E	1929-11-23
DBIC_INE_DANA_3910_03	DANA	3910 IV	5°28'N	79°57'E	1929-11-23
DBIC_ISW_DANA_3922_01	DANA	3922 V	3°45'S	56°33'E	1929-12-12
DBIC_ISW_DANA_3922_02	DANA	3922 V	3°45'S	56°33'E	1929-12-12
DELE_ISE_DANA_3184_01	DANA	3184 II	4°38'S	99°24'E	1929-09-09
DELE_ISE_DANA_3824_01	DANA	3824	0°08'S	97°15'E	1929-09-15
DFLE_INE_DANA_3827_01	DANA	3827 I	1°45'N	96°20'E	1929-09-17
DFLE_INE_DANA_3828_01	DANA	3828 I	1°53'N	95°07'E	1929-09-18
DGRA_ISE_DANA_3860_01	DANA	3860 XI XV	2°57'S	99°36'E	1929-10-20
DGRA_ISE_DANA_3860_02	DANA	3860 XI XV	2°57'S	99°36'E	1929-10-20
DGRA_ISE_DANA_3860_03	DANA	3860 XI XV	2°57'S	99°36'E	1929-10-20
DGRA_ISE_DANA_3860_04	DANA	3860 XI XV	2°57'S	99°36'E	1929-10-20
DGRA_ISE_DANA_3860_05	DANA	3860 XI XV	2°57'S	99°36'E	1929-10-20
DGRA_ISE_DANA_3860_06	DANA	3860 XI XV	2°57'S	99°36'E	1929-10-20
DGRA_ISE_DANA_3860_07	DANA	3860 XI XV	2°57'S	99°36'E	1929-10-20
DGRA_ISE_DANA_3860_08	DANA	3860 XI XV	2°57'S	99°36'E	1929-10-20
DGRA_ISE_DANA_3860_09	DANA	3860 XI XV	2°57'S	99°36'E	1929-10-20
DGRA_ISW_DANA_3926_01	DANA	3926 IV	8°27'S	50°54'E	1929-12-16
DLIL_ISW_DANA_3930_01	DANA	3930	11°55'S	49°55'E	1929-12-19
DLIL_ISW_DANA_3930_02	DANA	3930	11°55'S	49°55'E	1929-12-19
DLON_ISE_DANA_3809_01	DANA	3809 III	6°22'S	105°12'E	1929-09-04
DLON_ISE_DANA_3809_02	DANA	3809 III	6°22'S	105°12'E	1929-09-04
DLON_ISE_DANA_3809_03	DANA	3809 III	6°22'S	105°12'E	1929-09-04
DLON_ISE_DANA_3809_04	DANA	3809 III	6°22'S	105°12'E	1929-09-04
DLON_ISE_DANA_3809_05	DANA	3809 III	6°22'S	105°12'E	1929-09-04
DLON_ISE_DANA_3809_06	DANA	3809 III	6°22'S	105°12'E	1929-09-04
DLON_ISE_DANA_3809_07	DANA	3809 III	6°22'S	105°12'E	1929-09-04
DLON_ISE_DANA_3809_08	DANA	3809 III	6°22'S	105°12'E	1929-09-04
DLON_ISE_DANA_3809_09	DANA	3809 III	6°22'S	105°12'E	1929-09-04
DLON_ISE_DANA_3809_10	DANA	3809 III	6°22'S	105°12'E	1929-09-04
DLON_ISE_DANA_3809_11	DANA	3809 III	6°22'S	105°12'E	1929-09-04
DLON_ISE_DANA_3809_12	DANA	3809 III	6°22'S	105°12'E	1929-09-04
DLON_ISE_DANA_3809_13	DANA	3809 III	6°22'S	105°12'E	1929-09-04
DLON_ISE_DANA_3809_14	DANA	3809 III	6°22'S	105°12'E	1929-09-04

Identification				Geometric morphometrics						Genetics	
Specimen type (F, Fresh; M, Museum)	Genetic clade / Species (Van der Spoel et al., 1993)	LDA group	Integrative group	Ventral photo	Ventral 23LMs	Ventral 38LMs	Lateral photo	Lateral 15LMs	Lateral 49LMs	COI	28S
M unknown	*D. angulata*	N.A.	Unkn.	✓			✓	✓			
M unknown	*D. angulata*	N.A.	Unkn.	✓			✓	✓			
M unknown	*D. angulata*	N.A.	Unkn.	✓			✓				
M Step 4	*D. angulata*	Group 4	Group 4	✓			✓	✓	✓		
M unknown	*D. angulata*	N.A.	Unkn.	✓			✓				
M unknown	*D. angulata*	N.A.	Unkn.	✓			✓	✓			
M unknown	*D. angulata*	Amb.	Unkn.	✓	✓		✓				
M unknown	*D. angulata*	N.A.	Unkn.	✓			✓	✓			
M unknown	*D. angulata*	N.A.	Unkn.	✓			✓	✓			
M unknown	*D. angulata*	N.A.	Unkn.	✓			✓				
M unknown	*D. angulata*	N.A.	Unkn.	✓			✓				
M Step 4	*D. angulata*	Group 4	Group 4	✓	✓		✓	✓			
M unknown	*D. angulata*	N.A.	Unkn.	✓			✓	✓			
M Step 4	*D. angulata*	Group 4	Group 4	✓	✓	✓	✓				
M Step 4	*D. bicornis*	Group 3	Group 3	✓	✓		✓	✓	✓		
M Step 4	*D. bicornis*	Group 3	Group 3	✓			✓	✓	✓		
M unknown	*D. bicornis*	N.A.	Unkn.	✓			✓				
M Step 2	*D. bicornis*	Group 5	Group 5	✓	✓	✓	✓	✓	✓		
M Step 2	*D. bicornis*	Group 5	Group 5	✓	✓	✓	✓	✓			
M Step 4	*D. elegans*	Group 5	Group 5	✓	✓	✓	✓	✓	✓		
M unknown	*D. elegans*	Amb.	Unkn.	✓	✓	✓	✓	✓			
M unknown	*D. flexipes*	Amb.	Unkn.	✓	✓	✓	✓	✓			
M unknown	*D. flexipes*	Amb.	Unkn.	✓	✓		✓	✓			
M Step 4	*D. grayi*	Group 4	Group 4	✓	✓		✓				
M Step 4	*D. grayi*	Group 4	Group 4	✓	✓		✓	✓	✓		
M Step 4	*D. grayi*	Group 4	Group 4	✓	✓	✓	✓	✓			
M Step 4	*D. grayi*	Group 4	Group 4	✓	✓	✓	✓				
M Step 4	*D. grayi*	Group 4	Group 4	✓	✓	✓	✓	✓	✓		
M Step 4	*D. grayi*	Group 4	Group 4	✓	✓	✓	✓	✓	✓		
M Step 4	*D. grayi*	Group 4	Group 4	✓	✓	✓	✓	✓	✓		
M Step 4	*D. grayi*	Group 4	Group 4	✓	✓	✓	✓	✓	✓		
M Step 4	*D. grayi*	Group 4	Group 4	✓	✓	✓	✓				
M Step 4	*D. grayi*	Group 4	Group 4	✓	✓		✓	✓	✓		
M unknown	*D. limbata limbata*	Amb.	Unkn.	✓	✓	✓	✓	✓	✓		
M Step 4	*D. limbata limbata*	Group 3	Group 3	✓	✓	✓	✓	✓	✓		
M unknown	*D. longirostris*	N.A.	Unkn.	✓			✓	✓			
M Step 3	*D. longirostris*	Group 11	Group 11	✓	✓	✓	✓	✓	✓		
M Step 3	*D. longirostris*	Group 11	Group 11	✓			✓	✓	✓		
M Step 3	*D. longirostris*	Group 11	Group 11	✓	✓		✓	✓	✓		
M Step 3	*D. longirostris*	Group 11	Group 11	✓			✓	✓	✓		
M Step 3	*D. longirostris*	Group 11	Group 11	✓			✓	✓	✓		
M Step 3	*D. longirostris*	Group 11	Group 11	✓	✓	✓	✓	✓	✓		
M Step 3	*D. longirostris*	Group 11	Group 11	✓	✓	✓	✓	✓	✓		
M Step 3	*D. longirostris*	Group 11	Group 11	✓			✓	✓	✓		
M unknown	*D. longirostris*	N.A.	Unkn.	✓			✓	✓			
M Step 3	*D. longirostris*	Group 11	Group 11	✓	✓		✓	✓	✓		
M Step 3	*D. longirostris*	Group 11	Group 11	✓	✓	✓	✓	✓	✓		
M unknown	*D. longirostris*	N.A.	Unkn.	✓			✓	✓			
M unknown	*D. longirostris*	N.A.	Unkn.	✓			✓	✓			

TABLE S1. Continued

Sample information					
Specimen ID	Cruise	Station	Latitude	Longitude	Collection date
Indian Ocean					
DLON_ISE_DANA_3809_15	DANA	3809 III	6°22'S	105°12'E	1929-09-04
DLON_ISE_DANA_3809_16	DANA	3809 III	6°22'S	105°12'E	1929-09-04
DPAC_ISE_DANA_3824_01	DANA	3824	0°08'S	97°15'E	1929-09-15
DPAC_ISE_DANA_3824_02	DANA	3824	0°08'S	97°15'E	1929-09-15
DPAC_ISE_DANA_3824_03	DANA	3824	0°08'S	97°15'E	1929-09-15
DPAC_ISE_DANA_3824_04	DANA	3824	0°08'S	97°15'E	1929-09-15
DPAC_ISE_DANA_3824_05	DANA	3824	0°08'S	97°15'E	1929-09-15
DPAC_ISE_DANA_3844_01	DANA	3844 IV	12°05'S	96°45'E	1929-10-10
DPAC_ISE_DANA_3844_02	DANA	3844 IV	12°05'S	96°45'E	1929-10-10
DPAC_ISE_DANA_3850_01	DANA	3850 III	6°01'S	93°12'E	1929-10-14
DPAC_ISE_DANA_3850_02	DANA	3850 III	6°01'S	93°12'E	1929-10-14
DPAC_ISE_DANA_3850_03	DANA	3850 III	6°01'S	93°12'E	1929-10-14
DPAC_ISE_DANA_3850_04	DANA	3850 III	6°01'S	93°12'E	1929-10-14
DPAC_ISW_DANA_3920_01	DANA	3920 IX	1°12'S	62°19'E	1929-12-09
DPAC_ISW_DANA_3920_02	DANA	3920 IX	1°12'S	62°19'E	1929-12-09
DPAC_ISW_DANA_3920_03	DANA	3920 IX	1°12'S	62°19'E	1929-12-09
DPAC_ISW_DANA_3920_04	DANA	3920 IX	1°12'S	62°19'E	1929-12-09
DPAC_ISW_DANA_3920_05	DANA	3920 IX	1°12'S	62°19'E	1929-12-09
DPAC_ISW_DANA_3920_06	DANA	3920 IX	1°12'S	62°19'E	1929-12-09
DPAC_ISW_DANA_3920_07	DANA	3920 IX	1°12'S	62°19'E	1929-12-09
DPAC_ISW_DANA_3920_08	DANA	3920 IX	1°12'S	62°19'E	1929-12-09
DPAC_ISW_DANA_3920_09	DANA	3920 IX	1°12'S	62°19'E	1929-12-09
DPAC_ISW_DANA_3920_10	DANA	3920 IX	1°12'S	62°19'E	1929-12-09
DPAC_ISW_DANA_3920_11	DANA	3920 IX	1°12'S	62°19'E	1929-12-09
DPAC_ISW_DANA_3920_12	DANA	3920 IX	1°12'S	62°19'E	1929-12-09
DPAC_ISW_DANA_3922_01	DANA	3922 V	3°45'S	56°33'E	1929-12-12
DPAC_ISW_DANA_3922_02	DANA	3922 V	3°45'S	56°33'E	1929-12-12
DPAC_ISW_DANA_3922_03	DANA	3922 V	3°45'S	56°33'E	1929-12-12
DPAC_ISW_DANA_3922_04	DANA	3922 V	3°45'S	56°33'E	1929-12-12
DPAC_ISW_DANA_3922_05	DANA	3922 V	3°45'S	56°33'E	1929-12-12
DPAC_ISW_DANA_3922_06	DANA	3922 V	3°45'S	56°33'E	1929-12-12
DPAC_ISW_DANA_3922_07	DANA	3922 V	3°45'S	56°33'E	1929-12-12
DPAC_ISW_DANA_3922_08	DANA	3922 V	3°45'S	56°33'E	1929-12-12
DPAC_ISW_DANA_3922_09	DANA	3922 V	3°45'S	56°33'E	1929-12-12
DPAC_ISW_DANA_3922_10	DANA	3922 V	3°45'S	56°33'E	1929-12-12
DPAC_ISW_DANA_3922_11	DANA	3922 V	3°45'S	56°33'E	1929-12-12
DPAC_ISW_DANA_3922_12	DANA	3922 V	3°45'S	56°33'E	1929-12-12
DSOU_ISE_DANA_3860_01	DANA	3860	2°57'S	99°36'E	1929-10-20
DSOU_INW_TYRO_S15_01	leg. TYRO	B2-S1-5 N	12°05'N	54°54'E	1993-01-24
DSOU_INW_TYRO_S15_02	leg. TYRO	B2-S1-5 N	12°05'N	54°54'E	1993-01-24
DSOU_INW_TYRO_S15_03	leg. TYRO	B2-S1-5 N	12°05'N	54°54'E	1993-01-24
DSOU_INW_TYRO_S15_04	leg. TYRO	B2-S1-5 N	12°05'N	54°54'E	1993-01-24
DSOU_INW_TYRO_S15_05	leg. TYRO	B2-S1-5 N	12°05'N	54°54'E	1993-01-24
DSOU_INW_TYRO_S15_06	leg. TYRO	B2-S1-5 N	12°05'N	54°54'E	1993-01-24
DSOU_INW_TYRO_S15_07	leg. TYRO	B2-S1-5 N	12°05'N	54°54'E	1993-01-24
DSOU_INW_TYRO_SB21_01	leg. TYRO	B2-SB2-1 D	6°13'N	52°27'E	1993-01-15
DSOU_INW_TYRO_SB21_02	leg. TYRO	B2-SB2-1 D	6°13'N	52°27'E	1993-01-15
DSOU_INW_TYRO_SB21_03	leg. TYRO	B2-SB2-1 D	6°13'N	52°27'E	1993-01-15
DSOU_INW_TYRO_SB21_04	leg. TYRO	B2-SB2-1 D	6°13'N	52°27'E	1993-01-15

Identification				Geometric morphometrics						Genetics	
Specimen type (F, Fresh; M, Museum)	Genetic clade / Species (Van der Spoel et al., 1993)	LDA group	Integrative group	Ventral photo	Ventral 23LMs	Ventral 38LMs	Lateral photo	Lateral 15LMs	Lateral 49LMs	COI	28S
M unknown	*D. longirostris*	N.A.	Unkn.	✓			✓	✓			
M Step 3	*D. longirostris*	Group 11	Group 11	✓	✓						
M Step 4	*D. pacifica*	Group 4	Group 4	✓	✓	✓	✓				
M unknown	*D. pacifica*	N.A.	Unkn.	✓			✓	✓			
M unknown	*D. pacifica*	N.A.	Unkn.	✓			✓	✓			
M unknown	*D. pacifica*	Amb.	Unkn.	✓	✓		✓				
M Step 4	*D. pacifica*	Group 5	Group 5	✓	✓	✓	✓	✓			
M Step 4	*D. pacifica*	Group 4	Group 4	✓	✓	✓	✓	✓	✓		
M Step 4	*D. pacifica*	Group 4	Group 4	✓	✓		✓	✓	✓		
M Step 4	*D. pacifica*	Group 4	Group 4	✓	✓		✓	✓			
M Step 4	*D. pacifica*	Group 4	Group 4	✓	✓	✓	✓	✓			
M unknown	*D. pacifica*	N.A.	Unkn.	✓			✓				
M Step 4	*D. pacifica*	Group 4	Group 4	✓	✓		✓				
M Step 4	*D. pacifica*	Group 4	Group 4	✓	✓		✓	✓	✓		
M Step 4	*D. pacifica*	Group 4	Group 4	✓	✓		✓	✓	✓		
M Step 4	*D. pacifica*	Group 4	Group 4	✓	✓		✓	✓	✓		
M Step 4	*D. pacifica*	Group 4	Group 4	✓	✓		✓	✓	✓		
M Step 4	*D. pacifica*	Group 4	Group 4	✓	✓		✓				
M Step 4	*D. pacifica*	Group 4	Group 4	✓	✓	✓	✓	✓	✓		
M Step 4	*D. pacifica*	Group 4	Group 4	✓	✓		✓	✓	✓		
M Step 4	*D. pacifica*	Group 4	Group 4	✓	✓		✓				
M unknown	*D. pacifica*	N.A.	Unkn.	✓			✓				
M Step 4	*D. pacifica*	Group 4	Group 4	✓	✓		✓	✓	✓		
M Step 4	*D. pacifica*	Group 4	Group 4				✓	✓	✓		
M Step 4	*D. pacifica*	Group 4	Group 4	✓	✓		✓	✓	✓		
M unknown	*D. pacifica*	Amb.	Unkn.	✓	✓		✓	✓			
M Step 4	*D. pacifica*	Group 4	Group 4	✓	✓	✓	✓	✓			
M unknown	*D. pacifica*	Amb.	Unkn.	✓	✓		✓	✓			
M unknown	*D. pacifica*	Amb.	Unkn.	✓	✓		✓				
M unknown	*D. pacifica*	Amb.	Unkn.	✓	✓		✓				
M unknown	*D. pacifica*	Amb.	Unkn.	✓	✓		✓	✓			
M Step 4	*D. pacifica*	Group 4	Group 4	✓			✓	✓	✓		
M Step 4	*D. pacifica*	Group 5	Group 5	✓	✓		✓	✓	✓		
M unknown	*D. pacifica*	Amb.	Unkn.	✓	✓		✓	✓			
M Step 4	*D. pacifica*	Group 4	Group 4	✓	✓		✓	✓	✓		
M Step 4	*D. pacifica*	Group 4	Group 4	✓			✓	✓	✓		
M unknown	*D. souleyeti*	N.A.	Unkn.	✓			✓				
M Step 4	*D. souleyeti*	Group 11	Group 11	✓	✓	✓	✓	✓			
M Step 4	*D. souleyeti*	Group 3	Group 3	✓	✓	✓	✓	✓			
M unknown	*D. souleyeti*	Amb.	Unkn.	✓	✓	✓	✓	✓			
M Step 4	*D. souleyeti*	Group 3	Group 3	✓	✓	✓	✓	✓	✓		
M Step 4	*D. souleyeti*	Group 3	Group 3	✓	✓	✓	✓	✓	✓		
M Step 4	*D. souleyeti*	Group 11	Group 11	✓	✓	✓	✓	✓	✓		
M unknown	*D. souleyeti*	Amb.	Unkn.	✓	✓	✓	✓	✓	✓		
M Step 4	*D. souleyeti*	Group 3	Group 3	✓	✓	✓	✓	✓	✓		
M Step 4	*D. souleyeti*	Group 3	Group 3	✓	✓	✓	✓	✓	✓		
M Step 4	*D. souleyeti*	Group 3	Group 3	✓	✓	✓	✓	✓	✓		
M Step 4	*D. souleyeti*	Group 3	Group 3	✓	✓	✓	✓	✓	✓		

TABLE S1. Continued

Sample information					
Specimen ID	Cruise	Station	Latitude	Longitude	Collection date
Indian Ocean					
DSOU_INW_TYRO_SB21_05	leg. TYRO	B2-SB2-1 D	6°13'N	52°27'E	1993-01-15
DSOU_INW_TYRO_SB21_06	leg. TYRO	B2-SB2-1 D	6°13'N	52°27'E	1993-01-15
DSOU_INW_TYRO_US11_01	leg. TYRO	B1-US1-1 D	7°02'N	49°59'E	1992-07-19
DSOU_INW_TYRO_US11_02	leg. TYRO	B1-US1-1 D	7°02'N	49°59'E	1992-07-19
DSOU_INW_TYRO_US11_03	leg. TYRO	B1-US1-1 D	7°02'N	49°59'E	1992-07-19
DSOU_INW_TYRO_US11_04	leg. TYRO	B1-US1-1 D	7°02'N	49°59'E	1992-07-19
DSOU_INW_TYRO_US11_05	leg. TYRO	B1-US1-1 D	7°02'N	49°59'E	1992-07-19
DSOU_INW_TYRO_US11_06	leg. TYRO	B1-US1-1 D	7°02'N	49°59'E	1992-07-19
DSOU_INW_TYRO_US11_07	leg. TYRO	B1-US1-1 D	7°02'N	49°59'E	1992-07-19
DSOU_INW_TYRO_US15_01	leg. TYRO	B2-US1-5	7°51'N	50°35'E	1993-01-18
DSOU_INW_TYRO_US15_02	leg. TYRO	B2-US1-5	7°51'N	50°35'E	1993-01-18
DSOU_INW_TYRO_US15_03	leg. TYRO	B2-US1-5	7°51'N	50°35'E	1993-01-18
DSOU_INW_TYRO_US15_04	leg. TYRO	B2-US1-5	7°51'N	50°35'E	1993-01-18
DSOU_INW_TYRO_US15_05	leg. TYRO	B2-US1-5	7°51'N	50°35'E	1993-01-18
DSOU_INW_TYRO_US15_06	leg. TYRO	B2-US1-5	7°51'N	50°35'E	1993-01-18
DSOU_INW_TYRO_US15_07	leg. TYRO	B2-US1-5	7°51'N	50°35'E	1993-01-18
DSOU_INW_TYRO_US15_08	leg. TYRO	B2-US1-5	7°51'N	50°35'E	1993-01-18
DSOU_INW_TYRO_US15_09	leg. TYRO	B2-US1-5	7°51'N	50°35'E	1993-01-18
DSOU_INW_TYRO_US15_10	leg. TYRO	B2-US1-5	7°51'N	50°35'E	1993-01-18
DSOU_INW_TYRO_US15_11	leg. TYRO	B2-US1-5	7°51'N	50°35'E	1993-01-18
DSOU_INW_TYRO_US15_12	leg. TYRO	B2-US1-5	7°51'N	50°35'E	1993-01-18
DSOU_INW_TYRO_US15_13	leg. TYRO	B2-US1-5	7°51'N	50°35'E	1993-01-18
DSTI_ISE_DANA_3860_01	DANA	3860	2°57'S	99°36'E	1929-10-20
DSTI_ISE_DANA_3860_02	DANA	3860	2°57'S	99°36'E	1929-10-20
DSTI_ISE_DANA_3860_03	DANA	3860	2°57'S	99°36'E	1929-10-20
DSTI_ISE_DANA_3860_04	DANA	3860	2°57'S	99°36'E	1929-10-20
DSTI_ISE_DANA_3860_05	DANA	3860	2°57'S	99°36'E	1929-10-20
DSTI_ISE_DANA_3860_06	DANA	3860	2°57'S	99°36'E	1929-10-20
DSTI_ISE_DANA_3860_07	DANA	3860	2°57'S	99°36'E	1929-10-20
DSTI_ISE_DANA_3860_08	DANA	3860	2°57'S	99°36'E	1929-10-20
DTRI_INW_TYRO_BM1_01	leg. TYRO	B2-BM-1	12°45'N	43°14'E	1993-02-01
DTRI_INW_TYRO_BM1_02	leg. TYRO	B2-BM-1	12°45'N	43°14'E	1993-02-01
DTRI_INW_TYRO_BM1_03	leg. TYRO	B2-BM-1	12°45'N	43°14'E	1993-02-01
DTRI_INW_TYRO_BM1_04	leg. TYRO	B2-BM-1	12°45'N	43°14'E	1993-02-01
DTRI_INW_TYRO_BM1_05	leg. TYRO	B2-BM-1	12°45'N	43°14'E	1993-02-01
DTRI_INW_TYRO_BM1_06	leg. TYRO	B2-BM-1	12°45'N	43°14'E	1993-02-01
DTRI_INW_TYRO_BM1_07	leg. TYRO	B2-BM-1	12°45'N	43°14'E	1993-02-01
DTRI_INW_TYRO_BM1_08	leg. TYRO	B2-BM-1	12°45'N	43°14'E	1993-02-01
DTRI_INW_TYRO_GA11_01	leg. TYRO	B2-GA1-1	12°50'N	50°06'E	1993-01-27
DTRI_INW_TYRO_GA11_02	leg. TYRO	B2-GA1-1	12°50'N	50°06'E	1993-01-27
DTRI_INW_TYRO_GA11_03	leg. TYRO	B2-GA1-1	12°50'N	50°06'E	1993-01-27
DVUU_ISE_DANA_3184_01	DANA	3184 II	4°38'S	99°29'E	1929-09-09
DVUU_INE_DANA_3914_01	DANA	3914 V	4°02'N	77°08'E	1929-12-02
DVUU_INE_DANA_3914_02	DANA	3914 V	4°02'N	77°08'E	1929-12-02
Atlantic Ocean					
Ca_unc_ECO_91_1	GU1101	91	18°07'N	87°44'W	2011-01-31
Ca_unc_SB_NWA_3	NOAA PC201205	ST23P4	39°55'N	67°27'W	2012-09-04
Pacific Ocean					
Ca_unc_SB_GOC_1	MBARI GOC 2012	D342BW	24°22'N	109°13'W	2012-02-24
Ca_unc_SB_GOC_2	MBARI GOC 2012	D342BW	24°22'N	109°13'W	2012-02-24

Identification				Geometric morphometrics						Genetics	
Specimen type (F, Fresh; M, Museum)	Genetic clade / Species (Van der Spoel et al., 1993)	LDA group	Integrative group	Ventral photo	Ventral 23LMs	Ventral 38LMs	Lateral photo	Lateral 15LMs	Lateral 49LMs	COI	28S
M Step 4	*D. souleyeti*	Group 3	Group 3	✓	✓	✓	✓	✓	✓		
M Step 4	*D. souleyeti*	Group 3	Group 3	✓	✓	✓	✓	✓	✓		
M Step 4	*D. souleyeti*	Group 3	Group 3	✓	✓		✓	✓	✓		
M Step 4	*D. souleyeti*	Group 3	Group 3	✓	✓		✓	✓	✓		
M Step 4	*D. souleyeti*	Group 3	Group 3	✓	✓		✓	✓	✓		
M Step 4	*D. souleyeti*	Group 3	Group 3	✓			✓	✓	✓		
M Step 4	*D. souleyeti*	Group 3	Group 3	✓	✓		✓	✓	✓		
M Step 4	*D. souleyeti*	Group 3	Group 3	✓	✓	✓	✓	✓	✓		
M Step 4	*D. souleyeti*	Group 3	Group 3	✓	✓		✓	✓	✓		
M Step 4	*D. souleyeti*	Group 3	Group 3	✓	✓		✓	✓	✓		
M Step 4	*D. souleyeti*	Group 3	Group 3	✓	✓	✓	✓	✓	✓		
M Step 4	*D. souleyeti*	Group 3	Group 3	✓	✓		✓	✓	✓		
M unknown	*D. souleyeti*	Amb.	Unkn.	✓	✓		✓	✓			
M unknown	*D. souleyeti*	Amb.	Unkn.	✓	✓		✓				
M Step 4	*D. souleyeti*	Group 3	Group 3	✓	✓	✓	✓	✓	✓		
M unknown	*D. souleyeti*	Amb.	Unkn.	✓	✓		✓	✓			
M Step 4	*D. souleyeti*	Group 3	Group 3	✓	✓	✓	✓	✓	✓		
M Step 4	*D. souleyeti*	Group 3	Group 3	✓	✓	✓	✓	✓	✓		
M Step 4	*D. souleyeti*	Group 3	Group 3	✓	✓	✓	✓	✓	✓		
M Step 4	*D. souleyeti*	Group 3	Group 3	✓	✓	✓	✓	✓	✓		
M Step 4	*D. souleyeti*	Group 3	Group 3	✓	✓		✓	✓	✓		
M Step 4	*D. souleyeti*	Group 11	Group 11	✓	✓	✓	✓				
M Step 2	*D. striata*	Group 5	Group 5	✓	✓	✓	✓	✓			
M unknown	*D. striata*	N.A.	Unkn.	✓			✓	✓			
M Step 2	*D. striata*	Group 5	Group 5	✓			✓	✓	✓		
M Step 2	*D. striata*	Group 5	Group 5	✓	✓	✓	✓	✓	✓		
M Step 2	*D. striata*	Group 5	Group 5	✓	✓	✓	✓	✓	✓		
M Step 2	*D. striata*	Group 5	Group 5	✓	✓	✓	✓	✓	✓		
M Step 2	*D. striata*	Group 5	Group 5	✓	✓	✓	✓	✓			
M Step 2	*D. striata*	Group 5	Group 5	✓			✓	✓	✓		
M Step 4	*D. triangulata*	Group 8	Group 8	✓			✓	✓	✓		
M Step 4	*D. triangulata*	Group 11	Group 11	✓			✓	✓	✓		
M unknown	*D. triangulata*	Amb.	Unkn.	✓	✓		✓	✓	✓		
M unknown	*D. triangulata*	Amb.	Unkn.	✓	✓	✓	✓	✓	✓		
M Step 4	*D. triangulata*	Group 5	Group 5	✓	✓	✓	✓	✓	✓		
M unknown	*D. triangulata*	Amb.	Unkn.	✓	✓		✓	✓	✓		
M Step 4	*D. triangulata*	Group 5	Group 5	✓	✓	✓	✓	✓	✓		
M Step 4	*D. triangulata*	Group 11	Group 11	✓	✓	✓	✓	✓	✓		
M Step 4	*D. triangulata*	Group 11	Group 11	✓	✓	✓	✓	✓			
M Step 4	*D. triangulata*	Group 5	Group 5	✓			✓	✓	✓		
M Step 4	*D. triangulata*	Group 5	Group 5	✓	✓		✓	✓	✓		
M Step 4	*D. v. vanutrechti*	Group 11	Group 11	✓	✓	✓	✓	✓	✓		
M unknown	*D. v. vanutrechti*	Amb.	Unkn.	✓	✓		✓	✓			
M unknown	*D. v. vanutrechti*	Amb.	Unkn.	✓	✓		✓	✓	✓		
F outgroup	*Cavolinia uncinata*									MF048915	MF048968
F outgroup	*Cavolinia uncinata*									MF048916	MF048969
F outgroup	*Cavolinia uncinata*									MF048917	MF048970
F outgroup	*Cavolinia uncinata*									MF048918	MF048971

TABLE S2. Overview of 24 morphological *Diacavolinia* taxa according to Van der Spoel et al. (1993) and holo- and paratypes used in this study.

Diacavolinia species	Type locality	Type stored at	Types included in this study	Taxonomic description/ amendation
D. angulata	Indian	Laboratoire de Malacologie, Muséum d'Histoire Naturelle, Paris		Gray, 1850; Souleyet, 1852
D. aspina	Indian: 2°57'S 99°36'E	ZMUC, Copenhagen; NBC, Leiden		Van der Spoel et al., 1993
D. atlantica	Atlantic: 28°23.5'N 29°55.9'W	NBC, Leiden	Holotype	Van der Spoel et al., 1993
D. bandaensis	Pacific: 4°36.4'S 130°21.7'E	NBC, Leiden	Holotype, Paratypes	Van der Spoel et al., 1993
D. bicornis	Indian: 3°45'S 56°33'E	ZMUC, Copenhagen; NBC, Leiden	Paratypes	Van der Spoel et al., 1993
D. constricta	Atlantic: 28°27.5'N 29°51.2'W	NBC, Leiden	Holotype	Van der Spoel et al., 1993
D. deblainvillei	Atlantic: 38°45'N 72°20'W	NBC, Leiden	Holotype, Paratypes	Van der Spoel et al., 1993
D. deshayesi	Atlantic: 5°06'N 51°35'W	ZMUC, Copenhagen; NBC, Leiden	Paratypes	Van der Spoel et al., 1993
D. elegans	Pacific: 3°40.5'N 137°53'E	ZMUC, Copenhagen; NBC, Leiden	Paratypes	Van der Spoel et al., 1993
D. flexipes	Red Sea	Department of Zoology, University of Tel Aviv, ZMA		Van der Spoel, 1971; Van der Spoel et al., 1993
D. grayi	Pacific: 5°22.8'S 130°05'E	NBC, Leiden	Holotype, Paratypes	Van der Spoel et al., 1993
D. limbata f. *africana*	Atlantic: 29°48.1'N 29°57.5'W	NBC, Leiden	Holotype, Paratypes	D'Orbigny, 1836; Van der Spoel et al., 1993
D. limbata f. *limbata*	Atlantic: between 24-22°N and 30-33°W	Laboratoire de Malacologie, Muséum d'Histoire Naturelle, Paris		D'Orbigny, 1836
D. longirostris	Atlantic: 22°N *or* S	Could not be located		De Blainville, 1821
D. mcgowani	Pacific: 6°49'N 80°25'W	ZMUC, Copenhagen		Van der Spoel, 1973; Van der Spoel et al., 1993
D. ovalis	Atlantic: 38°50'N 72°25'W	NBC, Leiden	Holotype	Van der Spoel et al., 1993
D. pacifica	Pacific: 6°29.9'S 131°09.2'E	NBC, Leiden	Holotype, Paratypes	Van der Spoel et al., 1993
D. robusta	Pacific: 2°52'N 87°38'W	ZMUC, Copenhagen; NBC, Leiden		Van der Spoel et al., 1993
D. souleyeti	Indian: 2°57'S 99°36'E	ZMUC, Copenhagen; NBC, Leiden		Van der Spoel et al., 1993
D. strangulata	Probably in the Indo-Pacific	Could not be located		Deshayes, 1823
D. striata	Indian: 2°57'S 99°36'E	ZMUC, Copenhagen; NBC, Leiden	Paratypes	Van der Spoel et al., 1993
D. triangulata	Pacific: Philippine Sea	NBC, Leiden	Holotype, Paratypes	Van der Spoel et al., 1993
D. vanutrechti f. *meisenheimeri*	Pacific: 18°53'S 163°02.5'W	ZMUC, Copenhagen		Van der Spoel et al., 1993
D. vanutrechti f. *vanutrechti*	Pacific: 14°37'N 119°52'E	ZMUC, Copenhagen; NBC, Leiden	Paratypes	Van der Spoel et al., 1993

TABLE S3. Genetic distances (K2P + Γ) between *Diacavolinia* COI haplotypes and 28S alleles per group identified in this study, including *Cavolinia uncinata*. *N* indicates individuals included.

28S	Group 1 Atlantic	Group 3 Indo-Pacific	Group 4 Indo-Pacific	Group 5 Pacific	Group 6 Pacific	Group 7 Indian	Group 12 Pacific	Group 13 Indian	*C. uncinata* Atlantic	*C. uncinata* Pacific	COI
Between groups	0.0135	0.0036	-	0.0629	-	-	0.0083	-	0.0016	0.0077	**Within groups**
Group 1 (*N* = 35)		0.1859	-	0.4064	0.2559	0.2720	0.1903	0.2103	0.2506	0.2400	Group 1 (*N* = 56)
Group 3 (*N* = 17)	0.0035		-	0.4247	0.2419	0.2786	0.2070	0.2386	0.2590	0.2653	Group 3 (*N* = 21)
Group 4 (*N* = 78)	0.0241	0.0239		-	-	-	-	-	-	-	
Group 5 (*N* = 6)	0.0241	0.0263	0.0026		0.4162	0.4379	0.3926	0.4106	0.4052	0.3786	Group 5 (*N* = 6)
Group 6 (*N* = 1)	0.0034	0.0026	0.0242	0.0271		0.2912	0.2516	0.2655	0.2657	0.2559	Group 6 (*N* = 1)
Group 7 (*N* = 1)	0.0036	0.0017	0.0249	0.0271	0.0033		0.2395	0.2760	0.3078	0.3058	Group 7 (*N* = 1)
	-	-	-	-	-	-		0.1961	0.2415	0.2182	Group 12 (*N* = 3)
	-	-	-	-	-	-	-		0.1914	0.1832	Group 13 (*N* = 1)
C. unc. Atl (*N* = 2)	0.0450	0.0452	0.0465	0.0464	0.0460	0.0460	-	-		0.1082	*C. unc.* Atl (*N* = 2)
C. unc. Pac (*N* = 2)	0.0482	0.0490	0.0503	0.0495	0.0497	0.0497	-	-	0.0073		*C. unc.* Pac (*N* = 2)
Within groups	0.0011	0.0017	0.0005	0.0000	-	-	-	-	0.0033	0.0000	**Between groups**

TABLE S4. Overview of *Diacavolinia* groups identified in this study following the integrative taxonomic steps outlined in FIGURE 1. The Linear Discriminant Analysis (LDA) accuracy depicts the correspondence between geometric morphometric and genetic data (Step 1, S1), the correspondence between morphospace position of holo- and paratypes and their LDA identification (Step 2, S2), or the correspondence between estimated morphospace position and their LDA identification (Step 3, S3) following the morphometric assignment criteria (see text). Step 4 (S4) depicts the numbers of remaining specimens assigned to groups identified in Steps 1-3 using LDA. A = Atlantic; P = Pacific; I = Indian Ocean. See FIGURE 8 for taxonomic implications.

Assignment	Specimens				Stations	Steps 1 and 5	
Group (Evidence: G = Genetic; M = Morphometric)	Total	Atlantic	Pacific	Indian	Total	Ocean (*N* specimens)	LDA accuracy (*N*)
Atlantic							
Group 1 (G,M) Integrative species	276	276	0	0	58	S1: Atlantic (65) Atlantic sequences from Maas et al. (1993) (53)	100% (42/42)
Group 2 (M) Morphospecies	51	51	0	0	12		
Indo-Pacific							
Group 3 (G,M) Integrative species	100	0	66	34	27	S1: Pacific (15) S1: Indian (6)	92.9% (13/14)
Group 4 (G,M) Integrative species	172	0	123	49	35	S1: Pacific (75) S1: Indian (3)	95.9% (47/49)
Group 5 (G,M) Integrative species	64	0	48	16	18	S1: Pacific (6)	100% (5/5)
Group 6 (G,M) Integrative species	1	0	1	0	1	S1: Pacific (1)	
Group 7 (G,M) Integrative species	1	0	0	1	1	S1: Indian (1)	
Group 8 (M) Morphospecies	49	0	48	1	5		
Group 9 (M) Morphospecies	3	0	3	0	1		
Group 10 (M) Morphospecies	12	0	12	0	2		
Group 11 (M) Morphospecies	19	0	1	18	7		
Group 12 (G) Possible species	3	0	3	0	1	S5: Pacific sequences from Maas et al. (1993) identified as *D. vanutrechti* (3)	
Group 13 (G) Possible species	1	0	0	1	1	S5: Indian (1)	
Unknown	217	47	116	54			

Steps 2 and 3 Species according to Van der Spoel et al. (1993) (Ocean, *N* specimens)	LDA accuracy (*N*)	Step 4 Species according to Van der Spoel et al. (1993) (Ocean, *N* specimens)
S2: *D. deblainvillei* (A, 18) S2: *D. deshayesi* (A, 8) S2: *D. constricta* (A, 1) S2: *D. ovalis* (A, 1)	96.4% (27/28)	*D. deshayesi* (A, 30); *D. constricta* (A, 23); *D. longirostris* (A, 18); *D. angulata* (A, 15); *D. vanutrechti vanutrechti* (A, 15); *D. deblainvillei* (A, 14); *D. elegans* (Atl, 12); *D. strangulata* (A, 11); *D. ovalis* (A, 6); *D. limbata limbata* (A, 3); *D. vanutrechti meisenheimeri* (A, 2); *D. bicornis* (A, 1); Fresh specimens (A, 33)
S2: *D. limbata africana* (A, 5) S2: *D. atlantica* (A, 1)	100% (6/6)	*D. limbata limbata* (A, 31); *D. vanutrechti meisenheimeri* (A, 7); *D. atlantica* (A, 3); *D. constricta* (A, 2); *D. deshayesi* (A, 1); *D. strangulata* (A, 1)
S2: *D. vanutrechti vanutrechti* (P, 3) S2: *D. elegans* (P, 1)	75% (3/4)	*D. souleyeti* (I, 25); *D. vanutrechti vanutrechti* (P, 18); *D. vanutrechti meisenheimeri* (P, 16); *D. flexipes* (P, 13); *D. bicornis* (I, 2); *D. limbata limbata* (I, 1) *D. pacifica* (P, 11; I, 22); *D. angulata* (P, 17; I, 14); *D. grayi* (P, 5; I, 10); Fresh specimens (P, 15)
S2: *D. grayi* (P, 8); S2: *D. striata* (I, 7) S2: *D. bandaensis* (P, 6); S2: *D. pacifica* (P, 2); S2: *D. bicornis* (I, 2)	64% (16/25)	*D. pacifica* (P, 9; I, 2); *D. mcgowani* (P, 8); *D. elegans* (P, 4; I, 1); *D. triangulata* (P, 1; I, 4); *D. grayi* (P, 3); *D. angulata* (P, 1)
S2: *D. triangulata* (P, 16)	100% (16/16)	*D. longirostris* (P, 20); *D. pacifica* (P, 3); *D. triangulata* (P, 9; I, 1)
S3: *D. strangulata* (P, 3)	100% (3/3)	
S3: *D. mcgowani* (P, 7); S3: *D. longirostris* (P, 5)	100% (12/12)	
S3: *D. longirostris* (I, 11)	100% (11/11)	*D. elegans* (P, 1); *D. souleyeti* (I, 3); *D. triangulata* (I, 3); *D. vanutrechti vanutrechti* (I, 1)
		D. aspina (P, 1: ambiguous); *D. robusta* (Not available); *D. flexipes* (None from Type location: Red Sea)

6

Diversity and abundance of pteropods and heteropods along a latitudinal gradient across the Atlantic Ocean

Alice K. Burridge, Erica Goetze, Deborah Wall-Palmer,
Serena L. Le Double, Jef Huisman & Katja T.C.A. Peijnenburg

Abstract

Shelled pteropods and heteropods are two independent groups of holoplanktonic gastropods that are potentially good indicators of the effects of ocean acidification. Although insight into their ecology and biogeography is important for predicting species-specific sensitivities to ocean change, the species abundances and biogeographical distributions of pteropods and heteropods are still poorly known. Here, we examined abundance and distribution patterns of pteropods (euthecosomes, pseudothecosomes, gymnosomes) and heteropods at 31 stations along a transect from 46°N to 46°S across the open waters of the Atlantic Ocean (Atlantic Meridional Transect cruise AMT24). We collected a total of 7312 pteropod specimens belonging to at least 31 species. Pteropod abundances were low north of 40°N with <15 individuals per 1000 m^3, varied between 100 and 2000 ind./1000 m^3 between 30°N and 40°S, and reached >4000 ind./1000 m^3 just south of 40°S. This accounted for an estimated biomass of 3.2 mg m^{-3} south of 40°S and an average of 0.49 mg m^{-3} along the entire transect. Species richness of pteropods was highest in the stratified (sub)tropical waters between 30°N and 30°S, with a maximum of 15 species per station. The biogeographical distribution of pteropod assemblages inferred by cluster analysis was largely congruent with the distribution of Longhurst's biogeochemical provinces. Some pteropod species distributions were limited to particular oceanographic provinces, for example, subtropical gyres (e.g., *Styliola subula*) or warm equatorial waters (e.g., *Creseis virgula*). Other species showed much broader distributions between ~35°N and ~35°S (e.g., *Limacina bulimoides* and *Heliconoides inflatus*). We collected 1812 heteropod specimens belonging to 18 species. Highest heteropod abundances and species richness were found between 30°N and 20°S, with up to ~700 ind./1000 m^3 and a maximum of 14 species per station. Heteropods were not restricted to tropical and subtropical waters, however, as some taxa were also relatively abundant in subantarctic waters. Given the variation in distribution patterns among pteropod and heteropod species, it is likely that species will differ in their response to ocean changes.

Keywords:

Pteropods, Heteropods, Atlantic Ocean, Biogeography, Species diversity, Abundance, Biomass, Ocean acidification

This chapter was published as:

Burridge A.K., Goetze E., Wall-Palmer D., Le Double S., Huisman J., Peijnenburg K.T.C.A., in press. Diversity and abundance of pteropods and heteropods along a latitudinal gradient across the Atlantic Ocean. Progress in Oceanography, DOI: 10.1016/j.pocean.2016.10.001.

Introduction

Shelled pteropods and heteropods are holoplanktonic gastropods with aragonite shells that are vulnerable to the effects of ocean acidification (e.g., Bednaršek and Ohman, 2015; Gattuso et al., 2015; Wall-Palmer et al., 2016a). They are common components of the marine zooplankton and have highly diverse evolutionary histories, life strategies and morphologies. Through production of aragonitic shells, they are involved in biogenic carbon export from the surface to the deep ocean (Bednaršek et al., 2012a). However, especially in the open Atlantic Ocean, their species diversity and abundance are still poorly understood (e.g., Bé and Gilmer, 1977; Van der Spoel and Heyman, 1983; Richter and Seapy, 1999; Van der Spoel and Dadon, 1999; Bednaršek et al., 2012a). The pteropod distribution maps from Bé and Gilmer (1977) and Van der Spoel and Heyman (1983) are based on manual estimations of distributions based on synthesized presence-only data, precluding any quantitative comparisons within and between ocean basins. Gaining more insight into the current diversity and distribution of planktonic gastropods is important for measuring future changes in diversity and distribution, and for predicting species-specific sensitivities to ocean changes. New data on abundance will help estimate the biomass of holoplanktonic gastropods, about which little is known for many regions, including the open Atlantic Ocean. This is important for their incorporation as a plankton functional type in ecosystem models and to estimate their contribution to ocean carbon export in biogeochemical models (Bednaršek et al., 2012a).

The oceans appear to have more biodiversity and less homogeneous species communities than has long been assumed or expected (Angel, 1993; Norris, 2000). Biogeochemical provinces of the Atlantic Ocean provide a diverse range of ecological niches as well as barriers to dispersal for zooplankton taxa (e.g., Peijnenburg and Goetze, 2013; Andrews et al., 2014; Goetze et al., in press). For example, in *Cuvierina* pteropods, *C. cancapae* is endemic to the equatorial Atlantic and *C. atlantica* is restricted to the northern and southern subtropical gyres (Janssen, 2005; Burridge et al., 2015: Thesis chapter 3). Endemism of evolutionary lineages in the equatorial Atlantic is a pattern also observed in other plankton groups (e.g., Hirai et al., 2015; Goetze et al., in press). The species composition of planktonic ostracod assemblages also is more similar within ocean provinces (e.g., northern temperate, northern subtropical gyre and equatorial regions) than between provinces (Angel et al., 2007). Ocean warming and acidification may cause shifting species distributions in the plankton (e.g., Beaugrand et al., 2009; Provan et al., 2009), as well as (local) extinctions or adaptation to new conditions (e.g., Collins, 2012; Lohbeck et al., 2012, 2014).

Pteropods are a group of heterobranch gastropods (Jörger et al., 2010), a superorder comprised of the orders Thecosomata, also referred to as 'sea butterflies', and Gymnosomata, or 'sea angels' that play an important role in marine food webs (Lalli and Gilmer, 1989; Pierrot-Bults and Peijnenburg, 2015). According to the World Register of Marine Species (WoRMS), a total of 83 extant thecosome

species and 43 gymnosome species occur worldwide, and many fossil species also have been described (Janssen and Peijnenburg, 2014). Most taxa are between 0.05 and 2 cm in size and occur in the upper 300 m of the global ocean, although some species occur at bathypelagic depths (Bé and Gilmer, 1977; Van der Spoel and Dadon, 1999). Many species are known to be vertical migrators that move to shallower depths at night (Bé and Gilmer, 1977). Most thecosomes have aragonite shells, which they maintain as adults. They include the cavoliniid euthecosomes with uncoiled, bilaterally symmetrical shells (52 species), limaciniid euthecosomes with coiled shells (eight species), and pseudothecosomes, with coiled shells or a semi-soft pseudoconch without an aragonitic shell (23 species; Van der Spoel and Dadon, 1999). All thecosomes produce and deploy mucus webs to feed on microplankton (Gilmer and Harbison, 1986). Gymnosomes have larval shells, but shed them as they grow into adults. They are predators that feed exclusively or primarily on thecosomes (Lalli and Gilmer, 1989).

Heteropods or 'sea elephants', formally known as Pterotracheoidea, are a group of Caenogastropoda. According to WoRMS, this group consists of 35 extant species that occur in moderately low abundance in the global ocean, primarily at tropical and subtropical latitudes (Richter and Seapy, 1999). However, there is evidence that some taxa thrive in cold waters, e.g., south of Australia and during glacial periods in the geological past (Howard et al., 2011; Wall-Palmer et al., 2014). The vertical distribution of heteropods is not well understood, but they have been found to live at epipelagic and upper mesopelagic depths (e.g., Lalli and Gilmer, 1989; Richter and Seapy, 1999; Ossenbrügger, 2010). Heteropods are visual predators with well-developed eyes. To the extent that it is known, adults feed on other zooplankton and small fishes, and juveniles feed on phytoplankton and small zooplankton (Lalli and Gilmer, 1989; Seapy et al., 2003). The three heteropod families, Atlantidae, Carinariidae and Pterotracheidae, are highly diverse in size and body form. The Atlantidae have the highest species diversity (21 species; one additional species described by Wall-Palmer et al., 2016b), are generally less than 1 cm in size, are the least efficient swimmers of all heteropods, and can retract their bodies entirely into their keeled, dextrally coiled aragonite shells (Seapy et al., 2003). They are the most thoroughly sampled heteropod group in the southern subtropical Atlantic, with species densities of 410-1710 individuals per 1000 m^3 accounting for 80-99% of the total sampled heteropod community (Richter and Seapy, 1999). The Carinariidae (9 species) have a cylindrical body that is very large in relation to their shells, and can be as long as 50 cm (Lalli and Gilmer, 1989). The Pterotracheidae (5 species) only have larval shells, and have an elongated body that can reach a length of 33 cm in the Atlantic Ocean (Richter and Seapy, 1999). The Carinariidae and Pterotracheidae are thought to be more efficient swimmers than Atlantidae because of the relatively small body size and large shell of the latter group (Lalli and Gilmer, 1989).

In this study, we quantitatively sampled pteropods and heteropods from 46°N to 46°S along a transect of >12,000 km across the Atlantic Ocean, during Atlantic

Meridional Transect (AMT) cruise 24. The AMT is a multidisciplinary programme aimed at understanding biological, chemical, and physical oceanographic processes, with annual transect sampling across the Atlantic Ocean (Rees et al., 2015). Here we (1) assess species distributions, abundances and biomass of pteropods and heteropods at 31 sampling stations along the transect, (2) estimate biogeographical trends in species diversity, and (3) compare inter-station similarities in community structure with Longhurst's (1998) biogeochemical provinces. To our knowledge, this is the first paper to report quantitative abundance data of pteropods and heteropods across a large-scale latitudinal gradient in the Atlantic.

Methods

Sampling and sorting

Holoplanktonic gastropods were collected during the AMT24 expedition (United Kingdom to Falkland Islands) between 46°23'N and 46°05'S from September 28th to October 30th, 2014 (Table 1). We conducted oblique tows at night from the upper 311 (216-401) m at 31 stations, representing the epipelagic and upper mesopelagic zones. The stations were assigned to biogeochemical provinces according to Longhurst (1998) and Reygondeau et al. (2013; Table 1). We used a bongo net of 0.71 m diameter and 200 µm mesh size with a General Oceanics flowmeter (2030RC) mounted in the mouth of the net to measure the volume of seawater filtered during the tow. The flowmeter was calibrated both pre- and post-cruise. Bulk zooplankton samples were quantitatively split using a Folsom plankton splitter and one or more quantitative fractions were immediately preserved in 96% ethanol. The alcohol was replaced within 24 h of collection, and samples were stored at –20°C. Pteropods and heteropods were sorted from 25% or 50% of the quantitative zooplankton samples, depending on the bulk sample volume (Table 1).

Pteropod and heteropod material was sorted by species and counted after the expedition. The majority of taxa could be identified to species morphologically. However, we counted individuals in larval or juvenile growth stages separately if they could not be assigned to species because they lacked the morphological characters to distinguish between closely related species. This ambiguity occurred for juvenile *Cuvierina* euthecosomes (Bé et al., 1972), larval stages of *Diacria* and *Cavolinia* euthecosomes, *Peracle* pseudothecosomes, as well as larval stages of some atlantid heteropods. Some other taxa were registered only at the genus level because of their complex and unresolved taxonomies, including *Diacavolinia* euthecosomes, *Corolla* and *Gleba* pseudothecosomes, and *Pterotrachea* heteropods (Van der Spoel et al., 1993; Richter and Seapy, 1999; Van der Spoel and Dadon, 1999). Two formae of the euthecosome *Clio pyramidata*, forma *lanceolata* and forma *pyramidata*, were recorded together as *C. pyramidata* because these varieties were not found to be genetically distinct (Jennings et al., 2010), and likely represent a single species. We identified gymnosomes to order because we could not identify them to species following fixation in ethanol, and excluded them from

Table 1. Overview of sampling locations and tow information along AMT24 and corresponding CTD stations, surface temperatures and maximum chlorophyll *a* concentrations from the upper 300 m. The biogeochemical provinces of the sampling stations are based on Longhurst (1998) and Reygondeau et al. (2013): NADR (North Atlantic drift), NAST E (Northeast Atlantic subtropical gyre), NAST W (Northwest Atlantic subtropical gyre), NATR (North Atlantic tropical gyre), WTRA (Western tropical Atlantic), SATL (South Atlantic gyre), SSTC (Southern subtropical convergence), SANT (Subantarctic water ring), FKLD (Southwest Atlantic shelves).

Station	Sampling date	Latitude	Longitude	Max. depth [m]	Sorted water volume [m^3] (% of total vol.)	Surface temperature (-10 m) [°C]	Maximum chlorophyll *a* [mg/m^3]	Longhurst province
1	2014-09-28	46°23'N	10°58'W	NR	483 (50%)	19.3	0.748	NADR
2	2014-09-29	44°05'N	14°54'W	297	567 (50%)	20.4	0.583	NAST E
3	2014-09-30	41°46'N	18°44'W	382	491 (50%)	19.8	0.518	NAST E
4	2014-10-01	39°25'N	22°29'W	274	669 (50%)	21.0	0.584	NAST E
5	2014-10-03	34°45'N	26°37'W	364	538 (50%)	23.7	0.262	NAST W
6	2014-10-04	31°18'N	27°44'W	319	621 (50%)	24.5	0.126	NATR
7	2014-10-05	27°30'N	28°53'W	328	611 (50%)	26.7	0.123	NATR
8	2014-10-06	24°03'N	29°54'W	258	693 (50%)	26.7	0.147	NATR
9	2014-10-07	20°27'N	29°16'W	274	754 (50%)	26.6	0.154	NATR
10	2014-10-08	17°49'N	28°42'W	294	320 (25%)	26.8	0.240	NATR-WTRA
11	2014-10-09	14°12'N	27°56'W	305	342 (25%)	28.1	0.381	WTRA
12	2014-10-10	10°47'N	27°12'W	323	569 (50%)	28.3	0.192	WTRA
13	2014-10-11	7°17'N	26°30'W	329	686 (50%)	28.9	0.292	WTRA
14	2014-10-12	3°48'N	25°47'W	364	596 (50%)	28.0	0.262	WTRA
15	2014-10-13	0°05'N	25°01'W	341	637 (50%)	26.0	0.435	WTRA
16	2014-10-14	3°53'S	25°02'W	339	328 (25%)	26.0	0.329	WTRA
17	2014-10-15	7°28'S	25°07'W	266	353 (25%)	25.6	0.258	WTRA-SATL
18	2014-10-16	11°02'S	25°03'W	292	358 (25%)	25.4	0.175	SATL
19	2014-10-17	14°40'S	25°04'W	311	345 (25%)	24.7	0.249	SATL
20	2014-10-18	18°19'S	25°05'W	283	368 (25%)	23.4	0.176	SATL
21	2014-10-20	20°51'S	25°05'W	309	352 (25%)	22.9	0.165	SATL
22	2014-10-21	24°27'S	25°03'W	323	335 (25%)	22.0	0.143	SATL
23	2014-10-22	27°46'S	25°01'W	260	370 (25%)	20.5	0.172	SATL
24	2014-10-23	31°20'S	26°06'W	330	334 (25%)	18.5	0.500	SATL
25	2014-10-24	34°11'S	27°13'W	NR	227 (25%)	16.7	0.342	SATL
26	2014-10-25	37°54'S	28°44'W	372	308 (25%)	14.0	0.377	SSTC
27	2014-10-26	40°07'S	30°55'W	216	438 (25%)	13.2	0.321	SSTC
28	2014-10-27	41°29'S	33°52'W	228	422 (25%)	12.0	0.449	SSTC
29	2014-10-28	43°01'S	37°08'W	253	372 (25%)	11.6	0.406	SSTC
30	2014-10-29	44°37'S	40°42'W	350	301 (25%)	8.8	0.485	SANT-FKLD
31	2014-10-30	46°05'S	44°12'W	401	277 (25%)	9.3	0.528	SANT-FKLD

many subsequent analyses. The ratio between the abundances of gymnosomes, if present, and thecosomes was calculated to estimate the potential predation intensity by gymnosomes on thecosomes across the AMT24 transect. This ratio was calculated only for stations with more than 10 pteropod specimens.

Species diversity, abundance and biomass

To summarize the diversity of thecosomes and heteropods along AMT24, we calculated species richness *R*, Shannon-Wiener's diversity index *H'* and Pielou's evenness index *J'* at each station. Shannon-Wiener's *H'* is commonly used as a measure for species diversity in a community and accounts for abundance and evenness of the species present (Shannon and Weaver, 1949; Spellerberg and Fedor, 2003):

$$H' = -\sum_{i=1}^{R} (p_i \ln p_i)$$

In this formula, *R* is the species richness or total number of species, and p_i is the fraction of individuals belonging to species *i* relative to the total number of specimens. Pielou's evenness *J'* is derived from *H'* and quantifies how close in numbers or abundance each species is in an environment, given that there are at least two species present per location (Pielou, 1967):

$$J' = \frac{H'}{\ln R}$$

To assess trends in species diversity and abundance of thecosomes and heteropods, we analyzed our gastropod diversity and abundance data in relation to oceanographic data obtained during AMT24. Abundances of pteropods and heteropods were quantified in terms of individuals per 1000 m^3 of seawater filtered. Ocean temperature and chlorophyll *a* concentrations along AMT24 were obtained using a Sea-Bird Electronics 3P Temperature Sensor and a CTG Aquatracka MKIII Fluorometer. Oceanographic data were calibrated and archived by the British Oceanographic Data Centre (BODC). Sea surface temperature was measured at 10 m depth. Contour plots of temperature and chlorophyll *a* concentration in the upper 300 m were prepared in Ocean Data View 4 (Schlitzer, 2015). This depth range represents the zooplankton tow depth as well as the depth range of most pteropod and heteropod species. We examined whether species richness *R* showed a relationship with sea surface temperature and maximum chlorophyll *a* in the upper 300 m using regression analysis in the software package PAST 2.17 (Hammer et al., 2001).

We calculated the pteropod biomass in terms of total dry weight from the abundances and shell sizes using mostly genus-specific formulae from Bednaršek et al. (2012a). The formulae are presented in Table S1. These were only available for euthecosomes and gymnosomes, so we did not include shelled pseudothecosomes (*Peracle* species) and heteropods in our calculations. These formulae use estimated averages of shell length and width. Because some suggested size averages clearly overestimated the observed sizes along AMT24, we adjusted them to represent the collected speci-

mens along AMT24 (Table S1). We did this for *Clio cuspidata*, *C. pyramidata*, *C. pyramidata antarctica*, *C. pyramidata sulcata*, *Cuvierina* sp., *Styliola subula*, *Hyalocylis striata* and gymnosomes. Average sizes of *Clio recurva*, *Cavolinia gibbosa* and *Diacavolinia* were not indicated by Bednaršek et al. (2012a), so we used our own size estimates as well as their genus-level formulae to estimate their dry weight (using the *Cavolinia* formula for *Diacavolinia*). We used the formula for *Limacina helicina* (Bednaršek et al., 2012b) for all coiled euthecosomes. Bednaršek et al. (2012b) estimated that ~27% of the total carbon of *L. helicina antarctica* consisted of inorganic carbon.

Species composition

For subsequent analyses of inter-station similarities of species composition, sampling completeness and relative species dominance, we reduced our abundance dataset to exclude small sample sizes as follows. We excluded all stations with fewer than 10 thecosomes or heteropods, all larval and juvenile specimens that could be assigned to two or more species, and all identified species that only occurred at one selected station. The stations that were excluded from analyses of thecosome species composition were 1-4 and 31 because there were fewer than 10 specimens that could be identified to species or genus level. The thecosome species or genera that were excluded because they were observed at only one station were *Cavolinia gibbosa*, *Clio recurva*, *Diacria major*, *Gleba* and *Corolla*. *Cuvierina* juveniles and adults were binned into a single genus-level group because upon exclusion of the juveniles there would not be enough specimens (one adult: *Cuvierina atlantica*). For heteropods, we excluded stations 1-5, 12, 22, 24-26 and 30-31; also *Atlanta oligogyra* was excluded.

To examine whether the distributions of distinct species assemblages correspond with the distribution of Longhurst's (1998) biogeochemical provinces as defined by biogeochemistry and ecosystem dynamics, we quantified and visualized inter-station similarities of species composition and identified key species. For inter-station comparisons we performed a hierarchical cluster analysis, similarity profile analysis (SIMPROF), and non-metric multidimensional scaling analysis (nMDS) in PRIMER 6, without a priori assumptions (Clarke, 1993; Clarke and Warwick, 2001; Clarke and Gorley, 2006). To perform cluster analysis, SIMPROF and nMDS, we standardized and transformed (log [x + 1]) the abundance data and then calculated a Bray-Curtis similarity matrix. For the cluster analysis we used the group average setting. The significance of the clusters was tested with SIMPROF analyses using 1000 permutations and a significance level of $p < 0.05$. The nMDS ordinations were performed with 25 restarts. Furthermore, we created rank abundance curves based on the thecosome species abundances at each station in order to assess patterns of dominance across ocean biomes.

To assess sampling completeness, we created sample-based as well as individual-based rarefaction curves for thecosomes and heteropods in Primer 6 (Clarke and Gorley, 2006) and PAST 2.17 (Hammer et al., 2001). The sample-based curves were based on the Jacknife 2 index (Gotelli and Colwell, 2010) and only included non-transitional stations that belong to distinct biogeochemical provinces.

Results

Species abundance, biomass and diversity

We counted and identified a total of 7312 pteropods across all stations on the transect, traversing the northern temperate zone, the eastern side of the northern subtropical gyre, the equatorial upwelling zone, the southern subtropical gyre, the southern subtropical convergence and the northernmost part of the subantarctic (Figure 1A; Table 1). Among the pteropod specimens, there were 1028 uncoiled and 5980 coiled euthecosomes, 230 pseudothecosomes and 74 gymnosomes. Pteropod abundances were low (<15 ind./1000 m^3) north of 40°N and they were absent from station 3. Their abundance varied between 100 and 2000 ind./1000 m^3 between 30°N and 40°S. Abundances were highest at stations 27-29, just south of 40°S, with a maximum abundance of >4000 ind./1000 m^3 at station 28 (Figures 1B,C and 2A; Table S2). Coiled euthecosomes were particularly abundant in this high productivi-

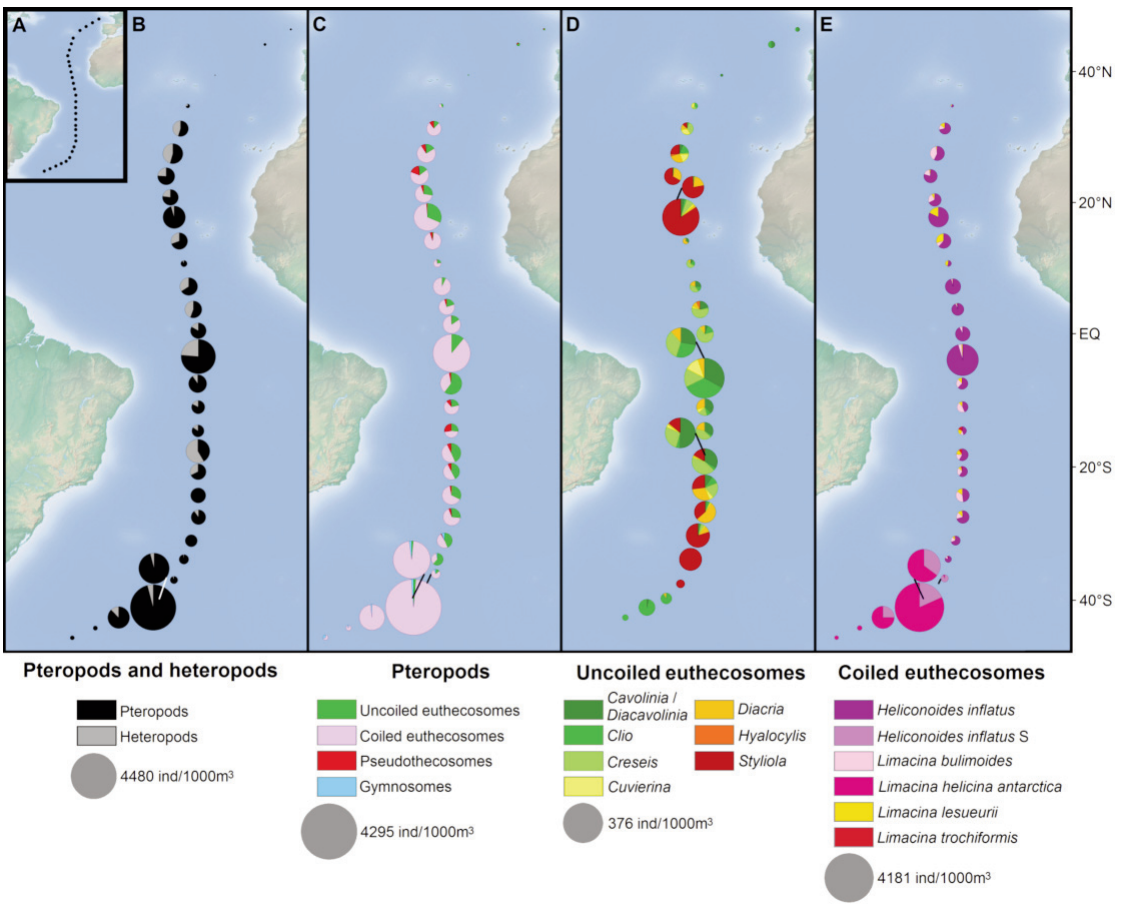

Figure 1. (A) Overview of pteropod and heteropod sampling locations along Atlantic Meridional Transect 24. (B-E) Distribution of (B) pteropods and heteropods, (C) euthecosome, pseudothecosome and gymnosome pteropods, (D) genera of uncoiled euthecosomes and (E) species of coiled euthecosomes along Atlantic Meridional Transect 24. The size of the pie charts is scaled according to the total abundance of the examined groups (size of the maximum abundance is shown in legend for each plot). True sampling locations are indicated with a white (B) or black (C-E) line if pie sizes did not allow placement at true locations.

ty area, while pseudothecosomes were more abundant in the subtropical gyres.

Gymnosomes feed almost exclusively on thecosomes. The ratio between gymnosomes, if present, and thecosomes (euthecosomes and pseudothecosomes) ranged from 0.005 to 0.019 in (sub)tropical waters between ~28°N and ~28°S (stations 7-23; Table S3). Gymnosomes were always present between ~32 and ~45°S (stations 24-30), with ratios between 0.012 and 0.091, suggesting higher potential predation intensity by gymnosomes on thecosomes at these southern stations than in (sub)tropical waters.

We observed taxa with strong preferences for particular oceanographic provinces, in particular among euthecosomes and pseudothecosomes (Figure 1C-E). In the equatorial province and in the subantarctic, the thecosome community consisted of one or two dominant species, and especially in the equatorial region a number of additional species occurred in low abundance. The relative species abundances were more equal in the subtropical gyres (Figure S1; abundances per species per station are listed in Table S2). Uncoiled euthecosomes were found between 46°N and 43°S (Figure 1D). Two *Clio* taxa, *C. pyramidata sulcata* and *C. pyramidata antarctica*, were restricted to the subantarctic, but were never dominant. *Clio pyramidata pyramidata/lanceolata* was found in all other regions along the transect. Key species that were most abundant in the subtropical gyres included *Creseis clava*, *Diacria danae* and *Styliola subula*, the latter of which was entirely absent in the equatorial upwelling region. Although *Cavolinia inflexa* was present across warm water environments, this species only occurred in high abundances in the southern gyre. *Creseis virgula* was found in the equatorial region and occurred nowhere else along the transect (Table S2). Coiled euthecosomes were found between 35°N and 46°S (Figure 1E). *Heliconoides inflatus* was abundant along the entire transect and did not show a clear preference for particular provinces. However, *H. inflatus* specimens in the subantarctic region were morphologically distinct from warm water *H. inflatus* specimens. Shells of the cold water form (listed as *H. inflatus* S herein) appeared to be coarser and thicker and, in contrast to the warm water form, they had a reddish hue along the whorls and aperture. *Limacina helicina antarctica* was dominant in subantarctic waters. *Limacina bulimoides* had a strong preference for the subtropical gyres, although it was also present in low numbers in the equatorial region. *Limacina lesueurii* was present throughout the warm water regions and *L. trochiformis* was only found in the southern gyre, though never in high numbers (maximum N = 9 at St. 20; Figure 1E). Most *Peracle* pseudothecosome species demonstrated a strong preference for the subtropical gyres (Figure 1C), but the

Figure 2. Basin-scale patterns of (A) pteropod abundance (individuals/1000 m^3), (B) pteropod biomass in terms of total dry weight (mg m^{-3}), (C) pteropod species richness R, (D) seawater temperature and (E) chlorophyll *a* concentrations in the upper 300 m of the water column, measured during Atlantic Meridional Transect cruise 24. Lines in (A) are interrupted in case of zero abundances. Because gymnosomes were not identified to the species level, they were not included in the calculation of species richness R in (C).

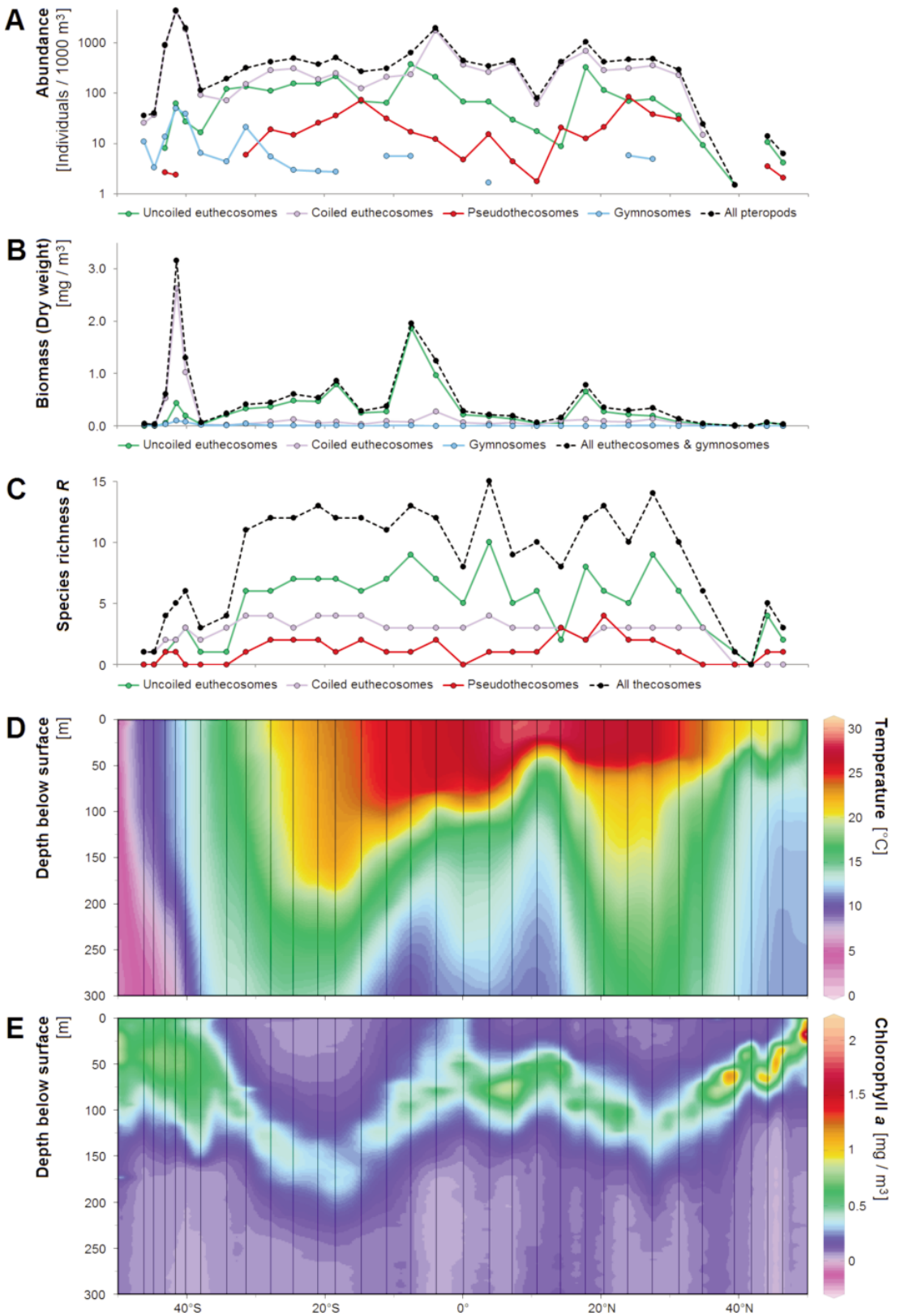
A
Abundance
[Individuals / 1000 m³]
1000
100
10
1
Uncoiled euthecosomes
Coiled euthecosomes
Pseudothecosomes
Gymnosomes
All pteropods
B
Biomass (Dry weight)
[mg / m³]
3.0
2.0
1.0
0.0
Uncoiled euthecosomes
Coiled euthecosomes
Gymnosomes
All euthecosomes & gymnosomes
C
Species richness R
15
10
5
0
Uncoiled euthecosomes
Coiled euthecosomes
Pseudothecosomes
All thecosomes
D
Depth below surface
[m]
0
50
100
150
200
250
300
Temperature [°C]
30
25
20
15
10
5
0
E
Depth below surface
[m]
0
50
100
150
200
250
300
40°S
20°S
0°
20°N
40°N
Chlorophyll a [mg / m³]
2
1.5
1
0.5
0

large, soft-bodied genera *Corolla* and *Gleba* were only found in cooler waters north of 40°N and south of 40°S in very low numbers (never more than $N = 2$ per station).

Areas with high chlorophyll *a* concentrations had the highest estimated pteropod biomass, except the northern temperate zone, where hardly any pteropods were captured (Figure 2B; Table S4). A total biomass of more than 3.1 mg m^{-3} in the upper ~300 m was reached in the southern subantarctic region, mainly caused by high abundances of *Limacina helicina antarctica* and *Heliconoides inflatus* S. Just south of the equator there was an estimated biomass of more than 1.9 mg m^{-3} because of high abundances of *Cavolinia inflexa* and *Clio pyramidata*. The median and average pteropod biomass across all stations along AMT24 was 0.28 mg m^{-3} and 0.49 mg m^{-3}, respectively.

The species richness of thecosomes was highest in the stratified (sub)tropical waters between ~30°N and ~30°S and was consistently high (11-13 species) in the southern gyre (Figure 2C,D), a pattern that was also evident from the Shannon-Wiener's diversity indices *H'* per station (Table S3). Uncoiled euthecosomes generally had a higher species richness than coiled euthecosomes and pseudothecosomes

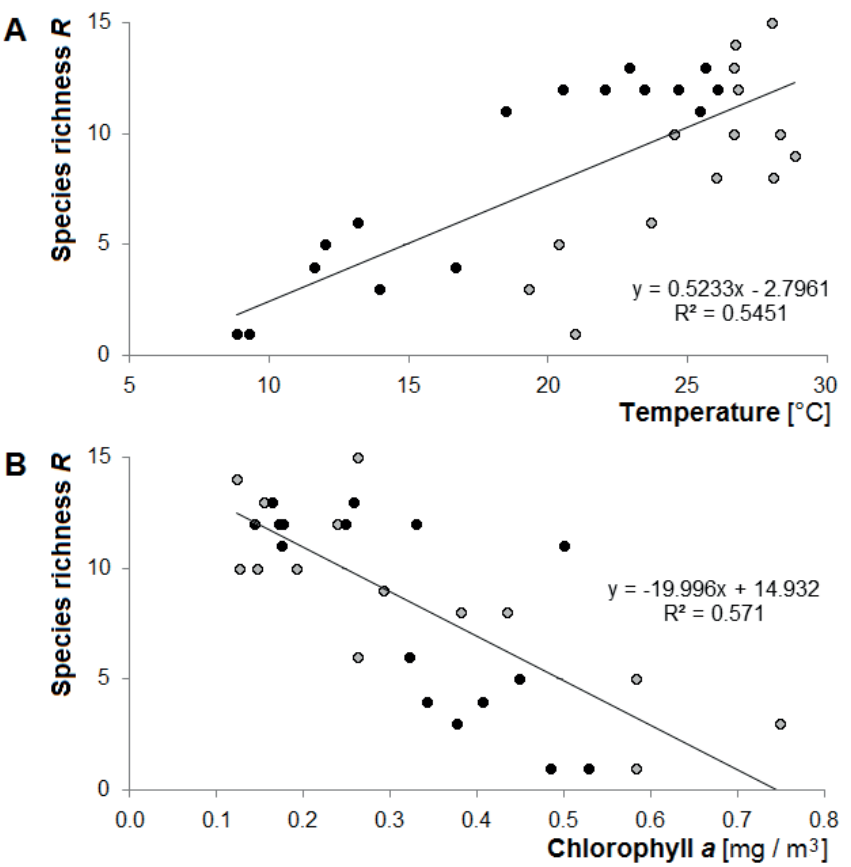

Figure 3. Relationships of species richness *R* of thecosome pteropods (euthecosomes and pseudothecosomes) with (A) sea surface temperature and (B) maximum chlorophyll *a* concentration in the upper 300 m of the water column. Lines are based on linear regression. Grey and black dots represent locations north and south of the equator, respectively.

(Figure 2C). Although most equatorial stations had slightly lower species richness than the gyre stations, the highest species richness (15 species) was observed close to the equator at station 14. Species richness showed a positive relationship with sea surface temperature (R^2 = 0.55; N = 30; p < 0.001; Figure 3A) and a negative relationship with chlorophyll *a* concentration at the deep chlorophyll maximum (R^2 = 0.57; N = 30; p < 0.001; Figure 3B). We note that sea surface temperature and chlorophyll *a* were only weakly correlated (R^2 = 0.28; N = 31; p < 0.01), and hence the degree of collinearity between these two explanatory variables was low. The species evenness *J'* was highest in the subtropical gyres, especially in the southern gyre (*J'* up to 0.84), when disregarding the high evenness values observed at the northern temperate stations 1, 2, and 5 because of their relatively low sample sizes. At equatorial stations 13-16 the evenness was lower (*J'* of 0.25-0.44) than in the gyres.

From the 1812 heteropods, a total of 1312 were atlantids, 325 were pterotracheids and 175 were carinariids. Heteropods were not found at stations 1-4 and 30-31. Highest heteropod species richness (up to 14 species) as well as abundances (maximum 704 ind./1000 m^3) were found in the (sub)tropical waters between ~30°N and ~20°S (Figure 4). A high abundance of heteropods (>100 ind./1000 m^3) was also found in the subantarctic region (Table S2). There were no clear patterns in species evenness along the transect except a lower evenness at stations 28-29 (*J'* of 0.10-0.37; Table S3).

Species composition

The cluster and SIMPROF analyses of thecosome species composition of the different stations along AMT24 resulted in six significant clusters (p < 0.05; Figure 5A). These

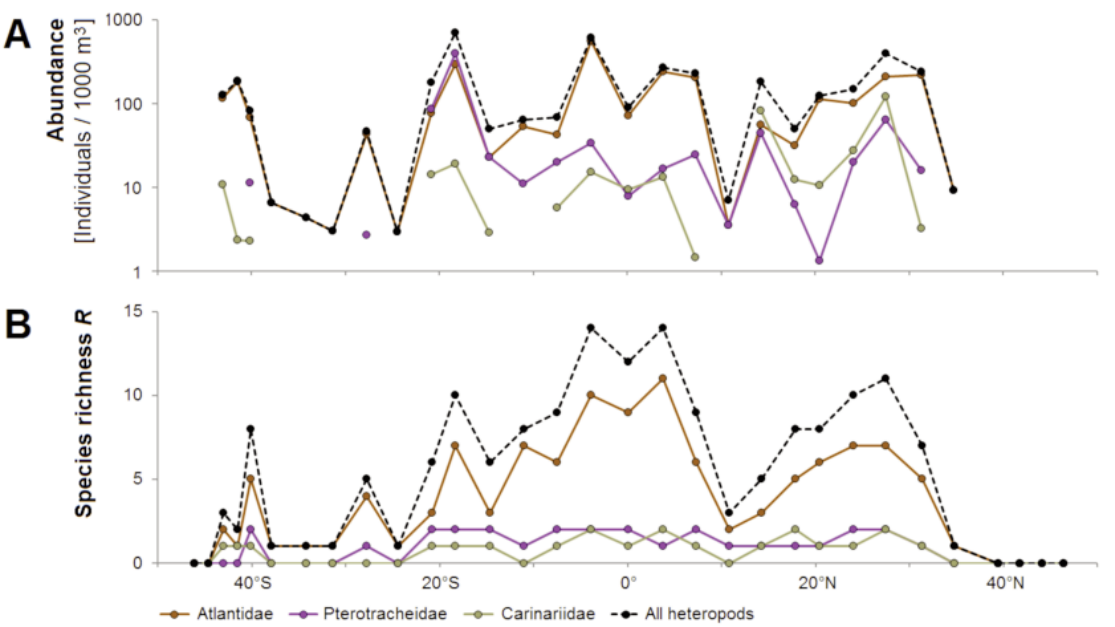

Figure 4. Basin-scale patterns of (A) heteropod abundance (individuals/1000 m^3), and (B) heteropod species richness *R*. Lines in (A) are interrupted in case of zero abundances.

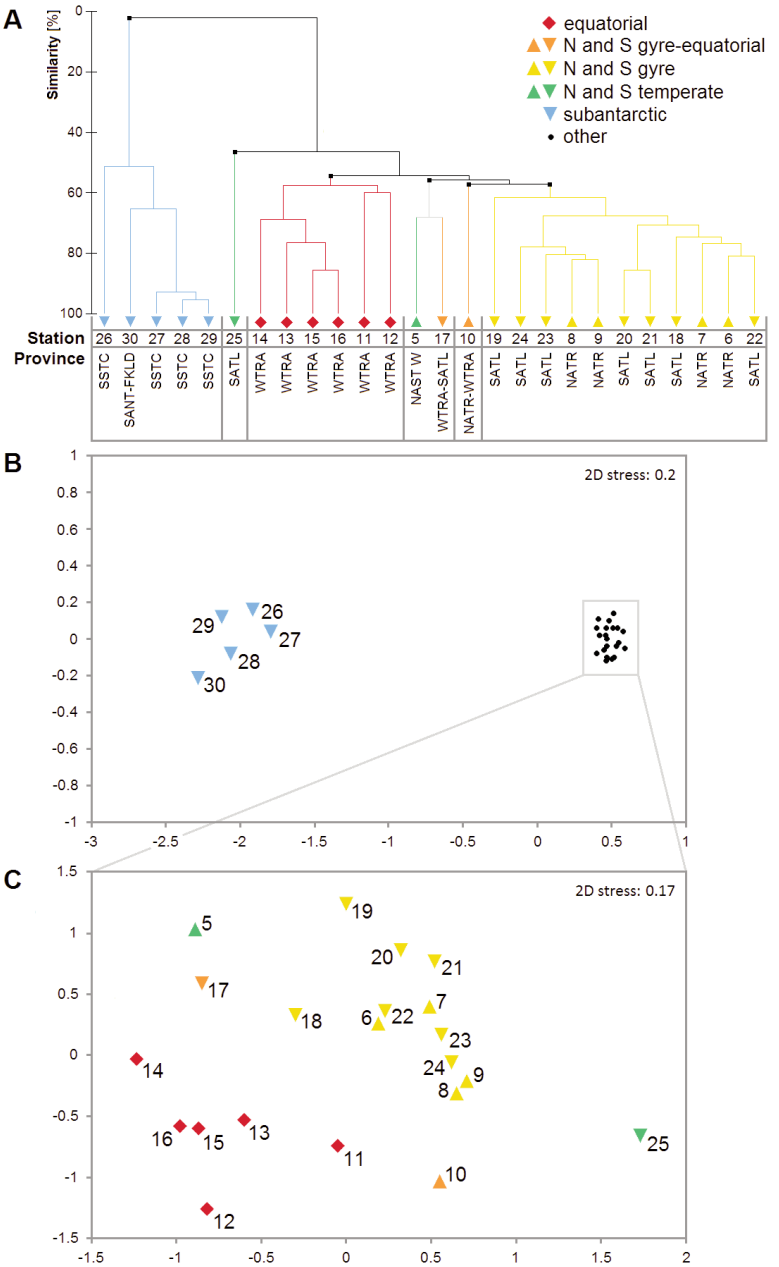

FIGURE 5. (A) Hierarchical cluster analysis of the stations according to their community composition of thecosome pteropods (euthecosomes and pseudothecosomes). The analysis is based on all stations with at least 10 specimens, and resulted in the indicated six significant clusters (SIMPROF $p < 0.05$). (B and C) nMDS ordination based on the community composition of thecosome pteropods, (B) using all stations with at least 10 specimens, and (C) excluding the subantarctic stations 26-30. Symbols are colored according to their geographic allocation, with upward pyramids for the northern hemisphere, downward pyramids for the southern hemisphere and diamonds for equatorial locations. The Longhurst provinces (Longhurst, 1998; Reygondeau et al., 2013) of the sampling stations are indicated in (A): NAST E (Northeast Atlantic subtropical gyral), NAST W (Northwest Atlantic subtropical gyral), NATR (North Atlantic tropical gyral), WTRA (Western tropical Atlantic), SATL (South Atlantic gyral), SSTC (South subtropical convergence), SANT (Subantarctic water ring), FKLD (Southwest Atlantic shelves).

results are further confirmed by the nMDS ordination, in which the six different clusters can be clearly recognized (Figure 5B,C). The species composition in the subantarctic region (St. 26-30) demonstrated almost no overlap with species compositions in other regions. The other clusters consisted of the equatorial stations (St. 11-16), the northern and southern gyres together (St. 6-9 and 18-23), the northern gyre-equatorial transition (St. 10), the southern subtropical convergence (St. 25), and the northern temperate zone and southern gyre-equatorial transition (St. 5 and 17) together. Because of the overlap between species compositions in the northern temperate and in the northern and southern gyre-equatorial transitions, the ordination of St. 5 and 17 may be an artefact of the gradual nature of the transitions between oceanographic provinces (Figure 5). According to the rarefaction curves of the equatorial, gyre and subantarctic stations, the major oceanographic provinces traversed during AMT24 were well-sampled for thecosomes (Figure S2A). Although transitions between oceanographic provinces were gradual, we were not able to thoroughly sample these areas at more than one location per transition (Figure S2B).

Heteropod species had a wider distribution than the subtropical gyres and equatorial regions: some of them also occurred in the subantarctic (Figures 1B and 4). This was the case for an exclusively subantarctic and yet undescribed *Atlanta* morphotype, listed as *Atlanta* species A herein (Wall-Palmer et al., 2016b). In particular, the taxa that produce very large adults, the carinariids and pterotracheids, had patchy distributions, with high numbers at a few stations and no or a few specimens at the adjacent stations (Table S2). It was therefore difficult to identify large-scale biogeographical distribution patterns among the heteropods. This patchy pattern was also reflected in rarefaction curves of heteropods, which were represented by fewer samples with at least 10 specimens compared to pteropods. Suboptimal sampling of the heteropods was demonstrated especially in the rarefaction curves representing the northern subtropical gyre and subantarctic stations (Figure S2C,D). We did not generate rarefaction curves for heteropods from northern and southern temperate stations because they contained too few (<6) specimens.

Discussion

General observations

We assessed pteropod and heteropod abundances, diversity and distributions in the Atlantic Ocean based on quantitative sampling along a basin-scale transect from 46°N to 46°S, crossing seven biogeochemical provinces. The AMT programme allowed us to combine zooplankton diversity and abundance data with ocean metadata from the same expedition, providing a rich oceanographic context to explain the observed patterns (e.g., Rees et al., 2015). Our results show that the species richness of both pteropods and heteropods was highest in the tropical and subtropical Atlantic. Pteropod abundance and biomass were highest just south of 40°S, and also reached high values near the equator (Figures 1 and 2; Tables S2 and S4). Some pteropod taxa showed strong preferences for particular oceanographic

provinces, for example for warm equatorial waters (e.g., *Creseis virgula*), subtropical gyres (e.g., *Styliola subula*), or in and south of the southern subtropical convergence zone (e.g., *Limacina helicina antarctica*). Other species occurred across a broad range of provinces (e.g., *Heliconoides inflatus* and *Limacina lesueurii*; Table S2). Most heteropods were restricted to warm waters, but some taxa also occurred in the subantarctic region.

We found no unexpected extremes in pteropod abundance along AMT24 (Figure 2A) and the rarefaction curves flattened with an increasing number of samples or individuals (Figure S2A,B), indicating that the pteropods in this study have been representatively sampled. However, it is likely that our net aperture (0.71 m) and mesh size (200 µm) are responsible for highly variable heteropod species counts, diversities and abundances across stations, and quantitative sampling of these larger taxa requires nets with larger apertures and mesh sizes (McGowan and Fraundorf, 1966; Wells, 1973; Wall-Palmer et al., 2016a). Hence, we will focus most of our discussion on pteropods.

Distribution and abundance

The biogeographical distributions of pteropod assemblages inferred by cluster analysis were largely congruent with the distribution of Longhurst's (1998) biogeochemical provinces for the period from September to November (Figure 5; Reygondeau et al., 2013). Our pteropod species distributions in the Atlantic Ocean also were comparable with those from the qualitative biogeographical synthesis of Bé and Gilmer (1977), however, there were some exceptions. According to Bé and Gilmer, *Limacina trochiformis* was most abundant in the equatorial province (WTRA). By contrast, we observed *L. trochiformis* only at station 14 (N = 3) in the equatorial province, but found much higher abundances throughout the south subtropical gyre. Exact localities upon which the distribution maps of Bé and Gilmer (1977) were based were not given, so we could not deduce if and where in the South Atlantic their samples were collected. We found a cold water variant of *Heliconoides inflatus* (*H. inflatus* S herein) in the subantarctic, but the distribution map from Bé and Gilmer (1977) most likely shows the broad equatorial and subtropical distribution of the warm water *H. inflatus* (listed as *Limacina inflata*) with a southern limit at ~40°S. The distribution of *Creseis virgula* was limited to the equatorial Atlantic in our study, but also occurred in the subtropical gyres according to Bé and Gilmer (1977). They also listed some species that were not found in our quantitative samples: the warm water species *Cavolinia tridentata* and the cold water species *Limacina retroversa*.

Because previous quantitative abundance data in provinces traversed by AMT24 are limited, our abundance data could only be compared to a few other pteropod studies. In October, St. 30 and 31 are within a transition zone between the Subantarctic water ring (SANT) and Southwest Atlantic shelves (FKLD) provinces (Reygondeau et al., 2013). Hunt et al. (2008) synthesized pteropod abundances in the Southern Ocean from tow data (1982-2006). In the mesozooplankton samples, they found low densities of *Limacina helicina antarctica* of only a few

tens of ind./1000 m^3 in October, both near the Antarctic Peninsula and south of Australia, which is comparable to the low densities of 25.3-36.5 ind./1000 m^3 of *L. helicina antarctica* that we found at St. 30 and 31 (45-46°S) in October. Much higher population densities of this species were found in the mid austral summer (January-February), with 103 to 104 ind./1000 m^3 at the Antarctic Peninsula and south of Australia, and even 105 ind./1000 m^3 near South Georgia (Hunt et al., 2008). Bednaršek et al. (2012b) report similar seasonal dynamics from the Antarctic Peninsula to South Georgia, with higher numbers of *L. helicina antarctica* in the austral summer and autumn than in the spring. We did find high densities of *L. helicina antarctica*, exceeding 103 to 104 ind./1000 m^3 in October, further up north at St. 27 and 28 (40-41°S), which may indicate that the growing season for this species started earlier at lower latitudes.

The total zooplankton abundance in the upper 200 m of the northeast Atlantic Ocean during July 1996 was characterized by Gallienne et al. (2001) by vertical hauls of 200 µm mesh size nets (aperture 0.57 m). They found low pteropod abundances of 0-75 ind./1000 m^3 between 39 and 47°N, comparable to 0-24.2 ind./1000 m^3 between 35 and 46°N in our study in late September/early October (St. 1-5). Gallienne et al. (2001) found higher summer abundances of 845-1730 ind./1000 m^3 at 37°N, whereas in our study higher abundances were found south of 31°N in early fall, which may again reflect seasonal variation.

In the Caribbean Sea, not sampled in our study, the average species abundances in the 239 µm mesh size net (aperture 1.0 m) used by Wells (1973) near Barbados resemble our findings in equatorial St. 14. For *Creseis virgula*, Wells (1973) found 16.9 ind./1000 m^3, which is highly comparable to the 18.4 ind./1000 m^3 in our study. For *Heliconoides inflatus*, Wells (1973) found 257.3 ind./1000 m^3 resembling the 239.8 ind./1000 m^3 in our study. The major difference was the high abundance of *Creseis conica* in the Caribbean (188.2 ind./1000 m^3) reported by Wells (1973; listed as *Creseis virgula conica*), whereas we found only 16.8 ind./1000 m^3 at our St. 14.

Plankton biomass in the global ocean

Qualitatively, the pteropod biomass distribution along AMT24 showed a similar large-scale pattern as the biomass distributions of many other mesozooplankton groups, with high zooplankton biomass in arctic and subantarctic waters, elevated biomass in the equatorial regions, and lowest biomass within the gyres (Moriarty and O'Brien, 2013). Quantitatively, however, biomass data from sampling locations between 10 and 500 m deep in various parts of the Atlantic Ocean as synthesized by Bednaršek et al. (2012a) point at a higher pteropod biomass (dry weight) in the Atlantic Ocean than in the Indian and Pacific oceans. This was true for the equatorial Atlantic north of Brazil, the Mediterranean Sea, and the subantarctic near South Georgia. Our data appear to confirm this. Compared to the global median pteropod biomass of 0.058 mg m^{-3} (only non-zero global data) reported by Bednaršek et al. (2012a), we found a much higher pteropod biomass per m^3 in the Atlantic Ocean (Figure 2B; median of 0.28 mg m^{-3}).

Latitudinal trends in species richness

The dominant paradigm for latitudinal diversity patterns in pelagic systems is a bimodal pattern of species richness, with maxima in the gyres, slightly lower richness in the equatorial province, and a sharp decrease of diversity towards the temperate and polar zones (e.g., Hillebrand, 2004a). Our pteropod data broadly support this pattern, and with the exception of one equatorial station, diversity at most stations in the equatorial province was slightly lower than in the gyres (Figure 2C). Many hypotheses have been formulated for advancing the ecological, biogeographic, and evolutionary understanding of the latitudinal diversity gradient, and for explaining why the gradient in the pelagic ocean differs from a steady increase of diversity towards the equator, the most widely recognized pattern in benthic and terrestrial environments (e.g., Angel, 1997; Gaston, 2000; Willig et al., 2003; Hillebrand, 2004a,b; Brayard et al., 2005). Examples of such conceptual models are the evolutionary speed hypothesis and geometric constraints hypothesis (Willig et al., 2003).

Several pelagic groups show latitudinal trends in species richness similar to pteropods, with the highest richness in the subtropical gyres. Such a pattern was reported for hydromedusans (Macpherson, 2002), euphausiids (Angel, 1997; Tittensor et al., 2010), pelagic decapods (Angel, 1997), ostracods (Angel, 1997; Angel et al., 2007), fish (Angel, 1997), foraminifera (Rutherford et al., 1999; Tittensor et al., 2010), and tintinnid ciliates (Dolan and Pierce, 2013). Several other pelagic taxa do not show a bimodal pattern with maximum species richness in the subtropical gyres, but display a diversity peak in the equatorial region or a diversity plateau across subtropical and tropical latitudes. Examples of equatorial maxima are found for salps (Macpherson, 2002) and hyperiid amphipods (Burridge et al., in press: Thesis chapter 7), and our data indicate that heteropods also show maximum species richness in equatorial waters. A wider diversity plateau across the tropics and subtropics was found for copepods (Woodd-Walker et al., 2002; Rombouts et al., 2009), siphonophore hydrozoans and cephalopods (Macpherson, 2002). Larvacean species diversity only had a clear peak in the northern gyre (Macpherson, 2002), and chaetognaths only demonstrated a peak in the southern gyre (Macpherson, 2002) with a distinct decrease in species diversity towards cold North Atlantic waters (42-59°N; Pierrot-Bults, 2008). However, the reported species diversities in the latter two groups were lower (maxima of up to ~50 and ~40 species, respectively) than for hydromedusans or crustaceans. Species diversities registered for pteropods were also comparatively low. Accurate estimates of pteropod species diversities may require more rigorous sampling efforts and more accurate assessments of species boundaries. Our anomaly of high diversity at equatorial station 14 was largely caused by the occurrence of pteropod taxa that are generally known to appear in low abundances and that were only sporadically collected along AMT24, e.g., *Diacavolinia* sp. and *Hyalocylis striata*. Repeated transect studies may compensate for such anomalies. Overall, the latitudinal diversity gradient varies among zooplankton groups, and appears to result from a complex interplay among ecological factors, highly diverse life history strategies and roles in the marine food web, as well as different evolutionary histories.

Conclusions

To our knowledge, this is the most comprehensive study of the diversity and abundance of planktonic gastropods across the Atlantic Ocean to date. We found close correspondence between our pteropod assemblages and Longhurst's (1998) biogeochemical provinces. On average, our results point to a substantially higher pteropod biomass in the Atlantic Ocean than in the Indian and Pacific oceans. The dominant paradigm of a bimodal pattern of species richness in pelagic systems, with maxima in the subtropical gyres, was broadly supported by our pteropod data. Our study provides only a snapshot in time, however. Thorough repeated sampling will be essential for examining large-scale, long-term trends in the diversity and abundance of planktonic gastropods, quantifying future changes, and predicting species-specific sensitivities to ocean changes.

Acknowledgements

We thank A.W. Janssen for his insights in taxonomy and comments on the manuscript, and M. Jungbluth, S. Cregeen and the AMT24 crew for their assistance at sea. We are grateful to M. Cusson for his advice on statistical analyses of species communities. A.K. Burridge was supported by funding through the KNAW (Royal Dutch Academy of Science) Ecology Fund UPS/297/Eco/1403J, the Netherlands Organisation for Scientific Research (NWO cruise participation grant, coordinated by the Royal Netherlands Institute for Sea Research [NIOZ]), and the Malacological Society of London Research Grant. E. Goetze and the fieldwork component of this study were supported by National Science Foundation (USA) grants OCE-1338959 and OCE-1255697. D. Wall-Palmer was funded by the Leverhulme Trust RPG-2013-363 (2014-2017) and a Martin-Fellowship from Naturalis Biodiversity Center (2015). Plankton collections made for this study were partially supported by the UK Natural Environment Research Council National Capability funding to Plymouth Marine Laboratory and the National Oceanography Centre, Southampton. This is contribution number 301 of the AMT programme.

References

Andrews K.R., Norton E.L., Fernandez-Silva I., Portner E., Goetze E., 2014. Multilocus evidence for globally distributed cryptic species and distinct populations across ocean gyres in a mesopelagic copepod. Molecular Ecology 23, 5462–5479.

Angel M.V., 1993. Biodiversity of the pelagic ocean. Conservation Biology 7, 760–772.

Angel M.V., 1997. Pelagic biodiversity. In: Ormond R.F.G., Gage J.R., Angel M.V. (Eds.), Marine Biodiversity, Patterns and Processes. Cambridge University Press, Cambridge, pp. 35–68.

Angel M.V., Blachowiak-Samolyk K., Drapun I., Castillo R., 2007. Changes in the composition of planktonic ostracod populations across a range of latitudes in the North-east Atlantic. Progress in Oceanography 73, 60–78.

Bé A.W.H., Gilmer R.W., 1977. A zoogeographic and taxonomic review of euthecosomatous Pteropoda. In: Ramsay A.T.S. (Ed.), Oceanic Micropaleontology 1. Academic Press, London, UK, pp. 733–808.

Bé A.W.H., MacClintock C., Currie D.C., 1972. Helical shell structure and growth of the pteropod *Cuvierina columnella* (Rang) (Mollusca, Gastropoda). Biomineralization Research Reports 4, 47–79.

Beaugrand G., Luczak C., Edwards M., 2009. Rapid biogeographical plankton shifts in the North Atlantic Ocean. Global Change Biology 15, 1790–1803.

Bednaršek N., Možina J., Vogt M., O'Brien C., Tarling G.A., 2012a. The global distribution of pteropods and their contribution to carbonate and carbon biomass in the modern ocean. Earth System Science Data 4, 167–186.

Bednaršek N., Ohman M.D., 2015. Changes in pteropod distributions and shell dissolution across a frontal system in the California Current System. Marine Ecology Progress Series 523, 93–103.

Bednaršek N., Tarling G.A., Fielding S., Bakker D.C.E., 2012b. Population dynamics and biogeochemical significance of *Limacina helicina antarctica* in the Scotia Sea (Southern Ocean). Deep-Sea Research II 59–60, 105–116.

Brayard A., Escarguel G., Bucher H., 2005. Latitudinal gradient of taxonomic richness: combined outcome of temperature and geographic mid-domain effects? Journal of Zoological Systematics and Evolutionary Research 43, 178–188.

British Oceanographic Data Centre (BODC). http://www.bodc.ac.uk

Burridge A.K., Goetze E., Raes N., Huisman J., Peijnenburg K.T.C.A., 2015. Global biogeography and evolution of *Cuvierina* pteropods. BMC Evolutionary Biology 15, 39. *Thesis chapter 3.*

Burridge A.K., Tump M., Vonk R., Goetze E., Peijnenburg K.T.C.A., in press. Diversity and distribution of hyperiid amphipods along a latitudinal gradient in the Atlantic Ocean. Progress in Oceanography, published online in 2016. *Thesis chapter 7.*

Clarke K.R., 1993. Non-parametric multivariate analyses of changes in community structure. Australian Journal of Ecology 18, 117–143.

Clarke K.R., Gorley R.N., 2006. PRIMER Version 6: User Manual/Tutorial. PRIMER-E, Plymouth, UK.

Clarke K.R., Warwick R.M., 2001. Change in Marine Communities: An Approach to Statistical Analysis and Interpretation. PRIMER-E, Plymouth, UK.

Collins S., 2012. Evolution on acid. Nature Geoscience 5, 310–311.

Dolan J.R., Pierce R.W., 2013. Diversity and distributions of tintinnids. In: Dolan J.R., Montagnes D.J.S., Agatha S., Wayne Coats D., Stoecker D.K. (Eds.), The Biology and Ecology of Tintinnid Ciliates: Models for Marine Plankton. John Wiley & Sons, Hoboken, pp. 214–243.

Gallienne C.P., Robins D.B., Woodd-Walker R.S., 2001. Abundance, distribution and size structure of zooplankton along a 20° west meridional transect of the northeast Atlantic Ocean in July. Deep-Sea Research II 48, 925–949.

Gaston K.J., 2000. Global patterns in biodiversity. Nature 405, 220–227.

Gattuso J.-P., Magnan A., Billé R., Cheung W.W.L., Howes E.L., et al., 2015. Contrasting futures for ocean and society from different anthropogenic CO_2 emissions scenarios. Science 349, aac4722 1–10.

Gilmer R.W., Harbison G.R., 1986. Morphology and field behavior of pteropod molluscs: feeding methods in the families Cavoliniidae, Limacinidae and Peraclididae (Gastropoda: Thecosomata). Marine Biology 91, 47–57.

Goetze E., Hüdepohl P.T., Chang C., Van Woudenberg L., Iacchei M., Peijnenburg K.T.C.A., in press. Ecological dispersal barrier across the equatorial Atlantic in a migratory planktonic copepod. Progress in Oceanography, published online in 2016.

Gotelli N.J., Colwell R.K., 2010. Estimating species richness. In: Magurran, A.E., McGill, B.J. (Eds.), Frontiers in Measuring Biodiversity. Oxford University Press, New York, pp. 39–54.

Hammer Ø., Harper D.A.T., Ryan P.D., 2001. PAST: paleontological statistics software package for education and data analysis. Palaeontologia Electronica 4, 1–9.

Hillebrand H., 2004a. On the generality of the latitudinal diversity gradient. American Naturalist 163, 192–211.

Hillebrand H., 2004b. Strength, slope, and variability of marine latitudinal gradients. Marine Ecology Progress Series 273, 251–267.

Hirai J., Tsuda A., Goetze E., 2015. Extensive genetic diversity and endemism across the global range of the oceanic copepod *Pleuromamma abdominalis*. Progress in Oceanography 138, 77–90.

Howard W.R., Roberts D., Moy A.D., Lindsay M.C.M., Hopcroft R.R., et al., 2011. Distribution, abundance and seasonal flux of pteropods in the Sub-Antarctic Zone. Deep-Sea Research II 58, 2293–2300.

Hunt B.V.P., Pakhomov E.A., Hosie G.W., Siegel V., Ward P., Bernard K.S., 2008. Pteropods in Southern Ocean ecosystems. Progress in Oceanography 78, 193–221.

Janssen A.W., 2005. Development of Cuvierinidae (Mollusca, Euthecosomata, Cavolinioidea) during the Cainozoic: a non-cladistic approach with a re-interpretation of Recent taxa. Basteria 69, 25–72.

Janssen A.W., Peijnenburg K.T.C.A., 2014. Holoplanktonic Mollusca: development in the Mediterranean basin during the last 30 million years and their future. In: Goffredo S., Dubinsky Z. (Eds.), The Mediterranean Sea: Its History and Present Challenges. Springer, Dordrecht, pp. 341–362.

Jennings R.M., Bucklin A., Ossenbrügger H., Hopcroft R.R., 2010. Species diversity of planktonic gastropods (Pteropoda and Heteropoda) from six ocean regions based on DNA barcode analysis. Deep-Sea Research II 57, 2199–2210.

Jörger K.M., Stöger I., Kano Y., Fukuda H., Knebelsberger T., Schrödl M., 2010. On the origin of Acochlidia and other enigmatic euthyneuran gastropods, with implications for the systematics of Heterobranchia. BMC Evolutionary Biology 10, 323.

Lalli C.M., Gilmer R.W., 1989. Pelagic Snails: The Biology of Holoplanktonic Gastropod Molluscs. Stanford University Press, Stanford, California.

Lohbeck K.T., Riebesell U., Collins S., Reusch T.B.H., 2012. Functional genetic divergence in high CO_2 adapted *Emiliana huxleyi* populations. Evolution 67, 1892–1900.

Lohbeck K.T., Riebesell U., Reusch T.B.H., 2014. Gene expression changes in coccolithophore *Emiliana huxleyi* after 500 generations of selection to ocean acidification. Proceedings of the Royal Society B 281, 20140003.

Longhurst A.R., 1998. Ecological Geography of the Sea. Academic Press, San Diego.

Macpherson E., 2002. Large-scale species-richness gradients in the Atlantic Ocean. Proceedings of the Royal Society B, 1715–1720.

McGowan J.A., Fraundorf V.J., 1966. The relationship between size of net used and estimates of zooplankton diversity. Limnology and Oceanography 11, 456–469.

Moriarty R., O'Brien T.D., 2013. Distribution of mesozooplankton biomass in the global ocean. Earth System Science Data 5, 45–55.

Norris R.D., 2000. Pelagic species diversity, biogeography, and evolution. Paleobiology 26, 236–258.

Ossenbrügger H., 2010. Distribution patterns of pelagic gastropods at the Cape Verde Islands. Semester thesis, Helmholz Centre for Ocean Research, Kiel.

Peijnenburg K.T.C.A., Goetze E., 2013. High evolutionary potential of marine zooplankton. Ecology and Evolution 3, 2765–2781.

Pielou E., 1967. The use of information theory in the study of diversity of biological populations. Proceedings of the 5th Berkeley Symposium on Mathematical Statistics and Probability, vol. 4, pp. 163–177.

Pierrot-Bults A.C., 2008. A short note on the biogeographic patterns of the Chaetognatha fauna in the North Atlantic. Deep-Sea Research II 55, 137–141.

Pierrot-Bults A.C., Peijnenburg K.T.C.A., 2015. Pteropods. In: Harff J., Meschede M., Petersen S., Thiede J. (Eds.), Encyclopedia of marine geosciences. Springer, Dordrecht, pp. 1–10.

Provan J., Beatty G.E., Keating S.L., Maggs C.A., Savidge G., 2009. High dispersal potential has maintained long-term population stability in the North Atlantic copepod *Calanus finmarchicus*. Proceedings of the Royal Society B 276, 301–307.

Rees A., Robinson C., Smyth T., Aiken J., Nightingale P., Zubkov M., 2015. 20 Years of the Atlantic Meridional Transect – AMT. Limnology and Oceanography Bulletin 24, 101–107.

Reygondeau G., Longhurst A., Martinez E., Beaugrand G., Antoine D., Maury O., 2013. Dynamic biogeochemical provinces in the global ocean. Global Biogeochemical Cycles 27, 1–13.

Richter G., Seapy R.R., 1999. Heteropoda. In: Boltovskoy, D. (Ed.), South Atlantic Zooplankton. Backhuys Publishers, Leiden, pp. 621–647.

Rombouts I., Beaugrand G., Ibanez F., Gasparini S., Chiba S., Legendre L., 2009. Global latitudinal variations in marine copepod diversity and environmental factors. Proceedings of the Royal Society B 276, 3053–3062.

Rutherford S., D'Hondt S., Prell W., 1999. Environmental controls on the geographic distribution of zooplankton diversity. Nature 400, 749–753.

Schlitzer R., 2015. Ocean Data View. http://odv.awi.de

Seapy R.R., Lalli C.M., Wells F.E., 2003. Heteropoda from western Australian waters. In: Wells F.E., Walker D.I., Jones D.S. (Eds.), The Marine Flora and Fauna of Dampier, Western Australia. Western Australian Museum, Perth, pp. 513–546.

Shannon C.E., Weaver W., 1949. The Mathematical Theory of Communication. University of Illinois Press, Urbana.

Spellerberg I.F., Fedor P.J., 2003. A tribute to Claude Shannon (1916–2001) and a plea for more rigorous use of species richness, species diversity and the 'Shannon-Wiener' index. Global Ecology and Biogeography 12, 177–179.

Tittensor D.P., Mora C., Jetz W., Lotze H.K., Ricard D., et al., 2010. Global patterns and predictors of marine biodiversity across taxa. Nature 466, 1098–1101.

Van der Spoel S., Bleeker J., Kobayasi H., 1993. From *Cavolinia longirostris* to twenty-four *Diacavolinia* taxa, with a phylogenetic discussion (Mollusca, Gastropoda). Bijdragen tot de Dierkunde 62, 127–166.

Van der Spoel S., Dadon J.R., 1999. Pteropoda. In: Boltovskoy D. (Ed.), South Atlantic Zooplankton. Backhuys Publishers, Leiden, pp. 649–706.

Van der Spoel S., Heyman R.P., 1983. A Comparative Atlas of Zooplankton: Biological Patterns in the Oceans. Springer, New York.

Wall-Palmer D., Burridge A.K., Peijnenburg K.T.C.A., 2016b. *Atlanta ariejansseni*, a new species of shelled heteropod from the Southern Subtropical Convergence Zone (Gastropoda, Pterotracheoidea). ZooKeys 604, 13–30.

Wall-Palmer D., Smart C.W., Hart M.B., Leng M.L., Borghini M., et al., 2014. Late Pleistocene pteropods, heteropods and planktonic foraminifera from the Caribbean Sea, Mediterranean Sea and Indian Ocean. Micropaleontology 60, 557–578.

Wall-Palmer D., Smart C.W., Kirby R., Hart M.B., Peijnenburg K.T.C.A., Janssen A.W., 2016a. A review of the ecology, palaeontology and distribution of atlantid heteropods (Caenogastropoda: Pterotracheoidea: Atlantidae). Journal of Molluscan Studies 82, 221–234.

Wells F.E., 1973. Effects of mesh size on estimation of population densities of tropical euthecosomatous pteropods. Marine Biology 20, 347–350.

Willig M.R., Kaufman D.M., Stevens R.D., 2003. Latitudinal gradients of biodiversity: pattern, process, scale, and synthesis. Annual Review of Ecology, Evolution, and Systematics 34, 273–309.

Woodd-Walker R.S., Ward P., Clarke A., 2002. Large-scale patterns in diversity and community structure of surface water copepods from the Atlantic Ocean. Marine Ecology Progress Series 236, 189–203.

World Register of Marine Species (WoRMS). http://www.marinespecies.org

Supplementary information

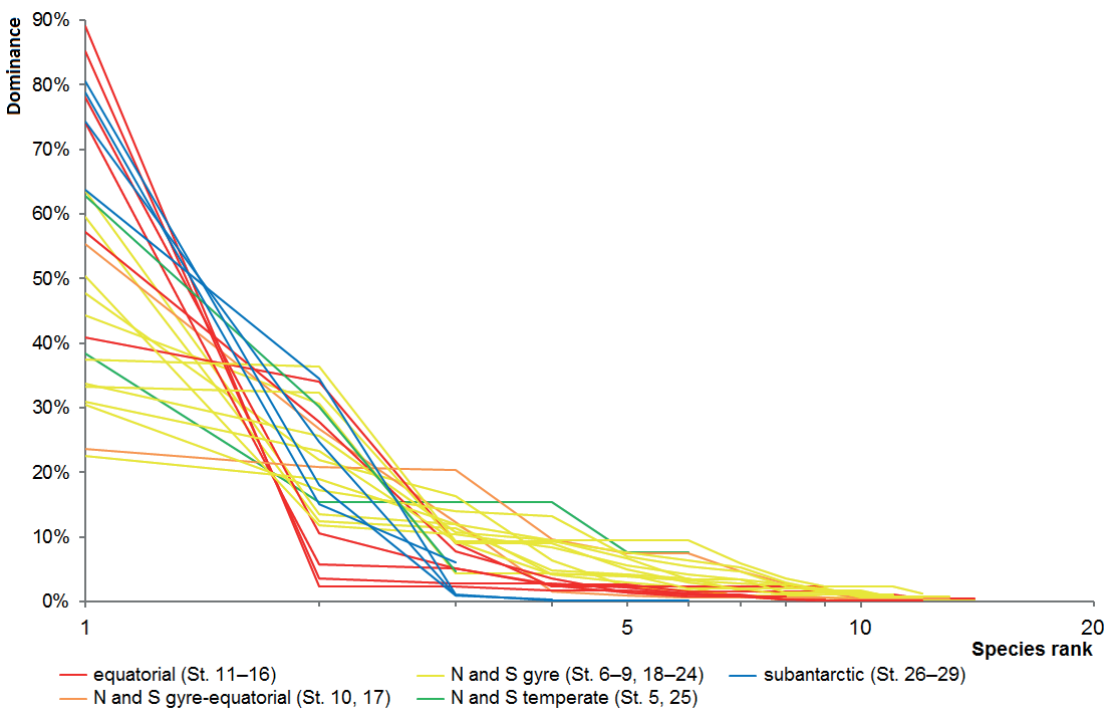

Figure S1. Rank abundance curves describing the distribution of thecosome species abundances for each station with at least 2 species and 10 specimens. Lines are colored according to the geographical location of the stations.

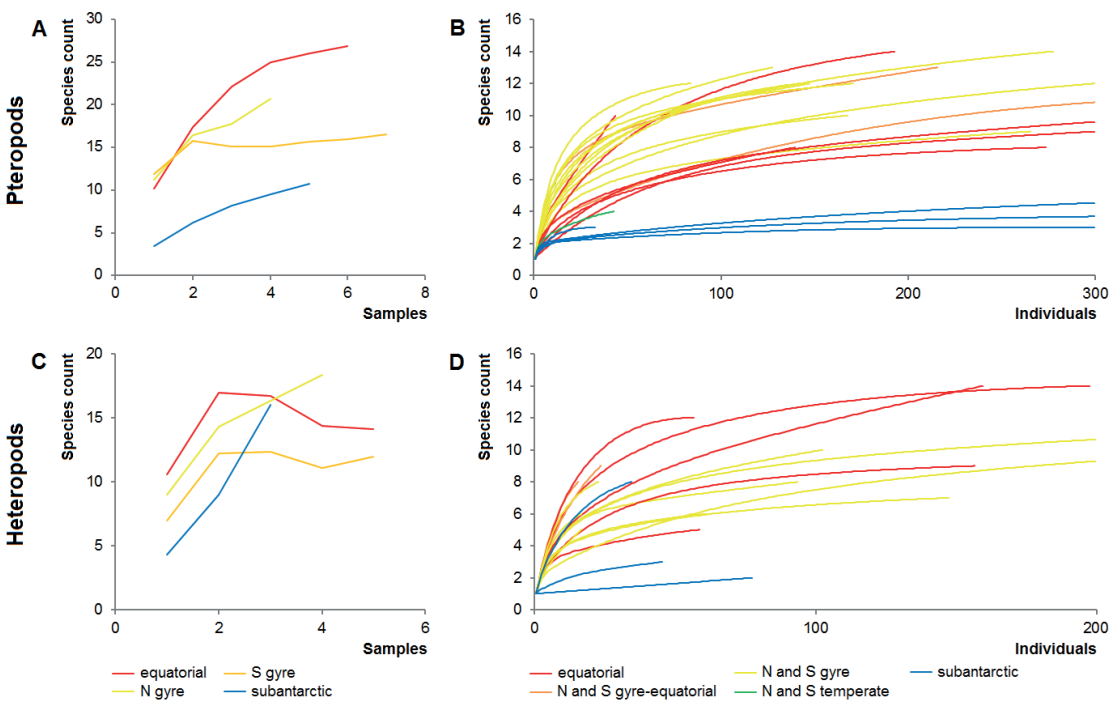

FIGURE S2. Sample-based (A and C) and individual-based (B and D) rarefaction curves for (A and B) thecosomes and (C and D) heteropods, based on all stations with at least 10 specimens. (B) and (D) show the first 300 and 200 individuals, respectively. Transitional stations 5, 10, 17 and 25 are not included in the sample-based rarefaction in (A and C). Lines are colored according to the geographical location of the stations.

TABLE S1. Formulae used to calculate the biomass of euthecosomes and gymnosomes by dry weight, as adjusted from Bednaršek et al. (2012a). L = shell length [mm], D = shell diameter [mm].

Species	Formula for dry weight [mg/ind.]	L or D [mm]	Remarks if different from Bednaršek et al. (2012)
Cavolinia inflexa	$0.28 \bullet 0.2152 \bullet L^{2.293}$	7	
Cavolinia uncinata	$0.28 \bullet 0.2152 \bullet L^{2.293}$	6.5	
Cavolinia gibbosa	$0.28 \bullet 0.2152 \bullet L^{2.293}$	6.5	*C. uncinata* size used: *C. gibbosa* was not indicated
Cavolinia sp juv	$0.28 \bullet 0.2152 \bullet L^{2.293}$	6.2	
Diacavolinia sp	$0.28 \bullet 0.2152 \bullet L^{2.293}$	4	*Cavolinia* formula and *C. longirostris* f. *strangulata* size used
Clio cuspidata	$0.28 \bullet 0.2152 \bullet L^{2.293}$	8	No fully grown specimens: mean L adjusted from 20 to 8 mm
Clio pyramidata pyramidata/ lanceolata	$0.28 \bullet 0.2152 \bullet L^{2.293}$	8	Mean L adjusted from 20 to 8 mm
Clio pyramidata sulcata	$0.28 \bullet 0.2152 \bullet L^{2.293}$	8	Mean L adjusted from 17 to 8 mm
Clio pyramidata antarctica	$0.28 \bullet 0.2152 \bullet L^{2.293}$	8	No fully grown specimens: mean L adjusted from 17 to 8 mm
Clio recurva	$0.28 \bullet 0.2152 \bullet L^{2.293}$	8	*Clio* formula used; *Clio recurva* was not indicated as a separate genus
Creseis clava	$0.28 \bullet \pi \bullet L^{(3*3/25)}$	6	
Creseis conica	$0.28 \bullet \pi \bullet L^{(3*3/25)}$	7	
Creseis virgula	$0.28 \bullet \pi \bullet L^{(3*3/25)}$	6	
Cuvierina sp	$0.28 \bullet \pi \bullet L^{(3*3/25)}$	6	Mostly juveniles: mean L adjusted from 10 to 6 mm
Diacria danae	$0.28 \bullet 0.2152 \bullet L^{2.293}$	1.7	
Diacria trispinosa	$0.28 \bullet 0.2152 \bullet L^{2.293}$	8	
Diacria major	$0.28 \bullet 0.2152 \bullet L^{2.293}$	10.7	
Diacria sp juv	$0.28 \bullet 0.2152 \bullet L^{2.293}$	5.9	*Diacria* spp. formula used
Hyalocylis striata	$0.28 \bullet \pi \bullet L^{(3*3/25)}$	3	Mean L adjusted from 8 to 3 mm
Styliola subula	$0.28 \bullet \pi \bullet L^{(3*3/25)}$	7	Mean L adjusted from 13 to 7 mm
Cavoliniidae sp	$0.28 \bullet \pi \bullet L^{(3*3/25)}$	4	
Heliconoides inflatus	$0.137 \bullet D^{1.5005}$	1	*Limacina helicina* formula used; mean D adjusted from 1.3 to 1 mm
Heliconoides inflatus S	$0.137 \bullet D^{1.5005}$	1.5	*Limacina helicina* formula used; mean D adjusted from 1.3 to 1.5 mm
Limacina bulimoides	$0.137 \bullet D^{1.5005}$	3	*Limacina helicina* formula used; mean D adjusted from 2 to 3 mm
Limacina helicina antarctica	$0.137 \bullet D^{1.5005}$	3	Mean D adjusted from 5 to 3 mm
Limacina lesueurii	$0.137 \bullet D^{1.5005}$	2	*Limacina helicina* formula used; mean D adjusted from 0.8 to 2 mm
Limacina trochiformis	$0.137 \bullet D^{1.5005}$	1.5	*Limacina helicina* formula used; mean D adjusted from 0.8 to 1.5 mm
Gymnosomata sp	$10^{(2.533*\log(L)-3.89095)} \bullet 1000$	3	Mean L adjusted from 12 to 3 mm

TABLE S2. Abundance data for pteropods and heteropods at each station during the AMT24 cruise. Units for abundance are individuals per 1000 m^3 of seawater filtered. Uncoiled euthecosomes are cavoliniids, coiled euthecosomes are limaciniids. *Clio pyramidata pyramidata/lanceolata* is labeled as *Clio pyr. pyr/lanceolata.* Numbers listed in bold report totals for that taxon. Results for heteropods (Pterotracheoidea) are also summed within each family.

Station	1	2	3	4	5	6	7	8	9	10	11	12	13
Total pteropod abundance	**6**	**14**	**0**	**1**	**24**	**292**	**472**	**466**	**414**	**1022**	**410**	**79**	**441**
Uncoiled euthecosomes	**4**	**11**	**0**	**1**	**9**	**35**	**77**	**69**	**113**	**322**	**9**	**18**	**29**
Cavolinia inflexa	2	5		1			3	1		6	3		7
Cavolinia uncinata												2	
Cavolinia gibbosa										3			
Cavolinia sp juv													
Diacavolinia sp							2						
Clio cuspidata	2	2										2	
Clio pyr. pyr./lanceolata		2			4	2	13		1	6		2	4
Clio pyramidata sulcata													
Clio recurva		2											
Clio pyramidata antarctica													
Creseis clava						13	2		1	6		2	10
Creseis conica					2								
Creseis virgula										16		7	1
Cuvierina sp					4	11	15	1		6			
Diacria danae						3	18	3	7			2	
Diacria trispinosa						2	2	16	9	3	6		6
Diacria major									1				
Diacria sp juveniles								1	5	3			
Hyalocylis striata							3						
Styliola subula						5	20	46	88	272			
Cavoliniidae sp												2	
Coiled euthecosomes	**0**	**0**	**0**	**0**	**15**	**225**	**352**	**307**	**280**	**687**	**380**	**60**	**408**
Heliconoides inflatus					9	161	201	244	190	562	234	32	390
Heliconoides inflatus S													
Limacina bulimoides					2	31	139	52	65		32	2	10
Limacina helicina antarctica													
Limacina lesueurii					4	34	11	12	25	125	114	26	7
Limacina trochiformis													
Pseudothecosomes	**2**	**4**	**0**	**0**	**0**	**31**	**38**	**84**	**21**	**12**	**20**	**2**	**4**
Corolla sp	2	4											
Gleba sp													
Peracle bispinosa									3	3			
Peracle diversa						10	20		4		3		
Peracle reticulata							7	9	4		3		1
Peracle valdiviae									1	9	15	2	
Peracle sp A								1					
Peracle sp B						3		20					1
Peracle sp C						6	3	19					
Peracle sp D						11	5	10					
Peracle sp E							3	3					
Peracle sp F								13	8				1
Peracle sp G								9	1				
Peracle sp H													
Peracle sp I													
Gymnosomes	**0**	**0**	**0**	**0**	**0**	**0**	**5**	**6**	**0**	**0**	**0**	**0**	**0**

14	15	16	17	18	19	20	21	22	23	24	25	26	27	28	29	30	31
340	435	1947	631	307	263	500	367	483	414	311	194	114	1929	4295	896	40	36
67	68	210	376	64	69	215	154	155	111	135	119	16	27	62	8	0	0
8	3	43	125	25	23	109	51	15	3	3							
		3															
														2			
5																	
		3	3														
2	11	55	127	6	3	8	6	15	5	3							
													5	17			
													21	43	8		
2			3	3	6	43	63	30		6							
17			8		23	14	3										
18	46	70	45	8													
3	2		45	3		8	3	9	3	3							
2		3	3	3	6	3	3	3	16								
5	6	21	17	6	6			3	22	12			2				
				11	3			39	22								
5																	
						30	26	42	41	108	119	16					
257	363	1725	232	206	122	247	185	310	278	150	70	91	1863	4181	872	36	25
240	336	1645	144	89	55	144	111	149	195	105	57						
												84	653	765	218		
8	22	55	59	92	14	43	48	113	46	27	9		5				
												6	1205	3417	654	36	25
3	5	24	28	25	29	35	17	48	32	12							
5					23	24	9		5	6	4						
15	5	12	17	31	72	35	26	15	19	6	0	0	0	2	3	0	0
														2			
2															3		
		3															
				14	9	3	20	12	14								
			3		46		6	3	5	3							
		6															
	2	3															
					3												
8			8	11	6	8											
			3														
				3		22											
3			3	3	9												
2	3																
						3				3							
2	0	0	6	6	0	3	3	3	5	21	4	6	39	50	13	3	11

TABLE S2. Continued

Station	1	2	3	4	5	6	7	8	9	10	11	12	13
Total heteropod abundance	**0**	**0**	**0**	**0**	**9**	**238**	**391**	**149**	**125**	**50**	**181**	**7**	**229**
Atlantidae	**0**	**0**	**0**	**0**	**9**	**219**	**208**	**101**	**113**	**31**	**56**	**4**	**203**
Atlanta echinogyra							2			12			
Atlanta fragilis									50				
Atlanta helicinoidea						6	2	1					3
Atlanta inclinata								6				2	
Atlanta lesueurii													
Atlanta oligogyra											6		
Atlanta peronii													
Atlanta rosea						56	151	45	21	9			6
Atlanta selvagensis					9	66	33	40	17	3			12
Atlanta tokiokai							3	6	7		3		47
Atlanta sp A													
Oxygyrus inflatus							11	1	1	3			6
Protatlanta souleyeti						89	7	1				2	
Protatlanta sculpta						2			16	3	38		130
Atlantidae sp											9		
Pterotracheidae	**0**	**0**	**0**	**0**	**0**	**16**	**64**	**20**	**1**	**6**	**44**	**4**	**25**
Firoloida desmarestia							10	3		6	44	4	12
Pterotrachea sp						16	54	17	1				13
Carinariidae	**0**	**0**	**0**	**0**	**0**	**3**	**120**	**27**	**11**	**12**	**82**	**0**	**1**
Pterosoma planum						3	100	27	11	6	82		
Carinaria pseudorugosa						20			6			1	12

14	15	16	17	18	19	20	21	22	23	24	25	26	27	28	29	30	31
270	90	603	68	64	49	704	176	3	46	3	4	6	82	185	126	0	0
240	72	555	42	53	23	294	77	3	43	3	4	6	68	182	116	0	0
2	24														3		
2	8	18		8		19	6		3				11				
2		9															
8		15	3	6													
2	3	6															
			6	11		3	3										
2	9	113	25			8	68	3	27				7				
91	5	152	3	6	6	3			3				2				
8	13	76															
												6	41	182	110		
54	3	43	3	17	3	3											
3	3	30	3	3	14	250			11	3			5				
65	5	91		3		8					4						
2													2		3		
17	8	34	20	11	23	391	85	0	3	0	0	0	11	0	0	0	0
17	3	27	6		12	11	63						5				
	5	6	14	11	12	381	23		3				7				
13	9	15	6	0	3	19	14	0	0	0	0	0	2	2	11	0	0
2	9	3	6		3	19	14										
	12											2	2	11			

TABLE S3. Species richness *R*, Shannon-Wiener's diversity index *H'*, Pielou's evenness index *J'* and the predator-prey ratio between the abundances of gymnosomes and thecosomes (euthecosomes and pseudothecosomes), calculated for all stations on the AMT24 cruise. Pteropod diversity indices include both euthecosomes and pseudothecosomes, but not gymnosomes. Zeros for *H'* are reported in grey because they are based on single specimens.

	Species richness *R*								Shannon-Wiener's diversity *H'*		Pielou's evenness index *J'*		
Station	Pteropods	Uncoiled euthecosomes	Coiled euthecosomes	Pseudothecosomes	Heteropods	Atlantidae	Pterotracheidae	Carinariidae	Pteropods	Heteropods	Pteropods	Heteropods	Pteropod predator-prey ratio
1	3	2	0	1	0	0	0	0	1.10		1.00		
2	5	4	0	1	0	0	0	0	1.49		0.93		
3	0	0	0	0	0	0	0	0					
4	1	1	0	0	0	0	0	0	0.00				
5	6	3	3	0	1	1	0	0	1.63	0.00	0.91		
6	10	6	3	1	7	5	1	1	1.37	1.44	0.59	0.74	
7	14	9	3	2	11	7	2	2	1.61	1.70	0.61	0.71	0.011
8	10	5	3	2	10	7	2	1	1.18	1.74	0.51	0.76	0.013
9	13	6	3	4	8	6	1	1	1.49	1.67	0.58	0.80	
10	12	8	2	2	8	5	1	2	1.22	1.96	0.49	0.94	
11	8	2	3	3	5	3	1	1	1.16	1.21	0.56	0.75	
12	10	6	3	1	3	2	1	0	1.54	1.04	0.67	0.95	
13	9	5	3	1	9	6	2	1	0.56	1.39	0.25	0.63	
14	15	10	4	1	14	11	1	2	1.18	1.80	0.44	0.68	0.005
15	8	5	3	0	12	9	2	1	0.85	2.25	0.41	0.91	
16	12	7	3	2	14	10	2	2	0.71	2.15	0.29	0.81	
17	13	9	3	1	9	6	2	1	1.98	1.85	0.77	0.84	0.009
18	11	7	3	1	8	7	1	0	1.66	1.92	0.69	0.92	0.019
19	12	6	4	2	6	3	2	1	2.09	1.63	0.84	0.91	
20	12	7	4	1	10	7	2	1	1.91	1.13	0.77	0.49	0.005
21	13	7	4	2	6	3	2	1	2.03	1.38	0.79	0.77	0.008
22	12	7	3	2	1	1	0	0	1.79	0.00	0.72		0.006
23	12	6	4	2	5	4	1	0	1.66	1.15	0.67	0.72	0.013
24	11	6	4	1	1	1	0	0	1.57	0.00	0.65		0.072
25	4	1	3	0	1	1	0	0	0.88	0.00	0.64		0.023
26	3	1	2	0	1	1	0	0	0.64	0.00	0.59		0.061

TABLE S3. Continued

	Species richness *R*								Shannon-Wiener's diversity *H'*		Pielou's evenness index *J'*		
Station	Pteropods	Uncoiled euthecosomes	Coiled euthecosomes	Pseudothecosomes	Heteropods	Atlantidae	Pterotracheidae	Carinariidae	Pteropods	Heteropods	Pteropods	Heteropods	Pteropod predator-prey ratio
27	6	3	3	0	8	5	2	1	0.74	1.56	0.41	0.75	0.021
28	5	2	2	1	2	1	0	1	0.56	0.07	0.35	0.10	0.012
29	4	1	2	1	3	2	0	1	0.63	0.41	0.45	0.37	0.015
30	1	0	1	0	0	0	0	0	0.00				0.091
31	1	0	1	0	0	0	0	0	0.00				

TABLE S4. Biomass of pteropods at each station on the AMT24 cruise, reported as dry weight [mg/m^3]. Uncoiled euthecosomes are cavoliniids, coiled euthecosomes are limaciniids. *Clio pyramidata pyramidata/lanceolata* is labeled as *Clio pyr. pyr./lanceolata*. Numbers listed in bold report totals for that taxon.

Station	1	2	3	4	5	6	7	8	9	10	11	12	13	14
Total pteropod biomass	**0.025**	**0.065**	**0.000**	**0.008**	**0.040**	**0.130**	**0.336**	**0.297**	**0.353**	**0.778**	**0.156**	**0.066**	**0.194**	**0.219**
Uncoiled euthecosomes	**0.025**	**0.065**	**0.000**	**0.008**	**0.036**	**0.073**	**0.194**	**0.210**	**0.271**	**0.653**	**0.057**	**0.050**	**0.130**	**0.175**
Cavolinia inflexa	0.011	0.028		0.008			0.017	0.008		0.033	0.015		0.038	0.044
Cavolinia uncinata												0.008		
Cavolinia gibbosa										0.014				
Cavolinia sp juv														
Diacavolinia sp							0.002							0.007
Clio cuspidata	0.015	0.012										0.012		
Clio pyr. pyr./lanceolata		0.012			0.026	0.011	0.093		0.009	0.044		0.012	0.031	0.012
Clio pyramidata sulcata														
Clio recurva		0.012												
Clio pyramidata antarctica														
Creseis clava						0.022	0.003		0.002	0.010		0.003	0.017	0.003
Creseis conica					0.003									0.030
Creseis virgula										0.026		0.012	0.002	0.031
Cuvierina sp					0.006	0.019	0.025	0.002		0.010				0.006
Diacria danae						0.001	0.004	0.001	0.001			0.000		0.000
Diacria trispinosa						0.011	0.012	0.113	0.066	0.022	0.041		0.041	0.036
Diacria major									0.018					
Diacria sp juv								0.005	0.019	0.011				
Hyalocylis striata							0.004							0.007
Styliola subula						0.009	0.035	0.082	0.155	0.482				
Cavoliniidae sp												0.003		
Coiled euthecosomes	**0.000**	**0.000**	**0.000**	**0.000**	**0.004**	**0.057**	**0.131**	**0.075**	**0.082**	**0.126**	**0.099**	**0.016**	**0.064**	**0.041**
Heliconoides inflatus					0.001	0.022	0.028	0.033	0.026	0.077	0.032	0.004	0.053	0.033
Heliconoides inflatus S														
Limacina bulimoides					0.001	0.022	0.099	0.037	0.046		0.023	0.001	0.007	0.006
Limacina helicina antarctica														
Limacina lesueurii					0.001	0.013	0.004	0.004	0.010	0.048	0.044	0.010	0.003	0.001
Limacina trochiformis														0.001
Gymnosomes	**0.000**	**0.000**	**0.000**	**0.000**	**0.000**	**0.000**	**0.010**	**0.012**	**0.000**	**0.000**	**0.000**	**0.000**	**0.000**	**0.003**

15	16	17	18	19	20	21	22	23	24	25	26	27	28	29	30	31
0.281	**1.238**	**1.951**	**0.373**	**0.280**	**0.866**	**0.532**	**0.607**	**0.446**	**0.411**	**0.235**	**0.068**	**1.301**	**3.159**	**0.606**	**0.033**	**0.041**
0.218	**0.964**	**1.867**	**0.274**	**0.245**	**0.790**	**0.468**	**0.481**	**0.362**	**0.328**	**0.211**	**0.029**	**0.194**	**0.429**	**0.057**	**0.000**	**0.000**
0.016	0.223	0.650	0.131	0.121	0.568	0.267	0.078	0.014	0.016							
	0.013															
	0.048												0.009			
	0.022	0.020														
0.078	0.389	0.903	0.040	0.021	0.058	0.040	0.106	0.038	0.021							
												0.032	0.118			
												0.146	0.302	0.057		
		0.005	0.005	0.010	0.073	0.105	0.050		0.010							
		0.015		0.041	0.024	0.005										
0.076	0.117	0.076	0.014													
0.003		0.076	0.005		0.014	0.005	0.015	0.005	0.005							
	0.001	0.001	0.001	0.001	0.001	0.001	0.001	0.003								
0.045	0.151	0.120	0.040	0.041			0.021	0.153	0.085			0.016				
			0.039	0.010			0.137	0.076								
					0.053	0.045	0.074	0.072	0.191	0.211	0.029					
0.064	**0.274**	**0.073**	**0.088**	**0.035**	**0.071**	**0.058**	**0.120**	**0.073**	**0.040**	**0.015**	**0.026**	**1.026**	**2.626**	**0.520**	**0.026**	**0.018**
0.046	0.225	0.020	0.012	0.008	0.020	0.015	0.020	0.027	0.014	0.008						
											0.021	0.164	0.193	0.055		
0.016	0.039	0.042	0.066	0.010	0.031	0.034	0.081	0.033	0.019	0.006		0.003				
											0.005	0.859	2.434	0.466	0.026	0.018
0.002	0.009	0.011	0.010	0.011	0.014	0.007	0.018	0.013	0.005							
				0.006	0.006	0.002		0.001	0.002	0.001						
0.000	**0.000**	**0.012**	**0.012**	**0.000**	**0.006**	**0.006**	**0.006**	**0.011**	**0.044**	**0.009**	**0.014**	**0.081**	**0.103**	**0.028**	**0.007**	**0.023**

7

Diversity and distribution of hyperiid amphipods along a latitudinal transect in the Atlantic Ocean

Alice K. Burridge, Marloes Tump, Ronald Vonk,
Erica Goetze & Katja T.C.A. Peijnenburg

Abstract

As commensals and parasitoids of gelatinous plankton, hyperiid amphipods play unique and important ecological roles in pelagic food webs. Because the diversity and biogeography of this group in oceanic waters is poorly known, we examined diversity and distribution patterns of hyperiids along a basin-scale meridional transect in the Atlantic Ocean (Atlantic Meridional Transect cruise 22). Hyperiids were collected from epipelagic and upper mesopelagic depths at 27 stations between 39°N and 45°S. A total of 70 species in 36 genera and 17 families were identified, the majority of which belonged to the epipelagic Physocephalata infraorder. We observed maximum species and genus richness in the equatorial upwelling region (up to 35 species, 27 genera per station; 7°N to 8°S), which appeared largely driven by increased diversity in the superfamily Platysceloidea, as well as a significant and positive relationship between species richness and sea surface temperature. Cluster analyses of hyperiid species assemblages along the transect broadly supported a division into gyral, equatorial, transitional, and subantarctic assemblages, congruent with Longhurst's biogeochemical provinces. Steepest transitions in hyperiid species composition occurred at the southern subtropical convergence zone (34-38°S). The majority of zooplankton groups show maximal diversity in subtropical waters, and our observations of equatorial maxima in species and genus richness for hyperiids suggest that the mechanisms controlling diversity in this group are distinct from other zooplanktonic taxa. These patterns may be driven by the distribution and diversity of gelatinous hosts for hyperiids, which remain poorly characterized at ocean basin scales. The data reported here provide new distributional records for epipelagic and upper mesopelagic hyperiids across six major oceanic provinces in the Atlantic Ocean.

Keywords:
Amphipods, Hyperiidea, Atlantic Ocean, Latitudinal diversity gradient, Biogeography

This chapter was published as:
Burridge A.K., Tump M., Vonk R., Goetze E., Peijnenburg K.T.C.A., in press. Diversity and distribution of hyperiid amphipods along a latitudinal gradient in the Atlantic Ocean. Progress in Oceanography, DOI: 10.1016/j.pocean.2016.08.003.

Introduction

The amphipod suborder Hyperiidea is an exclusively pelagic marine group, distributed from the sea surface to abyssopelagic depths worldwide. With 292 species currently described and accepted in the World Register of Marine Species (WoRMS), this peracarid crustacean group is a diverse component of the marine zooplankton. The majority of hyperiid species are commensals and parasitoids of gelatinous zooplankton (e.g., Harbison et al., 1977; Madin and Harbison, 1977; Laval, 1980), with tunicates, medusae, ctenophores, and siphonophores serving as primary hosts and additional associations reported for heteropod and pteropod molluscs and radiolarians (e.g., Harbison et al., 1977; Phleger et al., 1999; Gasca and Haddock, 2004). Characterization of host-parasite relationships is an active area of research (e.g., Gasca et al., 2015; Riascos et al., 2015), and some hyperiid genera and families appear to be restricted to particular host groups while others are less selective (e.g., Harbison et al., 1977; Madin and Harbison, 1977; Laval, 1980; Lavaniegos and Ohman, 1999). The association of the hyperiid with its host may encompass the entire life history or may be restricted to particular life stages of the amphipod. A small number of hyperiid amphipods, primarily in polar environments, are free-living, and they are often biomass dominants and important prey for seabirds (Bocher et al., 2001; Waluda et al., 2010), squids (Laptikhovsky, 2002), and fishes (Shreeve et al., 2009) in these ecosystems. Predatory fishes in other ecosystems also prey on commensal hyperiids, and they can make up a large fraction of their diets (Suntsov and Brodeur, 2008; Riascos et al., 2012; Choy et al., 2013). Hyperiids are routinely sampled in net-based oceanographic sampling programs, but their gelatinous hosts are largely destroyed by conventional sampling and preservation methods. As a result, Remotely Operated Vehicle (ROV) and scuba-based live observations of host-parasite associations derive largely from coastal areas (e.g., Monterey Bay, Gulf of California, Mediterranean Sea), while hyperiid diversity and distributions are known from a broader range of ocean ecosystems (e.g., Vinogradov et al., 1996; Zeidler and De Broyer, 2009).

Hyperiids are classified into two infraorders, the primarily bathypelagic and mesopelagic Physosomata and the epipelagic and mesopelagic Physocephalata (Vinogradov et al., 1996). The majority of hyperiid diversity is contained within the Physocephalata, with approximately 65% of extant species within the 20 families of this infraorder. Particularly diverse hyperiid families include the Scinidae (Physosomata; 45 species) and the Hyperiidae (Physocephalata; 29 species, WoRMS, 2016). Early workers recognized that many morphological features of hyperiids, such as mouthpart deformation (Dittrich, 1988), are correlated with their parasitoid association with gelatinous hosts, and may result from convergent evolution, with the suborder Hyperiidea then viewed as probably polyphyletic in origin (Pirlot, 1932; Vinogradov et al., 1996). Other morphological features, such as hypertrophied olfactory and visual systems, duplications of the eyes and an array of modifications to the appendages also likely derive from their pelagic life style (Harbison et al., 1977; Laval, 1980; Hurt et al., 2013; Baldwin Fergus et al., 2015).

Recent molecular phylogenetic studies of the Hyperiidea have supported monophyly of the infraorders as well as reciprocal monophyly of superfamilies Platysceloidea, Vibilioidea, and Phronimoidea within the Physocephalata, but also suggested novel placements for some groups (e.g., Paraphronimidae and Cystisomatidae; Browne et al., 2007; Hurt et al., 2013).

Our knowledge of the biogeography of hyperiids is limited, and most prior studies that report on the diversity of hyperiid assemblages in the Atlantic Ocean focus on particular ocean regions, often reporting species lists (e.g., Gasca, 2003, 2004, 2007). Characterizations of basin-scale patterns in the diversity and distribution of this group are rare (but see Tarling et al., 1995, southwest temperate Atlantic). Given the host-parasitoid relationship present for most hyperiid species, the large-scale patterns of hyperiid abundance and distribution are likely driven by gelatinous host abundance and diversity, as has been documented at the mesoscale in other ocean regions (e.g., Lavaniegos and Ohman, 1999; Lavaniegos and Hereu, 2009; Valencia et al., 2013). In other zooplankton groups, latitudinal diversity gradients often include subtropical maxima in diversity (species richness), with slightly lower diversity at equatorial latitudes, and dramatic declines poleward of the subtropical convergence zone (e.g., Reid et al., 1978; McGowan and Walker, 1993; Boltovskoy, 1998; Rutherford et al., 1999; Rombouts et al., 2009). A broad warm water plateau of species richness, across both subtropical and tropical waters, is another common latitudinal pattern observed in pelagic groups (e.g., Macpherson, 2002; Burridge et al., in press: Thesis chapter 6). Characterizing these broad-scale diversity gradients for different pelagic groups is important if we are to better understand the drivers of and controls on pelagic diversity (Macpherson, 2002; Beaugrand et al., 2013).

In this study, we report on the diversity and distribution of hyperiid amphipods across a continuous meridional transect in the Atlantic Ocean (39°N to 45°S) in order to assess large-scale biogeographic patterns and latitudinal diversity gradients for this group. The multidisciplinary Atlantic Meridional Transect programme (www.amt-uk.org, e.g., Rees et al., 2015) provided an ideal platform to sample hyperiid amphipods across a range of open ocean ecosystems (>12,000 km transect), and to examine distribution patterns within a rich oceanographic context. Our goals were to: (1) characterize the hyperiid species occurring in the epipelagic and upper mesopelagic zone across boreal to equatorial ocean provinces in the Atlantic Ocean, (2) test for the co-occurrence of species and identify recurring hyperiid assemblages within Atlantic ocean provinces, and (3) examine whether significant changes in species composition (biogeographical boundaries) are congruent with oceanographic gradients (temperature, salinity, chlorophyll *a*) and/or Longhurst's (1998) biogeochemical ocean provinces.

Methods

Sampling and identification

Bulk plankton samples were collected at 27 stations along Atlantic Meridional Transect Cruise 22 (AMT22) between October 16 and November 19, 2012 (Figure 1A; Table 1). Oblique tows were conducted with paired bongo (200 µm, 333 µm mesh) and Rectangular Midwater Trawl (RMT1, 333 µm mesh) plankton nets in the epipelagic and upper mesopelagic zone during night time at all stations except St. 42. Bongo tows were conducted on average between 319 m and the sea surface (range 150-488 m), while RMT tows were conducted over a shallower depth range (average maximum depth 152 m, range 62-216 m; Table 1). A LAT tag 1100 time-depth-recorder (LOTEK Wireless) was attached to the net frame to record the maximum depth of the tow. Tow durations averaged 50 min (range 38-90 min). Bulk samples were well-mixed and preserved in multiple jars. All hyperiid material examined in this study derived from the 333 µm nets (Bongo and RMT1) and was fixed in ethyl alcohol. Depending on the size of the total plankton sample, approximate fractions were examined for hyperiids, ranging from the entire original sample in oligotrophic waters, to 1 / 10 of the sample in very high biomass and low diversity regions (e.g., stations 64-74; see Table 1). Our approach was non-quantitative, and we therefore have focused our analyses primarily on species presence-absence, as well as on large-scale trends in diversity and species distributions. All hyperiids were counted and removed from the examined sample fraction. Hyperiids were identified based on the taxonomic keys of Bowman (1973), Bowman and Gruner (1973), Shih (1991), Vinogradov et al. (1996), and Zeidler (1999, 2003a,b, 2004a,b, 2006, 2009, 2012a,b, 2015). Representatives of all species were imaged using a Zeiss automated stacking light microscope. Voucher specimens were deposited in the Crustacea collection of Naturalis Biodiversity Center, Leiden, The Netherlands.

Conductivity-temperature-depth (CTD) casts in the upper 500 m of the water column were conducted at similar locations as the plankton tows. All plankton stations were matched to CTD casts based on geographic proximity. Seawater temperature and chlorophyll *a* concentration data were obtained using a Sea-Bird Electronics 3P Temperature Sensor and Chelsea MKIII Aquatracka Fluorometer, with data calibrated and archived by the British Oceanographic Data Centre (BODC).

Diversity and species assemblages

The species richness *R* and genus richness *D* for each station were used to summarize the diversity of hyperiid amphipods along the transect. We excluded juveniles of *Scina* sp. from the calculation of species richness because these specimens could not be confidently assigned. Lycaeidae sp. 1 was excluded from the calculation of genus diversity because this undescribed species shared morphological features of *Lycaea* as well as *Simorhynchotus* (Table S1). To gain insight into the underlying causes of the latitudinal trends in species richness, we tested for relationships between species diversity and environmental data by linear regression with species richness *R* as the dependent variable and sea surface temperature, chlorophyll *a*

Table 1. Collection information for all samples included in this study from Atlantic Meridional Transect 22. Samples indicated with an asterisk (*) by the Sample ID had sample sizes smaller than 30 specimens and were not included in statistical analyses. Oceanic provinces by Longhurst (1998) are given as NAST E (Northeast Atlantic subtropical gyral), NAST W (Northwest Atlantic subtropical gyral), NATR (North Atlantic tropical gyral), WTRA (Western tropical Atlantic), SATL (South Atlantic gyral), SSTC (South subtropical convergence), SANT (Subantarctic water ring), FKLD (Southwest Atlantic shelves).

AMT22 station	Sampling date	Latitude	Longitude	Net	Start tow	Max. depth [m]	Part of sample analyzed	Longhurst province
9*	2012-10-16	39°39'N	22°28'W	RMT1	3:23	174	1	NAST E
11*	2012-10-17	36°40'N	24°27'W	Bongo	3:17	306	1	NAST E
13	2012-10-18	34°21'N	27°38'W	RMT1	3:14	143	1/3	NAST W
17	2012-10-20	29°48'N	33°35'W	RMT1	2:45	195	1/3	NAST W
27	2012-10-25	17°42'N	36°27'W	Bongo	2:41	318	1/3	NATR
29	2012-10-26	15°18'N	34°40'W	RMT1	0:00	152	1	NATR
31	2012-10-27	12°14'N	32°23'W	Bongo	2:40	302	1/5	NATR
35	2012-10-29	6°37'N	28°19'W	Bongo	2:44	404	1	WTRA
37	2012-10-30	4°16'N	26°37'W	RMT1	0:01	216	1/2	WTRA
39	2012-10-31	1°08N	25°00'W	Bongo	2:40	339	1	WTRA
42	2012-11-01	2°55'S	25°01'W	RMT1	11:54	161	1	WTRA
43	2012-11-01	4°55'S	25°01W	Bongo	23:54	150	1	WTRA
45	2012-11-03	8°05'S	25°02'W	Bongo	2:42	488	1/2	WTRA
47	2012-11-03	11°18'S	25°03'W	RMT1	23:57	166	1	SATL
51	2012-11-06	18°30'S	25°06'W	Bongo	2:42	373	1	SATL
53	2012-11-08	20°06'S	24°31'W	Bongo	2:24	330	1	SATL
55	2012-11-09	22°57'S	25°00'W	Bongo	2:25	305	1	SATL
57	2012-11-09	25°29'S	25°00'W	RMT1	23:53	153	2/3	SATL
58	2012-11-11	28°22'S	25°28'W	RMT1	1:43	62	3/4	SATL
60	2012-11-12	30°01'S	27°43'W	RMT1	0:00	128	1	SATL
62	2012-11-14	34°07'S	33°30'W	Bongo	2:39	376	1	SATL-SSTC
64	2012-11-14	35°52'S	36°00'W	RMT1	23:53	132	3/16	SATL-SSTC
66	2012-11-16	38°05'S	39°19'W	Bongo	2:43	292	3/8	SSTC
68	2012-11-16	39°53'S	42°03'W	RMT1	23:57	146	3/8	SSTC
70	2012-11-18	42°08'S	45°36'W	Bongo	1:46	309	1/8	SSTC
72	2012-11-19	43°56'S	48°32'W	Bongo	1:45	281	1/10	SSTC
74	2012-11-19	45°30'S	51°21'W	Bongo	1:46	211	1/10	SANT-FKLD

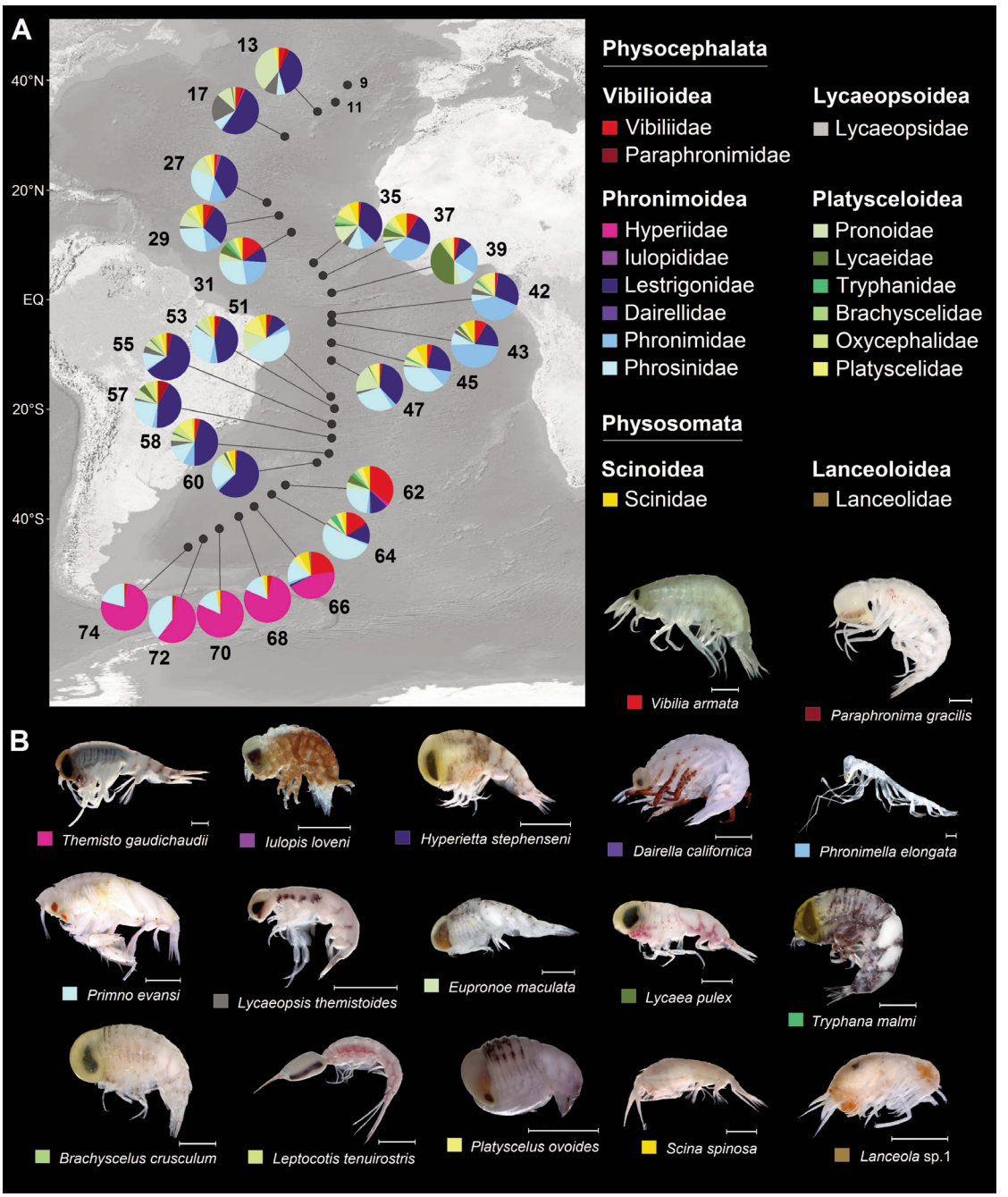

FIGURE 1. Overview of hyperiid diversity observed in open waters of the Atlantic Ocean. (A) Distribution of hyperiid families along Atlantic Meridional Transect 22. Piecharts indicate relative abundances of families at each station >30 specimens. (B) Most commonly found representatives of the 18 families that were sampled along Atlantic Meridional Transect cruise 22. Legend colors are arranged by infraorder and superfamily of hyperiids (following the current taxonomy as presented in the World Register of Marine Species: http://www.marinespecies.org). All scale bars represent 1 mm.

concentration at the deep chlorophyll maximum (DCM), or the integrated chlorophyll *a* concentration in the upper 300 m of the water column as independent variables using PAST 2.17 (Hammer et al., 2001). The sea surface temperature was represented by values sampled at 10 m depth in order to minimize missing data.

Comparisons of hyperiid assemblages across stations were conducted primarily with presence-absence based measures. We completed a second analysis incorporating species relative abundance, but only including stations for which the entire sample was examined (St. 29, 35, 39, 42, 43, 47, 53, 55, 60, 62). For all analyses, we reduced our dataset to exclude stations with small sample size (<30 specimens, stations 9 and 11). We also excluded the infraorder Physosomata because these species occur primarily at bathypelagic and mesopelagic depths (Vinogradov et al., 1996), and thus were inconsistently sampled in this study. We quantified inter-station similarities by means of hierarchical cluster analysis, similarity profile analysis (SIMPROF), and non-metric multidimensional scaling analysis (nMDS) in PRIMER 6 (Clarke, 1993; Clarke and Warwick, 2001; Clarke and Gorley, 2006). First, we used a Bray-Curtis similarity matrix derived from species presence-absence data including stations 13-74 and also, separately, for warm water stations 13-64. For the second analysis incorporating relative abundance, we used a Bray-Curtis similarity matrix based on standardized and transformed (log [x + 1]) species counts. The hierarchical cluster analyses were performed using the group average setting. We performed SIMPROF analyses to test the significance of the clusters using 1000 permutations and a significance level of $p < 0.05$. The nMDS ordinations were performed with 25 restarts. We inferred rank abundance curves in order to identify patterns of species dominance across ocean provinces and reported the most common species at each site.

Results

Diversity

A total of 3645 hyperiid specimens were counted and identified to 70 species belonging to 17 families (Figure 1A; Table S1). The most common species found along the AMT22 transect for each family are shown in Figure 1B. Sixty-six of the species sampled belonged to the Physocephalata infraorder (N = 3509 specimens), while four species belonged to the Physosomata (N = 136, including *Scina* specimens not identified to species). In our samples, Physocephalata were represented by four of the five described superfamilies, 15 of the 20 described families and 34 of the 56 described genera. Of the four Physocephalata superfamilies sampled, Platysceloidea was the most diverse (six families, 17 genera, 33 species), followed by Phronimoidea (six families, 14 genera, 25 species). The least diverse superfamilies were Vibilioidea (two families, two genera, seven species) and Lycaeopsoidea (one family, one genus, one species). The most abundant and diverse Physocephalata family was Lestrigonidae (N = 903; eight species). The Physosomata infraorder was represented by two superfamilies, each represented by a single family (Lanceolidae, Scinidae) and genus (Tables 2 and S1).

Hyperiid diversity was high in warm waters, with species richness *R* ranging from 15 to 36 species and genus diversity *D* from 13 to 27 genera at stations between 34°N and 36°S (Figure 2). Diversity peaked at stations located just north of the equator (4-15°N, St. 29, 31, 35, 37) with 29-36 species present in this region. In cooler waters south of 38°S (St. 66-74), hyperiid diversity declined to between three and nine species (Figure 2A; Table S1). A peak in species diversity associated with the equatorial upwelling region is apparent for Platysceloidea

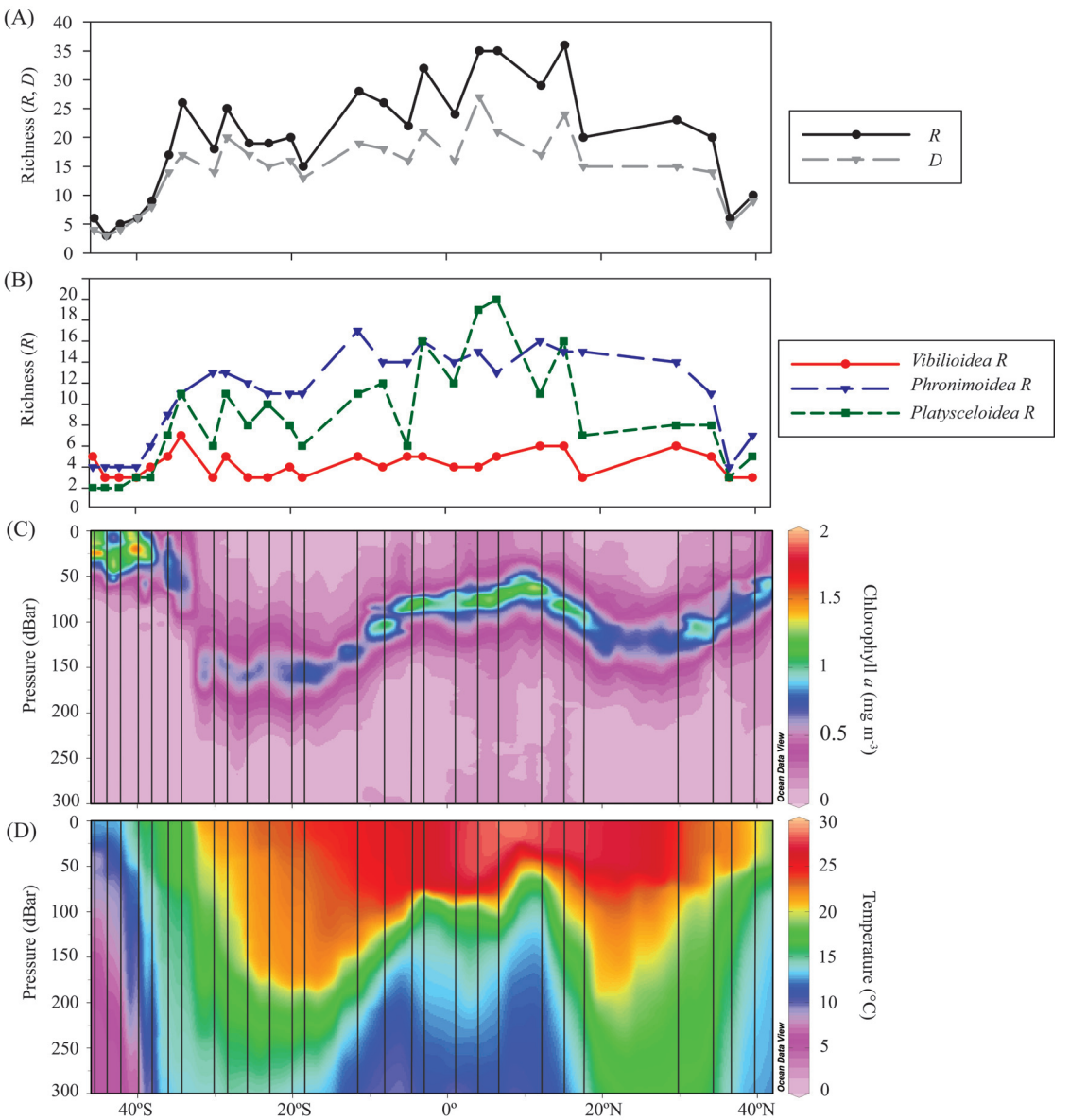

Figure 2. Basin-scale patterns of (A) total hyperiid species richness *R* and genus richness *D*, (B) species richness *R* of superfamilies Vibilioidea, Phronimoidea and Platysceloidea (Physocephalata), and (C,D) seawater temperature and chlorophyll *a* concentrations in the upper 300 m of the water column along AMT22. Vertical lines in (C) and (D) mark the sampling locations for this study.

TABLE 2. Overview of relative abundances of hyperiid species across six Longhurst ocean provinces sampled on Atlantic Meridional Transect cruise22 (AMT22). Species are listed by superfamily and family. Relative abundances report the percentage (%) of total specimens averaged within each oceanographic region. The first column per oceanographic region lists how common species are within that region: rare (R: <5.0% of total specimens averaged within that region); common (C: 5.0 – <15.0%); or abundant (A: = or >15.0%). The number of stations in which the species was found in each province is noted within brackets.

(Super)family	Species	NAST W St. 13, 17	%	NATR St. 27, 29, 31	%
Lycaeopsoidea					
Lycaeopsidae	*Lycaeopsis themistoides*	Common (2)	13.7	Rare (1)	1.2
Phronimoidea					
Dairellidae	*Dairella californica*				
Hyperiidae	*Hyperoche medusarum*				
	Hyperoche martinezii				
	Laxohyperia vespuliformis	Rare (1)	0.4		
	Themisto gaudichaudii				
	Themisto libellula				
Iulopididae	*Iulopis loveni*			Rare (1)	0.2
Lestrigonidae	*Hyperietta luzoni*	Rare (2)	3.4	Rare (1)	0.2
	Hyperietta stebbingi	Common (2)	6.0	Rare (3)	1.7
	Hyperietta stephenseni	Common (2)	5.6	Common (3)	7.3
	Hyperietta vosseleri	Rare (2)	2.6	Rare (1)	0.2
	Hyperioides longipes	Common (2)	6.8	Common (2)	6.8
	Lestrigonus bengalensis			Rare (1)	0.2
	Lestrigonus sp. 1	Abundant (2)	16.2	Common (3)	5.8
	Phronimopsis spinifera	Rare (2)	4.3	Rare (3)	2.2
Phronimidae	*Phronima atlantica*			Rare (2)	4.8
	Phronima sedentaria			Rare (3)	3.4
	Phronima solitaria				
	Phronima stebbingi	Rare (1)	0.4	Rare (2)	2.4
	Phronimella elongata			Rare (3)	4.8
Phrosinidae	*Anchylomera blossevillei*			Common (2)	6.3
	Phrosina semilunata	Rare (1)	1.3	Rare (3)	4.6
	Primno johnsoni			Rare (2)	0.7
	Primno evansi	Rare (2)	3.0	Common (2)	5.6
	Primno latreillei	Rare (2)	2.1	Common (3)	10.7
Platysceloidea					
Brachyscelidae	*Brachyscelus crusculum*			Rare (2)	1.7
	Brachyscelus globiceps				
	Brachyscelus macrocephalus				
	Brachyscelus sp. 1				
	Thamneus rostratus				
Lycaeidae	*Lycaea pulex*	Rare (1)	0.4	Rare (2)	2.2
	Lycaea serrata				
	Lycaea sp. 1				
	Lycaea sp. 2				
	Lycaeidae sp. 1				

WTRA St. 35, 37, 39, 42, 53, 45	%	SATL St. 47, 51, 53, 55, 57, 58, 60	%	SATL-SSTC St. 62, 64	%	SSTC, SANT-FKLD St. 66, 68, 70, 72, 74	%
Rare (3)	2.6	Rare (5)	2.3	Rare (1)	0.5		
Rare (1)	0.2			Rare (1)	0.5		
Rare (1)	0.1						
				Rare (1)	0.5		
				Rare (1)	0.5	Abundant (5)	76.9
				Rare (1)	0.5		
Rare (2)	0.8	Rare (3)	0.7	Rare (1)	1.0		
Common (5)	3.6	Rare (5)	1.6				
Common (6)	12.1	Common (7)	12.3	Common (2)	7.4		
Rare (4)	1.2	Rare (1)	0.4				
Rare (5)	1.7	Abundant (7)	21.7	Rare (2)	4.5	Rare (1)	0.1
Rare (5)	4.0	Common (7)	5.1	Rare (1)	0.5		
Rare (6)	3.0	Rare (6)	3.1				
Common (5)	7.1	Rare (2)	0.7	Rare (2)	1.5		
Common (6)	6.7	Rare (4)	0.5	Rare (1)	0.5		
Rare (3)	0.3	Rare (1)	0.1			Rare (1)	0.1
Common (6)	13.3	Rare (7)	2.6				
Common (6)	6.0	Common (5)	5.1				
Rare (6)	3.0	Common (5)	8.0	Rare (1)	3.5		
Rare (1)	2.2	Common (7)	6.8	Abundant (1)	18.3	Abundant (5)	17.9
Rare (6)	2.4	Rare (7)	4.8	Common (1)	14.9		
Rare (4)	2.0	Rare (1)	0.1	Rare (1)	1.0		
Rare (1)	0.1	Rare (1)	0.1	Rare (1)	0.5		
Rare (2)	0.2						
Rare (1)	0.1	Rare (1)	0.1				
Rare (1)	0.2						
Rare (3)	2.0	Rare (5)	1.2	Rare (1)	3.5		
Rare (1)	0.1						
Rare (3)	3.8						
Rare (1)	0.4						
Rare (2)	0.2						

Table 2. Continued

(Super)family	Species	NAST W St. 13, 17	%	NATR St. 27, 29, 31	%
Oxycephalidae	*Calamorhynchus pellucidus*			Rare (2)	0.5
	Cranocephalus scleroticus			Rare (1)	0.2
	Leptocotis tenuirostris				
	Oxycephalus piscator	Rare (1)	0.4		
	Rhabdosoma minor			Rare (1)	0.2
	Streetsia challengeri	Rare (1)	0.4	Rare (1)	0.2
	Streetsia mindanaònis				
	Streetsia porcella			Rare (2)	1.0
	Tullbergella cuspidata				
Platyscelidae	*Amphithyrus bispinosus*			Rare (1)	0.5
	Amphithyrus sculpturatus	Rare (1)	0.9		
	Platyscelus armatus	Rare (1)	0.4		
	Platyscelus crustulatus			Rare (1)	0.2
	Platyscelus ovoides	Rare (1)	0.4	Rare (3)	2.2
	Tetrathyrus forcipatus			Rare (2)	1.5
Pronoidae	*Eupronoe armata*	Rare (2)	3.8	Rare (3)	1.0
	Eupronoe maculata	Rare (1)	2.1	Common (3)	5.8
	Eupronoe minuta	Abundant (2)	17.9	Rare (2)	1.7
	Parapronoe campbelli	Rare (1)	0.4		
	Parapronoe crustulum			Rare (1)	0.2
	Parapronoe parva			Rare (1)	0.2
	Pronoe capito				
Tryphanidae	*Tryphana malmi*			Rare (1)	1.0
Vibilioidea					
Paraphronimidae	*Paraphronima gracilis*	Rare (2)	2.6	Rare (2)	2.2
Vibiliidae	*Vibilia armata*	Rare (2)	2.1	Common (2)	5.1
	Vibilia australis	Rare (2)	1.3	Rare (3)	1.0
	Vibilia borealis				
	Vibilia propinqua			Rare (2)	2.2
	Vibilia pyripes	Rare (1)	0.9		
	Vibilia stebbingi				

(Physocephalata), the most diverse superfamily in our data, with a maximum of 18 species present at station 35 (Figure 2B; Table S1). Phronimoidea (Physocephalata), the second most diverse superfamily in our study, showed a different pattern with highest species diversity observed between 29°N and 11°S at stations 17-47 (11-15 species). Species richness for this superfamily was between seven and 11 species in the central and southern parts of the southern gyre between 18 and 36°S at stations 51-64 (Figure 2B; Table S1). We found a significant and positive relationship between hyperiid species richness and sea surface temperature (R^2 = 0.65; N = 27; p < 0.001; Figure 3). However, there was no significant relationship between species richness and maximum chlorophyll *a* concentration (R^2 = 0.02; N = 27; p > 0.05) or between species richness and integrated chlorophyll *a* in the upper 300 m (R^2 = 0.14; N = 27; p > 0.05).

We found two species that have previously been reported to occur only in the Pacific and Indian oceans: *Scina curilensis* and *Tullbergella cuspidata* (Table S1). We

WTRA St. 35, 37, 39, 42, 53, 45	%	SATL St. 47, 51, 53, 55, 57, 58, 60	%	SATL-SSTC St. 62, 64	%	SSTC, SANT-FKLD St. 66, 68, 70, 72, 74	%
		Rare (1)	0.1				
Rare (1)	0.1						
Rare (1)	0.1	Rare (4)	1.2				
Rare (2)	0.2	Rare (4)	0.7				
Rare (1)	0.2	Rare (2)	0.2				
Rare (2)	0.4	Rare (2)	0.4	Rare (1)	0.5		
Rare (1)	0.1						
Rare (1)	0.1						
		Rare (1)	0.1				
Rare (2)	0.2						
Rare (4)	0.6	Rare (1)	0.8				
Rare (3)	0.8						
Rare (1)	0.1						
Rare (6)	3.8	Rare (6)	4.3	Rare (2)	4.0	Rare (2)	1.0
Rare (5)	2.6	Rare (2)	0.6				
Rare (4)	1.2	Rare (3)	2.5	Rare (1)	0.5		
Rare (6)	3.3	Common (6)	6.9	Rare (1)	0.5		
Rare (2)	0.2	Rare (6)	1.4	Rare (2)	2.0		
Rare (1)	0.2						
Rare (3)	0.4			Rare (2)	1.0		
Rare (2)	0.2						
Rare (2)	0.2						
Rare (4)	0.9			Rare (2)	3.5		
Rare (2)	0.3	Rare (6)	2.0	Rare (2)	1.0		
Rare (6)	3.8	Rare (2)	0.2	Common (2)	8.9	Rare (4)	1.9
Rare (2)	0.3	Rare (2)	0.6	Rare (1)	1.5	Rare (1)	0.1
Rare (4)	0.5						
		Rare (2)	0.4	Rare (1)	2.0	Rare (1)	0.1
Rare (1)	0.1			Rare (1)	2.0		
				Common (1)	13.4	Rare (2)	1.8

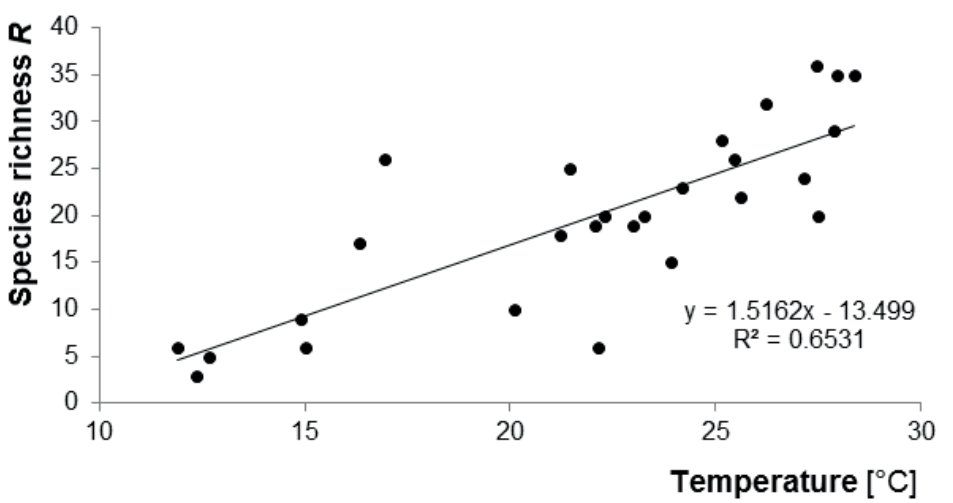

FIGURE 3. Relationship between hyperiid species richness *R* and sea surface temperature. Linear regression and R^2 value as reported in the legend.

also found six morphologically distinct hyperiids that may represent undescribed species, and are treated as species herein. These were listed as *Lanceola* sp. 1, *Lestrigonus* sp. 1, *Brachyscelus* sp. 1, *Lycaea* sp. 1 and 2, and Lycaeidae sp. 1.

Distribution patterns

Some of the well-sampled hyperiid families were present in both warm and cold waters along the AMT22 transect (Phrosinidae, Platyscelidae, Scinidae, Vibiliidae), while other families were restricted to warmer waters, occurring only as far south as 34°S (St. 62; Brachyscelidae, Lycaeidae, Oxycephalidae), 36°S (St. 64; Lycaeopsidae, Paraphronimidae, Pronoidae) or 38°S (St. 66; Lestrogonidae, Phronimidae). The Hyperiidae showed a different pattern: they were found sporadically in warm waters, but dominated in the subantarctic (St. 66-74; Figure 1A; Tables 2 and S1). Species distribution patterns were highly diverse (Table S1). Many hyperiid species were present across a broad warm water range, including *Eupronoe maculata*, *Hyperietta stephenseni*, *Lycaeopsis themistoides*, *Phronimella elongata*, *Phronimopsis spinifera* and *Primno latreillei*. Some species were restricted to locations in or near the equatorial region (e.g., *Vibilia borealis*) or the subtropical gyres (*Eupronoe minuta*). Other species were found only in the northern gyre and sometimes also in the (near-)equatorial region, but were absent from or very rare in the southern gyre (e.g., *Amphithyrus bispinosus*, *Hyperietta vosseleri*, *Parapronoe campbelli*, *Phronima stebbingi*, and *Primno johnsoni*). *Themisto gaudichaudii* and *Vibilia stebbingi* were found at southern transitional and subantarctic locations. Several species occurred across a wide range of warm and cold water regions along AMT22, sometimes with intermittent or disjunct distribution patterns. For example, *Vibilia armata* was absent in the central part of the southern gyre and *Primno evansi* was absent in the equatorial region. Such wide distribution patterns are questionable, and it is possible that some of these species represent a complex of morphologically similar, or cryptic, species.

Species assemblages

Hyperiid species composition differed significantly between stations along AMT22. The cluster and SIMPROF analyses based on species presence-absence identified three clusters ($p < 0.05$; Figure 4A), which are also apparent in the nMDS ordinations (Figure 4B,C). The species composition of subantarctic stations in the first cluster (St. 66, 68, 70, 72 and 74; 38-46°S) was most distinct from all other regions (15% similarity). A second cluster represented all stations from 13 to 64 except St. 62 (34°S), which was significantly distinct from all other stations in this analysis. The ordination of St. 64 may be artifactual, caused by the relatively small sample fraction that was examined at this station (Table 1). Stations 62 and 64 are located in southern temperate waters and represent transitional species assemblages between the southern subtropical gyre and subantarctic provinces. The equatorial stations 35, 37, 39, 42, 43 and 45 (7°N to 8°S) grouped together, although this cluster was not statistically significant (Figure 4). In analyses that included relative species abundance data and only included stations that were examined in their

entirety (11 stations, excluding the subantarctic region), we obtained three significant clusters ($p < 0.05$; FIGURE 5A). One cluster represented the equatorial upwelling region (St. 35, 39, 42, 43), another consisted of the northern and southern gyre stations combined (St. 29, 47, 51, 53, 55, 60), and the southern temperate St. 62 was distinct. These results were congruent with analyses based on presence-absence data only, but these analyses were better able to resolve the equatorial upwelling region as a distinct cluster (FIGURE 5).

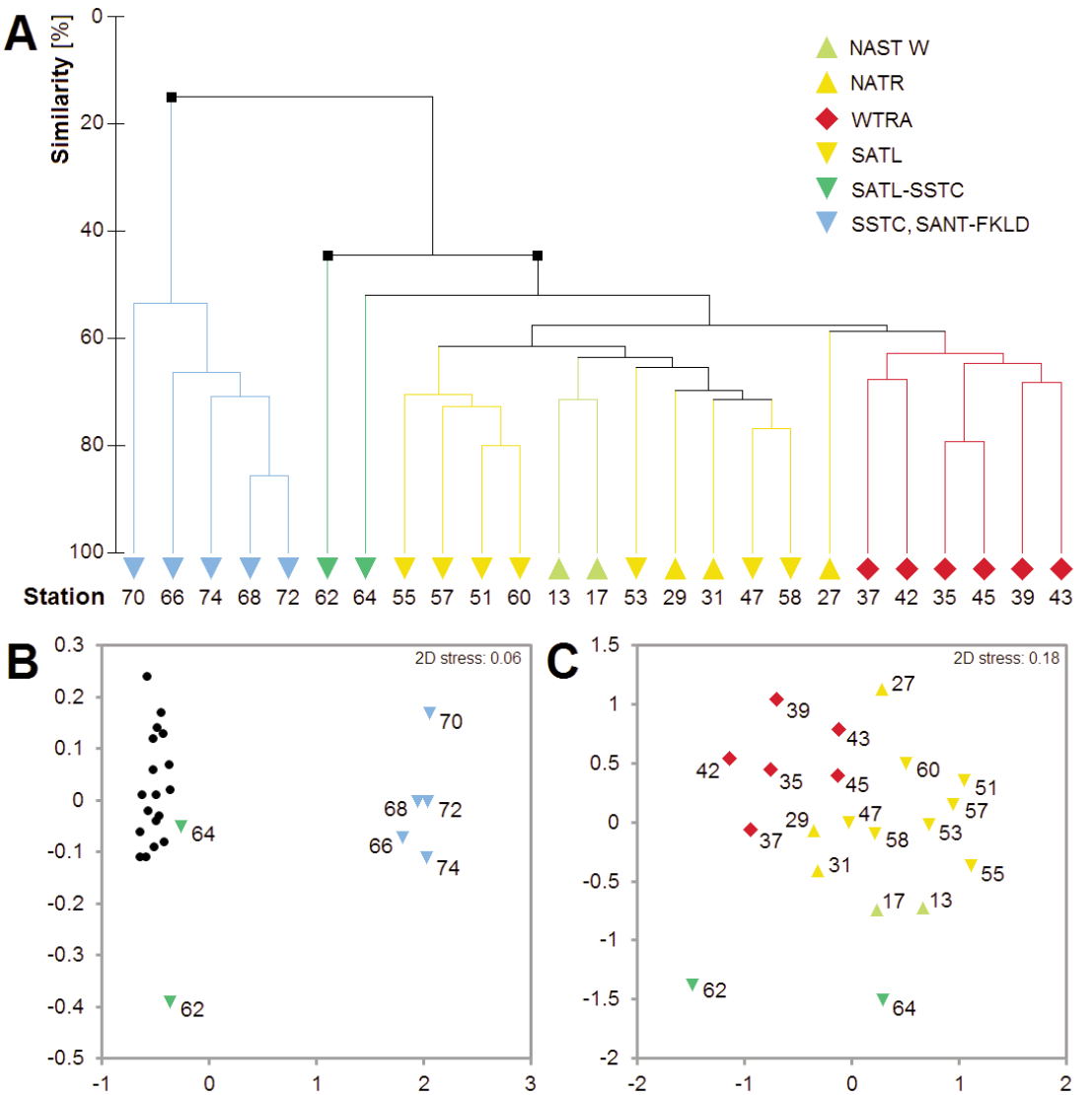

FIGURE 4. Species assemblages of Atlantic Physocephalata hyperiids based on presence-absence data for stations with >30 specimens. (A) Hierarchical cluster analysis of stations, according to their species composition. Three significant clusters are shown (SIMPROF $p < 0.05$). (B,C) Non-metric Multi-Dimensional Scaling (nMDS) ordination based on the species assemblage of hyperiids (B) using all stations, and (C) excluding the subantarctic stations 66, 68, 70, 72 and 74. Symbols are colored according to Longhurst provinces, with upward triangles for the northern hemisphere, downward triangles for the southern hemisphere and diamonds for equatorial locations.

The geographic distribution of hyperiid species assemblages corresponded to Longhurst's biogeochemical provinces (Longhurst, 1998), with seasonal positions as estimated by Reygondeau et al. (2013). Our analyses separated between the equatorial (western tropical Atlantic, WTRA), gyral (northwest Atlantic subtropical gyral, NAST W; north Atlantic tropical gyral, NATR; south Atlantic gyral, SATL), subantarctic (south subtropical convergence, SSTC; subantarctic water ring – southwest Atlantic shelves, SANT-FKLD), and temperate, transitional (SATL-SSTC) stations (Figures 4 and 5; Table 1). Stations from the NAST W province had similar species assemblages, although not significantly different from other gyre stations (Figure 4; Table 1).

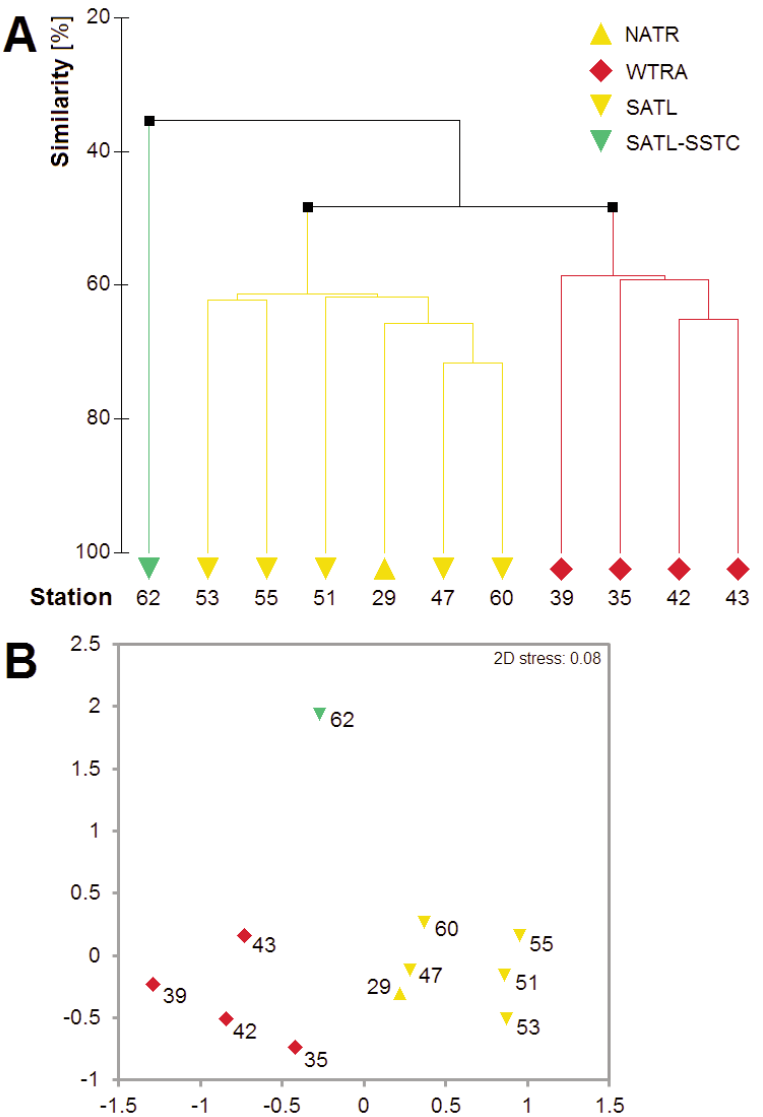

Figure 5. Species assemblages of Atlantic Physocephalata hyperiids based on relative abundance data for stations that were examined in their entirety (>30 specimens). (A) Hierarchical cluster analysis of stations, according to Physocephalata species composition and relative abundance (see Table 1). Three significant clusters are shown (SIMPROF $p < 0.05$). (B) nMDS ordination based on the species assemblage of hyperiids. Symbols are colored as in Figure 4.

An overview of species composition and relative abundance of hyperiids in six regions along the meridional transect is presented in Table 2. In the NAST W province (St. 13, 17), *Eupronoe minuta* (17.9%) and *Lestrigonus* sp. 1 (16.2%) were the most abundant species. *Primno latreillei* (10.7%), *Hyperietta stephenseni* (7.3%) and *Hyperioides longipes* (6.8%) were common in the NATR province (St. 27-31). In the equatorial WTRA province (St. 35-43), the most common species were *Phronimella elongata* (13.3%) and *Hyperietta stephenseni* (12.1%). In the southern gyre (SATL, St. 47-60), *Hyperioides longipes* (21.7%) and *Hyperietta stephenseni* (12.3%) were the most common species. The two samples from the southern transition zone (St. 62 and 64, SATL-SSTC) demonstrated a steep transition from species common in the southern gyre toward the subantarctic hyperiid assemblage. Across these stations combined, the most common species were *Primno evansi* (18.3%), *Primno latreillei* (14.9%) and *Vibilia stebbingi* (13.4%). In the subantarctic (SSTC, SANT-FKLD, St. 66-74), *Themisto gaudichaudii* was overwhelmingly dominant (76.9%), followed by *Primno evansi* (17.9%). The rank abundance curves confirmed a pattern of strong species dominance in the subantarctic, while there was never a dominant species (>50% per station) in the warm water regions, including southern transitional stations 62 and 64 (Figure S1).

Discussion

Hyperiid amphipods are an enigmatic macrozooplankton group and an important component of pelagic food webs. Despite their abundance in open ocean ecosystems from polar to tropical waters, hyperiid diversity and distribution patterns have not been characterized at basin-wide spatial scales. In this study, we examined the diversity and distribution of epipelagic and upper mesopelagic hyperiids along a meridional transect in the Atlantic Ocean spanning >80 degrees of latitude (39°N to 45°S). The majority of species sampled belonged to the Physocephalata infra-order, characterized by their large heads and eyes relative to their body length (Figure 1B). Across this transect, we identified 70 species from 17 families, of which six species represent putative undescribed species. We report new distributional records in the Atlantic Ocean for *Scina curilensis* and *Tullbergella cuspidata*, which were previously only reported from the Indo-Pacific.

Latitudinal diversity gradients

Overall, the dominant pattern in the latitudinal diversity gradient for hyperiids is a species diversity peak in the equatorial upwelling region, which is mainly caused by high equatorial diversity in the Platysceloidea hyperiids. Although this latitudinal pattern was also observed for salps (Macpherson, 2002), it is not the dominant pattern for latitudinal diversity gradients in the pelagic. A bimodal pattern of species richness is most commonly observed, with highest diversity in the subtropical gyres, (slightly) lower diversity in the equatorial upwelling zone, and a sharp decrease in species diversity poleward of the subtropical convergence (e.g., Rutherford et al., 1999; Brayard et al., 2005; Boyce et al., 2008; Dolan and Pierce, 2013). Such a pattern was reported for anthomedusan hydrozoans (Macpherson,

2002), cephalopods (Rosa et al., 2008) as well as for planktonic crustaceans, including euphausiids (Angel, 1997; Tittensor et al., 2010), decapods (Angel, 1997), and ostracods (Angel, 1997; Angel et al., 2007). Some fishes and microplanktonic groups also demonstrate this bimodal pattern, such as tuna and billfish (Boyce et al., 2008), tintinnid ciliates (Dolan and Pierce, 2013) and planktonic foraminifera (Rutherford et al., 1999; Tittensor et al., 2010). Finally, this pattern was observed for shelled pteropods along AMT24, a similar basin-scale transect in the Atlantic Ocean (Burridge et al., in press: Thesis chapter 6). A second latitudinal diversity pattern reported for some pelagic groups is of a broad plateau of species richness across subtropical and tropical waters (e.g., siphonophores and cephalopods; Macpherson, 2002). The Phronimoidea hyperiids in our study demonstrated this diversity plateau, with species richness relatively constant across warm waters of both subtropical gyres and the equatorial region (Figure 2B). Collectively, these studies demonstrate that basin-scale latitudinal diversity patterns differ among pelagic groups, and even among different superfamilies within hyperiid amphipods, suggesting that they may result from different drivers.

Because most hyperiid amphipods are commensal or parasitic on gelatinous hosts, their large-scale patterns in distribution, abundance, and diversity are likely driven substantially by host abundance and diversity (e.g., Madin and Harbison, 1977; Laval, 1980; Lavaniegos and Ohman, 1999; Gasca et al., 2007, 2015). In this study, we find some evidence that distribution patterns of hyperiids may be associated with distribution patterns of their respective hosts. However, we know that these fragile gelatinous plankton groups are not sampled adequately with plankton nets. Within Platysceloidea, the superfamily with a high equatorial peak in species diversity, the host-associations appear to be more specific than in the Phronimoidea superfamily, which had a broad warm water plateau in species richness (Figure 2B; Harbison et al., 1977, 1978; Madin and Harbison, 1977; Laval, 1980; Gasca et al., 2007, 2015). For example, the Lycaeidae family (Platysceloidea) is strongly associated with salp and pyrosome tunicates (e.g., Harbison, 1976; Madin and Harbison, 1977; Laval, 1980). The Lycaeidae family was most diverse in the equatorial region and contributed to the equatorial species diversity peak for Platysceloidea that was observed in this study (Figure 2B; Table S1). Likewise, salps show a peak in species diversity in equatorial waters (Macpherson, 2002) and salp blooms have been reported to be associated with increases in primary production (Stone and Steinberg, 2014) and upwelling of nutrients (Li et al., 2011) as occurs in the equatorial upwelling zone. We did not find prior reports in the literature suggesting a higher abundance of siphonophores or ctenophores in the equatorial region that may further explain the high equatorial diversity of Platysceloidea (but see Stemmann et al., 2008, for differences in abundance of gelatinous zooplankton between other oceanic regions worldwide). However, we noticed high abundances of pyrosomes, salps and other gelatinous plankton in the equatorial upwelling region along AMT22 (Peijnenburg and Goetze, unpubl. observations). In contrast, an example of less specific host associations at the family-level can be found in Hyperiidae (Phronimoidea),

with species known to associate with salp tunicates, ctenophores, scyphozoans, and antho- and leptomedusan hydrozoans (e.g., Harbison et al., 1977; Madin and Harbison, 1977; Laval, 1980; Lavaniegos and Ohman, 1999; Kruse et al., 2015). The tropical and subtropical plateau in species diversity of the Phronimoidea superfamily may be linked to this low host specificity.

Species assemblages and oceanography

Hyperiid species assemblages were distinct for gyral, equatorial, transitional, and subantarctic stations along AMT22 (Figures 4 and 5). The sharpest transition in hyperiid species composition occurred in the South Atlantic Ocean between the southern subtropical convergence and the subantarctic province, located at ~34-38°S. This transition consisted of a sudden drop in species diversity, with *Themisto gaudichaudii* and *Primno evansi* dominating in subantarctic waters (76.9 and 17.9% of the total assemblage; Table 2). The location of this transition is similar to that found for pteropods, which also showed dramatic declines in species richness poleward of the convergence zone along a similar AMT transect (AMT24; Burridge et al., in press: Thesis chapter 6). This region is characterized by a shift from oligotrophic waters with a deep DCM (150-200 m) and very low chlorophyll *a* concentrations (<0.6 mg/m^3 at the DCM) to well-mixed waters with shallow (<75 m) and high (>0.75 mg/m^3) maximum chlorophyll *a* concentrations. We found similar hyperiid species assemblages in the northern and southern subtropical gyres, a pattern also observed for assemblages of pteropods (Burridge et al., in press: Thesis chapter 6), copepod genera (Woodd-Walker et al., 2002), and cephalopod families (Rosa et al., 2008) within the Atlantic, as well as for several groups in the Pacific basin (e.g., Brinton, 1962; Williamson and McGowan, 2010). However, the northern and southern gyre ecosystems are not exact replicates of one another, as was reflected by the slightly lower hyperiid diversity and higher relative species dominance in the southern gyre (Figures 2 and S1).

The hyperiid species assemblage in the equatorial region occurred between ~7°N and 8°S, across a narrower latitudinal band than observed in some other zooplankton groups (e.g., Woodd-Walker et al., 2002; Angel et al., 2007; Hirai et al., 2015; Burridge et al., in press: Thesis chapter 6; Goetze et al., in press). Specifically, the location of the northern boundary of the equatorial hyperiid assemblage did not extend as far north as is commonly found for other zooplankton. Burridge et al. (in press: Thesis chapter 6) found a distinct equatorial assemblage between 14°N and 4°S with transitions at 18°N and 8°S for pteropod species along a similar Atlantic transect (AMT24, 2014). Angel et al. (2007) studied the inter-station similarities of ostracod assemblages in the North Atlantic and found that stations at 18°N, 10°N and 0° grouped closely together, suggesting that the equatorial species assemblage extended much farther north than was observed in hyperiids. For copepod genera, the equatorial assemblage occurred between 17.5°N and 7.5°S (Woodd-Walker et al., 2002). This narrower equatorial distribution for hyperiids may be a consequence of their dependence on gelatinous hosts, which serve as a micro-environment over large parts of the hyperiid life cycle (e.g., Laval, 1980).

However, little is known about species diversity and distribution patterns of gelatinous hosts across these Atlantic Ocean provinces (as shown by the distribution of the Jellyfish Database Initiative (JEDI) metadata sets in Condon et al., 2012), impeding our ability to assess whether the boundaries of distinct hyperiid species assemblages reflect those of their gelatinous hosts.

There are several limitations of the sampling in this study, and further work on hyperiids at ocean basin scales is justified. Our material was collected with the primary goal of providing specimens for molecular studies on marine zooplankton, and so while the 200 µm mesh net was handled quantitatively (e.g., calibrated flowmeter mounted in the net), the paired 333 µm mesh bongo net was intended for live collections of larger-bodied animals. Subsequent work should be conducted on a more quantitative collection of material, drawing from the initial taxonomic observations of this study. In addition, more information on the diversity and distribution of gelatinous hosts would enable greater inference from our observations on hyperiids. Although it may not be appropriate to attempt to quantify the gelatinous plankton in our net-collected samples, one fruitful way forward could be to examine the gut contents of hyperiids using a molecular approach in order to establish the taxonomic identities of hyperiid-host relationships (e.g., metabarcoding; Pompanon et al., 2012). Hyperiids often feed on host tissues (Laval, 1980), and DNA sequences from hyperiid stomach contents could reveal host identity in the majority of cases where net-collected animals have been disturbed from their hosts. Similar molecular diet studies have been very informative for detecting novel trophic links in other marine species (e.g., Deagle et al., 2009; Olsen et al., 2014; Albaina et al., 2016).

Conclusion

This study is among the first to examine large-scale diversity and distribution patterns of hyperiid amphipods across open waters of the Atlantic, and our data provide important new distributional records across six oceanic provinces. The latitudinal maximum in hyperiid species richness occurred in the equatorial upwelling region, and was largely driven by increases in the diversity of Platysceloidea hyperiids. We also observed a significant positive relationship between species richness and sea surface temperature at the basin scale. The dominant paradigm of a bimodal pattern of species richness in pelagic systems, with maxima in the subtropical gyres, was not supported by our data on hyperiids. Instead we propose that the large-scale patterns of hyperiid diversity are at least partly driven by gelatinous host abundance and diversity. However, limited knowledge of the diversity and distribution of gelatinous zooplankton hosts impedes our inferences regarding drivers of these basin-scale patterns in hyperiids. Species assemblages along AMT22 broadly supported a division into gyral, equatorial, transitional, and subantarctic hyperiid communities, congruent with Longhurst's (1998) biogeochemical provinces. Biogeographic distributions of hyperiids ranged from species that were endemic to specific regions (e.g., *Vibilia borealis*, *Eupronoe minuta*, *Hyperietta vosseleri*, *Vibilia stebbingi*), to species that occurred across broad warm

water ranges (e.g., *Hyperietta stephenseni*). Some species occurred in warm-, intermediate, as well as cold water regions (e.g., *Vibilia armata*, *Primno evansi*) often with disjunct distribution patterns. Such broadly distributed species may represent assemblages of cryptic or morphologically similar species, and would be interesting target species for future phylogeographic and taxonomic studies.

Acknowledgements

We thank the officers and crew of the RRS James Cook for supporting our zooplankton collections, K. van den Berg and K. Beentjes for help with imaging of hyperiid specimens, and J. Huisman for comments on the manuscript. This work was supported by a Netherlands Organisation for Scientific Research (NWO) cruise participation grant and VENI grant 863.08.024 to K.T.C.A. Peijnenburg. E. Goetze and the fieldwork for this study were supported under National Science Foundation (USA) grants OCE-1029478 and OCE-1338959. Plankton collections for this study were partially supported by the UK Natural Environmental Research Council National Capability funding to Plymouth Marine Laboratory and the National Oceanography Centre, Southampton. This is contribution number 304 of the Atlantic Meridional Transect Programme.

References

Albaina A., Aguirre M., Abad D., Santos M., Estonba A., 2016. 18S rRNA V9 metabarcoding for diet characterization: a critical evaluation with two sympatric zooplanktivorous fish species. Ecology and Evolution 6, 1809–1824.

Angel M.V., 1997. Pelagic biodiversity. In: Ormond R.F.G., Gage J.R., Angel M.V. (Eds.), Marine Biodiversity, Patterns and Processes. Cambridge University Press, Cambridge, pp. 35–68.

Angel M.V., Blachowiak-Samolyk K., Drapun I., Castillo R., 2007. Changes in the composition of planktonic ostracod populations across a range of latitudes in the North-east Atlantic. Progress in Oceanography 73, 60–78.

Baldwin Fergus J.L., Johnsen S., Osborn K.J., 2015. A unique apposition compound eye in the mesopelagic hyperiid amphipod *Paraphronima gracilis*. Current Biology 25, 473–478.

Beaugrand G., Rombouts I., Kirby R.R., 2013. Towards an understanding of the pattern of biodiversity in the oceans. Global Ecology and Biogeography 22, 440–449.

Bocher P., Cherel Y., Labat J.-P., Mayzaud P., Razouls S., Jouventin P., 2001. Amphipod-based food web: *Themisto gaudichaudii* caught in nets and by seabirds in Kerguelen waters, southern Indian Ocean. Marine Ecology Progress Series 223, 261–276.

Boltovskoy D., 1998. Pelagic biogeography: background, gaps and trends. In: Pierrot-Bults, A.C. (Ed.), Pelagic Biogeography ICoPB II. IOC/UNESCO, Paris, pp. 53–64.

Bowman T.E., 1973. Pelagic amphipods of the genus *Hyperia* and closely related genera (Hyperiidea: Hyperiidae). Smithsonian Contributions to Zoology 136, 1–76.

Bowman T.E., Gruner H.E., 1973. The families and genera of Hyperiidea (Crustacea: Amphipoda). Smithsonian Contributions to Zoology 146, 1–64.

Boyce D.G., Tittensor D.P., Worm B., 2008. Effects of temperature on global patterns of tuna and billfish richness. Marine Ecology Progress Series 355, 267–276.

Brayard A., Escarguel G., Bucher H., 2005. Latitudinal gradient of taxonomic richness: combined outcome of temperature and geographic mid-domain effects? Journal of Zoological Systematics 43, 178–188.

Brinton E., 1962. The distribution of Pacific euphausiids. Bulletin of the Scripps Institution of Oceanography of the University of California 8, 51–270.

British Oceanographic Data Centre (BODC) http://www.bodc.ac.uk

Browne W.E., Haddock S.H.D., Martindale M.Q., 2007. Phylogenetic analysis of lineage relationships among hyperiid amphipods as revealed by examination of the mitochondrial gene, cytochrome oxidase I (COI). Integrative and Comparative Biology 47, 815–830.

Burridge A.K., Goetze E., Wall-Palmer D., Le Double S.L., Huisman J., Peijnenburg K.T.C.A., in press. Diversity and abundance of pteropods and heteropods along a latitudinal gradient across the Atlantic Ocean. Progress in Oceanography, published online in 2016. *Thesis chapter 6.*

Choy C.A., Portner E., Iwane M., Drazen J.C., 2013. Diets of five important predatory mesopelagic fishes of the central North Pacific. Marine Ecology Progress Series 492, 169–184.

Clarke K.R., 1993. Non-parametric multivariate analyses of changes in community structure. Australian Journal of Ecology 18, 117–143.

Clarke K.R., Gorley R.N., 2006. PRIMER Version 6: User Manual/Tutorial. PRIMER-E, Plymouth, UK.

Clarke K.R., Warwick R.M., 2001. Change in Marine Communities: An Approach to Statistical Analysis and Interpretation. PRIMER-E, Plymouth, UK.

Condon R.H., Graham W.M., Duarte C.M., Pitt K.A., Lucas K.H., et al., 2012. Questioning the rise of gelatinous zooplankton in the world's oceans. BioScience 62, 160–169.

Deagle B.E., Kirkwood R., Jarman S.N., 2009. Analysis of Australian fur seal diet by pyrosequencing prey DNA in faeces. Molecular Ecology 18, 2022–2038.

Dittrich B., 1988. Studies on the life cycle and reproduction of the parasitic amphipod *Hyperia galba* in the North Sea. Helgoländer Meeresuntersuchungen 42, 79–98.

Dolan J.R., Pierce R.W., 2013. Diversity and distributions of tintinnids. In: Dolan J.R., Montagnes D.J.S., Agatha S., Wayne Coats D., Stoecker D.K. (Eds.), The Biology and Ecology of Tintinnid Ciliates: Models for Marine Plankton. John Wiley & Sons, Hoboken, pp. 214–243.

Gasca R., 2003. Hyperiid amphipods (Crustacea: Peracarida) in relation to a cold-core ring in the Gulf of Mexico. Hydrobiologia 510, 115–124.

Gasca R., 2004. Distribution and abundance of hyperiid amphipods in relation to summer mesoscale features in the southern Gulf of Mexico. Journal of Plankton Research 26, 993–1003.

Gasca R., 2007. Hyperiid amphipods of the Sargasso Sea. Bulletin of Marine Science 81, 115–125.

Gasca R., Haddock S.H.D., 2004. Associations between gelatinous zooplankton and hyperiid amphipods (Crustacea: Peracarida) in the Gulf of California. Hydrobiologia 530, 529–535.

Gasca R., Hoover R., Haddock S.H.D., 2015. New symbiotic associations of hyperiid amphipods (Peracarida) with gelatinous zooplankton in deep waters off California. Journal of the Marine Biological Association of the United Kingdom 95, 503–511.

Gasca R., Suárez-Morales E., Haddock S.H.D., 2007. Symbiotic associations between crustaceans and gelatinous zooplankton in deep and surface waters off California. Marine Biology 151, 233–242.

Goetze E., Hüdepohl P.T., Chang C., Van Woudenberg L., Iacchei M., Peijnenburg K.T.C.A., in press. Ecological dispersal barrier across the equatorial Atlantic in a migratory planktonic copepod. Progress in Oceanography, published online in 2016.

Hammer Ø., Harper D.A.T., Ryan P.D., 2001. PAST: paleontological statistics software package for education and data analysis. Palaeontologia Electronica 4, 1–9.

Harbison G.R., 1976. The development of *Lycaea pulex* Marion, 1874 and *Lycaea vincentii* Stebbing, 1888 (Amphipoda, Hyperiidea). Bulletin of Marine Science 26, 152–164.

Harbison G.R., Biggs D.C., Madin L.P., 1977. The associations of Amphipoda Hyperiidea with gelatinous zooplankton. II. Associations with Cnidaria, Ctenophora and Radiolaria. Deep-Sea Research 24, 465–488.

Harbison G.R., Madin L.P., Swanberg R., 1978. On the natural history and distribution of oceanic ctenophores. Deep-Sea Research 25, 233–256.

Hirai J., Tsuda A., Goetze E., 2015. Extensive genetic diversity and endemism across the global range of the oceanic copepod *Pleuromamma abdominalis*. Progress in Oceanography 138, 77–90.

Hurt C., Haddock S.H.D., Browne W.E., 2013. Molecular phylogenetic evidence for the reorganization of the Hyperiid amphipods, a diverse group of pelagic crustaceans. Molecular Phylogenetics and Evolution 67, 28–37.

Kruse S., Pakhomov E.A., Hunt B.V.P., Chikaraishi Y., Ogawa N.O., Bathmann U., 2015. Uncovering the trophic relationship between *Themisto gaudichaudii* and *Salpa thompsoni* in the Antarctic Polar Frontal Zone. Marine Ecology Progress Series 529, 63–74.

Laptikhovsky V., 2002. Diurnal feeding rhythm of the short-fin squid *Illex argentines* (Cephalopoda: Ommastrephidae) in the Falkland waters. Fisheries Research 59, 233–237.

Laval P., 1980. Hyperiid amphipods as crustacean parasitoids associated with gelatinous zooplankton. Oceanography and Marine Biology: An Annual Review 18, 11–56.

Lavaniegos B.E., Hereu C.M., 2009. Seasonal variation in hyperiid amphipod abundance and diversity and influence of mesoscale structures off Baja California. Marine Ecology Progress Series 394, 137–152.

Lavaniegos B.E., Ohman M.D., 1999. Hyperiid amphipods as indicators of climate change in the California current. In: Schram F.R., Von Vaupel Klein J.C. (Eds.), Proceedings of the Fourth International Crustacean Congress, 1998. Brill, Leiden, pp. 489–509.

Li K., Yin J., Huang L., Shang J., Lian S., Liu C., 2011. Distribution and abundance of thaliaceans in the northwest continental shelf of South China Sea, with response to environmental factors driven by monsoon. Continental Shelf Research 31, 979–989.

Longhurst A.R., 1998. Ecological Geography of the Sea. Academic Press, San Diego.

Macpherson E., 2002. Large-scale species-richness gradients in the Atlantic Ocean. Proceedings of the Royal Society B, 1715–1720.

Madin L.P., Harbison G.R., 1977. The associations of Amphipoda Hyperiidea with gelatinous zooplankton. I. Associations with Salpidae. Deep-Sea Research 24, 449–463.

McGowan J.A., Walker P.W., 1993. Pelagic diversity patterns. In: Ricklefs R.E., Schluter D. (Eds.), Species Diversity in Ecological Communities. University of Chicago Press, Chicago, pp. 203–214.

Olsen B.R., Troedsson C., Hadziavdic K., Pedersen R.B., Rapp H.T., 2014. A molecular gut content study of *Themisto abyssorum* (Amphipoda) from Arctic hydrothermal vent and cold seep systems. Molecular Ecology 23, 3877–3889.

Phleger C.F., Nelson M.M., Mooney B., Nichols P.D., 1999. Lipids of abducted Antarctic pteropods, *Spongiobranchaea australis*, and their hyperiid amphipod host. Comparative Biochemistry and Physiology Part B 124, 295–307.

Pirlot J.-M., 1932. Introduction á l'etude des Amphipodes Hyperides. Annales de l'Institut océanographique 12 (Pt 1), 1–361.

Pompanon F., Deagle B.E., Symondson W.O.C., Brown D.S., Jarman S.N., Taberlet P., 2012. Who is eating what: diet assessment using next generation sequencing. Molecular Ecology 21, 1931–1950.

Rees A., Robinson C., Smyth T., Aiken J., Nightingale P., Zubkov M., 2015. 20 Years of the Atlantic Meridional Transect – AMT. Limnology and Oceanography Bulletin 24, 101–107.

Reid, J.L., Brinton, E., Fleminger, A., Venrick, E.L., McGowan, J.A., 1978. Ocean circulation and marine life. In: Charnock H., Deacon G. (Eds.), Advances in Oceanography. Plenum Press, New York, pp. 65–130.

Reygondeau G., Longhurst A., Martinez E., Beaugrand G., Antoine D., Maury O., 2013. Dynamic biogeochemical provinces in the global ocean. Global Biogeochemical Cycles 27, 1–13.

Riascos J.M., Docmac F., Reddin C., Harrod C., 2015. Trophic relationships between the large scyphomedusa *Chrysaora plocamia* and the parasitic amphipod *Hyperia curticephala*. Marine Biology 162, 1841–1848.

Riascos J.M., Vergara M., Fajardo J., Villegas V., Pacheco A.S., 2012. The role of hyperiid parasites as a trophic link between jellyfish and fishes. Journal of Fish Biology 81, 1686–1695.

Rombouts I., Beaugrand G., Ibanez F., Gasparini S., Chiba S., Legendre L., 2009. Global latitudinal variations in marine copepod diversity and environmental factors. Proceedings of the Royal Society B 276, 3053–3062.

Rosa R., Dierssen H.M., Gonzalez L., Seibel B.A., 2008. Large-scale diversity patterns of cephalopods in the Atlantic open ocean and deep sea. Ecology 89, 3449–3641.

Rutherford S., D'Hondt S., Prell W., 1999. Environmental controls on the geographic distribution of zooplankton diversity. Nature 400, 749–753.

Shih C.T., 1991. Description of two new species of *Phronima* Latreille, 1802 (Amphipoda: Hyperiidea) with a key to all species of the genus. Journal of Crustacean Biology 11, 322–335.

Shreeve R.S., Collins M.A., Tarling G.A., Main C.E., Ward P., Johnston N.M., 2009. Feeding ecology of myctophid fishes in the northern Scotia Sea. Marine Ecology Progress Series 385, 221–236.

Stemmann, L., Youngbluth, M., Robert, K., Hosia, A., Picheral, M., et al., 2008. Global zoogeography of fragile macrozooplankton in the upper 100–1000 m inferred from the underwater video profiler. ICES Journal of Marine Science 65, 433–442.

Stone J.P., Steinberg D.K., 2014. Long-term time-series study of salp population dynamics in the Sargasso Sea. Marine Ecology Progress Series 510, 111–127.

Suntsov A.V., Brodeur R.D., 2008. Trophic ecology of three dominant myctophid species in the northern California Current region. Marine Ecology Progress Series 371, 81–96.

Tarling G.A., Ward P., Sheader M., Williams J.A., Symon C., 1995. Distribution patterns of macrozooplankton assemblages in the southwest Atlantic. Marine Ecology Progress Series 120, 29–40.

Tittensor D.P., Mora C., Jetz W., Lotze H.K., Ricard D., et al., 2010. Global patterns and predictors of marine biodiversity across taxa. Nature 466, 1098–1101.

Valencia B., Lavaniegos B.E., Giraldo A., Rodríguez-Rubio E., 2013. Temporal and spatial variation of hyperiid amphipod assemblages in response to hydrographic processes in the Panama Bight, eastern tropical Pacific. Deep-Sea Research I 73, 46–61.

Vinogradov M.E., Volkov A., Semenova T.N., 1996. Hyperiid Amphipods (Amphipoda, Hyperiidea) of the World Oceans. NH, USA, Science Publishers Inc., Lebanon, p. 632.

Waluda C.M., Collins M.A., Black A.D., Staniland I.J., Trathan P.N., 2010. Linking predator and prey behaviour: contrasts between Antarctic fur seals and macaroni penguins at South Georgia. Marine Biology 157, 99–112.

Williamson M., McGowan J.A., 2010. The copepod communities of the north and south Pacific central gyres and the form of species-abundance distributions. Journal of Plankton Research 32, 273–283.

Woodd-Walker R.S., Ward P., Clarke A., 2002. Large-scale patterns in diversity and community structure of surface water copepods from the Atlantic Ocean. Marine Ecology Progress Series 236, 189–203.

World Register of Marine Species, 2016 (WoRMS) www.marinespecies.org

Zeidler W., 1999. Review of the hyperiidean amphipod genus *Oxycephalus* Milne-Edwards (Crustacea: Amphipoda: Hyperiidea: Oxycephalidae). Invertebrate Taxonomy 13, 391–424.

Zeidler W., 2003a. A review of the hyperiidean amphipod superfamily Vibilioidea Bowman and Gruner, 1973 (Crustacea: Amphipoda: Hyperiidea). Zootaxa 280, 1–104.

Zeidler W., 2003b. A review of the hyperiidean amphipod family Cystisomatidae, Willemöes-Suhm, 1875 (Crustacea: Amphipoda: Hyperiidea). Zootaxa 141, 1–43.

Zeidler W., 2004a. A review of the hyperiidean amphipod superfamily Lycaeopsoidea Bowman & Gruner, 1973 (Crustacea: Amphipoda: Hyperiidea). Zootaxa 520, 1–18.

Zeidler W., 2004b. A review of the families and genera of the hyperiidean amphipod superfamily Phrominoidea, Bowman & Gruner, 1973 (Crustacea: Amphipoda: Hyperiidea). Zootaxa 567, 1–66.

Zeidler W., 2006. A review of the hyperiidean amphipod superfamily Archaeoscinoidea Vinogradov, Volkov & Semenova, 1982 (Crustacea: Amphipoda: Hyperiidea). Zootaxa 1125, 1–37.

Zeidler W., 2009. A review of the hyperiidean amphipod superfamily Lanceoloidea Bowman & Gruner, 1973 (Crustacea: Amphipoda: Hyperiidea). Zootaxa 2000, 1–117.

Zeidler W., 2012a. A new species of Mimonecteola (Crustacea: Amphipoda: Hyperiidea: Mimonecteolidae) from the Southern Ocean. Zootaxa 3308, 63–67.

Zeidler W., 2012b. A review of the hyperiidean amphipod families Mimonectidae and Proscinidae (Crustacea: Amphipoda: Hyperiidea: Scinoidea). Zootaxa 3533, 1–74.

Zeidler W., 2015. A review of the hyperiidean amphipod genus *Hyperoche Bovallius*, 1887 (Crustacea: Amphipoda: Hyperiidea: Hyperiidae), with the description of a new genus to accommodate *H. shihi* Gasca, 2005. Zootaxa 3905, 151–192.

Zeidler W., De Broyer C., 2009. Volume 3: Catalogue of the hyperiidean Amphipoda (Crustacea) of the Southern Ocean with distribution and ecological data. In: De Broyer C. (Ed.), Synopsis of the Amphipoda of the Southern Ocean. Bulletin van het Koninklijk Belgisch Instituut voor Natuurwetenschappen Vol. 79 Suppl. 1, Brussel, pp. 1–104.

Supplementary information

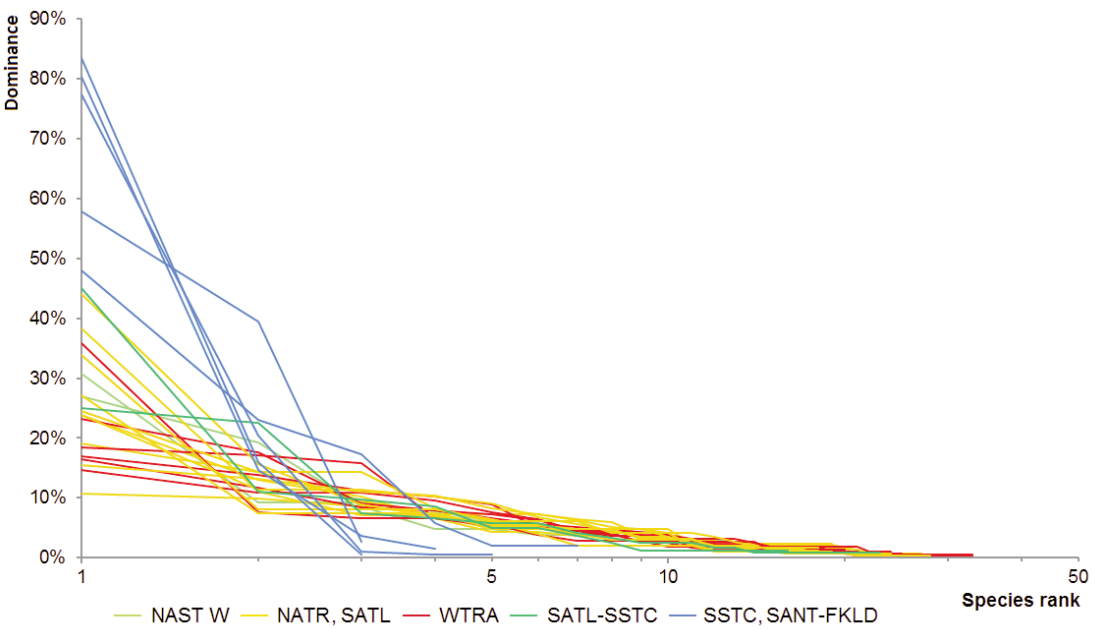

Figure S1. Rank abundance curves describing the distribution of relative Physocephalata hyperiid species abundances for each station with >30 specimens along AMT22. Lines are colored by Longhurst province, see legend and Figure 4.

TABLE S1. Hyperiid species richness *R*, genus diversity *G*, and raw specimen counts for the approximate sample fractions analyzed at each station during the AMT22 cruise. Numbers listed in bold report totals for that taxon.

Station		9	11	13	17	27	29	31	35	37	39	42
Part of sample analyzed		1	1	1/3	1/3	1/3	1	1/5	1	1/2	1	1
Species richness *R*												
Hyperiid amphipods		10	6	20	23	20	36	29	35	35	24	32
Physosomata	*excludes *Scina* sp	0	2	1	0	1	4	2	2	2	0	0
Physocephalata		10	4	19	23	19	32	27	33	33	24	32
Lycaeopsoidea		1	0	1	1	0	1	0	1	1	0	1
Phronimoidea		5	2	9	12	13	13	14	11	13	12	14
Platysceloidea		3	1	6	6	5	14	9	18	17	10	14
Vibilioidea		1	1	3	4	1	4	4	3	2	2	3
Genus diversity *D*												
Hyperiid amphipods		9	5	14	15	15	24	17	21	27	16	21
Physosomata		0	1	1	0	1	2	1	1	1	0	0
Physocephalata		9	4	13	15	14	22	16	20	26	16	21
Lycaeopsoidea		1	0	1	1	0	1	0	1	1	0	1
Phronimoidea		4	2	5	8	9	9	8	9	10	8	9
Platysceloidea	*excludes Lycaeidae sp 1	3	1	5	4	4	10	6	9	13	7	9
Vibilioidea		1	1	2	2	1	2	2	1	2	1	2
Counts												
Hyperiid amphipods		15	16	132	104	43	246	143	229	316	106	224
Physosomata		0	4	2	0	1	13	5	16	27	0	0
Lanceoloidea (Physosomata)		0	0	0	0	0	1	0	0	0	0	0
Lanceolidae	*Lanceola* sp 1						1					
Scinoidea (Physosomata)		0	4	2	0	1	12	5	16	27	0	0
Scinidae	*Scina curilensis*		2				7	4	7	22		
	Scina spinosa		2	2			4	1	9	5		
	Scina tullbergi					1	1					
	Scina sp											
Physocephalata		15	12	130	104	42	233	138	213	289	106	224
Lycaeopsoidea (Physocephalata)		2	0	12	20	0	5	0	10	4	0	10
Lycaeopsidae	*Lycaeopsis themistoides*	2		12	20		5		10	4		10
Phronimoidea (Physocephalata)		9	10	58	64	34	163	84	128	197	44	167
Dairellidae	*Dairella californica*									2		
Hyperiidae	*Hyperoche medusarum*											1
	Hyperoche martinezii											
	Laxohyperia vespuliformis				1							
	Themisto gaudichaudii	1										
	Themisto libellula											
Iulopididae	*Iulopis loveni*					1						
Lestrigonidae	*Hyperietta luzoni*			4	4			1		5		3
	Hyperietta stebbingi	1		12	2	2	4	1	25		2	4
	Hyperietta stephenseni	1	7	8	5	8	20	2	35	51	2	25
	Hyperietta vosseleri			3	3			1	1		2	8
	Hyperioides longipes		3	7	9		23	5	4	4	2	
	Lestrigonus bengalensis						1					
	Lestrigonus sp 1			10	28	4	17	3	9	7		23
	Phronimopsis spinifera			6	4	2	5	2	8	1	2	2
Phronimidae	*Phronima atlantica*					2		18		12	8	38
	Phronima sedentaria	5				2	6	6	4	21	6	20
	Phronima solitaria									1	1	1
	Phronima stebbingi				1		5	5				
	Phronimella elongata					1	17	2	18	67	7	31

43	45	47	51	53	55	57	58	60	62	64	66	68	70	72	74	Total
1	1/2	1	1	1	1	2/3	3/4	1	1	3/16	3/8	3/8	1/8	1/10	1/10	
22	26	28	15	20	19	19	25	18	26	17	9	6	5	3	6	
2	1	0	1	2	0	1	1	2	3	1	2	2	2	0	1	
20	25	28	14	18	19	18	24	16	23	16	7	4	3	3	5	
1	1	1	0	1	1	1	1	0	0	1	0	0	0	0	0	
12	12	15	9	9	9	10	11	11	9	7	4	2	2	2	2	
4	10	9	4	6	8	6	9	4	9	5	1	1	0	0	0	
3	2	3	1	2	1	1	3	1	5	3	2	1	1	1	3	
16	18	19	13	16	15	17	20	14	17	14	8	6	4	3	4	
1	1	0	1	1	1	1	1	1	1	1	2	2	1	0	1	
15	17	19	12	15	14	16	19	13	16	13	6	4	3	3	3	
1	1	1	0	1	1	1	1	0	0	1	0	0	0	0	0	
9	9	9	8	8	6	8	8	9	7	6	4	2	2	2	2	
4	6	7	3	4	6	6	8	3	7	4	1	1	0	0	0	
1	1	2	1	2	1	1	2	1	2	2	1	1	1	1	1	
82	171	290	52	92	103	63	150	107	126	85	57	282	181	38	192	3645
6	14	0	3	4	4	1	3	5	6	3	5	8	5	0	1	136
0	0	0	0	0	0	0	0	0	0	0	1	1	0	0	0	3
											1	1				
6	14	0	3	4	4	1	3	5	6	3	4	7	5	0	1	133
3				1				1	1							
3	14		3	1		1	3	2	1			3	1			
									3	1	3		2		1	
				2	4			2	1	2	1	4	2			
76	157	290	49	88	99	62	147	102	120	82	52	274	176	38	191	3509
2	2	6	0	1	5	1	6	0	0	1	0	0	0	0	0	87
2	2	6		1	5	1	6			1						
61	124	198	32	74	76	44	102	90	52	57	36	260	175	37	187	2563
									1							
									1							
									1		25	220	147	22	148	
									1							
		2			1		3			2						
1	6	1			3	1	7	1								
4	12	30	1	6	7	3	40	16	7	8						
2		3														
3	5	45	1	21	38	21	11	45	8	1	1					
3	1	10	3	8	11	2	7	2		1						
2	17	14	1	5	3		1	2								
12	6	5						1	2	1						
13	7	1		1		1	1		1							
		1									1					
14	5	2	2	4	1	1	11	1								

TABLE S1. Continued

Station		9	11	13	17	27	29	31	35	37	39	42
Part of sample analyzed		1	1	1/3	1/3	1/3	1	1/5	1	1/2	1	1
Counts												
Phrosinidae	*Anchylomera blossevillei*					1	25		14	23	7	3
	Phrosina semilunata	1			3	1	14	4	4	1	2	4
	Primno johnsoni					2		1				
	Primno evansi			6	1	6	17					
	Primno latreillei			2	3	2	9	33	6	2	3	4
Platysceloidea (Physocephalata)		**3**	**1**	**50**	**14**	**7**	**45**	**32**	**71**	**61**	**58**	**43**
Brachyscelidae	*Brachyscelus crusculum*						2	5	11	7	1	2
	Brachyscelus globiceps									1		
	Brachyscelus macrocephalus									1		1
	Brachyscelus sp 1								1			
	Thamneus rostratus									2		
Lycaeidae	*Lycaea pulex*				1			9	1	18		
	Lycaea serrata											1
	Lycaea sp 1								1	1	38	
	Lycaea sp 2										4	
	Lycaeidae sp 1								1			
Oxycephalidae	*Calamorhynchus pellucidus*						1	1				
	Cranocephalus scleroticus						1					
	Leptocotis tenuirostris									1		
	Oxycephalus piscator			1						1	1	
	Rhabdosoma minor						1			2		
	Streetsia challengeri				1		1				2	2
	Streetsia mindanaònis											1
	Streetsia porcella					1	3			1		
	Tullbergella cuspidata											
Platyscelidae	*Amphithyrus bispinosus*	1					2		1			1
	Amphithyrus sculpturatus			2					2	1		2
	Platyscelus armatus				1				4		2	
	Platyscelus crustulatus							1				1
	Platyscelus ovoides	1		1		1	5	3	5	13	3	11
	Tetrathyrus forcipatus	1				1	5		12	2	2	8
Pronoidae	*Eupronoe armata*			5	4	1	1	2	5	4	2	2
	Eupronoe maculata				5	3	15	6	17	4	3	7
	Eupronoe minuta			40	2		6	1	1			
	Parapronoe campbelli			1					2			
	Parapronoe crustulum		1				1		1	1		
	Parapronoe parva						1		1			
	Pronoe capito								1			1
Tryphanidae	*Tryphana malmi*							4	4	1		3
Vibilioidea (Physocephalata)		**1**	**1**	**10**	**6**	**1**	**20**	**22**	**4**	**27**	**4**	**4**
Paraphronimidae	*Paraphronima gracilis*		1	4	2		7	2		1		2
Vibiliidae	*Vibilia armata*	1		4	1		7	14	1	26	2	1
	Vibilia australis			2	1	1	1	2	2			
	Vibilia borealis								1		2	1
	Vibilia propinqua						5	4				
	Vibilia pyripes				2							
	Vibilia stebbingi											

43 1	45 1/2	47 1	51 1	53 1	55 1	57 2/3	58 3/4	60 1	62 1	64 3/16	66 3/8	68 3/8	70 1/8	72 1/10	74 1/10	Total
2	15	21	2			2	11	7								
4	17	32	12	9		5		9		7						
	23	24	3	10	7	3	8	2		37	9	40	28	15	39	
1	10	7	7	10	5	5	2	4	30							
6	**25**	**81**	**15**	**9**	**14**	**12**	**33**	**11**	**24**	**10**	**3**	**4**	**0**	**0**	**0**	**632**
							1		2							
					1				1							
					1											
2		2			1	3	2	2	7							
	1															
		1														
1																
		1		3		1	5									
			1		2	2	1									
				1		1										
		1					2		1							
					1											
	1						7									
	3															
2	7	15	7		3	1	8	2	5	3	3	4				
	4	4		1												
		18		2			1			1						
1	3	38	4	1	3		6	6	1							
	1	1	3	1	2	4		1	3	1						
	2								1	1						
	1															
	2								3	4						
7	**6**	**5**	**2**	**4**	**4**	**5**	**6**	**1**	**44**	**14**	**13**	**10**	**1**	**1**	**4**	**227**
		2	2	3	4	5	1		1	1						
5	5	1						1	9	9	1	10		1	2	
	1			1			4		3				1			
1																
		2					1			4					1	
1									4							
									27		12				1	

8

Discussion

To track the effects of ocean change on pelagic species diversity and distribution patterns, it is essential to better understand how current biodiversity evolved, what part of the biodiversity is where, and how closely related species can be distinguished. In this thesis, I aimed to better understand the diversity, distribution, and evolution of three groups of marine zooplankton. The focus of my PhD research was on pteropods (Chapters 2-6), but I also investigated the diversity and distribution patterns of another group of planktonic gastropods: the shelled heteropods (Chapter 6), and of a conspicuous group of planktonic arthropods: the hyperiid amphipods (Chapter 7). In doing so, the work reported in this thesis has contributed to several public reference databases containing genetic, biogeographic, and morphometric data of these taxa. One of the core challenges of my research was to accurately identify species and hence, I discuss the pros and cons of different methods I used or which could be applied in future research. I also discuss the potential of using pteropods as indicators of ocean acidification, including what open questions still need to be addressed and recommendations for future research.

Identifying species in the open ocean

The identification of species in my PhD research was largely based on an integrative approach. I used qualitative morphological identification based on taxonomic keys in Chapters 2, 6, and 7, applied quantitative geometric morphometric methods in Chapters 3, 4, and 5, and used DNA sequencing of specific genes to assess genetic relatedness in Chapters 2-5. Furthermore, I also used geographic information where available (Chapters 2-7). Species diversity in the plankton has likely been underestimated based on morphology only. Hence, genetic methods such as DNA barcoding are useful in revealing additional diversity, but they do not come without pitfalls (Bucklin et al., 2011, 2016; Peijnenburg and Goetze, 2013).

DNA barcoding is the use of short DNA sequences for species recognition and discrimination and has accelerated the rate of discovery of taxonomic diversity (Hebert et al., 2003). Barcoding of zooplankton taxa revealed additional clades that may represent new or previously discounted zooplankton species (Goetze, 2010; Blanco-Bercial et al., 2014; Cornils and Held, 2014; Laakman and Holst, 2014; Hirai et al., 2015a). Cytochrome Oxidase I (COI) is the most frequently used gene in animals and there is an extensive database available for comparison, but for zooplankton taxa it is very incomplete and samples are often not identified to species level (Benson et al., 2013). For COI, genetic distances are typically <3% within zooplankton species and >10% between species (Bucklin et al., 2011). However, a universal barcode to identify species defined by a standard barcoding gap of at least 2% divergence between COI sequences is not always applicable across different zooplankton groups. According to Hebert et al. (2003), 94.1% of the Cnidaria species possessed less than 2% of pairwise sequence divergence versus 1.9% of the species in other taxonomic groups, such as Annelida, Arthropoda, Chordata, Cnidaria, Mollusca, Nematoda, and Platyhelminthes. Another exceptional group in the marine zoo-

plankton are chaetognaths. A recent study by Marlétaz et al. (2017) showed that sequence divergence within a single population of the species *Sagitta elegans* could be as high as 17.8% for COI and up to 20.8% for all mitochondrial genes combined.

Defining a hard barcoding gap is difficult in pteropods because genetic differences between morphologically distinct taxa can be highly variable. Hence, an integrative taxonomic approach was needed to more accurately assess species boundaries. I applied this approach to assess species boundaries in *Cuvierina* and *Diacavolinia* (Chapters 3-5) based on a combination of two-dimensional geometric morphometric analyses of their shell shapes and DNA sequences of mitochondrial COI and nuclear 28S genes. For *Cuvierina* species, I additionally applied Ecological Niche Modelling (ENM) to quantitatively estimate the ecological tolerances of distinct morphotypes. Standard DNA barcoding failed to detect some incipient *Cuvierina* species, such as *C. cancapae*, which were found to be morphologically and ecologically different. DNA barcoding revealed three major mitochondrial clades that each would represent one species according to the barcoding gap species concept, with average pairwise genetic distances of 4.5-5.1% between clades (Chapter 3). The first clade represents specimens from the Atlantic Ocean. It consists of two morphotypes, *C. atlantica* and *C. cancapae*, differing in both shell ornamentation and shell shape, but which were not distinguished based on COI sequences (average pairwise genetic distance between morphotypes was 2.0%, similar to the genetic distance within morphotypes). Hence, we concluded that these morphotypes probably diverged recently. The clade representing the Indo-Pacific Ocean comprises *C. columnella*, *C. urceolaris*, and *C. tsudai* individuals sampled predominantly from the North Pacific Ocean. These morphotypes are closely related according to their COI sequences (average pairwise genetic distance was 1.7%) but they differ in shell ornamentation and shell shape. However, because there were very few genetic samples for *C. columnella* and *C. urceolaris*, I concluded that they should remain separate species based on their remarkably different shell shapes and ornamentations compared to *C. tsudai*. *Cuvierina pacifica* (0.8% average pairwise genetic distance) sampled exclusively in the South Pacific gyre differed both morphologically and genetically from the other *Cuvierina* species and was distinguished as a separate, third genetic clade based on COI sequences (Chapters 3 and 4). Former *C. pacifica* individuals that belong to the same Indo-Pacific genetic clade as *C. columnella* and *C. urceolaris* were described as the new species *C. tsudai* in Chapter 4.

COI sequences of *Diacavolinia* pteropods were highly diversified (Chapter 5). Pairwise genetic distances between mitochondrial clades were much larger for *Diacavolinia* (18.6-43.8% average pairwise genetic distance) than for *Cuvierina* taxa (4.5-5.1%), but pairwise differences within mitochondrial clades were comparable for *Diacavolinia* and *Cuvierina* (0.2-6.3% and 0.8-2.0% average pairwise genetic distance, respectively). Based only on COI, one could doubt whether *Diacavolinia* represents a single genus because pairwise genetic differences between clades were much larger than within other pteropod genera. However, results of the more conservative nuclear ribosomal genes 28S (Chapters 2 and 5) as well as 18S (Chapter 2) show that

Diacavolinia taxa are monophyletic and are all nested within *Cavolinia* rendering this latter genus paraphyletic. Moreover, COI sequences could not be obtained for all *Diacavolinia* taxa and not all taxa were resolved based on 28S sequences. Hence, it is clear that a lot of genetic diversity exists within *Diacavolinia* and *Cavolinia* clades, however, their taxonomy is still unresolved. Adding geometric morphometric information to the available genetic information proved useful in assessing species boundaries within *Diacavolinia*, resulting in the confirmation of described taxa or discovery of new taxa (Chapter 5). Using a species hypothesis based on a combination of data types, I found that no *Diacavolinia* species were shared between the Atlantic and Indo-Pacific oceans, two species were supported in the Atlantic Ocean in contrast to eight currently described, and a maximum of 11 species was present in the Indo-Pacific Ocean, comprising 13 of the currently described species. However, ENM was not applied to *Diacavolinia* taxa because some specimens could not be assigned with confidence to a species, for example, when no genetic and too little morphological information was available. Additionally, some species were extremely rare and did not allow for such methods. In Chapter 5, I found five such taxa, of which only one to three specimens were ever sampled at single locations in the world's oceans during multiple sampling expeditions between 1909 and 2012.

Methodological aspects

Throughout this thesis, specimens from the natural history collections at Naturalis Biodiversity Center in Leiden and the Zoological Museum of Copenhagen provided an essential initial framework for assessing species boundaries and represented a substantial source of information (Chapters 3-5). Historical samples from the 19th and 20th centuries, including specimens from the Danish DANA expeditions, which were thoroughly studied by A. Janssen (e.g., Janssen, 2005, 2007, 2010, 2012; Cahuzak and Janssen, 2010), were essential for use as reference samples and for increasing total sampling coverage for geometric morphometric purposes across the global ocean, especially in the Indian Ocean (e.g., Schmidt, 1934). Combined with fresh specimens for which morphometric as well as genetic information could be obtained, historical museum specimens enabled accurate assessment of species boundaries and matching of *Diacavolinia* morphotypes to actual species names. Museum samples were available for 23 of the 24 *Diacavolinia* taxa described by Van der Spoel et al. (1993), including holo- and/or paratypes for 14 taxa.

Computed tomography (CT) scanning allows the reconstruction of shells and internal structures at micrometer scale in 3D and the measurement of shell thickness, volume, density, and shape (Liew, 2014; Manno et al., 2017). Three-dimensional geometric morphometric analyses may be better able to distinguish between taxa than the two-dimensional geometric morphometric analyses used in this thesis (Chapters 3-5). However, it is more time-consuming to apply 3D compared to 2D morphometrics and standard workflows for data analysis are not available yet. Hence, depending on the research purpose, I do not think that 3D morphometric methods should completely replace 2D geometric morphometric methods.

In recent years, high-throughput or next-generation sequencing (NGS) methods have rapidly developed and have generated large volumes of genomic data on non-model organisms (Taylor and Harris, 2012). NGS-based DNA sequencing methods can be more sensitive than traditional Sanger sequencing of a few selected genes, and hence, would probably better resolve recently diverged or incipient species. For example, I hypothesize that for *Cuvierina*, additional genetic markers in the form of Single Nucleotide Polymorphisms (SNPs) scattered across the genome will provide enough information to distinguish genetically between ecologically distinct morphotypes (Chapter 3). Additionally, such NGS-based methods would circumvent the problem of specimens that did not amplify for particular genetic markers. Null amplifications of COI were a problem for one *Diacavolinia* clade and were probably due to mutations in primer regions (Chapter 5). Furthermore, another NGS-based technique, such as RNA-sequencing, could generate large amounts of transcriptomic data. These would allow phylogenomic analyses including genetic information of >1000 protein-coding genes, which could improve our understanding of the evolutionary history of pteropods. This would probably result in better resolution of higher taxonomic levels in the phylogeny of pteropods, such as the relation between the Euthecosomata, Pseudothecosomata, and Gymnosomata suborders. Their phylogenetic relationships remained unresolved based on three genetic markers (Chapter 2). It may also better resolve relationships between coiled and uncoiled euthecosome genera. The use of many slowly evolving protein-coding genes rather than a small subset of genes would homogenize long branches due to high rate variation within and between taxa, as was the case for *Limacina bulimoides* and *Heliconoides inflatus* (Chapter 2).

Metabarcoding is another emerging NGS method, used for large-scale taxonomic identification of complex samples via analysis of one or more homologous DNA regions (barcodes). It basically combines DNA-based identification methods with high throughput sequencing (Bucklin et al., 2016). Applications include estimation of zooplankton community composition and species discovery (Lindeque et al., 2013; De Vargas et al., 2015; Pearman and Irigoien, 2015), community composition of specific taxa (Hirai et al., 2015b; Wu et al., 2015), and estimation of spatio-temporal turnover (Brannock et al., 2016; Chain et al., 2016).

There are many advantages to the use of metabarcoding for identifying species in the marine zooplankton especially because large amounts of data can be generated in an efficient way, which has the potential of broadening the understanding of the diversity of different pelagic groups, assessment of ecosystem health, detection of impacts of climate change, and characterization of food webs (Bucklin et al., 2016; Leray and Knowlton, 2016). However, metabarcoding also has limitations compared to morphology with respect to identifying species in the marine zooplankton assemblage.

First, metabarcoding of marine zooplankton is hindered by a lack of taxonomic identification at lower taxonomic levels due to gaps in reference databases, reducing the confidence in assigning operational taxonomic units (OTUs) to species (Bucklin

et al., 2016; Leray and Knowlton, 2016). Hence, although metabarcoding can provide a broad assessment of zooplankton diversity, it cannot simply replace morphological species identifications and there is an urgent need for updating and building of reference databases for the marine zooplankton assemblage.

Second, although morphological analysis may underestimate biodiversity in the global ocean compared to metabarcoding because not all plankton taxa can be distinguished morphologically, metabarcoding may also fail to amplify certain species or even entire groups because of mutations in the primer regions, as was the case for certain *Diacavolinia* taxa (Chapter 5). For example, a comparative study between metabarcoding and microscopy demonstrated a high correspondence in community composition for zooplankton, but not for phytoplankton (Abad et al., 2016).

Third, unlike metabarcoding, species identification based on morphology enables the estimation of species abundances, because individual specimens are preserved and can be counted. Quantitative zooplankton species identification based on morphology enables conversion to biomass (Chapter 6). In metabarcoding, the number of sequence reads associated with an OTU can potentially estimate biomass (Lindeque et al., 2013). Several studies have shown a positive correlation between number of sequence reads and dry weight of the taxon (e.g., Hirai et al., 2015c). Sun et al. (2015) demonstrated a correspondence between low-abundance sequence reads and low-abundance species. However, these findings should be treated with caution because metabarcoding not always corresponds with morphological species abundance data (e.g., Mohrbeck et al., 2015). The relation between number of sequence reads and biomass is probably not linear and will be biased by species-specific differences in copy numbers of 28S and 18S in the genome. Hence, state-of-the-art metabarcoding remains at best a semi-quantitative method for assessing species abundances (Bik et al., 2012).

Fourth, diversity estimates based on metabarcoding result in a number of OTUs but it is unclear how this number relates to actual species diversity. This depends on the chosen similarity threshold based on the marker of choice, its sequence length, and intra- and interspecific degree of conservation for assignment of sequences to OTUs. Although assessing taxonomic diversity based on similarity thresholds is also possible when reference taxonomic information is not available, it is not clear how this number relates to the actual number of biological species (Brown et al., 2015). In this sense, the problem with fixed barcoding gaps persists. A threshold based on high similarity may overestimate taxon richness, and any threshold assumes that intraspecific variation is approximately equally distributed across taxonomic groups. Hence, an integrative approach remains critically important for taxonomic identification of new, closely related taxa based on combined information including biogeography and ecology.

Pteropods as indicators of ocean acidification

In recent years, pteropods have gained considerable attention because of their potential vulnerability to ocean acidification (e.g., Fabry et al., 2008). However, the

usefulness of pteropods as potential indicators of the effects of ocean acidification is compromised by limited historical context for understanding species-specific long-term exposure to variation in ocean chemistry (but see Janssen et al., 2016). The degree of pteropod vulnerability to ocean acidification is currently debated (Bednaršek et al., 2016a; Peck et al., 2016). Based on observations of *Limacina helicina* pteropods, Peck et al. (2016) conclude that shell dissolution is only happening if the periostracum, the outer protective layer, is damaged. If this is true, shelled pteropods may not be as vulnerable to ocean acidification as currently thought (e.g., Bednaršek et al., 2016b). All in all, future work may provide more insights into the sensitivity of different pteropod species to ocean acidification as well as the role of the periostracum.

A number of open questions regarding the effects of ocean acidification on shelled pteropods are discussed in the review paper by Manno et al. (2017). Some are addressed in this thesis. First, it is often still unknown whether genetically distinct forms can be morphologically separated and the other way round, and whether regional differences within pteropod species could be responsible for distinct physiological responses to ocean acidification. To improve the accuracy of knowledge of the taxonomy, evolution, and biogeography of pteropods, an evolutionary framework of pteropods was constructed (Chapter 2) and an integrative taxonomic approach was applied to delimit species within the pteropod genera *Cuvierina* (Chapters 3 and 4) and *Diacavolinia* (Chapter 5). Second, it would be informative to know species diversity and abundance patterns in relation to oceanographic parameters such as temperature, chlorophyll *a*-concentrations, and carbonate chemistry. For Chapter 6, species diversity and abundance data as well as water column properties were obtained by participation in a multidisciplinary oceanographic expedition across the Atlantic Ocean. Participation in this expedition led to new insights in species distributions and abundances based on ecological preferences, as well as in the interplay between species assemblages and water column properties, such as a positive correlation between species diversity and water temperature (AMT24; Rees et al., 2017). Ocean change may affect the distributions and abundances of pteropod species, which can be assessed by resampling zooplankton communities along a similar transect in the future.

Because different pteropod growth stages may have different tolerances to ocean acidification, historical records can be a valuable contribution to our understanding of the controls of ocean acidification on growth stage. To understand the historical context of ocean acidification and to monitor the potential effects of ocean change on shell mineralization, specimens from different time spans may be obtained from museum collections (e.g., Howes et al., 2017) or from sediment cores (e.g., Wall-Palmer et al., 2013). Although *Cuvierina* and *Diacavolinia* specimens obtained from museum collections were not used as such in Chapters 3-5, this is possible in future work. In a comparison of Mediterranean pteropod shell biometrics, thicker shells were observed in historical samples (1910 and 1921) compared to recent samples (2012) for Mediterranean *Cavolinia inflexa* and

Styliola subula (Howes et al., 2017). Time series in the Mediterranean Sea covering the period 1967-2003 showed a pH decline of 0.05 units, but this decline did not cause a decrease in local pteropod abundances (Howes et al., 2015). To study the in-life shell dissolution of pteropods from the Late Pleistocene, Wall-Palmer et al. (2013) used fossil *Heliconoides inflatus* specimens not affected by post-depositional shell dissolution. Marine sediment cores proved useful in determining that high in-life dissolution of shells due to low aragonite saturation levels in the past was accompanied by smaller shell sizes, indicating a reduction in calcification rate.

Apart from time series of shell biometrics using historical samples, shell dissolution in undersaturated basins or simulated laboratory conditions may be another measurement of the effects of ocean acidification on pteropods. Several experimental studies have been conducted to understand the consequences of short-term exposure to elevated CO_2 conditions. In-situ studies and laboratory incubations simulating the effects of future atmospheric CO_2 scenarios have mainly focused on shelled pteropods, but heteropods have received little attention thus far (Wall-Palmer et al., 2016). Reported potential implications of ocean acidification on shelled pteropods include shell degradation, reduced shell calcification rates, abnormal shell growth, metabolic suppression, and ultimately, reduced survival (Comeau et al., 2009, 2010a,b, 2012; Lischka et al., 2011; Bednaršek et al., 2012a,b; Lischka and Riebesell, 2012; Maas et al., 2012; Manno et al., 2012, 2015; Seibel et al., 2012; Gazeau et al., 2013). Effects of ocean acidification on larval stages of pteropods may be even more severe than effects on adults (Comeau et al., 2010a). An experiment in which larvae of Mediterranean *Cavolinia inflexa* were maintained at pH 8.1, 7.8, and 7.5 demonstrated that shells became malformed at pH 7.8, and that larvae did not make shells at pH 7.5 (Comeau et al., 2010a). However, because pteropods are notoriously difficult to maintain in the laboratory, resultant high mortality rates and unnatural behaviors may bias experimental study outcomes (Howes et al., 2014). Effects of culturing pteropods may be the inability of adults to feed, rapid sinking when not actively swimming, and shell damage during sampling (Peck et al., 2016; Manno et al., 2017). These issues require careful consideration in future designs for pteropod culturing, which are still developing (Howes et al., 2015).

Effects of ocean acidification on pteropod shells have also been examined using live animals collected directly from their natural environments (Bednaršek et al., 2012a, 2014, 2015). These authors demonstrated that impacts of ocean acidification on shell mineralization were also occurring in populations under supersaturated conditions in the Southern Ocean (Bednaršek et al., 2012a). This implies that regional declines of pteropod populations may occur sooner than currently projected. Pteropod studies from the California Current Ecosystem (CCE) indicated decreasing habitat suitability due to ocean acidification (Bednaršek et al., 2014, 2015). However, future experiments should consider that shell mineralization is not only affected by ocean acidification, but also by other synergistic stressors, including ocean warming, deoxygenation, and increased stratification (Kroeker et al., 2017; Manno et al., 2017).

Transcriptome-wide analyses are increasingly applied to understand the differences in physiological responses of pteropod species and populations to the effects of ocean acidification (Maas et al., 2015; Moya et al., 2016). For example, a study of the physiological response of *Clio pyramidata* to a 10-h exposure to elevated CO_2 (800 ppm) demonstrated differential gene expression patterns compared to ambient conditions (380 ppm; Maas et al., 2015). Some genes associated with aerobic metabolism were down-regulated, and some genes that may be associated with biomineralization were up-regulated. During a 3-day experiment, *Heliconoides inflatus* demonstrated a decrease in gross calcification in response to acidified conditions (pH 7.9) compared to control treatments (pH 8.1) despite up-regulation of genes potentially involved in calcification (Moya et al., 2016). This reflects the inability of pteropods to maintain calcification rates under acidified conditions. Moreover, a large number of genes related to nervous system structure and function were also up-regulated, potentially leading to altered behavior.

In conclusion, my thesis has revealed substantial genetic and taxonomic diversity in the marine zooplankton assemblage, with a special focus on pteropods. This taxonomic diversity is the result of their evolutionary history and ecological responses to environmental variation. I found that different species of pteropods and distinct species assemblages occur across distinct biogeochemical provinces of the global ocean. This supports the idea that there may be considerable biological variation in the sensitivities of these calcifying organisms to ocean acidification (Fabry et al., 2008). Hence, my studies urge for an accurate taxonomic resolution to study the response of pteropods, and more generally, of other marine zooplankton to environmental pressures. Biological variation within and among species should be taken into account in projections of the response of marine ecosystems to global change.

References

Abad D., Albaina A., Aguirre M., Laza-Martínez A., Uriarte I. et al., 2016. Is metabarcoding suitable for estuarine plankton monitoring? A comparative study with microscopy. Marine Biology 163, 149.

Bednaršek N., Feely R.A., Reum J.C.P., Peterson B., Menkel J. et al., 2014. *Limacina helicina* shell dissolution as an indicator of declining habitat suitability owing to ocean acidification in the California Current Ecosystem. Proceedings of the Royal Society B 281, 20140123.

Bednaršek N., Harvey C.J., Kaplan I.C., Feely R.A., Možina J., 2016b. Pteropods on the edge: Cumulative effects of ocean acidification, warming, and deoxygenation. Progress in Oceanography 145, 1–24.

Bednaršek N., Johnson J., Feely R.A., 2016a. Comment on Peck et al: Vulnerability of pteropod (*Limacina helicina*) to ocean acidification: shell dissolution occurs despite an intact organic layer. Deep-Sea Research II 127, 53–56.

Bednaršek N., Ohman M.D., 2015. Changes in pteropod distributions and shell dissolution across a frontal system in the California Current System. Marine Ecology Progress Series 523, 93–103.

Bednaršek N., Tarling G.A., Bakker D.C.E., Fielding S., Cohen A. et al., 2012b. Description and quantification of pteropod shell dissolution: a sensitive bioindicator of ocean acidification. Global Change Biology 18, 2378–2388.

Bednaršek N., Tarling G.A., Bakker D.C.E., Fielding S., Jones E.M. et al., 2012a. Extensive dissolution of live pteropods in the Southern Ocean. Nature Geoscience 5, 881–885.

Benson D.A., Cavanaugh M., Clark K., Karsch-Mizrachi I., Lipman D.J. et al., 2013. GenBank. Nucleic Acids Research 41, D36–D42.

Bik H.M., Porazinska D.L., Creer S., Caporaso J.G., Knight R., Thomas W.K., 2012. Sequencing our way towards understanding global eukaryotic biodiversity. Trends in Ecology and Evolution 27, 233–243.

Blanco-Bercial L., Cornils A., Copley N., Bucklin A., 2014. DNA barcoding of marine copepods: assessment of analytical approaches to species identification. PLoS Currents 6, doi: 10.1371/currents.tol.cdf8b74881f87e3b01d56b43791626d2

Brannock P.M., Ortmann A.C., Moss A.G., Halanych K.M., 2016. Metabarcoding reveals environmental factors influencing spatio-temporal variation in pelagic micro-eukaryotes. Molecular Ecology 25, 3593–3604.

Brown E.A., Chain F.J.J., Crease T.J., MacIsaac H.J., Cristenscu M., 2015. Divergence thresholds and divergent biodiversity estimates: can metabarcoding reliably describe zooplankton communities? Ecology and Evolution 5, 2234–2251.

Bucklin A., Lindeque P.K., Rodriguez-Ezpeleta N., Albaina A., Lehtiniemi M., 2016. Metabarcoding of marine zooplankton: prospects, progress and pitfalls. Journal of Plankton Research 38, 393–400.

Bucklin A., Steinke D., Blanco-Bercial L., 2011. DNA barcoding of marine metazoa. Annual Review of Marine Science 3, 471–508.

Cahuzak B., Janssen A.W., 2010. Eocene to Miocene holoplanktonic Mollusca (Gastropoda) of the Aquitaine Basin, southwest France. Scripta Geologica 141, 1–193.

Chain F.J.J., Brown E.A., MacIsaac H.J., Cristescu M.E., 2016. Metabarcoding reveals strong spatial structure and temporal turnover of zooplankton communities among marine and freshwater ports. Diversity and Distributions 22, 493–504.

Comeau S., Gattuso, J.-P., Nisumaa A.-M., Orr J., 2012. Impact of aragonite saturation state changes on migratory pteropods. Proceedings of the Royal Society B 279, 732–738.

Comeau S., Gorsky G., Alliouane S., Gattuso J.-P., 2010a. Larvae of the pteropod *Cavolinia inflexa* exposed to aragonite undersaturation are viable but shell-less. Marine Biology 157, 2341–2345.

Comeau S., Gorsky G., Jeffree R., Teyssié J.-L., Gattuso J.-P., 2009. Impact of ocean acidification on a key Arctic pelagic mollusk (*Limacina helicina*). Biogeosciences 6, 1877–1882.

Comeau S., Jeffree R., Teyssié J.-L., Gattuso J.-P., 2010b. Response of the Arctic pteropod *Limacina helicina* to projected future environmental conditions. PLoS ONE 5, e11362.

Cornils A., Held C., 2014. Evidence of cryptic and pseudocryptic speciation in the *Paracalanus parvus* species complex (Crustacea, Copepoda, Calanoida). Frontiers in Zoology 11, 19.

De Vargas C., Audic S., Henry N., Decelle J., Mahé F. et al., 2015. Eukaryotic plankton diversity in the sunlit ocean. Science 348, 1261605.

Fabry V.J., Seibel B.A., Feely R.A., Orr J.C., 2008. Impacts of ocean acidification on marine fauna and ecosystem processes. ICES Journal of Marine Science 65, 414–432.

Gazeau F., Parker L.M., Comeau S., Gattuso J.-P., O'Connor W.A. et al., 2013. Impacts of ocean acidification on marine shelled molluscs. Marine Biology 160, 2207–2245.

Goetze E., 2010. Species discovery in marine planktonic invertebrates through global molecular screening. Molecular Ecology 19, 952–967.

Hebert P.D.N., Ratnasingham S., deWaard J.R., 2003. Barcoding animal life: cytochrome *c* oxidase subunit 1 divergences among closely related species. Proceedings of the Royal Society B 270, Suppl. 1 S96–S99.

Hirai J., Kuriyama M., Ichikawa T., Hidaka K., Tsuda A., 2015b. A metagenetic approach for revealing community structure of marine planktonic copepods. Molecular Ecology Resources 15, 68–80.

Hirai J., Tsuda A., Goetze E., 2015a. Extensive genetic diversity and endemism across the global range of the oceanic copepod *Pleuromamma abdominalis*. Progress in Oceanography 138, 77–90.

Hirai J., Yasuike M., Fujiwara A., Nakamura Y., Hamaoka S. et al., 2015c. Effects of plankton net characteristics on metagenetic community analysis of metazoan zooplankton in a coastal marine ecosystem. Journal of Experimental Marine Biology and Ecology 469, 36–43.

Howes E.L., Bednaršek N., Büdenbender J., Comeau S., Doubleday A. et al., 2014. Sink and swim: a status review of thecosome pteropod culture techniques. Journal of Plankton Research 36, 299–315.

Howes E.L., Eagle R.A., Gattuso J.-P., Bijma J., 2017. Comparison of Mediterranean pteropod shell biometrics and ultrastructure from historical (1910 and 1921) and present day (2012) samples provides baseline for monitoring effects of global change. PLoS ONE 12, e0167891.

Howes E.L., Stemmann L., Assailly C., Irisson J.-O., Dima M. et al., 2015. Pteropod time series from the North Western Mediterranean (1967-2003): impacts of pH and climate variability. Marine Ecology Progress Series 531, 193–206.

Janssen A.W., 2005. Development of Cuvierinidae (Mollusca, Euthecosomata, Cavolinioidea) during the Cainozoic: a non-cladistic approach with a re-interpretation of Recent taxa. Basteria 69, 25–72.

Janssen A.W., 2007. Holoplanktonic Mollusca (Gastropoda) from the Gulf of Aqaba, Red Sea and Gulf of Aden (Late Holocene-Recent). The Veliger 49, 140–195.

Janssen A.W., 2010. Systematics and biostratigraphy of holoplanktonic Mollusca from the Oligo-Miocene of the Maltese Archipelago. Bollettino del Museo Regionale di Scienze Naturali Torino 28, 197–601.

Janssen A.W., 2012. Late Quaternary to Recent holoplanktonic Mollusca (Gastropoda) from bottom samples of the eastern Mediterranean Sea: systematics, morphology. Bollettino Malacologico 48, 1–105.

Janssen A.W., Sessa J.A., Thomas E., 2016. Pteropoda (Mollusca, Gastropoda, Thecosomata) from the Paleocene-Eocene Thermal Maximum (United States Atlantic Coastal Plain). Palaeontologia Electronica 19, 1–26.

Kroeker K.J., Kordas R.L., Harley C.D.G., 2017. Embracing interactions in ocean acidification research: confronting multiple stressor scenarios and context dependence. Biology Letters 13, 20160802.

Laakmann S., Holst S., 2014. Emphasizing the diversity of North Sea hydromedusae by combined morphological and molecular methods. Journal of Plankton Research 36, 64–76.

Leray M., Knowlton N., 2016. Censusing marine eukaryotic diversity in the twenty-first century. Philosophical Transactions of the Royal Society B 371, 20150331.

Liew T.-S., Kok A.C.M., Schilthuizen M., Urdy S., 2014. On growth and form of irregular coiled-shell of a terrestrial snail: *Plectostoma concinnum* (Fulton, 1901) (Mollusca: Caenogastropoda: Diplommatinidae). PeerJ 2, e383.

Lindeque P.K., Parry H.E., Harmer R.A., Somerfield P.J., Atkinson A., 2013. Next generation sequencing reveals the hidden diversity of zooplankton assemblages. PLoS ONE 8, e81327.

Lischka S., Büdenbender J., Boxhammer T., Riebesell U., 2011. Impact of ocean acidification and elevated temperatures on early juveniles of the polar shelled pteropod *Limacina helicina*: mortality, shell degradation, and shell growth. Biogeosciences 8, 919–932.

Lischka S., Riebesell U., 2012. Synergistic effects of ocean acidification and warming on overwintering pteropods in the Arctic. Global Change Biology 18, 3517–3528.

Maas A.E., Lawson G.L., Tarrant A.M., 2015. Transcriptome-wide analysis of the response of the thecosome pteropod *Clio pyramidata* to short-term CO_2 exposure. Comparative Biochemistry and Physiology, Part D 16, 1–9.

Maas A.E., Wishner K.F., Seibel B.A., 2012. Metabolic suppression in thecosomatous pteropods as an effect of low temperature and hypoxia in the eastern tropical North Pacific. Marine Biology 159, 1955–1967.

Manno C., Bednaršek N., Tarling G.A., Peck V.L., Comeau S. et al., 2017. Shelled pteropods in peril: assessing vulnerability in a high CO_2 ocean. Earth-Science Reviews 169, 132–145.

Manno C., Morata N., Primicerio R., 2012. *Limacina retroversa*'s response to combined effects of ocean acidification and sea water freshening. Estuarine, Coastal and Shelf Science 113, 163–171.

Manno C., Peck V.L., Tarling G.A., 2015. Pteropod eggs released at high pCO_2 lack resilience to ocean acidification. Scientific Reports 6, 25752.

Marlétaz F., Le Parco Y., Liu S., Peijnenburg K.T.C.A., 2017. Extreme mitogenomic variation in natural populations of chaetognaths. Genome Biology and Evolution 9, 1374–1384.

Mohrbeck I., Raupach M.J., Martínez Arbizu P., Knebelsberger T., Laakmann S., 2015. High-throughput sequencing–the key to rapid biodiversity assessment of marine metazoa? PLoS ONE 10, e0140342.

Moya A., Howes E.L., Lacoue-Labarthe T., Forêt S., Bishoy H. et al., 2016. Near-future pH conditions severely impact calcification, metabolism and the nervous system in the pteropod *Heliconoides inflatus*. Global Change Biology 22, 3888–3900.

Pearman J.K., Irigoien X., 2015. Assessment of zooplankton community composition along a depth profile in the central Red Sea. PLoS ONE 10, e0133487.

Peck V.L., Tarling G.A., Manno C., Harper E.M., Tynan E., 2016. Outer organic layer and internal repair mechanism protects pteropod *Limacina helicina* from ocean acidification. Deep-Sea Research II 127, 41–52.

Peijnenburg K.T.C.A., Goetze E., 2013. High evolutionary potential of marine zooplankton. Ecology and Evolution 3, 2765–2781.

Rees A.P., Nightingale P.D., Poulton A.J., Smyth T.J., Tarran G.A., Tilstone G.H., 2017. The Atlantic Meridional transect programme (1995-2016). Progress in Oceanography, in press.

Schmidt J. Dana-Report Vol. I 1932-1934: the Carlsberg foundation's oceanographic expedition round the world 1928-1939, and previous 'Dana' expeditions. C.A. Reitzels Vorlag, Oxford University Press, London.

Seibel B.A., Maas A.E., Dierssen H.M., 2012. Energetic plasticity underlies a variable response to ocean acidification in the pteropod, *Limacina helicina antarctica*. PLoS ONE 7, e30464.

Sun C., Zhao Y., Li H., Dong Y., MacIsaak H.J., Zhan A., 2015. Unreliable quantitation of species abundance based on high-throughput sequencing data of zooplankton communities. Aquatic Biology 24, 9–15.

Taylor H.R., Harris W.E., 2012. An emergent science on the brink of irrelevance: a review of the past 8 years of DNA barcoding. Molecular Ecology Resources 12, 377–388.

Van der Spoel S., Bleeker J., Kobayasi H., 1993. From *Cavolinia longirostris* to twenty-four *Diacavolinia* taxa, with a phylogenetic discussion (Mollusca, Gastropoda). Bijdragen tot de Dierkunde 62, 127–166.

Wall-Palmer D., Smart C.W., Kirby R., Hart M.B., Peijnenburg K.T.C.A., Janssen A.W., 2016. A review of the ecology, palaeontology and distribution of atlantid heteropods (Caenogastropoda: Pterotracheoidea: Atlantidae). Journal of Molluscan Studies 82, 221–234.

Wu S., Xiong J., Yu Y., 2015. Taxonomic resolutions based on 18S rRNA genes: a case study of subclass Copepoda. PLoS ONE 10, e0131498.

Summary

Marine biogeography and evolution: diversity patterns of planktonic gastropods and amphipods

Current changes in the oceans, including global warming and ocean acidification, are partially caused by human activity, unlike earlier episodes of change throughout geological history. Understanding and forecasting the responses of marine organisms to these changes is top priority for scientists, managers and policy makers. Yet, relatively little is known of the effects of ocean change on marine zooplankton. Ocean change affects species diversity and distributions, but different zooplankton taxa may not be equally affected. This thesis aims to fill this knowledge gap by contributing information regarding the taxonomy, genetic diversity, and biogeography of several selected marine zooplankton groups, providing baseline information that is needed to track the effects of ocean change on marine zooplankton. The study organisms in this thesis represent two groups of planktonic gastropods: pteropods (sea butterflies and sea angels) and heteropods (sea elephants), and a group of crustaceans: the hyperiid amphipods. Pteropods are uniquely suitable for the study of long-term evolutionary processes in the open ocean because their aragonite shells provide a good fossil record. They have been proposed as bioindicators to monitor the impacts of ocean acidification. Heteropods are another group of pelagic gastropods that independently colonized the pelagic. They are visual predators that prey upon shelled pteropods. Shelled heteropods have received little attention relative to pteropods, but are probably equally vulnerable to the effects of ocean acidification. Hyperiids represent a highly diverse and abundant group and are often commensals and parasitoids of gelatinous plankton. They play unique and important ecological roles in pelagic foodwebs.

The major questions that are being addressed in this thesis are:

(1) How can closely related pteropod species be distinguished?

(2) When did current pteropod biodiversity evolve?

(3) Which pteropod, heteropod, and hyperiid amphipod species are where in the Atlantic Ocean?

How can closely related pteropod species be distinguished?

To be used as bioindicators of ocean acidification, it is important to accurately assess species boundaries of pteropods, because different species are expected to respond differently to ocean changes. An integrative taxonomic approach based on combining morphological, genetic, and geographic information was applied to assess species boundaries in the circumglobal pteropod genera *Cuvierina* and *Diacavolinia* (Chapters 3, 4, and 5). The approach combined molecular phylogenetic analyses based on Cytochrome Oxidase I (COI) and 28S DNA sequences, geometric morphometric analyses of shells, as well as ecological niche modelling (only in Chapter 3). Museum samples provided an essential initial framework for assessing

species boundaries based on morphological information and a substantial source of information for increasing geographic coverage.

Based on geometric morphometric analyses, six morphotypes were distinguished within the genus *Cuvierina* (Chapter 3). These morphotypes had distinct ecological preferences and belonged to three major genetic clades. Using a fossil-calibrated phylogenetic analysis, it was estimated that these clades separated in the Late Oligocene and Early to Middle Miocene. Based on these findings, two previously distinguished subgenera of *Cuvierina* were rejected and a new species endemic to the Pacific Ocean was described (Chapter 4). Current consensus is that there exist two Atlantic, two Pacific and two Indo-Pacific *Cuvierina* species. These species can generally be distinguished based on their differences in shell shape and size, but more information is preferred to more confidently confirm their status as species. Because not all taxa were distinguished based on COI sequences, the number of genetic markers should be increased.

Diacavolinia is the most speciose genus of shelled pteropods with 24 described taxa. The measurements of several hundreds of freshly-collected and museum specimens including type specimens provided evidence for a reduction in the number of species to a maximum of 13 species (Chapter 5). The most important biogeographic barriers were between the Atlantic and Indo-Pacific oceans, and between the East and Central Pacific. These barriers are well-known for other zooplankton groups as well.

All in all, an integrative approach proved successful in distinguishing between pteropod species, although additional molecular markers are needed to more accurately distinguish between closely related taxa, as was demonstrated for *Cuvierina* and *Diacavolinia*. Moreover, some rare *Diacavolinia* taxa currently lack morphological and/or genetic information. Hence, additional sampling efforts are still needed, especially in the highly diverse Indo-Australian Archipelago and the East Pacific Ocean.

When did current pteropod biodiversity evolve?

Combined with molecular methods for phylogenetic inference, the fossil record improves our understanding of the evolution of pteropods by providing a framework of ages for certain shelled taxa. The phylogenetic relationships of 55 pteropod species (euthecosomes, pseudothecosomes, and gymnosomes) collected from all ocean basins and spanning the diversity of the group were inferred using time-calibrated molecular phylogenies based on combined analyses of COI, 28S, and 18S gene sequence data and information of the fossil record (Chapter 2). However, the phylogenetic relationships between (sub)orders euthecosomes, pseudothecosomes, and gymnosomes were not resolved based on the available information. The uncoiled euthecosomes were monophyletic, and within this group, *Creseis* was monophyletic, as well as all other uncoiled genera together. Most uncoiled genera were also supported, but *Clio* was polyphyletic, and *Diacavolinia* grouped within *Cavolinia*, rendering the latter genus paraphyletic. The coiled euthecosomes were not monophyletic contrary to the accepted morphology-based taxonomy, but indi-

vidual genera were. With the first occurrence of coiled euthecosomes estimated at 79–66 million years ago (mya), it was inferred that uncoiled euthecosomes evolved 51–42 mya and that most extant uncoiled genera originated 40–15 mya, with *Creseis* as the earliest diverging lineage at 41–38 mya. These findings are congruent with a molecular clock analysis using the Isthmus of Panama formation as an independent calibration. Although not all phylogenetic relationships could be resolved, the new data on the diversity and evolution of pteropods are an essential first step for their use as bio-indicators of the ongoing effects of ocean acidification. To improve phylogenetic resolution, especially at higher (order or suborder) levels, it will be necessary to increase the number of genetic markers substantially (e.g., by applying a phylogenomic approach). For future studies, it is also necessary to increase taxon sampling of pseudothecosome and gymnosome taxa, which were underrepresented in this study.

Which pteropod, heteropod, and hyperiid amphipod species are where in the Atlantic Ocean?

The distributions and abundances of many marine zooplankton species are still poorly known. Large collections of meso- and macrozooplankton material collected from the upper 300 m along a basin-scale meridional transect in the Atlantic Ocean between 46°N and 46°S contributed to the characterization of the diversity and distribution of pteropods, heteropods, and hyperiid amphipods (Chapters 6 and 7). Species richness of pteropods and heteropods was highest in the stratified (sub)tropical waters between ~30°N and ~30°S, a diversity pattern similar to that reported for other pelagic taxa (e.g., decapods, ostracods, and foraminifera) (Chapter 6). The diversity of pteropods and heteropods was lowest just south of 40°S. Along a similar transect, maximum species and genus richness of hyperiids occurred in the equatorial upwelling region between 7°N and 8°S (Chapter 7). The observations of equatorial instead of subtropical maxima in species and genus richness for hyperiids suggest that the mechanisms controlling diversity in this group are distinct from other zooplankton groups. These are probably influenced by the distribution and diversity of gelatinous hosts for hyperiids. The distributions of communities of pteropods, heteropods, and hyperiids were largely congruent with Longhurst's biogeochemical provinces. Repeated zooplankton sampling combined with environmental data collected along similar transects will be crucial to monitor changes in species diversity and distribution patterns in response to ocean change.

Future directions

Integrative taxonomy offers a more comprehensive framework for testing species hypotheses than DNA barcoding alone, because diverse and sometimes incomplete character and data types can be combined, and because the sole use of genetic information may sometimes fail to delimit actual species (Chapter 8). Novel research tools, despite their pitfalls, can help species identification and improve our evolutionary understanding of marine zooplankton. Three-dimensional geo-

metric morphometric analyses may better distinguish between taxa than the two-dimensional geometric morphometric analyses used in this thesis. Next-generation sequencing of genomes may better resolve species boundaries and phylogenetic relationships than traditional Sanger sequencing of a few selected genes. Meta-barcoding studies based on next-generation sequencing may improve our understanding of zooplankton communities not only in the epipelagic, but also at greater depths, of which still little is known. Furthermore, these methods may be applied to monitor seasonal variation as well as long-term changes in zooplankton communities in response to, e.g., climate change.

All published papers and data supporting the results of this thesis are freely available online, stored in the Dryad online repository and GenBank.

Samenvatting

Mariene biogeografie en evolutie: diversiteitspatronen van planktonische slakken en vlokreeften

De huidige veranderingen in de oceaan, zoals opwarming en oceaanverzuring, worden gedeeltelijk veroorzaakt door de mens, en zijn daarmee anders dan eerdere grootschalige veranderingen in de geologische geschiedenis van onze planeet. Het begrijpen en voorspellen van het effect van deze veranderingen heeft hoge prioriteit voor wetenschappers en beleidsmakers. Er is echter betrekkelijk weinig bekend over de effecten van deze veranderingen op het dierlijke plankton (ofwel zoöplankton) in zee, de organismen die aan de basis staan van vrijwel alle mariene voedselketens. Grootschalige verandering van de oceaan heeft invloed op de diversiteit en verspreidingspatronen van soorten, met verschillende effecten op verschillende groepen zoöplankton. Dit proefschrift onderzoekt de taxonomie, genetische diversiteit, en soortensamenstelling van enkele groepen marien zoöplankton en voorziet daarmee in basiskennis die nodig is om de effecten van verandering van de oceaan op marien zoöplankton te kunnen registreren. De onderzoeksorganismen in dit proefschrift zijn planktonische gastropoden (slakjes): de pteropoden (zeevlinders en zee-engelen) en heteropoden (zeeolifanten), alsook een groep crustaceeën (kreeftachtigen): de hyperiide amfipoden (vlokreeftjes). Pteropoden zijn bijzonder geschikt voor het bestuderen van langdurige evolutionaire processen in de open oceaan omdat hun schelpjes kunnen fossiliseren. Ze staan wereldwijd in de belangstelling als mogelijke bio-indicatoren om het effect van oceaanverzuring op kalkvormende organismen te kunnen meten. Heteropoden zijn een andere groep planktonische gastropoden die onafhankelijk de open waterkolom hebben gekoloniseerd. Het zijn visuele roofdieren en hun voedsel bestaat voornamelijk uit zeevlinders. Heteropoden hebben tot dusver minder aandacht gekregen van oceaanwetenschappers dan pteropoden, maar zijn waarschijnlijk even kwetsbaar voor de effecten van oceaanverzuring. Hyperiiden zijn een zeer diverse en veelvoorkomende groep amfipoden in het plankton en ze hebben vaak een parasitaire relatie met gastheersoorten zoals salpen. Ze spelen een unieke ecologische rol in voedselketens in de oceaan.

De belangrijkste vragen die in dit proefschrift aan bod komen zijn:

(1) Hoe kunnen nauw verwante soorten pteropoden worden onderscheiden?

(2) Wanneer is de huidige diversiteit aan pteropoden ontstaan?

(3) Welke soorten pteropoden, heteropoden en hyperiiden bevinden zich waar in de Atlantische Oceaan?

Hoe kunnen nauw verwante soorten pteropoden worden onderscheiden?

Om pteropoden te kunnen gebruiken als bio-indicatoren voor oceaanverzuring is het belangrijk om hun soortsgrenzen in kaart te brengen, want verschillende soorten kunnen op een verschillende manier reageren op veranderingen in de oceaan.

Een gecombineerde taxonomische benadering gebaseerd op zowel morfologische als genetische en geografische informatie is toegepast om soortsgrenzen te bepalen in de tropische en subtropische pteropodengenera *Cuvierina* en *Diacavolinia* (Hoofdstukken 3, 4 en 5). Deze aanpak omvatte moleculair fylogenetische analyses gebaseerd op DNA sequenties van de Cytochrome Oxidase I (COI) en 28S genen, geometrisch morfometrische analyses van schelpjes en het modelleren van ecologische niches (alleen in Hoofdstuk 3). Museummateriaal vormde de basis voor het bepalen van soortsgrenzen gebaseerd op morfologische informatie en was een belangrijke bron van informatie voor een betere geografische verspreiding van monsters.

Zes morfotypen van het genus *Cuvierina* konden worden onderscheiden gebaseerd op geometrisch morfometrische analyses van hun schelpjes (Hoofdstuk 3). Deze zes morfotypen hadden duidelijke ecologische voorkeuren en vormden samen drie genetische groepen. Volgens de evolutionaire stamboom aan de hand van fossielen en DNA zijn deze groepen ontstaan in het Laat-Oligoceen en Vroegtot Midden-Mioceen. Aan de hand van deze bevindingen werden twee voorheen gescheiden subgenera van *Cuvierina* verworpen. Ook werd een nieuwe soort beschreven die alleen voorkomt in de Pacifische Oceaan (Hoofdstuk 4). De huidige consensus is dat er twee Atlantische, twee Pacifische en twee Indo-Pacifische soorten *Cuvierina* bestaan. Deze soorten kunnen over het algemeen onderscheiden worden gebaseerd op hun verschillende schelpvormen en -afmetingen, maar meer informatie is wenselijk om hun soortenstatus verder te onderbouwen.

Diacavolinia is met 24 beschreven taxa het meest soortenrijke genus van de pteropoden met schelp. Metingen aan enkele honderden recent verzamelde of uit museumcollecties afkomstige individuen, waaronder type exemplaren, vormden bewijs voor een vermindering van het aantal soorten tot maximaal 13 (Hoofdstuk 5). De belangrijkste biogeografische barrières bevonden zich tussen de Atlantische en Indo-Pacifische oceanen en tussen de oostelijke en centrale Pacifische Oceaan. Deze barrières zijn ook beschreven aan de hand van verspreidingspatronen van andere zoöplanktongroepen.

Over het algemeen was de gecombineerde taxonomische aanpak succesvol in het onderscheiden van pteropodensoorten, maar meer moleculaire informatie is nodig om nauw verwante soorten nog beter te kunnen onderscheiden, zoals blijkt voor *Cuvierina* en *Diacavolinia* soorten. Bovendien is er voor sommige zeldzame *Diacavolinia*-soorten nog geen morfologische en/of genetische informatie beschikbaar. Daarvoor zijn meer samples nodig, vooral uit de zeer diverse Indo-Australische Archipelago en de Oost-Pacifische Oceaan.

Wanneer is de huidige diversiteit aan pteropoden ontstaan?

Fossielen bieden een leeftijdsreferentie voor bepaalde pteropodensoorten. Dankzij fossielen en gecombineerde analyses van COI, 28S en 18S sequenties konden de fylogenetische relaties van 55 pteropodensoorten (euthecosomen, pseudothecosomen en gymnosomen), verzameld uit alle oceanen en representatief voor de diversiteit van de groep, worden afgeleid (Hoofdstuk 2). De fylogenetische rela-

ties tussen de (sub)orders euthecosomen, pseudothecosomen en gymnosomen konden niet worden opgelost op basis van de beschikbare informatie. De ongewonden euthecosomen vormden een monofyletische groep, en binnen deze groep was *Creseis* monofyletisch, net als alle andere ongewonden genera bij elkaar. De meeste andere ongewonden genera werden ook ondersteund, maar *Clio* was polyfyletisch, en *Diacavolinia* groepeerde binnen *Cavolinia*, waarmee de laatste parafyletisch is. De gewonden euthecosomen waren niet monofyletisch, in tegenstelling tot de geaccepteerde, op morfologie gebaseerde taxonomie, maar individuele genera waren dat wel. In combinatie met het eerste fossiel van een gewonden euthecosoom van ca. 79–66 miljoen jaar oud kon worden afgeleid dat de ongewonden euthecosomen 51–42 miljoen jaar geleden evolueerden en dat de meeste huidige genera 40–15 miljoen jaar geleden ontstonden, met *Creseis* als het oudste genus van 41–38 van miljoen jaar oud. Deze bevindingen komen ongeveer overeen met een moleculaire klok gecalibreerd op basis van de formatie van het Isthmus van Panama. Hoewel niet alle evolutionaire relaties achterhaald konden worden, zijn de nieuwe data over de diversiteit en evolutie van pteropoden een belangrijke eerste stap voor hun gebruik als bio-indicatoren van de voortschrijdende effecten van oceaanverzuring. Om de evolutionaire stamboom van pteropoden verder op te lossen, moeten vooral meer soorten pseudothecosomen en gymnosomen worden toegevoegd.

Welke soorten pteropoden, heteropoden en hyperiiden bevinden zich waar in de Atlantische Oceaan?

Over de verspreiding en abundantie van veel soorten marien zoöplankton is nog weinig bekend. Grote collecties meso- en macrozoöplankton, verzameld langs een transect in de Atlantische Oceaan tussen 46° noorderbreedte (NB) en 46° zuiderbreedte (ZB) en tot 300 meter diep, hebben bijgedragen aan het karakteriseren van de diversiteit en verspreiding van pteropoden, heteropoden en hyperiide amfipoden (Hoofdstukken 6 en 7). De soortenrijkdom van pteropoden en heteropoden was het grootst in de gestratificeerde (sub)tropische wateren tussen ongeveer 30° NB en 30° ZB, een diversiteitspatroon vergelijkbaar met wat bekend is van andere planktonische groepen (zoals decapoden, ostracoden en foraminiferen) (Hoofdstuk 6). De diversiteit van pteropoden en heteropoden was het laagst ten zuiden van 40° ZB. Het maximum aantal soorten en genera van hyperiiden is gevonden rondom de evenaar tussen 7° NB en 8° ZB langs een vergelijkbaar transect (Hoofdstuk 7). Deze hoge biodiversiteit rondom de evenaar suggereert dat de mechanismen die de soortenrijkdom in hyperiiden reguleren anders zijn dan van de meeste andere zoöplanktongroepen die een hoge diversiteit vertonen over een veel bredere tropische en subtropische zone. Diversiteitspatronen van hyperiiden worden waarschijnlijk beïnvloed door de verspreiding en diversiteit van de gastheersoorten in het plankton waarvan veel hyperiiden afhankelijk zijn. De verspreidingspatronen van gemeenschappen van pteropoden, heteropoden en hyperiiden kwamen grotendeels overeen met Longhurst's biogeochemische provincies. Een herhaalde

zoöplanktonbemonstering in combinatie met omgevingsdata, verzameld langs vergelijkbare transecten, is noodzakelijk om veranderingen in soortendiversiteits- en verspreidingspatronen als gevolg van oceaanverandering te meten.

Toekomstig onderzoek

Een gecombineerde taxonomische aanpak biedt een steviger basis voor het onderscheiden van soorten dan identificaties die alleen op morfologie of DNA barcoding gebaseerd zijn. Door integratie van de verschillende benaderingen kunnen diverse en soms incomplete kenmerken gecombineerd worden om tot een goede identificatie te komen (Hoofdstuk 8). In toekomstig onderzoek kunnen nieuwe onderzoeksmethoden, ondanks hun tekortkomingen, de identificatie van soorten verder bevorderen en zo leiden tot een beter begrip van de evolutie van marien zoöplankton. Driedimensionale geometrisch morfometrische analyses onderscheiden waarschijnlijk beter tussen soorten dan de tweedimensionale geometrisch morfometrische analyses toegepast in dit proefschrift. Nauw verwante soorten kunnen met next-generation sequencing van het genoom beter worden onderscheiden dan met traditionele Sanger-sequencing van slechts een handvol genen. Metabarcoding, een methode gebaseerd op next-generation sequencing, kan bovendien onze kennis van zoöplanktongemeenschappen niet alleen in het bovenste deel van de oceaan vergroten, maar ook in de diepere oceaan waarover nog weinig bekend is. Daarnaast kunnen deze nieuwe methoden ook worden toegepast om langetermijnveranderingen in de soortensamenstelling van het zoöplankton als gevolg van bijvoorbeeld klimaatverandering te meten.

Alle gepubliceerde papers en data van dit proefschrift zijn gratis online beschikbaar en opgeslagen in de Dryad databank en GenBank.

Acknowledgements

First of all, I want to thank Katja Peijnenburg. Dear Katja, we first met during my BSc research project on pteropods at the University of Amsterdam in 2010. I also completed my first MSc project under your supervision in 2011, laying the foundations for the work that would result in this PhD thesis. As your very first PhD candidate I want to thank you for all your insights, positive conversations, all the times we visited conferences together, all the papers you stumbled upon that may somehow be interesting to cite in my own papers, and more than anything, your trust in me.

I thank my promotors Jef Huisman and Steph Menken from the Institute for Biodiversity and Ecosystem Dynamics at the University of Amsterdam for their advice and encouragement along the way.

I am grateful to members of the Naturalis Marine Biodiversity team and the former Marine Zoology department for the scientific discussions and not always equally scientific dinners. Dear Deborah Wall-Palmer, Remy van der Hulst, Marloes Tump and Serena Le Double, thank you for your great contributions to various papers. I enjoyed our collaboration. Dear Emma Otto, Diede Maas, Lisette Mekkes, Cas Retel, Aleksandra Dragozet, Thijs Bal, Renate Olie and Zoë van Kemenade, thank you for getting to know you. I also want to thank Willem Renema, Nicole de Voogd, Frank Wesselingh, Bert Hoeksema, Bastian Reijnen and Sancia van der Meij for their interest in my work. Although I often worked on this thesis from home, with one or two cats lying on my desk or on my lap, I thank Martien van Oijen for being my roommate at Naturalis.

I thank Erica Goetze from the University of Hawai´i at Mānoa for our collaboration, resulting in multiple publications. Dear Erica, I had a great time working with you and with Michelle Jungbluth during the Atlantic Meridional Transect 24 oceanographic expedition in 2014. I also thank all other scientists and crew members I met during this expedition.

Furthermore, I thank all members of my PhD committee for their interest in my work, all paper co-authors, all other colleagues at Naturalis and the Institute for Biodiversity and Ecosystem Dynamics whose valuable input helped me with different parts of this thesis, as well as all colleagues I met during my scientific outreach activities.

From a young age I have been interested in (marine) biology, long before I started my PhD project. With this in mind I am grateful to my biology teacher Yuri Robbers at the Stedelijk Gymnasium Leiden. I also thank Kjell Bjørklund for supervising my second MSc research project, for his recommendations, and for being a great mentor.

Continuous personal development and lifelong learning are very important to me. I thank my friends, family and acquaintances for their support. I especially thank my paranymphs Rebecca de Leeuw and Suzanne Veerman. A further list of names would be too extensive – you know who you are.

Last but not least: dear Mark Rog, words can’t describe how happy I am with you in my life.

Curriculum vitae

'Curiouser and curiouser!' cried Alice

Alice's Adventures in Wonderland, Lewis Carroll, 1865

Born in The Netherlands with Dutch and British nationalities, Alice Karen Burridge (July 16th, 1989) has always been a curious person. The subjects of her curiosity were diverse, but from an early age she could engage in what fascinated her for long stretches of time. Topics that fascinated her included astronomy, geology, history, garden life, cats, and the creatures hiding in the rocky shores of Devon. She was often found reading, writing stories, painting, or digging in the garden. After attending multiple primary and secondary schools she completed the Stedelijk Gymnasium in Leiden, The Netherlands, in 2007. Subjects included languages as well as sciences.

In 2007 she started her BSc studies in Earth Sciences at the University of Amsterdam. In her third year she pursued a minor in biological sciences, including paleoecology, aquatic ecology, and marine biology courses. Furthermore, she followed an elective course in relativity as well as courses in short story writing and impressionistic painting. Rather than choosing an earth science-focused individual research project to complete her BSc studies, she chose a project that would eventually get out of hand. Supervised by Dr. Katja Peijnenburg, she studied shell shapes of a group of pteropod snails (sea butterflies). She obtained her BSc degree Cum Laude in 2010.

In the same year she started her MSc studies in Biological Sciences, track Limnology & Oceanography, at the University of Amsterdam to further accommodate her interest in marine life. Upon following an array of courses in freshwater and marine biology as well as an elective course in astronomy, she pursued two research projects for which she was awarded an early-career research grant from the Malacological Society of London and an Erasmus scholarship. In her first project she returned to studying sea butterflies and learned how to work with genetic data. As part of this project she participated in a short student research cruise, organized by the University of Hawai'i at Mānoa, to collect fresh samples off the Hawai'ian coast. She presented the results of this project during the Young Systematists' Forum in London, earning the Best Presentation Prize. For her second

project she moved to Oslo, Norway, for seven months to study the diversity of radiolarians, marine microplankton, supervised by Professor Emeritus Kjell Rasmus Bjørklund at the University of Oslo and its Natural History Museum. In 2012 she obtained her MSc degree Cum Laude.

In September 2012 she started her PhD research on the diversity and evolution of marine zooplankton at Naturalis Biodiversity Center and the University of Amsterdam, supervised by Dr. Katja Peijnenburg. As part of her research she joined the Atlantic Meridional Transect #24 oceanographic expedition from England to the Falkland Islands in 2014, for which she obtained grants from the Dutch Royal Academy of Sciences (KNAW) and the Royal Netherlands Institute for Sea Research (NIOZ). On board she was part of the 'Zooplankton team' led by Dr. Erica Goetze (University of Hawai'i at Mānoa). She presented her work at conferences in Galway (Ireland), Honolulu (USA), London, Cambridge, Plymouth (UK), and Bergen (Norway). She also was a teaching assistant at the University of Amsterdam and supervised BSc and MSc student projects. Outreach activities were the Naturalis Biodiversity Center colloquium committee, Science Talks in Naturalis to communicate science to the general public, and a blog about her research activities: 'Alice's adventures underwater'.

Publications in peer-reviewed journals

Burridge A.K., Goetze E., Wall-Palmer D., Le Double S.L., Huisman J., Peijnenburg K.T.C.A., in press. Diversity and abundance of pteropods and heteropods along a meridional transect in the Atlantic Ocean. Progress in Oceanography, published online in 2016.

Burridge A.K., Tump M., Vonk R., Goetze E., Peijnenburg K.T.C.A., in press. Diversity and distribution of hyperiid amphipods along a latitudinal transect in the Atlantic Ocean. Progress in Oceanography, published online in 2016.

Burridge A.K., Hörnlein C., Janssen A.W., Hughes M., Bush S.L., Marlétaz F., Gasca R., Pierrot-Bults A.C., Michel E., Todd J.A., Young J.R., Osborn K.J., Menken S.B.J., Peijnenburg K.T.C.A., 2017. Time-calibrated molecular phylogeny of pteropods. PLoS ONE 12, e0177325.

Manno C., Bednaršek N., Tarling G.A., Peck V.L., Comeau S., Adhikari D., Bakker D.C.E., Bauerfeind E., Bergan J.A., Berning **M.I.**, Buitenhuis E., **Burridge A.K.**, Chierici M., Flöter S., Fransson A., Gardner J., Howes E., Keul N., Kimoto K., Kohnert P., Lawson G.L., Lischka S., Maas A., Mekkes L., Oakes R.L., Pebody C., Peijnenburg K.T.C.A., Seifert M., Skinner J., Thibodeau P.S., Wall-Palmer D., Ziveri P., 2017. Shelled pteropods in peril: assessing vulnerability in a high CO_2 ocean. Earth-Science Reviews 169, 132–145.

Wall-Palmer D., **Burridge A.K.**, Peijnenburg K.T.C.A., Janssen A., Kirby R., Hart M., Smart C., 2016. Evidence for the validity of *Protatlanta sculpta* (Gastropoda: Pterotracheoidea). Contributions to Zoology 85, 423–435.

Burridge A.K., Janssen A.W., Peijnenburg, K.T.C.A., 2016. Revision of the genus *Cuvierina* Boas, 1886 based on integrative taxonomic data, including the description of a new species from the Pacific Ocean (Gastropoda, Thecosomata). ZooKeys 619, 1–12.

Wall-Palmer D., **Burridge A.K.**, Peijnenburg K.T.C.A., 2016. *Atlanta jansseni*, a new species of shelled heteropod from the Southern Subtropical Convergence Zone (Gastropoda, Pterotracheoidea). ZooKeys 604, 13–30.

Burridge A.K., Goetze E., Raes N., Huisman J., Peijnenburg K.T.C.A., 2015. Global biogeography and evolution of *Cuvierina* pteropods. BMC Evolutionary Biology 15, 39.

Burridge A.K., Bjørklund K.R., Kruglikova S.B., Hammer Ø., 2014. Inter- and intraspecific morphological variation of four-shelled *Actinomma* taxa (Radiolaria) in polar and subpolar regions. Marine Micropaleontology 110, 50–71.

Burridge A.K., Bjørklund K.R., 2014. Inter- and intraspecific morphological variation of three Hexacontium (Radiolaria) species in three southern Norwegian fjords: *H. gigantheum*, *H. pachydermum* and *H. enthacanthum*. Marine Micropaleontology 110, 72–82.

Author addresses

Naturalis Biodiversity Center, P.O. Box 9517, 2300 RA Leiden, The Netherlands

Alice K. Burridge, Remy van der Hulst, Arie W. Janssen, Serena L. Le Double, Katja T.C.A. Peijnenburg, Annelies C. Pierrot-Bults, Niels Raes, Marloes Tump, Ronald Vonk, Deborah Wall-Palmer

Institute for Biodiversity and Ecosystem Dynamics (IBED), University of Amsterdam, P.O. Box 94248, 1090 GE Amsterdam, The Netherlands

Alice K. Burridge, Christine Hörnlein, Martin Hughes, Jef Huisman, Serena L. Le Double, Steph B.J. Menken, Katja T.C.A. Peijnenburg, Annelies C. Pierrot-Bults, Ronald Vonk

Koninklijk Nederlands Instituut voor Onderzoek der Zee (NIOZ), P.O. Box 140, 4400 AC Yerseke, The Netherlands

Christine Hörnlein

Natural History Museum (NHM), Cromwell Road, London SW7 5BD, UK

Martin Hughes, Ellinor Michel, Jonathan A. Todd

Smithsonian Institution National Museum of Natural History, 10th St. & Constitution Ave. NW, Washington, DC 20560, USA

Stephanie L. Bush, Karen J. Osborn

Monterey Bay Aquarium Research Institute (MBARI), 7700 Sandholdt Road, Moss Landing, CA 95039 & Monterey Bay Aquarium, 886 Cannery Row, Monterey, CA 93940, USA

Stephanie L. Bush, Karen J. Osborn

Molecular Genetics Unit, Okinawa Institute of 26 Science and Technology, Onna-son, 904-0495, Japan

Ferdinand Marlétaz

El Colegio de la Frontera Sur (ECOSUR), Unidad Chetumal, Av. Centenario Km 5.5, Quintana Roo 77014, Chetumal, Mexico

Rebeca Gasca

Department of Earth Sciences, University College London, Gower Street, London WC1E 6BT, UK

Jeremy R. Young

Department of Oceanography, University of Hawaii at Manoa, 1000 Pope Road, Honolulu, HI 96822, USA

Erica Goetze

School of Geography, Earth and Environmental Sciences, Plymouth University, Drake Circus, Plymouth, Devon PL4 8AA, UK

Deborah Wall-Palmer

Thesis co-authors and contributions

Chapter 2

A.K. Burridge, K.T.C.A. Peijnenburg, E. Michel, J.A. Todd and J.R. Young designed the study and A.W. Janssen provided methodological input. A.K. Burridge, C. Hörnlein, M. Hughes, S.L. Bush, R. Gasca and K.J. Osborn provided specimen photographs and A.W. Janssen provided illustrations of fossil species. A.K. Burridge, C. Hörnlein, M. Hughes, S.L. Bush and K. Osborn generated the DNA sequences. A.K. Burridge and F. Marlétaz performed the phylogenetic analyses. A.K. Burridge visualized the data. A.K. Burridge and K.T.C.A. Peijnenburg wrote the manuscript. C. Hörnlein, A.W. Janssen, M. Hughes, S.L. Bush, F. Marlétaz, R. Gasca, A.C. Pierrot-Bults, E. Michel, J.A. Todd, J.R. Young, K.J. Osborn, and S.B.J. Menken reviewed and edited the manuscript.

Chapter 3

A.K. Burridge and K.T.C.A. Peijnenburg designed the study. A.K. Burridge generated, analyzed and visualized the data. A.K. Burridge and N. Raes applied ecological niche modelling. A.K. Burridge and K.T.C.A. Peijnenburg wrote the manuscript. E. Goetze, N. Raes and J. Huisman reviewed and edited the manuscript.

Chapter 4

A.K. Burridge and K.T.C.A. Peijnenburg designed the study. A.K. Burridge generated, analyzed and visualized the data. A.K. Burridge and A.W. Janssen wrote the manuscript. K.T.C.A. Peijnenburg reviewed and edited the manuscript.

Chapter 5

A.K. Burridge and K.T.C.A. Peijnenburg designed the study. A.K. Burridge generated the geometric morphometric data and R. v/d Hulst generated the DNA sequences. A.K. Burridge analyzed and visualized the data and wrote the manuscript. R. v/d Hulst contributed to the Materials and Methods paragraph. K.T.C.A. Peijnenburg and E. Goetze reviewed and edited the manuscript.

Chapter 6

A.K. Burridge and K.T.C.A. Peijnenburg designed the study. A.K. Burridge, D. Wall-Palmer and S.L. Le Double generated the data. A.K. Burridge analyzed and visualized the data and wrote the manuscript. K.T.C.A. Peijnenburg, E. Goetze, D. Wall-Palmer and J. Huisman reviewed and edited the manuscript.

Chapter 7

K.T.C.A. Peijnenburg and R. Vonk designed the study. M. Tump generated the data. A.K. Burridge analyzed and visualized the data. A.K. Burridge, K.T.C.A. Peijnenburg, E. Goetze, R. Vonk and M. Tump wrote, reviewed and edited the manuscript.

‘But I have too deeply enjoyed the voyage, not to recommend any naturalist, although he must not expect to be so fortunate in his companions as I have been, to take all chances, and to start, on travels by land if possible, if otherwise, on a long voyage. He may feel assured, he will meet with no difficulties or dangers, excepting in rare cases, nearly so bad as he beforehand anticipates. In a moral point of view, the effect ought to be, to teach him good-humoured patience, freedom from selfishness, the habit of acting for himself, and of making the best of every occurrence. In short, he ought to partake of the characteristic qualities of most sailors. Travelling ought also to teach him distrust; but at the same time he will discover, how many truly kind-hearted people there are, with whom he never before had, or ever again will have any further communication, who yet are ready to offer him the most disinterested assistance.’

Charles Darwin after the voyage of the Beagle, 1836. Published in *The Voyage of the Beagle* (first published in 1909, New York: P.E. Collier).